

Introduction to Modern Solid State Physics

Yuri M. Galperin

FYS 448

Department of Physics, P.O. Box 1048 Blindern, 0316 Oslo, Room 427A
Phone: +47 22 85 64 95, E-mail: iouri.galperinefys.uio.no

Contents

I Basic concepts	1
1 Geometry of Lattices ...	3
1.1 Periodicity: Crystal Structures	3
1.2 The Reciprocal Lattice	8
1.3 X-Ray Diffraction in Periodic Structures	10
1.4 Problems	18
2 Lattice Vibrations: Phonons	21
2.1 Interactions Between Atoms	21
2.2 Lattice Vibrations	23
2.3 Quantum Mechanics of Atomic Vibrations	38
2.4 Phonon Dispersion Measurement	43
2.5 Problems	44
3 Electrons in a Lattice.	45
3.1 Electron in a Periodic Field	45
3.1.1 Electron in a Periodic Potential	46
3.2 Tight Binding Approximation	47
3.3 The Model of Near Free Electrons	50
3.4 Main Properties of Bloch Electrons	52
3.4.1 Effective Mass	52
3.4.2 Wannier Theorem → Effective Mass Approach	53
3.5 Electron Velocity	54
3.5.1 Electric current in a Bloch State. Concept of Holes.	54
3.6 Classification of Materials	55
3.7 Dynamics of Bloch Electrons	57
3.7.1 Classical Mechanics	57
3.7.2 Quantum Mechanics of Bloch Electron	63
3.8 Second Quantization of Bosons and Electrons	65
3.9 Problems	67

II Normal metals and semiconductors	69
4 Statistics and Thermodynamics ...	71
4.1 Specific Heat of Crystal Lattice	71
4.2 Statistics of Electrons in Solids	75
4.3 Specific Heat of the Electron System	80
4.4 Magnetic Properties of Electron Gas.	81
4.5 Problems	91
5 Summary of basic concepts	93
6 Classical dc Transport ...	97
6.1 The Boltzmann Equation for Electrons	97
6.2 Conductivity and Thermoelectric Phenomena.	101
6.3 Energy Transport	106
6.4 Neutral and Ionized Impurities	109
6.5 Electron-Electron Scattering	112
6.6 Scattering by Lattice Vibrations	114
6.7 Electron-Phonon Interaction in Semiconductors	125
6.8 Galvano- and Thermomagnetic	130
6.9 Shubnikov-de Haas effect	140
6.10 Response to “slow” perturbations	142
6.11 “Hot” electrons	145
6.12 Impact ionization	148
6.13 Few Words About Phonon Kinetics.	150
6.14 Problems	152
7 Electrodynamics of Metals	155
7.1 Skin Effect.	155
7.2 Cyclotron Resonance	158
7.3 Time and Spatial Dispersion	165
7.4 ... Waves in a Magnetic Field	168
7.5 Problems	169
8 Acoustical Properties...	171
8.1 Landau Attenuation.	171
8.2 Geometric Oscillations	173
8.3 Giant Quantum Oscillations.	174
8.4 Acoustical properties of semiconductors	175
8.5 Problems	180

CONTENTS	iii
9 Optical Properties of Semiconductors	181
9.1 Preliminary discussion	181
9.2 Photon-Material Interaction	182
9.3 Microscopic single-electron theory	189
9.4 Selection rules	191
9.5 Intraband Transitions	198
9.6 Problems	202
9.7 Excitons	202
9.7.1 Excitonic states in semiconductors	203
9.7.2 Excitonic effects in optical properties	205
9.7.3 Excitonic states in quantum wells	206
10 Doped semiconductors	211
10.1 Impurity states	211
10.2 Localization of electronic states	215
10.3 Impurity band for lightly doped semiconductors.	219
10.4 AC conductance due to localized states	225
10.5 Interband light absorption	232
III Basics of quantum transport	237
11 Preliminary Concepts	239
11.1 Two-Dimensional Electron Gas	239
11.2 Basic Properties	240
11.3 Degenerate and non-degenerate electron gas	250
11.4 Relevant length scales	251
12 Ballistic Transport	255
12.1 Landauer formula	255
12.2 Application of Landauer formula	260
12.3 Additional aspects of ballistic transport	265
12.4 $e - e$ interaction in ballistic systems	266
13 Tunneling and Coulomb blockage	273
13.1 Tunneling	273
13.2 Coulomb blockade	277
14 Quantum Hall Effect	285
14.1 Ordinary Hall effect	285
14.2 Integer Quantum Hall effect - General Picture	285
14.3 Edge Channels and Adiabatic Transport	289
14.4 Fractional Quantum Hall Effect	294

IV Superconductivity	307
15 Fundamental Properties	309
15.1 General properties	309
16 Properties of Type I ..	313
16.1 Thermodynamics in a Magnetic Field.	313
16.2 Penetration Depth	314
16.3 ...Arbitrary Shape	318
16.4 The Nature of the Surface Energy.	328
16.5 Problems	329
17 Magnetic Properties -Type II	331
17.1 Magnetization Curve for a Long Cylinder	331
17.2 Microscopic Structure of the Mixed State	335
17.3 Magnetization curves.	343
17.4 Non-Equilibrium Properties. Pinning.	347
17.5 Problems	352
18 Microscopic Theory	353
18.1 Phonon-Mediated Attraction	353
18.2 Cooper Pairs	355
18.3 Energy Spectrum	357
18.4 Temperature Dependence	360
18.5 Thermodynamics of a Superconductor	362
18.6 Electromagnetic Response	364
18.7 Kinetics of Superconductors	369
18.8 Problems	376
19 Ginzburg-Landau Theory	377
19.1 Ginzburg-Landau Equations	377
19.2 Applications of the GL Theory	382
19.3 N-S Boundary	388
20 Tunnel Junction. Josephson Effect.	391
20.1 One-Particle Tunnel Current	391
20.2 Josephson Effect	395
20.3 Josephson Effect in a Magnetic Field	397
20.4 Non-Stationary Josephson Effect	402
20.5 Wave in Josephson Junctions	405
20.6 Problems	407

21 Mesoscopic Superconductivity	409
21.1 Introduction	409
21.2 Bogoliubov-de Gennes equation	410
21.3 N-S interface	412
21.4 Andreev levels and Josephson effect	421
21.5 Superconducting nanoparticles	425
V Appendices	431
22 Solutions of the Problems	433
A Band structure of semiconductors	451
A.1 Symmetry of the band edge states	456
A.2 Modifications in heterostructures.	457
A.3 Impurity states	458
B Useful Relations	465
B.1 Trigonometry Relations	465
B.2 Application of the Poisson summation formula	465
C Vector and Matrix Relations	467

Part I

Basic concepts

Chapter 1

Geometry of Lattices and X-Ray Diffraction

In this Chapter the general static properties of crystals, as well as possibilities to observe crystal structures, are reviewed. We emphasize basic principles of the crystal structure description. More detailed information can be obtained, e.g., from the books [1, 4, 5].

1.1 Periodicity: Crystal Structures

Most of solid materials possess crystalline structure that means *spatial periodicity* or *translation symmetry*. All the lattice can be obtained by repetition of a building block called **basis**. We assume that there are 3 non-coplanar vectors \mathbf{a}_1 , \mathbf{a}_2 , and \mathbf{a}_3 that leave *all the properties* of the crystal unchanged after the shift as a whole by any of those vectors. As a result, any lattice point \mathbf{R}' could be obtained from another point \mathbf{R} as

$$\mathbf{R}' = \mathbf{R} + m_1\mathbf{a}_1 + m_2\mathbf{a}_2 + m_3\mathbf{a}_3 \quad (1.1)$$

where m_i are integers. Such a lattice of building blocks is called the **Bravais lattice**. The crystal structure could be understood by the combination of the properties of the building block (basis) and of the Bravais lattice. Note that

- There is no unique way to choose \mathbf{a}_i . We choose \mathbf{a}_1 as shortest period of the lattice, \mathbf{a}_2 as the shortest period not parallel to \mathbf{a}_1 , \mathbf{a}_3 as the shortest period not coplanar to \mathbf{a}_1 and \mathbf{a}_2 .
- Vectors \mathbf{a}_i chosen in such a way are called **primitive**.
- The volume cell enclosed by the primitive vectors is called the **primitive unit cell**.
- The volume of the primitive cell is \mathcal{V}_0

$$\mathcal{V}_0 = \underline{(\mathbf{a}_1[\mathbf{a}_2\mathbf{a}_3])} \quad (1.2)$$

The natural way to describe a crystal structure is a set of *point group operations* which involve operations applied around a point of the lattice. We shall see that symmetry provide important restrictions upon vibration and electron properties (in particular, spectrum degeneracy). Usually are discussed:

Rotation, C_n : Rotation by an angle $2\pi/n$ about the specified axis. There are *restrictions* for n . Indeed, if a is the lattice constant, the quantity $b = a + 2a \cos \phi$ (see Fig. 1.1) Consequently, $\cos \phi = i/2$ where i is integer.

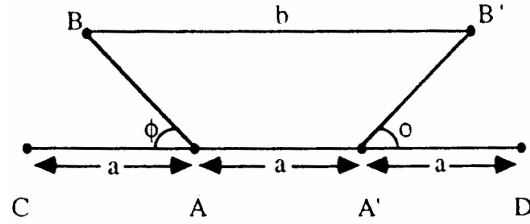


Figure 1.1: On the determination of rotation symmetry

Inversion, I : Transformation $\mathbf{r} \rightarrow -\mathbf{r}$, fixed point is selected as origin (lack of inversion symmetry may lead to piezoelectricity);

Reflection, σ : Reflection across a plane;

Improper Rotation, S_n : Rotation C_n , followed by reflection in the plane normal to the rotation axis.

Examples

Now we discuss few examples of the lattices.

One-Dimensional Lattices - Chains

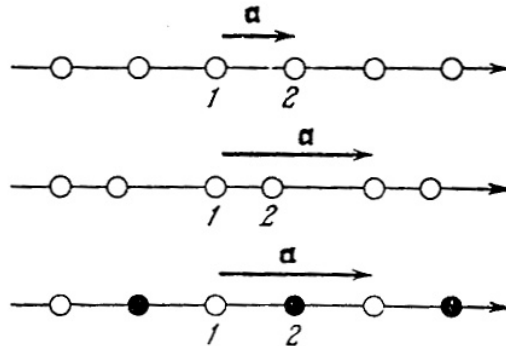


Figure 1.2: One dimensional lattices

1D chains are shown in Fig. 1.2. We have only 1 translation vector $|\mathbf{a}_1| = a$, $\mathcal{V}_0 = a$.

White and black circles are the atoms of different kind. a is a *primitive* lattice with one atom in a primitive cell; b and c are *composite* lattice with two atoms in a cell.

Two-Dimensional Lattices

There are 5 basic classes of 2D lattices (see Fig. 1.3)

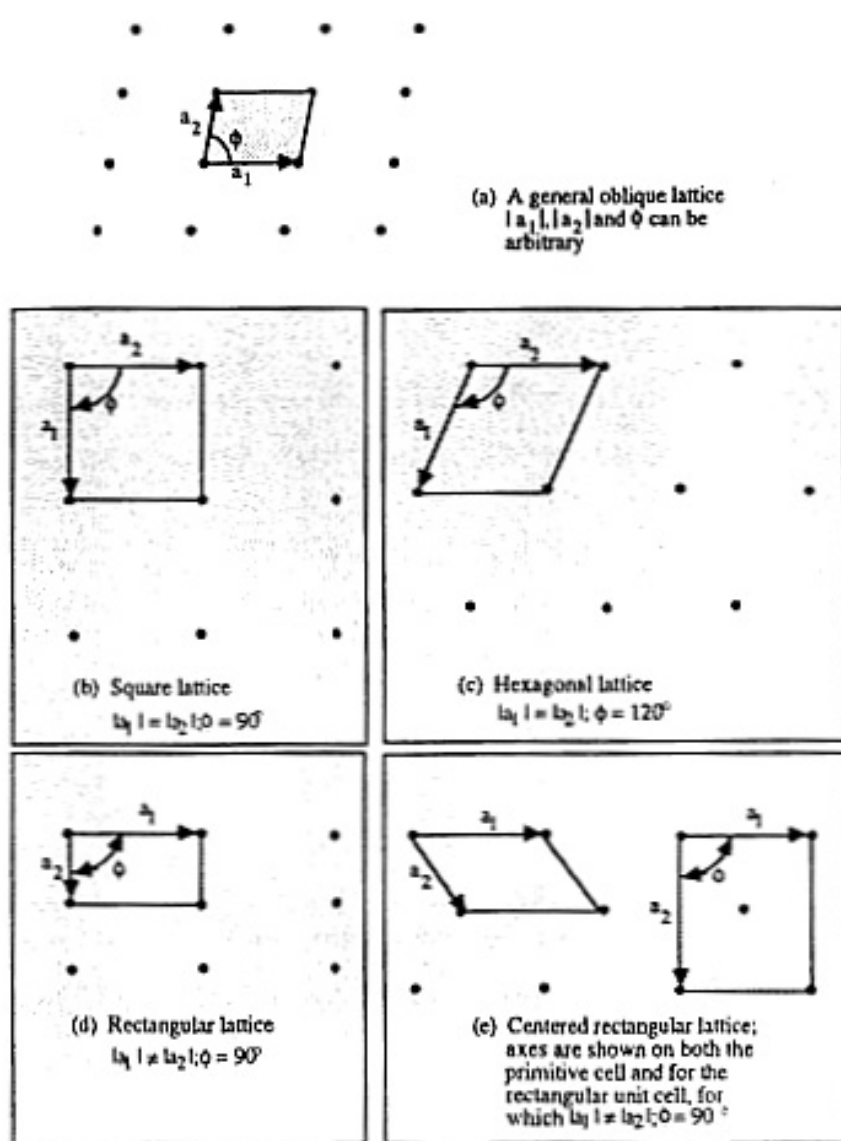


Figure 1.3: The five classes of 2D lattices (from the book [4]).

Three-Dimensional Lattices

There are 14 types of lattices in 3 dimensions. Several primitive cells are shown in Fig. 1.4. The types of lattices differ by the relations between the lengths a_i and the angles α_i .

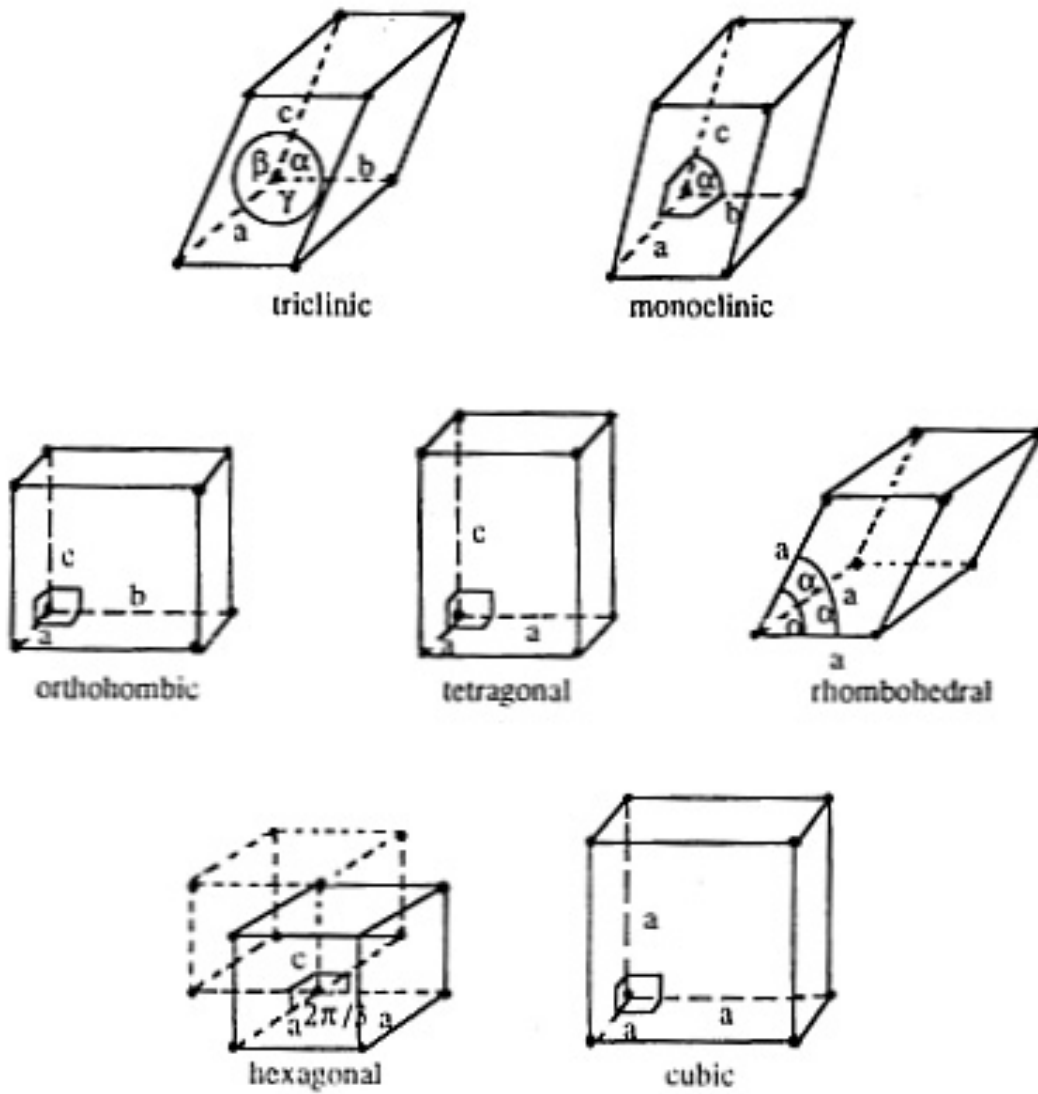


Figure 1.4: Types of 3D lattices

We will concentrate on cubic lattices which are very important for many materials.

Cubic and Hexagonal Lattices. Some primitive lattices are shown in Fig. 1.5. a , b , and c show cubic lattices. a is the *simple cubic lattice* (1 atom per primitive cell), b is the *body centered cubic lattice* ($1/8 \times 8 + 1 = 2$ atoms), c is *face-centered lattice* ($1/8 \times 8 + 1/2 \times 6 = 4$ atoms). The part c of the Fig. 1.5 shows hexagonal cell.

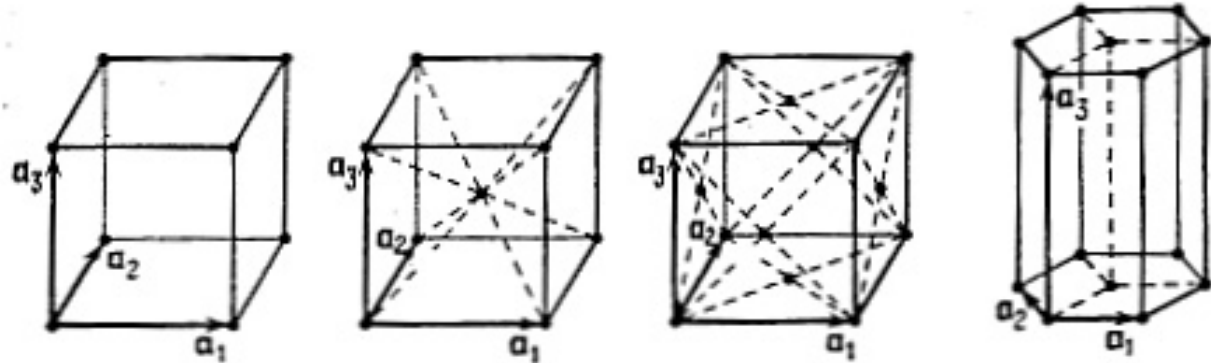


Figure 1.5: Primitive lattices

We shall see that discrimination between simple and complex lattices is important, say, in analysis of lattice vibrations.

The Wigner-Zeitz cell

As we have mentioned, the procedure of choose of the elementary cell is not unique and sometimes an arbitrary cell does not reflect the symmetry of the lattice (see, e. g., Fig. 1.6, and 1.7 where specific choices for cubic lattices are shown). There is a very convenient

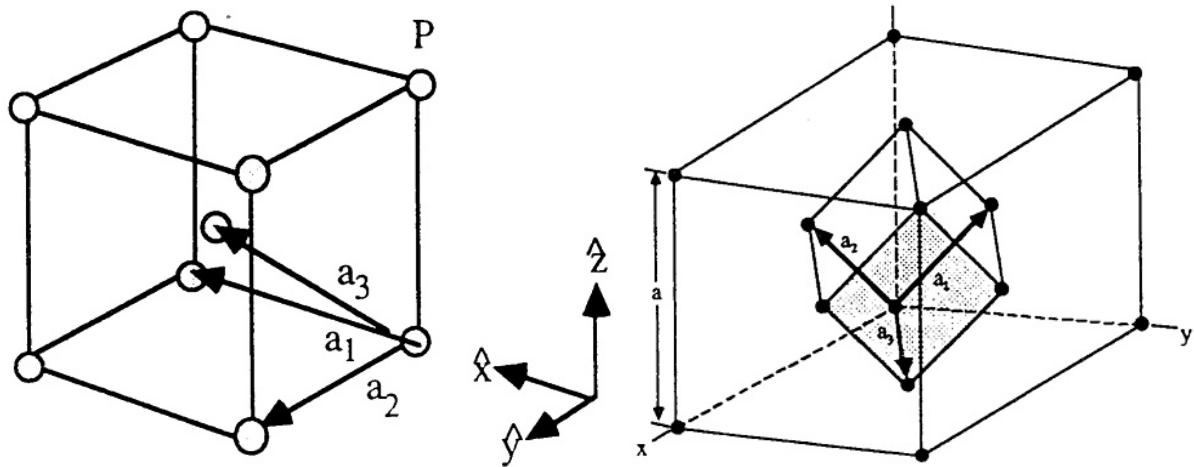


Figure 1.6: Primitive vectors for bcc (left panel) and (right panel) lattices.

procedure to choose the cell which reflects the symmetry of the lattice. The procedure is as follows:

1. Draw lines connecting a given lattice point to all neighboring points.
2. Draw bisecting lines (or planes) to the previous lines.

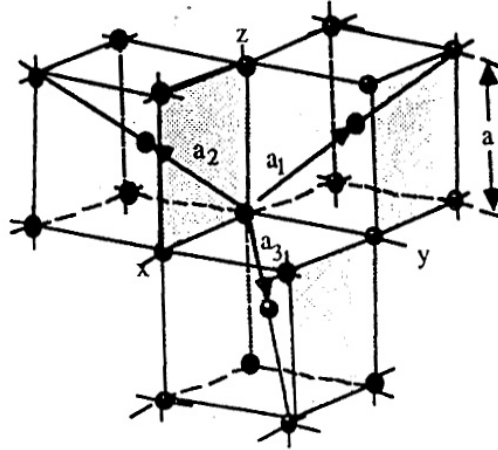


Figure 1.7: More symmetric choice of lattice vectors for bcc lattice.

The procedure is outlined in Fig. 1.8. For complex lattices such a procedure should be done for one of simple sublattices. We shall come back to this procedure later analyzing electron band structure.

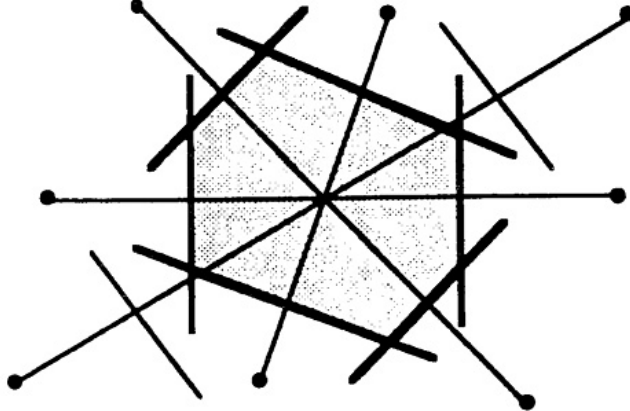


Figure 1.8: To the determination of Wigner-Zeitz cell.

1.2 The Reciprocal Lattice

The crystal periodicity leads to many important consequences. Namely, all the properties, say electrostatic potential V , are periodic

$$V(\mathbf{r}) = V(\mathbf{r} + \mathbf{a}_n), \quad \mathbf{a}_n \equiv n_1 \mathbf{a}_1 + n_2 \mathbf{a}_2 + n_3 \mathbf{a}_3. \quad (1.3)$$

It implies the Fourier transform. Usually the oblique co-ordinate system is introduced, the axes being directed along \mathbf{a}_i . If we denote co-ordinates as ξ_s having periods a_s we get

$$V(\mathbf{r}) = \sum_{k_1, k_2, k_3 = -\infty}^{\infty} V_{k_1, k_2, k_3} \exp \left[2\pi i \sum_s \frac{k_s \xi_s}{a_s} \right]. \quad (1.4)$$

Then we can return to Cartesian co-ordinates by the transform

$$\xi_i = \sum_k \alpha_{ik} x_k \quad (1.5)$$

Finally we get

$$V(\mathbf{r}) = \sum_{\mathbf{b}} V_{\mathbf{b}} e^{i\mathbf{b}\mathbf{r}}. \quad (1.6)$$

From the condition of periodicity (1.3) we get

$$V(\mathbf{r} + \mathbf{a}_n) = \sum_{\mathbf{b}} V_{\mathbf{b}} e^{i\mathbf{b}\mathbf{r}} e^{i\mathbf{b}\mathbf{a}_n}. \quad (1.7)$$

We see that $e^{i\mathbf{b}\mathbf{a}_n}$ should be equal to 1, that could be met at

$$\mathbf{b}\mathbf{a}_1 = 2\pi g_1, \quad \mathbf{b}\mathbf{a}_2 = 2\pi g_2, \quad \mathbf{b}\mathbf{a}_3 = 2\pi g_3 \quad (1.8)$$

where g_i are integers. It could be shown (see *Problem 1.4*) that

$$\mathbf{b}_g \equiv \mathbf{b} = g_1 \mathbf{b}_1 + g_2 \mathbf{b}_2 + g_3 \mathbf{b}_3 \quad (1.9)$$

where

$$\mathbf{b}_1 = \frac{2\pi[\mathbf{a}_2 \mathbf{a}_3]}{\mathcal{V}_0}, \quad \mathbf{b}_2 = \frac{2\pi[\mathbf{a}_3 \mathbf{a}_1]}{\mathcal{V}_0}, \quad \mathbf{b}_3 = \frac{2\pi[\mathbf{a}_1 \mathbf{a}_2]}{\mathcal{V}_0}. \quad (1.10)$$

It is easy to show that scalar products

$$\mathbf{a}_i \mathbf{b}_k = 2\pi \delta_{i,k}. \quad (1.11)$$

Vectors \mathbf{b}_k are called the basic vectors of the *reciprocal lattice*. Consequently, one can construct reciprocal lattice using those vectors, the elementary cell volume being $(\mathbf{b}_1 [\mathbf{b}_2, \mathbf{b}_3]) = (2\pi)^3 / \mathcal{V}_0$.

Reciprocal Lattices for Cubic Lattices. Simple cubic lattice (sc) has simple cubic reciprocal lattice with the vectors' lengths $b_i = 2\pi/a_i$. Now we demonstrate the general procedure using as examples body centered (bcc) and face centered (fcc) cubic lattices.

First we write lattice vectors for bcc as

$$\begin{aligned} \mathbf{a}_1 &= \frac{a}{2} (\mathbf{y} + \mathbf{z} - \mathbf{x}), \\ \mathbf{a}_2 &= \frac{a}{2} (\mathbf{z} + \mathbf{x} - \mathbf{y}), \\ \mathbf{a}_3 &= \frac{a}{2} (\mathbf{x} + \mathbf{y} - \mathbf{z}) \end{aligned} \quad (1.12)$$

where unit vectors \mathbf{x} , \mathbf{y} , \mathbf{z} are introduced (see Fig. 1.7). The volume of the cell is $\mathcal{V}_0 = a^3/2$. Making use of the definition (1.10) we get

$$\begin{aligned}\mathbf{b}_1 &= \frac{2\pi}{a}(\mathbf{y} + \mathbf{z}), \\ \mathbf{b}_2 &= \frac{2\pi}{a}(\mathbf{z} + \mathbf{x}), \\ \mathbf{b}_3 &= \frac{2\pi}{a}(\mathbf{x} + \mathbf{y})\end{aligned}\tag{1.13}$$

One can see from right panel of Fig. 1.6 that they form a *face-centered cubic* lattice. So we can get the Wigner-Zeitz cell for bcc reciprocal lattice (later we

shall see that this cell bounds the 1st Brillouin zone for vibration and electron spectrum). It is shown in Fig. 1.9 (left panel). In a very similar way one can show that *bcc lattice is the reciprocal to the fcc one*. The corresponding Wigner-Zeitz cell is shown in the right panel of Fig. 1.9.

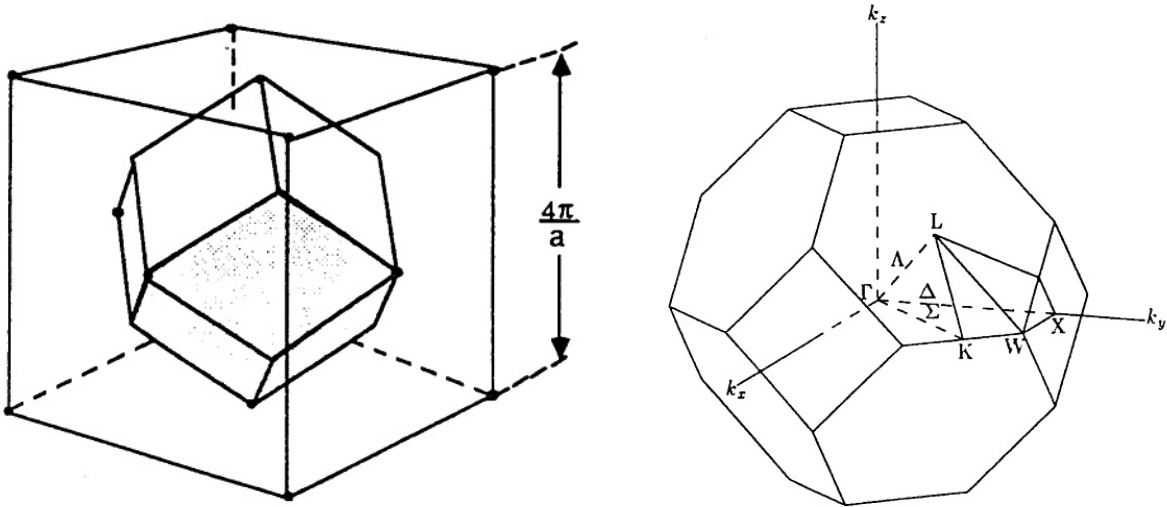


Figure 1.9: The Wigner-Zeitz cell for the bcc (left panel) and for the fcc (right panel) lattices.

1.3 X-Ray Diffraction in Periodic Structures

The Laue Condition

Consider a plane wave described as

$$\mathbf{F}(\mathbf{r}) = \mathbf{F}_0 \exp(i\mathbf{k}\mathbf{r} - \omega t)\tag{1.14}$$

which acts upon a periodic structure. Each atom placed at the point ρ produces a scattered spherical wave

$$\mathbf{F}_{sc}(\mathbf{r}) = f\mathbf{F}(\rho) \frac{e^{ikr}}{r} = f\mathbf{F}_0 \frac{e^{i\mathbf{k}\rho} e^{i(kr-\omega t)}}{r} \quad (1.15)$$

where $r = R - \rho \cos(\rho, \mathbf{R})$, \mathbf{R} being the detector's position (see Fig. 1.10). Then, we

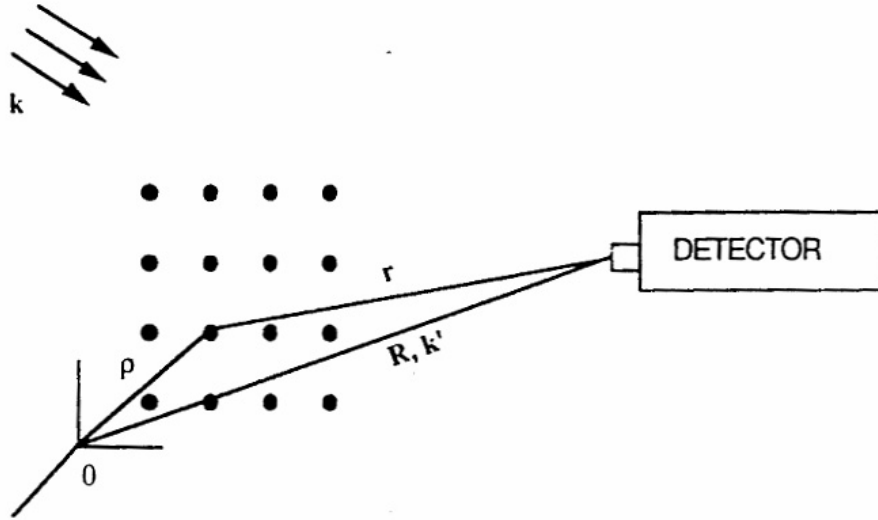


Figure 1.10: Geometry of scattering by a periodic atomic structure.

assume $R \gg \rho$ and consequently $r \approx R$; we replace r by R in the denominator of Eq. (1.15). Unfortunately, the phase needs more exact treatment:

$$\mathbf{k}\rho + kr = \mathbf{k}\rho + kR - k\rho \cos(\rho, \mathbf{R}). \quad (1.16)$$

Now we can replace $k\rho \cos(\rho, \mathbf{R})$ by $\mathbf{k}'\rho$ where \mathbf{k}' is the scattered vector in the direction of \mathbf{R} . Finally, the phase equal to

$$kR - \rho \Delta \mathbf{k}, \quad \Delta \mathbf{k} = \mathbf{k} - \mathbf{k}'.$$

Now we can sum the contributions of all the atoms

$$\mathbf{F}_{sc}(\mathbf{R}) = \sum_{m,n,p} f_{m,n,p} \left(\mathbf{F}_0 \frac{e^{i(kR-\omega t)}}{R} \right) [\exp(-i\rho_{m,n,p} \Delta \mathbf{k})] \quad (1.17)$$

If all the scattering factors $f_{m,n,p}$ are equal the only phase factors are important, and strong diffraction takes place at

$$\rho_{m,n,p} \Delta \mathbf{k} = 2\pi n \quad (1.18)$$

with integer n . The condition (1.18) is *just the same* as the definition of the reciprocal vectors. So, scattering is strong if the transferred momentum proportional to the reciprocal lattice factor. Note that the Laue condition (1.18) is just the same as the famous Bragg condition of strong light scattering by periodic gratings.

Role of Disorder

The scattering *intensity* is proportional to the amplitude squared. For $\mathbf{G} = \Delta\mathbf{k}$ where \mathbf{G} is the reciprocal lattice vector we get

$$I_{sc} \propto \left| \sum_i e^{i\mathbf{GR}_i} \right| \cdot \left| \sum_i e^{-i\mathbf{GR}_i} \right| \quad (1.19)$$

or

$$I_{sc} \propto \left| \sum_i 1 + \sum_i \sum_{j \neq i} e^{i\mathbf{G}(\mathbf{R}_i - \mathbf{R}_j)} \right|. \quad (1.20)$$

The first term is equal to the total number of sites N , while the second includes correlation. If

$$\mathbf{G}(\mathbf{R}_i - \mathbf{R}_j) \equiv \mathbf{GR}_{ij} = 2\pi n \quad (1.21)$$

the second term is $N(N - 1) \approx N^2$, and

$$I_{sc} \propto N^2.$$

If the arrangement is *random* all the phases cancel and the second term cancels. In this case

$$I_{sc} \propto N$$

and it is *angular independent*.

Let us discuss the role of a weak disorder where

$$\mathbf{R}_i = \mathbf{R}_i^0 + \Delta\mathbf{R}_i$$

where $\Delta\mathbf{R}_i$ is small *time-independent* variation. Let us also introduce

$$\Delta\mathbf{R}_{ij} = \Delta\mathbf{R}_i - \Delta\mathbf{R}_j.$$

In the vicinity of the diffraction maximum we can also write

$$\mathbf{G} = \mathbf{G}^0 + \Delta\mathbf{G}.$$

Using (1.20) and neglecting the terms $\propto N$ we get

$$\frac{I_{sc}(\mathbf{G}_0 + \Delta\mathbf{G})}{I_{sc}(\mathbf{G}_0)} = \frac{\sum_{i,j} \exp [i (\mathbf{G}^0 \Delta\mathbf{R}_{ij} + \Delta\mathbf{G} \mathbf{R}_{ij}^0 + \Delta\mathbf{G} \Delta\mathbf{R}_{ij})]}{\sum_{i,j} \exp [i \mathbf{G}^0 \Delta\mathbf{R}_{ij}]} \quad (1.22)$$

So we see that there is a *finite width* of the scattering pattern which is called *rocking curve*, the width being the characteristics of the amount of disorder.

Another source of disorder is a finite size of the sample (important for small semiconductor samples). To get an impression let us consider a chain of N atoms separated by a distance a . We get

$$\left| \sum_{n=0}^{N-1} \exp(ina\Delta k) \right|^2 \propto \frac{\sin^2(Na\Delta k/2)}{\sin^2(a\Delta k/2)}. \quad (1.23)$$

This function has maxima at $a\Delta k = 2m\pi$ equal to N^2 (l'Hopital's rule) the width being $\Delta k'a = 2.76/N$ (see *Problem 1.6*).

Scattering factor f_{mnp}

Now we come to the situation with complex lattices where there are more than 1 atoms per basis. To discuss this case we introduce

- The co-ordinate ρ_{mnp} of the initial point of unit cell (see Fig. 1.11).
- The co-ordinate ρ_j for the position of j th atom in the unit cell.

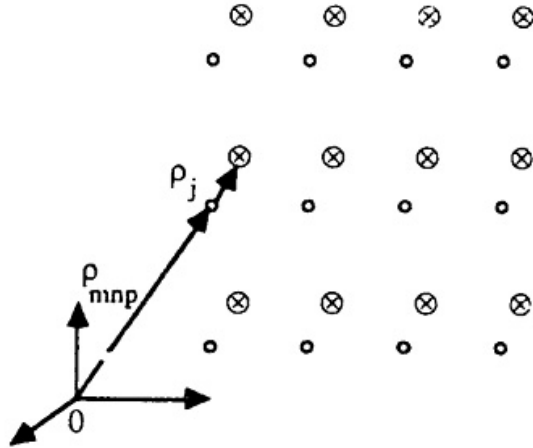


Figure 1.11: Scattering from a crystal with more than one atom per basis.

Coming back to our derivation (1.17)

$$\mathbf{F}_{sc}(\mathbf{R}) = \mathbf{F}_0 \frac{e^{i(kR - \omega t)}}{R} \sum_{m,n,p} \sum_j f_j \exp [-i(\rho_{m,n,p} + \rho_j) \Delta \mathbf{k}] \quad (1.24)$$

where f_j is in general different for different atoms in the cell. Now we can extract the sum over the cell for $\Delta \mathbf{k} = \mathbf{G}$ which is called the *structure factor*:

$$S_G = \sum_j f_j \exp [-i\rho_j \mathbf{G}] . \quad (1.25)$$

The first sum is just the same as the result for the one-atom lattice. So, we come to the rule

- *The X-ray pattern can be obtained by the product of the result for lattice sites times the structure factor.*

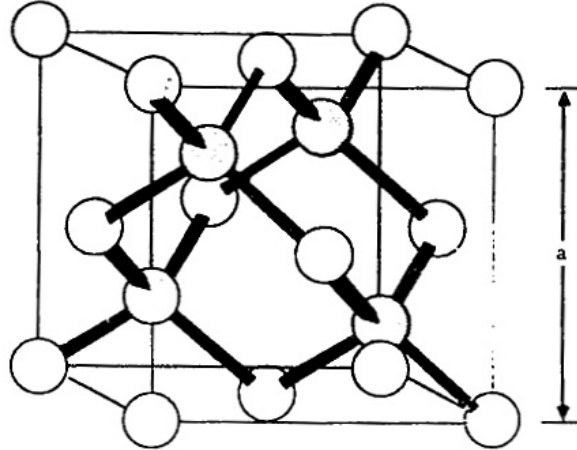


Figure 1.12: The two-atomic structure of inter-penetrating fcc lattices.

[

The Diamond and Zinc-Blend Lattices] Example: The Diamond and Zinc-Blend Lattices

To make a simple example we discuss the lattices with a two-atom basis (see Fig. 1.12) which are important for semiconductor crystals. The co-ordinates of two basis atoms are (000) and $(a/4)(111)$, so we have 2 inter-penetrating fcc lattices shifted by a distance $(a/4)(111)$ along the body diagonal. If atoms are identical, the structure is called the *diamond* structure (elementary semiconductors: Si, Ge, and C). If the atoms are different, it is called the *zinc-blend structure* (GaAs, AlAs, and CdS).

For the diamond structure

$$\begin{aligned}\rho_1 &= 0 \\ \rho_2 &= \frac{a}{4}(\mathbf{x} + \mathbf{y} + \mathbf{z}).\end{aligned}\tag{1.26}$$

We also have introduced the reciprocal vectors (see *Problem 1.5*)

$$\begin{aligned}\mathbf{b}_1 &= \frac{2\pi}{a}(-\mathbf{x} + \mathbf{y} + \mathbf{z}), \\ \mathbf{b}_2 &= \frac{2\pi}{a}(-\mathbf{y} + \mathbf{z} + \mathbf{x}), \\ \mathbf{b}_3 &= \frac{2\pi}{a}(-\mathbf{z} + \mathbf{x} + \mathbf{y}),\end{aligned}$$

the general reciprocal vector being

$$\mathbf{G} = n_1 \mathbf{b}_1 + n_2 \mathbf{b}_2 + n_3 \mathbf{b}_3.$$

Consequently,

$$S_G = f \left(1 + \exp \left[\frac{i\pi}{2}(n_1 + n_2 + n_3) \right] \right).$$

It is equal to

$$S_G = \begin{cases} 2f, & n_1 + n_2 + n_3 = 4k; \\ (1 \pm i)f, & n_1 + n_2 + n_3 = (2k+1); \\ 0, & n_1 + n_2 + n_3 = 2(2k+1). \end{cases} \quad (1.27)$$

So, the diamond lattice has some spots missing in comparison with the fcc lattice.

In the zinc-blend structure the atomic factors f_i are different and we should come to more understanding what do they mean. Namely, for X-rays they are due to Coulomb charge density and are proportional to the Fourier components of local charge densities. In this case one has instead of (1.27)

$$S_G = \begin{cases} f_1 + f_2, & n_1 + n_2 + n_3 = 4k; \\ (f_1 \pm if_2), & n_1 + n_2 + n_3 = (2k+1); \\ f_1 - f_2, & n_1 + n_2 + n_3 = 2(2k+1). \end{cases} \quad (1.28)$$

We see that one can extract a lot of information on the structure from X-ray scattering.

Experimental Methods

Here we review few most important experimental methods to study scattering. Most of them are based on the simple geometrical *Ewald construction* (see Fig. 1.13) for the vectors satisfying the Laue condition. The prescription is as follows. We draw the *reciprocal lattice*

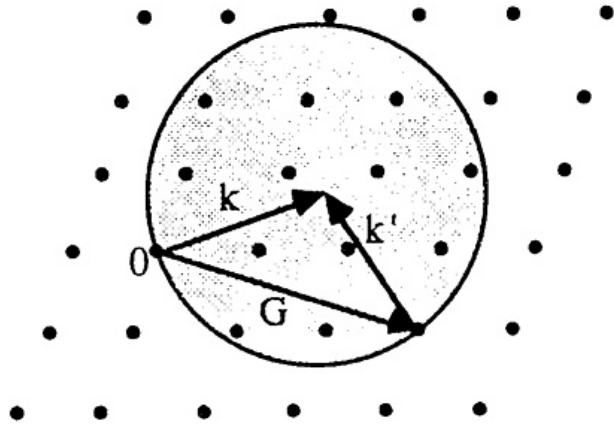


Figure 1.13: The Ewald construction.

(RL) and then an incident vector \mathbf{k} , $k = 2\pi/\lambda_X$ starting at the RL point. Using the tip as a center we draw a sphere. The scattered vector \mathbf{k}' is determined as in Fig. 1.13, the intensity being proportional to S_G .

The Laue Method

Both the positions of the crystal and the detector are *fixed*, a *broad* X-ray spectrum (from λ_0 to λ_1 is used). So, it is possible to find diffraction peaks according to the Ewald picture.

This method is mainly used to determine the *orientation* of a single crystal with a known structure.

The Rotating Crystal Method

The crystal is placed in a holder, which can rotate with a high precision. The X-ray source is fixed and monochromatic. At some angle the Bragg conditions are met and the diffraction takes place. In the Ewald picture it means the rotating of reciprocal basis vectors. As long as the X-ray wave vector is not too small one can find the intersection with the Ewald sphere at some angles.

The Powder or Debye-Scherrer Method

This method is very useful for powders or microcrystallites. The sample is fixed and the pattern is recorded on a film strip (see Fig. 1.14) According to the Laue condition,

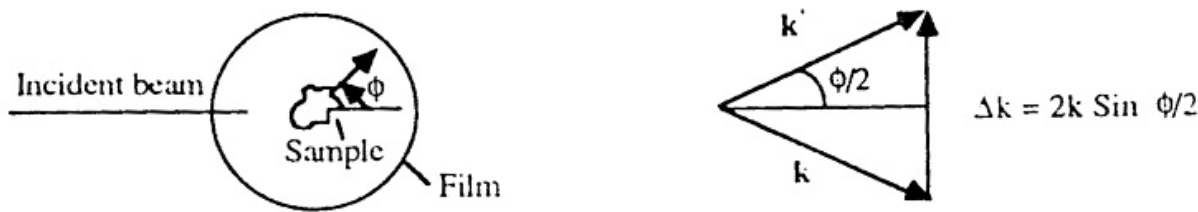


Figure 1.14: The powder method.

$$\Delta k = 2k \sin(\phi/2) = G.$$

So one can determine the *ratios*

$$\sin\left(\frac{\phi_1}{2}\right) : \sin\left(\frac{\phi_2}{2}\right) \dots \sin\left(\frac{\phi_N}{2}\right) = G_1 : G_2 \dots G_N.$$

Those ratios could be calculated for a given structure. So one can *determine* the structure of an unknown crystal.

Double Crystal Diffraction

This is a very powerful method which uses one very high-quality crystal to produce a beam acting upon the specimen (see Fig. 1.15).

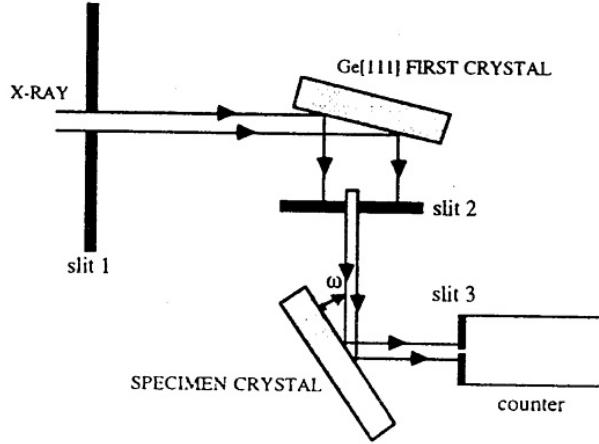


Figure 1.15: The double-crystal diffractometer.

When the Bragg angles for two crystals are the same, the narrow diffraction peaks are observed. This method allows, in particular, study epitaxial layer which are grown on the substrate.

Temperature Dependent Effects

Now we discuss the role of thermal vibration of the atoms. In fact, the position of an atom is determined as

$$\boldsymbol{\rho}(t) = \boldsymbol{\rho}_0 + \mathbf{u}(t)$$

where $\mathbf{u}(t)$ is the time-dependent displacement due to vibrations. So, we get an extra phase shift $\Delta\mathbf{k} \mathbf{u}(t)$ of the scattered wave. In the experiments, the average over vibrations is observed (the typical vibration frequency is 10^{12} s^{-1}). Since $u(t)$ is small,

$$\langle \exp(-\Delta\mathbf{k} \mathbf{u}) \rangle = 1 - i \langle \Delta\mathbf{k} \mathbf{u} \rangle - \frac{1}{2} \langle (\Delta\mathbf{k} \mathbf{u})^2 \rangle + \dots$$

The second item is equal to zero, while the third is

$$\langle (\Delta\mathbf{k} \mathbf{u})^2 \rangle = \frac{1}{3} (\Delta k)^2 \langle u^2 \rangle$$

(the factor $1/3$ comes from geometric average).

Finally, with some amount of cheating¹ we get

$$\langle \exp(-\Delta\mathbf{k} \mathbf{u}) \rangle \approx \exp \left[-\frac{(\Delta k)^2 \langle u^2 \rangle}{6} \right].$$

¹We have used the expression $1 - x = \exp(-x)$ which in general is not true. Nevertheless there is *exact* theorem $\langle \exp(i\varphi) \rangle = \exp[-\langle (\varphi)^2 \rangle / 2]$ for any Gaussian fluctuations with $\langle \varphi \rangle = 0$.

Again $\Delta\mathbf{k} = \mathbf{G}$, and we get

$$I_{sc} = I_0 e^{-G^2 \langle u^2 \rangle / 3} \quad (1.29)$$

where I_0 is the intensity from the perfect lattice with points ρ_0 . From the pure classical considerations,²

$$\langle u^2 \rangle = \frac{3k_B T}{m\omega^2}$$

where ω is the lattice vibrations frequency (10^{13} – 10^{14} s⁻¹). Thus,

$$I_{sc} = I_0 \exp \left[-\frac{k_B T G^2}{m\omega^2} \right]. \quad (1.30)$$

According to quantum mechanics, even at zero temperature there are zero-point vibrations with³

$$\langle u^2 \rangle = \frac{3\hbar}{2m\omega}.$$

In this case

$$I_{sc} = I_{0R} \exp \left[-\frac{\hbar G^2}{2m\omega} \right] \quad (1.31)$$

where I_{0R} is the intensity for a rigid classical lattice. For $T = 0$, $G = 10^9 \text{ cm}^{-1}$, $\omega = 2\pi \cdot 10^{14}$ s⁻¹, $m = 10^{-22}$ g the exponential factor is 0.997.

It means that vibrations do not destroy the diffraction pattern which can be studied even at high enough temperatures.

At the present time, many powerful diffraction methods are used, in particular, neutron diffraction. For low-dimensional structures the method of *reflection high energy electron diffraction* (RHEED) is extensively used.

1.4 Problems

1.1. Show that $(\mathbf{a}_1[\mathbf{a}_2\mathbf{a}_3]) = (\mathbf{a}_3[\mathbf{a}_1\mathbf{a}_2]) = (\mathbf{a}_2[\mathbf{a}_3\mathbf{a}_1])$.

1.2. Show that only $n = 1, 2, 3, 6$ are available.

1.3. We have mentioned that primitive vectors are not unique. New vectors can be defined as

$$\mathbf{a}'_i = \sum_k \beta_{ik} \mathbf{a}_k,$$

the sufficient condition for the matrix $\hat{\beta}$ is

$$\det(\beta_{ik}) = \pm 1. \quad (1.32)$$

Show that this equality is sufficient.

1.4. Derive the expressions (1.10) for reciprocal lattice vectors.

² $\langle E \rangle = m\omega^2 \langle u^2 \rangle / 2 = 3k_B T / 2$.

³ $\langle E \rangle = 3\hbar\omega / 4$.

- 1.5.** Find the reciprocal lattice vectors for fcc lattice.
- 1.6.** Find the width of the scattering peak at the half intensity due to finite size of the chain with N

Chapter 2

Lattice Vibrations: Phonons

In this Chapter we consider the dynamic properties of crystal lattice, namely lattice vibrations and their consequences. One can find detailed theory in many books, e.g. in [1, 2].

2.1 Interactions Between Atoms in Solids

The reasons to form a crystal from free atoms are manifold, the main principle being

- Keep the charges of the same sign apart
- Keep electrons close to ions
- Keep electron kinetic energy low by quantum mechanical spreading of electrons

To analyze the interaction forces one should develop a full quantum mechanical treatment of the electron motion in the atom (ion) fields, the heavy atoms being considered as fixed. Consequently, the total energy appears dependent on the atomic configuration as on external parameters. All the procedure looks very complicated, and we discuss only main physical principles.

Let us start with the discussion of the nature of *repulsive* forces. They can be due both to Coulomb repulsive forces between the ions with the same sign of the charge and to repulsive forces caused by inter-penetrating of electron shells at low distances. Indeed, that penetration leads to the *increase* of kinetic energy due to Pauli principle – the kinetic energy of Fermi gas increases with its density. The quantum mechanical treatment leads to the law $V \propto \exp(-R/a)$ for the repulsive forces at large distances; at intermediate distances the repulsive potential is usually expressed as

$$\Delta V(R) = A/R^{12}. \quad (2.1)$$

There are several reasons for atom *attraction*. Although usually the bonding mechanisms are mixed, 4 types of bonds are specified:

Ionic (or electrostatic) bonding. The physical reason is near complete transfer of the electron from the anion to the cation. It is important for the alkali crystals NaCl, KI, CsCl, etc. One can consider the interaction as the Coulomb one for point charges at the lattice sites. Because the ions at the first co-ordination group have opposite sign in comparison with the central one the resulting Coulomb interaction is an attraction.

To make very rough estimates we can express the interaction energy as

$$V_{ij} = \begin{cases} \lambda e^{-R/\rho} - \frac{e_*^2}{R} & \text{for nearest neighbors,} \\ \pm \frac{e_*^2}{R_{ij}} & \text{otherwise} \end{cases} \quad (2.2)$$

with $R_{ij} = Rp_{ij}$ where p_{ij} represent distances for the lattice sites; e_* is the effective charge. So the total energy is

$$U = L \left(z\lambda e^{-R/\rho} - \alpha \frac{e_*^2}{R} \right)$$

where z is the number of nearest neighbors while

$$\alpha = \sum'_{i,j} \frac{\pm}{p_{ij}}$$

is the so-called *Madelung constant*. For a linear chain

$$\alpha = 2 \left(1 - \frac{1}{2} + \frac{1}{3} - \dots \right) == 2 \ln(1+x)|_{x=1} = 2 \ln 2.$$

Typical values of α for 3D lattices are: 1.638 (zinc-blend crystals), 1.748 (NaCl).

Covalent (or homopolar) bonding. This bonding appears at small distances of the order of atomic length 10^{-8} cm. The nature of this bonding is pure quantum mechanical; it is just the same as bonding in the H_2 molecule where the atoms share the two electron with anti-parallel spins. The covalent bonding is dependent on the electron orbitals, consequently they are *directed*. For most of semiconductor compounds the bonding is mixed – it is partly ionic and partly covalent. The table of the ionicity numbers (effective charge) is given below Covalent bonding depends both on atomic orbital and on the distance – it exponentially decreases with the distance. At large distances universal attraction forces appear - van der Waal's ones.

Van der Waal's (or dispersive) bonding. The physical reason is the polarization of electron shells of the atoms and resulting dipole-dipole interaction which behaves as

$$\Delta V(R) = -B/R^6. \quad (2.3)$$

The two names are due i) to the fact that these forces has the same nature as the forces in real gases which determine their difference with the ideal ones, and ii) because they are

Crystal	Ionicity
Si	0.0
SiC	0.18
Ge	0.0
ZnSe	0.63
ZnS	0.62
CdSe	0.70
InP	0.42
InAs	0.46
InSb	0.32
GaAs	0.31
GaSb	0.36

Table 2.1: Ionicity numbers for semiconductor crystals.

determined by the same parameters as light dispersion. This bonding is typical for inert gas crystals (Ar, Xe, Cr, molecular crystals). In such crystals the interaction potential is described by the Lennard-Jones formula

$$V(R) = 4\epsilon \left[\left(\frac{\sigma}{R}\right)^{12} - \left(\frac{\sigma}{R}\right)^6 \right] \quad (2.4)$$

the equilibrium point where $dV/dR = 0$ being $R_0 = 1.09\sigma$.

Metallic bonding. Metals usually form closed packed fcc, bcc, or hcp structures where electrons are shared by all the atoms. The bonding energy is determined by a balance between the *negative* energy of Coulomb interaction of electrons and positive ions (this energy is proportional to e^2/a) and *positive* kinetic energy of electron Fermi gas (which is, as we will see later, $\propto n^{2/3} \propto 1/a^2$).

The most important thing for us is that, irrespective to the nature of the bonding, the general form of the binding energy is like shown in Fig. 2.1.

2.2 Lattice Vibrations

For small displacement on an atom from its equilibrium position one can expand the potential energy near its minimal value (see Fig. 2.1)

$$\begin{aligned} V(R) &= V(R_0) + \left(\frac{dV}{dR}\right)_{R_0} (R - R_0) + \frac{1}{2} \left(\frac{d^2V}{dR^2}\right)_{R_0} (R - R_0)^2 + \\ &+ \frac{1}{6} \left(\frac{d^3V}{dR^3}\right)_{R_0} (R - R_0)^3 + \dots \end{aligned} \quad (2.5)$$

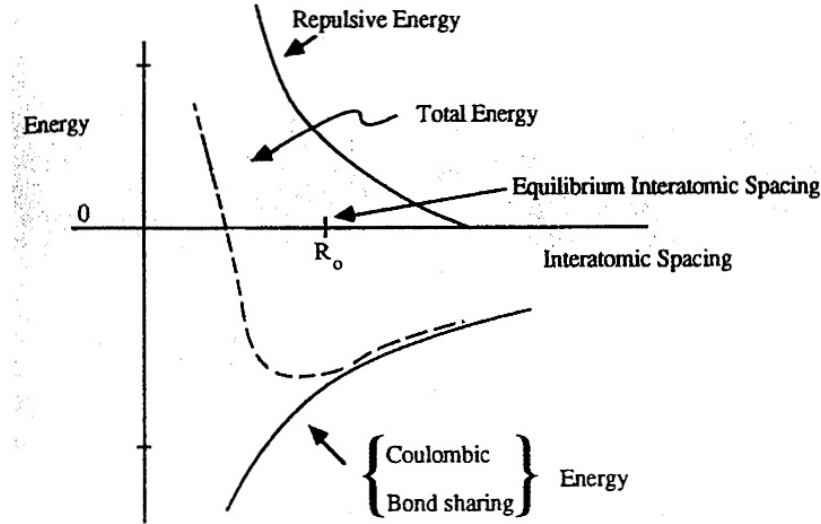


Figure 2.1: General form of binding energy.

If we expand the energy near the equilibrium point and denote

$$\left(\frac{d^2V}{dR^2}\right)_{R_0} \equiv C > 0, \quad \left(\frac{d^3V}{dR^3}\right)_{R_0} \equiv -2\gamma > 0$$

we get the following expression for the restoring force for a given displacement $x \equiv R - R_0$

$$F = -\frac{dV}{dx} = -Cx + \gamma x^2 \quad (2.6)$$

The force under the limit $F = -Cx$ is called *quasi elastic*.

One-Atomic Linear Chain

Dispersion relation

We start with the simplest case of one-atomic linear chain with nearest neighbor interaction (see Fig. 2.2) If one expands the energy near the equilibrium point for the n th atom and

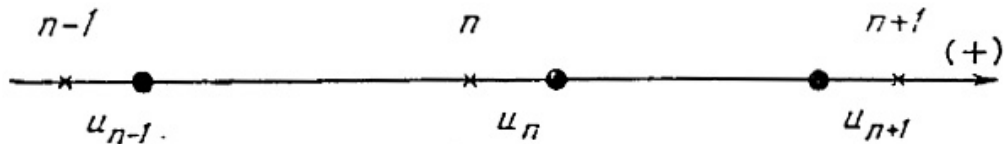


Figure 2.2: Vibrations of a linear one-atomic chain (displacements).

use quasi elastic approximation (2.6) he comes to the Newton equation

$$m\ddot{u}_n + C(2u_n - u_{n-1} - u_{n+1}) = 0. \quad (2.7)$$

To solve this *infinite* set of equations let us take into account that the equation does not change if we shift the system *as a whole* by the quantity a times an integer. We can fulfill this condition automatically by searching the solution as

$$u_n = A e^{i(qan - \omega t)}. \quad (2.8)$$

It is just a plane wave but for the *discrete co-ordinate* na . Immediately we get (see *Problem 2.1*)

$$\omega = \omega_m |\sin \frac{qa}{2}|, \quad \omega_m = 2\sqrt{\frac{C}{m}}. \quad (2.9)$$

The expression (2.9) is called the *dispersion law*. It differs from the dispersion relation for an homogeneous string, $\omega = sq$. Another important feature is that if we replace the wave number q as

$$q \rightarrow q' = q + \frac{2\pi g}{a},$$

where g is an integer, the solution (2.8) does not change (because $\exp(2\pi i \times \text{integer}) = 1$). Consequently, it is impossible to discriminate between q and q' and it is natural to choose the region

$$-\frac{\pi}{a} \leq q \leq \frac{\pi}{a} \quad (2.10)$$

to represent the dispersion law in the whole q -space. This law is shown in Fig. 2.3. Note that there is the *maximal frequency* ω_m that corresponds to the *minimal wave length*

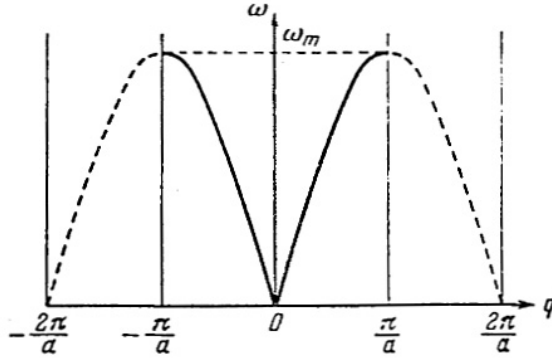


Figure 2.3: Vibrations of a linear one-atomic chain (spectrum).

$\lambda_{\min} = 2\pi/q_{\max} = 2a$. The maximal frequency is a typical feature of discrete systems vibrations.

Now we should recall that any crystal is *finite* and the translation symmetry we have used fails. The usual way to overcome the problem is to take into account that actual

number L of sites is large and to introduce *Born-von Karman* cyclic boundary conditions

$$u_{n\pm L} = n_n. \quad (2.11)$$

This condition make a sort of ring of a very big radius that physically does not differ from the long chain.¹ Immediately, we get that the wave number q should be *discrete*. Indeed, substituting the condition (2.11) into the solution (2.8) we get $\exp(\pm iqaL) = 1$, $qaL = 2\pi g$ with an integer g . Consequently,

$$q = \frac{2\pi}{a} \frac{g}{L}, \quad -\frac{L}{2} < g < \frac{L}{2} \quad (2.12)$$

(it is convenient to consider L as a large even number). So, for a linear chain, the wave number q takes L discrete values in the interval $(-\pi/a, \pi/a)$. Note that this interval is just the same as the Wigner-Zeitz cell of the one-dimensional reciprocal lattice.

Density of States

Because of the discrete character of the vibration states one can calculate *the number of states*, z , with different q in the frequency interval $\omega, \omega + d\omega$. One easily obtains (see *Problem 2.2*)

$$\frac{dz}{d\omega} = \frac{2L}{\pi} \frac{1}{\sqrt{\omega_m^2 - \omega^2}}. \quad (2.13)$$

This function is called the *density of states* (DOS). It is plotted in Fig. 2.4. We shall see

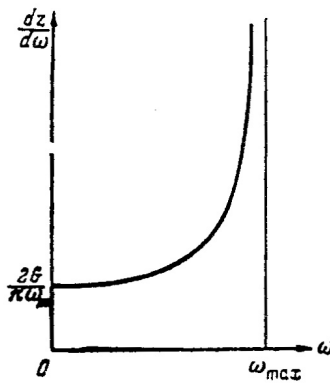


Figure 2.4: Density of states for a linear one-atomic chain.

that DOS is strongly dependent on the dimensionality of the structure.

¹Note that for small structures of modern electronics this assumption need revision. Violation of this assumption leads to the specific interface modes.

Phase and Group Velocity

Now we discuss the properties of long wave vibrations. At small q we get from Eq. (2.9)

$$\omega = sq, \quad (2.14)$$

where

$$s = a\sqrt{\frac{C}{m}} \quad (2.15)$$

is the sound velocity in a homogeneous elastic medium. In a general case, the sound velocity becomes q -dependent, i. e. there is the dispersion of the waves. One can discriminate between the phase (s_p) and group (s_g) velocities. The first is responsible for the propagation of the equal phase planes while the last one describes the energy transfer. We have

$$\begin{aligned} s_p &= \frac{\omega}{|q|} = s \left| \frac{\sin(aq/2)}{aq/2} \right|, \\ s_g &= \left| \frac{d\omega}{dq} \right| = s |\cos(aq/2)|. \end{aligned} \quad (2.16)$$

At the boundaries of the interval we get $s_p = (2/\pi)s$ while $s_g = 0$ (boundary modes cannot transfer energy).

Diatomeric Chain. Acoustic and Optical branches.

We use this case to discuss vibrations of compound lattices. Let us consider the chain shown in Fig. 2.5. One can see that the elementary cell contains 2 atoms. If we assume the

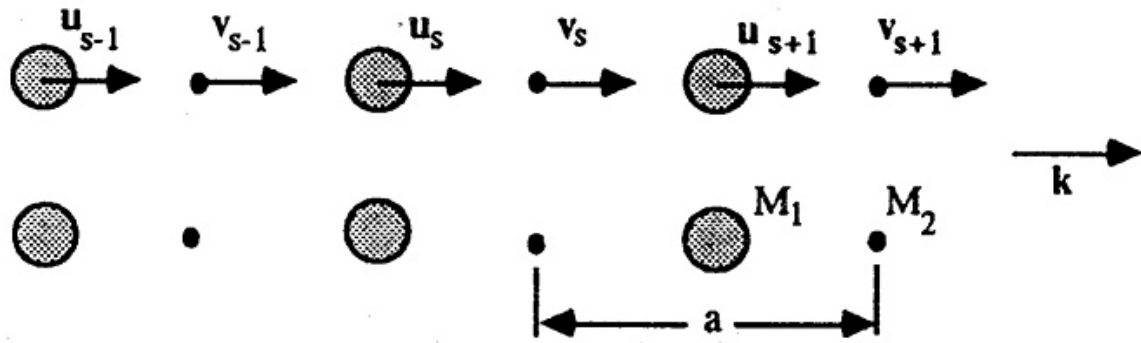


Figure 2.5: Linear diatomic chain.

elastic constants to be $C_{1,2}$ we come to the following equations of motion:

$$\begin{aligned} m_1 \ddot{u}_n &= -C_1(u_n - v_n) - C_2(u_n - v_{n-1}), \\ m_2 \ddot{v}_n &= -C_1(v_n - u_n) - C_2(v_n - u_{n-1}). \end{aligned} \quad (2.17)$$

It is natural to use once more the translation symmetry condition and search the solution as

$$u_n = A_u e^{i(qan - \omega t)}, \quad v_n = A_v e^{i(qan - \omega t)}. \quad (2.18)$$

After substitution to Eqs. (2.17) we get the set of equations for the constants A_i . To formulate these equations it is convenient to express these equations in a matrix form introducing the vector $\mathbf{A} \equiv (A_u \ A_v)$ and the so-called *dynamic matrix*

$$\hat{D} = \begin{pmatrix} \frac{C_1+C_2}{m_1+m_2} & -\frac{C_1+C_2 e^{-iaq}}{m_1} \\ -\frac{C_1+C_2 e^{iaq}}{m_2} & \frac{C_1+C_2}{m_1} \end{pmatrix} \quad (2.19)$$

The equation for \mathbf{A} has the form (see matrix notations in Appendix B)

$$\omega^2 \mathbf{A} - \hat{D} \mathbf{A} = \hat{0}. \quad (2.20)$$

This is homogeneous equation; it has a solution only if

$$\det(\omega^2 \hat{1} - \hat{D}) = 0. \quad (2.21)$$

This is just the equation which determines the eigenfrequencies. We get

$$\omega_{1,2}^2 = \frac{\omega_0^2}{2} \left[1 \mp \sqrt{1 - \gamma^2 \sin^2 \frac{aq}{2}} \right] \quad (2.22)$$

where

$$\omega^2 = \frac{(C_1 + C_2)(m_1 + m_2)}{m_1 m_2}, \quad \gamma^2 = 16 \left[\frac{C_1 C_2}{(C_1 + C_2)^2} \right] \left[\frac{m_1 m_2}{(m_1 + m_2)^2} \right].$$

The frequencies $\omega_{1,2}$ are real because $|\gamma| \leq 1$.

We see a very important difference with the case of monoatomic chain: there are 2 branches $\omega_{1,2}$ for a given value of q . The branches are shown in Fig. 2.6. The lower branch

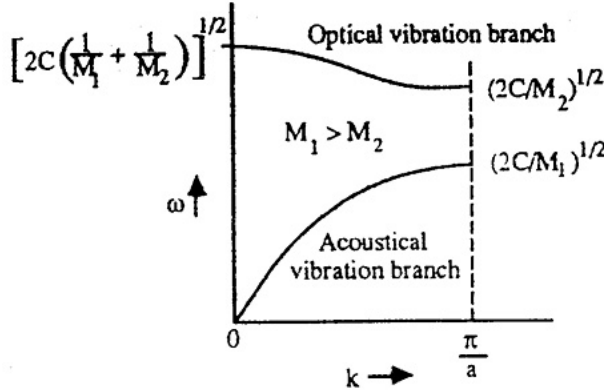


Figure 2.6: Optical and acoustic vibration branches.

is called the *acoustic branch* while the upper one is called the *optical branch*. To understand

the physical reason for these names let us consider the limits of zero and maximal q . We get

$$\begin{aligned}\omega_{ac}(0) &= 0, & \omega_{ac}(\pi/a) &= \frac{\omega_0}{\sqrt{2}} \sqrt{1 - \sqrt{1 - \gamma^2}}, \\ \omega_{opt}(0) &= \omega_0, & \omega_{opt}(\pi/a) &= \frac{\omega_0}{\sqrt{2}} \sqrt{1 + \sqrt{1 - \gamma^2}}.\end{aligned}\quad (2.23)$$

So, we have the inequality chain

$$\omega_{opt}(0) = \omega_0 > \omega_{opt}(\pi/a) > \omega_{ac}(\pi/a) > \omega_{ac}(0) = 0.$$

What happens in the degenerate case when $C_1 = C_2$, $m_1 = m_2$? This situation is illustrated in Fig. 2.7 Now we can discuss the structure of vibrations in both modes. From

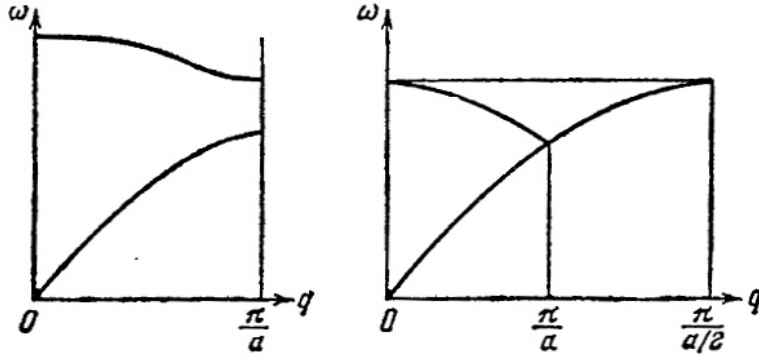


Figure 2.7: Degenerate case.

the dispersion equation (2.20) we get

$$\mathcal{P}_{ac,opt} = \frac{u_n}{v_{n ac,opt}} = \frac{A_u}{A_v} = \frac{C_1 + C_2 e^{-iqa}}{(C_1 + C_2) - m_1 \omega_{ac,opt}^2}. \quad (2.24)$$

At very long waves ($q \rightarrow 0$) we get (*Problem 2.3*)

$$\mathcal{P}_{ac} = 1, \quad \mathcal{P}_{opt} = -\frac{m_2}{m_1} \quad (2.25)$$

So, we see that in the acoustic mode all the atoms move next to synchronously, like in an acoustic wave in homogeneous medium. Contrary, in the optical mode; the gravity center remains unperturbed. In an ionic crystal such a vibration produce alternating *dipole moment*. Consequently, the mode is *optical active*. The situation is illustrated in Fig. 2.8.

Vibration modes of 3D lattices

Now we are prepared to describe the general case of 3D lattice. Assume an elementary cell with s different atoms having masses m_k . We also introduce the *main region* of the crystal

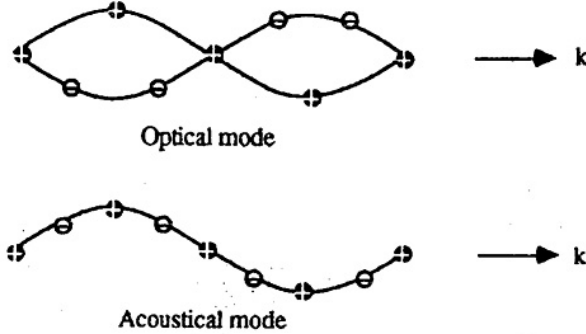


Figure 2.8: Transverse optical and acoustic waves.

as a body restricted by the rims $L\mathbf{a}_i$, the volume being $\mathcal{V} = L^3\mathcal{V}_0$ while the number of sites $N = L^3$. The position of each atom is

$$\mathbf{R}_n^k = \mathbf{a}_n + \mathbf{R}^k. \quad (2.26)$$

Here \mathbf{R}^k determines the atom's position within the cell. Similarly, we introduce displacements \mathbf{u}_n^k . The displacement-induced change of the potential energy Φ of the crystal is a function of all the displacements with a minimum at $\mathbf{u}_n^k = 0$. So, we can expand it as

$$\Phi = \frac{1}{2} \sum_{all} \Phi_{\alpha\beta} \left(\begin{array}{c} kk' \\ \mathbf{n}\mathbf{n}' \end{array} \right) u_{n\alpha}^k u_{n'\beta}^{k'} + \frac{1}{6} \sum_{all} \Phi_{\alpha\beta\gamma} \left(\begin{array}{c} kk'k'' \\ \mathbf{n}\mathbf{n}'\mathbf{n}'' \end{array} \right) u_{n\alpha}^k u_{n'\beta}^{k'} u_{n''\gamma}^{k''} \quad (2.27)$$

(Greek letters mean Cartesian projections). There are important relations between the coefficients Φ in Eq. (2.27) because the energy should not change if one shifts the crystal *as a whole*.

1. The coefficients are dependent only on the differences $\mathbf{n} - \mathbf{n}'$, $\mathbf{n} - \mathbf{n}''$, etc.

$$\Phi_{\alpha\beta} \left(\begin{array}{c} kk' \\ \mathbf{n}\mathbf{n}' \end{array} \right) = \Phi_{\alpha\beta} \left(\begin{array}{c} kk' \\ \mathbf{n} - \mathbf{n}' \end{array} \right). \quad (2.28)$$

2. The coefficient do not change if one changes the order of columns in their arguments

$$\Phi_{\alpha\beta} \left(\begin{array}{c} kk' \\ \mathbf{n}\mathbf{n}' \end{array} \right) = \Phi_{\alpha\beta} \left(\begin{array}{c} k'k \\ \mathbf{n}'\mathbf{n} \end{array} \right). \quad (2.29)$$

3. The sums of the coefficients over all the subscripts vanish.

$$\sum_{n'k'} \Phi_{\alpha\beta} \left(\begin{array}{c} kk' \\ \mathbf{n}\mathbf{n}' \end{array} \right) = 0, \quad \sum_{n'n''k'k''} \Phi_{\alpha\beta\gamma} \left(\begin{array}{c} kk'k'' \\ \mathbf{n}\mathbf{n}'\mathbf{n}''\mathbf{n}'' \end{array} \right) = 0. \quad (2.30)$$

Now we can formulate the Newton equations

$$m_k \ddot{u}_{n\alpha}^k = \sum_{n'k'\beta} \Phi_{\alpha\beta} \left(\begin{array}{c} kk' \\ nn' \end{array} \right) u_{n'\beta}^{k'} \quad (2.31)$$

As in 1D case, we search the solution as (it is more convenient to use symmetric form)

$$\tilde{u}_{n\alpha}^k = \frac{1}{\sqrt{m_k}} A_\alpha^k(q) e^{i(\mathbf{q}\mathbf{a}_n - \omega t)}. \quad (2.32)$$

Here we introduce wave vector \mathbf{q} . Just as in 1D case, we can consider it in a restricted region

$$-\pi < \mathbf{q}\mathbf{a}_i < \pi \quad (2.33)$$

that coincides with the definition of the first Brillouin zone (or the Wigner-Seitz cell). The wave vector \mathbf{q} is defined with the accuracy of an arbitrary reciprocal vector \mathbf{G} , the q -space is the same as the reciprocal lattice one.

Finally, we come to the equation (2.20) with

$$D_{\alpha\beta}^{kk'}(\mathbf{q}) = \sum_{n'} \frac{1}{\sqrt{m_k m_{k'}}} \Phi_{\alpha\beta} \left(\begin{array}{c} kk' \\ nn' \end{array} \right) e^{i\mathbf{q}(a_{n'} - a_n)} \quad (2.34)$$

This matrix equation is in fact the same as the set of $3s$ equations for $3s$ complex unknowns A_α^k . Now we come exactly to the same procedure as was described in the previous subsection. In fact, the dispersion equation has the form (2.21).

Let us discuss general properties of this equation. One can show (see *Problem 2.5*) that

$$D_{\alpha\beta}^{kk'} = \left[D_{\beta\alpha}^{k'k} \right]^*, \quad (2.35)$$

i. e. the matrix \hat{D} is *Hermitian*. Consequently, its eigenvalues are *real* (see Appendix B). One can show that they are also *positive* using the request of the potential energy to be minimal in the equilibrium.

The general way is as follows. One should determine $3s$ eigenvalues of the matrix \hat{D} for a given \mathbf{q} to get the values of $\omega_j(\mathbf{q})$. These values have to be substituted into Eq. (2.20) to find corresponding complex amplitudes $A_{j\alpha}^k(\mathbf{q})$ which are proportional to the eigenvectors of the dynamic matrix \hat{D} . One can show from its definition that in general case

$$\hat{D}(-\mathbf{q}) = \left[\hat{D}(\mathbf{q}) \right]^*. \quad (2.36)$$

That means important properties of solutions:

$$\omega_j(-\mathbf{q}) = \omega_j(\mathbf{q}), \quad A_{j\alpha}^k(-\mathbf{q}) = [A_{j\alpha}^k(\mathbf{q})]^*. \quad (2.37)$$

These properties are in fact the consequences of the *time reversibility* of the mechanical problem we discuss.

Finally, one can construct a set of iso-frequency curves $\omega_j(\mathbf{q}) = \text{const}$ which are periodic in \mathbf{q} -space the period being the reciprocal lattice vector \mathbf{G} . The symmetry of those curves are determined by the lattice symmetry.

In the end of this subsection, we analyze the long wave properties of 3D lattice. It is clear, that at $\mathbf{q} = 0$ the component of \hat{D} -matrix are *real*. If we put the real displacement $A_{j\beta}^k/\sqrt{m_k}$ to be k -independent and use the property (2.30) we readily get $\omega_j(0) = 0$ for all the 3 components $\alpha = 1, 2, 3$. So, there are 3 acoustic branches and 3s-3 optical ones. To describe their behavior we should write down the dynamic equation for real displacements for $\mathbf{q} = 0$ as

$$\omega^2(0)m_k \frac{A_\alpha^k(0)}{\sqrt{m_k}} = \sum_{k'\beta n'} \frac{1}{\sqrt{m_{k'}}} \Phi_{\alpha\beta} \left(\begin{array}{c} kk' \\ nn' \end{array} \right) A_\beta^{k'}(0) \quad (2.38)$$

and then sum over k (over the atoms in the primitive cell). Using the property (2.30)

$$\sum_{n'k'} \Phi_{\alpha\beta} \left(\begin{array}{c} kk' \\ nn' \end{array} \right) = 0$$

we get

$$\sum_k m_k u_{n\alpha}^k = 0, \quad (2.39)$$

i. e. the center of gravity for optical modes remains constant. A typical vibration spectrum is shown in Fig. 2.9

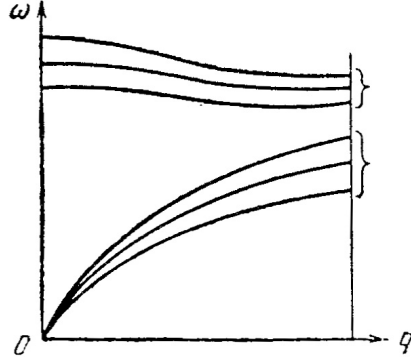


Figure 2.9: Typical vibration spectrum in 3D case.

Continual Approximation for Lattice Vibrations

To elucidate the difference between acoustic and optical vibrations we discuss here the long wave limit in continual approximation.

Acoustic vibrations

According to the theory of elasticity, one can write equations of motion as

$$\rho \frac{\partial^2 \mathbf{u}}{\partial t^2} = (\Upsilon + \Lambda) \operatorname{grad} \operatorname{div} \mathbf{u} + \Upsilon \nabla^2 \mathbf{u} \quad (2.40)$$

where ρ is the mass density while Υ, Λ are elastic constants. It is known that $\vartheta = \operatorname{div} \mathbf{u}(\mathbf{r}, t)$ is the relative *volume change* while $\boldsymbol{\varphi} = \frac{1}{2} \operatorname{curl} \mathbf{u}$ is the rotation angle. Taking into account that

$$\operatorname{curl} \operatorname{grad} \psi(\mathbf{r}) = 0, \operatorname{div} \operatorname{curl} \mathbf{k}(\mathbf{r}) = 0, \nabla^2 \equiv \operatorname{div} \operatorname{grad},$$

we can obtain the equations for the quantities $\vartheta, \boldsymbol{\varphi}$:

$$\frac{\partial^2 \vartheta}{\partial t^2} = s_l^2 \nabla^2 \vartheta, \quad (2.41)$$

$$\frac{\partial^2 \boldsymbol{\varphi}}{\partial t^2} = s_t^2 \nabla^2 \boldsymbol{\varphi}, \quad (2.42)$$

where

$$s_l = \sqrt{\frac{2\Upsilon + \Lambda}{\rho}}, \quad s_t = \sqrt{\frac{\Upsilon}{\rho}}. \quad (2.43)$$

If $\mathbf{u} = \mathbf{A} \exp(i\mathbf{qr} - i\omega t)$ we get

$$\begin{aligned} \vartheta &= \operatorname{div} \mathbf{u} = i\mathbf{q}\mathbf{u}, \\ \boldsymbol{\varphi} &= \frac{1}{2}[\mathbf{q}\mathbf{u}]. \end{aligned} \quad (2.44)$$

So, we see that the compression ϑ wave is *longitudinal* while the $\boldsymbol{\varphi}$ rotation wave is transversal. These waves are the analogs of 3 acoustic modes in a crystal. We can also calculate the number of the vibrations if we restrict ourselves with a cube with the side L and put zero boundary conditions. We get $\vartheta = A \sin(\omega t) \sin(q_x x) \sin(q_y y) \sin(q_z z)$ for each mode with $q_i = n_i \frac{\pi}{L}$. We have $\omega = q s = s \sqrt{q_x^2 + q_y^2 + q_z^2}$ for each branch. Consequently, the number of vibrations in the region $R, R + dR$ where $R = \sqrt{\sum_i n_i^2}$ is

$$g(\omega) d\omega = \sum_{l,t} \frac{4\pi R^2 dR}{8} = \frac{\mathcal{V}}{2\pi^2} \left(\frac{1}{s_l^3} + \frac{2}{s_t^3} \right) \omega^2 d\omega. \quad (2.45)$$

Optical vibrations

Consider a ionic crystal with 2 ions in a primitive cell with effective charges $\pm e^*$. Denoting the corresponding displacements as \mathbf{u}_\pm and the force constant as κ we get the following equations of motion

$$\begin{aligned} M_+ \frac{d^2 \mathbf{u}_+}{dt^2} &= -\kappa(\mathbf{u}_+ - \mathbf{u}_-) + e^* \mathbf{E}_e, \\ M_- \frac{d^2 \mathbf{u}_-}{dt^2} &= -\kappa(\mathbf{u}_- - \mathbf{u}_+) - e^* \mathbf{E}_e \end{aligned} \quad (2.46)$$

where \mathbf{E}_e is the effective electric field acting from the external sources and from other ions. Then, let us introduce reduced mass

$$\frac{1}{M_r} = \frac{1}{M_+} + \frac{1}{M_-}$$

and relative displacement $\mathbf{s} = \mathbf{u}_+ - \mathbf{u}_-$. Combining Eqs. (2.46) we obtain

$$M_r \frac{d^2 \mathbf{s}}{dt^2} = -\kappa \mathbf{s} + e^* \mathbf{E}_e. \quad (2.47)$$

Now one should express the effective field \mathbf{E}_e through \mathbf{s} to make all the set of equations complete. The effective field differs from *average* field, \mathbf{E} , by the contribution of the polarization, \mathbf{P} . In this way, we get the following set of equations for the normalized displacement $\mathbf{w} = \sqrt{N_0 M_r} \mathbf{s}$

$$\begin{aligned} \ddot{\mathbf{w}} + \gamma_{11} \mathbf{w} - \gamma_{12} \mathbf{E} &= 0 \\ \gamma_{12} \mathbf{w} + \gamma_{22} \mathbf{E} - \mathbf{P} &= 0, \\ \nabla(\mathbf{E} + 4\pi \mathbf{P}) &= 0. \end{aligned} \quad (2.48)$$

The coefficients γ_{ik} can be expressed through dielectric parameters of the crystal (see derivation below)

$$\gamma_{11} = \omega_0^2, \quad \gamma_{12} = \omega_0 \sqrt{\frac{\epsilon_0 - \epsilon_\infty}{4\pi}}, \quad \gamma_{22} = \frac{\epsilon_\infty - 1}{4\pi}. \quad (2.49)$$

Here

$$\omega_0^2 = \frac{\kappa}{M_r} - \frac{4\pi N_0 e^{*2} (\epsilon_\infty + 2)}{9M_r}, \quad (2.50)$$

While $\epsilon_0(\infty)$ are, respectively, static and high-frequency dielectric constants. Finally, we come to the set of equations

$$\begin{aligned} \frac{d^2 \mathbf{w}}{dt^2} &= -\omega_0^2 \mathbf{w} + \omega_0 \sqrt{\frac{\epsilon_0 - \epsilon_\infty}{4\pi}} \mathbf{E}, \\ \mathbf{P} &= \omega_0 \sqrt{\frac{\epsilon_0 - \epsilon_\infty}{4\pi}} \mathbf{w} + \frac{\epsilon_\infty - 1}{4\pi} \mathbf{E}. \end{aligned} \quad (2.51)$$

This is the final set of equation we should analyze. To do it we split the displacement \mathbf{w} into the potential \mathbf{w}_l ($\text{curl } \mathbf{w}_l = 0$) and solenoidal \mathbf{w}_t ($\text{div } \mathbf{w}_t = 0$) parts. It the absence of free charges

$$\text{div } \mathbf{D} = 0 \rightarrow \text{div } \mathbf{E} = -4\pi \text{div } \mathbf{P}.$$

Using (2.51) we get

$$\mathbf{E} = -\frac{\omega_0}{\epsilon_\infty} \sqrt{4\pi(\epsilon_0 - \epsilon_\infty)} \mathbf{w}_l.$$

Substituting this relation into the equations (2.51) and separating potential and solenoidal parts we get

$$\begin{aligned}\frac{d^2\mathbf{w}_t}{dt^2} &= -\omega_0^2 \mathbf{w}_t, \\ \frac{d^2\mathbf{w}_l}{dt^2} &= -\omega_0^2 \frac{\epsilon_0}{\epsilon_\infty} \mathbf{w}_l.\end{aligned}\quad (2.52)$$

Consequently, we come to the picture of longitudinal and transversal optical modes with

$$\frac{\omega_l}{\omega_t} = \sqrt{\frac{\epsilon_0}{\epsilon_\infty}} \quad (2.53)$$

(the *Lyddane-Sax-Teller relation*).

The ion motion in the transversal and longitudinal modes is shown in Fig. 2.10 taken from the book [4]. We see that the two types of optical vibrations differ because of the long-range electric forces which are produced only by *longitudinal* modes. Consequently, they are called *polar*. The difference between the frequencies of polar and non-polar modes depends on the crystal ionicity and allows one to estimate the latter.

Derivation of the constants γ_{ik}

In a cubic crystal, where polarizability is a scalar, we have

$$\mathbf{P} = N_0 \frac{e^* \mathbf{s} + \alpha \mathbf{E}}{1 - (4N_0\pi/3)\alpha} \quad (2.54)$$

and introduce the dielectric function ϵ according to the electrostatic equation for the displacement vector

$$\mathbf{D} = \mathbf{E} + 4\pi\mathbf{P} = \epsilon \mathbf{E}. \quad (2.55)$$

This function is dependent on the vibration frequency ω . We get

$$\mathbf{P} = \frac{\epsilon - 1}{4\pi} \mathbf{E}. \quad (2.56)$$

Actually, ϵ is frequency dependent and at high frequencies ions cannot react on the a.c. electric field. Let us denote this limit as ϵ_∞ and put for this limit $\mathbf{s} = 0$ in Eq. (2.54). Combining (2.54) for $\mathbf{s} = 0$ with (2.56) we get

$$\alpha = \frac{\epsilon_\infty - 1}{(4\pi N_0/3)(\epsilon_\infty + 2)}. \quad (2.57)$$

Then we can substitute it once more in Eq. (2.54) and get

$$\mathbf{P} = N_0 \frac{e^*(\epsilon_\infty + 2)}{3} \mathbf{s} + \frac{\epsilon_\infty - 1}{4\pi} \mathbf{E}. \quad (2.58)$$

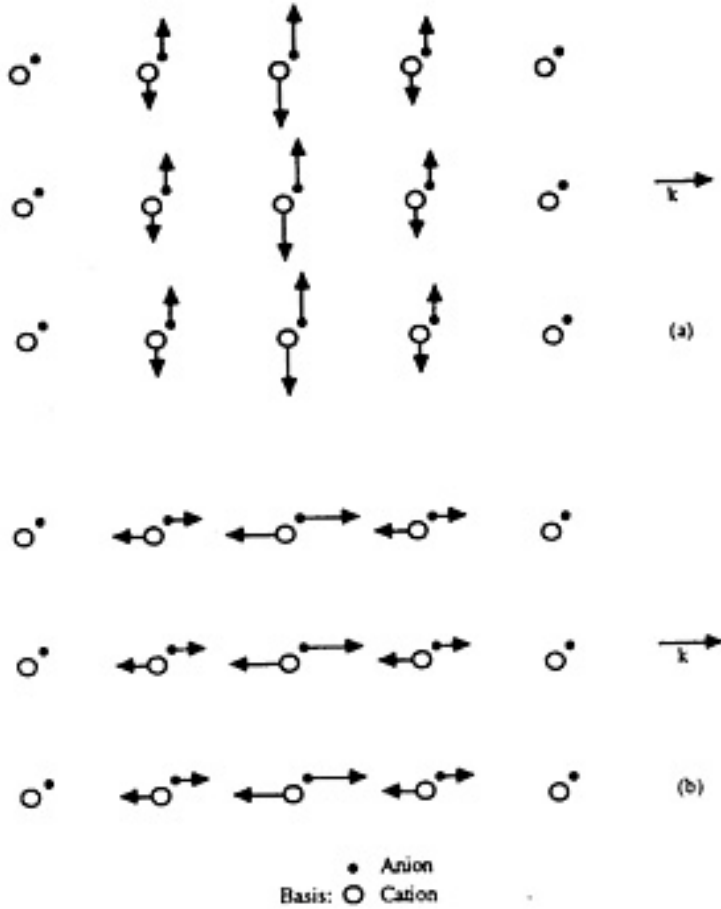


Figure 2.10: Optical modes of vibration of an ion crystal.

Making use of this equation we get

$$M_r \frac{d^2 \mathbf{s}}{dt^2} = -M_r \omega_0^2 \mathbf{s} + \frac{e^* (\epsilon_\infty + 2)}{4\pi} \mathbf{E} \quad (2.59)$$

where

$$\omega_0^2 = \frac{\kappa}{M_r} - \frac{4\pi N_0 e^{*2} (\epsilon_\infty + 2)}{9 M_r}. \quad (2.60)$$

Usually the normalized displacement $\mathbf{w} = \sqrt{N_0 M_r} \mathbf{s}$ is introduced, so finally we come to the set of equations

$$\begin{aligned} \frac{d^2 \mathbf{w}}{dt^2} &= -\omega_0^2 \mathbf{w} + \sqrt{\frac{N_0}{M_r}} e^* \frac{\epsilon_\infty + 2}{3} \mathbf{E}, \\ \mathbf{P} &= \sqrt{\frac{N_0}{M_r}} e^* \frac{\epsilon_\infty + 2}{3} \mathbf{w} + \frac{\epsilon_\infty - 1}{4\pi} \mathbf{E}. \end{aligned} \quad (2.61)$$

It is reasonable to introduce the *static* dielectric constant ϵ_0 from the request of vanishing of the right-hand side of Eq. (2.59):

$$\epsilon_0 - \epsilon_\infty = \frac{N_0}{M_r} e^{*2} \frac{4\pi(\epsilon_\infty + 2)^2}{9\omega_0^2}. \quad (2.62)$$

Thus we arrive to the set of equations to be analyzed.

Optical Vibration–Light Interaction

It is clear that optical vibrations in ionic compounds should interact with electromagnetic waves. To take this interaction into account one should add the Maxwell equations to the complete set of equations for the vibrations. We have²

$$\begin{aligned} [\nabla \times \mathbf{B}] &= \frac{1}{c} \left(\frac{\partial \mathbf{E}}{\partial t} + 4\pi \frac{\partial \mathbf{P}}{\partial t} \right), \\ [\nabla \times \mathbf{E}] &= -\frac{1}{c} \frac{\partial \mathbf{B}}{\partial t}, \\ (\nabla \cdot \mathbf{B}) &= 0, \\ \nabla \cdot (\mathbf{E} + 4\pi \mathbf{P}) &= 0, \\ \ddot{\mathbf{w}} + \gamma_{11}\mathbf{w} - \gamma_{12}\mathbf{E} &= 0, \\ \mathbf{P} &= \gamma_{12}\mathbf{w} + \gamma_{22}\mathbf{E}. \end{aligned} \quad (2.63)$$

Here \mathbf{B} is magnetic induction,

$$\gamma_{11} = \omega_0^2, \quad \gamma_{12} = \omega_0 \sqrt{\frac{\epsilon_0 - \epsilon_\infty}{4\pi}}, \quad \gamma_{22} = \frac{\epsilon_\infty - 1}{4\pi}. \quad (2.64)$$

We are interested in the transversal modes, so we search solutions proportional to $\exp(i\mathbf{qr} - i\omega t)$ with

$$\mathbf{E} \parallel \mathbf{P} \parallel \mathbf{w} \parallel \mathbf{x}, \quad \mathbf{B} \parallel \mathbf{y}, \quad \mathbf{q} \parallel \mathbf{z}. \quad (2.65)$$

The equations for the complex amplitudes are (Check!)

$$\begin{aligned} \frac{i\omega}{c} E - iqB + \frac{4\pi i\omega}{c} P &= 0, \\ iqE - \frac{i\omega}{c} B &= 0, \\ \gamma_{12}E + (\omega^2 - \gamma_{11})w &= 0, \\ \gamma_{22}E - P + \gamma_{12}w &= 0. \end{aligned} \quad (2.66)$$

Consequently, to get eigenfrequencies one should request

$$\det \begin{vmatrix} \omega/c & 4\pi\omega/c & -q & 0 \\ q & 0 & -\omega/c & 0 \\ \gamma_{12} & 0 & 0 & \omega^2 - \gamma_{11} \\ \gamma_{22} & -1 & 0 & \gamma_{12} \end{vmatrix} = 0. \quad (2.67)$$

²We use the so-called Gaussian system of units.

After the substitution of all the values of γ_{ik} we get

$$\omega^4 \epsilon_\infty - \omega^2 (\omega_t^2 + c^2 q^2) + \omega_t^2 c^2 q^2 = 0. \quad (2.68)$$

This equation is quadratic in ω^2 the roots being

$$\omega_{1,2} = \frac{1}{2\epsilon_\infty} (\omega_t^2 \epsilon_0 + c^2 q^2) \pm \sqrt{\frac{1}{4\epsilon_0^2} (\omega_t^2 \epsilon_0 + c^2 q^2)^2 - \omega_t^2 q^2 \left(\frac{c^2}{\epsilon_\infty} \right)}. \quad (2.69)$$

This spectrum is shown in Fig. 2.11. It is important that there is no possibility for the light

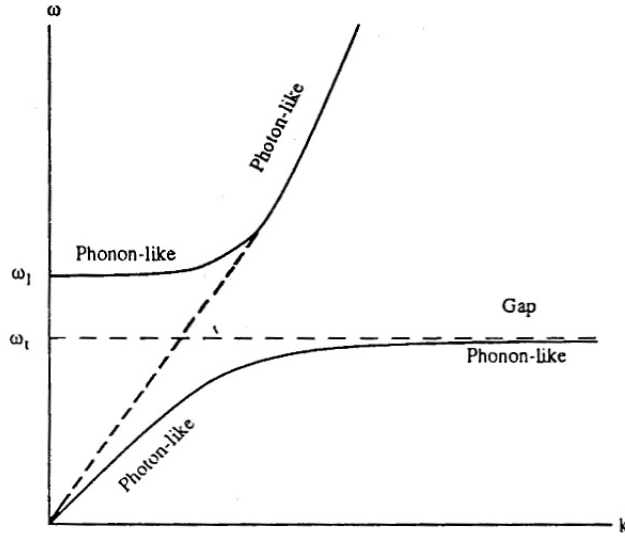


Figure 2.11: Coupled TO-photon modes. The broken lines – spectra without interaction.

with the frequencies between ω_t and ω_l to penetrate the crystal, it is completely reflected. The coupled TO-vibration-photon modes are often called the *polaritons*. One can easily understand that longitudinal model do not couple to the light.

2.3 Quantum Mechanics of Atomic Vibrations

Normal Co-ordinates for Lattice Vibrations

Now we formulate the dynamic equations in a universal form to prepare them to quantum mechanical description.

Let us introduce the eigenvectors $\mathbf{e}_{jk}(\mathbf{q})$ of the dynamical matrix \hat{D} which correspond to the eigenvalues $\omega_j^2(\mathbf{q})$. According to the definition of eigenvectors,

$$\sum_{k'\beta} D_{\alpha\beta}^{kk'}(\mathbf{q}) e_{jk'\beta}(\mathbf{q}) = \omega_j^2(\mathbf{q}) e_{jk\alpha}(\mathbf{q}).$$

According to the properties of Hermitian matrices, the eigenvectors are orthogonal and normalized,

$$\sum_{\alpha k} e_{jk\alpha} e_{j'k\alpha}^* = \delta_{jj'} \quad \sum_j e_{jk\alpha} e_{jk'\beta}^* = \delta_{kk'} \delta_{\alpha\beta}. \quad (2.70)$$

Also,

$$e_{jk\alpha}(\mathbf{q}) = e_{jk\alpha}^*(-\mathbf{q}). \quad (2.71)$$

The general displacements may differ from eigenvectors only by normalization. Consequently, it is convenient to expand the displacements in terms of the eigenvectors as

$$u_{n\alpha}^k(t) = \frac{1}{\sqrt{N m_k}} \sum_{\mathbf{q}j} e_{jk\alpha}(\mathbf{q}) a_j(\mathbf{q}, t) e^{i\mathbf{q}\mathbf{q}_n}. \quad (2.72)$$

The amplitudes $a_j(\mathbf{q}, t)$ are called the *normal co-ordinates* (or normal modes). One can prove that $a(-\mathbf{q}) = a^*(\mathbf{q})$ (otherwise we cannot obtain real displacements). The total number of the amplitudes is $3sN$ ($3s$ values for the mode's number j and N for the discrete \mathbf{q} number).

Now we calculate the kinetic energy of vibrations:

$$\mathcal{T} = \frac{1}{2} \sum_{n\alpha} m_k (\dot{u}_{n\alpha}^k)^2. \quad (2.73)$$

It is easy to show (see *Problem 2.6*) that it is equal to

$$\mathcal{T} = \frac{1}{2} \sum_{\mathbf{q}j} |\dot{a}_j(\mathbf{q}, t)|^2. \quad (2.74)$$

Now we come to the potential energy. After some calculations (see *Problem 2.7*) we get

$$\Phi = \frac{1}{2} \sum_{\mathbf{q}j} \omega_j^2(\mathbf{q}) |a_j(\mathbf{q}, t)|^2, \quad (2.75)$$

the total energy being

$$\mathcal{E} = \frac{1}{2} \sum_{\mathbf{q}j} [|\dot{a}_j(\mathbf{q}, t)|^2 + \omega_j^2(\mathbf{q}) |a_j(\mathbf{q}, t)|^2]. \quad (2.76)$$

We see that the total energy is the sum of the energies of *independent oscillators*. The quantities $a_j(\mathbf{q}, t)$ are called the *complex normal co-ordinates*. It is convenient to come to the so-called *real normal co-ordinates* to apply all the laws of mechanics. Usually, it is done with the help of the so-called *Pierls transform*. Let us introduce real co-ordinates $Q_j(\mathbf{q})$ and real canonic momentum $P_j(\mathbf{q}) \equiv \dot{Q}_j(\mathbf{q})$ with the help of the transform

$$\begin{aligned} a_j(\mathbf{q}) &= \frac{1}{2} [Q_j(\mathbf{q}) + Q_j^*(-\mathbf{q})] + \\ &+ \frac{i}{2\omega_j(\mathbf{q})} [\dot{Q}_j(\mathbf{q}) - \dot{Q}_j^*(-\mathbf{q})]. \end{aligned} \quad (2.77)$$

We observe that the condition $a_j(\mathbf{q}) = a_j^*(-\mathbf{q})$ is automatically met. Making use of the equality $\omega_j(-\mathbf{q}) = \omega_j(\mathbf{q})$ one can easily show that the co-ordinates Q_j obey the equation

$$\ddot{Q}_j(\pm\mathbf{q}) = -\omega_j^2(\mathbf{q})Q_j(\pm\mathbf{q}). \quad (2.78)$$

After very simple calculations (see *Problem 2.8*) we get

$$\mathcal{E} = \frac{1}{2} \sum_{\mathbf{q}j} \left[\dot{Q}_j^2(\mathbf{q}) + \omega_j^2(\mathbf{q})Q_j^2(\mathbf{q}) \right]. \quad (2.79)$$

Now we can use the general principles of mechanics and introduce canonic momenta as

$$P_j(\mathbf{q}) = \frac{\partial \mathcal{E}}{\partial \dot{Q}_j} = \dot{Q}_j(\mathbf{q}). \quad (2.80)$$

Finally, we can write down the classical Hamilton function of the system as

$$\mathcal{H}(Q, P) = \mathcal{E} = \sum_{\mathbf{q}j} \left[\frac{P_j^2(\mathbf{q})}{2} + \omega_j^2(\mathbf{q}) \frac{Q_j^2(\mathbf{q})}{2} \right]. \quad (2.81)$$

As a result, we have expressed the classical Hamiltonian as the one for the set of independent oscillators.

At the end of this section we express the displacement in terms of the canonic variables (later we will need this expression)

$$u_{n\alpha}^k = \frac{1}{\sqrt{Nm_k}} \sum_{\mathbf{q}j} \text{Re} \left\{ e_{j\alpha k}(\mathbf{q}) \left[Q_j(\mathbf{q}) + \frac{i}{\omega_j(\mathbf{q})} P_j(\mathbf{q}) \right] e^{i\mathbf{q}\mathbf{a}_n} \right\}. \quad (2.82)$$

Quantization of Atomic Vibrations: Phonons

The quantum mechanical prescription to obtain the Hamiltonian from the classical Hamilton function is to replace classical momenta by the operators:

$$\dot{Q}_j(\mathbf{q}) = P_j(\mathbf{q}) \rightarrow \hat{P}_j(\mathbf{q}) = \frac{\hbar}{i} \frac{\partial}{\partial Q_j(\mathbf{q})}. \quad (2.83)$$

Consequently we come to the Schrödinger equation

$$\hat{\mathcal{H}}(\hat{P}, Q) = \sum_{\mathbf{q}j} \left\{ -\frac{\hbar^2}{2} \frac{\partial^2}{\partial Q_j^2(\mathbf{q})} - \frac{1}{2} \omega_j^2(\mathbf{q})Q_j^2(\mathbf{q}) \right\}. \quad (2.84)$$

It is a sum of the Schrödinger equations for independent oscillators with the mass equal to 1, co-ordinate $Q_j(\mathbf{q})$ and eigenfrequency $\omega_j(\mathbf{q})$. It is known that in such a case the total wave function is the product of the one-oscillator functions. So, let us start with one-oscillator equation for the wave function ψ

$$-\frac{\hbar^2}{2} \frac{\partial^2 \psi}{\partial Q^2} + \frac{1}{2} \omega^2 Q^2 \psi = \varepsilon \psi. \quad (2.85)$$

Its solution is

$$\begin{aligned}\psi &= \psi_N(Q) = \left(\frac{\omega}{\pi\hbar}\right)^{1/4} \frac{1}{\sqrt{2^N N!}} e^{-\omega Q^2/2\hbar} H_N\left[\left(\frac{\omega}{\hbar}\right)^{1/2} Q\right], \\ \varepsilon &= \varepsilon_N = \hbar\omega(N + 1/2).\end{aligned}\quad (2.86)$$

Here N is the oscillator's quantum number, $H_N(\xi)$ is the Hermit polynom which is dependent on the dimensionless co-ordinate

$$\xi = Q\sqrt{\omega/\hbar}. \quad (2.87)$$

In the following we will need the matrix elements of the operators Q and \hat{P} defined as

$$\langle \alpha | \hat{A} | \beta \rangle \equiv \int_{-\infty}^{\infty} dQ \psi_{\alpha}^{*}(Q) \hat{A} \psi_{\beta}(Q).$$

According to the table of integrals,

$$\begin{aligned}\langle N' | \hat{Q} | N \rangle &= \sqrt{\frac{\hbar}{2\omega}} \times \begin{cases} \sqrt{N}, & \text{if } N' = N - 1, \\ \sqrt{N+1}, & \text{if } N' = N + 1, \\ 0, & \text{otherwise;} \end{cases} \\ \langle N' | \hat{P} | N \rangle &= i\sqrt{\frac{\hbar\omega}{2}} \times \begin{cases} -\sqrt{N}, & \text{if } N' = N - 1, \\ \sqrt{N+1}, & \text{if } N' = N + 1, \\ 0, & \text{otherwise.} \end{cases}\end{aligned}\quad (2.88)$$

The equations introduced above describe the quantum mechanical approach to the lattice vibrations. In the following we employ this system to introduce a very general and widely used concept of *secondary quantization*.

Second Quantization

In the Q -representation, the total wave function is the symmetrized product of the oscillator wave functions with quantum numbers $N_{j\mathbf{q}}$. Because it is impossible to discriminate between the modes with given $j\mathbf{q}$ the numbers $N_{j\mathbf{q}}$ completely describe the system.

To describe quasiparticles it is convenient to introduce operators which act directly upon the occupation numbers $N_{j\mathbf{q}}$. They are introduced as

$$\begin{aligned}b &= \left(\frac{\omega}{2\hbar}\right)^{1/2} \hat{Q} + i \left(\frac{1}{2\hbar\omega}\right)^{1/2} \hat{P}, \\ b^{\dagger} &= \left(\frac{\omega}{2\hbar}\right)^{1/2} \hat{Q} - i \left(\frac{1}{2\hbar\omega}\right)^{1/2} \hat{P}.\end{aligned}\quad (2.89)$$

One can show directly that

$$\begin{aligned}b\psi_N &= \sqrt{N}\psi_{N-1}, \\ b^{\dagger}\psi_N &= \sqrt{N+1}\psi_{N+1}.\end{aligned}\quad (2.90)$$

We see that the operator b^\dagger *increases* the occupation number by one while the operator b *decreases* this number also by one. Consequently, the operators are called *creation* and *annihilation* operators.

Let us consider the properties of the creation and annihilation operators in more details. According to quantum mechanics

$$Q\hat{P} - \hat{P}Q \equiv [Q, \hat{P}] = i\hbar. \quad (2.91)$$

Inserting in these commutation relations the definitions (2.89) we get

$$bb^\dagger - b^\dagger b = [b, b^\dagger] = 1 \quad (2.92)$$

This relation could be generalized for the case of different modes because the modes with different $j\mathbf{q}$ are independent under harmonic approximation. Consequently, the corresponding operators commute and we get

$$[b_j(\mathbf{q}), b_{j'}^\dagger(\mathbf{q})] = \delta_{jj'}\delta\mathbf{q}\mathbf{q}'. \quad (2.93)$$

So we come to the picture of independent particles. To be more precise, they are called *quasiparticles*.³ The quasiparticles obeying the commutation relations (2.93) are called *bosons*, they are described by the *Bose-Einstein* statistics.

Now we can insert the operators b , b^\dagger into the Hamiltonian (2.84). After very simple algebra (Check!) we get

$$\mathcal{H} = \sum_{j,\mathbf{q}} \frac{\hbar\omega_j(\mathbf{q})}{2} \left[b_j(\mathbf{q})b_j^\dagger(\mathbf{q}) + b_j^\dagger(\mathbf{q})b_j(\mathbf{q}) \right] = \sum_{j,\mathbf{q}} \hbar\omega_j(\mathbf{q}) \left[b_j^\dagger(\mathbf{q})b_j(\mathbf{q}) + 1/2 \right]. \quad (2.94)$$

Applying the product $b^\dagger b$ to the wave function ψ_N we get

$$b^\dagger b\psi_N = N\psi_N. \quad (2.95)$$

Consequently, the operator $b_j^\dagger(\mathbf{q})b_j(\mathbf{q})$ has eigenvalues $N_{j,\mathbf{q}}$.

Finally, it is useful to remember matrix elements of the creation and annihilation operators:

$$\langle N' | b | N \rangle = \sqrt{N}\delta_{N',N-1}, \quad \langle N' | b^\dagger | N \rangle = \sqrt{N+1}\delta_{N',N+1}. \quad (2.96)$$

As will be demonstrated in the following, the normal vibrations behave as *particles* with the energy $\hbar\omega_j(\mathbf{q})$ and *quasimomentum* $\hbar\mathbf{q}$. The quasiparticles are called *phonons*. The part *quasi* is very important for some reasons which we will discuss in detail later. In particular, we have obtained the effective Hamiltonian as sum of the independent oscillator Hamiltonians under the *harmonic approximation* where only quadratic in displacement terms are kept. The higher approximation lead to an *interaction* between the introduced *quasiparticles*. It will be shown that the conservation laws for the quasiparticle interaction

³We will see the reasons later.

differ from the ones for free particles, namely $\sum_i \hbar \mathbf{q}_i$ is conserved with the accuracy of the arbitrary reciprocal lattice vector \mathbf{G} .

It is convenient to introduce operators for lattice vibrations. Using definitions of the operators $b_{\mathbf{q}}$ and $b_{\mathbf{q}}^\dagger$ and Eq. (2.82) we obtain

$$\hat{u}_{n\alpha}^k(t) = \sqrt{\frac{\hbar}{2Nm_k}} \sum_{\mathbf{q}j} \frac{e_{j\alpha k}(\mathbf{q})}{\sqrt{\omega_{j\mathbf{q}}}} [b_{\mathbf{q}} e^{i\mathbf{q}\mathbf{a}_n - i\omega_{j\mathbf{q}}t} + b_{\mathbf{q}}^\dagger e^{-i\mathbf{q}\mathbf{a}_n + i\omega_{j\mathbf{q}}t}] . \quad (2.97)$$

2.4 Phonon Dispersion Measurement Techniques

Here be describe very briefly the main experimental techniques to investigate phonon spectra.

Neutron Scattering

In this method, neutron with the energy $E = p^2/2M_n$, $M_n = 1.67 \cdot 10^{-24}$ g are incident upon the crystal. The phonon dispersion is mapped exploiting the momentum-energy conservation law

$$\begin{aligned} E' - E &= \sum_{j,\mathbf{q}} \hbar\omega_j(\mathbf{q})(N'_{j\mathbf{q}} - N_{j\mathbf{q}}), \\ \mathbf{p}' - \mathbf{p} &= - \sum_{j,\mathbf{q}} \hbar\mathbf{q}(N'_{j\mathbf{q}} - N_{j\mathbf{q}}) + \hbar\mathbf{G}. \end{aligned} \quad (2.98)$$

The processes involving finite \mathbf{G} are called the *Umklapp* ones.

Zero Phonon Scattering

If no phonon are emitted or absorbed we have the same conditions as for X-ray scattering, the Laue condition $\mathbf{p}' - \mathbf{p} = \hbar\mathbf{G}$.

One Phonon Scattering

We get:

- Absorption:

$$\begin{aligned} E' &= E + \hbar\omega_j(\mathbf{q}), \\ \mathbf{p}' &= \mathbf{p} + \hbar\mathbf{q} + \hbar\mathbf{G}. \end{aligned} \quad (2.99)$$

- Emission:

$$\begin{aligned} E' &= E - \hbar\omega_j(\mathbf{q}), \\ \mathbf{p}' &= \mathbf{p} - \hbar\mathbf{q} + \hbar\mathbf{G}. \end{aligned} \quad (2.100)$$

Making use of the periodicity of the phonon spectra $\omega_j(\mathbf{q})$ we have

- Absorption:

$$\frac{\mathbf{p}'^2}{2M_n} = \frac{\mathbf{p}^2}{2M_n} + \hbar\omega_j \left(\frac{\mathbf{p} + \mathbf{p}'}{\hbar} \right),$$

- Emission

$$\frac{\mathbf{p}'^2}{2M_n} = \frac{\mathbf{p}^2}{2M_n} - \hbar\omega_j \left(\frac{\mathbf{p} - \mathbf{p}'}{\hbar} \right). \quad (2.102)$$

The equations allow one to analyze the phonon spectra.

Light Scattering

Usually the photons with $k \sim 10^5 \text{ cm}^{-1}$ are used that corresponds to the photon energy $\approx 1 \text{ eV}$. Because this wave vector is much less than the size of the Brillouin zone only central phonons contribute. The interaction with acoustic phonons is called *Brillouin scattering* while the interaction with optical modes is called the *Raman* one.

Once more one should apply the conservation laws. Introducing photon wave vector \mathbf{k} we get

$$\begin{aligned} \omega' &= \omega \pm \omega_j(\mathbf{q}), \\ \eta\mathbf{k}' &= \eta\mathbf{k} \pm \mathbf{q} + \mathbf{G} \end{aligned} \quad (2.103)$$

where η is the refractive index, + corresponds to a phonon absorption (the so-called anti-Stokes process) while – correspond to an emission (Stokes process). It is clear that $\omega_j(\mathbf{q}) \ll \omega$. Consequently, $|\mathbf{k}| \approx |\mathbf{k}'|$ and

$$q = 2\frac{\omega\eta}{c} \sin \frac{\theta}{2},$$

where θ is the scattering angle. The corresponding phonon frequency is determined as $\Delta\omega$.

2.5 Problems

- 2.1.** Derive the dispersion relation (2.9).
- 2.2.** Derive the expression (2.13).
- 2.3.** Derive Eq. (2.25).
- 2.4.** Prove the relation of the Section 4.
- 2.5.** Prove the relation (2.35).
- 2.6.** Prove the equation (2.74).
- 2.7.** Prove the expression (2.75) for the potential energy.
- 2.8.** Prove the expression (2.79).
- 2.9.** Prove the expression (2.90).

Chapter 3

Electrons in a Lattice. Band Structure.

In this chapter the properties of electron gas will be considered. Extra information can be found in many books, e. g. [1, 2].

3.1 General Discussion. Electron in a Periodic Field

To understand electron properties one should in general case solve the Schrödinger equation (SE) for the whole system of electrons and atoms including their interaction. There are several very important simplifications.

- The atomic mass M is much greater than the electron one m . So, for the beginning, it is natural to neglect the atomic kinetic energy, considering atoms as *fixed*. In this way we come to the SE for the many-electron wave function,

$$\left[-\frac{\hbar^2}{2m} \sum_i \nabla_i^2 + V(\mathbf{r}, \mathbf{R}) \right] \psi = \mathcal{E} \psi \quad (3.1)$$

where atomic co-ordinates are considered as *external parameters*

$$\psi(\mathbf{r}, \mathbf{R}), \quad \mathcal{E}(\mathbf{R}).$$

- We will see that the behavior of *interacting* electrons is very similar to the one of *non-interacting* particles (i. e. gas) in an external self-consistent field produced by the lattice ions and other electrons. It is very difficult to calculate this field but it is clear that it has *the same symmetry* as the lattice. So let us take advantage of this fact and study the general properties of the electron motion.

3.1.1 Electron in a Periodic Potential

Let us forget about the nature of the potential and take into account only the periodicity condition

$$V(\mathbf{r} + \mathbf{a}) = V(\mathbf{r}). \quad (3.2)$$

The one electron SE

$$-\frac{\hbar^2}{2m}\nabla^2\psi(\mathbf{r}) + V(\mathbf{r})\psi(\mathbf{r}) = \varepsilon\psi(\mathbf{r}) \quad (3.3)$$

should also have the solution $\psi(\mathbf{r} + \mathbf{a})$ corresponding to the *same energy*. Consequently, if the level ε is *non-degenerate* we get

$$\psi(\mathbf{r} + \mathbf{a}) = C\psi(\mathbf{r}), \quad C = \text{constant}. \quad (3.4)$$

According to the normalization condition $|C|^2 = 1$ one can write

$$C = e^{i\varphi(\mathbf{a})} \quad (3.5)$$

where φ is some real function of the lattice vector. Now we can apply the translation symmetry and make consequential displacements, \mathbf{a} and \mathbf{a}' . We get

$$C(\mathbf{a})C(\mathbf{a}') = C(\mathbf{a} + \mathbf{a}') \quad (3.6)$$

that means the φ -function should be *linear*

$$\varphi(\mathbf{a}) = \mathbf{p}\mathbf{a}/\hbar. \quad (3.7)$$

It is clear that vector \mathbf{p} is defined with the accuracy of $\hbar\mathbf{G}$ where \mathbf{G} is the reciprocal lattice vector.

Finally, the general form of the electron wave function in a lattice is

$$\psi(\mathbf{r}) = e^{i\mathbf{pr}/\hbar}u(\mathbf{r}) \quad (3.8)$$

where

$$u(\mathbf{r} + \mathbf{a}) = u(\mathbf{r}) \quad (3.9)$$

is a periodic function. The expression (3.8) is known as the *Bloch theorem*.

The Bloch function (3.8) is very similar to the plane wave, the difference being the presence of the modulation u . The vector \mathbf{p} is called *quasimomentum* because it is defined with the accuracy $\hbar\mathbf{G}$. Because of periodicity, we can consider only one cell in the reciprocal lattice space.

As in the situation with lattice vibrations, we apply cyclic boundary conditions, so the vector \mathbf{p} is a discrete variable:

$$p_i = \frac{2\pi\hbar}{L_i}n_i, \quad (3.10)$$

the number of states being

$$\prod_i \Delta n_i = \frac{\mathcal{V}}{(2\pi\hbar)^3} \prod_i \Delta p_i. \quad (3.11)$$

It means that the density of states is $\mathcal{V}/(2\pi\hbar)^3$. We will very often replace the sums over discrete states by the integrals

$$\mathcal{V} \sum_i \rightarrow \mathcal{V} \int \frac{2d^3p}{(2\pi\hbar)^3} \equiv \mathcal{V} \int (dp).$$

Here we have taken into account that an electron has spin 1/2, the projection to a given axis being $\pm 1/2$ that doubles the number of states. Thus, the energy levels are specified as $\varepsilon_l(\mathbf{p})$ where \mathbf{p} acquires N values where N is the number of primitive cells in the sample. Hence, the total number of states for a quantum number l is $2N$.

The functions $\varepsilon_l(\mathbf{p})$ are periodic in the reciprocal space, so they have maximal and minimal values and form bands. These bands can overlap or some energy gaps can exist.

Let us consider some other general properties of wave functions. If one writes down the complex conjugate to the Schrödinger equation and then replaces $t \rightarrow -t$ he gets the same equation with the Hamiltonian \mathcal{H}^* . But it is known that Hamiltonian is a Hermitian operator and $\mathcal{H} = \mathcal{H}^*$. It means that if

$$\psi_{l\mathbf{p}}(\mathbf{r}, t) = \exp[-i\varepsilon_l(\mathbf{p})t/\hbar] \psi_{l\mathbf{p}}(\mathbf{r})$$

is an eigenfunction of \mathcal{H} the function $\psi_{l\mathbf{p}}^*(\mathbf{r}, -t)$ is also the eigenfunction. At the same time, after the shift \mathbf{a} these functions acquire different factors, $e^{\pm i\mathbf{p}\mathbf{a}/\hbar}$ respectively. It means

$$\varepsilon_l(\mathbf{p}) = \varepsilon_l(-\mathbf{p}).$$

In the following we will specify the region of the reciprocal space in the same way as for lattice vibrations, namely, Brillouin zones (BZ). If the lattice symmetry is high enough the extrema of the functions $\varepsilon_l(\mathbf{p})$ are either in the center or at the borders of BZ.

3.2 Tight Binding Approximation

To get some simple example we consider the so-called tight-binding-approximation. Let us start with the 1D case and assume that the overlap of the electron shells is very small. Consequently, this overlap can be considered as perturbation and we start with the potential

$$V(x) = \sum U(x - na), \quad (3.12)$$

the SE equation being

$$-\frac{\hbar^2}{2m} \frac{d^2\psi}{dx^2} + \sum_n U(x - na) \psi(x) = \varepsilon \psi(x). \quad (3.13)$$

Let the exact wave functions be

$$\psi_p(x) = e^{ipx/\hbar} u_p(x)$$

with the eigenvalues $\varepsilon(p)$. We construct the so-called *Wannier* functions as

$$w_n(x) = \frac{1}{\sqrt{N}} \sum_p e^{-ipna/\hbar} \psi_p(x), \quad (3.14)$$

where N is the total number of atoms in the chain while p belongs to the 1st BZ. One can check (*Problem 3.1*) that the inverse transform is

$$\psi_p(x) = \frac{1}{\sqrt{N}} \sum_n e^{ipna/\hbar} w_n(x). \quad (3.15)$$

The Wannier functions are orthogonal and normalized (*Problem 3.2*).

It is important that the Wannier function w_n is large only near the n th ion position (without Bloch modulation it will be δ -function $\delta(x-na)$). Moreover, because of periodicity

$$w_n(x) = w_0(x - na).$$

Now we can substitute the function (3.15) into the exact SE and make the auxiliary transform

$$\mathcal{H} = \sum_n \left[-\frac{\hbar^2}{2m} \frac{d^2}{dx^2} + U(x - na) + h_n(x) \right]$$

where

$$h_n(x) \equiv V(x) - U(x - na)$$

between the *exact* potential $V(x)$ and the nearest atomic one. We get

$$\begin{aligned} \sum_n \left[-\frac{\hbar^2}{2m} \frac{d^2}{dx^2} + U(x - na) \right] e^{ikan} w_n(x) &+ \sum_n h_n(x) e^{ikan} w_n(x) = \\ &= \varepsilon(k) \sum_n e^{ikan} w_n(x). \end{aligned} \quad (3.16)$$

Here we have introduced the electron wave vector $k \equiv p/\hbar$.

The product

$$h_n(x) e^{ikan} w_n(x)$$

is small because it contains only the items $U(x - ma) w_n(x)$ for $m \neq n$, and we can neglect it as a zeroth approximation. As a result we get

$$w^{(0)} = \psi_0(x)$$

where $\psi_0(x)$ is the wave function of a free atom. Consequently

$$\varepsilon^{(0)}(p) = \varepsilon_0.$$

In the next approximation we put $w = w^{(0)} + w^{(1)}$ and find

$$\begin{aligned} \sum_n \left[-\frac{\hbar^2}{2m} \frac{d^2}{dx^2} + U(x - na) - \varepsilon_0 \right] e^{ikan} w_n^{(1)}(x) &= \\ = - \sum_n h_n(x) e^{ikan} w_n^{(0)}(x) + (\varepsilon(p) - \varepsilon_0) \sum_n e^{ikan} w_n^{(0)}(x). \end{aligned} \quad (3.17)$$

This is *non-uniform linear* equation for $w_n^{(1)}$. Since the Hamiltonian is Hermitian, Eq. (3.17) has a solution only if the r.h.s. is orthogonal to the solution of the corresponding *uniform* equation with the same boundary conditions. This solution is $w_n^{(0)}$.

As a result, we get

$$\varepsilon(p) - \varepsilon_0 = \frac{\sum_n h(n) e^{ikan}}{\sum_n I(n) e^{ikan}} \quad (3.18)$$

where

$$\begin{aligned} h(n) &= \int dx \psi_0^*(x) h_n(x) \psi_0(x - na), \\ I(n) &= \int dx \psi_0^*(x) \psi_0(x - na). \end{aligned} \quad (3.19)$$

The atomic wave function can be chosen as real, so $h(-n) = h(n)$, $I(-n) = I(n)$, both functions rapidly decrease with increasing n (small overlap!). Finally, we get (*Problem 3.3*)

$$\varepsilon - \varepsilon_0 = h(0) + 2[h(1) - h(0)I(1)] \cos(ka). \quad (3.20)$$

The 3D case is more complicated if there are more than 1 atom in a primitive cell. First, atoms' positions are connected by the symmetry transforms which differ from a simple translation. Second, atomic levels for higher momenta are degenerate. We discuss here the simplest case with 1 atom per a primitive cell and for *s*-states of the atoms having spherical symmetry. In this case we come to a similar expression

$$\varepsilon(p) - \varepsilon_0 = \frac{\sum_{\mathbf{n}} h(\mathbf{n}) e^{i\mathbf{k}\mathbf{n}}}{\sum_{\mathbf{n}} I(\mathbf{n}) e^{i\mathbf{k}\mathbf{n}}}. \quad (3.21)$$

In a bcc lattice taking into account nearest neighbors we get

$$\mathbf{a} = (a/2)(\pm 1, \pm 1, \pm 1),$$

and

$$\varepsilon(\mathbf{k}) - \varepsilon_0 = h(0) + 8W \cos(k_x a/2) \cos(k_y a/2) \cos(k_z a/2), \quad (3.22)$$

where $W = [h(1) - h(0)I(1)]$ is the characteristics of bandwidth. In a similar case of fcc lattice one gets (Check!)

$$\begin{aligned} \varepsilon(\mathbf{k}) - \varepsilon_0 &= h(0) + 4W [\cos(k_x a/2) \cos(k_y a/2) + \\ &+ \cos(k_y a/2) \cos(k_z a/2) + \\ &+ \cos(k_z a/2) \cos(k_x a/2)]. \end{aligned} \quad (3.23)$$

In a sc lattice one gets (*Problem 3.4*)

$$\varepsilon(\mathbf{k}) - \varepsilon_0 = h(0) + 2W [\cos(k_x a) + \cos(k_y a) + \cos(k_z a)] . \quad (3.24)$$

The physical meaning of the results is the spreading of atomic levels into narrow bands (Fig. 3.2)

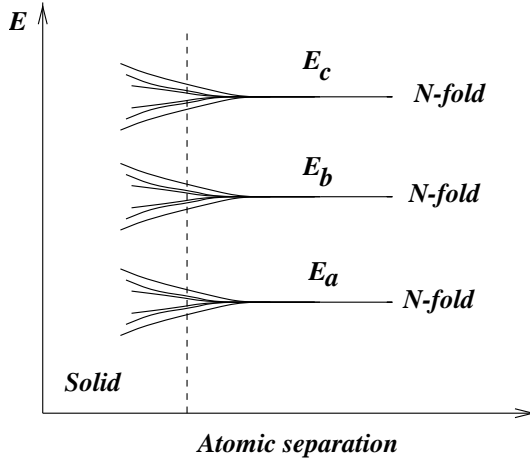


Figure 3.1: Spreading of atomic levels into bands

The tight binding approximation is useful when the overlap is small (transition and rare earth metals). Another application is to produce starting empirical formulas having proper symmetry.

3.3 The Model of Near Free Electrons

Now we come to the opposite limiting case where electrons are almost free. We start from 1D model for a very weak periodic potential. The starting approximation is a plane wave (we have in mind periodic boundary conditions)

$$\frac{1}{\sqrt{L}} e^{ikx} , \quad k = p/\hbar , \quad (3.25)$$

the energy being

$$\varepsilon^{(0)}(k) = \hbar^2 k^2 / 2m . \quad (3.26)$$

We can expand the periodic potential as

$$V(x) = \sum_n V_n e^{2\pi i n x / a} \quad (3.27)$$

where

$$V(k, k') = \frac{1}{L} \int dx V(x) e^{-i(k-k')x} = V_n \delta \left(k - k' - \frac{2\pi n}{a} \right) .$$

The first perturbation correction $\varepsilon^{(1)} = V_0$ is not important (shift of energy) while the second one is

$$\varepsilon^{(2)}(k) = \sum_{n \neq 0} \frac{|V_n|^2}{\varepsilon^{(0)}(k) - \varepsilon^{(0)}(k - 2\pi n/a)} \quad (3.28)$$

The perturbation theory is valid if $\varepsilon^{(2)} \ll \varepsilon^{(1)}$ that cannot be met at small denominators. At the same time, at $k \rightarrow \pi n/a$ the quantity $k' \rightarrow -\pi n/a$ and denominator tends to zero. Consequently, one has to use the perturbation theory for *degenerate states*. So let us recall the famous problem of quantum mechanics.

Assume that the functions ψ_i where $i = 1, 2$ correspond to the states 1, 2. We chose the wave function as their superposition,

$$\psi = A_1\psi_1 + A_2\psi_2.$$

Substituting this function into SE we get

$$A_1(\varepsilon_1 - \varepsilon)\psi_1 + V(A_1\psi_1 + A_2\psi_2) + A_2(\varepsilon_2 - \varepsilon)\psi_2 = 0.$$

Then we multiply the equation first by ψ_1^* and second by ψ_2^* . Integrating over x we get

$$\begin{aligned} (\varepsilon_1 - \varepsilon + V_0)A_1 + V_n A_2 &= 0, \\ V_n^* A_1 + (\varepsilon_2 - \varepsilon + V_0)A_2 &= 0. \end{aligned} \quad (3.29)$$

As a result, we get a quadratic equation for ε (we include the constant V_0 into this quantity):

$$\varepsilon^2 - (\varepsilon_1 + \varepsilon_2)\varepsilon + \varepsilon_1\varepsilon_2 - |V_n|^2 = 0,$$

which has solutions

$$\varepsilon = \frac{\varepsilon_1 + \varepsilon_2}{2} \pm \sqrt{\frac{(\varepsilon_1 - \varepsilon_2)^2}{4} + |V_n|^2}. \quad (3.30)$$

The sign is chosen from the request that far from the “dangerous” point ε should be close to ε_0 . As a result, the energy has a drop $2|V_n|$ near the points $k = \pm\pi n/a$. This situation is illustrated in Fig. 3.2

Because the energy spectrum is periodic in \mathbf{k} -space, it is convenient to make use of the periodicity of ε in k -space and to subtract from each value of k the reciprocal lattice vector in order to come within BZ. So we come from the left panel to the right one. We have once more the picture of bands with gaps in between, the gaps being small in comparison with the widths of the allowed bands.

In the 3D case the periodicity of the potential is taken into account by the expansion

$$V(\mathbf{r}) = \sum_{\mathbf{G}} V_{\mathbf{G}} e^{i\mathbf{Gr}}$$

where \mathbf{G} is the reciprocal lattice vector, the perturbation theory being destroyed at

$$\varepsilon^{(0)}(\mathbf{k}) = \varepsilon^{(0)}(\mathbf{k} - \mathbf{G}).$$

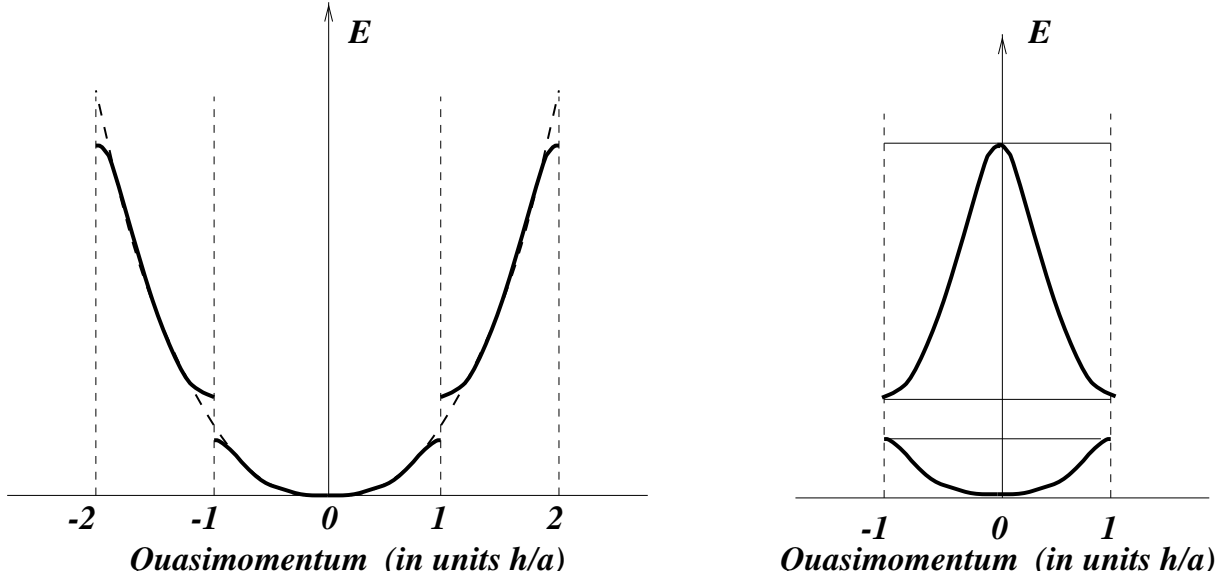


Figure 3.2: Energy spectrum in a weak periodic potential.

Substituting $\varepsilon^{(0)} = \hbar^2 k^2 / 2m$ we get

$$\mathbf{k}\mathbf{G} = G/2. \quad (3.31)$$

It is just the equation for the plane boundary of the BZ.

Thus the structure of BZ is extremely important for understanding of electron properties.

3.4 Main Properties of Bloch Electrons

3.4.1 Effective Mass

Let us discuss general properties on electrons in periodic potential. To make it as simple as possible we start with the case of a simple cubic crystal in the tight binding limit. From the expression (3.24) we see that there is a minimum \mathbf{b} in the BZ center $\mathbf{k} = 0$. Near the minimum expanding (3.24) for small product $k_i a \ll 1$ we get

$$\varepsilon = \varepsilon_b + Wk^2a^2, \quad k = \sqrt{k_x^2 + k_y^2 + k_z^2}, \quad (3.32)$$

where ε_b is the energy of the minimum. So the spectrum is just the same as the one of a particle with the *effective mass*

$$m_n^*(b) = \left(\frac{\partial^2 \varepsilon}{\partial p_x^2} \right)_b^{-1} = \frac{\hbar^2}{2Wa^2} \quad (3.33)$$

(the subscript n indicates that the material is of n -type, electron-like). Now we can analyze the BZ boundary \mathbf{a} with $k_i \approx \pi/a$. Substituting $k'_i = \pi/a - k_i$ and expanding (3.24) in powers of $k'_i a \ll 1$ we get

$$\varepsilon = \varepsilon_a - Wa^2 k'^2. \quad (3.34)$$

In a similar way, we get the expression for the effective mass

$$m_n^*(a) = -\frac{\hbar^2}{2Wa^2} \quad (3.35)$$

that is *negative*. Very often such a quasiparticle is called a *hole* (see later) and we define its mass as the electron mass with opposite sign. So, in a simple cubic crystal the hole mass, $m_p^* = |m_n^*|$, near the band top is the same as the electron mass near its bottom.

In the general case one can expand the energy as in l th band near an extremum as

$$\varepsilon_l(\mathbf{k}) = \frac{1}{2} \sum_{\alpha,\beta} \left(\frac{\partial^2 \varepsilon(\mathbf{k})}{\partial k_\alpha \partial k_\beta} \right)_0 (k_\alpha - k_{\alpha 0})(k_\beta - k_{\beta 0}) \quad (3.36)$$

and introduce the *inverse effective mass tensor*

$$(m^{-1})_{\alpha\beta} = \left(\frac{\partial^2 \varepsilon(\mathbf{k})}{\partial k_\alpha \partial k_\beta} \right)_0 \quad (3.37)$$

This 2nd-order tensor can be transformed to its principal axes.

3.4.2 Wannier Theorem → Effective Mass Approach

Now we come to a very important concept of solid state physics which allows one to treat electrons in a periodic field like ordinary particles - to the so-called *effective mass approach*.

We know that the energy in a given band is periodic in the \mathbf{k} -space that is the same as the reciprocal lattice space. So we can expand

$$\varepsilon_l(\mathbf{k}) = \sum_{\mathbf{a}} c_{\mathbf{a}} e^{i\mathbf{k}\mathbf{a}} \quad (3.38)$$

where \mathbf{a} are lattice vectors (Check!). How does the operator

$$\exp(\mathbf{a}\nabla)$$

act upon the Bloch function? One can immediately show that it is just the operator, which shifts the co-ordinate by \mathbf{a} (*Problem 3.5*):

$$\exp(\mathbf{a}\nabla)\psi_l(\mathbf{r}) = \psi_l(\mathbf{r} + \mathbf{a}). \quad (3.39)$$

Then we come to the very important formula:

$$\varepsilon_l(-i\nabla)\psi_l(\mathbf{r}) = \varepsilon_l(\mathbf{k})\psi_l(\mathbf{r}). \quad (3.40)$$

This relation is called the *Wannier theorem*. It is valid only if the spectrum is non-degenerate in the point \mathbf{k} .

So we come to the following prescription. As far as we know the spectrum $\varepsilon_l(\mathbf{k})$, we can replace $\mathbf{k} \rightarrow -i\nabla$ in the SE (which can also contain external fields) and analyze the electron's quantum dynamics. If we return to the situation where quadratic expansion is possible we come to the problem of a particle with (anisotropic) effective mass which can strongly differ from the free electron mass m_0 .

It is important to note that the prescription has essentially *single-band character*, it needs a very serious generalization if the bands are degenerate (or the gaps are narrow and interband transitions are possible). It is important in many situations in semiconductor crystals and we will come back to this point in the corresponding Section.

3.5 Electron Velocity

Let us calculate quantum mechanical average electron velocity $\langle \mathbf{v} \rangle$ in a Bloch state $\gamma \equiv l\mathbf{k}$. For a free electron one would obtain

$$\langle \mathbf{v} \rangle = \frac{1}{m_0} \langle \mathbf{p} \rangle = -\frac{i\hbar}{m_0} \langle \gamma | \nabla | \gamma \rangle = \frac{\hbar \mathbf{k}}{m_0}.$$

It is natural that for a quantum particle the average velocity is just the *group* velocity of the wave package representing quantum particle,

$$\mathbf{v} = \frac{\partial \varepsilon}{\partial \mathbf{p}} = \frac{1}{\hbar} \frac{\partial \varepsilon}{\partial \mathbf{k}} \quad (3.41)$$

(see *Problem 3.6*).

We see that if the spectrum is determined by quadratic expansion we get the usual expression for a particle with the mass m^* . In an external field we get the Newton equation

$$m^* \frac{\partial \mathbf{v}}{\partial t} = \mathbf{F}.$$

3.5.1 Electric current in a Bloch State. Concept of Holes.

Suppose that the electron has the charge $-e$ (we suppose e to be positive). The electric current is

$$\mathbf{j}_\gamma = -e \mathbf{v}_\gamma. \quad (3.42)$$

We know that $\varepsilon(-\mathbf{k}) = \varepsilon(\mathbf{k})$. Consequently, $\mathbf{v}(-\mathbf{k}) = -\mathbf{v}(\mathbf{k})$ and one can easily show that

$$\sum \mathbf{v}(\mathbf{k}) = 0 \quad (3.43)$$

where summation is performed inside the BZ. To get the total current one should multiply the equation (3.42) by 2 (number of spin projections). Taking into account relation (3.43)

one can prove that *the total current of completely filled band vanishes*. It is a very important statement. It remains valid also in an external electric field (if the field is small enough and electrons are not transferred to higher bands).

If the band is only filled partly, the total current is determined by the difference of filled states with \mathbf{k} and $-\mathbf{k}$. To formulate the current we introduce the occupation factor $\nu_n(\mathbf{k}, s)$ which is equal to 1 if the state with the quasimomentum $\hbar\mathbf{k}$ and spin s is *occupied* and 0 otherwise. One can also introduce the occupation number of *holes* as

$$\nu_p(\mathbf{k}, s) = 1 - \nu_n(\mathbf{k}, s)$$

which characterizes the probability of *empty* states. The current can be expressed as

$$\mathbf{j} = -e \sum_{\mathbf{k}, s} \nu_n(\mathbf{k}, s) \mathbf{v}(\mathbf{k}) = e \sum_{\mathbf{k}, s} \nu_p(\mathbf{k}, s) \mathbf{v}(\mathbf{k})$$

(the current of a completely filled band is zero!). So we can express the current of a partly full band as the current of *holes* with the charge $+e > 0$.

To get a more deep analogy let us calculate the *energy current* due to the flux of electrons and holes. Characterizing the energy current in a state \mathbf{k} as $\mathbf{v}[\varepsilon(\mathbf{k}) - e\varphi]$ where φ is the electric potential we get

$$\begin{aligned} \mathbf{w} &= \sum_{\mathbf{k}, s} \nu_n(\mathbf{k}, s) [\varepsilon(\mathbf{k}) - e\varphi] \mathbf{v}(\mathbf{k}) = \sum_{\mathbf{k}, s} [1 - \nu_p(\mathbf{k}, s)] [\varepsilon(\mathbf{k}) - e\varphi] \mathbf{v}(\mathbf{k}) = \\ &= \sum_{\mathbf{k}, s} [\varepsilon(\mathbf{k}) - e\varphi] \mathbf{v}(\mathbf{k}) + \sum_{\mathbf{k}, s} \nu_p(\mathbf{k}, s) [-\varepsilon(\mathbf{k}) + e\varphi] \mathbf{v}(\mathbf{k}) \end{aligned} \quad (3.44)$$

So we see that holes can be considered as particles with the energy $-\varepsilon(\mathbf{k})$. The usual way to treat the quasiparticles near the top of the band where the expansion (3.34) is valid is to define the hole energy as

$$\varepsilon_p(\mathbf{k}) = \varepsilon_a - \varepsilon_n(\mathbf{k}), \quad m_p = -m_n > 0$$

where subscript n characterizes an electron variable. In such a way we come to the description of the particles with the charge e and effective mass m_p .

3.6 Band Filling and Classification of Materials

We have discussed the picture of allowed bands and forbidden gaps. Now we are prepared to discuss the actual presence of electrons in these bands.

One can discuss the following variants.

1. There is one atom per cell. Consequently, at $T = 0$ the band is *half-full*.
2. One atom per cell and 2 electrons per atom. The band is full, there is a band gap and the next band is empty.

3. There are two atoms per cell and each atom contributes 1 electron. The same as in the previous case.

In the case 1 the material has high conductivity at very low temperatures, it is a *metal*. The cases 2 and 3 correspond to *insulators*, their conductivity exponentially decreases at low temperatures. This is shown in Fig. 3.3

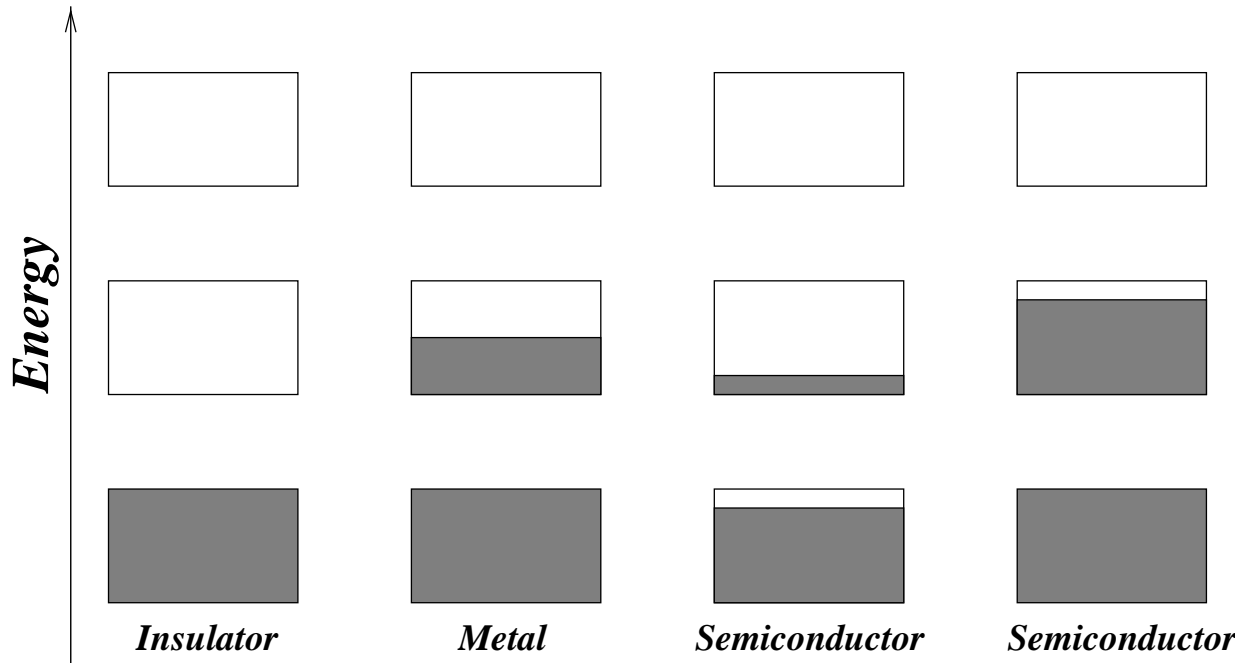


Figure 3.3: Electron occupation of bands (schematically).

All this scheme is valid if the bands do not overlap. If the bands overlap the conduction is usually metallic (see Fig. 3.4). Such materials are often called *semimetals* if effective number of carriers is small. A typical example of semimetals is Bi.

The *semiconductors* are defined as insulators with small forbidden gaps. At finite temperatures some electrons are excited from the lower *valence* band to the upper, *conduction* one. So there are holes in the valence band and the electrons in the conduction one. Such semiconductor is called *intrinsic*. The modern way to produce materials for electronics is to “*dope*” semiconductor material with impurity atoms which introduce carriers in a controllable way.

The impurity level are usually situated in the forbidden gap. If the impurity level are situated near the bottom of conduction band the atom are ionized at low enough temperatures and provide extra electrons to the band (such impurities are called *donors*). Contrary, if the levels are near the top of the valence band they take electrons from the band producing holes (they are called *acceptors*).

We will come back to this classification later to describe special features of different materials.

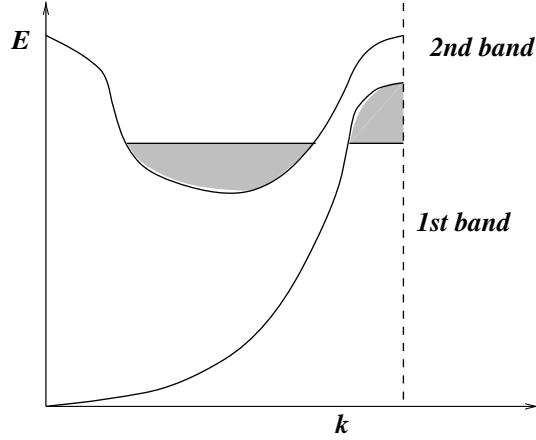


Figure 3.4: The case of band overlap.

3.7 Dynamics of Bloch Electrons

Now we discuss dynamic properties of Bloch electrons both classical and quantum.

3.7.1 Classical Mechanics

As we have seen, under the *one band approximation* the Bloch electron can be described as a particle with the classical Hamilton function

$$\mathcal{H}(\mathbf{p}, \mathbf{r}) = \varepsilon(\mathbf{p}) + \mathcal{U}(\mathbf{r}), \quad \mathbf{p} = \hbar\mathbf{k}.$$

Here $\mathcal{U}(\mathbf{r})$ is the total potential energy due to external fields. To take account of magnetic field one should replace the momentum \mathbf{p} by the *kinematic* one¹

$$\mathbf{p} \rightarrow \mathbf{P} = p + \frac{e}{c}\mathbf{A}(\mathbf{r})$$

where \mathbf{A} is the *vector-potential* of the magnetic field which is connected with the magnetic field \mathbf{H} by the relation

$$\mathbf{H} = \text{curl } \mathbf{A}.$$

Consequently, we have

$$\mathcal{H}(\mathbf{p}, \mathbf{r}) = \varepsilon \left[\mathbf{p} + \frac{e}{c} \mathbf{A}(\mathbf{r}) \right] + \mathcal{U}(\mathbf{r}), \quad \mathbf{p} = \hbar\mathbf{k}$$

where

$$\mathcal{U}(\mathbf{r}) = U(\mathbf{r}) - e\varphi(\mathbf{r}),$$

¹Remember that we denote the electron charge as $-e$.

U is the potential energy due to non-electric fields (like deformation), while φ is the electrostatic potential. To analyze the dynamics one should use classical Hamilton equations

$$\dot{\mathbf{r}} = \mathbf{v} = \frac{\partial \mathcal{H}}{\partial \mathbf{p}}, \quad \dot{\mathbf{p}} = -\frac{\partial \mathcal{H}}{\partial \mathbf{r}}.$$

The first equation reduces to the one we have discussed earlier,

$$\mathbf{v} = \frac{\partial \varepsilon}{\partial \mathbf{p}}$$

while the second one needs more care because the vector-potential is \mathbf{r} -dependent. We get

$$\dot{p}_i = -\frac{\partial}{\partial x_i} \varepsilon \left[\mathbf{p} + \frac{e}{c} \mathbf{A}(\mathbf{r}) \right] - \frac{\partial \mathcal{U}(\mathbf{r})}{\partial x_i}.$$

The first item is

$$-\frac{e}{c} \sum_k \frac{\partial \varepsilon}{\partial p_k} \frac{\partial A_k}{\partial x_i} = -\frac{e}{c} \sum_k v_k \frac{\partial A_k}{\partial x_i}.$$

We will consider for simplicity the case of a *homogeneous* magnetic field. It is convenient to choose the so-called *Landau gauge*

$$\mathbf{A} = \begin{pmatrix} 0 \\ Hx \\ 0 \end{pmatrix}, \quad \mathbf{H} = H\hat{\mathbf{z}}. \quad (3.45)$$

In this case we have

$$-\frac{e}{c} v_y \frac{\partial A_y}{\partial x} = -\frac{e}{c} v_y H_z = -\frac{e}{c} [\mathbf{v} \times \mathbf{H}]_x.$$

As a result, we come to the very usual formula

$$\dot{\mathbf{p}} = (-e) \left(\mathbf{E} + \frac{1}{c} [\mathbf{v} \times \mathbf{H}] \right) - \nabla U(\mathbf{r}), \quad \mathbf{E} = -\nabla \varphi(\mathbf{r}). \quad (3.46)$$

which is just the Newton law for the particle with the charge $-e$.

In the absence of external the electric field and the potential U , as one can easily show, energy is conserved. Indeed

$$\frac{d\varepsilon}{dt} = \frac{\partial \varepsilon}{\partial \mathbf{p}} \frac{\partial \mathbf{p}}{\partial t} = -\frac{e}{c} (\mathbf{v} [\mathbf{v} \times \mathbf{H}]) = 0.$$

So we have 2 integrals of motion,

$$\varepsilon = \text{const}, \quad p_z = \text{const}.$$

Thus we come to a geometric picture: one should take the surface $\varepsilon(\mathbf{p}) = \text{const}$ and intersect this surface by the plane $p_z = \text{const}$. The resulting line is just the electron orbit in \mathbf{p} -space.

It is clear that the result is strongly dependent on the *shape* of the surface $\varepsilon(\mathbf{p}) = \text{const}$. In semiconductors usually only the electrons near band extrema are important and all the orbits are *closed* lines.

The situation is much more rich in metals where the number of conduction electrons is large and (because of the Pauli principle) at small temperatures they occupy the states below the certain energy which is called the *Fermi level* ϵ_F . The electrons near the surface

$$\varepsilon(\mathbf{p}) = \epsilon_F$$

(the *Fermi surface*, FS) are most important for all the properties of metals. If the Fermi surface is confined within one BZ it is called *closed*. In general, FS can touch the boundaries of the BZ. In this case it is called *open*. The examples of closed and open FS in 2D case are shown in Fig. 3.5 while some FS in 3D case are shown in Fig. 3.6 and Fig. 3.7.

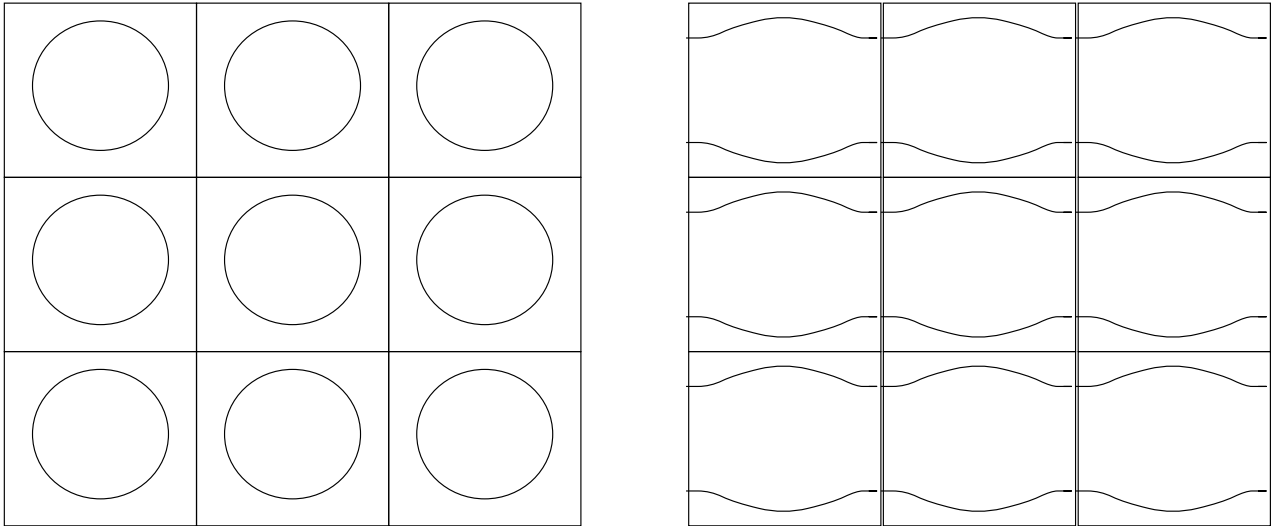


Figure 3.5: Closed and open FS in two-dimensional case (examples).

The closed orbits can be both electron- and hole-like. *Electron* orbits are the ones with the velocity $\mathbf{v} = \nabla_{\mathbf{p}}\varepsilon(\mathbf{p})$ is directed “outside” the orbit, the hole ones have to velocity directed “inside”. It easy to show that it is just the same definition as we have used previously (see later). If the magnetic field is tilted with respect to the symmetry axes both closed and open orbits can exist (see Fig. 3.8).

To study the motion in momentum space one can introduce the element

$$dp \equiv \sqrt{(dp_x)^2 + (dp_y)^2}.$$

Taking squares of Eq. (3.46) for p_x and p_y and adding them we get

$$\frac{dp}{dt} = \frac{e}{c} H v_{\perp}, \quad \text{or} \quad dt = \frac{c}{eH} \frac{dp}{v_{\perp}}.$$

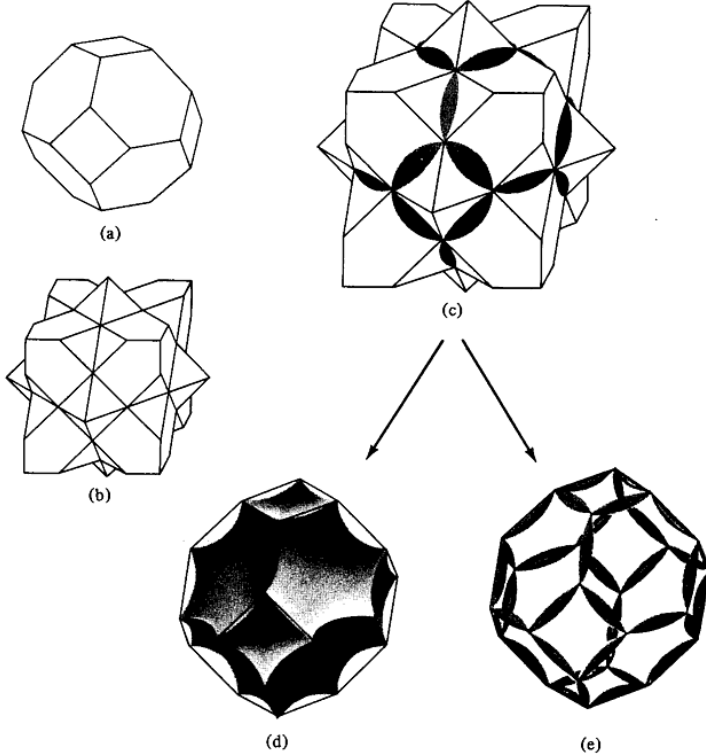


Figure 3.6: (a) 1st BZ for a fcc crystal (Al). (b) 2nd BZ for a fcc crystal. (c) The free electron sphere for a trivalent fcc Bravais lattice. It completely encloses the 1st zone, passing through and beyond the 2nd zone into the third and (at the corners) ever slightly into the fourth. (d) Portion of the free electron surface in the second zone when translated into the 1st zone. The convex surface encloses holes. (e) portion of the free electron sphere in the 3d zone when translated into the 1st zone. The surface encloses electrons.

If the orbit is closed we immediately get the expression for the period through the integral along the orbit

$$T = \frac{c}{eH} \oint \frac{dp}{v_{\perp}}.$$

This period can be easily expressed in terms of the orbit's area S

$$S(p_z) = \left[\int dp_x dp_y \right]_{p_z=\text{const}}.$$

To do this integral we can take 2 contours corresponding to ε and $\varepsilon + d\varepsilon$, the width in \mathbf{p} -space in the normal direction being

$$d\varepsilon |\partial\varepsilon/\partial\mathbf{p}_{\perp}|^{-1} = d\varepsilon/v_{\perp}. \quad (3.47)$$

Thus

$$S = \int d\varepsilon \oint \frac{dp}{v_{\perp}}.$$

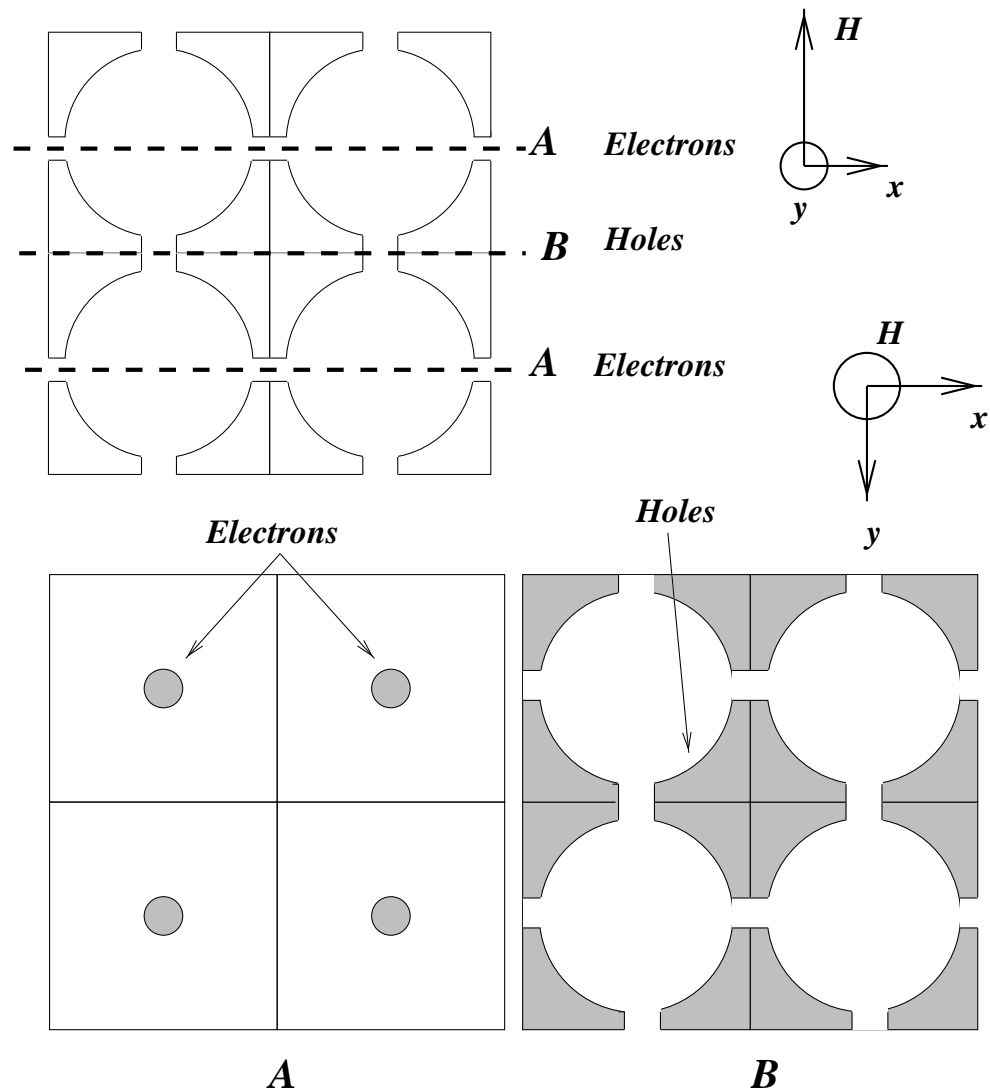


Figure 3.7: Possible FS for a cubic metal. Lower panel: Left part - electron orbits, right part - hole ones.

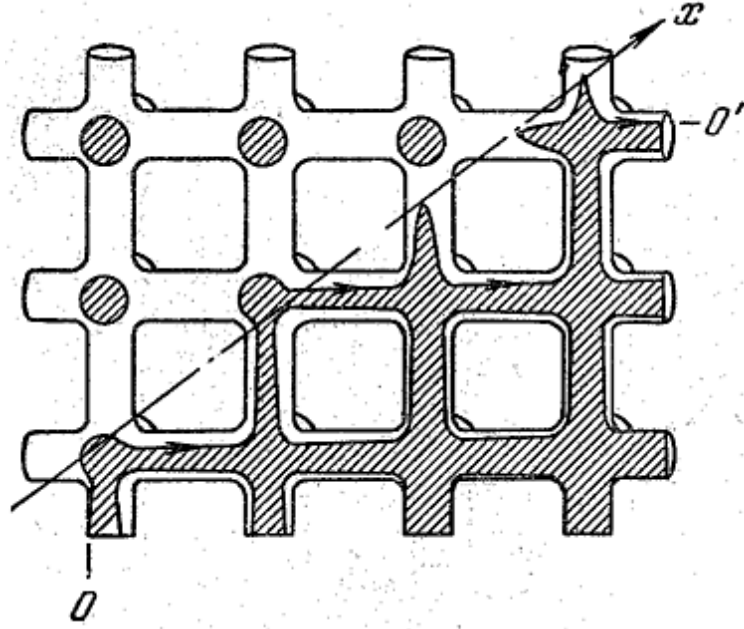


Figure 3.8: Electron orbits for tilted magnetic field.

Finally, we get the following formula for the *cyclotron frequency*

$$\omega_c = \frac{eH}{cm_c}, \text{ where } m_c(\varepsilon, p_z) = \frac{1}{2\pi} \left[\frac{\partial S}{\partial \varepsilon} \right]_{p_z}$$

is the *cyclotron effective mass*. For a free electron $\varepsilon = (p_z^2 + \mathbf{p}_\perp^2)/2m_0$, and

$$S(p_z) = \pi \mathbf{p}_\perp^2 = 2\pi m_0 \varepsilon - \pi p_z^2, \text{ and } m_c = m_0.$$

Thus, the cyclotron mass appears constant. The same holds for all the quasiparticles with isotropic and quadratic spectrum $\varepsilon(\mathbf{p})$. Returning to real space, one can rewrite the equation of motion as

$$d\mathbf{p} = -\frac{e}{c} [\mathbf{dr} \times \mathbf{H}].$$

We see that the projection of the motion in the real space on the plane normal to \mathbf{H} can be obtained by the substitution

$$x \rightarrow \frac{cH}{e} p_y, \quad y \rightarrow \frac{cH}{e} p_x.$$

Also remains the motion along \mathbf{z} -axis with the velocity $v_z = \partial \varepsilon / \partial z$.

Now we discuss one very useful trick to calculate the properties of electrons in a magnetic field. Namely, let us introduce the *time* of the motion along the orbit as

$$t_1 = \frac{c}{eH} \int \frac{dp}{v_\perp}$$

One should keep in mind that it is not the real time but some function of the point in the \mathbf{p} -space. We get

$$\frac{2}{(2\pi\hbar)^3} \int dp_x dp_y dp_z = \frac{2}{(2\pi\hbar)^3} \frac{eH}{c} \int dp_z d\varepsilon dt_1$$

Here we have used the relation (3.47). This trick will be extensively used later.

Cyclotron resonance.

Now we discuss one of the ways to measure the characteristics of electron spectra. Let us assume that the electron with effective mass m moves in a weak a.c. electric field

$$\mathbf{E} = \mathbf{E}_0 \exp(-i\omega t), \quad \mathbf{E}_0 \parallel \hat{\mathbf{x}}$$

and in a constant magnetic field $\mathbf{H} \parallel \hat{\mathbf{z}}$. We get

$$\begin{aligned} -i\omega mv_x &= -eE_x - \frac{e}{c}v_y H, \\ -i\omega mv_y &= \frac{e}{c}v_x H. \end{aligned}$$

To solve this set it is convenient to introduce the complex velocity $v \equiv v_x + iv_y$ and get

$$i(\omega - \omega_c)v = eE_x.$$

We see that at $\omega \rightarrow \omega_c$ the amplitude of velocity increases. It means that electron absorbs the energy from the electric field. To get more adequate theory of the *cyclotron resonance* one needs to take into account relaxation (we will come back to this problem later). The cyclotron resonance is a very useful tool to determine the cyclotron effective mass.

3.7.2 Quantum Mechanics of Bloch Electron

An electron with isotropic quadratic spectrum

We start our considerations with the simplest case of where the periodic potential can be taken into account by the effective mass approximation (we will denote it as m). We also use the Landau gauge (3.45). To get the SE² one can replace \mathbf{p} in the classical Hamilton function with the operator $\hat{\mathbf{p}} = -i\hbar\nabla$

$$-\frac{\hbar^2}{2m} \left[\frac{\partial^2 \psi}{\partial x^2} + \left(\frac{\partial}{\partial y} + \frac{ieHx}{c} \right)^2 \psi + \frac{\partial^2 \psi}{\partial z^2} \right] = \varepsilon \psi. \quad (3.48)$$

It is convenient to search the solution as

$$\psi(\mathbf{r}) = \varphi(x) e^{i(k_y y + k_z z)}.$$

²We ignore for a while the electron spin.

Substituting this expression into (3.48) we get the equation for $\varphi(x)$ (Check!)

$$-\frac{\hbar^2}{2m} \frac{\partial^2 \varphi}{\partial x^2} + \frac{1}{2} m \omega_c^2 (x - x_0)^2 \varphi = \varepsilon_1 \varphi$$

where ω_c is the cyclotron frequency,

$$x_0 = -a_H^2 k_y, \quad a_H = \sqrt{\frac{c\hbar}{eH}}, \quad \varepsilon_1 = \varepsilon - \frac{\hbar^2 k_z^2}{2m}.$$

The quantity a_H is often called the magnetic length or Landau length. Finally we came to the SE for a harmonic oscillator and we can write down both the energies and wave functions:

$$\varepsilon_1 = \varepsilon_N \equiv \hbar \omega_c (N + 1/2), \quad (3.49)$$

the so-called Landau levels,

$$\varphi(x) = \frac{1}{\sqrt{a_H}} \exp \left[-\frac{1}{2} \left(\frac{x - x_0}{a_H} \right)^2 \right] H_N \left(\frac{x - x_0}{a_H} \right) \quad (3.50)$$

where H_N is the Hermite polynomial. We see that the electron states in a magnetic field could be specified by the set of quantum numbers $\alpha = N, k_y, k_z$, the energy levels

$$\varepsilon_\alpha = \varepsilon_N + \frac{\hbar^2 k_z^2}{2m} \quad (3.51)$$

being dependent only on N, k_z .

One can ask: why the co-ordinates x and y are not equivalent? The reason is that the wave functions (3.50) correspond to the energy independent of k_y . Consequently, any function of the type

$$\sum_{k_y} C(k_y) \psi_{N,k_y,k_z}$$

corresponds to the same energy and one can chose convenient linear combinations to get correct asymptotic behavior.

General case.

The spectrum (3.51) has a very simple form for the case of any isotropic quadratic spectrum. Nevertheless it is possible to obtain important results even in the case of very complicated FS if we are interested in the Landau levels for large quantum numbers N . In this case one can expect that one can use the *Bohr-Sommerfeld* quantization procedure. Indeed, in the presence of magnetic field, as we have seen the *kinematic* momentum operator is

$$\mathbf{P} = -i\hbar \nabla + \frac{e}{c} \mathbf{A}.$$

Consequently,

$$P_x = -i\hbar\partial/\partial x, \quad P_y = -i\hbar\partial/\partial y + (e/c)Hx,$$

the commutator being

$$[P_x, P_y] = i\pi\hbar\frac{eH}{c}.$$

One can see that the co-ordinate

$$Y = -\frac{c}{eH}P_x$$

is canonically conjugated to P_y ,

$$[P_y, Y] = i\hbar.$$

Now we can directly apply the quantization rule

$$\left| \oint P_y dY \right| = \frac{c}{eH} \left| \oint P_y dP_x \right| = \frac{cS}{eH} = 2\pi\hbar[N + \gamma(N)].$$

Here $\gamma(N)$ is a slow function of N , $0 < \gamma < 1$. It is easy to show that the distance between the levels is just $\hbar\omega_c$. Indeed, neglecting $\gamma(N) - \gamma(N-1)$ we get

$$\frac{c}{eH} \frac{\partial S(\varepsilon)}{\partial \varepsilon} \Delta\varepsilon = 2\pi\hbar.$$

3.8 Second Quantization of Bosons and Electrons

Now we briefly discuss the way to describe many-electron states by the occupation numbers. Such a procedure was introduced for phonons which are *Bose* particles and we first generalize that procedure.

In general case, the total wave function of bosons is symmetric in replacement of the particles. Thus it can be expressed as a symmetric product of individual wave functions

$$\Phi_{N_1 N_2 \dots} = \left(\frac{N_1! N_2! \dots}{N!} \right)^{1/2} \sum_P \varphi_{p_1}(\xi_1) \varphi_{p_2}(\xi_2) \dots \varphi_{p_N}(\xi_N), \quad (3.52)$$

where p_i label the states, φ_{p_i} are while the sum is calculated over all the permutations of $\{p_i\}$. The coefficient is introduced to make the total function normalized:

$$\int |\Phi|^2 \prod_i d\xi_i = 1.$$

The main idea is to consider $\Phi_{N_1 N_2 \dots}$ as a function of the *occupation numbers* N_i . Assume that we have an arbitrary one-particle symmetric operator

$$F^{(1)} = \sum_a f_a^{(1)} \quad (3.53)$$

where $f_a^{(1)}$ acts only upon the functions of ξ_a . It is clear that acting upon $\Phi_{N_1 N_2 \dots}$ it changes the state of only one particle. So it is reasonable to introduce the operators with matrix elements

$$(b_i)_{N_i}^{N_i-1} = \sqrt{N_i}, \quad (b_i^\dagger)_{N_i-1}^{N_i} = [(b_i)_{N_i}^{N_i-1}]^* = \sqrt{N_i} \quad (3.54)$$

It is just annihilation and creation operators introduced earlier. The operator (3.53) can be expressed in terms of the creation-annihilation operators as

$$F^{(1)} = \sum_{ik} f_{ik}^{(1)} b_i^\dagger b_k \quad (3.55)$$

where

$$f_{ik}^{(1)} = \int \varphi_k^*(\xi_1) f^{(1)}(\xi_1) \varphi_k(\xi) d\xi_1. \quad (3.56)$$

One can easily prove this relation comparing both diagonal and off-diagonal matrix elements of the operators. A 2-particle symmetric operator

$$F^{(2)} = \sum_{ab} f_{ab}^{(2)} \quad (3.57)$$

where $f_{ab}^{(2)}$ acts upon the functions of the variables ξ_a and ξ_b can be expressed as

$$F^{(2)} = \sum_{iklm} f_{lm}^{ik} b_i^\dagger b_k^\dagger b_l b_m \quad (3.58)$$

where

$$f_{lm}^{ik} = \int \varphi_i^*(\xi_1) \varphi_k^*(\xi_2) f^{(2)}(\xi_1, \xi_2) \varphi_l(\xi_1) \varphi_m(\xi_2) d\xi_1 d\xi_2. \quad (3.59)$$

Now we turn to the Fermi statistics to describe electrons. According to the Pauli principle, the total wave function should be *anti-symmetric* over all the variables. So the occupation numbers could be 0 or 1. In this case we get instead of (3.52)

$$\Phi_{N_1 N_2 \dots} = \frac{1}{\sqrt{N!}} \sum_P (-1)^P \varphi_{p_1}(\xi_1) \varphi_{p_2}(\xi_2) \dots \varphi_{p_N}(\xi_N) \quad (3.60)$$

where all the numbers p_1, p_2, \dots, p_N are *different*. The symbol $(-1)^P$ shows that odd and even permutations enter the expression (3.60) with opposite signs (we take the sign '+' for the term with $p_1 < p_2 < \dots < p_N$). Note that the expression (3.60) can be expressed as the determinant of the matrix with the elements $M_{ik} = (N!)^{-1/2} \varphi_{p_i}(\xi_k)$ which is often called the *Slater determinant*.

The diagonal matrix elements of the operator $F^{(1)}$ are

$$\bar{F}^{(1)} = \sum_i f_{ii}^{(1)} N_i \quad (3.61)$$

just as for the Bose particles. But off-diagonal elements are

$$(F^{(1)})_{0_i 1_k}^{1_i 0_k} = \pm f_{ik}^{(1)} \quad (3.62)$$

where the sign is determined by the parity of the total number of particles in the states between the i and k ones.³ Consequently, for Fermi particles it is convenient to introduce the annihilation and creation operators as

$$(a_i)_1^0 = (a_i^\dagger)_0^1 = (-1)^{\sum_{l=1}^{i-1} N_l}. \quad (3.63)$$

We immediately get (Check!) the commutation rules for the Fermi operators:

$$\begin{aligned} \left\{ a_i, a_k^\dagger \right\} &\equiv a_i a_k^\dagger + a_i^\dagger a_k = \delta_{ik}, \\ \{a_i, a_k\} &= \left\{ a_i^\dagger, a_k^\dagger \right\} = 0. \end{aligned} \quad (3.64)$$

The product of Fermi operators are

$$a_i^\dagger a_i = N_i, \quad a_i a_i^\dagger = 1 - N_i. \quad (3.65)$$

One can express all the operators for Fermi particles exactly in the same way as the Bose ones, Eqs. (3.55), (3.58).

3.9 Problems

- 3.1.** Derive Eq. (3.15).
- 3.2.** Prove the orthogonality of the Wannier functions.
- 3.3.** Derive expression (3.16).
- 3.4.** Derive expression (3.24).
- 3.5.** Prove the identity (3.39).
- 3.6.** Prove the formula (3.41).

³Note that for Bose particles similar matrix elements are $(F^{(1)})_{N_{i-1}, N_k}^{N_i, N_k-1} = f_{ik}^{(1)} \sqrt{N_i N_k}$.

Part II

Normal metals and semiconductors

Chapter 4

Statistics and Thermodynamics of Phonons and Electrons

In this Chapter we discuss thermodynamics of crystal lattice.

4.1 Specific Heat of Crystal Lattice

From the classical statistical physics, the average kinetic energy per degree of freedom is

$$\bar{\varepsilon}_k = \frac{1}{2}k_B T,$$

the total energy being

$$\bar{\varepsilon} = \bar{\varepsilon}_{\text{pot}} + \bar{\varepsilon}_{\text{kin}} = 2\bar{\varepsilon}_{\text{kin}}.$$

As a result, the total energy is

$$\mathcal{E} = 3N_0 \cdot \bar{\varepsilon}_{\text{kin}} = 3RT,$$

where R is the Rydberg constant while N_0 is the Avogadro one. As a result, the specific heat is

$$c_V = 3R = 5.96 \text{ kal/K} \cdot \text{mole}. \quad (4.1)$$

This relation is violated at low temperatures as far as the temperature becomes less than the so-called *Debye* temperature (which is for most of solids is within the interval 100-400 K), namely it decreases with the temperature decrease. To understand this behavior one should apply quantum mechanics.

Let us calculate the average electron energy from the point of view of quantum mechanics. We have seen that normal vibrations can be described as quasiparticles with the energy

$$\varepsilon_N = \hbar\omega(N + 1/2),$$

where we have omitted the indices \mathbf{q} and j which characterize a given oscillator. The probability to find the oscillator in the state N is

$$w_N = \frac{e^{-\varepsilon_N/k_B T}}{\sum_N e^{-\varepsilon_N/k_B T}}.$$

The average energy is

$$\bar{\varepsilon} = \frac{\sum_N \varepsilon_N e^{-\varepsilon_N/k_B T}}{\sum_N e^{-\varepsilon_N/k_B T}}.$$

To demonstrate the way to calculate the average energy we introduce the *partition function* as

$$Z = \sum_{N=0} e^{-\varepsilon_N/k_B T}. \quad (4.2)$$

We get

$$\bar{\varepsilon} = -d \ln Z / d\beta, \quad \beta = 1/k_B T.$$

From the definition (see *Problem 4.1*)

$$Z = \frac{e^{-\hbar\omega/2k_B T}}{1 - e^{-\hbar\omega/k_B T}}.$$

Making use of this formula we get

$$\bar{\varepsilon} = \frac{\hbar\omega}{2} + \hbar\omega N(\omega), \quad N(\omega) = \frac{1}{e^{\hbar\omega/k_B T} - 1} \quad (4.3)$$

where $N(\omega)$ is the *Planck function*. The first item is energy-independent while the second one is just the average energy of bosons with zero chemical potential. In general the Bose distribution has the form

$$\frac{1}{\exp\left[\frac{\varepsilon - \zeta}{k_B T}\right] - 1}$$

where ζ is *chemical potential* which is equal to the derivative of the free energy:

$$\left(\frac{\partial \mathcal{F}}{\partial N}\right)_{T,V} = \zeta.$$

Usually the chemical potential is determined by the conservation of the particles' number.

The number of phonons is not conserved: they can be created or annihilated in course of interactions. Therefore their should be determined from the condition of *equilibrium*, i. e. from the request of minimum of free energy. As a result, for phonons $\zeta = 0$. The Planck function determines the *equilibrium* number of phonons with a given frequency. Such a picture allows one to consider the phonons as *elementary excitations* over the zero-point vibration energy

$$\mathcal{E}_0 = (1/2) \sum_{j\mathbf{q}} \hbar\omega_j(\mathbf{q}).$$

To get the total energy one should sum (4.3) over all the frequencies and vibration branches. It is convenient to express this sum through the DOS according to the general definition

$$g(\omega) = \sum_{j,\mathbf{q}} \delta [\omega - \omega_j(\mathbf{q})]. \quad (4.4)$$

We get

$$E = \int_0^\infty g(\omega) \hbar\omega N(\omega) d\omega.$$

In the first approximation let us assume that the frequencies of the optical branches are \mathbf{q} -independent and equal to ω_{j0} . Consequently, the summation is just the multiplication by the Planck function $N(\omega_{j0})$. For acoustic modes we use the Debye model (see Section 2.2.4). Introducing the average sound velocity s_0 as

$$\frac{1}{s_0^3} = \frac{1}{3} \left(\frac{1}{s_l^3} + \frac{2}{s_t^3} \right)$$

we get the following contribution of acoustic modes

$$\mathcal{E}_{ac} = \frac{3\mathcal{V}\hbar}{2\pi^3 s_0^3} \int_0^{\omega_D} d\omega \frac{\omega^3}{e^{\hbar\omega/k_B T} - 1}$$

where the so-called Debye frequency is determined from the condition of the total number of modes to be equal to $3N$ for all acoustic branches,

$$3N = \int_0^{\omega_D} g(\omega) d\omega.$$

From this equation

$$\omega_D = s_0 \left(\frac{6\pi^2}{\mathcal{V}_0} \right)^{1/3}, \quad q_D = \frac{\omega_D}{s_0}$$

where V_0 is the cell volume. The order-of-magnitude estimate for the maximal wave vector q_D is π/a . So according to the so-called *Debye model* all the values of \mathbf{q} are confined in a sphere with the radius q_D . Usually, the *Debye temperature* is introduced as

$$\Theta = \frac{\hbar\omega_D}{k_B} = \frac{\hbar s_0}{k_B} \left(\frac{6\pi^2}{\mathcal{V}_0} \right)^{1/3}.$$

The typical value of this temperature can be obtained from the rough estimate $a = 10^{-8}$ cm, $s_0 = 10^5$ cm/s. We get $\omega_D = 10^{13}$ s⁻¹, $\Theta = 100$ K. It is conventional also to introduce the temperatures corresponding to optical branches as

$$\Theta_j = \frac{\hbar\omega_{j0}}{k_B}.$$

These energies are of the order of $10^2 - 10^3$ K. Finally, we get the following expression for the internal energy

$$\mathcal{E} = \mathcal{E}_0 + Nk_B T \left[3\mathcal{D}\left(\frac{\Theta}{T}\right) + \sum_{j=4}^{3s} \frac{\Theta_j/T}{e^{\Theta_j/T} - 1} \right] \quad (4.5)$$

where the *Debye function* $\mathcal{D}(z)$ is

$$\mathcal{D}(z) = \frac{3}{z^3} \int_0^z \frac{x^3 dx}{e^x - 1}. \quad (4.6)$$

At high temperatures, $T \gg \Theta_j$ (and, consequently, $T \gg \Theta$) we get $z \ll 1$ in Eq. (4.6) and then expand the integrand in powers of x . We see that $\mathcal{D}(0) = 1$. The item under the sum sign in Eq (4.5) are equal to 1, and we get for the sum $3s - 3$. consequently, we get the classical expression

$$\mathcal{E} = \mathcal{E}_0 + 3sNk_B T$$

that leads to the classical expression (4.1) for the specific heat. At low temperatures we immediately see that optical modes give exponentially small contributions and we can discard them. At the same time, we can replace the upper limit of the integral in (4.6) by infinity. Taking into account that

$$\int_0^\infty \frac{x^3 dx}{e^x - 1} = \frac{\pi^4}{15}$$

we get

$$\mathcal{E} = \mathcal{E}_0 + \frac{\pi^2 \mathcal{V} (k_B T)^4}{10 \hbar^3 s_0^3}$$

that leads to the following expression for the specific heat

$$c_V = \frac{12\pi^4 k_B}{5} \left(\frac{T}{\Theta} \right)^3.$$

The Debye model is very good for low temperatures where only long wave acoustic modes are excited. The acoustic contribution to the specific heat can be expressed through the derivative of the Debye function. We have

$$\frac{c_{ac}}{3k_B N} = 3 \left(\frac{T}{\Theta} \right)^3 \int_0^{\Theta/T} \frac{x^4 dx}{e^x - 1}.$$

This function is shown in Fig. 4.1 One can see that really the border between the classical and quantum region corresponds to $T \leq \Theta/3$ rather than to $T \leq \Theta$. The physical reason is strong frequency dependence of phonon DOS. In real life, DOS behavior is much more complicated because of the real band structure effects. The experimental DOS for NaCl is shown in Fig. 4.2 (upper panel), the dash curve showing Debye approximation. Usually, people still fit the results on specific heat by Debye approximation but assume that the Debye temperature, Θ , is temperature dependent. The dependence $\Theta(T)$ is shown in Fig. 4.2 (lower panel)

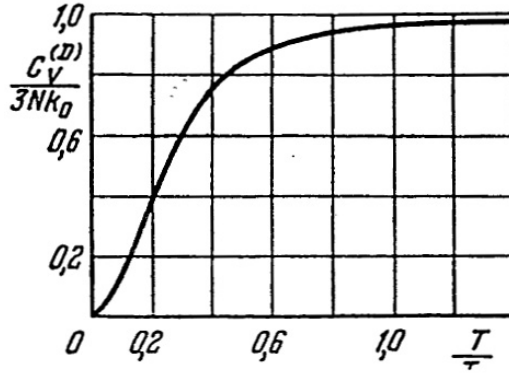


Figure 4.1: Temperature dependence of acoustic contribution to the specific heat.

4.2 Statistics of Electrons in Solids

Now we turn to the electron system in thermodynamic equilibrium. As we have seen, the electron state for a given energy band is characterized by the quantum number \mathbf{k} , the average number of electrons in this state being

$$f_0(\varepsilon_{\mathbf{k}}) = \frac{1}{\exp\left(\frac{\varepsilon_{\mathbf{k}} - \zeta}{k_B T}\right) + 1}. \quad (4.7)$$

The function (4.7) is called the *Fermi-Dirac function*. The *chemical potential* ζ is determined by the normalization condition

$$N = \sum_{\mathbf{k}} \frac{1}{\exp\left(\frac{\varepsilon_{\mathbf{k}} - \zeta}{k_B T}\right) + 1}. \quad (4.8)$$

The summation here should be done also over spin indices. The equation (4.8) defines the dependence of the chemical potential ζ on the electron density $n = N/\mathcal{V}$. It is also convenient to introduce the density of electron states with the formula similar to Eq. (4.4)

$$g(\varepsilon) = 2 \sum_{\mathbf{k}} \delta(\varepsilon - \varepsilon_{\mathbf{k}}) \quad (4.9)$$

where we have taken into account spin degeneracy. We get

$$n = \int_0^{\infty} g(\varepsilon) f_0(\varepsilon) d\varepsilon. \quad (4.10)$$

For the quadratic spectrum with the effective mass m we have (see *Problem 4.2*)

$$g(\varepsilon) = \frac{\sqrt{2}}{\pi^2} \frac{m^{3/2}}{\hbar^3} \sqrt{\varepsilon}. \quad (4.11)$$

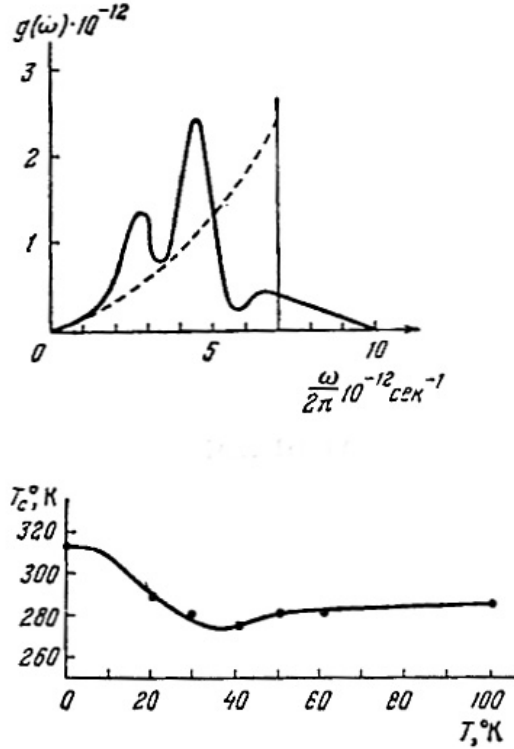


Figure 4.2: DOS and effective Debye temperature for NaCl .

Inserting this formula to the normalization condition (4.10) and introducing the dimensionless chemical potential $\zeta^* = \zeta/k_B T$ we get the following equation for ζ^*

$$n = \frac{\sqrt{2}}{\pi^2} \frac{(mk_B T)^{3/2}}{\hbar^3} \mathcal{F}_{1/2}(\zeta^*)$$

where $\mathcal{F}_{1/2}(z)$ is a particular case of the *Fermi integrals*

$$\mathcal{F}_n(z) = \int_0^\infty \frac{x^n dx}{e^{x-z} + 1}.$$

Degenerated Electron Gas

Now we discuss the important limiting cases. The first one is the case for good metals or highly doped semiconductors in which the density of conduction electrons is large. The large density of conduction electrons means that $\zeta^* \gg 1$. That leads to the following approximate presentation for the Fermi function

$$f_0(\varepsilon) = \Theta(\zeta - \varepsilon)$$

where

$$\Theta(x) = \begin{cases} 1, & \text{if } x > 0, \\ 0, & \text{if } x < 0 \end{cases}$$

is the Heaviside unit step function. In this approximation we easily get

$$\zeta_0 = \frac{\hbar^2 k_F^2}{2m} = \frac{\hbar^2}{2m} (3\pi^2 n)^{2/3}.$$

This quantity is often called the *Fermi level* because it is just the border between the full and empty states. We will also use this word and denote it as ϵ_F . To get temperature dependent corrections one should calculate the integral in Eq. (4.10) more carefully. One obtains (see *Problem 4.3*)

$$\zeta = \epsilon_F \left[1 - \frac{\pi^2}{12} \left(\frac{k_{BT}}{\epsilon_F} \right)^2 \right].$$

Now we can check when our approximation is really good. To do it let us request that the second item in the brackets to be small. We get

$$\frac{\epsilon_F}{k_{BT}} = \frac{\hbar^2 (3\pi^2 n)^{2/3}}{2mk_{BT}} \gg 1. \quad (4.12)$$

So we see that the gas is degenerate at big enough electron density and small effective mass. Note that the criterion has the *exponential* character and inequality (4.12) can be not too strong (usually 5-7 is enough). In a typical metal $n \approx 10^{22} \text{ cm}^{-3}$, $m \approx 10^{-27} \text{ g}$, and at room temperature $\frac{\epsilon_F}{k_{BT}} \approx 10^2$.

Non-Degenerate Electron Gas

Now we discuss the situation when the electron density in the conduction band is not very high and the electrons are non-degenerate. It means that $\zeta < 0$, $\exp(-\zeta^*) \gg 1$. In this case the Fermi distribution tends to the *Maxwell-Boltzmann* distribution

$$f_0(\varepsilon) \approx e^{\zeta^*} e^{-\varepsilon/k_{BT}}$$

where

$$\begin{aligned} \mu^* &= \ln \left[\frac{4\pi^3 \hbar^3 n}{(2\pi m k_{BT})^{3/2}} \right], \\ e^{\zeta^*} &= \frac{4\pi^3 \hbar^3 n}{(2\pi m k_{BT})^{3/2}}. \end{aligned} \quad (4.13)$$

We see that the chemical potential of non degenerate electron gas is strongly temperature dependent. The degeneracy for room temperature is intermediate at $n \approx 10^{19} \text{ cm}^{-3}$.

These formulas are not very interesting in typical semiconductors because electrons are taken from impurities which can be partly ionized. So the dependence n vs. T remains unknown. To get insight into the problem let us consider the band scheme of a typical semiconductor with one donor level ε_D and one accepter one ε_A , Fig. 4.3 (the origin of energies is the bottom of the conduction band). The most important feature is that in

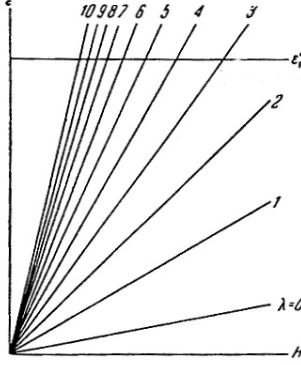


Figure 4.3: Band scheme of a typical semiconductor.

such situation we have both electrons (in the conduction band) and holes (in the valence band). The occupation factor for holes is

$$f'_0(\varepsilon) = 1 - f_0(\varepsilon) = \frac{1}{e^{\frac{\zeta - \varepsilon}{k_B T}} + 1}.$$

It is natural to call the function $f'(\varepsilon)$ as the Fermi function of holes. According to our prescription for energies, the electron energy in the conduction band is $\varepsilon = \hbar^2 k^2 / 2m_n$, at the donor level $\varepsilon = -\varepsilon_D$, at the accepter level $\varepsilon = -\varepsilon_A$, while in the valence band $\varepsilon = -\varepsilon_G - \varepsilon'$ where ε_G is the width of the forbidden gap while $\varepsilon' = \hbar^2 k'^2 / 2m_p$. If we also introduce the *hole chemical potential*, $\zeta' = -\varepsilon_G - \zeta$ we come to exactly the same form for the hole Fermi function as for electrons with the replacement $\varepsilon \rightarrow \varepsilon'$, $\zeta \rightarrow \zeta'$. To get the position of the chemical potential now we should apply the neutrality condition

$$\text{number of electrons} = \text{number of holes}$$

which reads

$$\int_{c.b.} g_n(\varepsilon) f_0(\varepsilon) d\varepsilon + \sum_A \frac{1}{e^{\frac{-\varepsilon_A - \zeta}{k_B T} + 1}} = \int_{v.b.} g_p(\varepsilon') f_0(\varepsilon') d\varepsilon' + \sum_D \frac{1}{e^{\frac{\varepsilon_D + \zeta}{k_B T} + 1}}.$$

This equation is strongly simplified if both electrons and holes obey the Boltzmann statistics. Denoting $A = \exp(\zeta^*) \ll 1$ and assuming that $\exp(\zeta^* + \varepsilon_G/k_B T) \gg 1$ we get

$$\nu_n A + \frac{n_A}{\frac{1}{A} \exp\left(-\frac{\varepsilon_A}{k_B T}\right) + 1} = \nu_p A^{-1} e^{-\frac{\varepsilon_G}{k_B T}} + \frac{n_D}{A \exp\left(+\frac{\varepsilon_D}{k_B T}\right) + 1} \quad (4.14)$$

where we have introduced

$$\nu_{n,p} = \frac{(2\pi m_{n,p} k_B T)^{3/2}}{4\pi^3 \hbar^3}.$$

Even now we have a rather complicated situation which depends on the relation between the energies and the temperature. In the following we analyze few most important cases.

Intrinsic semiconductor

It is the simplest case where there is no both donors and acceptors. From the Eq. (4.14) we have

$$\begin{aligned} A &= \left(\frac{m_p}{m_n} \right)^{3/4} \exp \left(-\frac{\varepsilon_G}{2k_B T} \right), \\ \zeta &= -\frac{\varepsilon_G}{2} + \frac{3}{4} k_B T \ln \left(\frac{m_p}{m_n} \right). \end{aligned} \quad (4.15)$$

We see that the chemical potential in an intrinsic semiconductor is close to the middle of the forbidden gap. Concentrations of the electrons and holes are the same

$$n_i = n_T \exp \left(-\frac{\varepsilon_G}{2k_B T} \right), \quad n_T = \sqrt{\nu_n \nu_p}.$$

The concentration n_T for the room temperature and the free electron mass is $2.44 \cdot 10^{19}$ cm⁻³, it scales as $(m_n m_p)^{3/4} T^{3/2}$.

Extrinsic semiconductor

Let us assume that only donors are present and $\varepsilon_G \gg \varepsilon_D$. In this case we get from Eq. (4.14)

$$\nu_n A \left(A e^{\frac{\varepsilon_D}{k_B T}} + 1 \right) = n_D.$$

At very low temperatures the first term is the most important one, and

$$A = \sqrt{\frac{n_D}{\nu_n}} e^{-\frac{\varepsilon_D}{2k_B T}}.$$

We see that the chemical potential is near the middle of the distance between the donor level and the bottom of the conduction band, the concentration in the conduction band being

$$n_n \approx \frac{n_D}{A} e^{-\frac{\varepsilon_D}{k_B T}} = \sqrt{\nu_n n_D} e^{-\frac{\varepsilon_D}{2k_B T}}.$$

At high temperatures we get

$$A = \frac{n_D}{\nu_n}, \quad n_n \approx n_D.$$

The result is clear enough: at high temperature all the donors are ionized while at low temperatures electrons “freeze-out” into the donor states. The situation in accepter semiconductor is just the mirror one.

4.3 Specific Heat of the Electron System

Now we calculate the specific heat of the electron sub-system. Just as in the case of phonons, we have

$$\mathcal{E} = \int_0^\infty \varepsilon g(\varepsilon) f_0(\varepsilon) d\varepsilon. \quad (4.16)$$

Making use of the *Problem 4.3* we can write the integral in the universal form

$$I = \int_0^\infty \chi(\varepsilon) f(\varepsilon) d\varepsilon = \int_0^\infty \varphi(\varepsilon) \left(-\frac{\partial f_0}{\partial \varepsilon} \right) d\varepsilon \quad (4.17)$$

with

$$\varphi(\varepsilon) = \int_0^\varepsilon \chi(x) dx.$$

In our case,

$$\varphi(\varepsilon) = \frac{(2m)^{3/2}}{5\pi^2 \hbar^3} \varepsilon^{5/2}.$$

Then exactly as in the *Problem 4.3* we obtain

$$\mathcal{E} = \frac{(2m)^{3/2}}{5\pi^2 \hbar^3} \zeta^{5/2} \left[1 - \frac{5\pi^2}{8} \left(\frac{k_B T}{\epsilon_F} \right)^2 \right].$$

According to the same problem, the chemical potential ζ is also temperature-dependent, and

$$\zeta^{5/2} = \epsilon_F^{5/2} \left[1 - \frac{5\pi^2}{24} \left(\frac{k_B T}{\epsilon_F} \right)^2 \right].$$

Making use of this equation, we get the final result

$$\mathcal{E} = \frac{(2m)^{3/2}}{5\pi^2 \hbar^3} \epsilon_F^{5/2} \left[1 + \frac{5\pi^2}{12} \left(\frac{k_B T}{\epsilon_F} \right)^2 \right].$$

Finally, we get

$$c_V = \frac{\sqrt{2}}{3} \frac{m^{3/2}}{\hbar^3} \sqrt{\epsilon_F k_B^2 T}. \quad (4.18)$$

We see that $c_V \propto T$, it goes to zero at $T \rightarrow 0$ (the *Nernst theorem*). The physical meaning of Eq. (4.18) is very simple - only the electrons in the narrow layer $k_B T$ could be excited; their number being $g(\epsilon_F)k_B T$ while the contribution of each one to the specific heat being k_B .

It is interesting to compare electron and phonon contributions to specific heat. At room temperature and $\epsilon_F \approx 1$ eV we get that the electron contribution is only few percents in comparison with the phonon one. But *it is not the case at low temperatures* where the phonon contribution goes like T^3 while the electron one is $\propto T$.

For the Boltzmann statistics one can substitute the Boltzmann distribution function into Eq.(4.16). The result is (see *Problem 4.4*)

$$c_V = (3/2)n k_B.$$

4.4 Magnetic Properties of Electron Gas.

Now we will discuss the basic magnetic properties of electron gas. We start from the recalling of the main thermodynamic relations for magnetics.

Basic thermodynamic relations.

In a magnetic field \mathbf{H} a sample acquires the magnetic moment \mathbf{M} . For a volume dV one can introduce *magnetization*

$$d\mathbf{M} = \mathbf{M}(\mathbf{H}) dV.$$

The derivative

$$\chi = \left(\frac{dM}{dH} \right)_{H=0}$$

is called magnetic susceptibility. It is a dimensionless quantity. According to the thermodynamics, the change of the internal energy is

$$d\mathcal{E} = dQ + dA$$

where $dQ = T dS$ is the transferred heat (S is the entropy) while dA is the work with the system, $dA = -\mathbf{M} d\mathbf{H}$. Finally

$$d\mathcal{E} = T dS - M dH.$$

Consequently, for the *free energy* $\mathcal{F} = \mathcal{E} - TS$ we get

$$d\mathcal{F} = -S dT - M dH,$$

and

$$S = - \left(\frac{\partial \mathcal{F}}{\partial T} \right)_H, \quad M = - \left(\frac{\partial \mathcal{F}}{\partial H} \right)_T, \quad \chi = - \left(\frac{\partial^2 \mathcal{F}}{\partial H^2} \right)_{T;H=0}.$$

So, the main quantity is the free energy.

Magnetic susceptibility of a molecular system.

Classical theory.

Now suppose that the gas consists of the molecules with magnetic momenta \mathbf{l}_A (we reproduce the *Langevin theory* of a paramagnet gas). As it is known, the average magnetic moment in this model is

$$\langle l \rangle = l_A \mathcal{L} \left(\frac{l_A H}{k_B T} \right), \quad \mathcal{L}(x) = \coth(x) - \frac{1}{x} \quad (4.19)$$

is the *Langevin function* (see *Problem 4.4*). At low fields or at high temperatures one can expand this function as $\mathcal{L}(x) \approx x/3$ and get

$$M = n \langle l \rangle = \chi H, \quad \chi = \frac{l_A^2 n}{3 k_B T}.$$

Note that we have reproduced the *Curie law* $\chi \propto 1/T$, which is pure classical.

Quantum theory.

According to the quantum mechanics, the angles between the magnetic moment and the magnetic field can take only discrete values. To take into account quantum effects one should recall that for an electron in the atomic stationary state the orbital momentum projection is $\mathcal{L}_z = \hbar l$ where l is the *magnetic quantum number*, the magnetic momentum being $M_z = \mu_B l$ where

$$\mu_B = \frac{e\hbar}{2mc} = 0.927 \cdot 10^{-20} \text{ erg/Oe}$$

is the *Bohr magneton*. A free electron also posses the spin momentum $s_z = \pm \hbar/2$ and magnetic momentum μ_B (note that the ratio M_z/L_z for a free electron is twice greater than for the orbital motion).

To get the total momentum, one should sum the orbital and spin momenta *in a vector form*. As a result, the magnetic moment is not parallel to the mechanical one. We do not come here deeply into quantum mechanics of a spin. Let us just mention that the result is that there is a quantum number j for a total mechanical momentum which is equal to $\hbar\sqrt{j(j+1)}$, the magnetic momentum being

$$\mu_j = \mu_B g_L j, \quad g_L = 1 + \frac{j(j+1) + s(s+1) - l(l+1)}{2j(j+1)}.$$

Here g_L is the so-called *Lande factor*, l is the orbital quantum number (the total orbital moment being $\hbar\sqrt{l(l+1)}$), while $s = \pm 1/2$ is the spin quantum number. As a result, there are $2j+1$ discrete orientations with the angles ϑ_m determined by the condition $\cos \vartheta_m = m/j$ where magnetic quantum number m takes the values $j, j-1, \dots, -j+1, -j$. The energy in magnetic field is determined as

$$-\mu_j H \cos \vartheta_m = -\mu_B H g_L m$$

The average magnetic moment could be calculated just as in the *Problem 4.4* with the only difference that we have discrete sums instead of integrals

$$\langle \mu \rangle = \mu_B g_L \frac{\partial}{\partial \alpha} \left[\ln \left(\sum_{m=-j}^j e^{\alpha m} \right) \right] \quad (4.20)$$

where $\alpha = \mu_B g_L H / k_B T$. In weak field $\alpha \ll 1$, and

$$\chi = \frac{\mu_{eff}^2 n}{3k_B T}, \quad \mu_{eff} = \mu_B g_L \sqrt{j(j+1)}. \quad (4.21)$$

Paramagnetism of Free Electrons (Pauli Paramagnetism).

Now we are prepared to discuss the magnetic susceptibility of a gas of near free electrons. In this case the orbital moment $l = 0$, $j = s = 1/2$ and $g_L = 2$. Consequently one could

expect quite big magnetic susceptibility according to Eq. (4.21). *This statement strongly contradicts with the experiment* - in fact the susceptibility is small. This very important problem was solved by *Pauli* in 1927 and it was just the beginning of quantum theory of metals. The key idea is that the electrons have Fermi statistics and one should calculate the average in Eq. (4.20) taking into account the Pauli principle.

To make such a calculation let us recall that the electron energy in a magnetic field depends on the momentum orientation

$$\varepsilon_{\pm} = \varepsilon \mp \mu_B H.$$

Consequently

$$M = M_+ - M_- = \frac{\mu_B}{2} \int [f_0(\varepsilon_+) - f_0(\varepsilon_-)] g(\varepsilon) d\varepsilon.$$

(the factor 1/2 is due to the fact that we have introduced the DOS $g(\varepsilon)$ including spin factor 2). For small magnetic fields we can expand the square brackets and get

$$\chi = \mu_B^2 \int \left(-\frac{\partial f_0(\varepsilon)}{\partial \varepsilon} \right) g(\varepsilon) d\varepsilon.$$

To get the final formula one should take into account that

$$\int \left(-\frac{\partial f_0(\varepsilon)}{\partial \varepsilon} \right) g(\varepsilon) d\varepsilon = \frac{\partial n}{\partial \zeta},$$

i. e. the derivative of electron concentration with respect to the chemical potential. This quantity is often called the *thermodynamic density of states*. So we get

$$\chi = \mu_B^2 \frac{\partial n}{\partial \zeta}.$$

Now the magnetic susceptibility can be calculated for any limiting case. For example, the temperature-dependent part for a strongly degenerate gas (see *Problem 4.5*)

$$\chi = \mu_B^2 g(\epsilon_F) \left[1 - \frac{\pi^2}{12} \left(\frac{k_B T}{\epsilon_F} \right)^2 \right]. \quad (4.22)$$

We see very important features: at low temperatures the main part of magnetic susceptibility is temperature-independent. Comparing the free electron susceptibility (4.22) with the Langevin one (4.21) we see that for electrons the role of characteristic energy plays the Fermi energy ϵ_F . For the Boltzmann gas we return to the formula (4.21).

Paramagnet Resonance (Electron Spin Resonance)

We take the opportunity to discuss here a very important tool of the modern solid state physics to investigate the properties of both the conduction electrons and the electrons

belonging to impurity centers. As we have seen, in an atomic electron the level's splitting in the magnetic field is proportional to the Lande factor g_L . In a solid state electron there is also *spin-orbital interaction*, as well as the interaction with the lattice. So one could introduce instead of the Lande factor the so-called spectroscopic factor g_s which effectively describes the level's splitting. This factor is often called simply *g-factor*. In general case $g_s \neq 2$, it can be anisotropic and also depend on the magnetic field direction.

Under the external magnetic field the levels split. In simplest case, the electron level splits into doublet corresponding to $s = \pm 1$, in general case the splitting-can be much more complicated. It is important that in any case the selection rule for a *dipole magnetic transitions* $\Delta m = \pm 1$. So one can study *resonant absorption* of electromagnetic field in the sample obeying the condition

$$\hbar\omega = g_s\mu_B H.$$

Consequently, one can determine the behavior of *g-factor* which is a very instructive quantity. The position and width of the resonant peaks allows one to make many conclusions on the symmetry of the local field in a crystal, interaction with neighboring magnetic atoms and with the lattice vibrations, etc.

The very similar picture hold for atomic nuclei in a crystal, the corresponding approach is called the *nuclear magnetic resonance* (NMR).

Phenomenological theory of EPR.

Here we show a very simple theory of EPR (Bloch, 1946). If \mathbf{M} is the magnetization vector and \mathbf{L} is the mechanical momentum of a volume unit, we have the following equation of motion

$$\frac{d\mathbf{L}}{dt} = [\mathbf{M} \times \mathbf{H}]$$

(just the sum of equations for different particles). According to very general concepts of quantum mechanics

$$\mathbf{M} = \gamma \mathbf{L}, \quad \gamma = \frac{eg_s}{2mc}.$$

So we get the close vector equation for \mathbf{M}

$$\frac{d\mathbf{M}}{dt} = \gamma [\mathbf{M} \times \mathbf{H}] . \quad (4.23)$$

To get explicit results let us assume that

$$\mathbf{H} = \mathbf{H}_0 + \mathbf{H}_1 \exp(-i\omega t), \quad \mathbf{H}_0 \parallel z, \quad \mathbf{H}_1 \parallel \mathbf{x}.$$

The solution can be expressed in the form

$$\mathbf{M} = \mathbf{M}_0 + \mathbf{M}_1 \exp(-i\omega t), \quad \mathbf{M}_0 \parallel z.$$

We get instead of Eq. (4.23)

$$\begin{aligned} -i\omega M_x &= \gamma M_{1y} H_0 \\ -i\omega M_y &= \gamma(M_z H_{1x} - M_x H_0) \approx \gamma(M_{0z} H_{1x} - M_x H_0) \\ -i\omega M_{1z} &= -\gamma M_{1y} H_{1x} \approx 0 \end{aligned} \quad (4.24)$$

where we keep only linear in the field \mathbf{H}_1 terms. Solving this equation we get

$$\chi_x = \frac{M_x}{H_x} = \frac{\chi_0}{1 - (\omega/\omega_0)^2}$$

where

$$\chi_0 = \frac{M_{0z}}{H_z}, \quad \omega_0 = \gamma H_0.$$

We see that at $\omega \rightarrow \omega_0$ $\chi_x \rightarrow \infty$ (note that the relaxation is neglected).

Diamagnetism of Atoms and Electrons (Landau Diamagnetism).

Now we are going to show that there is also *diamagnetic* contribution to the magnetic response which is usually masked by more strong paramagnetism.

Gas of atoms.

Let us start from an isolated atom with Z electrons which is place in a magnetic field $\mathbf{H} \parallel \mathbf{z}$. According to the *Larmor theorem* the influence of magnetic field is the rotation around z -axis with the *Larmor frequency*

$$\omega_L = eH/2mc.$$

The corresponding magnetic moment is $-\mu\mathbf{H}$. Consequently, if we introduce the mechanical momentum l we come to a universal relation

$$\mu = \frac{e}{2mc}l.$$

Taking into account that

$$l = m\omega_L \sum_{i=1}^Z \sqrt{(x_i^2 + y_i^2)}$$

we come to the following expression for *diamagnetic* susceptibility

$$\chi_d = \frac{n\mu}{H} = \frac{e^2 n}{4mc^2} \sum_{i=1}^Z \overline{(x_i^2 + y_i^2)}.$$

The order of magnitude estimate for $\sum_{i=1}^Z \overline{(x_i^2 + y_i^2)}$ is Za^2 . If we compare this result with the Langevin paramagnetic response $\mu_B^2 n/k_B T$ we get

$$\frac{\chi_d}{\chi_p} \approx Z \frac{k_0 T}{e^2/a}.$$

Usually this ration is 10^{-2} at room temperature.

Free electrons. Classical theory.

One can imagine that such a description holds for electrons. Indeed, a free electron's orbit moves along a circle in the plane normal to \mathbf{H} , the radius being

$$r_c = \frac{mcv_\perp}{eH} = \frac{v_\perp}{\omega_c} \quad (4.25)$$

where

$$\omega_c = \frac{eH}{mc} \quad (4.26)$$

is the *cyclotron frequency*. Note that $\omega_c = 2\omega_L$, where the Larmor frequency ω_L was introduced earlier. The corresponding magnetic moment is

$$\mu = \frac{er_c v_\perp}{2c} = \frac{mv_\perp^2/2}{H}.$$

Making use of the classical statistics, namely assuming $\overline{mv_\perp^2}/2 = k_B T$, we get

$$\chi = n \frac{k_B T}{H^2}.$$

It is clear that we have got a wrong equation, because it is charge-independent. It is interesting that the wrong result is due to the assumption that *all* the electrons have circular orbits. It appears that surface orbits which are not circles contribute to the surface current. So we will be more careful and show that according to classical physics one should get zero susceptibility for free electrons.

Let us introduce the *vector-potential* $\mathbf{A}(\mathbf{r})$ of the magnetic field as

$$\mathbf{H} = \text{curl} \mathbf{A}.$$

For $\mathbf{H} \parallel \mathbf{z}$ we have $\mathbf{A} \parallel \mathbf{y}$, $A_y = xH$. The classical Hamilton function is

$$\mathcal{H} = \frac{1}{2m} \left(\mathbf{p} + \frac{e}{c} \mathbf{A} \right)^2 + \mathcal{U}(\mathbf{r}) \quad (4.27)$$

where $\mathcal{U}(\mathbf{r})$ is the potential energy (remember that we denote the electron charge as $-e$). The partition function is

$$Z = \left[\int (dp) \int_V (dr) \exp \left(-\frac{\mathcal{H}}{k_B T} \right) \right]^N \quad (4.28)$$

where N is the total number of particles. The free energy is, as usual,

$$\mathcal{F} = -k_B T \ln Z.$$

One can shift the integration variables \mathbf{p} in Eq. (4.28) by $(e/c)\mathbf{A}(\mathbf{r})$, the shift being \mathbf{p} -independent. We come to the conclusion that the partition function is *field-independent* and $\chi = 0$.

Electron gas. Quantum theory. Quantum mechanics changes the situation completely. To understand the result let us apply a uniform magnetic field and assume that we have taken into account the periodic potential by the effective mass approximation. As was shown, the electron states in a magnetic field could be specified by the set of quantum numbers $\alpha = N, k_y, k_z$, the energy levels

$$\varepsilon_\alpha = \varepsilon_N + \frac{\hbar^2 k_z^2}{2m} = \hbar\omega_c(N + 1/2) + \frac{\hbar^2 k_z^2}{2m} \quad (4.29)$$

being dependent only on N, k_z .

To obtain thermodynamic functions one should calculate the density of states in a magnetic field. First we should count the number of the values k_y corresponding to the energy ε_α (the so-called *degeneracy factor*). As usual, we apply cyclic boundary conditions along y and z -axes and get

$$k_y = \frac{2\pi}{L_y} n_y, \quad k_z = \frac{2\pi}{L_z} n_z.$$

At the same time, we assume that the solution exists only in the region

$$0 < |x_0| < L_x.$$

So, the degeneracy factor is

$$\frac{L_y}{2\pi} k_y^{\max} = \frac{L_y}{2\pi a_H^2} x_0^{\max} = \frac{L_y L_x}{2\pi a_H^2}. \quad (4.30)$$

This is very important relation which shows that one can imagine Landau states as cells with the area a_H^2 . We will come back to this property later.

Now it is easy to calculate density of states treating the k_z variable as for the usual 1D motion

$$\frac{2|k_z|L_z}{2\pi} = \frac{2\sqrt{2m}L_z}{2\pi\hbar}\sqrt{\varepsilon - \hbar\omega_c(N + 1/2)}$$

for each state with a given N . Finally, the total number of states for a given spin is

$$Z_s(\varepsilon) = \sum_N Z_{sN}(\varepsilon) = \frac{2\sqrt{2m}}{(2\pi)^2 \hbar a_H^2} \sum_N \sqrt{\varepsilon - \hbar\omega_c(N + 1/2)}$$

where one has to sum over all the values of N with non-negative $\varepsilon - \hbar\omega_c(N + 1/2)$. The total number of states is $Z(\varepsilon) = 2Z_s(\varepsilon)$. To get DOS one should differentiate this equation with respect to ε . the result is

$$g_s(\varepsilon) = \frac{dZ(\varepsilon)}{d\varepsilon} = \frac{\sqrt{2m}}{(2\pi)^2 \hbar a_H^2} \sum_N \frac{1}{\sqrt{\varepsilon - \hbar\omega_c(N + 1/2)}}.$$

To take the spin into account one should add the spin splitting

$$\pm \mu_B g_s H$$

to the energy levels (4.29). If we ignore the spin splitting we can assume spin degeneracy and multiply all the formulas by the factor 2. We take it into account automatically using $g(\varepsilon) = 2g_s(\varepsilon)$.

The behavior of the density of states could be interpreted qualitatively in the following way. The Landau levels as functions of magnetic field for a given value of p_z are shown in Fig. 4.4. They form the so-called *Landau fan*. The Fermi level is also shown. At low

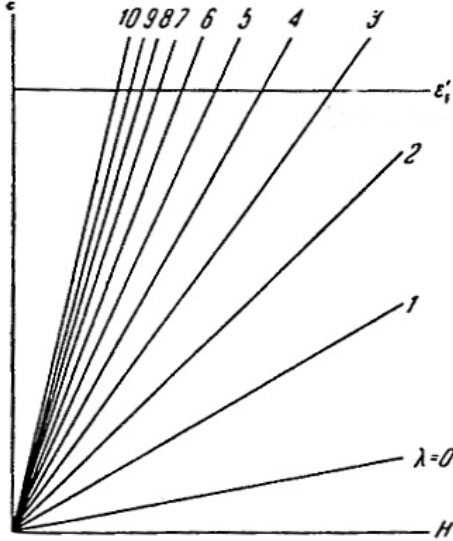


Figure 4.4: Landau levels as functions of H .

magnetic fields its dependence on magnetic field is very weak. We see that if magnetic field is small many levels are filled. Let us start with some value of magnetic field and follow the upper filled level N . As the field increases, the slopes of the "fan" also increase and at a given threshold value H_N for which

$$\varepsilon_N(H_N) = \epsilon_F.$$

As the field increases the electrons are transferred from the N -th Landau level to the other ones. Then, for the field H_{N-1} determined from the equation $\varepsilon_{N-1}(H_{N-1}) = \epsilon_F$ the $(N-1)$ becomes empty. We get

$$H_N \approx \frac{m_c c \epsilon_F}{e \hbar} \frac{1}{N}, \text{ so } \Delta \left(\frac{1}{H} \right) \approx \frac{e \hbar}{m_c c \epsilon_F}.$$

We see that electron numbers at given levels oscillate with magnetic field and one can expect the oscillating behavior of all the thermodynamic functions. To illustrate the oscillations the functions

$$\tilde{Z}(x) = \sum_N \sqrt{x - N - \frac{1}{2}}$$

as well as the difference between its classical limit $(2/3)x^{3/2}$ are plotted in Fig. 4.5.

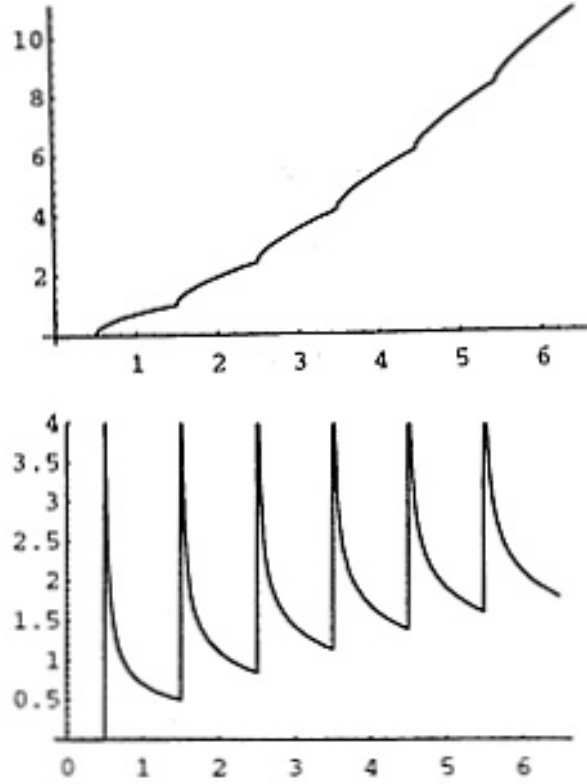


Figure 4.5: Number of filled states as a function of the energy.

Quantitative theory of magnetic susceptibility.

Now we are prepared to calculate the magnetic susceptibility. Using the known formula for the entropy of the Fermi gas we get the following expression for the free energy

$$\mathcal{F} = n\zeta - k_B T \int_{\varepsilon_0}^{\infty} \ln \left[1 + e^{\frac{\zeta-\varepsilon}{k_B T}} \right] g(\varepsilon) d\varepsilon = n\zeta - \int_{\varepsilon_0}^{\infty} f_0(\varepsilon) Z(\varepsilon) d\varepsilon .$$

Here $\varepsilon_0 = \hbar\omega_c/2$ and we have integrated by parts. Making the second integration by part we get

$$\mathcal{F} = n\zeta - \int_{\varepsilon_0}^{\infty} \left(-\frac{\partial f_0}{\partial \varepsilon} \right) \Phi(\varepsilon) d\varepsilon \quad (4.31)$$

where

$$\Phi(\varepsilon) = \sum_N \int_{\varepsilon_N}^{\varepsilon} Z_N(\varepsilon) d\varepsilon .$$

The behavior of the function $\Phi(\varepsilon)$ depends on the number of levels which are present in the summation over N . One can derive the auxiliary formula (see Appendix B)

$$K(x) = \sum_N (x - n - 1/2)^{3/2} = \frac{2}{5}x^{5/2} - \frac{1}{16}x^{1/2} - \frac{3}{8\pi^2} \sum_{l=1}^{\infty} \left[\sin(2\pi lx) S\left(\sqrt{4lx}\right) + \cos(2\pi lx) C\left(\sqrt{4lx}\right) \right].$$

As a result the function Φ in (4.31) is

$$\Phi(\varepsilon) = AK \left(\frac{\varepsilon}{\hbar\omega_c} \right), \quad A = \frac{(2m)^{3/2}(\hbar\omega_c)^{5/2}}{3\pi^2\hbar^3}.$$

At strong degeneracy

$$\left(-\frac{\partial f_0}{\partial \varepsilon} \right) \approx \delta(\varepsilon - \epsilon_F)$$

and we see that the free energy oscillates in magnetic field, the period of the l -th item being $\hbar\omega_c/l$. At the same time, at

$$k_B T \gg \hbar\omega_c$$

the oscillations are smeared, and

$$\mathcal{F} = n\epsilon_F - A \left[\frac{2}{5} \left(\frac{\epsilon_F}{\hbar\omega_c} \right)^{5/2} - \frac{1}{16} \left(\frac{\epsilon_F}{\hbar\omega_c} \right)^{1/2} \right].$$

The second item is field-independent, and we get

$$\chi = -\frac{\partial^2 \mathcal{F}}{\partial H^2} = -\frac{1}{3} \frac{\sqrt{2}}{\pi^2} \left(\frac{m_0}{m} \right)^2 \frac{m^{3/2} \mu_B^2 \epsilon_F}{\hbar^3}.$$

One can easily show that the ratio of this diamagnetic susceptibility to the Pauli paramagnetic one is

$$\frac{1}{3} \left(\frac{m_0}{m} \right)^2.$$

This ratio can be large in semiconductors.

In the opposite limiting case,

$$k_B T \leq \hbar\omega_c$$

the oscillations of the free energy and of the susceptibility are pronounced. It is the so-called *de Haas-van Alphen* oscillations which were first observed in Bi (1930). It is very important effect to determine the characteristics of the *Fermi surface of metals*. A typical shape of these oscillations is shown in Fig. 4.6. In a non-degenerate gas we have the Boltzmann distribution instead of the Fermi one and we get (Check!)

$$\mathcal{F} = n\zeta - \frac{A\hbar\omega_c}{k_B T} e^{\zeta^*} \sum_{N=0}^{\infty} \left(\frac{\varepsilon}{\hbar\omega_c} - N - \frac{1}{2} \right)^{3/2} e^{-\varepsilon/k_B T}. \quad (4.32)$$

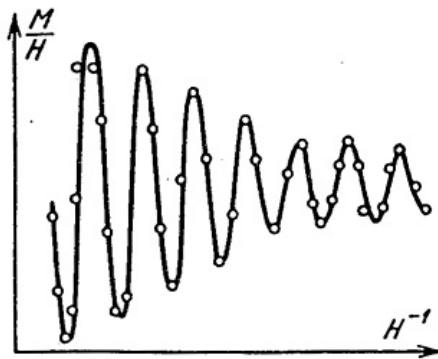


Figure 4.6: De Haas-van Alphen oscillations.

Then we easily get (*Problem 4.6*)

$$\mathcal{F} = n\zeta - \frac{3\sqrt{\pi}}{4} A \left(\frac{k_B T}{\hbar\omega_c} \right)^{5/2} e^{\zeta^*} \left[\frac{2ze^z}{1 - e^{-2z}} \right] \quad (4.33)$$

where $z = \hbar\omega_c/2k_B T$. The only magnetic field dependence is due to the last factor. At low magnetic fields we can expand the expression in square brackets as $1 - z^2/6$. Differentiating with respect to magnetic field we get

$$\chi = -\frac{1}{3} \left(\frac{m_0}{m} \right)^2 \frac{\mu_B n}{k_B T}.$$

So we come to the conclusion that the relation between the diamagnetic and paramagnetic parts holds also for non degenerate gas.

4.5 Problems

- 4.1.** Calculate the partition function for a harmonic oscillator.
- 4.2.** Prove the expression (4.11).
- 4.3.** Calculate temperature-dependent corrections to the chemical potential of a Fermi gas.
- 4.4.** Calculate specific heat for the Boltzmann gas.
- 4.5.** Derive expression (4.22) for magnetic susceptibility.
- 4.6.** Derive the formula (4.33) for magnetic susceptibility of Boltzmann gas.

Chapter 5

Summary of basic concepts

In this very short chapter we discuss main concepts of the first, introductory part of the course and try to understand their range of applicability.

1. The first concept was **translation symmetry** of crystalline materials. This concept allowed us to classify the structure of crystals and to formulate the basic theory of *lattice vibrations*. It was shown that *under harmonic approximation* one can introduce normal co-ordinates of lattice displacements which are independent. In fact, because of translation symmetry, these displacements propagate as plane waves which are characterized by the *wave vector* \mathbf{q} and frequency $\omega(\mathbf{q})$. The *dispersion law* $\omega(\mathbf{q})$ is *periodic* in \mathbf{q} -space, the period being the *reciprocal lattice vector* \mathbf{G} which can be constructed from the basis \mathbf{b}_i as $\mathbf{G} = \sum_i n_i \mathbf{b}_i$ where n_i are integers. Consequently, one can chose a basic volume in the reciprocal lattice space (the Brillouin zone, BZ). The properties of the dispersion law $\omega(\mathbf{q})$ are determined by the crystal structure, in particular, by the number s of atoms in a primitive cell. There are 3 acoustic branches and $3s - 3$ optical ones.

It is clear that the exact periodicity is not the case in real life because i) all the samples are finite, and ii) many important systems are inhomogeneous. Consequently, this approach do not take into account *surface states*, *interface states*. Moreover, the imperfections of the crystal lattice (defects, impurities) lead to violation of the translation symmetry and, as a result, to *scattering* of the waves. As a result, if the degree of disorder is large, all the picture developed above needs important corrections. In particular, some *localized* modes can appear which are completely beyond the scope of Part 1.

2. The properties of the lattice waves allowed us to introduce the central concept of solid state physics - **the concept of quasiparticles**. Namely, the lattice vibrations can be described as a set of quasiparticles (**phonons**) with quasimomentum $\hbar\mathbf{q}$ and energy $\hbar\omega_j(\mathbf{q})$. They can be treated as the Bose particles with zero chemical potential, the only (but very important) difference being that (as we will see later) in all the interaction processes quasimomenta \mathbf{q} are conserved with the accuracy of \mathbf{G} .

Remember, that all the formulation is base on the harmonic approximation. The lattice anharmonicity leads to the interaction between quasiparticles. This interaction together with the scattering by defects lead to the *dumping* of quasiparticles. It means that a quasiparticle is not exact eigenvalue of the total Hamiltonian of the system and the quasi-

momentum $\hbar\mathbf{q}$ is not exact quantum number. Physically, the quasiparticles have finite *mean free path* ℓ that is the characteristic distance of the wave function dumping due to all the interactions. The length ℓ is very important property for all the transport phenomena. One can understand that the concept of quasiparticles can be valid only if

$$q_{ph} \gg \frac{1}{\ell_{ph}}.$$

Another formulation of this inequality is that the wave length $2\pi/q$ should be much less than the mean free path ℓ . Indeed, quantum system should have enough space to form a stationary state. In most situation this condition holds because the anharmonicity is rather weak (we will estimate it later). Nevertheless, there are some important situations where phonons could not be considered as independent quasiparticles. In particular, phonons can interact with electrons. In some situations this interaction appears strong enough to form bound states -*polarons*. It is clear that in such a situation the concept of independent weakly interacting phonons fails.

3. The translation symmetry influences strongly upon the electron system. As we have seen, the concept of **Bloch electrons** can be developed. The main advantage is that the periodic potential created by the lattice and other electrons in the first approximation leads only to the *renormalization* of the electron spectrum from $\mathbf{p}^2/2m_0$ to more complicated function $\varepsilon(\mathbf{p})$ which is periodic in \mathbf{p} -space

$$\varepsilon(\mathbf{p} + \mathbf{G}) = \varepsilon(\mathbf{p}).$$

Again, we come to next to independent quasiparticles with the quasimomentum ($\mathbf{k} = \mathbf{p}/\hbar$ confined in the BZ. As in the case of phonons, electrons have several energy bands, $\varepsilon_j(\mathbf{p})$.

The most important for applications feature is that one can treat the function

$$\mathcal{H}(\mathbf{p}, \mathbf{r}) = \varepsilon_j \left(\mathbf{p} + \frac{e}{c} \mathbf{A}(\mathbf{r}) \right) + U(\mathbf{r}) - e\varphi(\mathbf{r})$$

as the Hamiltonian to describe the motion of a Bloch electron in external fields. This is very important statement because it allows one to analyze the electron motion in external fields. Its range of applicability is limited mainly by *one-band approximation* - it is implicitly assumed that *interband transitions* do not take place due to external fields. In particular this approach fails if the frequency ω of external field is close to the $|\varepsilon_i(\mathbf{p}) - \varepsilon_j(\mathbf{p})|$ for a given \mathbf{p} . One can see that one cannot use the simplified effective mass approach for the case of *degenerate bands* in semiconductors (one should bear in mind that there are some special methods to treat this case, we will discuss some of them later). Another criterion is that the typical spatial scale of motion, \mathcal{L} , should be greater than the lattice constant a . Indeed, the Bloch state is formed at the distances much greater than a , and external fields should not interfere with the formation of the electron state. The latter criterion is, in fact, dependent of the problem under consideration. Suppose that we are interested in the formation of a bound state Bloch electron+impurity with Coulomb potential. It is the typical problem of

semiconductor physics. Substituting the Hamiltonian $\hat{\mathbf{p}}^2/2m + e\varphi = \hat{\mathbf{p}}^2/2m - e^2/\epsilon r$ with the effective mass m to the SE we get the effective *Bohr radius*

$$a_B = \frac{\hbar^2 \epsilon}{me^2} = a_B^0 \frac{m_0}{m} \epsilon = 0.53 \frac{m_0}{m} \epsilon, \text{ \AA}.$$

In this case the criterion for one-band approximation is $a_B \gg a$. This criterion can be met only in materials with small effective mass and large dielectric constant ϵ . For the so-called deep levels. as well as for some interface states this approach is not valid.

The electron states as the phonon ones can be destroyed by the impurity scattering, as well as by electron-phonon and electron-electron interaction. Form the first glance, electron should interact with each other via very strong Coulomb forces and it is impossible for them to be near independent. Nevertheless, i) the total system is electrically neutral, and ii) electrons effectively screen electric fields. As a result, Coulomb interaction appears mostly included in the self-consistent potential and the remaining effects can be not important for many actual problems. We will come back to the electron-electron interaction in the following parts.

At the same time, there are important physical situations where the interaction play crucial role and change the ground state of the system. One example is the formation of the polaron (electron+phonon) states, another one is the formation of a superconductor states. The properties of superconductors will be discussed in a special Part.

Up to now, we have described the electron states as *stationary solutions* $\psi = e^{i\mathbf{k}\mathbf{r}} u_k(\mathbf{r})$ of the SE. To describe the transport it is useful to form a *package* of the electrons with the quasimomenta \mathbf{p} , $\mathbf{p}+\Delta\mathbf{p}$. According to the uncertainty principle,

$$\Delta p \Delta r \approx \hbar.$$

Now, if we want to localize the quasiparticle, the uncertainty Δr should be, at least, less than the mean free path ℓ . The upper limit for Δp is p . So, we come to the criterion

$$p \gg \frac{\hbar}{\ell}.$$

For a typical metal $p \approx \hbar/a$, and we get $\ell \gg a$. There is another important criterion which is connected with the *life-time* τ_φ with the respect of the phase destruction of the wave function. The energy difference $\Delta\varepsilon$ which can be resolved cannot be greater than \hbar/τ_φ . In the most cases $\Delta\varepsilon \approx k_B T$, and we have

$$k_B T \gg \frac{\hbar}{\tau_\varphi}.$$

Note that elastic scattering does not contribute to the phase destruction.

The previous part of the course has outlined the physics of independent quasiparticles which are very often called the *elementary excitations*.

Chapter 6

Classical dc Transport in Electron and Phonon Systems

In this chapter we discuss transport properties of bulk normal conductors and insulators.

6.1 The Boltzmann Equation for Electrons

General Form

The description of quasiparticles as wave packages allows one to introduce the *non-equilibrium distribution function* $f(\mathbf{p}, \mathbf{r})$ which is the average occupation number for the state \mathbf{p} at the point \mathbf{r} . In the absence of external fields and interactions this function is equal to the equilibrium one, f_0 . Otherwise it becomes time dependent, and one can write

$$\frac{df}{dt} = I(f)$$

where $I(f) \equiv (\partial f / \partial t)_{\text{coll}}$ is called the *collision integral*. One can write the l.h.s. as

$$\frac{\partial f}{\partial t} + \frac{\partial f}{\partial \mathbf{r}} \frac{\partial \mathbf{r}}{\partial t} + \frac{\partial f}{\partial \mathbf{p}} \frac{\partial \mathbf{p}}{\partial t}.$$

Using the Newton equation we can write the previous formula as

$$\frac{\partial f}{\partial t} + \mathbf{v} \frac{\partial f}{\partial \mathbf{r}} - e \left(\mathbf{E} + \frac{1}{c} [\mathbf{v} \times \mathbf{H}] \right) \frac{\partial f}{\partial \mathbf{p}}.$$

The collision integral describes transitions between the states with different \mathbf{p} due to collisions. It can be specified if one knows the collision probability $W(\mathbf{p}, \mathbf{p}')$. Indeed, the change of the distribution induced by the collisions is

$$\text{decrease: } - \sum_{\mathbf{p}'} W(\mathbf{p}, \mathbf{p}') f(\mathbf{p}) [1 - f(\mathbf{p}')] \rightarrow \text{"out" term,}$$

$$\text{increase: } \sum_{\mathbf{p}'} W(\mathbf{p}', \mathbf{p}) f(\mathbf{p}') [1 - f(\mathbf{p})] \rightarrow \text{"in" term.}$$

The first term describes the scattering processes in which the electron *leaves* the state \mathbf{p} while the second one describes the processes where an electron comes to the state \mathbf{p} from other states \mathbf{p}' . The factors $[1 - f(\mathbf{p})]$ takes account of the Pauli principle. So

$$I(f) = \sum_{\mathbf{p}'} \{W(\mathbf{p}', \mathbf{p}) f(\mathbf{p}') [1 - f(\mathbf{p})] - W(\mathbf{p}, \mathbf{p}') f(\mathbf{p}) [1 - f(\mathbf{p}')]\}. \quad (6.1)$$

Finally, we get the *Boltzmann equation* for electrons

$$\frac{\partial f}{\partial t} + \mathbf{v} \frac{\partial f}{\partial \mathbf{r}} - e \left(\mathbf{E} + \frac{1}{c} [\mathbf{v} \times \mathbf{H}] \right) \frac{\partial f}{\partial \mathbf{p}} = I(f). \quad (6.2)$$

Let us investigate general properties of the collision integral. It is clear that if the system is in equilibrium the collision integral should vanish, $I(f_0) \equiv 0$. Making use of the relation

$$1 - f_0(\varepsilon) = f_0(\varepsilon) \exp \left(\frac{\varepsilon - \zeta}{k_B T} \right)$$

we get the general property

$$W(\mathbf{p}', \mathbf{p}) \exp \left(\frac{\varepsilon}{k_B T} \right) = W(\mathbf{p}, \mathbf{p}') \exp \left(\frac{\varepsilon'}{k_B T} \right)$$

where $\varepsilon = \varepsilon(\mathbf{p})$, $\varepsilon' = \varepsilon(\mathbf{p}')$. For any elastic scattering

$$W(\mathbf{p}', \mathbf{p}) = W(\mathbf{p}, \mathbf{p}')$$

and we get

$$I(f) = \sum_{\mathbf{p}'} W(\mathbf{p}, \mathbf{p}') [f(\mathbf{p}') - f(\mathbf{p})]. \quad (6.3)$$

We see that the Pauli principle is not important for elastic collisions because it is met automatically. Now we will discuss one important collision mechanism to show the main properties of the transport, namely, the impurity scattering. This mechanism is important at low temperatures and in rather dirty materials.

Impurity scattering

Under the Born approximation, the scattering probability for impurities is

$$W(\mathbf{p}, \mathbf{p}') = \frac{2\pi}{\hbar} |V_{\mathbf{pp}'}|^2 \delta [\varepsilon(\mathbf{p}) - \varepsilon(\mathbf{p}')] \quad (6.4)$$

where $V_{\mathbf{pp}'}$ is the matrix elements of the impurity potential

$$V(\mathbf{r}) = \sum_i v(\mathbf{r} - \mathbf{R}_i) \quad (6.5)$$

which is the sum of the potentials v of the individual impurities between the Bloch states

$$\frac{1}{\sqrt{\mathcal{V}}} e^{i\mathbf{k}\mathbf{r}} u_{\mathbf{k}}(\mathbf{r}), \quad \mathbf{k} \equiv \frac{\mathbf{p}}{\hbar}.$$

Substituting (6.5) into the expression for matrix elements we get

$$\begin{aligned} V_{\mathbf{pp}'} &= \mathcal{V}^{-1} \sum_i \int v(\mathbf{r} - \mathbf{r}_i) e^{i(\mathbf{k}-\mathbf{k}')\mathbf{r}} u_{\mathbf{k}'}^*(\mathbf{r}) u_{\mathbf{k}}(\mathbf{r}) d^3 r \\ &= \mathcal{V}^{-1} \sum_i e^{i(\mathbf{k}-\mathbf{k}')\mathbf{R}_i} \int v(\mathbf{r}) u_{\mathbf{k}'}^*(\mathbf{r}) u_{\mathbf{k}}(\mathbf{r}) e^{i(\mathbf{k}-\mathbf{k}')\mathbf{r}} d^3 r \\ &= \mathcal{V}^{-1} \sum_i e^{i(\mathbf{k}-\mathbf{k}')\mathbf{R}_i} v_{\mathbf{p}'\mathbf{p}}. \end{aligned}$$

Here we have assumed all the impurity atoms be of the same kind and their positions in the primitive cells are equivalent. So we have shifted the origin of the frame of reference for each cell by an appropriate lattice vector. Now we can calculate the scattering probability (6.4). We get

$$\frac{2\pi}{\hbar} \frac{1}{\mathcal{V}^2} \int \mathcal{V}(dp') |v_{\mathbf{p}'\mathbf{p}}|^2 \delta[\varepsilon(\mathbf{p}) - \varepsilon(\mathbf{p}')] \sum_{i,k} e^{i(\mathbf{k}-\mathbf{k}')(\mathbf{R}_i-\mathbf{R}_k)}$$

where we replaced the summation over the discrete quasimomenta by the integration

$$\sum_{\mathbf{p}'} \rightarrow \mathcal{V} \int (dp') \equiv \frac{2\mathcal{V}}{(2\pi\hbar)^3} \int d^3 p'.$$

The last sum can be strongly simplified because the positions of the impurities are *random* the distance between them is much greater than interatomic spacing a . So we can average over their positions and the only terms important are the ones with $i = k$ (the other oscillate strongly, their contribution being very small). As a result,

$$\overline{\sum_{i,k} e^{i(\mathbf{k}-\mathbf{k}')(\mathbf{R}_i-\mathbf{R}_k)}} = N_{\text{imp}}$$

where N_{imp} is the number of impurities. Finally, we get the following collision integral

$$I(f) = \frac{2\pi}{\hbar} n_i \int (dp') |v_{\mathbf{p}'\mathbf{p}}|^2 \delta[\varepsilon(\mathbf{p}) - \varepsilon(\mathbf{p}')] [f(\mathbf{p}') - f(\mathbf{p})] \quad (6.6)$$

where we introduced the impurity concentration as $n_i = N_{\text{imp}}/\mathcal{V}$.

Now we change the variables from \mathbf{p}' to the energy ε' and the surface S' defined as $\varepsilon(\mathbf{p}') = \varepsilon'$. We get

$$\frac{2}{(2\pi\hbar)^3} d^3 p' = \frac{2}{(2\pi\hbar)^3} dS' dp'_\perp = \frac{2}{(2\pi\hbar)^3} dS' \frac{d\varepsilon'}{|\partial\varepsilon'/\partial\mathbf{p}'|} = d\varepsilon' (ds'_{\varepsilon'})$$

where we have denoted

$$(ds_\varepsilon) \equiv \frac{2}{(2\pi\hbar)^3} \frac{dS}{v}.$$

Note that the density of states is given by the expression

$$g(\varepsilon) = \int_{S_\varepsilon} (ds_\varepsilon)$$

where the integral is calculated over the surface of constant energy $\varepsilon(\mathbf{p})$. Using the above mentioned notations we can then apply the δ -function to integrate over the ε' . The result has a simple form

$$I(f) = \frac{2\pi}{\hbar} n_i \int_{S_{\varepsilon'}} (ds_{\varepsilon'}) |v_{\mathbf{p}'\mathbf{p}}|^2 [f(\mathbf{p}') - f(\mathbf{p})]. \quad (6.7)$$

The Transport Relaxation Time

Now we demonstrate a very useful representation of the collision integral that makes the solution of the Boltzmann equation rather simple. Let us assume that the deviation from equilibrium is small, so that

$$f = f_0 + f_1, \quad |f_1| \ll f_0.$$

Because $I(f_0) = 0$ we have $I(f) = I(f_1)$. To get explicit results we assume that the spectrum $\varepsilon(\mathbf{p})$ is isotropic. Consequently $p = p'$, $v_{\mathbf{p}'\mathbf{p}}$ depends only on the angle between \mathbf{p} and \mathbf{p}' , the surface S is a sphere and the integration is in fact performed over the solid angle.

It is convenient to write the function f_1 as

$$f_1 = -\mathbf{n} \cdot \mathbf{f}(\varepsilon), \quad \mathbf{n} \equiv \mathbf{p}/p \quad (6.8)$$

is the unit vector directed along \mathbf{p} . In this case

$$I(f) = f(\varepsilon) \int \frac{d\Omega'}{4\pi} W(\theta) (\cos(\widehat{\mathbf{p}'\mathbf{f}}) - \cos(\widehat{\mathbf{p}\mathbf{f}}))$$

where Ω' is the solid angle in the \mathbf{p}' -space, $\theta \equiv \widehat{\mathbf{p}, \mathbf{p}'}$ is the angle between \mathbf{p} and \mathbf{p}' , while (Check!)

$$W(\theta) = \pi \frac{n_i |v(\theta)|^2}{\hbar} g(\varepsilon). \quad (6.9)$$

Then we can transform the integral as follows. Choose the polar axis \mathbf{z} along the vector \mathbf{p} . Now let us rewrite the equation

$$\mathbf{p}' \cdot \mathbf{f} = p'_z f_z + \mathbf{p}'_\perp \cdot \mathbf{f}_\perp$$

as

$$\cos(\widehat{\mathbf{p}}, \widehat{\mathbf{f}}) = \cos(\widehat{\mathbf{p}'}, \widehat{\mathbf{p}}) \cos(\widehat{\mathbf{f}}, \widehat{\mathbf{p}}) + \sin(\widehat{\mathbf{p}'}, \widehat{\mathbf{p}}) \sin(\widehat{\mathbf{f}}, \widehat{\mathbf{p}}) \cos \varphi_{\mathbf{p}'_\perp, \mathbf{f}_\perp}. \quad (6.10)$$

Here $\varphi_{\mathbf{p}'_\perp, \mathbf{f}_\perp}$ is the angle between the projections of \mathbf{p}' and \mathbf{f} to the plane normal to \mathbf{p} . Note that the angle $\widehat{\mathbf{p}, \mathbf{p}'} = \theta$. The second term in (6.10) vanishes after integration over $\varphi_{\mathbf{p}'_\perp, \mathbf{f}_\perp}$. Finally we get

$$I(f) = -\frac{f_1}{\tau_{\text{tr}}} = -\frac{f - f_0}{\tau_{\text{tr}}}$$

where

$$\frac{1}{\tau_{\text{tr}}} = \frac{1}{2} \int_0^\pi W(\theta) (1 - \cos \theta) \sin \theta d\theta. \quad (6.11)$$

The quantity τ_{tr} is called the *transport relaxation time*. In many situations the Boltzmann equation is represented in the form

$$\frac{\partial f}{\partial t} + \mathbf{v} \frac{\partial f}{\partial \mathbf{r}} - e \left(\mathbf{E} + \frac{1}{c} [\mathbf{v} \times \mathbf{H}] \right) \frac{\partial f}{\partial \mathbf{p}} = \quad (6.12)$$

Here we have shown that this form is *exact* for elastic impurity scattering if the non-equilibrium function can be expressed as (6.8). One should remember that we have made several important simplifications:

- Isotropic spectrum;
- Elastic scattering;
- The form (6.8) for the non-equilibrium distribution function.

All these assumptions are important and in some cases they can be wrong. Nevertheless the form (6.12) allows one to get good order-of-magnitude estimates and we will extensively use it.

6.2 Conductivity and Thermoelectric Phenomena.

DC Electric Conductivity

Let us apply the outlined approach to calculate the conductivity of a conductor. Namely, let us assume that a weak stationary electric field \mathbf{E} is applied to the sample. The Boltzmann equation has the form

$$-e \left(\mathbf{E} \cdot \frac{\partial f}{\partial \mathbf{p}} \right) = -\frac{f - f_0}{\tau_{\text{tr}}}. \quad (6.13)$$

Because the field is weak we can assume that

$$f = f_0 + f_1, \quad f_1 \propto E, \quad |f_1| \ll f_0$$

and we can replace $f \rightarrow f_0$ in the l.h.s. and get $e(\mathbf{E} \cdot \mathbf{v})(-\partial f_0 / \partial \varepsilon)$. Immediately we get

$$f_1 = e(\mathbf{E} \cdot \mathbf{v}) \tau_{\text{tr}} (\partial f_0 / \partial \varepsilon).$$

We see that it has just the form of (6.8) that justifies our approach. Now we calculate the current as

$$\mathbf{j} = -e \int (dp) \mathbf{v} f_1 = e^2 \int (dp) \tau_{\text{tr}} \mathbf{v} (\mathbf{E} \cdot \mathbf{v}) \left(-\frac{\partial f_0}{\partial \varepsilon} \right) \quad (6.14)$$

(the function f_0 is even in \mathbf{p} and does not contribute to the current). Again, we can average over the surface of a constant energy as

$$\int M(\mathbf{p})(dp) = \int d\varepsilon \int_{S_\varepsilon} M(\mathbf{p}) (ds_\varepsilon) = \int d\varepsilon g(\varepsilon) \langle M(\mathbf{p}) \rangle_\varepsilon$$

where

$$\langle M(\mathbf{p}) \rangle_\varepsilon \equiv \frac{\int_{S_\varepsilon} M(\mathbf{p}) (ds_\varepsilon)}{g(\varepsilon)}. \quad (6.15)$$

In the case of an isotropic spectrum the average (6.15) is just the average over the angles. Finally for the isotropic spectrum we get Ohm's law $\mathbf{j} = \sigma \mathbf{E}$ with

$$\sigma = e^2 \int d\varepsilon \left(-\frac{\partial f_0}{\partial \varepsilon} \right) g(\varepsilon) D(\varepsilon) \quad (6.16)$$

where

$$D(\varepsilon) = \frac{1}{3} \langle v^2 \tau_{\text{tr}} \rangle_\varepsilon$$

is the partial *diffusivity* for the electrons with the given energy.

Indeed, consider a gas of electrons with the mean free time τ and mean free path $\ell = v\tau$. Let the density of electrons, n_e be non-uniform along the \mathbf{x} -axis. In this case the flux of the electrons through 1 cm^2 of the surface normal to \mathbf{x} is equal

$$i_D(x) = \int n_e(x - \ell \cos \theta) v \cos \theta \frac{d\Omega}{4\pi}$$

where θ is the angle between \mathbf{v} and \mathbf{x} while ℓ is the electron mean free path, $\ell = v\tau_{\text{tr}}$. Here we have taken into account that the electrons have arrived at the point with coordinate x from the point with the coordinate $x - \ell \cos \theta$ in a ballistic way. As a result, non-compensated current is

$$i_D = -\frac{\partial n_e}{\partial x} \frac{\ell v}{2} \int_{-1}^1 \cos^2 \theta d(\cos \theta) = -\frac{\ell v}{3} \frac{\partial n_e}{\partial x}.$$

According to the definition of the diffusivity (diffusion coefficient), we get $D = \ell v / 3 = v^2 \tau_{\text{tr}} / 3$.

In the case of Fermi statistics where $(-\partial f_0/\partial \varepsilon) = \delta(\varepsilon - \epsilon_F)$ we get the *Drude formula* (*Problem 6.2*)

$$\sigma_0 = e^2 D(\epsilon_F) g(\epsilon_F) = \frac{ne^2 \tau_{\text{tr}}}{m}. \quad (6.17)$$

The first expression is known as the *Einstein relation*.

If the degeneracy is not so strong, the energy dependence of the factor $D(\varepsilon)$ becomes important. This is just the case for semiconductors. We will come back to this problem after the analysis of important scattering mechanisms which determine the dependence $\tau_{\text{tr}}(\varepsilon)$.

In general anisotropic case the Ohms law has the form

$$\mathbf{j} = \hat{\sigma} \mathbf{E}, \quad \text{or} \quad j_i = \sum_k \sigma_{ik} E_k.$$

The *conductivity tensor* $\hat{\sigma}$ can be calculated with the help of the relation (6.16) if the *diffusivity tensor*

$$D_{ik} = \langle v_i I^{-1} v_k \rangle_\varepsilon$$

is known. Here the formal "inverse collision operator" is introduced which shows that one should in fact solve the Boltzmann equation.

AC Conductivity

Solving the Boltzmann equation for the perturbation $\propto \exp(-i\omega t)$ we obtain

$$\sigma(\omega) = \sigma_0 \frac{1}{\langle \tau_{\text{tr}} \rangle} \left\langle \frac{\tau_{\text{tr}}}{1 - i\omega\tau_{\text{tr}}} \right\rangle.$$

Here angular brackets mean

$$\langle A \rangle = \frac{\int d\varepsilon \varepsilon^{3/2} A(\varepsilon) (\partial f_0 / \partial \varepsilon)}{\int d\varepsilon \varepsilon^{3/2} (\partial f_0 / \partial \varepsilon)}.$$

The real part of this expression,

$$\text{Re } \sigma(\omega) = \sigma_0 \frac{1}{\langle \tau_{\text{tr}} \rangle} \left\langle \frac{\tau_{\text{tr}}}{1 + \omega^2 \tau_{\text{tr}}^2} \right\rangle,$$

represents ac loss in the sample, while imaginary part is the contribution to dielectric function. The typical scale for the momentum relaxation time is about $10^{-12}\text{--}10^{-14}$ s. Consequently, frequency dependence is important at microwave frequencies.

Thermoelectric Phenomena

Now we demonstrate another kind of problems which appear if a *temperature gradient* is created in the sample. In this case the temperature is a slow function of co-ordinates and can be expressed as

$$T(\mathbf{r}) = T_1 + (\mathbf{r} - \mathbf{r}_1) \nabla T, \quad T_1 \equiv T(\mathbf{r}_1).$$

If the characteristic scale of the spatial variation of the temperature, $T/|\nabla T|$, is large in comparison with the scale at which temperature is formed (that is usually the phonon mean free path, ℓ_{ph}) one can assume that at any point the distribution is close to equilibrium one,

$$f_0(\varepsilon, \mathbf{r}) = \left[\exp \left(\frac{\varepsilon - \zeta(\mathbf{r})}{k_B T} \right) + 1 \right]^{-1} \quad (6.18)$$

Here we take into account that the chemical potential ζ is also coordinate-dependent, since it depends on the temperature. Consequently, we get

$$\nabla_{\mathbf{r}} f_0 = \left(-\frac{\partial f_0}{\partial \varepsilon} \right) \left[\nabla \zeta(\mathbf{r}) + \frac{\varepsilon - \zeta}{T} \nabla T(\mathbf{r}) \right].$$

Thus in the l.h.s. of the Boltzmann equation we get

$$\left[(\mathbf{v} \cdot \nabla \zeta) + \frac{\varepsilon - \zeta}{T} (\mathbf{v} \cdot \nabla T) \right] \left(-\frac{\partial f_0}{\partial \varepsilon} \right).$$

Comparing this expression with the corresponding l.h.s. of Eq. (6.13) of the Boltzmann equation in the case of electric field we observe that an additional effective $\delta \mathbf{E} = \nabla(\zeta/e)$ electric field appears, the total field being

$$\mathbf{E}^* = \nabla \left(\frac{\zeta}{e} - \varphi \right) = -\nabla \varphi^*.$$

The quantity $\varphi^* = \varphi - \zeta/e$ is called the *electrochemical potential*. This quantity rather than the pure electric potential φ describes the transport. In the following we will assume that the static electric field includes this correction. Thus the first item leads to the extra contribution to the Ohmic current and finally $j = \sigma \mathbf{E}^*$. As for the second one, we can plug it into the equation

$$\mathbf{v} \cdot \nabla_{\mathbf{r}} f_0(\mathbf{r}) = \frac{\varepsilon - \zeta}{T} (\mathbf{v} \cdot \nabla T) \left(-\frac{\partial f_0}{\partial \varepsilon} \right) = -\frac{f - f_0}{\tau_{\text{tr}}}$$

to get

$$f_1 = \tau_{\text{tr}} \frac{\varepsilon - \zeta}{T} (\mathbf{v} \cdot \nabla T) \frac{\partial f_0}{\partial \varepsilon}. \quad (6.19)$$

Now we substitute this expression into Eq. (6.14) and calculate the current. The result can be expressed as $\mathbf{j}_T = -\eta \nabla T$ with

$$\eta = -\frac{e}{T} \int d\varepsilon g(\varepsilon) D(\varepsilon) (\varepsilon - \zeta) \left(-\frac{\partial f_0}{\partial \varepsilon} \right). \quad (6.20)$$

This expression differs strongly from the corresponding expression for the conductivity by the factor $(\varepsilon - \zeta)$ under the integral. Indeed, assume that the temperature is zero, so $(-\partial f_0/\partial \varepsilon) = \delta(\varepsilon - \epsilon_F)$. We see that $\eta = 0$. At finite temperatures, some electrons are excited above the Fermi level forming quasi-electron excitations and leaving quasi-hole ones below the Fermi level. Both quasiparticles are dragged by the temperature gradient in the *same* direction, but they have *different* charges. Consequently, there is almost exact compensation of the contributions, the remainder has the order of $k_B T/\epsilon_F$. Indeed, because $(-\partial f_0/\partial \varepsilon)$ is a sharp function we can expand the integrand as

$$g(\varepsilon)D(\varepsilon) = g(\epsilon_F)D(\epsilon_F) + (\varepsilon - \zeta) \left[\frac{d}{d\varepsilon} (g(\varepsilon)D(\varepsilon)) \right]_{\varepsilon=\epsilon_F} .$$

Note that $\epsilon_F \equiv \zeta(T = 0)$. The contribution of the first item vanishes after substitution to Eq. (6.20). To calculate the second contribution we extract the constant factor

$$(gD)'_F \equiv [(d(g(\varepsilon)D(\varepsilon))/d\varepsilon)]_{\varepsilon=\epsilon_F}$$

out of the integral. In the remaining intergral, we introduce a new variable, $\gamma \equiv k_B T(\varepsilon - \zeta)$, and extend the limits of integration over γ to $-\infty, \infty$. We are left with the integral

$$\eta = \frac{ek_B^2 T}{4} (gD)'_F \int_{-\infty}^{\infty} \frac{\gamma^2 d\gamma}{\cosh^2 \gamma / 2}$$

The results is

$$\eta = \frac{\pi^2}{9} e k_B^2 T (gD)'_F .$$

This is the well known Cutler-Mott formula.

There are some important comments in connection with this formula.

- The thermoelectric coefficient is proportional to the *first* power of the charge. Consequently, it feels the type of the carriers and provides the way to determine it from the experiment.
- In the case of non-degenerate materials the thermoelectric coefficient is much more sensitive to the dependence of $D(\epsilon_F)$ on the energy than the conductivity because it contains the derivative.
- If there are several kinds of carriers the behavior of thermoelectric coefficient becomes rich and very instructive to understand what happens.

Thermoelectric effects have important applications. Indeed, we have seen that in our simplest case the current can be written as

$$\mathbf{j} = \sigma \mathbf{E}^* - \eta \nabla T .$$

If the circuit is open $\mathbf{j} = 0$ and we obtain the *thermoelectric field*

$$\mathbf{E}^* = \alpha \nabla T, \quad \alpha = \frac{\eta}{\sigma}.$$

The quantity α is called the *differential thermo-e.m.f.* or *Seebeck coefficient*. Indeed, the voltage across the sample is

$$V = \int_1^2 \alpha(d\mathbf{r} \cdot \nabla T) = \int_{T_1}^{T_2} \alpha(T) dT.$$

To measure this voltage one should prepare the *thermocouple*, i. e. system depicted in Fig. 6.1. It should contain 2 branches fabricated from different materials. The voltage

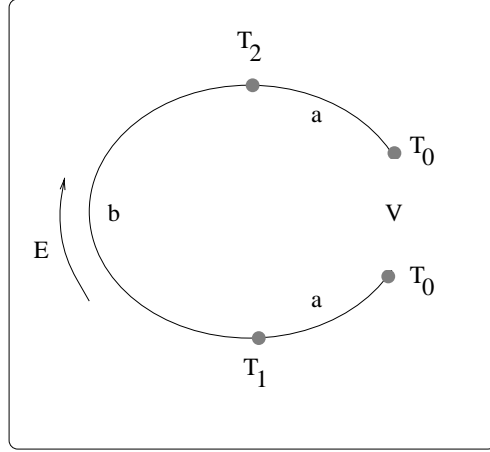


Figure 6.1: The scheme of thermocouple.

measured between the leads is

$$V_T = \int_{T_1}^{T_2} [\alpha_a(T) - \alpha_b(T)] dT.$$

We see that it is a relative effect, to measure absolute thermo-e.m.f. one branch is made of a superconductor.

6.3 Energy Transport

Now we discuss the energy transport in an electron system in the presence of electric field and temperature gradient. First we should define the energy flux. There are 2 conventional ways to express the charge and energy currents, \mathbf{j} and \mathbf{w} , respectively. The first one is to express both currents through the field \mathbf{E}^* and ∇T . In this way

$$\begin{aligned} \mathbf{j} &= \sigma \mathbf{E}^* - \eta \nabla T; \\ \mathbf{w} - \varphi^* \mathbf{j} &= \gamma \mathbf{E}^* - \beta \nabla T. \end{aligned} \tag{6.21}$$

The quantity $\mathbf{w} - \varphi^* \mathbf{j}$ has a physical meaning of the *heat* flux since we subtract the “convective” energy flux $\varphi^* \mathbf{j} = (\zeta - \epsilon\varphi)\langle \mathbf{v} \rangle$ from the total energy flux.

More usual way is to express the electric field and the energy flux through the current \mathbf{j} and ∇T . In this case we get

$$\begin{aligned}\mathbf{E}^* &= \rho \mathbf{j} + \alpha \nabla T; \\ \mathbf{w} - \varphi^* \mathbf{j} &= \Pi \mathbf{j} - \kappa \nabla T.\end{aligned}\tag{6.22}$$

It is clear that

$$\rho = \frac{1}{\sigma}, \quad \alpha = \frac{\eta}{\sigma}, \quad \Pi = \frac{\gamma}{\sigma}, \quad \kappa = \beta + \Pi\eta.$$

The quantity ρ is called *resistivity*, κ is called *thermal conductivity*, while Π is called the *Peltier coefficient*.

The physical nature of the differential thermo-e.m.f. has been already discussed. The nature of the Peltier coefficient can be visualized if one induces a current through the boundary between two materials at a given temperature. If $\Pi_1 \neq \Pi_2$ the fluxes are different and it means that some energy is taken from the contact or it is given to the contact. So, one has the way to cool, or to heat special regions. This is very important property for applications.

Due to fundamental *Onsager relations* all the thermoelectric coefficients can be expressed through only one, say differential thermo-e.m.f. α .

Assume that some generalized forces X_i are applied to the system. They induce currents

$$J_i = \sum_k Q_{ik} X_k$$

where the quantities Q_{ik} are called the *kinetic coefficients*. They are defined so that the entropy production can be expressed as

$$\dot{S} = - \sum_i J_i X_i.$$

The Onsager relations follow from the fact that the entropy production must be positive. Consequently, the tensor \hat{Q} must be *symmetric*,¹

$$Q_{ik} = Q_{ki}.$$

To apply the Onsager relations we have to specify forces and currents. In our case, both the divergence of the energy flux, $-\operatorname{div} \mathbf{w}$, and the Joule heating $\mathbf{j} \mathbf{E}^*$ contribute to the entropy production. Consequently,

$$\dot{S} = - \int \frac{\operatorname{div} \mathbf{w}}{T} dV + \int \frac{\mathbf{j} \mathbf{E}^*}{T} dV.$$

¹In the presence of a magnetic field they should be generalized, see below.

Integrating the first term by parts we get

$$\dot{S} = \int \mathbf{w} \nabla \left(\frac{1}{T} \right) d\mathcal{V} + \int \frac{\mathbf{j} \mathbf{E}^*}{T} d\mathcal{V}.$$

We see that the generalized forces are

$$-\frac{\mathbf{E}^*}{T}, \quad -\nabla \left(\frac{1}{T} \right).$$

Thus the kinetic coefficients for our problem are

$$\begin{aligned} -\sigma T, & -\eta T^2, \\ -\gamma T, & -\beta T^2. \end{aligned}$$

Applying the Onsager relations we obtain $\gamma = \eta T$. Using a similar approach for the Eqs. (6.22), we get $\Pi = \alpha T$. Combining the above equalities we get $\varkappa = \beta - T\eta\alpha$. The second contribution to the thermal conductivity is always small in the degenerate gas (*Problem 6.5*). Consequently, to analyze the thermal conductivity of a metal it is enough to calculate β .

In fact, \varkappa is determined both by electrons and phonons. Here we are interested only in the electron contribution which is usually the main one in typical metals if the temperature is not too low.

One can estimate the coefficient β from the kinetic equation in a similar way as we have done to the thermo-e.m.f. We use the formula (6.19) for the distribution function and take into account that the energy flux transferred by one electron is $(\varepsilon - \zeta)\mathbf{v}$. As a result, instead of Eq. (6.20) we get

$$\varkappa \approx \beta = \frac{1}{T} \int d\varepsilon g(\varepsilon) D(\varepsilon) (\varepsilon - \zeta)^2 \left(-\frac{\partial f_0}{\partial \varepsilon} \right).$$

In the case of strong degeneracy we get

$$\varkappa = \frac{\pi^2}{9} k_B^2 T g(\epsilon_F) D(\epsilon_F).$$

It is interesting to calculate the ratio

$$\frac{\varkappa}{T\sigma} = \frac{\pi^2 k_B^2}{3e^2}.$$

This relation is called the *Wiedemann-Franz law* while its r.h.s. is called the *Lorenz number*. This law is derived under assumptions of isotropic spectrum and elastic scattering. One can show that only the last one is necessary.

So we see that all the characteristics of the d.c. transport are determined by the energy dependence of the quantity $D(\varepsilon)$, i.e. by the energy dependence of the transport relaxation time. If the relaxation time is described by a power law

$$\tau_{\text{tr}}(\varepsilon, T) \propto T^a \varepsilon^r \quad \rightarrow \quad D(\varepsilon, T) \propto T^a \varepsilon^{r+1}$$

we get from Eq. (6.16) $\sigma \propto T^a$ for the degenerate gas. For the Boltzmann gas with the distribution $f_0 \propto \exp(-\varepsilon/k_B T)$ substituting $D(\varepsilon, T) = D_0(T)(\varepsilon/k_B T)^{r+1}$, $g(\varepsilon) = g(T)(\varepsilon/k_B T)^{1/2}$ we obtain

$$\sigma = \frac{e^2 D(T) n_e}{k_B T} \frac{\int_0^\infty x^{r+3/2} e^{-x} dx}{\int_0^\infty x^{1/2} e^{-x} dx} = \frac{e^2 D(T) n_e}{k_B T} \frac{\Gamma(r+5/2)}{\Gamma(3/2)} \propto T^{a+r}.$$

Here $\Gamma(x)$ is the Γ -function.

In the next section we will discuss the scattering processes in more detail and then we come back to the case of semiconductors to discuss the temperature dependencies of the kinetic coefficients.

6.4 Scattering by Neutral and Ionized Impurities.

In the following we will not perform very cumbersome calculations to solve the Boltzmann equation. Rather we will outline the main physics and obtain important estimates. The main goal is to learn how to make those estimates.

To study scattering it is convenient to determine the *scattering cross section*. The simplest idea one can use is that the atom is neutral and behaves as a hard sphere. Nevertheless, in many important situations it is not the case, the atom is *ionized* and has an electric charge.

The very important concept is that the electrons in the vicinity of the impurity atom rearrange to *screen the potential*. Consequently, one should calculate the electric potential which acts upon the electrons from the Poisson equation

$$\epsilon \nabla^2 \varphi = -4\pi e n'_e$$

where $-en'_e$ is the excess electric charge while ϵ is the dielectric constant. The boundary condition for this equation is

$$\varphi = \frac{Ze}{\epsilon r} \quad \text{at } r \rightarrow 0.$$

Now we should remember that in the presence of electric potential the chemical potential ζ is changed to the electrochemical one, $\zeta - e\varphi$. Consequently,

$$n'_e = n_e(\zeta - e\varphi) - n_e(\zeta) \approx -e\varphi \frac{\partial n_e}{\partial \zeta}. \quad (6.23)$$

Finally, the Poisson equation has the form

$$\nabla^2 \varphi - \frac{\varphi}{r_s^2} = 0 \quad (6.24)$$

where

$$r_s = \left(\frac{4\pi e^2}{\epsilon} \frac{\partial n_e}{\partial \zeta} \right)^{-1/2}. \quad (6.25)$$

The solution of the Eq. (6.24) has the form (*Problem 6.6*)

$$\varphi = \frac{Ze}{r} e^{-r/r_s}, \quad (6.26)$$

so the quantity r_s is called the *screening length*.

Now let us estimate the screening length. In a degenerate gas, we get $n_e \propto p_F^3 \propto \epsilon_F^{3/2}$. So

$$\frac{\partial n_e}{\partial \zeta} = \frac{3}{2} \frac{n_e}{\epsilon_F}$$

and

$$r_s = \left(\frac{6\pi e^2 n_e}{\epsilon \epsilon_F} \right)^{-1/2} \equiv r_{TF}.$$

This is the so-called *Thomas-Fermi length*, r_{TF} . For a typical metal we get

$$\frac{1}{r_{TF}} \sim \left(e^2 \frac{p_F^3 m}{\hbar^3 p_F^2} \right)^{1/2} = \frac{p_F}{\hbar} \left(\frac{e^2}{\hbar v_F} \right)^{1/2}.$$

The ratio $e^2/\hbar v_F$ has a clear physical meaning - it is just the ratio of the typical potential energy e^2/\bar{r} to the typical kinetic energy $p_F^2/2m$. Indeed, in a typical metal, $\bar{r} \sim \hbar/p_F$ and

$$\frac{e^2/\bar{r}}{p_F^2/m} \sim \frac{e^2}{\hbar v_F}.$$

This ratio is or the order 1 because the metal is “glued” by the conduction electrons. Consequently, we get that the screening length in a typical metal is of the order of the interatomic distance a and one comes back to the model of hard spheres.

There two important things to be mentioned.

- We have assumed that the electron response is *local*, i. e. the electron density $n'_e(\mathbf{r})$ feels the potential at the same point. In fact, it is not the case because the resulting electrical potential φ varies sharply in space, and the self-consistent approach (6.23) fails. In general,

$$n'_e(\mathbf{r}) = -e \int K(\mathbf{r} - \mathbf{r}') \varphi(\mathbf{r}') dV'.$$

The function K cannot be derived from classical considerations because the typical spatial scale of the potential variation appears of the order of the de Broglie wave length \hbar/p . We will come back to this problem later in connection with the quantum transport. The function $K(r)$ reads (in the isotropic case)

$$K(r) = -g(\epsilon_F) \frac{p_F^3}{(\pi \hbar)^3} \left[\frac{\cos(2k_F r)}{(2k_F r)^3} - \frac{\sin(2k_F r)}{(2k_F r)^4} \right].$$

We see that the response oscillates in space that is a consequence of the Fermi degeneracy (*Friedel oscillations*). These oscillations are important for specific effects but if we are interested in the distances much greater than k_F^{-1} the oscillations are smeared and we return to the picture of the spheres of atomic scale. So one can use the Thomas-Fermi approximation to get estimates.

- In the expression (6.23) we have assumed linear response to the external potential. In typical metals it is the case but in some semiconductors with small electron density one needs some generalizations (not enough electrons to screen). We will come back to the problem discussing hopping transport in semiconductors.

If the electrons are non-degenerate one should plug into the general expression (6.25) the Boltzmann distribution function

$$f_0(\varepsilon) = \exp\left(\frac{\zeta - \varepsilon}{k_B T}\right)$$

to get $\partial n_e / \partial \zeta = n_e / k_B T$. As a result

$$r_s \equiv r_D = \left(\frac{4\pi e^2 n_e}{\epsilon k_B T}\right)^{-1/2},$$

the quantity r_D is called the *Debye-Hukkel* length. One can get

$$\frac{r_D}{\bar{r}} = \sqrt{\frac{k_B T}{4\pi e^2 / \epsilon \bar{r}}},$$

so the estimate differs from the Thomas-Fermi length by the presence $k_B T$ instead of the Fermi energy ϵ_F .

Now we can make a very rough estimate of the conductivity of a typical metal. We get

$$\sigma \sim \frac{n_e e^2 \tau}{m} \sim \frac{n_e e^2 \ell}{p_F} \sim \frac{n_e}{n_i} \frac{e^2}{p_F Q}.$$

Here we have taken into account that

$$\ell = \frac{1}{n_i Q}$$

where Q is the effective cross section. Making use of the estimates

$$Q \sim (\hbar/p_F)^2, \quad e^2 \sim \hbar v_F, \quad n_i/n_e \sim c_i$$

where c_i is the atomic impurity concentration (the numbers of electrons and atoms are the same) we get

$$\sigma \sim 10^{16} / c_i \text{ s}^{-1}.$$

To analyze the situation with the Boltzmann gas one should be more careful because the energy dependence of the relaxation time is important. In this case both a typical de Broglie wave length $\sim \hbar/p$ and the screening length r_s appear much greater than a typical interatomic distance, a . Consequently, while calculating the matrix element $|v(\theta)|$ for scattering against charged impurities one can forget about the periodic potential and

just calculate the matrix element of the potential (6.26) between the plane wave states. As a result, (*Problem 6.7*),

$$W(\theta) = 4\pi n_i v \left[\frac{e^2/\epsilon}{2\epsilon(1 - \cos\theta) + \hbar^2/2mr_s^2} \right]^2. \quad (6.27)$$

After substitution of the cross section in the definition of the transport relaxation time (6.11) we get

$$\tau_{\text{tr}} = \frac{\epsilon^2 m^2 v^3}{2\pi e^4 n_i \Phi(\eta)} = \frac{\sqrt{2m}\epsilon^2 \varepsilon^{3/2}}{\pi e^4 n_i \Phi(\eta)} \quad (6.28)$$

where

$$\Phi(\eta) = \ln(1 + \eta) - \frac{\eta}{1 + \eta}, \quad \eta = \frac{4m^2 v^2 r_s^2}{\hbar^2} = \frac{8m\varepsilon r_s^2}{\hbar^2}.$$

We observe if the screening is neglected $r_s \rightarrow \infty$ than the the transport relaxation time $\tau_{\text{tr}} \rightarrow 0$, and the transport relaxation rate diverges (long-range potential!). The function $\Phi(\eta)$ slowly depends on the energy, so

$$\tau_{\text{tr}} \propto \varepsilon^{3/2}.$$

6.5 Electron-Electron Scattering

Now we estimate the electron-electron scattering, and as usual, we start from the case of Fermi gas. Suppose that particle 1 is excited outside the Fermi sea, the first-order decay is as follows from Fig. 6.2: Particle 1 interacts with particle 2 inside the Fermi shpere, and both subsequently make transitions to states 1' and 2' outside the Fermi sphere (Pauli principle!). According to the momentum conservation law,

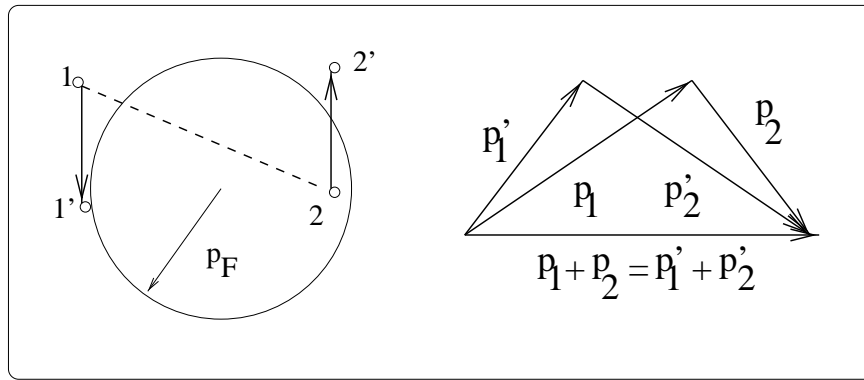


Figure 6.2: Scattering processes for electron-electron interaction.

$$\mathbf{p}_1 + \mathbf{p}_2 = \mathbf{p}'_1 + \mathbf{p}'_2,$$

and, as we have seen,

$$p_1, p'_1, p'_2 > p_F; \quad p_2 < p_F.$$

The momentum conservation law is shown graphically in the right panel of Fig. 6.2. One should keep in mind that the planes $(\mathbf{p}_1, \mathbf{p}_2)$ and $(\mathbf{p}'_1, \mathbf{p}'_2)$ are not the same, they are shown together for convenience. To get the scattering probability for particle 1 one should integrate over the intermediate momenta \mathbf{p}_2 and \mathbf{p}'_1 ,

$$W \propto \int \delta(\varepsilon_1 + \varepsilon_2 - \varepsilon'_1 - \varepsilon'_2) (dp_2) (dp'_1)$$

since \mathbf{p}'_2 is fixed by the momentum conservation. The energy conservation law actually determines the angle between \mathbf{p}'_1 and \mathbf{p}'_2 for given absolute values of these vectors. Consequently, the rest is to integrate over $p_2 = |\mathbf{p}_2|$ and $p'_1 = |\mathbf{p}'_1|$.

Let p_1 be close to p_F . It means that all the momenta are close to p_F and the angles with the resultant vector $\mathbf{p}_1 + \mathbf{p}_2$ are almost the same. So let us assume cosines of these angles to be the same and from the relation between the projections write down

$$p'_1 \approx p_1 + p_2 - p'_2.$$

Now let us recall that $p'_2 > p_F$. Consequently, $p'_1 < p_1 + p_2 - p_F$. But at the same time, $p'_1 > p_F$. Thus

$$p_1 + p_2 - p_F > p_F, \quad \text{or} \quad p_2 > 2p_F - p_1.$$

But from the Pauli principle, the upper limit for p_2 is p_F . As a result, we come to the following chain of inequalities

$$0 > p_2 - p_F > p_F - p_1, \quad 0 < p'_1 - p_F < (p_1 - p_F) + (p_2 - p_F).$$

Finally,

$$\int dp_2 dp'_1 = \int_{-\alpha_1}^0 d\alpha_2 \int_0^{\alpha_1 + \alpha_2} d\alpha'_1 = \frac{\alpha_1^2}{2}$$

where we have introduced $\alpha_i = p_i - p_F$. Now we should remember that $\varepsilon - \epsilon_F = v_F(p - p_F)$. So $W \propto (\varepsilon - \epsilon_F)^2$. The simplest way to estimate τ is to use the dimensionality approach. Indeed, the average potential and kinetic energies are of the order of ϵ_F . Consequently, the only quantity which is proportional to $(\varepsilon - \epsilon_F)^2$ and has the time dimensionality is

$$\tau \sim \frac{\hbar \epsilon_F}{(\varepsilon - \epsilon_F)^2}. \quad (6.29)$$

We came to an important conclusion: the quasiparticles near the Fermi level, $|\varepsilon - \epsilon_F| \ll \epsilon_F$, can be treated as free particles provided

$$\frac{\hbar}{(\varepsilon - \epsilon_F)\tau} \approx \frac{\varepsilon - \epsilon_F}{\epsilon_F} \ll 1.$$

The typical value for the quasiparticle energy is $k_B T \ll \epsilon_F$. This is why the electron-electron interaction can be treated in the leading approximation in a self-consistent approximation which results in a renormalization of the particle mass, $m_0 \rightarrow m^*$, and in a relatively weak damping with the rate τ^{-1} .

Substituting (6.29) in the Drude formula we easily get the estimate of the conductivity, limited by the electron-electron scattering

$$\sigma \sim \frac{n_e e^2 \hbar \epsilon_F}{m(k_B T)^2} \sim 10^{16} \left(\frac{\epsilon_F}{k_B T} \right)^2 \text{ s}^{-1}.$$

Note that electron-electron interaction is the typically *inelastic* one. Electron-electron interaction is usually unimportant for the Boltzmann gas (not too many electrons!). One should also know that disorder drastically increases the electron-electron interaction. We will discuss this problem later.

6.6 Scattering by Lattice Vibrations

Now we come to a very important point - to the electron phonon interaction which leads to many important consequences including superconductivity.

Interaction Hamiltonian (Estimates for Metals)

There are several mechanisms of electron-phonon interaction. First, the deformed lattice creates a polarization \mathbf{P} , the polarization charge being $\text{div } \mathbf{P}$. Consequently, one can write down the interaction energy as

$$-e \int Q(\mathbf{r} - \mathbf{r}') \text{div } \mathbf{P}(\mathbf{r}') d\mathcal{V}'.$$

In the absence of screening, $Q(\mathbf{r} - \mathbf{r}') \propto |\mathbf{r} - \mathbf{r}'|^{-1}$ but *in a typical metal* the screening makes it local. As a result the estimate of $Q(\mathbf{r} - \mathbf{r}')$ is $Q(\mathbf{r} - \mathbf{r}') \approx a^2 \delta(\mathbf{r} - \mathbf{r}')$. The polarization, in its turn, is of the order of $n_a e \mathbf{u}$ where n_a is the atomic density which is of the order of the electron one while \mathbf{u} is the displacement vector. If

$$\mathbf{u}(\mathbf{r}, t) = \sum_{\mathbf{q}} [\mathbf{u}_{\mathbf{q}} e^{i\mathbf{q} \cdot \mathbf{r} - i\omega_{\mathbf{q}} t} + \mathbf{u}_{\mathbf{q}}^* e^{-i\mathbf{q} \cdot \mathbf{r} + i\omega_{\mathbf{q}} t}] ,$$

then \mathbf{q} th Fourier component of the quantity $\text{div } \mathbf{P}(\mathbf{r})$ has the estimate $i n_a e (\mathbf{q} \cdot \mathbf{u}) \approx i(\omega_{\mathbf{q}}/s) n_a e u$. Here we consider the case of acoustic phonons when $q = \omega_{\mathbf{q}}/s$ and s is sound velocity.

Finally, we the following estimate for the Fourier component of the interaction potential

$$U_{\mathbf{q}} \sim ie^2 a^2 n_a \frac{\omega_{\mathbf{q}}}{s} u_{\mathbf{q}} . \quad (6.30)$$

In the following we use the second quantization scheme. According to this approach, phonon system is characterized by number of phonons, $N_{\mathbf{q},j}$, having the wave vector \mathbf{q} and belonging to the branch j , so the state is specified as $|V_{\mathbf{q},j}\rangle$. The so-called phonon annihilation (or creation) operators $b_{\mathbf{q}}, b_{\mathbf{q}}^{\dagger}$ are defined by the properties

$$b|N\rangle = \sqrt{N}|N-1\rangle \quad b^{\dagger}|N\rangle = \sqrt{N+1}|N+1\rangle,$$

the commutation rules being

$$bb^{\dagger} - b^{\dagger}b \equiv [b, b^{\dagger}]_{-} = 1.$$

The creation and annihilation operators for different modes *commute*. It is easy to check the following important properties of the creation and annihilation operators,

$$\begin{aligned} b^{\dagger}b|N\rangle &= N|N\rangle, \\ \langle N'|b|N\rangle &= \sqrt{N}\delta_{N',N-1}, \quad \langle N'|b^{\dagger}|N\rangle = \sqrt{N+1}\delta_{N',N+1}. \end{aligned}$$

The interaction Hamiltonian in terms of electron creation and annihilation operators can be written as

$$\mathcal{H}_{\text{int}} = \sum_{\mathbf{k}\mathbf{k}'} \langle \mathbf{k}' | U(\mathbf{r}) | \mathbf{k} \rangle a_{\mathbf{k}'}^{\dagger} a_{\mathbf{k}} = \sum_{\mathbf{k}\mathbf{k}'} a_{\mathbf{k}'}^{\dagger} a_{\mathbf{k}} \sum_{j\mathbf{q}} \left[C_j(\mathbf{q}) \langle \mathbf{k}' | e^{i\mathbf{qr}} | \mathbf{k} \rangle b_{\mathbf{q}} + C_j^*(\mathbf{q}) \langle \mathbf{k}' | e^{-i\mathbf{qr}} | \mathbf{k} \rangle b_{\mathbf{q}}^{\dagger} \right].$$

Here $C_j(\mathbf{q})$ absorbs proportionality coefficients between the perturbation potential and normal coordinates.

From the properties of Bloch functions and lattice vibrations one can prove (Check!) that

$$\langle \mathbf{k}' | e^{i\mathbf{qr}} | \mathbf{k} \rangle = \sum_{\mathbf{G}} \delta(\mathbf{k}' - \mathbf{k} \mp \mathbf{q} - \mathbf{G}) \equiv \Delta_{\mathbf{k}', \mathbf{k} + \mathbf{q}} \quad (6.31)$$

where \mathbf{G} are the reciprocal lattice vectors. Finally we can express the interaction Hamiltonian as

$$\begin{aligned} \mathcal{H}_{\text{int}} &= \sum_{j\mathbf{q}\mathbf{k}\mathbf{k}'} a_{\mathbf{k}'}^{\dagger} a_{\mathbf{k}} \left[C_j(\mathbf{q}) \Delta_{\mathbf{k}', \mathbf{k} + \mathbf{q}} b_{\mathbf{q}} + C_j^*(\mathbf{q}) \Delta_{\mathbf{k}', \mathbf{k} - \mathbf{q}} b_{\mathbf{q}}^{\dagger} \right] \\ &= \sum_{j\mathbf{q}\mathbf{k}\mathbf{k}'} C_j(\mathbf{q}) \Delta_{\mathbf{k}', \mathbf{k} + \mathbf{q}} a_{\mathbf{k}'}^{\dagger} a_{\mathbf{k}} b_{\mathbf{q}} + \text{h.c.} \end{aligned} \quad (6.32)$$

Here h.c. stands for Hermitian conjugate. The form (6.32) is very illustrative to show the important transitions.

We can specify the following processes

- Phonon emission:

$$\begin{aligned} \text{electron} &: \text{scattered, } \mathbf{k} \rightarrow \mathbf{k}' = \mathbf{k} - \mathbf{q} + \mathbf{G} \\ \text{phonon} &: \text{created with the momentum } \hbar\mathbf{q}. \\ \text{matrix element} &: M_{\mathbf{k}, \mathbf{k}'}^{+} = C_{\mathbf{q}}^* \sqrt{N_{\mathbf{q}} + 1} \langle \mathbf{k}' | e^{-i\mathbf{qr}} | \mathbf{k} \rangle \\ \text{operator form} &: \sum_{\mathbf{G}} C_{\mathbf{q}}^* a_{\mathbf{k}'}^{\dagger} a_{\mathbf{k}} b_{\mathbf{q}}^{\dagger} \delta(\mathbf{k}' - \mathbf{k} + \mathbf{q} - \mathbf{G}). \end{aligned} \quad (6.33)$$

- Phonon absorption

$$\begin{aligned}
 \text{electron} &: \text{scattered}, \quad \mathbf{k} \rightarrow \mathbf{k}' = \mathbf{k} + \mathbf{q} + \mathbf{G} \\
 \text{phonon} &: \text{absorbed with the momentum } \hbar\mathbf{q}. \\
 \text{matrix element} &: M_{\mathbf{k}, \mathbf{k}'}^- = C_{\mathbf{q}} \sqrt{N_{\mathbf{q}}} \langle \mathbf{k}' | e^{i\mathbf{qr}} | \mathbf{k} \rangle \\
 \text{operator form} &: \sum_{\mathbf{G}} C_{\mathbf{q}} a_{\mathbf{k}'}^\dagger a_{\mathbf{k}} b_{\mathbf{q}} \delta(\mathbf{k}' - \mathbf{k} - \mathbf{q} - \mathbf{G})
 \end{aligned} \tag{6.34}$$

To estimate the quantities $C_{\mathbf{q}}$ one has to substitute to Eq. (6.30) the expression for $\mathbf{u}_{\mathbf{q}}$, i. e. to express the lattice displacement in terms of phonon annihilation and creation operators, b and b^\dagger , respectively. For a simple lattice the coefficients $\mathbf{u}_{\mathbf{q}}$ acquire the following operator form:

$$\hat{\mathbf{u}}_{\mathbf{q}} \rightarrow \sqrt{\frac{\hbar}{2\omega_{\mathbf{q}}NM}} \mathbf{e}_{\mathbf{q}} b_{\mathbf{q}}, \quad \hat{\mathbf{u}}_{\mathbf{q}}^* \rightarrow \sqrt{\frac{\hbar}{2\omega_{\mathbf{q}}NM}} \mathbf{e}_{\mathbf{q}} b_{\mathbf{q}}^\dagger.$$

Here N is the number of atoms in the sample, M is the atomic mass, $\mathbf{e}_{\mathbf{q}}$ is the unit vector parallel to $\mathbf{u}_{\mathbf{q}}$. We have taken into account only one acoustic mode. This procedure leads to the following estimate for $C(\mathbf{q})$

$$C_{\mathbf{q}} \sim i \frac{e^2 a^2 n_a \omega}{\sqrt{NM} s} \sqrt{\frac{\hbar}{\omega}} \sim i \sqrt{\frac{\hbar n_a \omega}{\mathcal{V} n_a M}} \frac{e^2 a^2 n_a}{s} \sim i n_a a^3 \frac{e^2}{a} \frac{1}{s \sqrt{M}} \sqrt{\frac{\hbar \omega}{\mathcal{V} n_a}} \sim i \sqrt{\frac{\hbar \omega}{\mathcal{V} m n_a}} p_F. \tag{6.35}$$

Here $n_a = N/\mathcal{V}$, we have taken into account that $n_a a^3 \sim 1$, $e^2/a \sim \epsilon_F \sim p_F^2/2m$, $s\sqrt{M} \sim v_F \sqrt{m}$.

Transition Probability

Now we can construct the transition probabilities from the Fermi golden rule,

$$W_{fi} = \frac{2\pi}{\hbar} |M_{fi}|^2 \delta(\varepsilon_f - \varepsilon_i)$$

where the subscripts i, f stand for the initial and final state, respectively.

For simplicity we assume here that $\mathbf{G} = 0$, that is the case for the most interesting situations (see later). For the case (6.33) we get

$$W_{\mathbf{k}-\mathbf{q}, \mathbf{k}}^+ = \frac{2\pi}{\hbar} |C_{j\mathbf{q}}|^2 (N_{\mathbf{q}} + 1) \delta[\varepsilon(\mathbf{k} - \mathbf{q}) - \varepsilon(\mathbf{k}) + \hbar\omega_j(\mathbf{q})].$$

The probability of the absorption process (6.34) is

$$W_{\mathbf{k}+\mathbf{q}, \mathbf{k}}^- = \frac{2\pi}{\hbar} |C_{j\mathbf{q}}|^2 N_{\mathbf{q}} \delta[\varepsilon(\mathbf{k} + \mathbf{q}) - \varepsilon(\mathbf{k}) - \hbar\omega_j(\mathbf{q})].$$

for the absorption one. The total probability for the $\mathbf{k} \rightarrow \mathbf{k} - \mathbf{q}$ transitions for a given phonon branch is then:

$$\begin{aligned}
 W_{\mathbf{k}-\mathbf{q} \leftarrow \mathbf{k}} &= (2\pi/\hbar) |C_{\mathbf{q}}|^2 \\
 &\times \left\{ \underbrace{(N_{\mathbf{q}} + 1) \delta[\varepsilon(\mathbf{k} - \mathbf{q}) - \varepsilon(\mathbf{k}) + \hbar\omega_{\mathbf{q}}]}_{\text{emission}} + \underbrace{N_{-\mathbf{q}} \delta[\varepsilon(\mathbf{k} - \mathbf{q}) - \varepsilon(\mathbf{k}) - \hbar\omega_{\mathbf{q}}]}_{\text{absorption}} \right\}.
 \end{aligned} \tag{6.36}$$

To get the probability of the reverse transition, $W_{\mathbf{k} \leftarrow \mathbf{k}-\mathbf{q}}$, one should first replace $\mathbf{k} \rightarrow \mathbf{k} + \mathbf{q}$ and then $\mathbf{q} \rightarrow -\mathbf{q}$. We get

$$W_{\mathbf{k} \leftarrow \mathbf{k}-\mathbf{q}} = (2\pi/\hbar) |C_{\mathbf{q}}|^2 \times \left\{ \underbrace{(N_{-\mathbf{q}} + 1)\delta[\varepsilon(\mathbf{k} - \mathbf{q}) - \varepsilon(\mathbf{k}) - \hbar\omega_{\mathbf{q}}]}_{\text{emission}} + \underbrace{N_{\mathbf{q}}\delta[\varepsilon(\mathbf{k} - \mathbf{q}) - \varepsilon(\mathbf{k}) + \hbar\omega_{\mathbf{q}}]}_{\text{absorption}} \right\}. \quad (6.37)$$

To construct the transition rate *from* the state \mathbf{k} one has to multiply Eq. (6.36) by the factor $f_{\mathbf{k}}(1 - f_{\mathbf{k}-\mathbf{q}})$ and then sum over the phonon brancehs j and wave vectors \mathbf{q} . The transtion rate *to* the state \mathbf{k} is given by multiplication of Eq. (6.37) by the factor $f_{\mathbf{k}-\mathbf{q}}(1 - f_{\mathbf{k}})$ with subsequent similar summation. Finally we come to the following collision integral

$$I = \frac{2\pi}{\hbar} \sum_{j\mathbf{q}} |C_j(\mathbf{q})|^2 [F_{\mathbf{k},\mathbf{k}-\mathbf{q}}^+ \delta(\varepsilon_{\mathbf{k}-\mathbf{q}} - \varepsilon_{\mathbf{k}} - \hbar\omega_{j\mathbf{q}}) + F_{\mathbf{k},\mathbf{k}-\mathbf{q}}^- \delta(\varepsilon_{\mathbf{k}-\mathbf{q}} - \varepsilon_{\mathbf{k}} + \hbar\omega_{j\mathbf{q}})] \quad (6.38)$$

where

$$\begin{aligned} F_{\mathbf{k},\mathbf{k}-\mathbf{q}}^+ &= f_{\mathbf{k}}(1 - f_{\mathbf{k}-\mathbf{q}})N_{-\mathbf{q}j} - f_{\mathbf{k}-\mathbf{q}}(1 - f_{\mathbf{k}})(N_{-\mathbf{q}j} + 1), \\ F_{\mathbf{k},\mathbf{k}-\mathbf{q}}^- &= f_{\mathbf{k}}(1 - f_{\mathbf{k}-\mathbf{q}})(N_{\mathbf{q}j} + 1) - f_{\mathbf{k}-\mathbf{q}}(1 - f_{\mathbf{k}})N_{\mathbf{q}j}. \end{aligned} \quad (6.39)$$

Now we start from rough estimates and then derive the relaxation rate more carefully.

Relaxation Time for Phonon Scattering.

Rough Estimate.

To get a rough estimate we first understand that the maximal phonon frequency is ω_D that corresponds to $q_D \sim \pi/a \sim k_F$. One has the estimate $\hbar\omega_D \sim \hbar s\pi/a \sim sp_F$. So there are two limiting cases which differ by the relation between $\hbar\omega_D$ and $k_B T$.

1. At high temperature,

$$k_B T \gg \hbar\omega_D,$$

the most probable are the processes with high-frequency phonons, $\omega \approx \omega_D$, and we can use the classical limit for the Planck function

$$N_{\mathbf{q}} \approx \frac{k_B T}{\hbar\omega_{\mathbf{q}}} \approx \frac{k_B T}{\hbar\omega_D} \gg 1.$$

We see that all the items in the collision integral have the same order. The integral over the \mathbf{q} is of the order

$$\frac{q_D^3}{\epsilon_F} \sim \frac{mp_F}{\hbar^3}.$$

Using the estimate (6.35) for the coefficient $C_{\mathbf{q}}$ we get

$$\frac{1}{\tau_{\text{tr}}} \sim \frac{1}{\hbar} p_F^2 \frac{\hbar\omega_D}{mn_a} \frac{k_B T}{\hbar\omega_D} \frac{mp_F}{\hbar^3} \sim \frac{k_B T}{\hbar}.$$

The estimate for conductivity is

$$\sigma = \frac{n_e e^2 \tau}{m} \sim \frac{p_F^2}{m \hbar k_B T} \frac{\epsilon_F}{k_B T} \sim 10^{16} \frac{\epsilon_F}{k_B T} \text{ s}^{-1}.$$

2. At low temperatures where

$$k_B T \ll \hbar \omega_D$$

the thermal phonons with $\hbar \omega \sim k_B T$ are most important, their wave vector being

$$q_T \sim k_B T / \hbar s.$$

We see that $q_T \ll k_F$. So these collisions are strongly *inelastic* - the change of the excitation energy (with respect to the Fermi level) is of the order of the excitation energy itself, while the change of momentum is relatively small. The δ -function in the conservation laws can be written as

$$\delta \left[\frac{\mathbf{p}^2}{2m} - \frac{(\mathbf{p} - \hbar \mathbf{q})^2}{2m} \pm \hbar \omega_{\mathbf{q}} \right] = \delta \left[\frac{\hbar \mathbf{p} \mathbf{q}}{m} - \frac{\hbar^2 q^2}{2m} \pm \hbar \omega_{\mathbf{q}} \right] = \frac{m}{\hbar p q} \delta \left[\cos \vartheta - \frac{\hbar q}{2p} \pm \frac{ms}{q} \right].$$

We see that both the items under the δ -function are small (the second one is of the order $ms/p_F \sim s/v_F \ll 1$). The integral over \mathbf{q} splits into the integral over the length of the wave vector and over the angles. Thus the δ -function gives 1 after the integration over the angles because it requests $|\cos \vartheta| \ll 1$. Finally, we get the following estimate

$$\frac{1}{\tau} \sim \frac{1}{\hbar} \frac{p_F^2 \hbar \omega}{mn_a} \frac{m}{\hbar p_F q} q^3 \sim \frac{1}{\hbar} \frac{p_F^2 \hbar \omega}{mn_a} \frac{ms}{p_F \hbar \omega} \left(\frac{\omega}{s} \right)^3 \sim \frac{1}{\hbar} \frac{p_F^2 k_B T}{m(p_F/\hbar)^3} \frac{ms}{p_F k_B T} \frac{(k_B T)^3}{\hbar^3 s^3} \sim \frac{k_B T}{\hbar} \left(\frac{k_B T}{\hbar \omega_D} \right)^2.$$

This is the good estimate for the escape relaxation time. To get the estimate one should multiply this quantity by the characteristic value of

$$1 - \cos \theta \approx \theta^2/2 \sim (\hbar q/p_F)^2 \sim (k_B T/\hbar \omega_D)^2.$$

As a result,

$$\frac{1}{\tau_{\text{tr}}} \sim \frac{k_B T}{\hbar} \left(\frac{k_B T}{\hbar \omega_D} \right)^4$$

and the conductivity acquires an extra factor $(\hbar \omega_D/k_B T)^4$:

$$\sigma \sim 10^{16} \frac{\epsilon_F}{k_B T} \left(\frac{\hbar \omega_D}{k_B T} \right)^4 \text{ s}^{-1}.$$

We see that for small-angle scattering the transport time is much longer than the escape time. It is interesting that in the expression for the thermal conductivity one can study the relaxation of the energy flux. For the energy flux, every collision is effective and the proper estimate for the relaxation rate is the escape time τ . As a result, the Wiedemann-Franz law is not valid any more, and

$$\frac{\kappa}{T \sigma} \sim \frac{k_B^2}{e^2} \left(\frac{k_B T}{\hbar \omega_D} \right)^2.$$

Derivation of the Relaxation Time. ²

Now we outline the procedure of more rigorous derivation of the relaxation rate which includes the summation over \mathbf{q}

$$\sum_{\mathbf{q}} \rightarrow \frac{\mathcal{V}}{(2\pi)^3} \int_{q_{\min}}^{q_{\max}} q^2 dq \int_0^\pi \sin \vartheta d\vartheta \int_0^{2\pi} d\varphi$$

where q_{\min} and q_{\max} are determined by the conservation laws, $\vartheta \equiv (\widehat{\mathbf{q}}, \mathbf{k})$.

First, one should prove the relaxation time approximation, i.e. that

$$I(f_1) \propto f_1.$$

To prove it let us (as we have done earlier) search the solution as

$$f_1 = -\mathbf{n}\mathbf{f}(\varepsilon) = -f \cos(\widehat{\mathbf{f}, \mathbf{k}}), \quad \mathbf{n} \equiv \mathbf{k}/k$$

and chose the polar axis \mathbf{z} along the vector \mathbf{k} . In our notations

$$1 - \cos(\widehat{\mathbf{k}, \mathbf{k} - \mathbf{q}}) = (\mathbf{q} \cdot \mathbf{k})/qk = \cos \vartheta.$$

As in the case of impurity scattering, it is convenient to use the relation

$$\mathbf{f}\mathbf{q} = f_z q_z + \mathbf{f}_{\perp} \mathbf{q}_{\perp},$$

or

$$\begin{aligned} \cos(\widehat{\mathbf{f}, \mathbf{q}}) &= \cos(\widehat{\mathbf{k}, \mathbf{q}}) \cos(\widehat{\mathbf{f}, \mathbf{k}}) + \sin(\widehat{\mathbf{k}, \mathbf{q}}) \sin(\widehat{\mathbf{f}, \mathbf{k}}) \cos \varphi_{q,f} \\ &= \cos \vartheta \cos(\widehat{\mathbf{f}, \mathbf{k}}) + \sin \vartheta \sin(\widehat{\mathbf{f}, \mathbf{k}}) \cos \varphi_{q,f}. \end{aligned}$$

Now we can integrate this equation over $\varphi_{q,f}$ taking into account that the angle $(\widehat{\mathbf{f}, \mathbf{k}})$ is $\varphi_{q,f}$ -independent.(see Fig. 6.3). We get

$$\int \cos(\widehat{\mathbf{f}, \mathbf{q}}) d\varphi = 2\pi \cos \vartheta \cos(\widehat{\mathbf{f}, \mathbf{k}}).$$

The term $\cos(\widehat{\mathbf{f}, \mathbf{k}})$ can be extracted from the integral over \mathbf{q} and we have proved that $I(f_1) \propto f_1$.

Finally, after neglecting of the term proportional to s/v we get

$$\begin{aligned} \frac{1}{\tau_{\text{tr}}} &= -\frac{(2\pi)^2}{\hbar} \frac{\mathcal{V}}{(2\pi)^3} \int_{q_{\min}}^{q_{\max}} q^2 dq |C(q)|^2 \frac{m}{\hbar^2 k q} \frac{q}{k} \int_0^\pi \sin \vartheta \cos \theta d\vartheta \\ &\quad \times [N_q \delta(q/2k + \cos \theta) - (N_q + 1) \delta(q/2k - \cos \theta)] \\ &= \frac{\mathcal{V}}{8\pi^2} \frac{m}{\hbar^2 k^3} \int_{q_{\min}}^{q_{\max}} |C(q)|^2 (2N_q + 1) q^3 dq. \end{aligned} \tag{6.40}$$

²Optional section

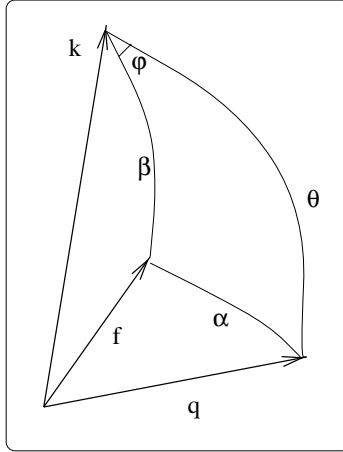


Figure 6.3: The arrangement of angles.

The result is determined by its limits determined by the conservation law and by the phonon spectrum. We have $q_{\min} = 0$ while

$$q_{\max} = \min(q_D, 2k), \quad \omega_{\max} = \max(\omega_D, 2ks).$$

At high temperature, at $\hbar\omega_{\max} \leq k_B T$, as was shown, $N_q \approx k_B T / \hbar s$ and we get

$$\frac{1}{\tau_{\text{tr}}} \propto \frac{1}{k^3} \int^{q_D} q \frac{k_B T}{\hbar s q} q^3 dq \propto \frac{T q_D^4}{k^3} \begin{cases} q_D^4 & \text{for } q_D < 2k \\ (2k)^4 & \text{for } q_D > 2k \end{cases} \propto T \begin{cases} \varepsilon^{-3/2} \\ \varepsilon^{1/2} \end{cases}$$

That is consistent with the rough estimates given above. The last case is important for semiconductors with low values of k . Remember that for the Boltzmann gas the typical value of $\hbar k$ is $\sqrt{mk_B T}$. Indeed,

$$\frac{\hbar sk}{k_B T} \approx \sqrt{\frac{ms^2}{k_B T}}, \quad ms^2 \rightarrow 0.1 \text{ K.}$$

In typical metals, $k \sim k_F \sim q_D$, and at low temperatures we meet the case $\hbar\omega_{\max} \leq k_B T$. This case is much more tricky because the collisions are *inelastic* and we cannot use the expression (6.11) for the relaxation time. Actually, one should linearize the collision integral (6.38). The main steps of the derivation are given below.

We transform the collision integral as follows. First we denote $f_{\mathbf{k}} = f_1 + \varphi_1$, $f_{\mathbf{k}-\mathbf{q}} = f_2 + \varphi_2$, where $f_{i,k}$ are equilibrium functions, and then linearize with respect to φ_i . We get

$$\begin{aligned} F_{\mathbf{k},\mathbf{k}-\mathbf{q}}^+ &= f_{\mathbf{k}}(1 - f_{\mathbf{k}-\mathbf{q}})N_{-\mathbf{q}} - f_{\mathbf{k}-\mathbf{q}}(1 - f_{\mathbf{k}})(N_{-\mathbf{q}} + 1) \\ &\rightarrow [\varphi_1(1 - f_2) - \varphi_2 f_1] N - [\varphi_2(1 - f_1) - \varphi_1 f_2] (N + 1) \\ &= \varphi_1 [N(1 - f_2) + f_2(N + 1)] - \varphi_2 [Nf_1 + (N + 1)(1 - f_1)] \\ &= \varphi_1 (N + f_2) - \varphi_2 (N + 1 - f_1) \end{aligned}$$

for the phonon emission and

$$\begin{aligned} F_{\mathbf{k}, \mathbf{k}-\mathbf{q}}^- &= f_{\mathbf{k}}(1 - f_{\mathbf{k}-\mathbf{q}})(N_{\mathbf{q}} + 1) - f_{\mathbf{k}-\mathbf{q}}(1 - f_{\mathbf{k}})N_{\mathbf{q}} \\ &\rightarrow (\varphi_1(1 - f_2) - \varphi_2 f_1)(N + 1) - (\varphi_2(1 - f_1) - \varphi_1 f_2)N \\ &= \varphi_1((N + 1)(1 - f_2) + f_2 N) - \varphi_2((N + 1)f_1 + N(1 - f_1)) \\ &= \varphi_1(N + 1 - f_2) - \varphi_2(N + f_1) \end{aligned}$$

for the absorption. Then we search solution in a form

$$\varphi(\mathbf{k}) = a(\mathbf{k}) \left(-\frac{\partial f_0}{\partial \varepsilon} \right) = \frac{a(\mathbf{k})}{k_B T} f_0(1 - f_0)$$

where $a(\mathbf{k})$ weakly depends on the energy, but strongly depends on the direction of \mathbf{k} . As a result, we have

$$k_B T F_{\mathbf{k}, \mathbf{k}-\mathbf{q}}^+ = a_1 f_1(1 - f_1)(N + f_2) - a_2 f_2(1 - f_2)(N + 1 - f_1) \rightarrow \text{emission}$$

To get a similar formula for absorption one should make a similar substitution. The result can be obtained from that above by the replacement $N \leftrightarrow N + 1$, $f \leftrightarrow 1 - f$,

$$a_1 f_1(1 - f_1)(N + 1 - f_2) - a_2 f_2(1 - f_2)(N + f_1)$$

and then replace $1 \leftrightarrow 2$ in the δ -functions to take into account the conservation law. Finally,

$$k_B T F_{\mathbf{k}, \mathbf{k}-\mathbf{q}}^- = a_1 f_2(1 - f_2)(N + 1 - f_1) - a_2 f_1(1 - f_1)(N + f_2) \rightarrow \text{absorptiom}$$

Combining with the expression for the emission and absorption we get

$$\frac{(a_1 - a_2)}{k_B T} [f_2(1 - f_2)(N + 1 - f_1) + f_1(1 - f_1)(N + f_2)].$$

Fragments in the square brackets are

$$N + 1 - f_1 = \frac{e^\nu}{e^\nu - 1} - \frac{1}{e^\nu + 1} = N f_1 (e^{x+\nu} + e^\nu - e^\nu + 1) = N \frac{f_1}{f_2},$$

$$N + f_2 = \frac{1}{e^\nu - 1} + \frac{1}{e^{x+\nu} + 1} = N f_2 (e^{x+\nu} + 1 + e^\nu - 1) = (N + 1) \frac{f_2}{f_1}$$

where $x = (\varepsilon - \zeta)/k_B T$, $\nu = \hbar\omega/k_B T$. Finally, we get in the brackets

$$N f_1(1 - f_2) + (N + 1) f_2(1 - f_1) = 2N f_1(1 - f_2)$$

and the integrand in the collision integral becomes proportional to

$$\frac{2N f_1(1 - f_2)}{k_B T} (a_1 - a_2).$$

We see that only thermal phonons are important since the integrand of the collision operator decreases exponentially at $\nu \gg 1$. As a result, we have proved the estimates made above. Unfortunately, the relaxation time approximation is not exact in this case and one should solve the Boltzmann equation numerically.

Umklapp-Processes³

It was a sort of cheating in our previous calculations of the electron-electron scattering. Indeed, suppose that we have only electrons which do not know anything about the lattice. How can the total momentum of the whole electron system relax?

To understand this important problem one should remember that there are processes where the quasimomentum is not conserved but there is a momentum transfer $\hbar\mathbf{G}$. To analyze the situation more carefully we write down the collision integral

$$\begin{aligned} I(f) = & - \int W_{\mathbf{p}_1 \mathbf{p}_2}^{\mathbf{p}'_1 \mathbf{p}'_2} \left[f_{\mathbf{p}_1} f_{\mathbf{p}_2} (1 - f_{\mathbf{p}'_1}) (1 - f_{\mathbf{p}'_2}) - f_{\mathbf{p}'_1} f_{\mathbf{p}'_2} (1 - f_{\mathbf{p}_1}) (1 - f_{\mathbf{p}_2}) \right] \\ & \times \delta(\varepsilon_1 + \varepsilon_2 - \varepsilon'_1 - \varepsilon'_2) (dp_2) (dp'_1). \end{aligned} \quad (6.41)$$

Here we assume that the momentum \mathbf{p}'_2 is determined by the conservation law

$$\mathbf{p}_1 + \mathbf{p}_2 = \mathbf{p}'_1 + \mathbf{p}'_2 + \hbar\mathbf{G}$$

and one should integrate over the remaining 2 variables. Because the process is inelastic we search the non-equilibrium function f_1 as

$$f_1(\mathbf{p}) = a(\mathbf{p}) \left(-\frac{\partial f_0}{\partial \varepsilon} \right) = \frac{a(\mathbf{p})}{k_B T} f_0 (1 - f_0). \quad (6.42)$$

We have 4 terms proportional to a . The terms proportional to $a(\mathbf{p}_1) \equiv a_1$ are

$$-\frac{a_1}{k_B T} f_1 (1 - f_1) \left[f_2 (1 - f'_1) (1 - f'_2) + f'_1 f'_2 (1 - f_2) \right]$$

where all the functions are the equilibrium Fermi ones. Using the detailed balance equation

$$f_1 f_2 (1 - f'_1) (1 - f'_2) - f'_1 f'_2 (1 - f_1) (1 - f_2) = 0$$

we transform the previous equation as (Check!)

$$-\frac{a_1}{k_B T} f_1 f_2 (1 - f'_1) (1 - f'_2).$$

The same transformation can be done with all other terms and we get the following combinations in the collision integral (6.41).

$$\frac{1}{k_B T} f_1 f_2 (1 - f'_1) (1 - f'_2) (a_1 + a_2 - a'_1 - a'_2).$$

If we assume that $a \propto p_i$ we get that the last bracket vanishes because of the momentum conservations. Consequently, we have no relaxation and a finite current in the absence of

³Optional section

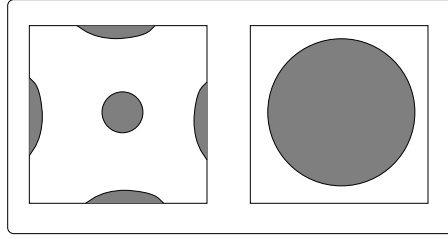


Figure 6.4: The Fermi surfaces of alkali metals and semimetals.

any field. To get a finite answer one should take into account the processes with finite \mathbf{G} , the so-called *Pierls Umklapp processes*.

We have seen that if \mathbf{p}_1 is close to the Fermi surface all other momenta are also close to the Fermi surface, all the vectors being in the BZ. Thus to get a finite resistance one should request

$$\max(|\mathbf{p}_1 + \mathbf{p}_2 - \mathbf{p}'_1 - \mathbf{p}'_2|) = \hbar G_{\min}$$

or

$$4 \max p_F(\mathbf{n}) > \hbar G_{\min}.$$

This relation is definitely met if the FS reaches the boundary of the BZ. The same is true for the metals with near-spherical FS because the volume of the FS is equal to 1/2 of the BZ volume (half full band). It means that the radius of the FS is greater than 1/2 of the reciprocal lattice vector.

In semimetals like Bi the FS contains quasi-electron and quasi-hole valleys and electron-electron interaction is important for inter-valley transitions (see Fig. 6.4).

The situation is more complicated for electron-phonon collisions. We have assumed the phonons to be equilibrium. It means that we assume some effective mechanism to create equilibrium in the phonon gas, say, scattering of phonons by defects or phonon-phonon interaction including Umklapp processes. If the metal is very pure and the temperature is low the only scattering mechanism for phonons is their scattering by the electrons. Consequently, one should construct the Boltzmann equation for phonons

$$\frac{\partial N_{\mathbf{q}}}{\partial t} + \frac{\partial \omega(\mathbf{q})}{\partial \mathbf{q}} \frac{\partial N_{\mathbf{q}}}{\partial \mathbf{r}} = I_{ph}(N_{\mathbf{q}}).$$

The collision integral with electrons has the form

$$I_{ph-e} = \int W [f_1(1-f_2)(N_{\mathbf{q}} + 1) - (1-f_1)f_2 N_{\mathbf{q}}] \delta(\varepsilon_1 - \varepsilon_2 - \hbar\omega_{\mathbf{q}}) (dp_1)$$

Again, we can search the solution for electrons as (6.42) and for phonon in the form

$$N_1(\mathbf{q}) = b(\mathbf{q}) \left(-\frac{\partial N_0}{\partial (\hbar\omega)} \right) = \frac{b(\mathbf{q})}{k_B T} N_0 (1 + N_0).$$

As a result, we get

$$I \approx \int W f_{10}(1 - f_{20})(N_{\mathbf{q}0} + 1)(a_1 - a_2 - b) (dp_1).$$

Again, if $a \propto p_i$, $b \propto \hbar q_i$ we get zero. Physically, it means the sum of electron and phonon quasimomenta conserve. As a result, we have a persistent motion of electrons accompanied by a "phonon wind". Again, we need the Umklapp processes to get finite electric and thermal conductivity. At high temperatures it is not a problem to find such processes. But at low temperatures the momenta of thermal phonons are small, and one can neglect the phonon quasimomenta in the conservation law

$$\mathbf{p}_1 - \mathbf{p}_2 - \hbar \mathbf{q} = \hbar \mathbf{G}.$$

So we come to the criterion

$$2 \max p_F(\mathbf{n}) > \hbar G_{\min}$$

that cannot be met if the FS does not touch the BZ boundary. That changes all the kinetics because thermal phonons cannot take the electron momentum. Consequently, we need high-frequency phonons with $q \sim q_D$, their number being proportional to $\exp(-T_0/T)$ where $T_0 \sim \hbar \omega_D / k_B$. The resulting situation appears very tricky. To get an insight, let us come to the picture of extended BZs periodic in the reciprocal space. If the FS is open the electron momenta relaxation is just a diffusion along this surface and we have shown that

$$\tau_e \sim \frac{1}{\omega_D} \left(\frac{\hbar \omega_D}{k_B T} \right)^5.$$

If the FS is closed, Umklapp processes mean *hops* between different branches. As a result, we get

$$\frac{1}{\tau_u} \sim \omega_D \underbrace{\left(\frac{k_B T_0}{\hbar \omega_D} \right)^3 e^{-T_0/T}}_{\text{number of phonons}} \cdot \underbrace{\frac{k_B T}{\hbar \omega_D}}_{\text{part of time}}.$$

The last factor is just the part of time which electron spends near the region to which it can hop. Indeed, $\delta p \approx k_B T / s$, and $\delta p / p_F \sim k_B T / \hbar \omega_D$. The total relaxation time is a sum

$$\tau' = \tau_e + \tau_u$$

of the diffusion time over the closes surface and the time τ_u , the longest being most important. Note that here we add partial times rather than rates. The reason is that the scattering events take place sequentially.

As a result, we come to a crossover between the power and exponential temperature dependencies. Remember that all this physics is relevant only to very clean metals, otherwise impurity scattering is the most important at low temperatures.

Temperature Dependence of Resistivity in Metals

Now we review the temperature dependence of the conductivity of metals. We have assumed recently that only one scattering mechanism is important. In real life there is a mixture of the mechanisms, the interplay being temperature dependent. If we assume the mechanisms to be independent the *resistivities* ρ are approximately additive because one should sum the scattering *rates*. So, according to the results of Boltzmann equation, at low temperatures

$$\rho = c + \underbrace{aT^2}_{\text{e-e}} + \underbrace{bT^5}_{\text{e-ph}}$$

(except alkali metals) while at high temperatures phonon scattering is the most important and

$$\rho = AT.$$

The corresponding dependences of the thermal conductivity are

$$\kappa^{-1} = dT^{-1} + fT + gT^2, \quad \text{and} \quad \kappa = \text{const.}$$

The temperature dependence of the resistivity of semiconductors is more tricky because the electron concentration is temperature dependent. We will come back to this problem later.

It is also important to know, that at very low temperatures quantum contribution to resistivity becomes important. This contribution cannot be analyzed with the help of the Boltzmann equation and we will also discuss it later.

6.7 Electron-Phonon Interaction in Semiconductors

Acoustic Phonons

Deformational interaction

Usually, the interaction with acoustic phonons in semiconductors is expressed in terms of the so-called *deformation potential*. For long waves one can describe the crystal as an elastic continuum, the deformation being characterized by the *strain tensor*

$$\hat{u} \rightarrow u_{ik} = \frac{1}{2} \left(\frac{\partial u_i}{\partial x_k} + \frac{\partial u_k}{\partial x_i} \right).$$

The strain changes the distances between atoms and, as a result, the electron energies change. A typical picture of the change of the forbidden gap width under the influence of an acoustic vibration is shown in Fig. (6.5). Note that the strain leads to a different influence than an electric field which shifts both bands in the same direction. Consequently, one can expand the position, say, of the bottom of the conduction band as

$$\mathcal{E}_c(\hat{u}) = \mathcal{E}_c(0) + \sum_{ik} \Lambda_{ik} u_{ik}.$$

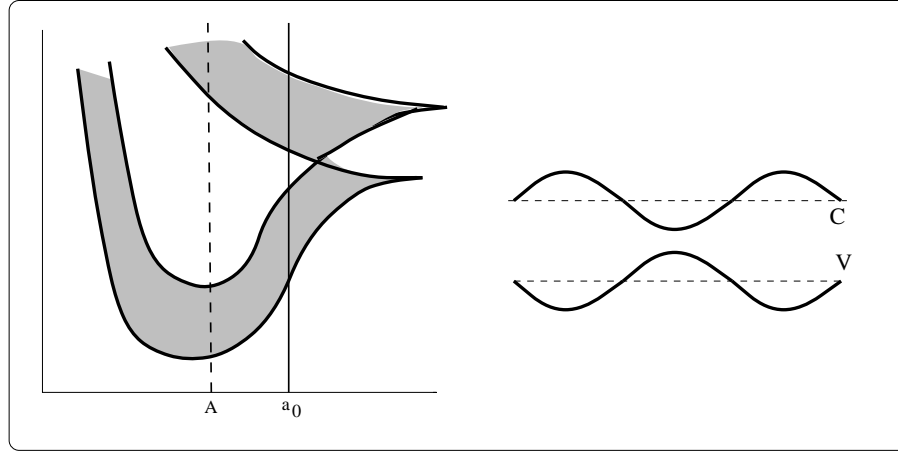


Figure 6.5: The variation of the forbidden gap.

One can show that in a cubic crystal off-diagonal components of the *deformation potential* tensor $\hat{\Lambda}$ vanish. Moreover, because all the axis are equivalent, $\Lambda_{ii} = \Lambda$ and we get

$$\mathcal{E}_c(\hat{u}) = \mathcal{E}_c(0) + \Lambda \text{ div } \mathbf{u}. \quad (6.43)$$

Consequently, we come to the interaction energy of the form (6.30)

$$U_{\mathbf{q}} \sim \Lambda i \mathbf{q} \mathbf{u}_{\mathbf{q}}.$$

The only difference is the replacement of the estimate $e^2 a^2 n_a$ by the deformation potential Λ . As a result, the interaction constant $C(\mathbf{q})$ can be expressed as

$$|C(\mathbf{q})|^2 = \frac{\Lambda^2 q^2 \hbar}{2NM\omega_{\mathbf{q}}} \propto q.$$

The deformation potential can be calculated for a real band structure and measured experimentally. The selection rules for electron-phonon transitions are determined by the symmetry.

Piezoelectric interaction.

Piezoelectric materials (ZnS, ZnSe, CdS, etc.) are ionic crystals without inversion symmetry. The strain u_{ik} induces in such crystals the electric polarization with the components

$$P_i = \sum_{kl} \beta_{i,kl} u_{kl}.$$

where $\hat{\beta}$ is called the *piezoelectric tensor*. The corresponding electric potential is determined from the Poisson equation

$$-\sum_{ik} \epsilon_{ik} \frac{\partial^2 \varphi}{\partial x_i \partial x_k} + 4\pi \sum_{ikl} \frac{\partial}{\partial x_i} \beta_{i,kl} \frac{\partial}{\partial x_k} u_l = 0.$$

If we assume

$$\varphi = \varphi_{\mathbf{q}} e^{i\mathbf{qr}}, \quad \mathbf{u} = \mathbf{u}_{\mathbf{q}} e^{i\mathbf{qr}}$$

we get

$$\varphi_{\mathbf{q}} = \frac{4\pi \sum_{ikl} \beta_{i,kl} q_i q_k u_{\mathbf{q}l}}{\sum_{ik} \epsilon_{ik} q_i q_k}.$$

Specifying the polarization vector $\mathbf{e}_j(\mathbf{q})$ and the unit vector of the propagation direction $\mathbf{n} = \mathbf{q}/q$ we get

$$-e\varphi_{\mathbf{q}} = Gu_0, \quad G(\mathbf{q}) = -\frac{4\pi e \sum_{ikl} \beta_{i,kl} n_i n_k e_{jl}(\mathbf{q})}{\sum_{ik} \epsilon_{ik} n_i n_k}$$

Comparing this expression with the expression (6.43) we see that for a given \mathbf{q} one should replace

$$\sum_{ik} \Lambda_{ik} n_i e_k \rightarrow G(\mathbf{q})/q.$$

We see that the corresponding scattering factors $|C(\mathbf{q})|^2$ behave as $q/q^2 \propto 1/q$. It means that at low temperatures piezoelectric interaction is more important than the deformational one. Since piezoelectric interaction is mediated by electric fields their screening by charge carriers at $q \lesssim r_s^{-1}$ can be important.

Optical Phonons

In non-polar materials one can also characterize the interaction as

$$\mathcal{H}_{e-ph} = \Lambda_0 u$$

where u is the relative displacement of the atoms in the basis. Much more interesting is the interaction in polar crystals where, as we have seen, optical phonons produce electric fields. In these materials the displacement $\mathbf{s} = \mathbf{u}_+ - \mathbf{u}_-$, see Sec. 2.2, page 33 for notations, creates the polarization (*Problem 6.8*)

$$\mathbf{P} = \sqrt{\frac{N_0 M_r \omega_l^2}{4\pi \epsilon^*}} (\mathbf{u}_+ - \mathbf{u}_-) \quad (6.44)$$

where

$$\frac{1}{\epsilon^*} = \frac{1}{\epsilon_\infty} - \frac{1}{\epsilon_0}.$$

We take into account only longitudinal vibrations which effectively interact with the electrons. Then,

$$\nabla^2 \varphi = 4\pi \operatorname{div} \mathbf{P} = \sqrt{\frac{4\pi N_0 M_r \omega_l^2}{\epsilon^*}} \operatorname{div} (\mathbf{u}_+ - \mathbf{u}_-).$$

Then, as usual, we expand the displacements in terms of the normal co-ordinates

$$\mathbf{u}_j^k(\mathbf{r}) = \frac{1}{\sqrt{NM_k}} \sum_{\mathbf{q}j} \mathbf{e}_{jk}(\mathbf{q}) \mathbf{b}_j(\mathbf{q}, t) e^{i\mathbf{qr}} \quad (6.45)$$

and take into account that at long waves the center of gravity does not move,

$$\sqrt{M_1}\mathbf{e}_{j1} + \sqrt{M_2}\mathbf{e}_{j2} = 0, \quad \mathbf{e}_{j1}^2 + \mathbf{e}_{j2}^2 = 1.$$

As a result,

$$\mathbf{e}_{j1} = \sqrt{\frac{M_1}{M_1 + M_2}}\mathbf{i}_j, \quad \mathbf{e}_{j2} = -\sqrt{\frac{M_2}{M_1 + M_2}}\mathbf{i}_j.$$

Finally we substitute these expressions to Eqs. (6.45) for \mathbf{u}_\pm and get (*Problem 6.9*)

$$\phi = -i\sqrt{\frac{4\pi\omega_l^2}{\epsilon^*}} \sum_{\mathbf{q}} \frac{1}{q} (b_{\mathbf{q}} e^{i\mathbf{qr}} - b_{\mathbf{q}}^* e^{-i\mathbf{qr}}) \quad (6.46)$$

Using the second quantization procedure (page 41) we arrive at the famous *Frölich Hamiltonian*

$$\mathcal{H}_{e-ph} = \frac{1}{\sqrt{\mathcal{V}}} \sum_{\mathbf{q}, j} \frac{M_j}{q} a_{\mathbf{p}-\hbar\mathbf{q}}^\dagger a_{\mathbf{p}} (b_{\mathbf{q}j} + b_{\mathbf{q}j}^\dagger) \quad (6.47)$$

with

$$M_j^2 = 2\pi e^2 \hbar \omega_{l,j} / \epsilon^*.$$

Sometimes it is expressed as

$$M^2 = \frac{4\pi\alpha\hbar(\hbar\omega_l)^{3/2}}{\sqrt{2m}}, \quad \alpha = \frac{e^2}{\hbar\epsilon^*} \sqrt{\frac{m}{2\hbar\omega_l}}.$$

The dimensionless constant α is called the *polaron constant*.

Now we can analyze the conservation laws $\varepsilon_{\mathbf{k}\pm\mathbf{q}} = \varepsilon_{\mathbf{k}} \pm \hbar\omega_l$ which can be rewritten as

$$\frac{\hbar^2 q^2}{2m} \pm \frac{\hbar^2 k q \cos \vartheta}{2m} \mp \hbar\omega_l = 0.$$

The roots of this equation are

$$q_1 = -k \cos \vartheta \pm \sqrt{k^2 \cos^2 \vartheta + k_0^2}, \quad q_2 = -k \cos \vartheta \pm \sqrt{k^2 \cos^2 \vartheta - k_0^2}$$

where $\hbar^2 k_0^2 / 2m = \hbar\omega_l$.

1. If $k \gg k_0$ we get for both absorption and emission the old conditions $q_{\min} = 0$, $q_{\max} = 2k$. At high temperatures, $k_B T \gg \hbar\omega_l$ the scattering is elastic, and we return to the same expression as for acoustic phonons. Using Eq. (6.40) we get

$$\tau_{tr} = \frac{\sqrt{2}}{2} \frac{\hbar^2 \epsilon^*}{e^2 \sqrt{m k_B T}} \varepsilon^{3/2} \propto T^{-1} \varepsilon^{3/2}.$$

2. The case of low temperatures,

$$\hbar\omega_l \gg k_B T,$$

is more tricky. In this case only absorption processes can take place, and

$$q_{\min} = \sqrt{k^2 + k_0^2} - k \quad (\vartheta = 0), \quad q_{\max} = \sqrt{k^2 + k_0^2} + k \quad (\vartheta = \pi).$$

It is clear, that the scattering is strongly inelastic and in general one cannot use the relaxation time approximation. Nevertheless, some simplification does exist. Indeed, note that the ratio of the emission and absorption probabilities is

$$(N_q + 1)/N_q \approx \exp(\hbar\omega_l/k_B T) \gg 1.$$

So if the electron absorbs an optical phonon it should immediately emit another one. As a result, the change of energy appears small while the change of the quasimomentum is large. One can get the result taking into account only the absorption processes. The corresponding δ -function is

$$\delta\left(\frac{\hbar^2 q^2}{2m} + \frac{\hbar^2 k q \cos \vartheta}{2m} - \frac{\hbar^2 k_0^2}{2m}\right) = \frac{m}{\hbar^2 k q} \delta\left(\frac{q^2 - k_0^2}{2kq} + \cos \vartheta\right)$$

while the relaxation time can be obtained as

$$\begin{aligned} \frac{1}{\tau_{\text{tr}}} &= \frac{1}{8\pi^2} \frac{m}{\hbar^2 k^3} \int_{q_{\min}}^{q_{\max}} w(q) N_q \frac{q^2 - k_0^2}{q} q^2 dq \\ &\approx (e^2 m \omega_l / \hbar^2 \epsilon^* k^3) \exp(-\hbar\omega_l/k_B T) \underbrace{\left[2k \sqrt{k^2 + k_0^2} - k_0 \ln \frac{\sqrt{k^2 + k_0^2} + k}{\sqrt{k^2 + k_0^2} - k} \right]}_{\approx (4/3)k^3/k_0}. \end{aligned}$$

Expanding this expression in powers of k/k_0 we get

$$\tau_{\text{tr}} = \frac{2\sqrt{2}}{2} \frac{\hbar^2 \epsilon^*}{e^2 \sqrt{m \hbar \omega_l}} \exp\left(\frac{\hbar\omega_l}{k_B T}\right).$$

This scattering is very weak. Note that it is not the case of the so-called *hot* electrons with high energies, which can emit optical phonons.

The polaron.⁴

We take the opportunity to demonstrate the role of interaction when it cannot be considered as weak. Let us consider the interaction of an electron with optical phonons. According to quantum mechanics, the change of the ground state energy due to interaction is

$$\mathcal{E}_n - \mathcal{E}_n^{(0)} = \langle n | \mathcal{H}_{\text{int}} | n \rangle + \sum_{m \neq n} \frac{|\langle m | \mathcal{H}_{\text{int}} | n \rangle|^2}{\mathcal{E}_n^{(0)} - \mathcal{E}_0^{(0)}}.$$

⁴Optional section

Consider the interaction with a polarized crystal. At $T = 0$ only emission of phonons is possible. We have $N_q = 0$, $N'_q = 1$, $\mathbf{k}' = \mathbf{k} - \mathbf{q}$. The diagonal matrix element is zero because it contains the same number of phonons. As a result, we get

$$\begin{aligned}\varepsilon_{\mathbf{k}} - \varepsilon_{\mathbf{k}}^{(0)} &= \sum_{\mathbf{q}} \frac{|\langle 1, \mathbf{k} - \mathbf{q} | -e\Phi | 0, \mathbf{k} \rangle|^2}{\frac{\hbar^2 k^2}{2m} - \frac{\hbar^2 (\mathbf{k} - \mathbf{q})^2}{2m} - \hbar\omega_l} \\ &= \frac{2\pi e^2 \hbar\omega_l}{\epsilon^*} \int \frac{(dq)}{q^2} \left(\frac{\hbar^2 k^2}{2m} - \frac{\hbar^2 (\mathbf{k} - \mathbf{q})^2}{2m} - \hbar\omega_l \right)^{-1}.\end{aligned}$$

As usual we introduce polar co-ordinates with the axis along \mathbf{k}

$$(dq) \rightarrow (2\pi)^{-2} q^2 dq \sin\vartheta d\vartheta; \quad \mathbf{k}\mathbf{q} = kq \cos\vartheta$$

and expand the integrand in powers of k . The integral can be calculated easily, and the result is

$$\varepsilon_{\mathbf{k}} = \frac{\hbar^2 k^2}{2m} - \alpha \left(\hbar\omega_l + \frac{\hbar^2 k^2}{12m} \right) \equiv -\alpha \hbar\omega_l + \frac{\hbar^2 k^2}{2m_{pol}}$$

where α has been introduced in the previous section as the polaron constant while

$$m_{pol} = \frac{m}{1 - \alpha/6} \approx m(1 + \alpha/6).$$

All these considerations are good only when $\alpha \ll 1$. We have

Material	α
InSb	0.015
InP	0.080
CdTe	0.39
CdS	0.65

Consequently, the interaction for the two last materials is strong and one cannot use the perturbation theory in the simplest way. The qualitative conclusions are that interaction with phonons leads to the shift of the energy levels (the relative shift is α at $\alpha \ll 1$) and to its "dressing" - increase of the effective mass.

6.8 Galvano- and Thermomagnetic Phenomena

The Physical Reason

The external magnetic field distort electron trajectories. Its influence is strong if the characteristic radius of cyclotron orbit, $r_c = v_{\perp}/\omega_c$, is less than the mean free path ℓ at which all the kinetic coefficients are formed. One can treat the distortion as an effective decrease of the mean free path ℓ . To estimate the influence of a weak magnetic field on

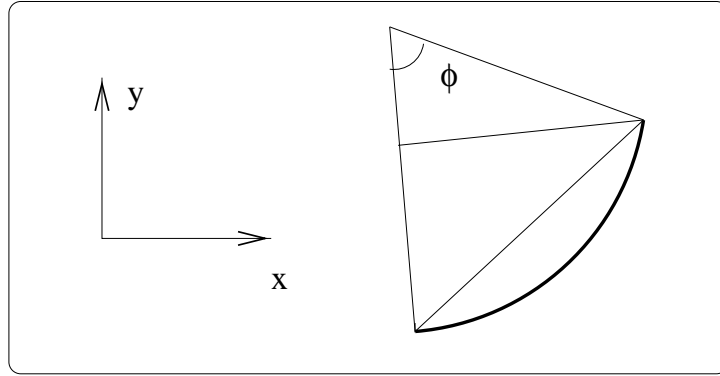


Figure 6.6: A trajectory fragment..

the resistance one can compare the path between two scattering centers along the circle $r_c\phi$ (see Fig. 6.6) with the distance $2r_c \sin \phi/2$. The difference is $\sim r_c \phi^3$. If we put $r_c \phi \sim \ell$ we get

$$\Delta\rho/\rho \sim (\ell/r_c)^2 \sim (\omega_c\tau)^2.$$

Another effect that one can expect is the creation of a current perpendicular to the electric and magnetic field direction. Indeed, under the influence of magnetic field an electron moves in the $[\mathbf{E} \times \mathbf{H}]$ direction by the distance

$$\sim r_c(1 - \cos \phi) \approx (1/2)r_c\phi^2 \sim \ell(\ell/r_c) \sim \ell(\omega_c\tau).$$

As a result, one can expect creation of off-diagonal components of the conductivity tensor with

$$|\sigma_{xy}| \sim \sigma_0(\omega_c\tau).$$

To get the results in strong magnetic fields is more tricky and we will do it later.

Conductivity Tensor. Calculations.

Simplified version for isotropic case

In a magnetic field the Boltzmann equation reads

$$\left\{ (\mathbf{v}\nabla_r) - e \left(E + \frac{1}{c} [\mathbf{v} \times \mathbf{H}] \right) \nabla_p \right\} f + \frac{f - f_0}{\tau_{\text{tr}}} = 0.$$

We look for a solution as

$$f = f_0 + (\mathbf{v} \cdot \mathbf{G}), \quad |\mathbf{G}| \propto E.$$

We have

$$\left(-\frac{e}{c} [\mathbf{v} \times \mathbf{H}] \frac{\partial}{\partial \mathbf{p}} + \frac{1}{\tau_{\text{tr}}} \right) (\mathbf{v} \cdot \mathbf{G}) = e \frac{\partial f_0}{\partial \varepsilon} (\mathbf{E} \cdot \mathbf{v}). \quad (6.48)$$

As we'll check, for a given ε the vector \mathbf{G} is independent of the direction of \mathbf{p} and depends only on the energy $\varepsilon = p^2/2m$. Since $\partial\varepsilon/\partial\mathbf{p} = \mathbf{v}$ we have

$$\frac{\partial(\mathbf{v} \cdot \mathbf{G})}{\partial\mathbf{p}} = \frac{\mathbf{G}}{m} + \mathbf{v} \left(\mathbf{v} \cdot \frac{d\mathbf{G}}{d\varepsilon} \right) .$$

Since

$$[\mathbf{v} \times \mathbf{H}] \cdot \mathbf{v} \left(\mathbf{v} \cdot \frac{d\mathbf{G}}{d\varepsilon} \right) = 0$$

we get

$$\frac{\mu}{c} ([\mathbf{v} \times \mathbf{H}] \cdot \mathbf{G}) + (\mathbf{v} \cdot \mathbf{G}) = e\tau_{\text{tr}}(\mathbf{v} \cdot \mathbf{E}) \frac{\partial f_0}{\partial \varepsilon} \quad (6.49)$$

where

$$\mu(\varepsilon) = \frac{|e|\tau_{\text{tr}}(\varepsilon)}{m} \quad (6.50)$$

is the partial electron *mobility*. It is natural to look for a solution of the equation (6.49) in the form

$$\mathbf{G} = \alpha\mathbf{E} + \beta\mathbf{H} + \gamma[\mathbf{H} \times \mathbf{E}] .$$

Substitution this form to (6.49) and using the equality $([\mathbf{v} \times \mathbf{H}] \cdot \mathbf{H}) = 0$ we get

$$\begin{aligned} \alpha \frac{\mu}{c} ([\mathbf{v} \times \mathbf{H}] \cdot \mathbf{E}) + \gamma \frac{\mu}{c} \{ (\mathbf{H} \cdot \mathbf{E})(\mathbf{v} \cdot \mathbf{H}) - H^2(\mathbf{v} \cdot \mathbf{E}) \\ + \alpha(\mathbf{v} \cdot \mathbf{E}) + \beta(\mathbf{v} \cdot \mathbf{H}) + \gamma(\mathbf{v} \cdot [\mathbf{H} \times \mathbf{E}]) \} = e\tau_{\text{tr}}(\mathbf{v} \cdot \mathbf{E}) \frac{\partial f_0}{\partial \varepsilon} . \end{aligned}$$

Then we can collect the coefficients at $(\mathbf{v} \cdot \mathbf{E})$, $(\mathbf{v} \cdot \mathbf{H})$ and $(\mathbf{v} \cdot [\mathbf{H} \times \mathbf{E}])$. We have

$$\begin{aligned} \alpha - \gamma \frac{\mu}{c} H^2 &= e\tau_{\text{tr}} \left(\frac{\partial f_0}{\partial \varepsilon} \right) , \\ \gamma \frac{\mu}{c} (\mathbf{H} \cdot \mathbf{E}) + \beta &= 0 , \\ \alpha \frac{\mu}{c} + \gamma &= 0 . \end{aligned} \quad (6.51)$$

As a result, (*Problem 6.8*)

$$\mathbf{G} = e\tau_{\text{tr}} \frac{\partial f_0}{\partial \varepsilon} \frac{\mathbf{E} + (\mu/c)^2(\mathbf{H} \cdot \mathbf{E}) \cdot \mathbf{H} + (\mu/c)[\mathbf{E} \times \mathbf{H}]}{1 + \mu^2 H^2 / c^2} . \quad (6.52)$$

The quantity $\mu H/c$ is nothing else than the product $\omega_c \tau_{\text{tr}}$. We see that in the presence of magnetic field there is a current along the direction of $[\mathbf{E} \times \mathbf{H}]$. The conductivity tensor is easily calculated from the expression

$$j_i = -e \int \frac{2d^3p}{(2\pi\hbar)^3} v_i \sum_k v_k G_k .$$

For an isotropic spectrum, we get $\sigma_{zz} = \sigma_0$,

$$\sigma_{xx} = \sigma_{yy} = \frac{ne^2}{m} \left\langle \frac{\tau_{\text{tr}}}{1 + \omega_c^2 \tau_{\text{tr}}^2} \right\rangle ,$$

while

$$\sigma_{xy} = -\sigma_{yx} = \frac{ne^2}{m} \left\langle \frac{\omega_c \tau_{\text{tr}}^2}{1 + \omega_c^2 \tau_{\text{tr}}^2} \right\rangle .$$

Here the average $\langle A \rangle$ is understood as

$$\langle A \rangle \equiv \frac{\int A(\mathbf{p})(-\partial f_0 / \partial \varepsilon) (dp)}{\int (-\partial f_0 / \partial \varepsilon) (dp)} .$$

Note that denominator of this expression is nothing else than *thermodynamic density of states*,

$$g_T \equiv \partial n_e / \partial \zeta \quad (6.53)$$

where n_e is the electron density while ζ is the chemical potential.

General case ⁵

In the presence of a magnetic field, see Sec. 3.7.1, it is convenient to introduce two different variables instead of p_x and p_y – the energy ε and the “trajectory time” defined as

$$t_1 = \frac{c}{eH} \int \frac{dl}{v_\perp} . \quad (6.54)$$

This is not a real time, but rather a function of \mathbf{p} defined by the equation of motion $\dot{\mathbf{p}} = -(e/c)[\mathbf{v} \times \mathbf{H}]$. According to our previous treatment,

$$\int dp_x dp_y = \int d\varepsilon \int dl/v_\perp \quad \text{or} \quad \int dp_x dp_y dp_z = \frac{eH}{c} \int dt_1 d\varepsilon dp_z .$$

In the presence of external fields the l.h.s. of the Boltzmann equation can be written as

$$\frac{\partial f}{\partial t_1} \frac{\partial t_1}{\partial t} + \frac{\partial f}{\partial p_z} \frac{\partial p_z}{\partial t} + \frac{\partial f}{\partial \varepsilon} \frac{\partial \varepsilon}{\partial t}$$

where we consider the quantities t_1 , p_z , ε as independent variables. Since

$$\frac{\partial \varepsilon}{\partial t} = \mathbf{v} \cdot \frac{d\mathbf{p}}{dt} = -\mathbf{v} \cdot \left(\frac{e}{c} [\mathbf{v} \times \mathbf{H}] + e\mathbf{E} \right) = -e(\mathbf{v} \cdot \mathbf{E}) , \quad \frac{dp_z}{dt} = -eE_z ,$$

and in a *weak* (comparing to vH/c) electric field $\partial t_1 / \partial t = 1$ we arrive at the Boltzmann equation

$$\frac{\partial f}{\partial t} - eE_z \frac{\partial f}{\partial p_z} - e(\mathbf{v} \cdot \mathbf{E}) \frac{\partial f}{\partial \varepsilon} = I_{\text{col}}(f) . \quad (6.55)$$

⁵Optional section

As usual, we search the solution as

$$f = f_0 + a \left(-\frac{\partial f_0}{\partial \varepsilon} \right).$$

The function f_0 depends only on the energy, and we get in the linear approximation

$$\frac{\partial a}{\partial t_1} - I(a) = -e(\mathbf{v} \cdot \mathbf{E}). \quad (6.56)$$

We should solve this equation with proper boundary conditions. In the case of closed orbits it is just the periodicity while for open orbits the function should be finite. We need to analyze the solution of this equation in different cases.

To make estimates we use the relaxation time approximation to get

$$\frac{\partial a}{\partial t_1} + \frac{a}{\tau} = -e(\mathbf{v}(t_1) \cdot \mathbf{E}). \quad (6.57)$$

The general solution is

$$a(t_1) = \int_c^{t_1} -e(\mathbf{v}(t_2) \cdot \mathbf{E}) e^{-(t_1-t_2)/\tau} dt_2.$$

If the orbits are *closed* one should apply the periodic conditions

$$a(t_1) = a(t_1 + T)$$

In this case one has to put $c = -\infty$ (*Problem 6.11*). The electric current is

$$\begin{aligned} j_i &= -e \int v_i f (dp) = -\frac{2e^2 H}{(2\pi\hbar)^3 c} \int d\varepsilon \left(-\frac{\partial f_0}{\partial \varepsilon} \right) \int dp_z dt_1 v_i a(\varepsilon, p_z, t) = \\ &= -\frac{2e^3 H}{(2\pi\hbar)^3 c} \int d\varepsilon \left(-\frac{\partial f_0}{\partial \varepsilon} \right) \int_{-p_F}^{p_F} dp_z \int_0^T dt_1 v_i(t_1) \int_{-\infty}^{t_1} dt_2 \sum_k v_k(t_2) e^{-(t_1-t_2)/\tau} E_k. \end{aligned}$$

We see that the conductivity is a tensor with the components

$$\sigma_{ik} = -\frac{2e^3 H}{(2\pi\hbar)^3 c} \int d\varepsilon \left(-\frac{\partial f_0}{\partial \varepsilon} \right) \int_{-p_F}^{p_F} dp_z \int_0^T dt_1 v_i(t_1) \int_{-\infty}^{t_1} dt_2 \sum_k v_k(t_2) e^{-(t_1-t_2)/\tau}.$$

Now we assume that $\mathbf{E} \perp \mathbf{H}$ and i, k are x, y -components. If the spectrum is isotropic,

$$v_x = v_\perp \cos \omega_c t_1, \quad v_y = -v_\perp \sin \omega_c t_1, \quad \omega_c = -\frac{eH}{mc}.$$

Now we can extract v_\perp and analyze

$$\left\{ \begin{array}{c} I_x \\ I_y \end{array} \right\} = \int_0^T dt_1 \left\{ \begin{array}{c} \cos \omega_c t_1 \\ -\sin \omega_c t_1 \end{array} \right\} \int_{-\infty}^{t_1} dt_2 e^{-(t_1-t_2)/\tau} (E_x \cos \omega_c t_2 - E_y \sin \omega_c t_2)$$

It is convenient to employ an auxiliary integral

$$\begin{aligned} \int_{-\infty}^{t_1} dt_2 e^{t_2/\tau} e^{i\omega_c t_2} &= e^{t_1/\tau} e^{i\omega_c t_1} \frac{\tau^{-1} - i\omega_c}{\tau^{-2} + \omega_c^2} = \\ &= e^{t_1/\tau} \frac{1}{\tau^{-2} + \omega_c^2} [(\tau^{-1} \cos \omega_c t_1 + \omega_c \sin \omega_c t_1) + i(\tau^{-1} \sin \omega_c t_1 - \omega_c \cos \omega_c t_1)]. \end{aligned}$$

Finally, we come to the integral

$$\begin{aligned} \left\{ \begin{array}{l} I_x \\ I_y \end{array} \right\} &= \int_0^T dt_1 \left\{ \begin{array}{l} \cos \omega_c t_1 \\ -\sin \omega_c t_1 \end{array} \right\} \times \\ &\times [E_x(\tau^{-1} \cos \omega_c t_1 + \omega_c \sin \omega_c t_1) - E_y(\tau^{-1} \sin \omega_c t_1 - \omega_c \cos \omega_c t_1)]. \end{aligned}$$

Finally we get

$$\left\{ \begin{array}{l} j_x \\ j_y \end{array} \right\} = -\frac{2e^3 H}{(2\pi\hbar)^3 c} \frac{T}{2} \int d\varepsilon \left(-\frac{\partial f_0}{\partial \varepsilon} \right) \frac{1}{\tau^{-2} + \omega_c^2} \left\{ \begin{array}{l} \tau^{-1} E_x + \omega_c E_y \\ -\omega_c E_x + \tau^{-1} E_y \end{array} \right\} \int dp_z v_\perp^2.$$

We have used the integrals

$$\begin{aligned} \int_0^T \cos^2 \omega_c t dt &= \int_0^T \sin^2 \omega_c t dt = \frac{T}{2}, \\ \int_0^T \cos \omega_c t \sin \omega_c t dt &= 0. \end{aligned}$$

For degenerate electrons the integral over the energy locates the internal integral to the Fermi surface, the last integral being

$$\int_{-p_F}^{p_F} v_\perp^2 dp_z = \frac{1}{m^2} \int_{-p_F}^{p_F} \int (p_F^2 - p_z^2) dp_z = \frac{4}{3} \frac{p_F^2}{m^2}.$$

The final result is

$$\hat{\sigma}_\perp = \frac{n_e e^2}{m} \frac{1}{\tau^{-2} + \omega_c^2} \left(\begin{array}{cc} \tau^{-1} & \omega_c \\ -\omega_c & \tau^{-1} \end{array} \right).$$

Weak Magnetic Field

In weak magnetic fields, when

$$\omega_c \tau \ll 1$$

we get

$$\hat{\sigma}_\perp = \sigma_0 \left(\begin{array}{cc} 1 & \omega_c \tau \\ -\omega_c \tau & 1 \end{array} \right).$$

The typical configuration to measure off-diagonal components of the conductivity tensor is shown in Fig. (6.7). In general

$$\begin{aligned} j_x &= \sigma_{xx} E_x + \sigma_{xy} E_y, \\ j_y &= \sigma_{yx} E_x + \sigma_{yy} E_y. \end{aligned} \tag{6.58}$$

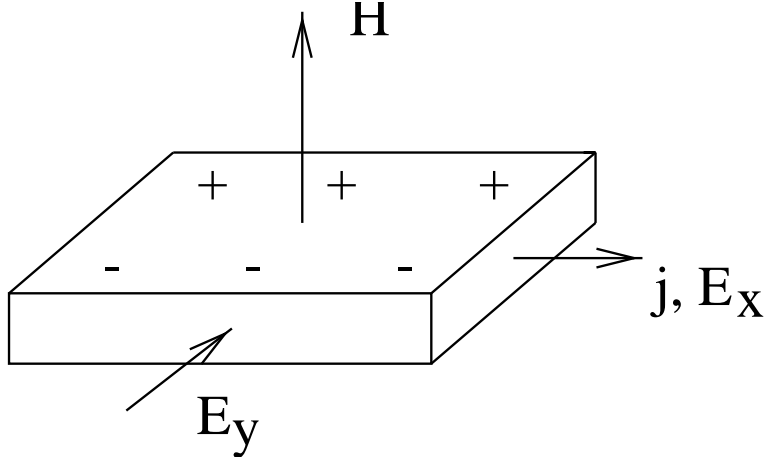


Figure 6.7: Arrangement to measure off-diagonal conductivity components.

If the circuit in y -direction is open we have $j_y = 0$. As a result, a field

$$E_y = -\frac{\sigma_{xy}}{\sigma_{xx}} E_x \quad (6.59)$$

appears, the current density being

$$j = j_x = \rho_{xx} E_x = \frac{\sigma_{xx}^2 + \sigma_{xy}^2}{\sigma_{xx}} E_x.$$

We have taken into account that

$$\sigma_{xx} = \sigma_{yy}, \quad \sigma_{xy} = -\sigma_{yx}.$$

Thus,

$$E_y = -\frac{\sigma_{xy}}{\sigma_{xx}^2 + \sigma_{xy}^2} j.$$

The creation of a transverse field directed along $[\mathbf{E} \times \mathbf{H}]$ is called the *Hall effect*. The *Hall coefficient* is defined as

$$R = \frac{E_y}{H j_x} = -\frac{\sigma_{xy}}{(\sigma_{xx}^2 + \sigma_{xy}^2) H}.$$

As we see, at weak magnetic field

$$R = -\frac{\omega_c \tau}{H \sigma_o} = \frac{1}{n_e e c}. \quad (6.60)$$

We came to the conclusion that the Hall coefficient depends only on the electron density. It is not the case in real materials because we have canceled the factor τ which in real life depends on the energy, directions, etc. In non-degenerate semiconductors the Hall coefficient becomes dependent on the scattering mechanisms. Usually, it is taken into account by introduction the *Hall factor* in Eq. (6.60). The resistivity component $\rho_{xx} = 1/\sigma_0$ in a weak field because $|\sigma_{xy}| \ll \sigma_{xx}$.

High Magnetic Field.

The results obtained above can be used to get estimates also in the case of high magnetic fields. But we will make more rigorous calculations because many results can be obtained for an arbitrary energy spectrum.

First, we introduce a specific perturbation theory to solve the Boltzmann equation in strong magnetic fields, i.e. expansion in power of $\gamma = (\omega_c \tau)^{-1}$. We write the function a as

$$a = \sum_k a_k, \quad a_k \sim \gamma^k$$

and substitute the Boltzmann equation (6.56)

$$\begin{aligned} \partial a_0 / \partial t_1 &= 0, \\ \partial a_1 / \partial t_1 - I(a_0) &= -e(\mathbf{v}\mathbf{E}), \\ \partial a_2 / \partial t_1 - I(a_1) &= 0, \dots \end{aligned}$$

The solutions are:

$$\begin{aligned} a_0 &= C_0, \\ a_1 &= \int_0^{t_1} [I(C_0) - e(\mathbf{v}(t_2)\mathbf{E})] dt_2 + C_1, \dots \\ a_k &= \int_0^{t_1} [I(a_{k-1}) - e(\mathbf{v}(t_2)\mathbf{E})] dt_2 + C_k \dots \end{aligned}$$

Then we average all the equations over the time taking into account that $\overline{\partial a / \partial t_1} = 0$. As a result,

$$-\overline{I(a_0)} = -e(\overline{\mathbf{v}\mathbf{E}}), \quad \overline{I(a_{k \neq 0})} = 0.$$

These equations determine the constant items C_i . Now we proceed with calculation of the conductivity tensor.

Closed Orbits

In this case $\overline{v_x} = \overline{v_y} = 0$, and C_0 depends only on $\overline{v_z} E_z$. Consequently, we are interested in a_1 and we can substitute

$$\frac{dp_x}{dt} = -\frac{e}{c} v_y H, \quad \frac{dp_y}{dt} = \frac{e}{c} v_x H. \quad (6.61)$$

As a result,

$$a_1 = \frac{c}{H} \int_0^{t_1} dt_2 \left(E_y \frac{dp_x}{dt_2} - E_x \frac{dp_y}{dt_2} \right) - e \int_0^{t_1} dt_2 v_z(t_2) E_z + \text{const}(\mathbf{v}).$$

Now it is very simple to calculate σ_{xy} . Let us calculate, say, j_x for the Fermi gas. We have

$$\begin{aligned} j_x &= \frac{2He^2}{(2\pi\hbar)^3 c} \int dp_z \int_0^\tau v_x(t_1) a_1 dt_1 = \frac{2e}{(2\pi\hbar)^3} \int dp_z \int_0^\tau a(t_1) \frac{dp_y}{dt_1} dt_1 \\ &= \frac{2e}{(2\pi\hbar)^3} \int dp_z \left[\int_0^\tau dt_1 (p_x(t_1) - p_x(0)) E_y \frac{c}{H} \frac{dp_y}{dt_1} + \text{vanishing items} \right]. \end{aligned}$$

The result is

$$\sigma_{xy} = \frac{2ec}{(2\pi\hbar)^3 H} \int dp_z \int_0^\tau dt_1 p_x \frac{dp_y}{dt_1} = \frac{2ec}{(2\pi\hbar)^3 H} \underbrace{\int dp_z \oint p_x dp_y}_{\text{volume}}.$$

The result can be expressed through the densities of electron-like and hole-like excitations:

$$\sigma_{xy} = -\frac{ec}{H} (n_e - n_h).$$

The physical reason is that the Lorenz force has different signs for electrons and holes and the *Hall effect feels the sign of charge carriers*. It is very important that the result is independent on scattering mechanisms and the shape of the surfaces $\varepsilon = \text{const}$. Actually, it is the most common way to determine the carriers' density.

Another conclusion is that there is no linear in γ contributions to the diagonal components of the conductivity tensor. Finally, we come to the following structure of the conductivity tensor

$$\sigma_{ik} = \begin{pmatrix} \gamma^2 a_{xx} & \gamma a_{xy} & \gamma a_{xz} \\ \gamma a_{yx} & \gamma^2 a_{yy} & \gamma a_{yz} \\ \gamma a_{zx} & \gamma a_{zy} & a_{zz} \end{pmatrix}$$

while the resistivity tensor $\hat{\rho} = (\hat{\sigma})^{-1}$ is

$$\rho_{ik} = \begin{pmatrix} b_{xx} & \gamma^{-1} b_{xy} & b_{xz} \\ \gamma^{-1} b_{yx} & b_{yy} & b_{yz} \\ b_{zx} & b_{zy} & b_{zz} \end{pmatrix}.$$

The case of compensated materials with $n_e = n_h$ (like Bi) needs a special treatment.

Note that the components of the conductivity tensor should meet the Onsager principle which in the presence of the magnetic field reads as

$$\sigma_{ik}(\mathbf{H}) = \sigma_{ki}(-\mathbf{H})$$

(the reason is that the Onsager principle is derived by use the symmetry with respect to time reversion. Under such a transform magnetic field changes its sign).

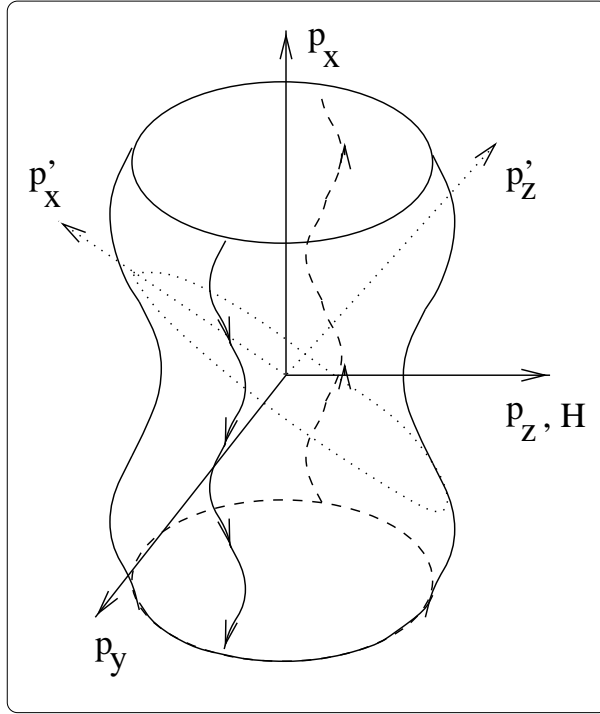


Figure 6.8: The case of open orbits..

Open Orbits

The case of open orbits is more tricky. To understand what happens let us consider the case shown in Fig. 6.8. We observe that the trajectory in p_z -direction is infinite while in p_y direction it is finite. Taking the average of the equations of motion (6.61) we get

$$\bar{v}_y = -\frac{c}{eH} \lim_{T_1 \rightarrow \infty} \left[\frac{p_x(T_1) - p_x(0)}{T_1} \right] \neq 0, \quad \bar{v}_x = 0.$$

As a result, the quantity a_0 contains a component $\propto E_y$, and the component σ_{yy} is not small. As a result,

$$\sigma_{ik} = \begin{pmatrix} \gamma^2 a_{xx} & \gamma a_{xy} & \gamma a_{xz} \\ \gamma a_{yx} & a_{yy} & a_{yz} \\ \gamma a_{zx} & a_{zy} & a_{zz} \end{pmatrix}.$$

One can see from Fig. 6.8 that the conductivity tensor strongly depends on the tilt angle of the magnetic field, having a sharp crossover at $\theta \rightarrow 0$. The schematic angular dependencies of the Hall coefficient and transverse resistivity are shown in Fig. 6.9. .

Thermomagnetic Effects.

It is clear that the temperature gradient also produces electric currents, and a magnetic field leads to off-diagonal transport. As we have seen these currents are produced by the

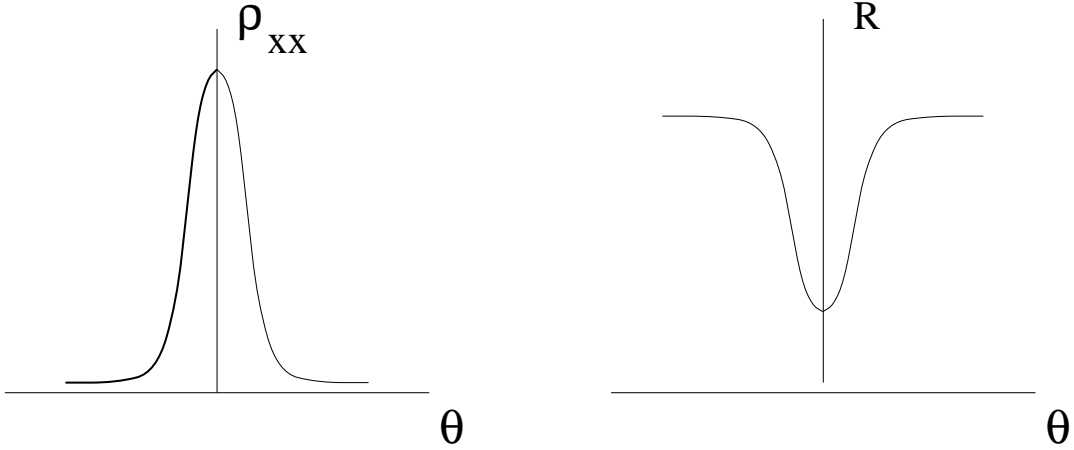


Figure 6.9: Crossover from closed to open orbits.

”effective force” $(\varepsilon - \zeta)\nabla T/T$. As a result, all the kinetic coefficients become tensors. According to the Onsager principle

$$\rho_{ik}(\mathbf{H}) = \rho_{ki}(-\mathbf{H}), \quad \varkappa_{ik}(\mathbf{H}) = \varkappa_{ki}(-\mathbf{H}), \quad \Pi_{ik}(\mathbf{H}) = T\alpha_{ki}(-\mathbf{H}).$$

Consequently, we have 36 kinetic coefficients which obey 15 Onsager relations. It is clear that 21 independent components lead to a very complicated picture and usually people study simplest cases. For example, in an isotropic material in a weak magnetic field one can write

$$\begin{aligned} \mathbf{j} &= \rho\mathbf{E} + R[\mathbf{H} \times \mathbf{j}] + \alpha\nabla T + N[\mathbf{H} \times \nabla T], \\ \mathbf{w} - \mathbf{j}\zeta &= \Pi\mathbf{j} + B[\mathbf{H} \times \mathbf{j}] - \varkappa\nabla T + L[\mathbf{H} \times \nabla T]. \end{aligned} \quad (6.62)$$

According to the Onsager principle, $B = NT$. The expressions (6.62) describe many effects. For example, suppose that $\nabla_x T = 0$, $j_y = 0$, $w_y = 0$, but $j_x \neq 0$. In this case we get

$$\frac{\partial T}{\partial y} = \frac{B}{\varkappa} H j_x$$

(the *Ettingshausen effect*). Another effect is creation of a field E_y by the gradient $\partial T/\partial x$ (the *Nernst effect*)

$$E_y = NH(\partial T/\partial x).$$

All these effects have important applications. In high magnetic fields all the coefficients become field-dependent.

6.9 Shubnikov-de Haas effect

Oscillations similar to the de Haas-van Alphen effect, see Sec. 4.4, exist also for kinetic coefficients. Although quantum transport is out of the scope of the present part of the course we will discuss the main picture.

Kinetic coefficients depend both on the density of states and on the scattering probability. We have seen that DOS oscillated because of the energy quantization. The scattering probability, in its term, is also dependent on the density of states, as well on the scattering matrix element. Consequently, it also oscillates in magnetic field, and it appears that the last contribution is the most important. The quantum oscillations of conductivity is called the *Shubnikov-de Haas effect*. Similar oscillations are also present for thermo.magnetic coefficients. Quantum oscillations of kinetic coefficients are widely used for investigation of the properties of metals and semiconductors.

Let us outline main principles of these effects. To take the electric field into account one should analyze the SE in crossed electric and magnetic field ($\mathbf{H} \parallel \mathbf{z}$, $\mathbf{E} \parallel x$)

$$-\frac{\hbar^2}{2m} \frac{\partial^2 \psi}{\partial x^2} + \frac{1}{2m} \left(\frac{\hbar}{i} \frac{\partial}{\partial y} + \frac{e}{c} Hx \right)^2 \psi - \frac{\hbar^2}{2m} \frac{\partial^2 \psi}{\partial z^2} + (eEx - \varepsilon) \psi = 0.$$

We can also search the solution as

$$\varphi(x) \exp(ik_y y + ik_z z).$$

The equation for φ has the form

$$-\frac{\hbar^2}{2m} \frac{d^2 \varphi}{dx^2} + \left[\frac{1}{2m} \left(\frac{eH}{c} \right)^2 x^2 + \left(\frac{\hbar eH}{mc} k_y + eE \right) x + \frac{\hbar^2 (k_y^2 + k_z^2)}{2m} - \varepsilon \right] \varphi = 0.$$

The result can be expressed just in the same way as for the case $E = 0$ with the additional terms

$$\varepsilon_\nu^E = \varepsilon_N + \frac{\hbar^2 k_z^2}{2m} + \delta\varepsilon, \quad \delta\varepsilon = -a_H^2 e E k_y - \frac{mc^2}{2} \left(\frac{E}{H} \right)^2$$

for the energy and

$$x_0^E = x_0 + \delta x_0, \quad \delta x_0 = -\frac{e E a_H^2}{\hbar \omega_c}.$$

for the oscillator center x_0 (see Sec. 3.7.2).

Now we introduce the following concept. Assume that the electron in the state ν is situated at the point x_0^E . The electric current is

$$j_x = -e \sum'_{\nu, \nu'} \{ f_0(\varepsilon_\nu^E) [1 - f_0(\varepsilon_{\nu'}^E)] W_{\nu\nu'}^E - f_0(\varepsilon_{\nu'}^E) [1 - f_0(\varepsilon_\nu^E)] W_{\nu'\nu}^E \}.$$

The prime over the sum means that the state ν has $x_0^E < 0$, while the state ν' has $x_0^E > 0$. Then we expand the expression up to the linear in E term and get

$$\sigma_{xx} = e^2 \sum_{\nu, \nu'} \left(-\frac{\partial f_0(\varepsilon_\nu)}{\partial \varepsilon_v} \right) \frac{(x_0 - x_0')^2}{2} W_{\nu\nu'}.$$

This formula has an explicit physical meaning. Indeed, the quantity

$$\frac{(x_0 - x'_0)^2}{2} W_{\nu\nu'}$$

is just the contribution of the states ν, ν' to the 2D diffusion coefficient in the plane (x, y) . thus we come to the old formula

$$\sigma = e^2 \int d\varepsilon g(\varepsilon) D(\varepsilon) \left(-\frac{\partial f_0}{\partial \varepsilon} \right)$$

where both $g(\varepsilon)$ and $D(\varepsilon)$ should be calculated with the help of quantum mechanics:

$$g(\varepsilon) = \sum_{\nu} \delta(\varepsilon - \varepsilon_{\nu}), \quad D(\varepsilon) = \frac{1}{g(\varepsilon)} \sum_{\nu, \nu'} \delta(\varepsilon - \varepsilon_{\nu}) \frac{(x_0 - x'_0)^2}{2} W_{\nu\nu'}.$$

One can see that the result is strongly dependent on the scattering mechanism and oscillates in the case of the Fermi statistics.

6.10 Response to “slow” perturbations

In this section we will discuss electron response to low-frequency perturbation which vary slowly in space.

Consider electron gas in a weak ac electric field $\mathbf{E}(\mathbf{r}, t)$. Let us separate odd and even in \mathbf{p} parts of the electron distribution function,

$$f(\mathbf{p}) = f^+(\mathbf{p}) + f^-(\mathbf{p}), \quad f^{\pm}(-\mathbf{p}) = \pm f^{\pm}(\mathbf{p}).$$

The key point of the following consideration is that the relaxation rates for the odd and even in \mathbf{p} components can be very much different. Indeed, elastic processes do not affect any function dependent only on the energy, and the average distribution function

$$F(\epsilon) = \langle f(\mathbf{p}) \rangle_{\epsilon} \equiv \frac{\int(d\mathbf{p}) f^+(\mathbf{p}) \delta(\epsilon_{\mathbf{p}} - \epsilon)}{\int(d\mathbf{p}) \delta(\epsilon_{\mathbf{p}} - \epsilon)}$$

is not effected by elastic scattering.

Assuming that inelastic processes are weak, we leave in the equation for f^- only elastic processes in the collision operator. As a result,

$$\frac{\partial f^-}{\partial t} + \mathbf{v} \frac{\partial f^-}{\partial \mathbf{r}} + e\mathbf{E} \frac{\partial f^+}{\partial \mathbf{p}} + \frac{f^-}{\tau_{\text{tr}}} = 0. \quad (6.63)$$

Such a procedure is not correct for f^+ because the main part of f^+ depends only on the electron energy. Thus one has to write

$$\frac{\partial f^+}{\partial t} + \mathbf{v} \frac{\partial f^+}{\partial \mathbf{r}} + e\mathbf{E} \frac{\partial f^-}{\partial \mathbf{p}} + I\{f^+\} = 0, \quad (6.64)$$

where the collision operator includes inelastic processes. Now let us assume

$$\omega\tau_{\text{tr}} \ll 1, \quad q\ell \ll 1$$

and solve Eq. (6.63),

$$f^-(\mathbf{p}) = -\tau_{\text{tr}}\mathbf{v}\frac{\partial f^+}{\partial \mathbf{r}} - e\tau_{\text{tr}}\mathbf{E}\frac{\partial f^+}{\partial \mathbf{p}}, \quad (6.65)$$

then substitute into Eq. 6.64 and average over the constant energy surface. One can show that the difference between $f^+(\mathbf{p})$ and $F(\epsilon_{\mathbf{p}})$ can be neglected if

$$eE\tau_{\text{tr}} \ll \bar{p}.$$

Neglecting this difference we arrive at the following equation for $F(\epsilon)$.

$$\frac{\partial F_1}{\partial t} - D_{ik}(\epsilon)\frac{\partial^2 F_1}{\partial x_i \partial x_k} + \langle I\{F_1\}\rangle_\epsilon = eD_{ik}(\epsilon)\frac{\partial E_k}{\partial x_i}\frac{\partial f_0}{\partial \epsilon}. \quad (6.66)$$

Here we have introduced $F_1 = F(\epsilon) - f_0(\epsilon)$ and

$$D_{ik} = \langle v_i \tau_{\text{tr}} v_k \rangle_\epsilon.$$

The typical estimate for the third term in Eq. 6.64 is F_1/τ_{in} where τ_{in} is the *inelastic* relaxation time. Thus the solution of Eq. (6.66) depends on the dimensionless quantities

$$\omega\tau_{\text{in}}, \quad q^2 D\tau_{\text{in}}.$$

Because usually in semiconductors at low temperatures

$$\tau_{\text{in}} \gg \tau_{\text{tr}}$$

these quantities can be large even at $\omega\tau_{\text{tr}}, q\ell \ll 1$.

Very low frequencies, $\omega\tau_{\text{in}}, q^2 D\tau_{\text{in}} \ll 1$.

In this case the third term in l.h.s. of Eq 6.66 is most important and one has to vanish this term. That can be done assuming that

$$F_1(\epsilon, \mathbf{r}, t) \propto f_0(\epsilon) = A(\mathbf{r}, t)f_0(\epsilon).$$

Multiplying this equation by the density of states $g(\epsilon)$ and integrating over the energies we get

$$A(\mathbf{r}, t) = n(\mathbf{r}, t)/n_0.$$

Here $n(\mathbf{r}, t)$ is the time- and position dependent electron density. In this way (in the isotropic case) we get

$$\frac{\partial n}{\partial t} - D\frac{\partial^2 n}{\partial x^2} = eD\frac{\partial E_x}{\partial x} \left(-\frac{\partial n_0}{\partial \zeta} \right). \quad (6.67)$$

Here ζ is the chemical potential while

$$D_{ik} = \frac{1}{n_0} \int d\epsilon g(\epsilon) f_0(\epsilon) D_{ik}(\epsilon).$$

Moving all the terms into l.h.s. we get instead of Eq. 6.67

$$\frac{\partial n}{\partial t} + \frac{1}{e} \frac{\partial}{\partial x} \left(-eD \frac{\partial n}{\partial x} + e^2 D \frac{\partial n}{\partial \zeta} E_x \right) = 0. \quad (6.68)$$

This is nothing else than the charge conservation law

$$e \frac{\partial n}{\partial t} + \operatorname{div} \mathbf{j} = 0.$$

Indeed, due to Einstein relation

$$\sigma = e^2 D \frac{\partial n_0}{\partial \zeta}$$

we have a usual expression for the current density'

$$j_x = \sigma E_x - eD \frac{\partial n}{\partial x}.$$

We conclude that at

$$\omega \tau_{\text{in}} \ll 1, \quad q^2 \tau_{\text{tr}} \tau_{\text{in}} \ll 1$$

one can employ very simple diffusion description of the response.

In the end of this section let us obtain a simplified expression for dielectric function at low frequencies. Let us assume that one applies an external field with the electrical induction

$$\mathbf{D}_e \exp(iqx - i\omega t) + \text{h.c.}$$

Then all the quantities are $\propto \exp(iqx - i\omega t)$, and one obtains

$$j = -iq(eDn + \sigma\phi), \quad (6.69)$$

the charge conservation law being

$$(-i\omega + q^2 D)n + e^{-1}q^2 \sigma\phi = 0. \quad (6.70)$$

Here n , and ϕ are Fourier components of the concentration and the potential, respectively. To relate the potential ϕ to the external field one has to employ Poisson equation

$$i\mathbf{q}\mathbf{D} = 4\pi en, \quad \mathbf{D} = -i\epsilon_0 \mathbf{q}\phi + \mathbf{D}_e.$$

We get

$$\epsilon_0 q^2 \phi + i\mathbf{q}\mathbf{D}_e = 4\pi en.$$

Now we can substitute n from Eq. (6.70) as

$$n = -\frac{1}{e} \frac{q^2 \sigma}{q^2 D - i\omega} \phi$$

to get

$$q^2 \phi \epsilon_0 \frac{-i\omega + q^2 D + 1/\tau_m}{-i\omega + q^2 D} = -i\mathbf{q}\mathbf{D}_e.$$

Here

$$\tau_m \equiv \epsilon_0 / 4\pi\sigma$$

is the well known Maxwell relaxation time. Having in mind that $\mathbf{E} = -i\mathbf{q}\phi$ and $\mathbf{E} = \mathbf{D}_e/\epsilon(\mathbf{q}, \omega)$ we get

$$\epsilon(\mathbf{q}, \omega) = \epsilon_0 \frac{-i\omega + q^2 D + 1/\tau_m}{-i\omega + q^2 D}. \quad (6.71)$$

As $\omega \rightarrow 0$

$$\epsilon(\mathbf{q}, 0) = \epsilon_0 \frac{q^2 + \kappa^2}{q^2}$$

where

$$\kappa^2 = \frac{4\pi\sigma}{\epsilon_0 D} = \frac{4\pi e^2}{\epsilon_0} \frac{\partial n_0}{\partial \zeta}$$

is the square of inverse static screening length.

6.11 “Hot” electrons

Now let us come back to the static case and discuss the difference between the function $F(\epsilon)$ and the equilibrium function $f_0(\epsilon)$. For this case let us calculate the second approximation in the electric field. Using (6.65) for the spatially uniform case we get

$$e\mathbf{E} \frac{\partial f^-}{\partial \mathbf{p}} + I\{f^+ - f_0\} = 0.$$

Now we can average this equation over the constant energy surface,

$$\langle e\mathbf{E} \frac{\partial f^-}{\partial \mathbf{p}} \rangle_e + \langle I\{f^+ - f_0\} \rangle_e = 0.$$

Substituting f^- from (6.65) and neglecting the difference between f^+ and its average over the constant energy surface we get

$$-e^2 E_i E_k \frac{1}{g(\epsilon)} \frac{\partial}{\partial \epsilon} g(\epsilon) D_{ik}(\epsilon) \frac{\partial F(\epsilon)}{\partial \epsilon} + \langle I\{F(\epsilon)\} \rangle_e = 0. \quad (6.72)$$

The first item in l.h.s. has a meaning of the power transferred from the field to the electrons with a given energy ϵ . The second term is the relaxation rate for the isotropic part of the non-equilibrium distribution function.

Let us calculate the relaxation rate of the power transferred from the field to the electrons with a given energy. We have

$$\langle I\{F(\epsilon)\}\rangle_e = \frac{1}{g(\epsilon)} \int (d\mathbf{p}) (d\mathbf{p}') \delta(\epsilon - \epsilon_{\mathbf{p}}) [W_{\mathbf{p}\mathbf{p}'} F(\epsilon_{\mathbf{p}}) - W_{\mathbf{p}'\mathbf{p}} F(\epsilon_{\mathbf{p}'})].$$

Let us replace $\mathbf{p} \rightarrow \mathbf{p}'$ and take a symmetric combination of the expressions. We get

$$\begin{aligned} \langle I\{F(\epsilon)\}\rangle_e &= \frac{1}{2g(\epsilon)} \int (d\mathbf{p}) (d\mathbf{p}') [\delta(\epsilon - \epsilon_{\mathbf{p}}) - \delta(\epsilon - \epsilon_{\mathbf{p}'})] \\ &\quad \times [W_{\mathbf{p}\mathbf{p}'} F(\epsilon_{\mathbf{p}}) - W_{\mathbf{p}'\mathbf{p}} F(\epsilon_{\mathbf{p}'})] \\ &\approx \frac{1}{2g(\epsilon)} \frac{\partial}{\partial \epsilon} \int (d\mathbf{p}) (d\mathbf{p}') (\epsilon_{\mathbf{p}'} - \epsilon_{\mathbf{p}}) \delta(\epsilon - \epsilon_{\mathbf{p}}) \\ &\quad \times [W_{\mathbf{p}\mathbf{p}'} F(\epsilon_{\mathbf{p}}) - W_{\mathbf{p}'\mathbf{p}} F(\epsilon_{\mathbf{p}'})]. \end{aligned}$$

Then let us take into account that

$$W_{\mathbf{p}'\mathbf{p}} = W_{\mathbf{p}\mathbf{p}'} \exp\left(\frac{\epsilon_{\mathbf{p}} - \epsilon_{\mathbf{p}'}}{kT}\right)$$

and expand it up to the first order in the energy difference,

$$W_{\mathbf{p}'\mathbf{p}} = W_{\mathbf{p}\mathbf{p}'} \left[1 + \frac{\epsilon_{\mathbf{p}} - \epsilon_{\mathbf{p}'}}{kT}\right].$$

Expanding also the distribution function we get finally

$$\langle I\{F(\epsilon)\}\rangle_e = -\frac{1}{g(\epsilon)} \frac{\partial}{\partial \epsilon} g(\epsilon) \frac{kT}{\tau_{\epsilon}} \left(1 + kT \frac{\partial}{\partial \epsilon}\right) F(\epsilon). \quad (6.73)$$

Here

$$\frac{1}{\tau_{\epsilon}(\epsilon)} = \frac{1}{g(\epsilon)} \int (d\mathbf{p}) (d\mathbf{p}') \delta(\epsilon - \epsilon_{\mathbf{p}}) W_{\mathbf{p}\mathbf{p}'} \left(\frac{\epsilon_{\mathbf{p}} - \epsilon_{\mathbf{p}'}}{kT}\right)^2 \quad (6.74)$$

has a meaning of the *energy relaxation rate*.

Energy relaxation rate for electron-phonon scattering

To give an example let us discuss the energy relaxation rate for electron-phonon collisions. Substituting the transition probability for the case of deformational-potential scattering one can re-write the collision operator through a dimensionless variable $x = \epsilon/kT$,

$$\langle I\{F(\epsilon)\}\rangle_e = -\frac{\sqrt{\pi}}{2\tau_{\epsilon}} \frac{1}{\sqrt{x}} \frac{d}{dx} x^2 \left(1 + \frac{d}{dx}\right) F(x), \quad (6.75)$$

where

$$\tau_{\epsilon} = \frac{\pi^{3/2} \hbar^4 \rho}{4\sqrt{2} \Lambda m^{5/2} \sqrt{kT}}.$$

The typical ratio

$$\frac{\tau_{\epsilon}}{\tau_{\text{tr}}} = \left(\frac{kT}{s\sqrt{mkT}}\right)^2 = \frac{kT}{ms^2} \gg 1.$$

Thus, scattering by acoustic phonons is a *quasi-elastic* process.

Non-equilibrium distribution function

Now we can substitute the expression for collision operator into Eq. (6.72). Assuming $\tau_{\text{tr}}(\epsilon) = \tau_{\text{tr}}(kT) \cdot x^s$ we get

$$\frac{1}{\sqrt{x}} \frac{d}{dx} \left[h x^{s+3/2} \frac{dF}{dx} + x^2 \left(1 + \frac{d}{dx} F \right) \right] = 0. \quad (6.76)$$

Here

$$h \equiv \frac{2}{\sqrt{\pi}} \frac{e^2 E_i E_k D_{ik}(kT) \tau_\epsilon}{(kT)^2}$$

is the so-called *heating parameter*. It has a transparent physical meaning. Having in mind Einstein relation for non-degenerate electron gas,

$$\sigma = e^2 n_0 D / kT,$$

we can express h as

$$h \sim \frac{\sigma E^2 \tau_\epsilon}{n_0 k T},$$

that is as the ratio of the energy absorbed during the relaxation time to the average energy.

We have

$$(h x^{s+1/2} + x^2) \frac{dF}{dx} + x^2 F = \text{constant} = 0. \quad (6.77)$$

Indeed, at large x the function F must vanish as well as its derivative. The general solution of Eq. (6.77) is

$$F(x) = \exp \left(- \int_A^x d\xi \frac{\xi^2}{\xi^2 + h \xi^{3/2+s}} \right),$$

the constant A being determined from the normalization condition

$$n = kT g(kT) \int dx \sqrt{x} F(x).$$

In many cases electron-electron scattering is very much important. To take it into account one has to add the proper collision operator. Electron-electron collisions do not remove the energy form the electronic system. However, they redistribute electrons between different energy levels leading to establishment of the Maxwell distribution with some effective temperature, T_e . We arrive at the qualitative picture of heating shown in Fig. 6.10

If

$$\tau_{ee} \ll \tau_\epsilon$$

one can think that the distribution function is $\propto \exp(-\epsilon/kT_e)$ and substitute

$$F(x) \propto \exp \left(-\frac{T}{T_e} x \right)$$

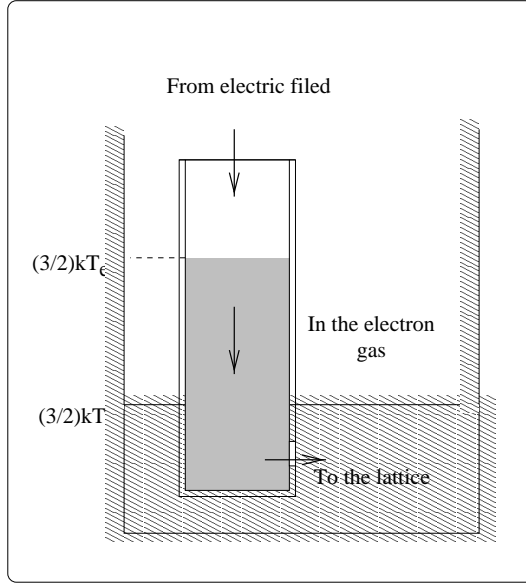


Figure 6.10: Schematic representation of the carrier energy balance.

into Eq. (6.77). We get

$$\left[x^2 - (hx^{s+3/2} + x^2) \frac{T}{T_e} \right] \exp\left(-\frac{T}{T_e}x\right) = 0. \quad (6.78)$$

To determine T_e one can use the energy balance, i.e. multiply Eq. (6.78) by the dimensionless “energy” x , integrate over x , and then solve the equation for the ratio T/T_e . Introducing new variable as, $x = (T_e/T)y$ and making integration over y we obtain the equation for $\theta \equiv T_e/T$

$$\theta - h\theta^{s-1/2} \frac{\Gamma(s+7/2)}{\Gamma(4)} - 1 = 0. \quad (6.79)$$

For example, at $s = 1/2$

$$T_e/T = 1 + h.$$

Electron heating is important in many devices. It leads to important limitations in electron mobility, as well as to a specific time response (e. g. to the so-called “overshoot”).

6.12 Impact ionization

We have assumed earlier that the charge carrier remains in the same band. At large fields ($E \geq 10^5$ V/cm) this assumption breaks down. A typical process of band-to-band impact ionization is shown in Fig. 6.11. The most common is impact ionization of shallow impurities where the critical field is very low. Indeed, the ionization energy of shallow impurities in Ge is about 10^{-2} eV, and the breakdown occurs at the fields of few V/cm. In Fig. 6.12 $I - V$ curves of n -Ge are shown in the temperature range 4.2-54.2 K. One

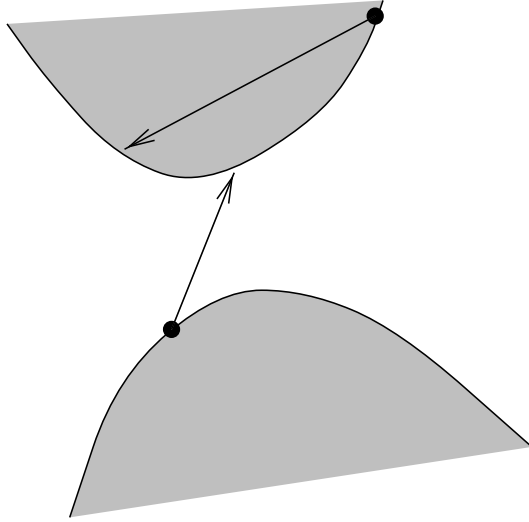


Figure 6.11: The impact ionization process where a high energy electron scatters from a valence band electron producing 2 conduction band electrons and a a hole.

clearly observed a threshold in the current which is masked at large temperatures as the impurities become ionized. The onset of the breakdown is shown more clearly in Fig. 6.13 where the reciprocal Hall coefficient and Hall mobility are shown. The decrease of Hall mobility is due to crossover to lattice scattering from the impurity one as the electron energy increases.

The breakdown is governed by the equation

$$\begin{aligned} \frac{dn}{dt} = & A_T(N_D - N_A) + A_I n [N_D - (N_A + n)] \\ & - B_T n (N_A + n) - B_I n^2 (N_A + n). \end{aligned} \quad (6.80)$$

Here A_T and A_I are the coefficients for thermal and impact ionization processes, $B_T(T, E)$ is the coefficient of thermal recombination of a single electron with an ionized donor, while $B_I(T, E)$ is the coefficient for the *Auger process* in which two electrons collide at an ionized donor, one being captured with the other taking the excess energy. This term is not important at small n . To understand the formula above note that $N_D - N_A$ is the concentration of uncompensated donors, $N_A + n$ is the concentration of ionized donors and $N_D - (N_A + n)$ is the concentration of neutral donors. The concentrations of neutral acceptors and holes are assumed to be negligible.

At small $n \ll N_A$ we obtain for the steady state concentration

$$n_0 = \frac{A_T(N_D - N_A)}{B_T N_A - A_I(N_D - N_A)}.$$

At a proper electric field, E_b , the denominator vanishes, this is just the breakdown point. It can be found from the expression

$$B_T(T, E_b) N_A = A_I(E_b)(N_D - N_A),$$

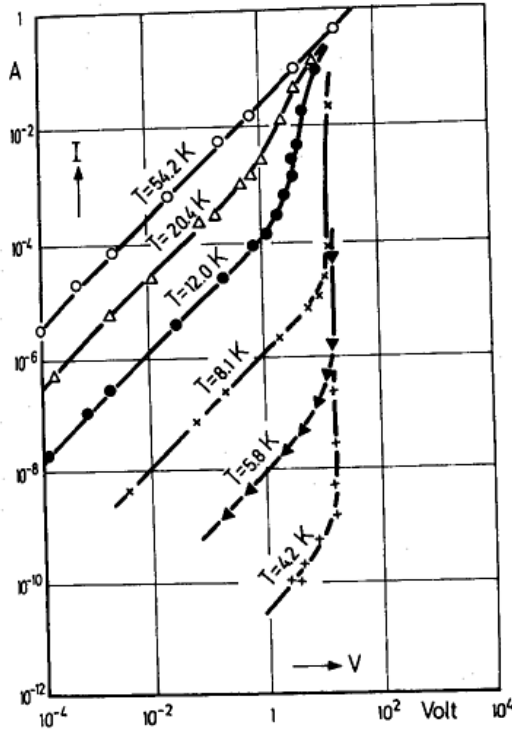


Figure 6.12: Current-voltage curves of n -Ge at low temperatures.

it depends only on the degree of compensation N_A/N_D . If one defines a time constant,

$$\tau = \frac{n_0}{A_T(N_D - N_A)},$$

then Eq. (6.80) can be re-written as

$$-\frac{dn}{dt} = \frac{n - n_0}{\tau},$$

so the recovery from breakdown must be exponential, it has been studied experimentally.

Impact breakdown is often accompanied by instabilities of $I - V$ curves.

6.13 Few Words About Phonon Kinetics.

In most of our consideration we have assumed the phonon distribution to be equilibrium. Actually, phonon system form a thermal bath for electrons. Such a assumption is based on the belief that phonons have efficient enough scattering which brings them to the equilibrium. Consequently, the temperature T is just the temperature of the phonon system.

At the same time, phonon distribution can be non-equilibrium. In particular, it is the case when a temperature gradient exists. To analyze the phonon kinetics one can

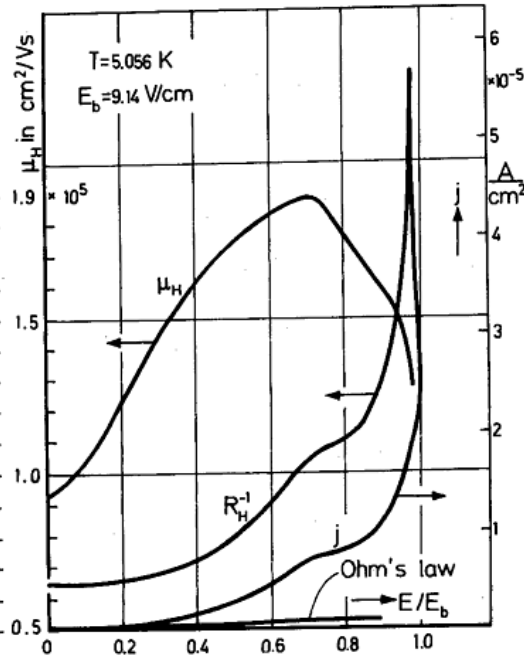


Figure 6.13: Impact ionization at low temperatures in n -Ge doped by Sb ($N_D - N_A = 2.2 \times 10^{14} \text{ cm}^{-3}$). The current density, reciprocal Hall coefficient and Hall mobility are shown, as well as extrapolated Ohm's law.

investigate the Boltzmann equation for phonons

$$\frac{\partial N}{\partial t} + s_g \frac{\partial N}{\partial \mathbf{r}} = I_{ph}(N, f), \quad s_g \equiv \frac{\partial \omega}{\partial \mathbf{q}}$$

where the collision integral is determined by the scattering processes. The most important of them are

- *Phonon-phonon processes.* These processes are rather complicated in comparison with the electron-electron ones because the number of phonons does not conserve. Consequently, along with the scattering processes ($2 \rightarrow 2$) there are processes ($2 \rightarrow 1$) and ($1 \rightarrow 2$). Scattering processes could be normal (N) or Umklapp ones. Their frequency and temperature dependencies are different ($\tau_N^{-1} \propto T\omega$, $\tau_U^{-1} \propto \exp(\Theta/T)$).
- *Scattering by static defects.* Usually it is the Rayleigh scattering (scattering by imperfections with the size less than the wave length, $\tau^{-1} \propto \omega^4$).
- *Scattering phonons by electrons.*

All these processes make the phonon physics rather complicated. We are not going to discuss it in detail. Rather we restrict ourselves with few comments.

Probably most important phenomenon is phonon contribution to thermal conductivity. Indeed, phonon flux transfers the energy and this contribution in many cases is the

most important. If one introduced the phonon transport relaxation time, τ_{ph} , the phonon contribution can be derived in the same way as for electrons. The result is

$$\kappa_{ph} = \int d\omega \hbar\omega g_{ph}(\omega) D_{ph}(\omega) \frac{\partial N_\omega}{\partial T}$$

where

$$D_{ph}(\omega) = \frac{1}{3} \langle s_g I^{-1} s_g \rangle_\omega$$

is the phonon diffusion coefficient. As we have discussed, N-processes cannot lead to finite thermal conductivity and one take into account defect scattering, or Umklapp-processes. Usually, the phonon thermal conductivity increases with the decrease of the temperature. Nevertheless, at low temperatures the phonon mean free path becomes of the order of the sample size, and boundary scattering appears very important. It is the case in many devices of modern electronics.

In very clean materials, the impurity scattering appears ineffective both for phonons and electrons. In this case at low temperatures (when Umklapp processes are not important) electron and phonon systems strongly interact (*electron-phonon drag*). As a result, the kinetics becomes rather complicated and very interesting.

6.14 Problems

6.1. An electron with an energy spectrum

$$\varepsilon(\mathbf{p}) = \frac{p_x^2}{2m_x} + \frac{p_y^2}{2m_y} + \frac{p_z^2}{2m_z}$$

is placed into a magnetic field parallel to **z**-axis. Find the cyclotron effective mass and compare it with the density-of-states effective mass defined as

$$g(\varepsilon) = \frac{\sqrt{2}m_d^{3/2}\varepsilon^{1/2}}{\pi^2\hbar^3}.$$

6.2. Derive the Drude formula.

6.3. Assume that the electrons obey Boltzmann statistics,

$$f_0(\varepsilon) = \exp\left(\frac{\zeta - \varepsilon}{T}\right),$$

and that

$$\tau_{tr}(\varepsilon, T) \propto \varepsilon^r.$$

Expressing the transport relaxation time as

$$\tau_{tr}(\varepsilon, T) = \tau_0(T)(\varepsilon/kT)^r$$

find the expressions for Drude conductance at $\omega\tau_0 \ll 1$ and $\omega\tau_0 \gg 1$.

6.4. Compare thermopower $\alpha = \eta/\sigma$ for degenerate and non-degenerate electron gas. Assume

$$\tau_{\text{tr}}(\varepsilon, T) = \tau_0(T)(\varepsilon/kT)^r.$$

6.5. Using the Wiedemann-Franz law compare the coefficients κ and β for a typical metal.

6.6. Derive the expression (6.26) for the screened Coulomb potential.

$$\varphi = \frac{Ze}{r} e^{-r/r_s},$$

6.7. Derive the expression (6.27).

$$W(\theta) = 4\pi n_i v \left[\frac{e^2/\epsilon}{2\varepsilon(1 - \cos\theta) + \hbar^2/2mr_s^2} \right]^2$$

6.8. Derive Eq. (6.44) for the polarization.

6.9. Derive Eq. (6.46).

6.10. Derive the expression for the solution of the Boltzmann equation

$$\mathbf{G} = e\tau_{\text{tr}} \frac{\partial f_0}{\partial \varepsilon} \frac{\mathbf{E} + (\mu/c)^2(\mathbf{H}\mathbf{E})\mathbf{H} + (\mu/c)[\mathbf{E}\mathbf{H}]}{1 + \mu^2 H^2/c^2}.$$

Use this expression to calculate the conductivity tensor.

6.11. Derive the condition $c = -\infty$ for Eq. (6.56).

6.12. Using the expression (6.71) find imaginary part of $1/\epsilon(\mathbf{q}, \omega)$ which is responsible for damping of the wave of electrical polarization.

Chapter 7

Electrodynamics of Metals

In this Chapter we discuss ac properties of metals.

7.1 Skin Effect.

Normal Skin Effect.

Assume that the sample is placed in an external ac electromagnetic field. The Maxwell equations read

$$\operatorname{curl} \mathbf{E} = -\frac{1}{c} \frac{\partial \mathbf{H}}{\partial t}, \quad \operatorname{curl} \mathbf{H} = \frac{4\pi}{c} \mathbf{j}.$$

As a starting point we assume that $\mathbf{j} = \sigma \mathbf{E}$ and consider the arrangement shown in Fig. 7.1: $\mathbf{E} \parallel \mathbf{y}$, $\mathbf{H} \parallel \mathbf{z}$, the propagation direction is \mathbf{x} . Let all the fields be proportional to

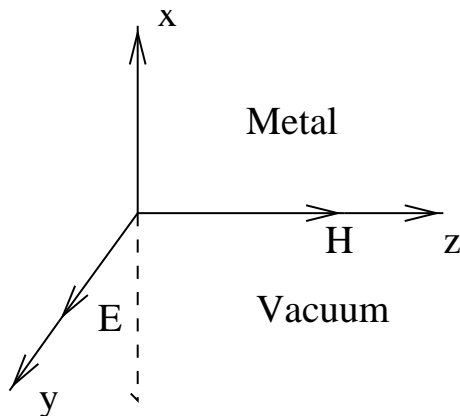


Figure 7.1: Arrangement for the calculation of the skin-effect.

$\exp [i(qx - \omega t)]$. We get the following equations

$$iqE_y = i\frac{\omega}{c}H_z, \quad -iqH_z = \frac{4\pi}{c}\sigma E_y.$$

Combining these equations we get

$$q^2 = 4\pi i \omega \sigma / c^2 \rightarrow q = \sqrt{4\pi i \omega \sigma / c^2} = (1+i) \sqrt{2\pi \omega \sigma / c^2} = q_1 + iq_2.$$

We see that the wave damps in the metal, the penetration depth being

$$\delta = \frac{1}{q_2} = \frac{c}{\sqrt{2\pi \omega \sigma}}. \quad (7.1)$$

Usually the surface impedance is introduced as a sheet resistance of a surface layer

$$Z = E_y(0) / \int_0^\infty j_y dx \equiv R - iX.$$

The active (R) and reactive (X) components can be measured by monitoring the amplitude and phase of the reflected wave. The part R is responsible for the heating of the metal (surface quenching). Using the Maxwell equations we can rewrite

$$Z = \frac{E_y(0)}{-(c/4\pi)H_z|_0^\infty} = \frac{4\pi}{c} \frac{E_y(0)}{H_z(0)} = \frac{4\pi \omega}{c^2} \frac{\omega}{q}.$$

Substituting (7.1) we get

$$R = X = \sqrt{\frac{2\pi\omega}{\sigma c^2}}.$$

Anomalous Skin Effect.

Let us consider the expression (7.1) in more detail. At low temperatures σ increases and in clean metals it can be large. So the skin depth decreases (at least at high frequencies). On the other hand, the mean free path ℓ *increases* with the decrease of the temperature. Finally, one can face the violation of the simple expression $\mathbf{j} = \sigma \mathbf{E}$ we have employed. Indeed, this expression can be valid only if all the fields change slowly at the scale of ℓ .

Now we consider the case $\delta \ll \ell$ that leads to the *anomalous skin effect* (London, 1940). The picture of the fragment of the electron orbit near the surface is shown in Fig. 7.2. Only the electrons with small component v_x contribute to the interaction with the field (the other ones spend a very small part of time within the region where the field is present). Introducing the spherical co-ordinate system with the polar axis along \mathbf{x} we estimate $d\Omega \sim \delta/\ell$, and the solid angle element being

$$d\Omega \sim 2\pi \sin \theta d\theta \approx 2\pi \delta/\ell, \quad (\theta \approx \pi/2).$$

The effective density of electrons participating in the interaction is

$$n_{\text{eff}} \sim n_e \frac{d\Omega}{4\pi} \sim n_e \delta/\ell.$$

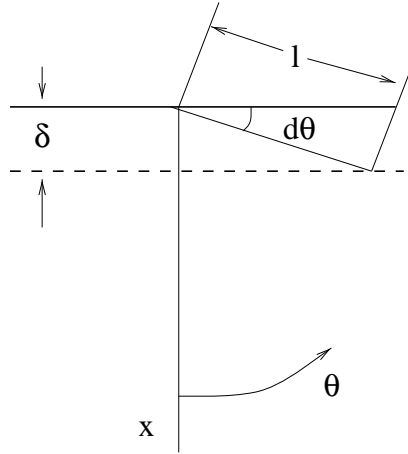


Figure 7.2: On the anomalous skin-effect.

So, we come to the conclusion that the effective conductivity should also contain the factor $\sim \delta/\ell$, while the complex coefficient cannot be determined by these simple considerations. It can be shown by exact calculation that

$$\sigma_{\text{eff}} = \sigma_0 \frac{ib}{q\ell}$$

where q is the wave vector while $b \sim 1$. This estimate means that the mean free path ℓ is replaced by the imaginary quantity i/q . Now we can use the expression

$$q = \sqrt{4\pi i \omega \sigma_{\text{eff}} / c^2}$$

and get (*Problem 7.1*)

$$q = \left[\frac{4\pi \omega \sigma_0 b}{c^2 \ell} \right]^{1/3} e^{i\pi/3}. \quad (7.2)$$

Consequently,

$$\delta = \frac{1}{\text{Im } q} = \frac{2}{\sqrt{3}} \left(\frac{c^2 \ell}{4\pi \sigma_0 b} \right)^{1/3}. \quad (7.3)$$

The surface impedance could be found as

$$Z = \frac{4\pi \omega}{c^2 q} = \left(\frac{2}{b} \right)^{1/3} \left(\frac{\pi \omega}{c^2} \right)^{2/3} \left(\frac{\ell}{\sigma_0} \right)^{1/3} (1 - \sqrt{3}).$$

We get: $Z \propto \omega^{2/3}$, $X = R\sqrt{3}$. It is important that the conductivity σ_0 enters only in the combination σ_0/ℓ which is determined only by the electron spectrum. The typical dependence of the surface conductance R on $\sqrt{\sigma_0}$ is shown in Fig. 7.3. This dependence is confirmed by the experiment.

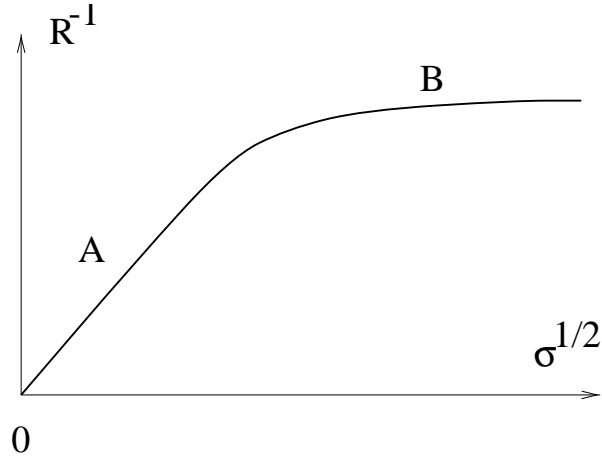


Figure 7.3: Dependence of the surface conductance on the bulk conductivity.

Finally, let us estimate the border between the normal skin effect and the anomalous one. From the criterion $\delta \approx \ell$ we get

$$\omega \sim c^2 p_F / (2\pi n_e e^2 \ell^3).$$

For $n_e \sim 10^{22} \text{ cm}^{-3}$, $p_F \sim 10^{-19} \text{ g}\cdot\text{cm}/\text{s}$ we get

$$\omega \sim 10^{-2} \ell^{-3}, \text{ s}^{-1}$$

where ℓ is measured in cm. For $\ell \sim 10^{-3} \text{ m}$ we get $\omega \sim 10^7 \text{ s}^{-1}$. We do not demonstrate here quite complicated procedure of solution of the Boltzmann equation.

7.2 Cyclotron Resonance

Now we consider the case where an external magnetic field is also applied. To understand the physical picture let us look at Fig. 7.4. Assume that the field is strong enough and

$$r_c \ll \ell.$$

In this case electrons move along helicoidal lines, the projection to x, y -plane being shown in the picture. If the frequency ω of the external electromagnetic field is high and the temperature is low the condition

$$\delta \ll r_c$$

is also met. The main physics is connected with the possibility for some electrons to return into the skin layer while the most part of time they spend in a field-free region. We understand that if the frequency ω equals to ω_c the returning electrons are each time accelerated by the electromagnetic field. This is the source of the cyclotron resonance in metals (Azbel, Kaner, 1956). It is clear that the resonance condition depends on the orbit shape and one can study the latter observing the resonance.

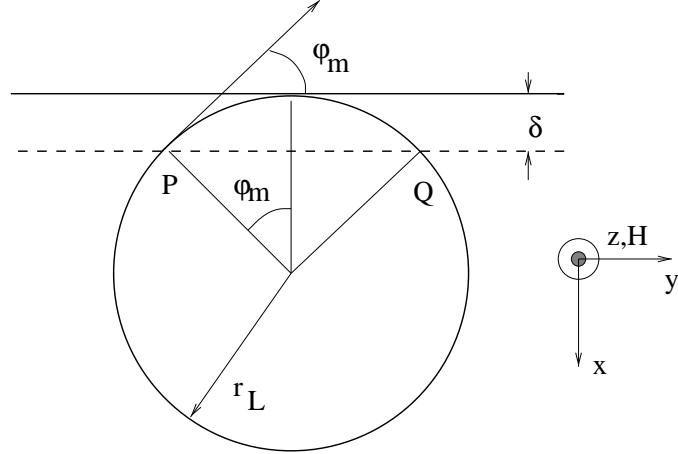


Figure 7.4: On the cyclotron resonance in metals.

To estimate the effect we write down the *non-stationary* Boltzmann equation

$$\frac{\partial f}{\partial t} + \frac{\partial f}{\partial t_1} + \mathbf{v} \frac{\partial f}{\partial \mathbf{r}} - e E_z \frac{\partial f}{\partial p_z} - e(\mathbf{v} \cdot \mathbf{E}) \frac{\partial f}{\partial \epsilon} = -\frac{f - f_0}{\tau}.$$

where the “trajectory time” t_1 was introduced by Eq. (6.54). It is important that the relaxation time approximation is *exact* in this case. The reason is that the only small group of electrons is important and “in” term of the collision integral is much less than the “out” one. Consequently, in this equation

$$\frac{1}{\tau(\mathbf{p})} = \sum_{\mathbf{p}'} W_{\mathbf{p}, \mathbf{p}'} \delta(\epsilon_{\mathbf{p}} - \epsilon_{\mathbf{p}'}).$$

Considering the electric field, \mathbf{E} as small, we put

$$f = f_0 + a \left(-\frac{\partial f_0}{\partial \epsilon} \right)$$

and get

$$\frac{\partial a}{\partial t_1} + (-i\omega + \tau^{-1})a + \mathbf{v} \frac{\partial a}{\partial \mathbf{r}} = -e(\mathbf{v} \cdot \mathbf{E}).$$

Now we remember the characteristic method to solve partial differential equations. Namely, we can write

$$dt_1 = \frac{dx}{v_x} = \frac{dy}{v_y} = \frac{da}{-e(\mathbf{v} \cdot \mathbf{E}) - (-i\omega + \tau^{-1})a}.$$

The first two equations give the electron trajectory

$$\mathbf{r}(t_2) - \mathbf{r}(t_1) = \int_{t_1}^{t_2} \mathbf{v}(t_3) dt_3.$$

It corresponds to the instant position of the electron which feels the field $\mathbf{E}(\mathbf{r}(t_i))$. As a result, we get the equation

$$\frac{\partial a}{\partial t_1} + (-i\omega + \tau^{-1})a = -e\mathbf{v}(t_1)\mathbf{E}(\mathbf{r}(t_1))$$

The solution is

$$a(\mathbf{r}, t_1) = -e \int_c^{t_1} \mathbf{v}(t_2)\mathbf{E}(\mathbf{r}(t_2)) \exp [(-i\omega + \tau^{-1})(t_2 - t_1)] dt_2$$

where the integration constant can be taken from the boundary conditions. As we have seen, if the orbit does not touch the surface one can put $c = -\infty$.¹ It is important, that we are interested in the function a at a given point \mathbf{r} at the time t_1 . So we should pick up the electrons with

$$\mathbf{r}(t_2) = \mathbf{r} + \int_{t_1}^{t_2} \mathbf{v}(t_3) dt_3.$$

Now we come to the result for the current

$$j_i = e^2 \int (ds_F) v_i \sum_k \int_{-\infty}^{t_1} v_k(t_2) E_k(\mathbf{r}(t_2)) \exp [(-i\omega + \tau^{-1})(t_2 - t_1)] dt_2. \quad (7.4)$$

This is the general formula and we need to specify all the dependencies. We will not do all the calculations. Rather we will make the order-of-magnitude estimates.

Consider the orbit depicted in Fig. 7.4. If we introduce the maximal angle φ_m for

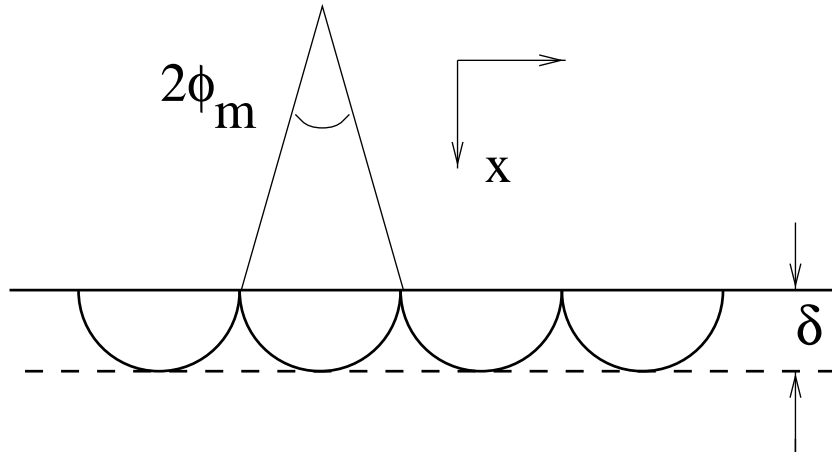


Figure 7.5: Surface orbits.

effective interaction region, we get

$$\delta = r_c(1 - \cos \varphi_m), \quad \text{or} \quad r_c \varphi_m^2 \sim \delta \quad \rightarrow \quad \varphi_m \sim \sqrt{\frac{\delta}{r_c}}.$$

¹The electrons which touch the surface are not important for the resonance, they produce a background current.

The length of the orbit inside the skin layer is $\approx 2r_c\varphi_m$, the duration time being $2r_c\varphi_m/v_y$. This is very short period in comparison with the total time $\mathcal{T} = 2\pi/\omega_c$ between successive excursions to the interaction region. As a result, $\int_{-\infty}^{t_1}$ in Eq. (7.4) splits into the sum of the contributions corresponding to each excursion. It is important, that the only difference between the contributions is the factors $\exp(-kw)$ where

$$w = \mathcal{T}(\tau^{-1} - i\omega) \quad (7.5)$$

while $k = 1, 2, \dots$. Finally, the integral is proportional to

$$(2r_c\varphi_m/v_y)(1 + e^{-w} + e^{-2w} + \dots) = \frac{2r_c\varphi_m}{v_y} \frac{1}{1 - e^{-w}}.$$

The remaining integral over the FS can be written as

$$\int dS_F \rightarrow \int \frac{d\Omega}{K(\theta, \varphi)}$$

where $K(\theta, \varphi)$ is the so-called *Gaussian curvature* which is just the product $K = (R_1 R_2)^{-1}$, $R_{1(2)}$ is the principal radius of curvature at the point with the direction θ, φ of the normal (see Fig. 7.6).

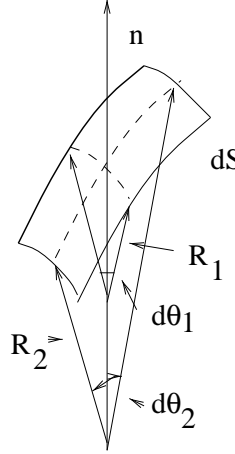


Figure 7.6: The definition of the Gaussian curvature.

Now we can estimate the integral. We see that the important electrons move along the sample's surface. So the integral over $d\theta$ is of the order of

$$v_x \max/v \quad \text{or} \quad (v_y/v)\varphi_m.$$

Finally, after the integration over θ we get the contribution $v_y\varphi_m/vK(\varphi)$, where $K(\varphi) \equiv K(\pi/2, \varphi)$. Picking up everything, we get

$$j_i \sim \frac{2e^2}{(2\pi\hbar)^3} \int \frac{d\varphi}{v} \frac{2r_c\varphi_m}{v_y} \frac{v_y\varphi_m}{vK(\varphi)} \frac{v_i v_k E_k}{1 - e^{-w}}.$$

Substituting the estimate for φ_m we get

$$(\sigma_r)_{ik}(\omega, H) \sim \frac{2e^2}{(2\pi\hbar)^3} \int d\varphi \frac{\delta}{1 - e^{-w}} \frac{n_i n_k}{K(\varphi)}.$$

Here $\mathbf{n} \equiv \mathbf{v}/v$. In the absence of external magnetic field $w \rightarrow \infty$ and we return to the result

$$\sigma_r(\omega, 0) \sim \sigma_0 \delta / \ell$$

for the anomalous skin-effect.

Now we should remember that there are electrons which reach the sample's surface. Most important are the ones shown in Fig. 7.5. To estimate the corresponding contribution of these electrons we take into account that $n_{\text{eff}} \sim n_e \varphi_m \sim n_e \sqrt{\delta/r_c}$. One could write the usual estimate for the conductivity using the effective number of electrons. But this result appears wrong because it does not take into account that there is finite fraction of diffuse scattering from the surface. If this fraction is β one can write

$$\sigma_s \sim \sigma_0 \frac{\varphi_m}{1 + \beta\mu}$$

where μ is the number of the reflections from the surface along the path ℓ . This factor takes into account the momentum transfer to the surface. We have

$$\mu \sim \frac{\ell}{r_c \varphi_m} \sim \sqrt{\frac{\ell^2}{\delta r_c}} \gg 1.$$

The fraction β has also the estimate $\beta \sim \varphi_m$ for a surface with atomic roughness. So, for an estimate, we can put $\beta\mu \sim \ell/r_c \gg 1$, and

$$\sigma_s \sim \sigma_0 \frac{\varphi_m}{\beta\mu} \sim \sigma_0 \frac{\varphi_m}{\varphi_m \mu} \sim \sigma_0 \frac{\sqrt{\delta r_c}}{\ell}$$

As a result, we see that if the factor $(1 - e^{-w})^{-1}$ is of the order 1, and $\sigma_s \gg \sigma_r$. Then we can proceed as follows. Introducing $\alpha \equiv \sigma_r/\sigma_s \ll 1$ we write effective conductivity as

$$\sigma_{\text{eff}} \sim \sigma_0 \frac{\sqrt{\delta r_c}}{\ell} (1 + \alpha)$$

and substitute it to the self-consistent equation for the penetration depth (7.2). The result is

$$\delta \sim \left(\frac{c^2 \ell}{\omega \sigma_0} \right)^{2/5} \frac{1}{r_c^{1/5}} \frac{1}{(1 + \alpha)^{2/5}}$$

and

$$Z \sim \frac{\omega \delta}{c^2} \sim \left(\frac{\omega}{c^2} \right)^{3/5} \left(\frac{\ell}{\sigma_0} \right)^{2/5} \frac{1}{r_c^{1/5}} \left(1 - \frac{2}{5}\alpha \right).$$

From this expression the ratio

$$\frac{Z_r}{Z} \sim \sqrt{\frac{\delta}{r_c}} \sim \left(\frac{c^2 \ell}{\omega \sigma_0 r_c^3} \right)^{1/5} \ll 1.$$

Now we can estimate the resonant part in more detail. To do this we should analyze the integral

$$B_{ik} = \int_0^{2\pi} \frac{n_i n_k}{K(\varphi)} \frac{d\varphi}{1 - e^{-w(\varphi)}}$$

In the denominator we have

$$1 - e^{-w} = 1 - \exp \left[\frac{2\pi i \omega}{\omega_c} \right] \exp \left[-\frac{2\pi}{\omega_c \tau} \right]$$

Because $\omega_c \tau \gg 1$ we have the resonances at $\omega/\omega_c = k$ where k is an integer.

The complication is that ω_c depends on φ . To clarify the situation let us recall that $\omega_c = eH/mc$ where

$$m(p_z) = \frac{1}{2\pi} \left[\frac{\partial S(p_z, \varepsilon)}{\partial \varepsilon} \right]_{\epsilon_F}.$$

We are interested in the points where $v_x = 0$ since only such electrons spend long time near the surface. These points are connected by the dash line in Fig. 7.7.

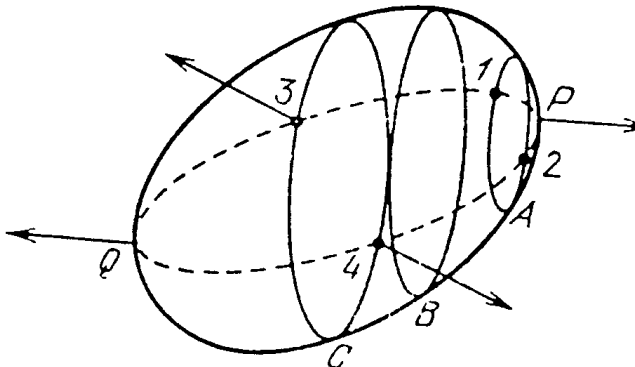


Figure 7.7: Momentum space geometry for the cyclotron resonance. Several orbits (A, B, C) in planes $p_z = \text{const}$ perpendicular to the magnetic field direction are shown on a closed Fermi surface with inversion symmetry. Most of the absorption comes from a narrow band centered about the contour (dashed line) where the velocity of the electrons is parallel to the surface, e.g., at the two points marked 3 and 4 on the central section C , or at those marked 1 and 2 on orbit A . These two points coalesce at the elliptic limiting points P and Q where the velocity is parallel to the magnetic field.

The problem is that the effective mass is not constant along this line because the energy spectrum is not quadratic. So, only small fraction of the trajectories can be important,

i.e. the ones near the sections with maximum density of states, or with extremal *effective mass*. Suppose that we are near the k -th resonance

$$\omega = k\omega_{\text{ext}}, \quad \text{where } \omega_{\text{ext}} = eH/m_{\text{ext}}c.$$

It is the case for some magnetic field H_k . Usually the frequency is fixed while people change the magnetic field and monitor the absorption. Thus, if $\Delta \equiv (H - H_k)/H_k$; we can write

$$\omega_c = \frac{\omega}{k} [1 + \Delta + b(\varphi - \varphi_0)^2]$$

where the angle φ_0 specifies the direction for the extremum effective mass while b is a dimensionless constant of the order 1. In this case, expanding e^{-w} where w is given by Eq. (7.5) in powers of $(\omega_c\tau)^{-1}$, $(\varphi - \varphi_0)^2$, Δ we get

$$1 - e^{-w} \approx w + 2\pi ik \approx 2\pi k [(\omega\tau)^{-1} + \Delta + b(\varphi - \varphi_0)^2].$$

The integral being determined by the vicinity of φ_0 , and we get

$$B_{ik} = \frac{n_i(\varphi_0)n_k(\varphi_0)}{K(\varphi_0)} \int_{-\infty}^{\infty} \frac{dx}{2\pi ika[x^2 + \Delta/b - i/b\omega_c\tau]} \equiv B_{ik}^{(0)}(\varphi_0)I.$$

In fact, according to Fig. 7.7 there are 2 points of the intersection between the extreme cross section and the line $v_x = 0$. The integrals I are the same while one should take the sum of the factors $B_{ik}^{(0)}(\varphi_0)$ in both points (3 and 4).

The integral I depends on the relation between the parameters Δ and $(\omega\tau)^{-1}$. At $b > 0$

$$I = \begin{cases} -i \left(2k\sqrt{\Delta b}\right)^{-1}, & \Delta > 0 \\ \left(2k\sqrt{\Delta b}\right)^{-1}, & \Delta < 0. \end{cases} .$$

At $b < 0$

$$I = \begin{cases} \left(2k\sqrt{\Delta|b|}\right)^{-1}, & \Delta > 0 \\ i \left(2k\sqrt{\Delta|b|}\right)^{-1}, & \Delta < 0. \end{cases}$$

We see that the result depends on the character of extreme (maximum or minimum). The resonant contribution is maximal at $\Delta \sim (\omega\tau)^{-1}$: $I_{\max} \sim (1/k)\sqrt{\omega\tau}$ For $k \sim 1$ it means $I_{\max} \sim \sqrt{\omega_c\tau}$. Consequently, at the maximum the ratio Z_r/Z acquires the extra large factor $\sqrt{\omega_c\tau}$, and

$$\left[\frac{Z_r}{Z} \right]_{\max} \sim \frac{\sqrt{\delta\ell}}{r_c}.$$

This ratio could be in principle large but usually is rather small.

The procedure employed is valid at $\omega_c\tau \gg 1$. In the opposite limiting case the oscillatory part of the impedance is exponentially small.

In real metals there are many interesting manifestations of the cyclotron resonance corresponding to different properties of FS. A typical experimental picture is shown in Fig. 7.8.

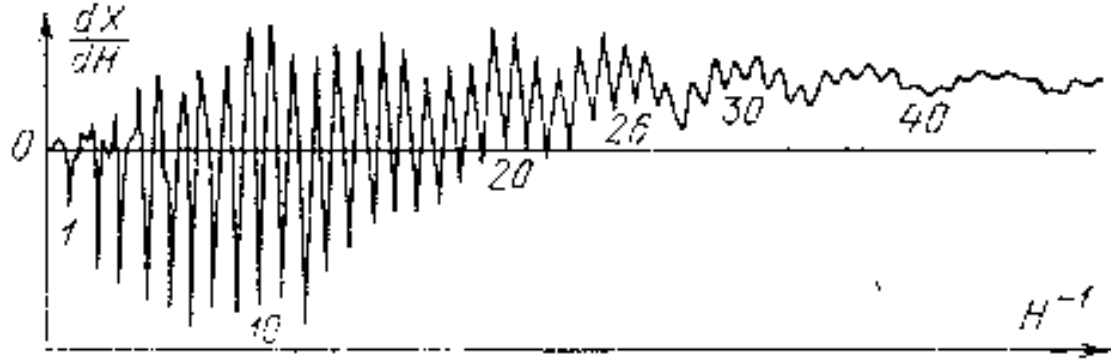


Figure 7.8: Typical experimental picture of the cyclotron resonance.

7.3 Time and Spatial Dispersion

General Considerations

In general, the current density $\mathbf{j}(\mathbf{r}, t)$ is determined by the electric field in the vicinity of the point \mathbf{r} and at previous times $t_1 < t$

$$\mathbf{j}(\mathbf{r}, t) = \int d\mathcal{V}_1 \int_{-\infty}^t dt_1 \sigma(\mathbf{r} - \mathbf{r}_1, t - t_1) \mathbf{E}(\mathbf{r}_1, t_1).$$

After Fourier transform we get

$$\mathbf{j}(\mathbf{q}, \omega) = \sigma(\mathbf{q}, \omega) \mathbf{E}(\mathbf{q}, \omega)$$

where $\sigma(\mathbf{q}, \omega)$ should be analytical function of ω in the upper half-space to keep the causality. Making use of the Boltzmann equation in the relaxation time approximation we get

$$\sigma_{ik}(\mathbf{q}, \omega) = e^2 \int (dp) \frac{v_i v_k}{i(\mathbf{q}\mathbf{v} - \omega) + \tau^{-1}} \left(-\frac{\partial f_0}{\partial \epsilon} \right).$$

In the case $q \rightarrow 0$, $\omega \rightarrow 0$ we return to the expression for the static conductivity. We see that there are 3 parameters with the dimension of frequency: qv , ω , and τ^{-1} . At

$$qv, \omega \ll \tau^{-1}$$

we return to the static case. In the general case we can write

$$\frac{1}{i(\mathbf{q}\mathbf{v} - \omega) + \tau^{-1}} = \frac{-i(\mathbf{q}\mathbf{v} - \omega) + \tau^{-1}}{(\mathbf{q}\mathbf{v} - \omega)^2 + \tau^{-2}} = \frac{1}{qv} \frac{-i(\cos \vartheta - \omega/qv) + (qv\tau)^{-1}}{(\cos \vartheta - \omega/qv)^2 + (qv\tau)^{-2}}$$

where ϑ is the angle between \mathbf{q} and \mathbf{v} . The case of strong *spatial dispersion* corresponds to

$$q\bar{v} \gg \omega, \tau^{-1}.$$

We see that σ_{\perp} (i.e. for the direction perpendicular to \mathbf{q}) strongly differs from σ_{\parallel} . Indeed

$$\sigma_{\perp} \sim e^2 \int d\varepsilon g(\varepsilon) \left(-\frac{\partial f_0}{\partial \varepsilon} \right) \int \frac{\sin \vartheta d\vartheta d\varphi}{4\pi} \frac{v^2 \sin^2 \vartheta \cos^2 \varphi}{qv} \pi \delta \left(\cos \vartheta - \frac{\omega}{qv} \right) \sim \frac{3\pi}{4} \frac{\sigma_0}{q\ell}.$$

This result is connected to the estimates which have been made in concern with the anomalous skin-effect. For σ_{\parallel} and $\omega\tau \ll 1$ we get

$$\sigma_{\parallel} \sim e^2 \int d\varepsilon g(\varepsilon) \left(-\frac{\partial f_0}{\partial \varepsilon} \right) \int \frac{\sin \vartheta d\vartheta}{2} \frac{v^2 \cos^2 \vartheta}{qv} \frac{(qv\tau)^{-1}}{(\cos \vartheta - \omega/qv)^2 + (qv\tau)^{-2}} \sim 3 \frac{\sigma_0}{(q\ell)^2}.$$

The limiting case

$$\omega \gg qv, \tau^{-1}$$

is called the *time dispersion* one. We get next to isotropic conductivity

$$\sigma(\omega) \sim e^2 \int d\varepsilon g(\varepsilon) \left(-\frac{\partial f_0}{\partial \varepsilon} \right) \int \frac{\sin \vartheta d\vartheta d\varphi}{4\pi} \frac{v^2 \sin^2 \vartheta \cos^2 \varphi}{-i\omega} \sim -\frac{\sigma_0}{i\omega\tau}.$$

If we apply the Drude formula, we get

$$\sigma(\omega) = i \frac{\epsilon}{4\pi} \frac{\omega_p^2}{\omega}, \quad \text{where } \omega_p^2 = \frac{4\pi n_e e^2}{\epsilon m} \quad (7.6)$$

is the *plasma frequency*. This term is connected with the plasma oscillations in an electron gas. Indeed, let us consider longitudinal oscillations. We get the Poisson equation

$$\operatorname{div} \mathbf{D} = \epsilon \operatorname{div} \mathbf{E} = -4\pi e(\delta n_e).$$

Then we can apply the continuity equation,

$$-e \frac{\partial n_e}{\partial t} + \operatorname{div} \mathbf{j} = 0 \rightarrow ie\omega(\delta n_e) + \sigma(\mathbf{q}, \omega)i(\mathbf{q}\mathbf{E}^*) = 0.$$

Here

$$\mathbf{E}^* = -\nabla(\varphi - \zeta/e) = \mathbf{E} + (1/e)(\partial\zeta/\partial n_e)\nabla(\delta n_e) = \mathbf{E} + (eg_T)^{-1}i\mathbf{q}(\delta n_e).$$

As a result, we come to the equation for (δn_e)

$$\left(ie\omega - \frac{\sigma}{eg_T} q^2 \right) (\delta n_e) + \sigma i(\mathbf{q}\mathbf{E}) = 0$$

Consequently,

$$\delta n_e = -\sigma(\mathbf{q}, \omega) \frac{(\mathbf{q}\mathbf{E})}{e[\omega + iD(\mathbf{q}, \omega)q^2]}, \quad \text{and} \quad \left[\epsilon + i \frac{4\pi\sigma(\mathbf{q}, \omega)}{\omega + iD(\mathbf{q}, \omega)q^2} \right] \mathbf{E} = \mathbf{0}.$$

Here we have denoted

$$D(\mathbf{q}, \omega) = \frac{\sigma(\mathbf{q}, \omega)}{e^2 g_T}$$

As a result, we get the following dispersion law for the waves in a gas

$$\epsilon_{\text{eff}} = \epsilon + i \frac{4\pi\sigma(\mathbf{q}, \omega)}{\omega + iD(\mathbf{q}, \omega)q^2} = 0.$$

Substituting (7.6) we get

$$iD(\mathbf{q}, \omega)q^2 = -\frac{\epsilon}{4\pi e^2 g_T} \frac{\omega_p^2}{\omega} q^2 = -\frac{\omega_p^2}{\omega} (qR)^2$$

and come to the dispersion equation

$$1 - \frac{\omega_p^2}{\omega^2} \frac{1}{1 - (\omega_p^2/\omega^2)(qR)^2} = 0.$$

At $qR \ll 1$ we get plasma oscillations. If we expand the relation (7.6) in powers of qv/ω and put $\omega = \omega_p$ we obtain the dispersion law for plasma waves (*plasmons*), see *Problem 7.2*.

In a quasi static limiting case $\omega \ll qv_F$ we get

$$\epsilon_{\text{eff}} = \epsilon \frac{q^2 + R^{-2}}{q^2}$$

i.e. the static screening.

The Jellium Model

Now we introduce a very simple but instructive model of the electron-ion response to the external field. This model is very useful to treat the nature of electron-electron interaction in superconductors, as well to make estimates.

As we have seen in the previous section, the effective dielectric function with respect to longitudinal perturbations has the form

$$\epsilon_{\text{eff}}(\mathbf{q}, \omega) = \epsilon + i \frac{4\pi\sigma(\mathbf{q}, \omega)}{\omega + iD(\mathbf{q}, \omega)q^2}.$$

This expression is valid for both ions and electrons and one should sum the contributions to the conductivity. At the same time, one should remember, that the masses for electrons and ions are different, and for important frequencies the inequality

$$\omega_i = \sqrt{\frac{4\pi Ze^2}{\epsilon M}} \ll qv_F, \quad \omega \ll \omega_p = \sqrt{\frac{4\pi e^2}{\epsilon m}}$$

is met. As a result, we obtain

$$\epsilon_{\text{eff}}(\mathbf{q}, \omega) = \epsilon \left(1 - \frac{\omega_i^2}{\omega^2} + \frac{R^{-2}}{q^2} \right) = \epsilon \left(\frac{\omega^2(q^2 + R^{-2}) - \omega_i^2 q^2}{\omega^2 q^2} \right)$$

or

$$\frac{1}{\epsilon_{\text{eff}}(\mathbf{q}, \omega)} = \frac{1}{\epsilon} \frac{q^2}{q^2 + R^{-2}} \left(1 + \frac{\omega_q^2}{\omega^2 - \omega_q^2} \right), \quad \omega_q^2 = \omega_i^2 \frac{q^2}{R^{-2} + q^2}.$$

For long waves, $\omega_q \sim \omega_i/R \sim v_F \sqrt{m/M}$, i.e. of the order of the sound velocity. We see that the effective matrix elements of the electron-electron interaction $4\pi e^2/q^2 \epsilon_{\text{eff}}(\mathbf{q}, \omega)$ has two parts - Coulomb repulsion (1st term) and attraction for small frequencies.

7.4 Electromagnetic Waves in High Magnetic Fields.

We came to the conclusion that in the absence of magnetic field an electromagnetic wave decays in the metal. External magnetic field changes drastically the situation because non-dissipative off diagonal part of conductivity exceeds the diagonal one.

To analyze the wave propagation one needs to solve the Maxwell equations which in the absence of the displacement current and for the fields proportional to $\exp(iqx - \omega t)$ read as (*Problem 7.3*)

$$\sum_k (q^2 \delta_{ik} - q_i q_k) E_k = \frac{4\pi i \omega}{c^2} \sum_k \sigma_{ik}(\mathbf{q}, \omega) E_k. \quad (7.7)$$

Before starting our analysis let us specify the conductivity tensor. The Boltzmann equation for the a -function has the form

$$[i(\mathbf{q}\mathbf{v} - \omega) + \tau^{-1}] a + \frac{\partial a}{\partial t_1} = -e(\mathbf{v}\mathbf{E}).$$

We see that if

$$qv_F, \omega \ll \omega_c \quad \text{or} \quad \omega \ll \omega_c, \quad qr_c \ll 1$$

both time and spatial dispersion are unimportant, and one can use the static conductivity tensor. The dispersion equation is

$$\det \left[q^2 \delta_{ik} - q_i q_k - \frac{4\pi i \omega}{c^2} \sigma_{ik} \right] = 0. \quad (7.8)$$

If the FS is closed and the numbers of electrons and holes are not equal we get

$$\det \begin{vmatrix} q^2 & -4\pi i \omega c^{-2} \sigma_{xy} & -4\pi i \omega c^{-2} \sigma_{xz} \\ 4\pi i \omega c^{-2} \sigma_{xy} & q_z^2 & -q_y q_z - 4\pi i \omega c^{-2} \sigma_{yz} \\ 4\pi i \omega c^{-2} \sigma_{xz} & -q_y q_z + 4\pi i \omega c^{-2} \sigma_{yz} & q_y^2 - 4\pi i \omega c^{-2} \sigma_{zz} \end{vmatrix} = 0.$$

Here we have assumed that the vector \mathbf{q} is in the (y, z) -plane, the angle $(\widehat{\mathbf{q}, \mathbf{z}})$ being θ and have taken into account only the terms of 0-th and 1-st orders in $(\omega_c \tau)^{-1}$. Because the largest element in the last row is σ_{zz} we come to the estimate for small enough $q \sim \sqrt{4\pi\omega c^{-2}\sigma_{xy}}$

$$q^2 \sim 4\pi\omega c^{-2}\sigma_{xy} \sim 4\pi\omega c^{-2}\sigma_{yz} \ll 4\pi\omega c^{-2}\sigma_{zz}.$$

As a result, the dispersion equation simplifies as

$$q^2 q_z^2 + (4\pi i\omega c^{-2}\sigma_{xy})^2 = 0.$$

Taking into account that $q_z = q \cos \theta$ we get

$$\omega = \frac{c^2 q^2 \cos \theta}{4\pi |\sigma_{xy}|} = \frac{c H q^2 \cos \theta}{4\pi e |n_e - n_h|}.$$

According to the last row of the matrix (7.7) we have $E_z \ll E_x, E_y$. Then from the first row we get

$$q^2 E_x - 4\pi i\omega c^{-2}\sigma_{xy} E_y = 0 \rightarrow E_x = i \cos \theta E_y.$$

So the wave is polarized elliptically. This wave is called the *helicon*. There are also waves of other kinds in metals in magnetic field.

There are different experimental methods to study electromagnetic excitations in metals. One of them is measurements of the surface impedance in thin plates. Changing magnetic field people change the wavelength of the waves and it is possible to observe resonances when the sample's thickness is an integer times the wavelength. Another approach is to study the interference between the electromagnetic wave and the wave which has passed through a thin plate.

7.5 Problems

7.1. Derive the equation (7.3).

$$\delta = \frac{1}{\text{Im } q} = \frac{2}{\sqrt{3}} \left(\frac{c^2 \ell}{4\pi \sigma \omega_0 b} \right)^{1/3}.$$

7.2. Derive the dispersion law for plasmons.

7.3. Derive the dispersion relation for electromagnetic waves in metals.

$$\det \left[q^2 \delta_{ik} - q_i q_k - \frac{4\pi i\omega}{c^2} \sigma_{ik} \right] = 0.$$

Chapter 8

Acoustical Properties of Metals and Semiconductors.

8.1 Landau Attenuation.

There is another useful approach to study high-frequency properties of good conductors - to induce an acoustic wave and measure its attenuation (or its velocity). The main advantage is that acoustic wave propagate inside the conductors without sufficient damping.

The interaction between the acoustic waves and the electrons can be written as

$$\delta\varepsilon(\mathbf{p}, \mathbf{r}) = \Lambda_{ik}(\mathbf{p})u_{ik}(\mathbf{r}) + e\varphi(\mathbf{r})$$

where the potential φ should be determined from the Poisson equation. As far as for good conductors $\omega \ll \sigma$ and $q \ll R^{-1}$ one can show that it is enough to request the *neutrality condition* $\delta n_e = 0$ that is the same as $e\varphi(\mathbf{r}) = -\langle \Lambda_{ik}(\mathbf{p}) \rangle_{\epsilon_F} u_{ik}(\mathbf{r})$. As a result, we get

$$\delta\varepsilon(\mathbf{p}, \mathbf{r}) = [\Lambda_{ik}(\mathbf{p}) - \langle \Lambda_{ik}(\mathbf{p}) \rangle_{\epsilon_F}] u_{ik}(\mathbf{r}) \equiv \lambda_{ik}(\mathbf{p})u_{ik}(\mathbf{r}).$$

We see that it is possible to produce an effective force varying as $\exp(i\mathbf{qr} - \omega t)$ and in such a way investigate the Fourier components of electronic response. The Boltzmann equation for the electrons in the field of a sound wave has the form

$$[i(\mathbf{qv} - \omega) + \tau^{-1}] a = \sum_{ik} \lambda_{ik}(\mathbf{p})(\mathbf{v}\nabla)u_{ik}(\mathbf{r}).$$

If we express

$$\sum_{ik} \lambda_{ik}(\mathbf{p})u_{ik} = i\frac{1}{2} \sum_{ik} \lambda_{ik}(\mathbf{p})(q_i u_k + q_k u_i) = i \sum_{ik} \lambda_{ik}(\mathbf{p})q_i u_k = iq\lambda u$$

(where u is the displacement, $\lambda = \sum_{ik} \lambda_{ik}(\mathbf{p})n_i e_k$, \mathbf{e} is the polarization vector of the wave, while $\mathbf{n} = \mathbf{q}/q$) we obtain

$$[i(\mathbf{qv} - \omega) + \tau^{-1}] a = -(\mathbf{qv})q\lambda u.$$

One can immediately express the absorbed power through the distribution function. Indeed,

$$Q = \int (dp) \dot{\varepsilon} f = \int (dp) \dot{\varepsilon}(\mathbf{p}) a(\mathbf{p}) \left(-\frac{\partial f_0}{\partial \varepsilon} \right) = \int d\varepsilon g(\varepsilon) \left(-\frac{\partial f_0}{\partial \varepsilon} \right) \langle \dot{\varepsilon}(\mathbf{p}) a(\mathbf{p}) \rangle_\varepsilon.$$

This expression should also be averaged over the period $2\pi/\omega$ of the sound wave. This average is calculated in a complex form

$$\begin{aligned} \overline{A(t)B(t)} &= \frac{\omega}{2\pi} \int_0^{2\pi/\omega} (Ae^{-i\omega t} + A^* e^{i\omega t}) (Be^{-i\omega t} + B^* e^{i\omega t}) \\ &= AB^* + A^* B = 2 \operatorname{Re}(AB^*). \end{aligned} \quad (8.1)$$

So, for Fermi electrons at low temperature we obtain

$$\begin{aligned} \bar{Q} &= 2g(\epsilon_F) \operatorname{Re} \langle (-i\omega\delta\varepsilon)^* a \rangle_{\epsilon_F} = 2\omega q^2 g(\epsilon_F) \lambda^2 |u|^2 \operatorname{Re} \left\langle \frac{(\mathbf{q}\mathbf{v})}{i(\mathbf{q}\mathbf{v} - \omega) + \tau^{-1}} \right\rangle_{\epsilon_F} \\ &= 2\omega q^2 g(\epsilon_F) \lambda^2 |u|^2 \left\langle \frac{(\mathbf{q}\mathbf{v})\tau^{-1}}{(\mathbf{q}\mathbf{v} - \omega)^2 + \tau^{-2}} \right\rangle_{\epsilon_F}. \end{aligned}$$

The most interesting case is the one of the so-called short-wave sound

$$q\ell \gg 1$$

which can be met in pure conductors at low temperatures. In this case we see that only the electrons with

$$\mathbf{q}\mathbf{v} \approx \omega \rightarrow v_{\mathbf{q}} \approx s \quad (8.2)$$

are important. This condition has a straightforward physical meaning: because $v_F \gg s$ most of electrons feel rapidly oscillating field produced by the acoustic wave, the average interaction being small. The electrons with $\mathbf{q}\mathbf{v} \approx \omega$ move in resonance with the wave and they feel a slow varying field. The damping due to the resonant electrons is called the *Landau damping*, it has been analyzed at first for plasma waves. In the Landau damping region

$$\left\langle \frac{(\mathbf{q}\mathbf{v})\tau^{-1}}{(\mathbf{q}\mathbf{v} - \omega)^2 + \tau^{-2}} \right\rangle_{\epsilon_F} \approx \pi \frac{\omega}{qv_F} = \pi \frac{s}{v_F}.$$

As a result

$$Q \approx 2\omega q^2 g(\epsilon_F) \lambda^2 |u|^2 \pi \frac{s}{v_F}.$$

Usually, the attenuation coefficient is measured which is determined as

$$\Gamma = \frac{Q}{\mathcal{E}_{ac}s}$$

where \mathcal{E}_{ac} is the energy density in the wave

$$\mathcal{E}_{ac} = 2\rho\omega^2 \overline{u(\mathbf{r}, t)^2}/2 = 2\rho\omega^2 |u^2|$$

while ρ is the crystal density. We get

$$\Gamma = \frac{2\omega q^2 g(\epsilon_F) \lambda^2 |u|^2 \pi (s/v_F)}{2\rho \omega^2 |u^2| s} = \pi \frac{g(\epsilon_F) \lambda^2}{\rho s^2} q \frac{s}{v_F}.$$

Since λ is of the order of a typical electron energy, for rough estimates we can put $\lambda \sim \epsilon_F$, $\rho s^2 \sim M n_a s^2 \sim n_e \epsilon_F$. So

$$\pi \frac{g(\epsilon_F) \lambda^2}{\rho s^2} \sim 1$$

and $\Gamma/q \sim s/v_F \ll 1$. The coefficient Γ characterizes spatial decay of the wave:

$$\frac{\partial \mathcal{E}_{ac}}{\partial x} = -\Gamma \mathcal{E}_{ac}.$$

Thus, we have proved that acoustic waves have relatively small damping.

8.2 Geometric Oscillations

The short wave regime is very useful to study the Fermi surface. Indeed, only the electrons with \mathbf{v} almost perpendicular to \mathbf{q} are important. As a result, only small parts of the electron orbit in a magnetic field contributes to attenuation.

To illustrate the situation we analyze the case

$$\mathbf{q} \perp \mathbf{H}, \quad qr_c \ll 1, \quad \omega_c \tau \gg 1.$$

An electronic orbit is shown in Fig. 8.1. The dashed lines show the planes where wave's

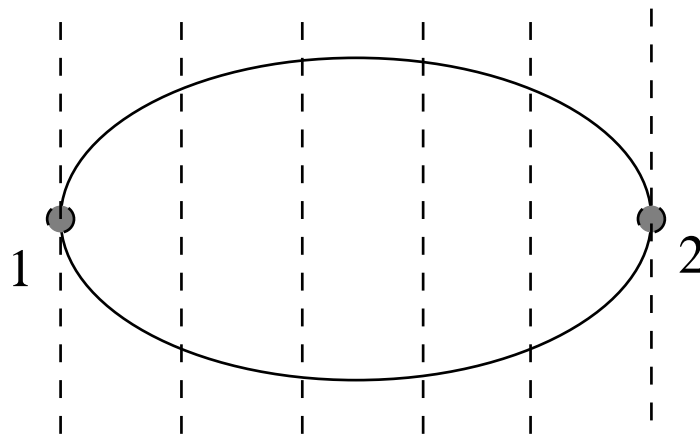


Figure 8.1: On the geometric oscillations.

phases are equal. An electron spends different time near these planes, the longest being near the points 1 and 2. These points are the ones where the interaction is most important.

Now let us assume that a function is extreme for a given phase difference

$$\varphi = \int_{t_{(1)}}^{t_{(2)}} (\mathbf{q}\mathbf{v}) dt.$$

Then, if the number of wavelengths at the orbit's diameter is changed by an integer n the phase difference is changed by $2\pi n$. Let us direct the x -axis along \mathbf{q} . Then, from the equation of motion

$$\frac{dp_y}{dt} = \frac{e}{c} H v_x$$

we obtain

$$\varphi = \frac{cq}{eH} [p_y^{(2)} - p_y^{(1)}].$$

Consequently, if $\varphi \gg 1$ the a -function oscillates with magnetic field, the period being

$$\Delta \left(\frac{1}{H} \right) = \frac{2\pi e}{cq} \frac{1}{p_y^{(2)} - p_y^{(1)}}.$$

In fact, the difference $p_y^{(2)} - p_y^{(1)}$ depends on p_z , and genuine oscillations correspond to the extreme cross sections with respect to $p_y^{(2)} - p_y^{(1)}$. As a result, the oscillations are relatively small (as in the case of the cyclotron resonance). The effect is more pronounced for open orbits.

The geometric oscillations provide a very powerful way to measure diameters of the FS.

8.3 Giant Quantum Oscillations.

Quantum transport is out of the scope of this part of the course. Nevertheless, we will consider a very beautiful quantum effect of giant oscillations of the sound absorption.

As we know, in a quantizing magnetic field the energy spectrum consists of the Landau bands

$$\varepsilon(N, p_z) = \varepsilon_N + p_z^2/2m, \quad \varepsilon_N = \hbar\omega_c(N + 1/2).$$

The energy-momentum conservation laws for the phonon absorption require

$$\varepsilon_{N'} + (p_z + \hbar q_z)^2/2m = \varepsilon_N + p_z^2/2m + \hbar\omega \rightarrow \hbar\omega_c(N' - N) + \hbar p_z q_z/2m = \hbar\omega.$$

For realistic sound frequency this condition can be met only for $N' = N$, and we get

$$p_z = m\omega/q_z = msq/q_z = ms/\cos\theta, \quad \theta \equiv \angle(\mathbf{q}, \mathbf{H}). \quad (8.3)$$

Consequently, one can control the value of p_z changing the propagation direction.

The Landau bands are shown in Fig. 8.2. The value of p_z corresponding to the condition (8.3) is denoted as p .

On the other hand, only the region near the FS (the layer of the thickness $\sim k_B T$) contributes to the absorption, the corresponding regions for p_z are hatched. If the value

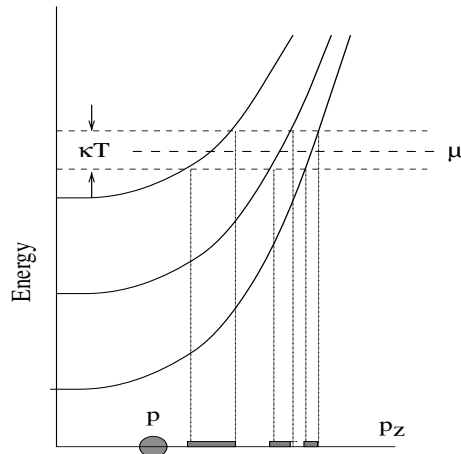


Figure 8.2: Landau levels.

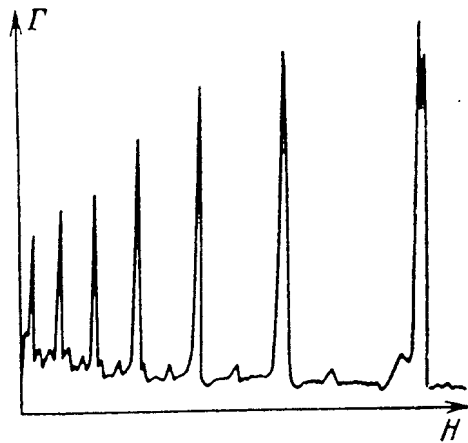


Figure 8.3: Giant oscillations of sound attenuation.

p is outside these regions, the absorption is very small. If magnetic field is changed the regions move along the p_z -axis. As a result, the attenuation coefficient Γ experiences giant oscillations. The typical experimental picture is shown in Fig. 8.3.

The giant oscillations provide a useful tool for investigation of the FS.

8.4 Acoustical properties of semiconductors

In the previous section we discussed the case when $q\ell \gg 1$. However, in typical semiconductor materials the opposite inequality,

$$q\ell \ll 1,$$

is usually met. The reason is that ionized doping impurities produce rather strong scattering, and the typical electron velocity is much less than in a metal.

The condition actually $q\ell \ll 1$ means that one can use a hydrodynamic approach which we used to describe response to “slow” perturbations. Thus we can write

$$\mathbf{j} = \sigma_0 \mathbf{E} - eD\nabla(\delta n)$$

where δn is the variation in the electron density. In the stationary state $\mathbf{j} = 0$ and

$$\delta n = -\frac{\sigma_0}{eD}\varphi.$$

Here ϕ is the electrical potential, so that

$$\mathbf{E} = -\nabla\varphi.$$

In the case of piezoelectric interaction, the second relation between δn and φ can be extracted from the *Poisson equation*

$$\operatorname{div} \mathbf{D} = 4\pi e(\delta n). \quad (8.4)$$

Here \mathbf{D} is the electrical induction,

$$\mathbf{D} = \epsilon \mathbf{E} + 4\pi \mathbf{P}$$

where \mathbf{P} is the polarization created by the acoustic wave. The piezoelectric interaction mechanism is clarified in Fig. 8.4. To get a quantitative description let us write the free energy of the deformed crystal (at *fixed electric field* \mathbf{E}) as

$$\tilde{F}(T, \mathbf{E}) \equiv F(T, \mathbf{D}) - \frac{\mathbf{ED}}{4\pi} = F_0 + \frac{1}{2}c_{iklm}u_{ik}u_{lm} - \frac{1}{8\pi}\epsilon_{ik}E_iE_k + \beta_{i,kl}E_iu_{kl}. \quad (8.5)$$

Here summation over repeated subscripts is assumed, c_{iklm} is the so-called elastic moduli tensor while

$$u_{ik} = \frac{1}{2} \left(\frac{\partial u_i}{\partial x_k} + \frac{\partial u_k}{\partial x_i} \right)$$

is the strain tensor. Tensor $\beta_{i,kl}$ describes the piezoelectric interaction.

According to general principles, the stress tensor is

$$\sigma_{ik} = \left. \frac{\partial \tilde{F}}{\partial u_{ik}} \right|_{\mathbf{E}=\text{const}} = c_{iklm}u_{lm} + \beta_{l,km}E_l. \quad (8.6)$$

The electric induction is

$$D_i = -4\pi \left. \frac{\partial \tilde{F}}{\partial E_i} \right|_{u_{ik}=\text{const}} = \epsilon_{ik}E_k - 4\pi\beta_{i,kl}u_{kl}. \quad (8.7)$$

Now we can substitute Eq. (8.6) into the elasticity equation,

$$\rho \frac{\partial^2 u_i}{\partial t^2} = \frac{\partial \sigma_{ik}}{\partial x_k}$$

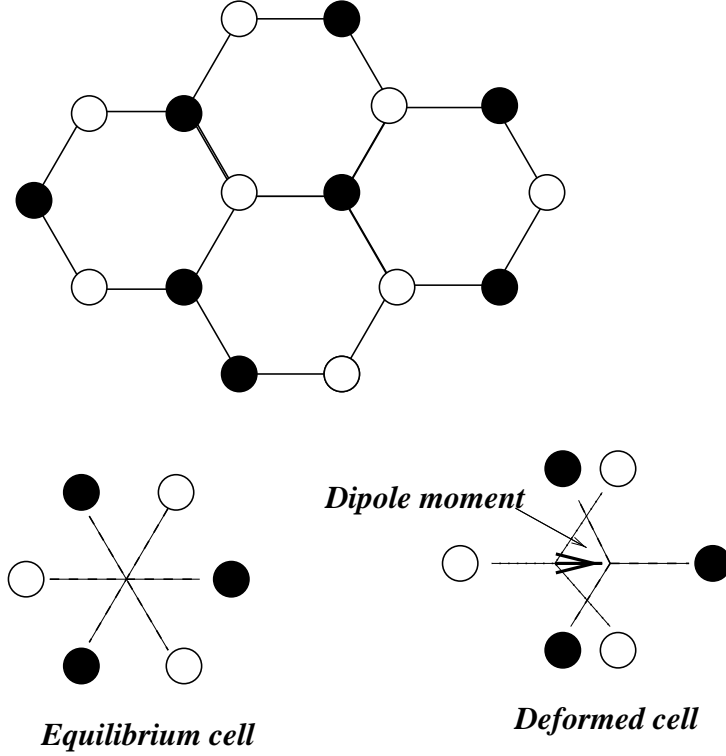


Figure 8.4: A plain ionic lattice without symmetry center. After deformation “center of gravities” of positive and negative triangle do not coincide, and as a result a dipole moment appears. Polarization \mathbf{P} is just the dipole moment of the unit volume.

to get

$$\rho \frac{\partial^2 u_i}{\partial t^2} = c_{iklm} \frac{\partial u_{lm}}{\partial x_k} + \beta_{l,ik} \frac{\partial E_l}{\partial x_k} \quad (8.8)$$

This equation should be solved together with the Poisson equation (8.4) and the continuity equation,

$$e \frac{\partial \delta n}{\partial t} + \operatorname{div} \mathbf{j} = 0. \quad (8.9)$$

Now let us assume for simplicity that the wave is propagating along a principal axis of the crystal (axis x). For a traveling wave all the quantities should be proportional to

$$\exp(i\omega t + iqx).$$

Thus the continuity equation can be written as

$$(-i\omega + Dq^2)(\delta n) + \frac{\sigma}{e} q^2 \phi = 0. \quad (8.10)$$

As a result, one can re-write the full set of equations as

$$\begin{array}{lll} (cq^2 - \rho\omega^2)u - \beta q^2 \phi & = 0 & \text{Elasticity} \\ 4\pi\beta q^2 u + \epsilon q^2 \phi - 4\pi e(\delta n) & = 0 & \text{Poisson} \\ \sigma q^2 \phi + (-i\omega + Dq^2) e(\delta n) & = 0 & \text{Continuity} \end{array} \quad (8.11)$$

A non-trivial solution of this set exists only if the determinant of the corresponding matrix vanishes. After some straightforward algebra the secular equation can be written as

$$\frac{q^2 - q_0^2}{q^2} \left[\frac{1 + (qR)^2 - i\omega\tau_m}{(qR)^2 - i\omega\tau_m} \right] = -\chi, \quad (8.12)$$

where $q_0 = \omega/w = \omega\sqrt{\rho/c}$,

$$R = \left[\frac{4\pi e^2}{\epsilon} \left(\frac{\partial n}{\partial \epsilon_F} \right) \right]^{-1/2}$$

is the screening length,

$$\tau_m = \frac{\epsilon}{4\pi\sigma}$$

is the Maxwell relaxation time, while

$$\chi = \frac{4\pi\beta^2}{\epsilon c}$$

is the so-called piezoelectric coupling constant.

Since usually $\chi \ll 1$ it is naturally to use an iteration procedure. If one puts $\chi = 0$, then Eq. (8.12) is decoupled into two equations. The 1st one yields

$$q^2 = q_0^2 \rightarrow q = \pm q_0,$$

so it describes usual acoustic waves propagating along (against) the x -axis.

The 2nd one yields

$$q = \frac{i}{R} \sqrt{1 - i\omega\tau_m},$$

it describes overdamped electron density waves.

In the general case it is natural to look for the solution as

$$q = q_0 + q_1, \quad |q_1| \ll q_0,$$

where $\text{Im } q_1$ characterizes the (amplitude) attenuation of the wave while the power attenuation is

$$\Gamma = 2 \text{Im } q = 2 \text{Im } q_1.$$

One easily obtains

$$\frac{2q_1}{q_0} = -\chi \frac{(qR)^2 - i\omega\tau_m}{1 + (qR)^2 - i\omega\tau_m} \quad (8.13)$$

to get

$$\Gamma = \chi q_0 \frac{\omega\tau_m}{(1 + q_0^2 R^2)^2 + (\omega\tau_m)^2}. \quad (8.14)$$

The qualitative picture of such a dependence is straightforward - at low frequencies there is a compensation of electrical and diffusion current, the attenuation being proportional to

Joule heat, ω^2 . At large frequencies the charge has no time to redistribute in the field of the acoustic wave.

One can see that the dependence Γ vs. ω has a maximum at

$$\omega = \omega_{\max} = s/R,$$

the maximal attenuation being

$$\Gamma_{\max} = \chi \frac{w}{R} \frac{\omega_{\max} \tau_m}{4 + (\omega_{\max} \tau_m)^2}$$

This maximum depends on the product $\omega_{\max} \tau_m$ reaching the absolute maximum

$$\Gamma_0 = \chi \frac{s}{4R}$$

at $\omega_{\max} \tau_m = 2$. Frequency dependences of the absorption are shown in Fig. 8.5

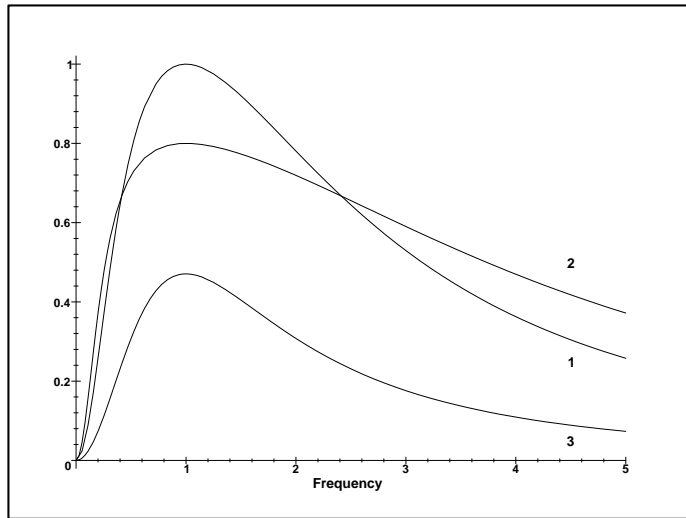


Figure 8.5: Dependences of the reduced attenuation coefficient, Γ/Γ_0 , on the reduced frequency, ω/ω_{\max} for $\omega_{\max} \tau_m = 2$ (curve 1), 4 (curve 2) and 0.5 (curve 3).

If the sample is a part of a closed loop with the transport current density j one can re-write the variation of the transport current as

$$\delta \mathbf{j} = e(\delta n) \mathbf{v}_d, \quad \mathbf{v}_d \equiv \frac{1}{e} \left. \frac{\partial \mathbf{j}}{\partial n} \right|_{\mathbf{E}=\text{const}}.$$

Substituting this expression to the equations above we obtain

$$\Gamma = \chi q_0 \frac{(\omega - \mathbf{q}_0 \mathbf{v}_d) \tau_m}{(1 + q_0^2 R^2)^2 + (\omega - \mathbf{q}_0 \mathbf{v}_d)^2 \tau_m^2}. \quad (8.15)$$

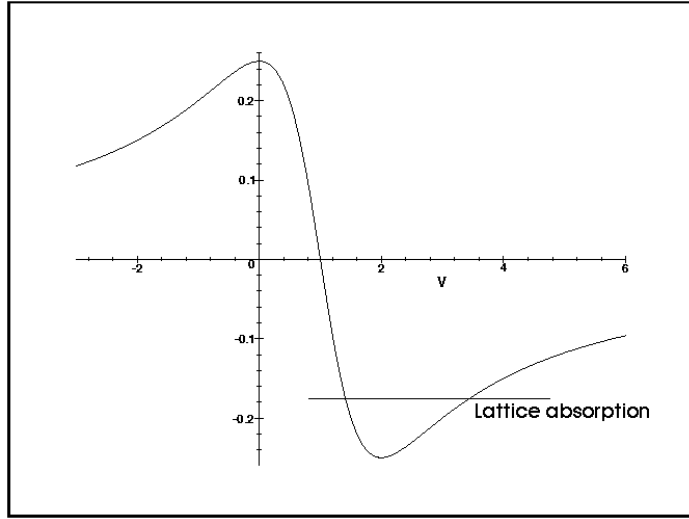


Figure 8.6: Dependences of the reduced attenuation coefficient on the reduced drift velocity, $V = v_d/w$, for $\omega_{\max}\tau_m = 2$. Horizontal line indicates the attenuation due to defects and lattice vibrations.

This dependence is shown in Fig. 8.6. One can see that at $|v_d| \geq s$ the attenuation coefficient changes its sign. That means *amplification* of acoustic waves by the charge carriers drift. If the gain is larger than the attenuation due to defects and lattice vibrations, then the sample can generate acoustic waves (phonons). Such a system placed in an acoustic resonator is an acoustic analog of the laser.

8.5 Problems

- 8.1.** Compare electrical and mechanical energies carried by the wave in a piezodielectric.
- 8.2.** Find the relation between the amplitudes of electric fields and deformation for the case of acoustic wave in a piezoelectric semiconductor.
- 8.3.** Find dc current induced by an acoustic wave in a non-degenerate piezoelectric semiconductor.

Hint: A dc current appears in the second approximation in the wave amplitude. Thus

$$j_{dc} = \langle \sigma E - eD(\partial \delta n / \partial x) \rangle_{\text{time}} \approx \langle (\delta \sigma) E \rangle = (\sigma/n) \langle (\delta n) E \rangle .$$

Chapter 9

Optical Properties of Semiconductors

9.1 Preliminary discussion

Basic equations

The Maxwell equations (ME) for electric field, \mathbf{E} , magnetic field \mathbf{H} , as well as for the corresponding inductions $\mathbf{D} = \epsilon\mathbf{E}$ and $\mathbf{B} = \mu\mathbf{H}$ read

$$\begin{aligned}\nabla \times \mathbf{E} + \frac{1}{c} \frac{\partial \mathbf{B}}{\partial t} &= 0 \\ \nabla \times \mathbf{H} - \frac{1}{c} \frac{\partial \mathbf{D}}{\partial t} &= \frac{4\pi}{c} \mathbf{J} \\ \nabla \cdot \mathbf{D} &= 4\pi\rho \\ \nabla \cdot \mathbf{B} &= 0.\end{aligned}\tag{9.1}$$

It is convenient to introduce scalar, ϕ and vector, \mathbf{A} potentials as

$$\begin{aligned}\mathbf{E} &= -\frac{1}{c} \frac{\partial \mathbf{A}}{\partial t} - \nabla\phi \\ \mathbf{B} &= \nabla \times \mathbf{A}.\end{aligned}\tag{9.2}$$

In this way we automatically meet the first and the last ME. The potentials are not unique, they can be replaced by new ones,

$$\begin{aligned}\mathbf{A}' &= \mathbf{A} + \nabla\chi \\ \phi' &= \phi - \frac{1}{c} \frac{\partial\chi}{\partial t},\end{aligned}\tag{9.3}$$

without changing of the physical field, \mathbf{E} and \mathbf{B} . For many cases, the so-called Lorentz gauge is convenient. In that case we put

$$\nabla \cdot \mathbf{A}' + \frac{1}{c} \frac{\partial\phi'}{\partial t} = 0.$$

Then one can re-write ME as

$$\begin{aligned}\nabla^2 \mathbf{A} - \frac{1}{c^2} \frac{\partial^2 \mathbf{A}}{\partial t^2} &= -\frac{4\pi}{c} \mathbf{J} \\ \nabla^2 \phi - \frac{1}{c^2} \frac{\partial^2 \phi}{\partial t^2} &= -4\pi\rho.\end{aligned}\quad (9.4)$$

At $\mathbf{J} = 0$ one can put $\nabla \cdot \mathbf{A}' = 0$, $\phi' = 0$, and we get the solution

$$\mathbf{A}(\mathbf{r}, t) = \mathbf{A}_0 \{ \exp[i(\mathbf{k}\mathbf{r} - \omega t)] + c.c. \}, \quad (9.5)$$

the fields being

$$\begin{aligned}\mathbf{E} &= -2(\omega/c)\mathbf{A}_0 \sin(\mathbf{k}\mathbf{r} - \omega t) \\ \mathbf{B} &= -2\mathbf{k} \times \mathbf{A}_0 \sin(\mathbf{k}\mathbf{r} - \omega t).\end{aligned}\quad (9.6)$$

The Poynting vector (power flux) is

$$\mathbf{S} = \frac{c}{4\pi} [\mathbf{E} \times \mathbf{H}] = \frac{1}{\pi} \frac{ck^2}{\sqrt{\epsilon\mu}} \hat{\mathbf{k}} |\mathbf{A}_0|^2 \sin^2(\mathbf{k}\mathbf{r} - \omega t).$$

Its time average is

$$\langle \mathbf{S} \rangle = \hat{\mathbf{k}} \frac{c}{\sqrt{\epsilon\mu}} \frac{\epsilon\omega^2}{2\pi c^2 \mu} |\mathbf{A}_0|^2.$$

Here $c/\sqrt{\epsilon\mu}$ is the velocity of light, $k = \omega\sqrt{\epsilon\mu}/c$ is the wave vector of light.

The energy density is

$$W \equiv \left| \frac{S \sqrt{\epsilon\mu}}{c} \right| = \frac{\epsilon\omega^2}{2\pi c^2 \mu} |\mathbf{A}_0|^2.$$

That can be expressed in terms of N_ω photons in the volume \mathcal{V} according to the relation

$$W = \frac{\hbar\omega N_\omega}{\mathcal{V}}.$$

Thus, the relation between the wave amplitude and photon density is

$$|\mathbf{A}_0|^2 = \frac{2\pi\hbar\mu c^2}{\epsilon\omega} \frac{N_\omega}{\mathcal{V}}. \quad (9.7)$$

9.2 Photon-Material Interaction

Now we can formulate a macroscopic theory of photon-material interaction. Substituting into (9.1) $\mathbf{J} = \sigma\mathbf{E}$ and eliminating \mathbf{B} we get the following equation for \mathbf{E}

$$\nabla^2 \mathbf{E} = \frac{\epsilon\mu}{c^2} \frac{\partial^2 \mathbf{E}}{\partial t^2} + \frac{4\pi\sigma\mu}{c^2} \frac{\partial \mathbf{E}}{\partial t}. \quad (9.8)$$

Looking for the plane wave solution now we obtain *complex* k ,

$$k = \frac{\omega}{c} \sqrt{\epsilon\mu + i\frac{4\pi\sigma}{\omega}}. \quad (9.9)$$

Now it is time to introduce the complex *refractive index*

$$\mathcal{N} = n + i\beta,$$

so that

$$k = n\frac{\omega}{c} + i\beta\frac{\omega}{c}.$$

We have

$$\mathcal{N} = \sqrt{\epsilon\mu + i\frac{4\pi\sigma}{\omega}}. \quad (9.10)$$

In this way, in the media placed at $z > 0$, the solution has the form

$$\mathbf{E} = \mathbf{E}_0 \exp \left[i\omega \left(\frac{nz}{c} - t \right) \right] \exp \left(-\frac{\beta\omega z}{c} \right). \quad (9.11)$$

The quantity $\alpha \equiv 2\beta\omega/c$ is called the (power) absorption coefficient.

At the interface one has partial reflection. Consider an interface between the vacuum and the material at $z > 0$. Then the solution in the vacuum is

$$\mathbf{E}_1 \exp \left[i\omega \left(\frac{nz}{c} - t \right) \right] + \mathbf{E}_2 \exp \left[-i\omega \left(\frac{nz}{c} + t \right) \right],$$

while in the material it is given by (9.11). Matching the boundary conditions at $z = 0$ for electric field

$$\mathbf{E}_0 = \mathbf{E}_1 + \mathbf{E}_2.$$

From the continuity of the tangential component of magnetic induction we get (using ME)

$$(n + i\beta)\mathbf{E}_0 = \mathbf{E}_2 - \mathbf{E}_1.$$

Combining the boundary conditions, we obtain

$$R \equiv \left| \frac{\mathbf{E}_1}{\mathbf{E}_2} \right|^2 = \frac{(n-1)^2 + \beta^2}{(n+1)^2 + \beta^2}. \quad (9.12)$$

Measuring α and R we find optical constants n and β .

Drude-Zener theory

Having in mind Eq. (9.10) and putting $\epsilon = \mu = 1$ we can introduce the *complex dielectric function*

$$\epsilon(\omega) = 1 + i \frac{4\pi}{\omega} \sigma(\omega). \quad (9.13)$$

Using the linearized Boltzmann equation and relaxation time approximation one obtains

$$\sigma(\omega) \equiv \sigma_1 + i\sigma_2 = \frac{\sigma_0}{1 + i\omega\tau}, \quad \sigma_0 = \frac{ne^2\tau}{m}.$$

In this way the optical functions are

$$\begin{aligned} n^2 - \beta^2 &= 1 - \frac{\omega_p^2\tau^2}{1 + \omega^2\tau^2} \\ n\beta &= \frac{\omega_p^2\tau}{\omega(1 + \omega^2\tau)}. \end{aligned} \quad (9.14)$$

Here

$$\omega_p = \sqrt{\frac{4\pi ne^2}{m}}$$

is the plasma frequency. Let us discuss some limits of these equations

$$\begin{aligned} (n + \beta)(n - \beta) &= 1 - \omega_p^2\tau^2 \\ 2n\beta &= \omega_p^2\tau/\omega. \end{aligned}$$

As both n and β increase as $\omega \rightarrow 0$

$$n \approx \beta \approx (2\pi\sigma_0/\omega)^{1/2}.$$

From this expression one finds the *skin depth*

$$\delta = c/\omega\beta = (c^2/2\pi\sigma_0\omega)^{1/2} = \sqrt{\frac{\omega_p^2\tau}{\omega}}.$$

Large frequencies, $\omega\tau \gg 1$

$$\text{Re } \epsilon \approx 1 - (\omega_p/\omega)^2, \quad \text{Im } \epsilon \approx 1/\omega\tau.$$

At ω close to ω_p (plasma edge) both n and β become very small, and the reflection coefficient is close to unity. For the frequencies above the plasma edge the material is essentially transparent. Frequency dependence of the reflectivity is shown in Fig. 9.1

To construct a quantum theory, one needs to allow for the conservation laws which include both energy and momentum transfer. Thus we employ *second-order* perturbation theory. The corresponding processes are shown in Fig. 9.2

One can find a discussion in the book [3], Sec. 11.10.

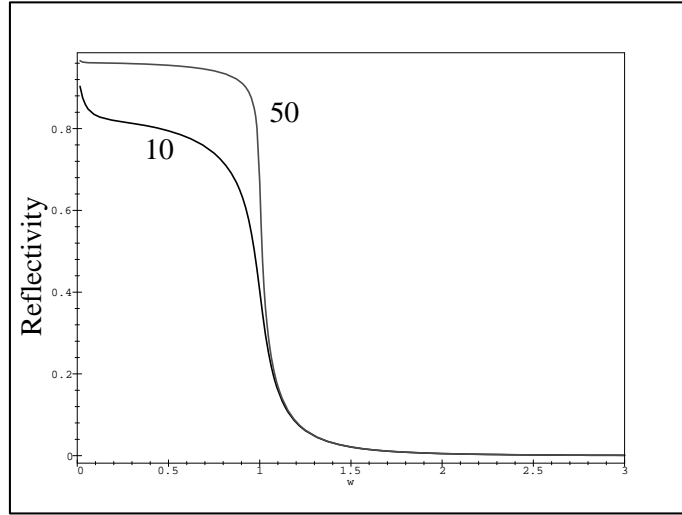


Figure 9.1: Dependence of the reflection coefficient on the reduced frequency, $w = \omega/\omega_p$. Numbers near the curves indicate values of $\omega_p\tau$.

Cyclotron resonance and Faraday effect

Consider propagation of a *polarized light* through a transparent medium containing free electrons with the effective mass m in a magnetic field \mathbf{H} . The simplest equation for electron velocity, \mathbf{v} , has the form

$$m \left(\dot{\mathbf{v}} + \frac{1}{\tau} \mathbf{v} \right) = -eE_0 \vec{\eta}_{\pm} e^{i\omega t} - \frac{e}{c} \mathbf{v} \times \mathbf{H}. \quad (9.15)$$

Here the polarization vector is

$$\vec{\eta}_{\pm} = \frac{1}{\sqrt{2}} (1, \pm i, 0).$$

Solving the vector set (9.15) and defining

$$j_x = \sigma E = -env_x$$

we obtain

$$\sigma_{\pm} = \sigma_0 \frac{1 - i(\omega \pm \omega_c)\tau}{(1 - i\omega\tau)^2 + \omega_c^2\tau^2} \quad (9.16)$$

One can see that the absorption given by

$$\operatorname{Re} \sigma_{\pm} = \sigma_0 \frac{1 + (\omega_c \pm \omega)^2\tau^2}{[(1 + (\omega_c^2 - \omega^2)\tau^2)^2 + 4\omega^2\tau^2]} = \frac{\sigma_0}{1 + (\omega_c \mp \omega)^2\tau^2}.$$

is maximal (at $\omega_c\tau \gg 1$) if ω close to ω_c (cyclotron resonance). It is strongly dependent on the polarization because $\sigma \approx \sigma_0$ for left-polarized wave and almost vanishes for the

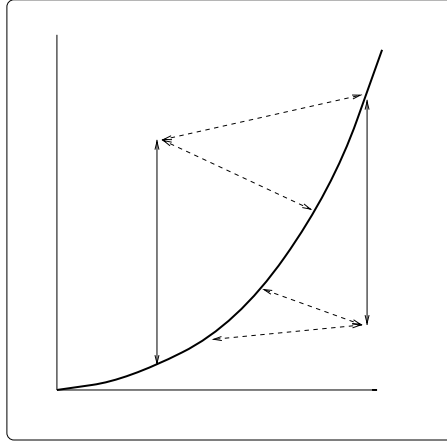


Figure 9.2: Scheme of phonon-assisted transitions. Solid curve is the electron dispersion law. Straight solid lines show optical transitions while dashed line show transitons involving phonons.

right-polarized one. This is the way to study the carrier's charge because cyclotron mass is proportional to e .

Introducing the complex refractive index,

$$n_{\pm} = \text{Re} \left\{ \sqrt{\epsilon - \frac{4\pi}{\omega} \sigma_{\pm}} \right\},$$

we can decouple a plane wave into a sum of left- and right- circularly polarized waves having the phases

$$\phi_{\pm} = \omega \left(\frac{n_{\pm} z}{c} - t \right).$$

Then the complex amplitude of the field is

$$\begin{aligned} E_x &= E_0 \exp \left(i \frac{\phi_+ + \phi_-}{2} \right) \cos \left(\frac{\phi_+ - \phi_-}{2} \right), \\ E_y &= -E_0 \exp \left(i \frac{\phi_+ + \phi_-}{2} \right) \sin \left(\frac{\phi_+ - \phi_-}{2} \right). \end{aligned}$$

Consequently, the angle between the polarization plane the x -axis is determined from the relation

$$\tan \theta = \frac{\text{Re}\{E_y\}}{\text{Re}\{E_x\}} = -\tan \left(\frac{\phi_+ - \phi_-}{2} \right).$$

If damping is small than one can neglect $\text{Re}\{\sigma\}$ and express the rotation angle through $\sigma^{(i)} \equiv \text{Im}\{\sigma\}$ as

$$\theta = \frac{\omega d}{c} (n_+ - n_-) = \frac{2\pi d}{c} \frac{2\sigma_-^{(i)} \sigma_+^{(i)}}{n_+ + n_-}.$$

As a result, we get at $\omega, \omega_c \gg 1/\tau$

$$\theta = \frac{\pi e^2 n H d}{c^2 m^2 \omega^2 (n_+ + n_-)}$$

This expression is independent of τ and can be used to determine the effective mass.

Lattice reflectivity in polar semiconductors

Lattice reflectivity can be modeled by the oscillator equation

$$m\ddot{x} + m\gamma\dot{x} + m\omega_0^2 x = eE_1 \exp(-i\omega t).$$

The dipole moment of the unit volume is

$$4\pi P = \epsilon(\omega) E_1 = 4\pi n e x = \frac{\omega_p^2}{\omega_0^2 - \omega^2 - i\omega\gamma} \epsilon E_1.$$

Here ϵ is a residual contribution to dielectric constant while n is the density of oscillators. Thus

$$\epsilon(\omega) = \epsilon_\infty + \frac{\omega_p^2}{\omega_0^2 - \omega^2 - i\omega\gamma} \epsilon. \quad (9.17)$$

Introducing static dielectric constant $\epsilon_0 \equiv \epsilon(0)$ we get

$$\epsilon(\omega) = \epsilon_\infty + \frac{\omega_0^2}{\omega_0^2 - \omega^2 - i\omega\gamma} (\epsilon_0 - \epsilon_\infty). \quad (9.18)$$

The dependence of the reflection coefficient on the reduced frequency is shown in Fig. 9.3. The minimum in that dependence corresponds to

$$\frac{\omega}{\omega_o} = \sqrt{\frac{\epsilon_0 - 1}{\epsilon_\infty - 1}} \approx \sqrt{\frac{\epsilon_0}{\epsilon_\infty}}.$$

From the Lyddane-Sachs-Teller relation

$$\frac{\omega_l}{\omega_o} = \sqrt{\frac{\epsilon_0}{\epsilon_\infty}}$$

we identify ω_0 as the frequency of the transverse optical phonons, while the minimum corresponds to longitudinal phonons.

Kramers-Kronig relation

Let us introduce complex conductivity as

$$j(\omega) = \sigma(\omega) E(\omega).$$

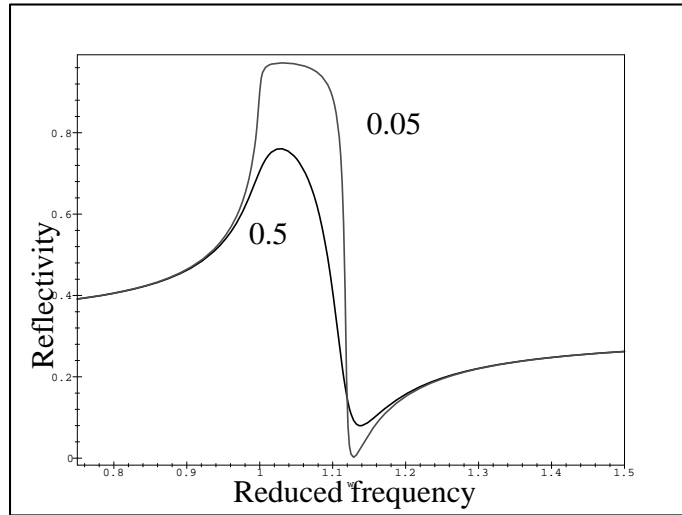


Figure 9.3: Dependence of the reflection coefficient on the reduced frequency, $w = \omega/\omega_0$. Numbers near the curves indicate values of γ/ω_0 . $\epsilon_\infty = 12$, $\epsilon_0 = 15$.

In time representation, one can write

$$j(t) = \int dt' \sigma(t - t') E(t') , \quad (9.19)$$

and

$$\sigma(t) = \frac{1}{2\pi} \int_{-\infty}^{\infty} dt \sigma(\omega) e^{-i\omega t}$$

must be real. Thus,

$$\begin{aligned} \sigma(-\omega) &= \sigma^*(\omega) , \quad \text{or} \\ \operatorname{Re} \sigma(-\omega) &= \operatorname{Im} \sigma(\omega) , \quad \operatorname{Im} \sigma(-\omega) = -\operatorname{Re} \sigma(\omega) . \end{aligned}$$

The important point is *causality* and one must define

$$\sigma(t) = 0 \quad \text{at} \quad t < 0 .$$

Thus the integration limits in (9.19) should be (t, ∞) . Using also the property $\sigma(\omega) \rightarrow 0$ as $\omega \rightarrow \infty$ one can prove that the function $\sigma(\omega)$ is regular in the ω -upper semi-plane.

Now let us consider a contour integral

$$\oint \frac{\sigma(\xi) d\xi}{\xi - \omega}$$

along the contour shown below. The integral must vanish. Thus

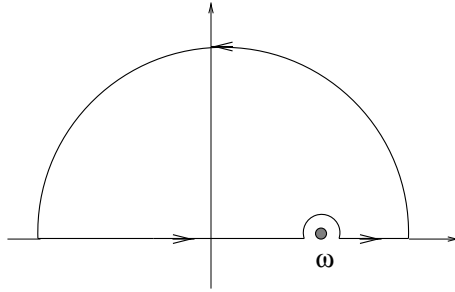


Figure 9.4: Integration circuit.

$$P \int \frac{\sigma(\xi) d\xi}{\xi - \omega} - i\pi\sigma(\omega) = 0 .$$

As a result,

$$\begin{aligned} \operatorname{Re} \sigma(\omega) &= \frac{1}{\pi} P \int_{-\infty}^{\infty} \frac{\operatorname{Re} \sigma(\xi)}{\xi - \omega} d\xi \\ \operatorname{Im} \sigma(\omega) &= -\frac{1}{\pi} P \int_{-\infty}^{\infty} \frac{\operatorname{Im} \sigma(\xi)}{\xi - \omega} d\xi . \end{aligned} \quad (9.20)$$

These relations can be generalized for a dielectric function $\epsilon(\omega)$. An important consequence - summation rules. For example, we know that at $\omega \gg \omega_p$, $\beta \rightarrow 0$, and

$$\epsilon(\omega) - \operatorname{Re} \epsilon(\infty) = -\omega_p^2/\omega^2 .$$

Thus

$$\omega_p^2 = \lim_{\omega \rightarrow \infty} \{\omega^2 [1 - \epsilon(\omega)]\} .$$

Using Kramers-Kronig relation one can show that if $\operatorname{Im} \epsilon(\omega)$ decays faster than ω^{-3} than

$$\omega_p^2 = \frac{2}{\pi} \int_0^\infty \xi \operatorname{Im} \epsilon(\xi) d\xi .$$

9.3 Microscopic single-electron theory

The Hamiltonian has the form

$$\mathcal{H} = \frac{1}{2m} \left[\hat{\mathbf{p}} + \frac{e}{c} \mathbf{A}(\hat{\mathbf{r}}) \right]^2 + e\phi + U(\mathbf{r}) . \quad (9.21)$$

An important point that momentum and co-ordinate *do not commute*. Using the relation

$$[f(\hat{\mathbf{r}}), \hat{\mathbf{p}}] = i\hbar \frac{\partial}{\partial \hat{\mathbf{r}}} f(\hat{\mathbf{r}})$$

we can rewrite Eq. (9.21) as

$$\mathcal{H} = \frac{p^2}{2m} + \frac{e}{mc} \mathbf{A} \cdot \mathbf{p} - \frac{ie\hbar}{2mc} \nabla \cdot \mathbf{A} + \frac{e^2}{2mc^2} \mathbf{A}^2 + e\phi + U(\mathbf{r}). \quad (9.22)$$

Hereby we will use semiclassical radiation theory as most simple. Namely, we shall consider the radiation as a classical field and use the time-dependent perturbation theory which yields scattering rates.

Let us chose the gauge $\nabla \mathbf{A} = \phi = 0$. Assume the radiation field to be small, such as the linear term

$$|(ie\hbar/mc)\mathbf{A} \cdot \nabla| / |(h^2/2m)\nabla^2| \sim eA/pc \ll 1.$$

Thus one can decouple the Hamiltonian as $\mathcal{H} = \mathcal{H}_0 + \mathcal{H}'$ where

$$\begin{aligned} \mathcal{H}_0 &= -\frac{\hbar^2}{2m} \nabla^2 + U(\mathbf{r}) \\ \mathcal{H}' &= \frac{ie\hbar}{mc} \mathbf{A} \cdot \nabla. \end{aligned} \quad (9.23)$$

The Fermi golden rule leads to the expressions for the scattering rate

$$W(i) = \frac{2\pi}{\hbar} \sum_f |\langle f | \mathcal{H}' | i \rangle|^2 \delta(E_f - E_i \mp \hbar\omega) \quad (9.24)$$

where - corresponds to photon absorption while + is for emission.

Here we have to specify in what we are interested in. If we are interested what happens with the electrons we have of sum over the phonon distribution. It can be written as the product $N = N_\omega g_{ph}(\omega)$ where

$$g_{ph}(\omega) = \frac{\omega^2}{2\pi^2 \hbar \tilde{c}^3}$$

is the photon density of states, $\tilde{c} \equiv c/\sqrt{\epsilon\mu}$. Thus we specify the amplitude as

$$|\mathbf{A}_0|^2 d\omega = \frac{2\pi\hbar c^2}{\omega\epsilon} N_\omega g_{ph}(\omega) d\omega$$

to get the following expression for the transition probability with absorption,

$$W^{(a)}(\omega) = \frac{4\pi^2 e^2 N_\omega g_{ph}(\omega)}{m^2 \omega \epsilon} \left| \int d^3 r \psi_{\mathbf{p}'}^* \exp(i\mathbf{k}\mathbf{r}) \hat{p}_A \psi_{\mathbf{p}}^* \right|^2. \quad (9.25)$$

Here \hat{p}_A is the projection of the electron momentum to the direction of \mathbf{A} . Define photon intensity as

$$I(\omega) = \mathcal{V} \hbar^2 \omega N_\omega g_{ph}(\omega)$$

we can write the final expression as

$$W^{(a)}(\omega) = \frac{4\pi^2 e^2 I(\omega)}{m^2 \mathcal{V} \omega^2 \hbar^2 \epsilon} \left| \int d^3 r \psi_{\mathbf{p}'}^* \exp(i\mathbf{k}\mathbf{r}) \hat{p}_A \psi_{\mathbf{p}}^* \right|^2. \quad (9.26)$$

For the situation when one is interested in light absorption it is necessary to sum over the electron states. The result can be expressed through electron density of states, g_{el} ,

$$W^{(a)}(\omega) = \frac{4\pi^2 e^2 N_\omega g_{el}(E_f)}{m^2 \omega \epsilon} \left| \int d^3r \psi_{\mathbf{p}'}^* \exp(i\mathbf{k}\mathbf{r}) \hat{p}_A \psi_{\mathbf{p}}^* \right|^2. \quad (9.27)$$

It is important that the transition is almost “vertical”, one can neglect the photon wave vector, and

$$\hbar\omega = \frac{p^2}{2} \left(\frac{1}{m_e} + \frac{1}{m_h} \right).$$

The only result of quantum theory of radiation is that it changes $N_\omega \rightarrow N_\omega + 1$ in the expression for the emission rate (spontaneous emission).

9.4 Selection rules

The selection rules are dependent on the matrix element

$$M_{if} = \left| \int d^3r \psi_f^* e^{i\mathbf{k}_{ph}\mathbf{r}} \hat{p}_A \psi_i^* \right|^2.$$

Usually one can put $e^{i\mathbf{k}\mathbf{r}} \approx 1$ (dipole approximation). Indeed,

$$\frac{1}{m} \langle f | \mathbf{p} | i \rangle = \frac{d}{dt} \langle f | \mathbf{r} | i \rangle = i\omega_{if} \langle f | \mathbf{r} | i \rangle, \quad \hbar\omega_{if} = E_i - E_f.$$

When the states have Bloch form $\psi_{\mathbf{k}l} = e^{i\mathbf{k}\mathbf{r}} u_{\mathbf{k}l}(\mathbf{r})$ the explicit expression for dipole matrix element is

$$M_{if} = \hbar\mathbf{k} \int \psi_{\mathbf{k}'l'}^* \psi_{\mathbf{k}l} d^3r - i\hbar \int u_{\mathbf{k}'l'}^* (\nabla u_{\mathbf{k}l}) e^{i(\mathbf{k}-\mathbf{k}')\mathbf{r}} d^3r. \quad (9.28)$$

Interband transitions

Bulk materials

Consider *band-to-band transition* in direct gap materials. The first item in r.h.s. of Eq. (9.28) is 0 (Bloch states are orthogonal!). The last term requires $\mathbf{k} = \mathbf{k}'$ because central-cell functions are periodic. Thus we are left with vertical transitions with matrix elements

$$\langle u_{c\mathbf{k}} | p_A | u_{v\mathbf{k}} \rangle$$

where c, v denotes conduction (valence) band. For near band-edge transitions one can use the function in the BZ center. We have the following specification of the states

- Conduction band:

$$u_{c0} = |s\rangle$$

spherically symmetric.

- Valence band:

- Heavy holes:

$$\begin{aligned} |3/2, 3/2\rangle &= -\frac{1}{\sqrt{2}}(|p_x\rangle + i|p_y\rangle) \uparrow \\ |3/2, -3/2\rangle &= \frac{1}{\sqrt{2}}(|p_x\rangle - i|p_y\rangle) \downarrow \end{aligned}$$

- Light holes:

$$\begin{aligned} |3/2, 1/2\rangle &= -\frac{1}{\sqrt{6}}[|p_x\rangle + i|p_y\rangle) \downarrow - 2|p_z\rangle \uparrow] \\ |3/2, -1/2\rangle &= \frac{1}{\sqrt{6}}[|p_x\rangle - i|p_y\rangle) \uparrow + 2|p_z\rangle \downarrow] \end{aligned}$$

Remember that

$$\begin{aligned} |p_x\rangle &= \sqrt{\frac{3}{4\pi}} \sin \theta \cos \phi, \\ |p_y\rangle &= \sqrt{\frac{3}{4\pi}} \sin \theta \sin \phi, \\ |p_z\rangle &= \sqrt{\frac{3}{4\pi}} \cos \theta. \end{aligned}$$

Symmetry allows the transitions

$$\langle p_x | p_x | s \rangle = \langle p_y | p_y | s \rangle = \langle p_z | p_z | s \rangle.$$

Thus measuring the matrix elements in the units of $\langle p_x | p_x | s \rangle$ we obtain

$$\begin{aligned} \langle HH | p_x | s \rangle &= \langle HH | p_y | s \rangle = 1/\sqrt{2} \\ \langle LH | p_x | s \rangle &= \langle LH | p_y | s \rangle = 1/\sqrt{6} \\ \langle LH | p_x | s \rangle &= 2/\sqrt{6}, \quad \langle LH | p_z | s \rangle = 0. \end{aligned} \tag{9.29}$$

These rules have important implications for polarization dependencies of the light absorption.

Quantum wells

The discussion above can be generalized for quantum wells. Two facts are important

- The central-cell functions are only weakly effected by confining potential.

- The absorption at low enough frequencies is important only in the well region because barriers have wide gaps. The states are

$$\begin{aligned}\psi_c^n &= \frac{1}{\sqrt{AW}} e^{i\mathbf{k}_e \cdot \mathbf{r}} g_c^n(z) u_{c\mathbf{k}_e}^n \\ \psi_v^m &= \frac{1}{\sqrt{AW}} e^{i\mathbf{k}_h \cdot \mathbf{r}} \sum_\nu g_v^{\nu m}(z) u_{v\mathbf{k}_h}^{\nu m}.\end{aligned}\quad (9.30)$$

Thus we have

$$M_{if}^{2D} = \frac{1}{AW} \sum_\nu \langle g_v^{\nu m} | g_c^n \rangle \int d^2 \rho e^{i(\mathbf{k}_e - \mathbf{k}_h) \cdot \mathbf{r}} \langle u_{v\mathbf{k}_h}^{\nu m} | p_A | u_{c\mathbf{k}_e}^n \rangle \quad (9.31)$$

For symmetric confining potentials,

$$\sum_\nu \langle g_v^{\nu m} | g_c^n \rangle \approx \delta_{nm}.$$

The main difference is replacement of the 3D density of states

$$g_{el}^{3D}(\epsilon) = \frac{\sqrt{2}m^{3/2}(\epsilon - E_g)^{1/2}}{\pi \hbar^3}$$

by its 2D analog

$$\frac{g_{el}^{2D}}{W} = \frac{m_r}{\pi \hbar^2 W} \sum_{nm} \langle g_v^m | g_c^n \rangle \Theta(E_n m - \hbar\omega), \quad E_{nm} = E_{gap} + E_c^n + E_v^m.$$

Here m_r is reduced effective mass, $m_r^{-1} = m_e^{-1} + m_h^{-1}$.

Before summarizing, let us introduce a relation between the scattering rate and absorption coefficient. We have,

$$W^{(a)} = \alpha \tilde{c} N_\omega,$$

Consequently,

$$\alpha = \frac{W^{(a)}}{\tilde{c} N_\omega}.$$

Summary

Now we can give a summary for interband transitions.

Bulk semiconductors

$$\begin{aligned}\alpha(\hbar\omega) &= \frac{4\pi e^2 \hbar}{m^2 c \eta(\hbar\omega)} |\mathbf{a} \cdot \mathbf{p}_{if}|^2 g_{3D}(\hbar\omega), \\ g_{el}(\hbar\omega) &= \frac{\sqrt{2}(m_r)^{3/2}(\hbar\omega - E_g)^{1/2}}{\pi^2 \hbar^3} \quad (\text{parabolic bands}).\end{aligned}\quad (9.32)$$

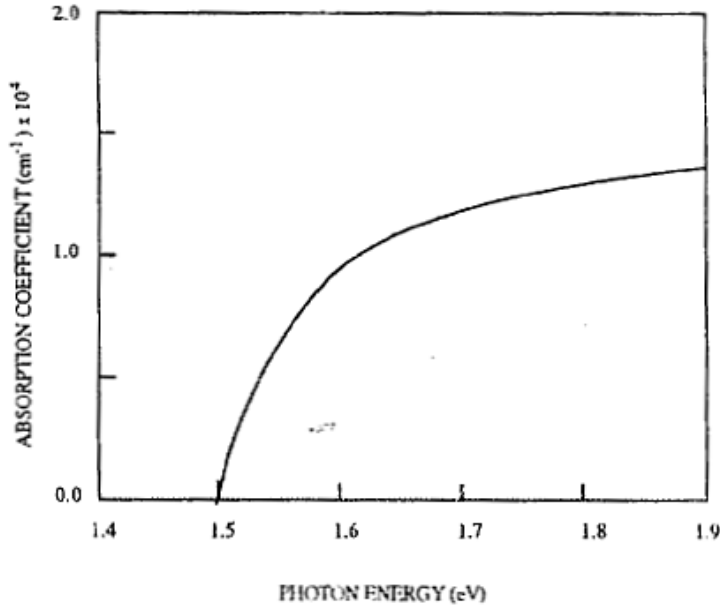


Figure 9.5: Absorption coefficient in GaAs. Note that excitonic effect can change the results inside the bandgap.

Here $\mathbf{a} \cdot \mathbf{p}_{if}$ denotes the dipole matrix element, \mathbf{a} is the polarization vector, while η is the refractive index of the material.

Quantum Well

$$\begin{aligned}\alpha(\hbar\omega) &= \frac{4\pi e^2 \hbar}{m^2 c \eta(\hbar\omega)} |\mathbf{a} \cdot \mathbf{p}_{if}|^2 \frac{g_{2D}}{W} \sum_{nm} f_{nm} \Theta(E_{nm} - \hbar\omega), \\ g_{2D} &= m_r / \pi \hbar^2,\end{aligned}\quad (9.33)$$

f_{nm} represent the overlap between n and m sub-band overlap functions.

The recombination rate for a bulk material is

$$W_{\text{em}} = \frac{4\pi e^2}{m^2 c \eta \omega \epsilon} |\mathbf{a} \cdot \mathbf{p}_{if}|^2 (N_\omega + 1) g_{\text{ph}}(\hbar\omega). \quad (9.34)$$

The total photon density of states if photons are emitted in 3D space is

$$g_{\text{ph}}(\hbar\omega) = \frac{2\omega^2}{2\pi^2 \hbar c^2}$$

where coefficient 2 allows for 2 transverse modes for each \mathbf{q} . This expression can be easily modified for quantum wells. Some experimental results are shown in Figs. 9.5 and 9.6

Important feature is $1/W$ dependence in the case of quantum well. It is a consequence of the assumption that the wave function is localized inside the well. In real life the upper states are spread outside the well, see Fig. 9.7.

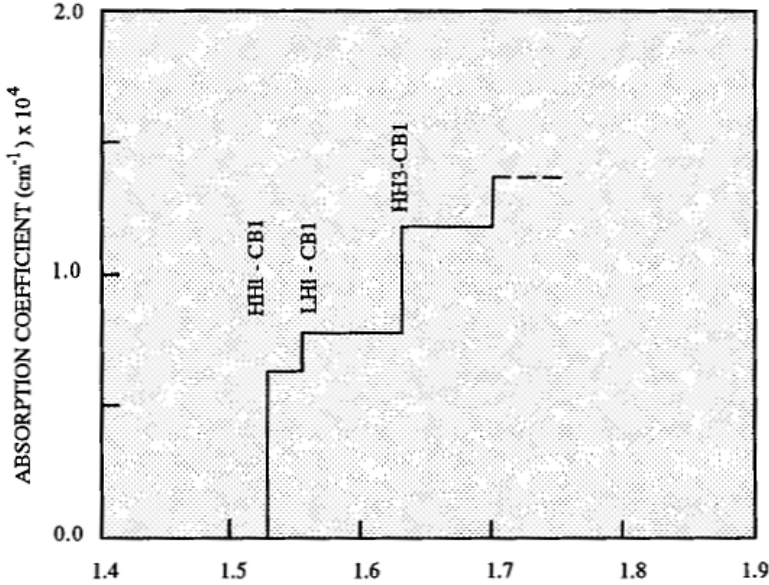


Figure 9.6: The same for 100 Å GaAs/Al_{0.3}Ga_{0.7}As quantum well structure for in-plane polarized light. The HH transition is ≈ 3 times stronger than LH transition in this polarization. The higher sub-bands become closer spaced and eventually one gets bulk absorption coefficient.

Few words about semiconductor lasers

A typical band profile to get a lasing effect is shown in Fig. 9.8. The main requirement is to compensate losses by gain $G(\hbar\omega)$, $\Gamma G = \alpha_{\text{loss}}$. Here Γ is the so-called optical confinement factor which is just the fraction of optical intensity in the active region. We have calculated the rates assuming that initial state is occupied but final is empty. What we need, is to average the result in a proper way to extract relative number of such configurations. In general, one has quasi-Fermi distributions for electrons and holes,

$$f_{e(h)} = \left[1 + \exp \left(\pm \frac{E - \mu_{e(h)}}{kT} \right) \right]^{-1},$$

the result being

$$\begin{aligned} G(\hbar\omega) &= \frac{4\pi e^2}{m^2 c \eta \omega} \int \frac{d^3 p}{(2\pi\hbar)^3} |\mathbf{a} \cdot \mathbf{p}_{if}|^2 \\ &\times [f_e(E_e(\mathbf{p})) + f_h(E_h(\mathbf{p})) - 1] \delta [E_e(\mathbf{p}) - E_h(\mathbf{p}) - \hbar\omega]. \end{aligned} \quad (9.35)$$

Here we calculate the difference between (induced) emission and absorption rates. It can be positive only if

$$f_e(E_e(\mathbf{p})) + f_h(E_h(\mathbf{p})) > 1$$

(population inversion). One gets a very similar form for a quantum well by replacement the states $|\mathbf{p}\rangle \rightarrow |n, \mathbf{p}_\parallel\rangle$. In general, one has also to sum over the angular momentum

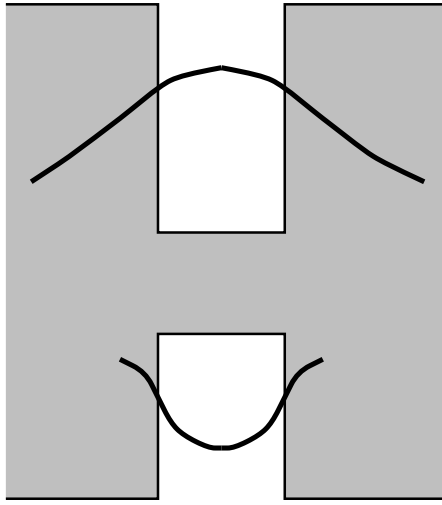


Figure 9.7: Schematic structure of wave functions.

states of the holes. In the most cases, the most important are the transitions with $m = n$. The main directions to obtain lasing – increase of optical confinement, of reduced density of states (quantum wells!!)

An important feature is the *threshold current* that is the product of the electron charge eR_{rec} where R_{rec} is the recombination rate due to spontaneous photon emission and non-radiative processes. It must be as small as possible, and people try to decrease them. An important contribution which can be optimized is Auger processes, Fig. 9.9 They can be direct or phonon-assisted (trap-assisted, etc). Auger processes are very harmful for lasing.

Indirect interband transitions

When the energy and momentum conservation law cannot be met, then *indirect transitions* come into play. Let us consider a situation when phonon energy is less than direct gap. However, there are states at some other values of \mathbf{p} where the energy conservation can be met. In this case the necessary momentum can be supplied by a phonon in course of phonon-assisted transition. One has to pay for that because this process involves 2nd order perturbation theory.

Let us consider an example, Fig. 9.10 We have to employ the second-order perturbation theory,

$$W = \frac{2\pi}{\hbar} \int \left| \sum_n \frac{\langle f | \mathcal{H}_{\text{int}} | n \rangle \langle n | \mathcal{H}_{\text{int}} | i \rangle}{E_i - E_n} \right|^2 \delta(E_f - E_i) \frac{d^3 p}{(2\pi\hbar)^3} , .$$

The interaction Hamiltonian is a sum of the contributions of electron-photon and electron-phonon interaction,

$$\mathcal{H}_{\text{int}} = \mathcal{H}_{\text{ph}} + \mathcal{H}_{\text{ep}} .$$

Both combinations shown in Fig. 9.10 can contribute. In any case, indirect transitions

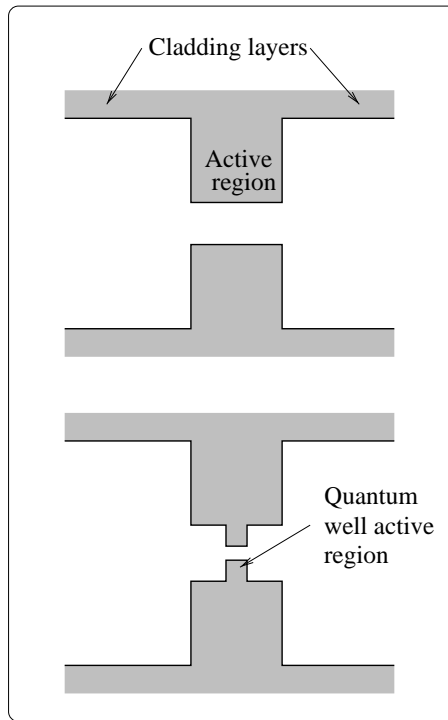


Figure 9.8: Typical band profiles used for bulk (upper panel) and quantum well (lower panel) lasers. The width of the active region dimensions in the quantum well $\leq 100 \text{ \AA}$, while in double heterostructure laser it is $\geq 0.1 \mu\text{m}$.

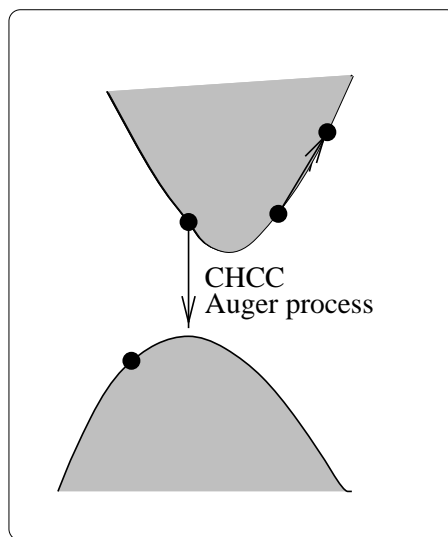


Figure 9.9: A typical Auger process. A reverse one is called impact ionization.

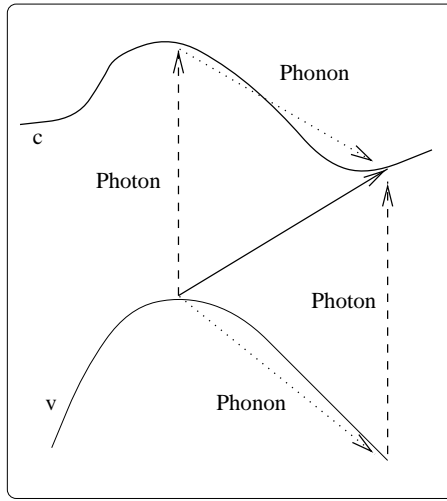


Figure 9.10: A typical indirect transition.

lead to an additional small coefficient corresponding to electron-phonon coupling. One can trace that comparing the absorption profiles for GaAs and Si, Fig. 9.11.

9.5 Intraband Transitions

Bulk semiconductors

Intraband transitions must involve a phonon, or some other scattering mechanism. The second-order process is very much similar to the one discussed above. It is very important for lasers because it is responsible for losses in cladding areas.

Quantum wells

A remarkable feature - possibility of intraband (but inter-subband) transitions in the lowest order. Consider 2 subbands with wave functions

$$\psi^i = g^i(z) e^{i\mathbf{k}\rho} u_{n\mathbf{k}}^i(\mathbf{r}).$$

The functions $g_i(z)$ are orthogonal, while the central cell functions are essentially the same for all the subbands. Thus

$$\mathbf{p}_{if} = -\frac{i\hbar}{W} \int g^{2*}(z) e^{-i\mathbf{k}\rho} \mathbf{a} \nabla g^1(z) e^{i\mathbf{k}\rho} d^2\rho dz.$$

If \mathbf{k} is in the ρ -plane, then the matrix element is 0. However, if the light is polarized in z -plane, then

$$\mathbf{p}_{if} = -\frac{i\hbar}{W} \int g^{2*}(z) \hat{z} \frac{\partial}{\partial z} g^1(z) d^2\rho dz.$$

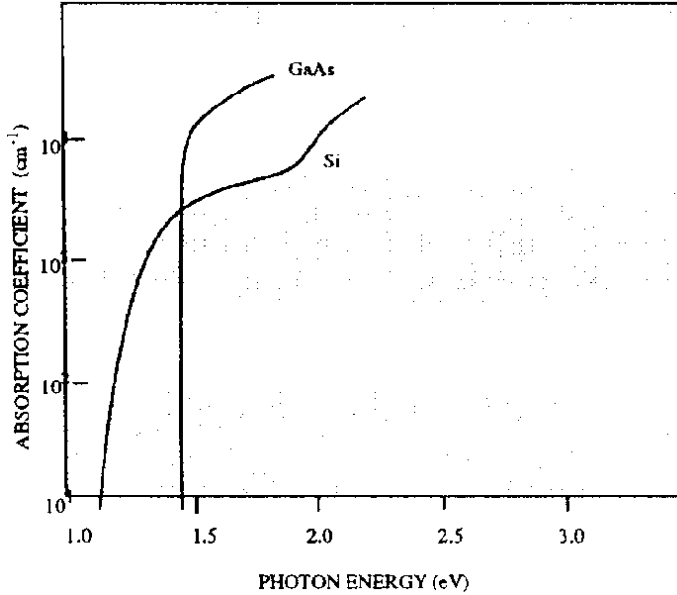


Figure 9.11: Absorption coefficient of Si and GaAs.

If the states have opposite parities, then the integral is finite, and

$$\mathbf{p}_{if} \approx \frac{\hbar}{W} .$$

Finally, we get

$$W_{\text{abs}} = \frac{4\pi^2 e^2 N_\omega}{m^2 \omega \epsilon} \frac{1}{W} \sum_f |\mathbf{p}_{if}|^2 \delta(E_f - E_i - \hbar\omega) f(E_i) [1 - f(E_f)] .$$

Assuming that only one subband is filled and introducing electron concentration as

$$N_c = \sum_f \delta(E_f - E_i - \hbar\omega) f(E_i)$$

we could obtain the result. However, in 2D case the joint density of states is infinite in the resonance if both subbands have the same dispersion law. Usually, a Gaussian broadening is assumed,

$$g(E) = \frac{1}{(1.44\pi\sigma)^{1/2}} \exp \left[-\frac{(E - E_{12})^2}{1.44\sigma} \right] .$$

Physics of the broadening is rather complicated (disorder, phonon-related processes). Any way, we get

$$\alpha(\hbar\omega) = \frac{4\pi^2 e^2}{m^2 c \eta \omega} \frac{|\mathbf{p}_{if}|^2}{W} \frac{1}{(1.44\pi\sigma)^{1/2}} \exp \left[-\frac{(E - E_{12})^2}{1.44\sigma} \right] ,$$

What is important that the absorption is strongly dependent on the *polarization* of the incoming light. If electric field is parallel to the 2D plane then there is a weak free-electron

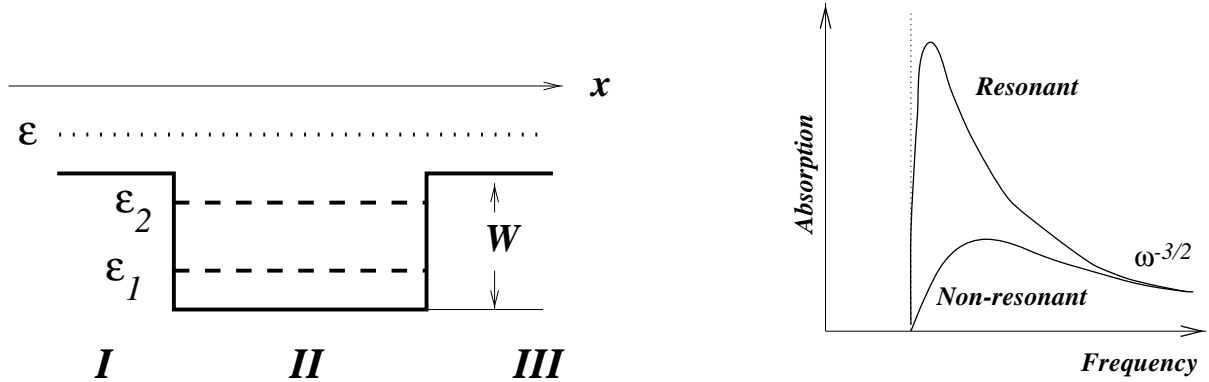


Figure 9.12: Energy profile of a quantum well (left panel) and schematic behavior of absorption coefficient (right panel).

absorption. The resonant absorption discussed above is possible only if the light is polarized *perpendicular* to 2D gas. The selection rules (for symmetric quantum wells with isotropic spectrum) imply that the transition can take place only between the states with *opposite* parity, otherwise

$$\mathbf{p}_{if} \propto \int dz \psi_M^*(z) \frac{d\psi_N(z)}{dz} = 0.$$

Note that this rule is opposite to the case of interband transitions.

In the wells with finite depth, there is a continuum spectrum above discrete states. In such a situation, a properly polarized light can induce transitions from discrete to continuum states, i. e. lead to *photoionization*.

Let us sketch the calculation for a rectangular well with the depth W (Fig. 9.12). For a scattering state in the continuum spectrum, the wave function for the incoming energy ϵ can be written as

$$\psi_\epsilon = \begin{cases} \exp(ikz) + R \exp(-ikz) & \text{in the region I} \\ B \exp(iKz) + C \exp(-iKz) & \text{in the region II} \\ T \exp(ikz) & \text{in the region III} \end{cases}. \quad (9.36)$$

Here

$$k^2 = \frac{2m\epsilon}{\hbar^2}, \quad K^2 = \frac{2m(W + \epsilon)}{\hbar^2}.$$

Then we have to match both the functions and their derivatives at two boundaries. For example,

$$B = \frac{2k(k + K)}{(K + k)^2 + (K - k)^2 \exp(2iKa)}.$$

It is clear that at small k ($k \ll K$) the coefficient B (as well as C and T) are small. Thus the electrons are reflected from the well. However, at $Ka = s\pi/2$, $s = 1, 2, \dots$ we have

$$B = c = 1/2.$$

That means full penetration - the well behaves as Fabri-Perot resonator for de Broglie waves. As a result, these “resonant” states are very important. Only for these states overlap of wave functions is significant.

Now let us discuss the behavior of the absorption close to the threshold ($\hbar\omega = W$), i.e. for small ε . One can show that for the so-called non-resonant wells with

$$\sqrt{2mW} \neq s\hbar/a$$

the absorption is small and proportional to $\sqrt{\hbar\omega - W + \varepsilon_1}$, while for the resonant ones it is proportional to $(\hbar\omega - W + \varepsilon_1)^{-1/2}$.

Above we ignored frequency dependence of dielectric function which might be important near resonant transitions. The account of these effects is beyond the scope of this course.

Interband transitions in a magnetic field

In a magnetic field, *Landau levels* are formed in the conduction and valence bands, the energies (for parabolic bands) being

$$\epsilon_n = \left(n + \frac{1}{2}\right)\hbar\omega_c + \frac{p_z^2}{2m}; \quad n = 0, 1, 2, \dots, \quad (9.37)$$

where

$$\omega_c = \frac{eB}{mc}. \quad (9.38)$$

Thus the band edge moves to give the energy gap as

$$E_g(B) = E_g(0) + \frac{e\hbar}{2m_r}B, \quad \frac{1}{m_r} \equiv \left(\frac{1}{m_e} + \frac{1}{m_h}\right). \quad (9.39)$$

Thus, the fundamental edge must be shifted $\propto B$. There is also *spin splitting*,

$$\Delta E_{\pm} = g\mu_B B_z, \quad \mu_B = e\hbar/2m_0c.$$

Now let us estimate the absorption coefficient. As it is well known, the quantum numbers of an electron in a magnetic field are $\{n, p_y, p_z\}$. One can easily show that because one can neglect the photon wave vector the dipole matrix element can be expressed as

$$\mathcal{P}_{vc} = \frac{e}{mc} A_0 |\mathbf{e}\mathbf{p}_{vc}|^2 \delta_{p_y, p'_y} \delta_{p_z, p'_z} \delta_{nn'}.$$

Thus the transition probability is

$$W_{vc} = \frac{2\pi}{\hbar} \frac{e^2 |A_0|^2 |\mathbf{e}\mathbf{p}_{vc}|^2}{m^2 c^2} \sum_n \int \int \frac{dp_y dp_z}{\pi^2 \hbar^2} \delta \left[\hbar\omega - E_g - (n + 1/2) \frac{eH}{m_r c} + \frac{p_z^2}{2m_r c} \right].$$

The following calculation is straightforward. We use the following simplifications

$$\int dp_y = L_x eH/c,$$

$$\int dp_z \delta \left[A - \frac{p_z^2}{2m_r} \right] = L_z \sqrt{m_r/2A}.$$

Finally,

$$\alpha = \frac{e^2 \omega_c}{m^2 \omega n c} |\mathbf{e} \mathbf{p}_{vc}|^2 \left(\frac{2m_r}{\hbar^2} \right)^{3/2} \sum_N \frac{1}{\sqrt{\hbar\omega - E_g - (\hbar e H / m_r c)(N + 1/2)}} \quad (9.40)$$

Thus, there are *maxima* at

$$\hbar\omega_{\max} - E_g - (\hbar e H / m_r c)(N + 1/2) = 0.$$

9.6 Problems

9.1. Calculate dipole matrix element for the transitions between the subbands in a rectangular quantum well of width W with infinite potential barriers. Assume that light is polarized perpendicular to the well.

9.2. Make a similar calculation for a parabolic confinement

$$U(z) = (1/2)m\omega^2 z^2.$$

Define ω from the request that the typical spread of the ground state wave function is W and compare the result with the case of rectangular confinement.

9.7 Excitons

In the previous discussion we employed the independent electron approximation. The effect of other electrons enters only through the occupation probabilities without altering eigenvalues of the electronic problem. Now we turn to the role of electron-electron (electron-hole) interaction.

Consider a simple example.

Excitonic states are known since 1931 (Frenkel). Further work – Peierls, Wannier, Elliot, Knox. In bulk materials the binding energy is very low and such states can be observed only in pure materials and used for their characterization. In poorer quality samples these states merge with band-to-band transitions.

In heterostructures, due to spatial confinement, the binding energy increases. The oscillator strength is also increased. Thus one observes sharp *excitonic transitions*. These energy positions can be tuned by electronics and optics. Implications - high-speed modulation of optical signals, optoelectronic switches, etc. In particular, one can tune exciton transitions

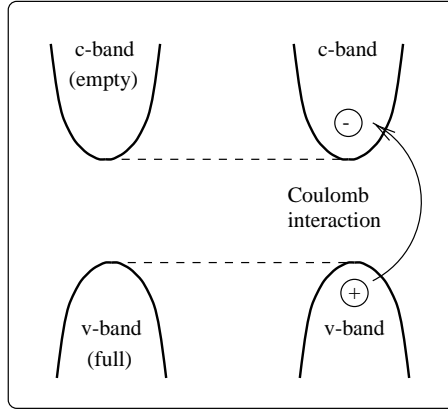


Figure 9.13: The band structure of independent electrons (left) and Coulomb electron-hole interaction which would modify the band picture (right).

- by application of a transverse electric field (quantum confined Stark effect);
- “bleaching” of exciton transition by high electron-hole density.

9.7.1 Excitonic states in semiconductors

There are two types of excitons – Frenkel (small radius) and Wannier-Mott (large radius). We will discuss the latters because they are relevant to semiconductors. For them we use the effective mass theory for the envelope function,

$$\left(-\frac{\hbar^2}{2m_e} \nabla_e^2 - \frac{\hbar^2}{2m_h} \nabla_h^2 - \frac{e^2}{\epsilon |\mathbf{r}_e - \mathbf{r}_h|} \right) \psi_{\text{ex}} = E \psi_{\text{ex}}. \quad (9.41)$$

Then we introduce new co-ordinates

$$\begin{aligned} \mathbf{r} &= \mathbf{r}_e - \mathbf{r}_h, & \mathbf{R} &= \frac{m_e \mathbf{r}_e + m_h \mathbf{r}_h}{m_e + m_h} \\ \mathbf{k} &= \frac{m_e \mathbf{k}_e + m_h \mathbf{k}_h}{m_e + m_h}, & \mathbf{K} &= \mathbf{k}_e - \mathbf{k}_h \end{aligned} \quad (9.42)$$

to get

$$\mathcal{H} = \frac{\hbar^2 K^2}{2(m_e + m_h)} + \left\{ \frac{\hbar^2 k^2}{2m_r} - \frac{e^2}{2|\mathbf{r}|} \right\}. \quad (9.43)$$

Here m_r is the reduced mass. The 1st term gives solution

$$\psi_{\text{cm}} = \exp(i\mathbf{KR}).$$

The second leads to the hydrogen atom problem,

$$\left\{ \frac{\hbar^2 k^2}{2m_r} - \frac{e^2}{2|\mathbf{r}|} \right\} F(\mathbf{r}) = EF(\mathbf{r}).$$

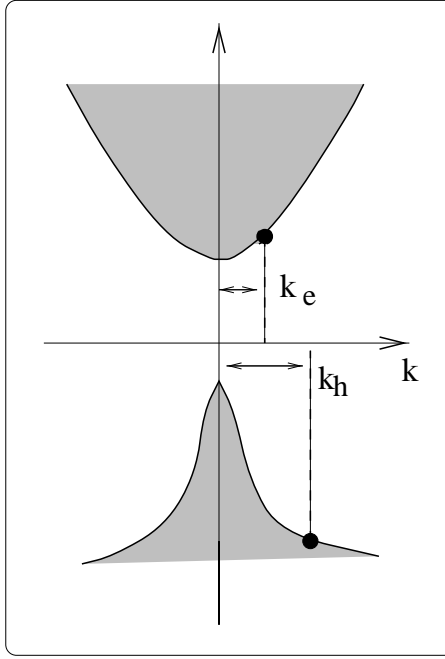


Figure 9.14: Schematic picture of an exciton in Bloch representation.

As a result

$$\psi_{n\mathbf{K}} = e^{i\mathbf{KR}} F_n(\mathbf{r}) \phi_c(\mathbf{r}_e) \phi_v(\mathbf{r}_h) \quad (9.44)$$

where $\phi_{c,v}$ are central cell functions. The eigenvalues are

$$E_{n\mathbf{K}} = E_n + \frac{\hbar^2 K^2}{2(m_e + m_h)}, \quad E_m = -\frac{m_r e^4}{2\epsilon^2 \hbar^2} \frac{1}{n^2}. \quad (9.45)$$

Typically, $E_1 = 2 - 6$ meV.

We need to develop a perturbation theory to find an interaction between light and excitons. In general,

$$\mathcal{H}_e = \mathcal{H}_0 + \frac{1}{2} \sum_{i \neq j} \frac{e^2}{\epsilon |\mathbf{r}_i - \mathbf{r}_j|}.$$

Because of translational symmetry,

$$\psi_{\text{ex}}(\{\mathbf{r}_i + \mathbf{a}\}) = e^{i\mathbf{Ka}} \psi_{\text{ex}}(\{\mathbf{r}_i\}),$$

where \mathbf{a} is the lattice vector. Thus the proper basis functions are

$$\Phi_{c\alpha_e;v\alpha_h} \quad (9.46)$$

where $\alpha_{c(v)} \equiv \{\mathbf{k}, S\}$ describes momentum and spin state of the electron or hole, see Fig. 9.14. The excitonic state then can be constructed as a linear combination of the

building blocks (9.46),

$$\psi_{\text{ex}}^{\beta} = \sum_{\mathbf{k}} A_{\beta}(\mathbf{k}) \Phi_{c,\mathbf{k}-\mathbf{K}/2,S_e;v,\mathbf{k}+\mathbf{K}/2,S_h}^{\beta} \quad (9.47)$$

where the set of quantum numbers $\beta \equiv \{n, l, m\}$ characterizes the energy eigenvalue index and angular momentum indices, respectively.

Now we employ the generalized effective mass approximation assuming that the exciton has large scale and the coefficients $A_{\beta}(\mathbf{k})$ are localized in \mathbf{k} -space. In this way we come back to the real space,

$$F_{\beta}(\mathbf{r}) = \sum_{\mathbf{k}} A_{\beta}(\mathbf{k}) e^{i\mathbf{kr}}$$

which obeys the hydrogen-like equation

$$\left[E_{cv}(-i\nabla, \mathbf{K}) - \frac{e^2}{\epsilon|\mathbf{r}|} \right] F_{\beta}(\mathbf{r}) = E_{\text{ex}} F_{\beta}(\mathbf{r}) . \quad (9.48)$$

Here

$$E_{cv}(-i\nabla, \mathbf{K}) \equiv E_c(\mathbf{k} + \mathbf{K}/2) - E_v(\mathbf{k} - \mathbf{K}/2)|_{\mathbf{k} \rightarrow -i\nabla} .$$

Note that ϵ is a quite complicated function which can strongly differ from static dielectric function at large carrier concentrations.

In the case of simple parabolic bands the solution is simple and coincides with given above. Namely,

$$E_n^{\text{ex}} = E_g - R_{\text{ex}}/n^2, \quad R_{\text{ex}} = m_r e^4 / 2\hbar^2 \epsilon^2 .$$

The envelope ground state wave function is

$$F_{100} = \frac{1}{\sqrt{\pi a_{\text{ex}}^3}} e^{-r/a_{\text{ex}}}, \quad a_{\text{ex}} = (\epsilon m_0 / m_r) a_B . \quad (9.49)$$

Here $a_B = 0.529$ Å is the Bohr radius. The typical value of a_{ex} is about 100 Å, \gg than the lattice constant a .

9.7.2 Excitonic effects in optical properties

The transition rate from the ground state ψ_0 to the excitonic state $\psi_{\mathbf{K}}$ (according to the Fermi golden rule) is

$$W = \frac{2\pi}{\hbar} \left(\frac{eA}{mc} \right)^2 \delta_{\mathbf{K}} \left| \sum_{\mathbf{k}} A(\mathbf{k}) \mathbf{a} \mathbf{p}_{cv}(\mathbf{k}) \right|^2 \delta(E_{\text{ex}} - E_0 - \hbar\omega) .$$

Assuming that \mathbf{p}_{cv} is \mathbf{k} independent, we arrive at

$$W = \frac{2\pi}{\hbar} \left(\frac{eA}{mc} \right)^2 \delta_{\mathbf{K}} |\mathbf{a} \mathbf{p}_{if}|^2 \left| \sum_{\mathbf{k}} A(\mathbf{k}) \right|^2 \delta(E_{\text{ex}} - E_0 - \hbar\omega) . \quad (9.50)$$

From the definition,

$$\sum_{\mathbf{k}} A_{\beta}(\mathbf{k}) = F_{\beta}(0).$$

Finally, for the ground state we have

$$W = \frac{2\pi}{\hbar} \left(\frac{eA}{mc} \right)^2 \delta_{\mathbf{K}} |\mathbf{ap}_{if}|^2 \frac{\delta(E_{\text{ex}} - E_0 - \hbar\omega)}{\pi a_{\text{ex}}^3 n^3}. \quad (9.51)$$

In a realistic case, δ -function is broadened.

An important note is that we have a selection rule $\mathbf{K} = 0$. This is why the transition is discrete even though the excitonic states are extended.

As a result, we arrive at the following picture. Inside the gap there are sharp excitonic lines with intensities proportional to n^{-3} . They become closer and closer as n increases. One can introduce exciton density of states as

$$g_{\text{ex}} = 2(\partial n / \partial E) = n^3 / R_{\text{ex}}.$$

Then it is easy to re-write the absorption coefficient α inside the gap through α_F – the absorption coefficient without excitonic effects,

$$\alpha|_{\hbar\omega \approx E_g} = \alpha_F \frac{2\pi R_{\text{ex}}^{1/2}}{(E_g - \hbar\omega)^{1/2}}. \quad (9.52)$$

Thus α reaches a constant at the band edge. Above the gap one can obtain

$$\alpha = \alpha_F \frac{\pi x e^{\pi x}}{\sinh \pi x}, \quad x = \left(\frac{R_{\text{ex}}}{\hbar\omega - E_g} \right)^{1/2}.$$

Far enough from the edge the result tends to the one for the absence of the excitonic effects. A typical experimental plot is shown in Fig. 9.15 Very instructive is luminescence at low temperatures where electrons and holes freeze out in the excitonic states. Here one can clearly observe free excitons, as well as various bound excitons.

9.7.3 Excitonic states in quantum wells

To illustrate peculiarities of the quantum wells let us consider first a shallow H-like center in a well $0 \leq z \leq a$. We have to solve SE of the type

$$-\frac{\hbar^2}{2m} \nabla^2 \Psi - \frac{e^2}{\epsilon \sqrt{x^2 + y^2 + (z - z_0)^2}} \Psi = \varepsilon_i \Psi. \quad (9.53)$$

Here we assume that the structure has the same dielectric constant of all the parts. Such an assumption is good for heterostructures but fails for MOS systems. Also it is assumed that the effective mass approach is valid.

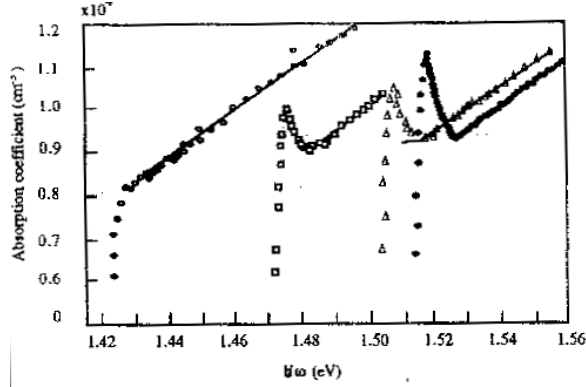


Figure 9.15: Measured absorption in GaAs at the temperatures 294, 186, 90, and 21 K. At room temperature the excitonic transitions merge with band-to-band absorption.

The boundary conditions for infinite potential are

$$\Psi(0) = \Psi(a) = 0.$$

Let us consider a simplified situation when

$$a_B \gg a. \quad (9.54)$$

Then one can neglect the item $(z - z_0)^2$ in Eq. 9.53. In this case the variables z and $\rho = \sqrt{x^2 + y^2}$ are decoupled, and

$$\Psi = \phi(\rho)\chi(z).$$

The solution of the 2D problem (see e. g. [6]) lead to eigenvalues $-\varepsilon_0/(i - 1/2)^2$ where $\varepsilon = me^4/2\epsilon^2\hbar^2$ is the 3D Rydberg energy. Thus

$$\varepsilon_{N,i} = \varepsilon_s N^2 - \frac{\varepsilon_0}{(i - 1/2)^2}, \quad \varepsilon_s = \frac{\pi\hbar^2}{2ma^2}. \quad (9.55)$$

According to inequality (9.54), $\varepsilon_0 \ll \varepsilon_s$. That means that each level of size quantization has impurity satellites. It is important that for all the $N \neq 1$ impurity states overlap with continuous spectrum of lower sub-bands. Consequently, it has a finite life time even in the absence of collisions.

In the limiting case (9.54) the energy of ground state is 4 times larger than in the 3D case. Beyond his limit the energy is between ε_0 and $4\varepsilon_0$, it depends on the position z_0 . As a result, a sort of “impurity band” appears. Another assumption which was used is the infinite potential. It is valid until

$$a_B \gg \delta = \frac{\hbar}{\sqrt{m(W - \varepsilon_1)}}.$$

In the opposite case the calculations are rather cumbersome, especially when effective masses within the well and the barrier are different.

Now we can re-formulate the results for the excitons. In this case SE has the form

$$\left(-\frac{e^2}{2m_e} \nabla_e^2 - \frac{e^2}{2m_h} \nabla_h^2 \right) \Psi - \frac{e^2}{\epsilon \sqrt{(x_e - x_h)^2 + (y_e - y_h)^2 + (z_e - z_h)^2}} \Psi = \varepsilon_{\text{ex}} \Psi. \quad (9.56)$$

Under the condition (9.54) we can also drop z -dependent part of the denominator. Thus we are left with 2D problem. It is natural to introduce new variables

$$\mathbf{R} = \frac{m_e \boldsymbol{\rho}_e + m_h \boldsymbol{\rho}_h}{m_e + m_h}, \quad \boldsymbol{\rho} = \boldsymbol{\rho}_e - \boldsymbol{\rho}_h.$$

Consequently,

$$\Psi(\mathbf{r}_e, \mathbf{r}_h) = \psi_N(z_e) \psi_M(z_h) \exp(i\mathbf{K}\mathbf{R}) \Phi(\rho).$$

As a result, the equation for Φ differs from similar equation for an impurity state by the replacement

$$m \rightarrow m_r = \frac{m_e m_h}{m_e + m_h},$$

and

$$\varepsilon_{\text{ex}} = -\frac{m_r e^4}{\epsilon(i - 1/2)^2}.$$

In many materials (Si, A^{III}B^V) because of the presence of both light and heavy holes there are 2 type of excitons.

In general, the Hamiltonian for relative motion has the form

$$\begin{aligned} \mathcal{H} = & -\frac{\hbar^2}{2m_r} \left(\frac{1}{\rho} \frac{\partial}{\partial \rho} \rho \frac{\partial}{\partial \rho} + \frac{1}{\rho^2} \frac{\partial^2}{\partial \phi^2} \right) - \frac{\hbar^2}{2m_e} \frac{\partial^2}{\partial z_e^2} - \frac{\hbar^2}{2m_h} \frac{\partial^2}{\partial z_h^2} \\ & - \frac{e^2}{\epsilon |\mathbf{r}_e - \mathbf{r}_h|} + V_{ew}(z_e) + V_{hw}(z_h) \end{aligned}$$

where $V_{iw}(z_i)$ are confining potentials. There is no simple analytical solution for this equation. Moreover, the parabolic approximation is usually bad for hole states in GaAlAs heterostructures. It is also important to allow for screening. So numerical methods are usual.

The expressions for the absorption coefficient are similar, however one must use correct matrix elements. The important quantity is the oscillator strength defined as

$$f_{nm} = \frac{2}{(2\pi)^2 m E_{nm}^{\text{ex}}} \left| \int d^2 k G_{nm}(\mathbf{k}) \mathbf{a} \mathbf{p}_{nm}(\mathbf{k}) \right|^2.$$

Here

$$\mathbf{p}_{nm}(\mathbf{k}) = \sum_{\mu\nu} \int d^2 \rho U_0^\nu(\boldsymbol{\rho}) \hat{\mathbf{p}} U_0^\mu(\boldsymbol{\rho}) \int dz g_n^\mu(z) g_m^\nu(k, z) \quad (9.57)$$

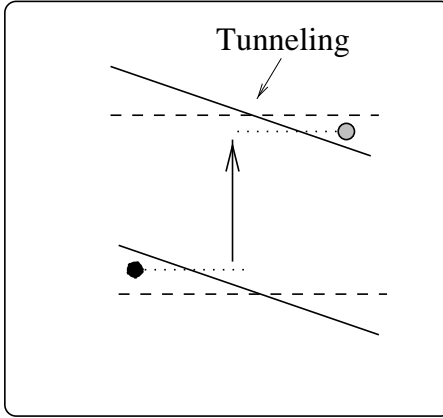


Figure 9.16: On the Franz-Keldysh effect.

while G_{nm} are the coefficients of expansion of the exciton wave function in terms of the basis in \mathbf{k} -space,

$$|\psi^{\text{ex}}\rangle = \sum_{nm} \int d^2k |n, \mathbf{k}\rangle |n, -\mathbf{k}\rangle G_{nm}(\mathbf{k}).$$

Then, as usual,

$$\alpha_{nm} = \frac{4\pi^2 e^2 \hbar}{\eta mcW} \sum_{nm} f_{nm} \delta(E_{nm}^{\text{ex}} - \hbar\omega).$$

Oscillator strength is substantially increased because of exciton confinement. More exact theoretical treatment is given e. g. in the book [6].

Quantum confined Stark effect

Consider optical absorption in the presence of an external electric field. The electrical field pulls apart electron-hole pairs which causes the broadening of the exciton peak and a shift of the peak to lower energies (Franz-Keldysh effect, Fig. 9.16). In heterostructures, the most interesting is *transverse* field because it allows to tune exciton transitions. The presence of the large barriers helps the electron and hole to be together and the transition takes place up to the fields ≤ 100 kV/cm.

The electric field

1. Changes inter-subband separations;
2. Pushes electrons and holes to opposite directions making the energy separations smaller. Due to the separations of electron and holes in space the exciton binding energy decreases.

The first effect is usually much more important. Let us make a crude estimate valid at small electric field. The Hamiltonian can be written as

$$\mathcal{H} = \mathcal{H}_0 + eFz,$$

where F is the electric field. The first perturbative correction is

$$\Delta E^{(1)} = \langle \psi_1 | eFz | \psi_1 \rangle = 0$$

because the ground state is *even*. The second order correction for the ground state in a square well is

$$\Delta E^{(2)} = \frac{1}{24\pi^2} \left(\frac{15}{\pi^2} - 1 \right) \frac{me^2 F^2 W^4}{\hbar^2}.$$

One has to optimize the well width W because in wide wells the absorption goes down, the optimum being at $W \sim 100$ Å.

Chapter 10

Ac transport and optics in doped semiconductors

10.1 Impurity states

A typical energy level diagram is shown on Fig. 10.1 Shallow levels allow a universal

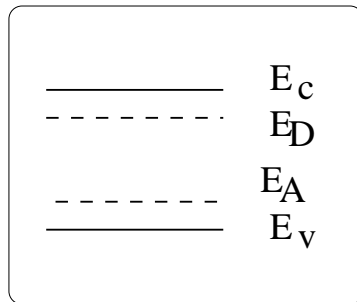


Figure 10.1: band diagram of a semiconductor.

description because the spread of wave function is large and the potential can be treated as from the point charge,

$$U(r) = e^2/\epsilon r.$$

To find impurity states one has to treat Schrödinger equation (SE) including periodic potential + Coulomb potential of the defect.

Extremum at the center of BZ

Then for small k we have

$$E_n(k) = \frac{\hbar^2 k^2}{2m}.$$

We look for solution of the SE

$$(\mathcal{H}_0 + U)\psi = E\psi$$

in the form

$$\psi = \sum_{n'k'} B_{n'}(\mathbf{k}') \phi_{n'k'}(\mathbf{r}),$$

where $\phi_{n'k'}(\mathbf{r})$ are Bloch states. By a usual procedure (multiplication by $\phi_{nk}^*(\mathbf{r})$ and integration over \mathbf{r}) we get the equation

$$\begin{aligned} [E_n(\mathbf{k}) - E] B_n(\mathbf{k}) + \sum_{n'k'} U_{n'k'}^{nk} B_{n'}(\mathbf{k}) &= 0 \\ U_{n'k'}^{nk} &= \frac{1}{V} \int u_{nk}^* u_{n'k'} e^{i(k'-k)\mathbf{r}} U(\mathbf{r}) d\mathbf{r}. \end{aligned}$$

Then, it is natural to assume that $B(\mathbf{k})$ is nonvanishing only near the BZ center, and to replace central cell functions u by their values at $\mathbf{k} = 0$. These function rapidly oscillate within the cell while the rest varies slowly. Then within each cell

$$\int_{\text{cell}} u_{n0}^* u_{n'0} d\mathbf{r} = \delta_{nn'}$$

because Bloch functions are orthonormal. Thus,

$$\begin{aligned} [E_n(\mathbf{k}) - E] B_n(\mathbf{k}) + \sum_{n'} U(\mathbf{kk}') B_n(\mathbf{k}') &= 0 \\ U(\mathbf{kk}') &= \frac{1}{V} \int e^{i(\mathbf{k}-\mathbf{k}')\mathbf{r}} U(r) d\mathbf{r} = -\frac{4\pi e^2}{\epsilon V |\mathbf{k} - \mathbf{k}'|^2}. \end{aligned}$$

Finally we get

$$\left[\frac{\hbar^2 k^2}{2m} - E \right] B_n(\mathbf{k}) - \frac{4\pi e^2}{\epsilon V} \sum_{\mathbf{k}'} \frac{1}{|\mathbf{k} - \mathbf{k}'|^2} B_n(\mathbf{k}')$$

where one can integrate over \mathbf{k} in the infinite region (because $B_n(\mathbf{k})$ decays rapidly).

Coming back to the real space and introducing

$$F(\mathbf{r}) = \frac{1}{\sqrt{V}} \sum_{\mathbf{k}} B_n(\mathbf{k}) e^{i\mathbf{kr}}$$

we come to the SE for a hydrogen atom,

$$\left[-\frac{\hbar^2}{2m} \nabla^2 - \frac{e^2}{\epsilon r} \right] F(r) = E F(r).$$

Here

$$\begin{aligned} E_t &= -\frac{1}{t^2} \frac{e^4 m}{2\epsilon^2 \hbar^2}, \quad t = 1, 2 \dots \\ F(r) &= (\pi a^3)^{-1/2} \exp(-r/a), \quad a = \hbar^2 \epsilon / m e^2. \end{aligned}$$

For the total wave function one can easily obtain

$$\psi = u_{n0}(\mathbf{r}) F(\mathbf{r}).$$

The results are summarized in the table.

Material	ϵ	m/m_0	E_{1s} (th.) (meV)	E_{1s} (exp.) (meV)
GaAs	12.5	0.066	5.67	Ge: 6.1 Si: 5.8 Se: 5.9 S: 6.1 S: 5.9
InP	12.6	0.08	6.8	7.28
CdTe	10	0.1	13	13.*

Table 10.1: Characteristics of the impurity centers.

Several equivalent extrema

Let us consider silicon for example. The conduction band minimum is located at $k_z = 0.85(2\pi/a)$ in the [100] direction, the constant energy surfaces are ellipsoids of revolution around [100]. There must be 6 equivalent ellipsoids according to cubic symmetry. For a given ellipsoid,

$$E = \frac{\hbar^2}{2m_\ell}(k_z - k_z^0)^2 + \frac{\hbar^2}{2m_t}(k_x^2 + k_y^2).$$

Here $m_\ell = 0.916m_0$, $m_t = 0.19m_0$. According to the effective mass theory, the energy levels are N -fold degenerate, where n is the number of equivalent ellipsoids. In real situation, these levels are split due to short-range corrections to the potential. These corrections provide inter-extrema matrix elements. The results for an arbitrary ration $\gamma = m_t/m_\ell$ can be obtained only numerically by a variational method (Kohn and Luttinger). The trial function was chosen in the form

$$F = (\pi a_\parallel a_\perp^2)^{-1/2} \exp \left\{ - \left[\frac{x^2 + y^2}{a_\perp^2} + \frac{z^2}{a_\parallel} \right]^{1/2} \right\},$$

and the parameters a_i were chosen to minimize the energy at given γ . Excited states are calculated in a similar way. The energies are listed in table 10.1.

Material	E_{1s} (meV)		E_{2p_0} (meV)
Si (theor.)		31.27	11.51
Si(P)	45.5	33.9	32.6
Si(As)	53.7	32.6	31.2
Si(Sb)	42.7	32.9	30.6
Ge(theor/)		9.81	4.74
Ge(P)	12.9	9.9	4.75
Ge(As)	14.17	10.0	4.75
Ge(Sb)	10.32	10.0	4.7

Table 10.2: Donor ionization energies in Ge and Si. Experimental values are different because of chemical shift

Impurity levels near the point of degeneracy

Degeneracy means that there are $t > 1$ functions,

$$\phi_{n\mathbf{k}}^j, \quad j = 1, 2..t$$

which satisfy Schrödinger equation without an impurity. In this case (remember, $\mathbf{k} \approx 0$),

$$\psi = \sum_{j=1}^t F_j(\mathbf{r}) \phi_{n0}^j(br) .$$

The functions F_j satisfy matrix equation,

$$\sum_{j'=1}^t \left[\sum_{\alpha,\beta=1}^3 H_{jj'}^{\alpha\beta} \hat{p}_\alpha \hat{p}_\beta + U(\mathbf{r}) \delta_{jj'} \right] F_{j'} = EF_j . \quad (10.1)$$

If we want to include spin-orbital interaction we have to add

$$\mathcal{H}_{so} = \frac{1}{4m_0^c c^2} [\boldsymbol{\sigma} \times \nabla V] \cdot \hat{\mathbf{p}} .$$

Here $\boldsymbol{\sigma}$ is the spin operator while V is periodic potential. In general \mathcal{H} -matrix is complicated. Here we use the opportunity to introduce a simplified (the so-called invariant) method based just upon the symmetry.

For simplicity, let us start with the situation when spin-orbit interaction is very large, and split-off mode is very far. Then we have 4-fold degenerate system. Mathematically, it can be represented by a pseudo-spin 3/2 characterized by a pseudo-vector \mathbf{J} .

There are only 2 invariants quadratic in \mathbf{p} , namely $\hat{\mathbf{p}}^2$ and $(\hat{\mathbf{p}} \cdot \mathbf{J})^2$. Thus we have only two independent parameters, and traditionally the Hamiltonian is written as

$$\mathcal{H} = \frac{1}{m_0} \left[\frac{\hat{\mathbf{p}}^2}{2} \left(\gamma_1 + \frac{5}{2}\gamma \right) - \gamma(\hat{\mathbf{p}} \cdot \mathbf{J})^2 \right] . \quad (10.2)$$

That would be OK for spherical symmetry, while for cubic symmetry one has one more invariant, $\sum_i \hat{p}_i^2 J_i^2$. As a result, the Hamiltonian is traditionally expressed as

$$\mathcal{H} = \frac{1}{m_0} \left[\frac{\hat{\mathbf{p}}^2}{2} \left(\gamma_1 + \frac{5}{2}\gamma_2 \right) - \gamma_3(\hat{\mathbf{p}} \cdot \mathbf{J})^2 + (\gamma_3 - \gamma_2) \sum_i \hat{p}_i^2 J_i^2 \right] . \quad (10.3)$$

This is the famous Luttinger Hamiltonian. Note that if the lattice has no inversion center there also linear in \mathbf{p} terms.

Now we left with 4 coupled Schrödinger equations (10.1). To check the situation, let us first put $U(\mathbf{r}) = 0$ and look for solution in the form

$$F_j = A_j(\mathbf{k}/k) e^{i\mathbf{kr}}, \quad k \equiv |\mathbf{k}| .$$

The corresponding matrix elements can be obtained by substitution $\hbar\mathbf{k}$ instead of the operator \hat{p} into Luttinger Hamiltonian. The Hamiltonian (10.2) does not depend on the direction of \mathbf{k} . Thus let us direct \mathbf{k} along z axis and use representation with diagonal J_z^2 . Thus the system is decoupled into 4 independent equation with two different eigenvalues,

$$E_\ell = \frac{\gamma_1 + 2\gamma}{2m_0} \hbar^2 k^2, \quad E_h = \frac{\gamma_1 - 2\gamma}{2m_0} \hbar^2 k^2.$$

If

$$\gamma_1 \pm 2\gamma > 0$$

both energies are positive (here the energy is counted inside the valence band) and called the light and heavy holes. The effective masses are

$$m_{\ell(h)} = m_0 / (\gamma_1 \pm \gamma).$$

The calculations for the full Luttinger Hamiltonian (10.3) require explicit form of \mathbf{J} -matrices. Its solutions lead to the anisotropic dispersion law

$$E_{\ell,h} = \frac{\hbar^2}{2m_0} \left\{ \gamma_1 k^2 \pm 4 [\gamma_2^2 k^4 + 12(\gamma_3^2 - \gamma_2^2)(k_x^2 k_y^2 + k_y^2 k_z^2 + k_z^2 k_x^2)]^{1/2} \right\}.$$

The parameters of Ge and Si are given in the Table 10.1

Material	γ_1	γ_2	γ_3	Δ	ϵ
Ge	4.22	0.39	1.44	0.044	11.4
Si	13.35	4.25	5.69	0.29	15.4

Table 10.3: Parameters of the Luttinger Hamiltonian for Ge and Si

The usual way to calculate acceptor states is variational calculation under the spherical model (10.2). In this case the set of 4 differential equations can be reduced to a system of 2 differential equations containing only 1 parameter, $\beta = m_\ell/m_h$.

10.2 Localization of electronic states

What happens when the number of doping impurities is large and their wave functions overlap?

Narrow bands and Mott transition

As a simple example, consider an ordered lattice of impurities, the potential being

$$V(\mathbf{r}) = \sum_j U(\mathbf{r} - \mathbf{r}_j).$$

Assume that we know the eigenstates ϕ_n and eigenvalues, E_n , of a single-impurity problem. Here we shall use single-band approximation, and therefore ignore Bloch (central-cell) factors. Also, we assume the impurity bandwidth is less than the spacing between E_n and restrict ourselves by the lowest level, E_0 . Along the tight-binding method, we can expand the wave functions in terms of the above eigenvalues,

$$\psi = \sum_j a_j \phi(\mathbf{r} - \mathbf{r}_j), \quad \sum_j |a_j|^2 = 1,$$

the energy being

$$E = \sum_{\mathbf{m}} e^{i\mathbf{km}} I(\mathbf{m}).$$

The only important property of the *overlap integrals*, $I(m)$ is that it is small (tight-binding approximation!).

In this way we get energy bands. For example, for a simple cubic lattice

$$E = 2I(b_0) \sum_i \cos(k_i b_0)$$

where here b_0 denotes the lattice constant for impurity lattice. Expanding near $\mathbf{k} = 0$ we get

$$E(k) = 6I(b_0) - I(b_0)k^2 b_0^2$$

the effective mass being $m^* = \hbar^2/2Ib_0^2$. As the lattice constant increases, $I(b_0) \propto \exp(-\beta b_0/a)$ where β is a number of the order 1.

According to our model, each impurity adds one electron, and each state possesses 2-fold spin degeneracy. Thus the impurity lattice is a *metal*.

Is this correct? In principle, no, because we neglected electron-electron interaction. In fact, two electrons at the same site repel each other the energy can be estimated as $U_0 \approx e^2/a$. If U_0 is comparable with the bandwidth $\sim I(b_0)$, then one must allow for the interaction. At large b_0 the band is narrow and this is the case. Let us plot the electron terms as a function of $1/b_0$. The insulator-to-metal transition of this kind is usually called the Mott transition.

Anderson transition

We come back to single-electron approximation and concentrate on disorder. Suppose that impurities are still ordered, but depths of the potential wells are random, Fig. (10.3). The effective Hamiltonian has the form

$$\mathcal{H} = \sum_j \epsilon_j a_j^+ a_j + \sum_{m,j \neq 0} I(m) a_j^+ a_{j+m}.$$

The energies ϵ are assumed to be uncorrelated and random, the distribution being

$$P(\epsilon) = \begin{cases} 1/A & , |\epsilon| < A/2 \\ 0 & , |\epsilon| > A/2 \end{cases}$$

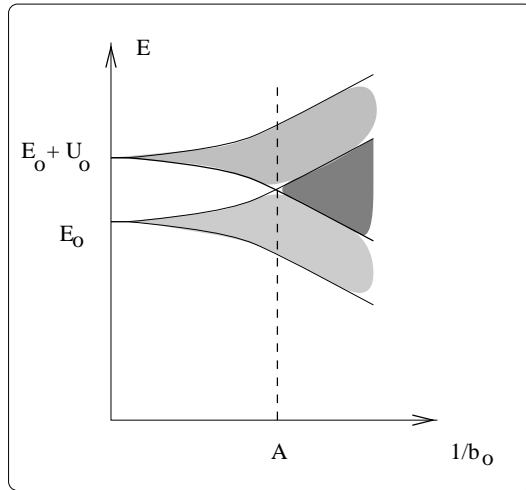


Figure 10.2: Dependence of electron bands on impurity sublattice period b_0 . To the left of point A is an insulator, to the right a metal.

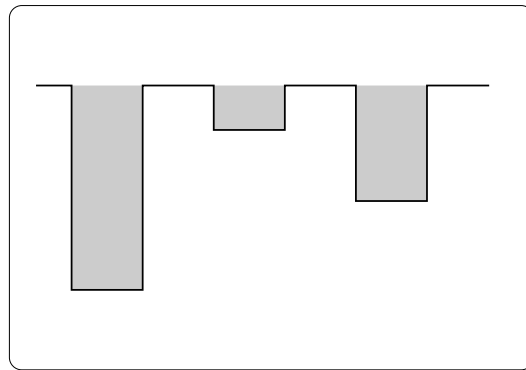


Figure 10.3: Potential wells in the Anderson model.

Anderson has formulated the following criterion for localization. Let us place a particle at the site i and study its decay in time due to quantum smearing of the wave packet. The state is called extended if $|\psi_i(t)|^2 \rightarrow 0$ at $t \rightarrow \infty$.

The *Anderson model* has one dimensionless parameter, W/I , where I is the overlap integral for nearest neighbors. In a 3D system there is a critical value, A_c/I , at which delocalized states begin to appear in the middle band. In 1D case the states are localized *at any disorder*. 2D case is a marginal, the states being also localized at any disorder.

Two-state model

Now let us turn to 3D case and try to discuss Anderson result in a simplified form. Namely, consider two potential wells. When isolated, they can be characterized by the energies ϵ_1

Lattice	x_c	$4/x_c$	A_c/I
Diamond	0.43	9.3	8.0
Simple cubic	0.31	12.9	15

Table 10.4: Percolation thresholds and critical values A_c/I obtained numerically for different lattices

and ϵ_2 and wave functions ϕ_1 and ϕ_2 . At $\epsilon_1 = \epsilon_2$ the wave functions are

$$\Psi_{I,II} = \frac{1}{\sqrt{2}}(\phi_1 \pm \phi_2),$$

the energy difference being $E_I - E_{II} = 2I$. This solution is reasonably good at $|\epsilon_1 - \epsilon_2| \ll I$. In general,

$$\psi_{I,II} = c_1\phi_1 \pm c_2\phi_2,$$

and we have a matrix Schrödinger equation,

$$\begin{pmatrix} \Delta/2 - E & I \\ I^* & -\Delta/2 - E \end{pmatrix}.$$

Here the origin for energy is taken at $(\epsilon_1 + \epsilon_2)/2$, while $\Delta \equiv \epsilon_1 - \epsilon_2$. The secular equation is thus

$$E^2 - (\Delta/2)^2 - |I|^2 = 0 \rightarrow E_{I,II} = \pm \sqrt{(\Delta/2)^2 + |I|^2}.$$

Consequently,

$$E_I - E_{II} = \sqrt{\Delta^2 + 4|I|^2}. \quad (10.4)$$

The ratio

$$\frac{c_1}{c_2} = \frac{I}{\Delta/2 \pm \sqrt{(\Delta/2)^2 + I^2}}.$$

Thus at $\Delta \gg I$ either c_1 or c_2 is close to 1, and collectivization does not occur.

Now, following Thouless, let us chose a band

$$\delta/2 \leq \epsilon \leq \delta/2, \quad \delta \sim I$$

and call the sites *resonant* if their energy falls into the band. Then let us look for *connected* resonant states which share a site. Non-resonant sites can be disregarded as $I \ll W$.

It is clear that it must be a threshold in the quantity W/I where the transition takes place. If one assumes that the connected cluster is a 1D chain, then the bandwidth is $4I$. In such a model,

$$\frac{A_c}{I} = \frac{4}{x_c}$$

where x_c is the *percolation threshold* for the site problem. This is quite a good estimate, see the Table 10.2 Finally, one arrives at the following profile of density-of-states (DOS) for the Anderson model, Fig. 10.4

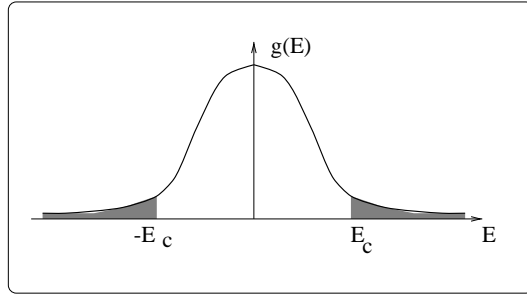


Figure 10.4: Density of states in the Anderson model. Localized states are shaded. Mobility edges are denoted as E_c .

10.3 Impurity band for lightly doped semiconductors.

The material is called lightly doped if there is only a small overlap between electronic states belonging to different impurities, $Na^3 \ll 1$. Here N is the impurity concentration while a is the localization length. In lightly doped materials conductivity vanished *exponentially* as $T \rightarrow 0$.

Let us start with a material with only one type of impurities, say *n*-type. At $T = 0$ each of donors must have an electron, the missing electron represents an *elementary excitation*. An excitation can be localized at any donor, the energies being slightly different. The reasons are

- If one removes an electron, the remaining positive charges polarize the neutral donor located in vicinity. That contributes to donor ionization energy, the contribution being dependent on the configuration of neutral neighbors.
- There is a quantum overlap between the donors being excited.

The first mechanism is usually more important for realistic semiconductors having compensating impurities.

Now let us assume that there are also acceptors which capture electrons from the donors and are fully occupied $T = 0$. Thus we have neutral donors, negatively charged acceptors and an equal number of positively charged donors. These randomly distributed charges create a fluctuating random potential which localizes the electronic states.

Let us count the energy ϵ_i of i -th donor from the energy of an isolated donor, $-E_0$. We have

$$\epsilon_i = \frac{e^2}{\kappa} \left[\sum_l^{\text{acc}} \frac{1}{|\mathbf{r}_i - \mathbf{r}_l|} - \sum_{k \neq i}^{\text{don}} \frac{1 - n_k}{|\mathbf{r}_i - \mathbf{r}_k|} \right].$$

The occupation numbers have to be determined to minimize the free energy (at $T = 0$ – electrostatic energy).

A typical dependence of the Fermi level μ on the degree of compensation, $K = N_A/N_D$, is shown in Fig. 10.5 Below we discuss limiting cases of small and large K .

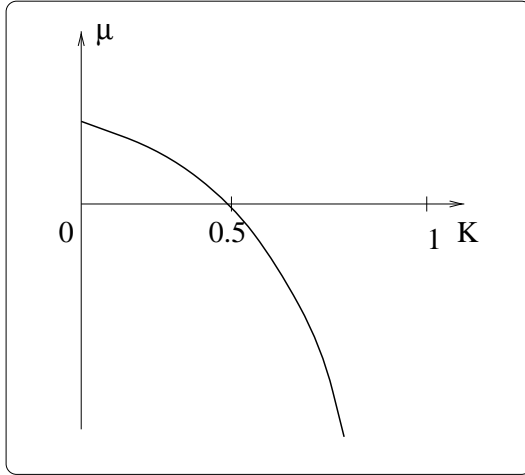


Figure 10.5: Position of the Fermi level μ as a function of the degree of compensation, K .

Low degree of compensation

At $K \ll 1$ most of donors keep their electrons, and only a small number is empty and charged positive. Each acceptor carries a negative charge, the concentration of charged donors is equal to N_A .

A positive charged hole will be located as close as possible to a negative acceptor. Thus, it occupies the donor the most closed to an acceptor. In a first approximation, each acceptor can be regarded as immersed in an infinite sea of donors. Transporting a hole from a donor situated near a charged acceptor to infinity requires work of order $e^2/\kappa r_D$, where r_D is the average distance between the donors.

To get a quantitative theory one has to add more input. Namely, there are some acceptor without holes, and some acceptors having 2 holes. Indeed, some acceptors do not have a close donors (Poisson distribution), so they bind holes very weakly. So holes prefer to find another acceptor with more close donors even at the expense to become a second hole. To illustrate the situation let us consider a configuration shown in Fig. 10.6,a. The work necessary to remove a hole equals to

$$e^2/\kappa r - e^2/2\kappa r = e^2/2\kappa,$$

it becomes large at small r .

It is curious that an acceptor cannot bind more than 2 holes. Consider a configuration shown in Fig. 10.6,b. The energy of attraction to the acceptor equals $\sqrt{3}e^2/\kappa l$ while the repulsion energy from two other holes is $2e^2/\kappa l$. We end at the following situation. There are 3 configurations – 0-complexes (negative) where there is no ionized donor near a particular acceptor, 1-complexes (neutral), and 2-complexes (positive). So the neutrality condition which fixes the Fermi level is actually

$$N_0(\mu) = N_2(\mu).$$

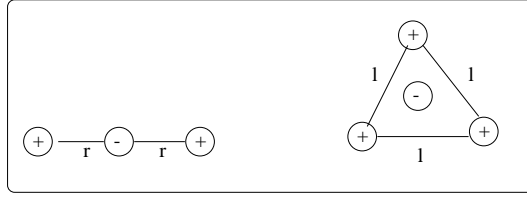


Figure 10.6: Donor-acceptor configurations.

For 0-complex, there must be *no donors* within the sphere of radius $r_\mu = e^2/\kappa\mu$ from a fixed acceptor, the probability being $\exp(-4\pi N_D r_\mu^3/3)$. Thus,

$$N_0(\mu) = N_A \exp\left(-\frac{4\pi}{3} \frac{e^6 N_D}{\kappa^3 \mu^3}\right).$$

It is much more difficult to find number of 2-complexes. Let us estimate it *from above*, $N_2^>(\mu)$, as a concentration of pairs of donors whose additional energies ϵ_1 and ϵ_2 exceed μ when *both donors* are ionized. This estimate is larger because

- it could be another close donor which initiates a 1-complex,
- it can be more than one pair of donors near a given acceptor.

Let us put the origin of coordinates at acceptor site and suppose that a donor is located at \mathbf{r}_1 . The average number of donors in the element $d\mathbf{r}_2$ is equal to $N_D d\mathbf{r}_2$. Thus, the number of pairs with $r_2 \geq r_1$ is

$$N_D \int_{r_2 > r_1} d\mathbf{r}_2 \Theta[\epsilon_1(\mathbf{r}_1, \mathbf{r}_2) - \mu] \Theta[\epsilon_2(\mathbf{r}_1, \mathbf{r}_2) - \mu].$$

Here

$$\epsilon_{1,2} = \frac{e^2}{\kappa} \left[\frac{1}{|\mathbf{r}_{1,2}|} - \frac{1}{|\mathbf{r}_1 - \mathbf{r}_2|} \right].$$

To get the total concentration of pairs one has to multiply it by N_D and integrate over \mathbf{r}_1 , and finally multiply by N_A . As a result,

$$N_2^>(\mu) = N_A N_D^2 \int d\mathbf{r}_1 \int_{r_2 > r_1} d\mathbf{r}_2 \Theta[\epsilon_1(\mathbf{r}_1, \mathbf{r}_2) - \mu] \Theta[\epsilon_2(\mathbf{r}_1, \mathbf{r}_2) - \mu].$$

This estimate is very close to exact result. Integration yields

$$N_2^>(\mu) = 7.14 \cdot 10^{-4} N_A (4\pi N_D r_\mu^3/3)^2.$$

Using this estimate and solving the neutrality equation one obtains

$$\mu = 0.61\epsilon_D, \quad \epsilon_D = e^2/\kappa r_D = (e^2/\kappa)(4\pi N_D/3)^{1/3}.$$

Now let us discuss the shape of the peak. The majority of donors are far from few acceptors, so there must be a sharp peak at $-E_0$. The tails of $g(\epsilon)$ above the Fermi level falls with the characteristic energy ϵ_D . Consequently, near the Fermi level

$$g(\epsilon) \propto N_A/\epsilon_D.$$

Long-range potential

Above we did not take into account electrostatic interaction between the complexes. It is small indeed because $N_0 \ll N_D$. However, the interaction leads to an additional dispersion of the peak.

An average fluctuations of charge produce an average potential of order $e^2 N_0^{1/3} / \kappa$. We shall show that *long-range* fluctuations are much more important. Let us introduce fluctuations of the complex concentrations for 0- and 2-complexes,

$$\xi_i(\mathbf{r}) = N_i(\mathbf{r}) - \langle N_i(\mathbf{r}) \rangle .$$

We consider the fluctuations as uncorrelated,

$$\begin{aligned} \langle \xi_0(\mathbf{r}) \xi_0(\mathbf{r}') \rangle &= \langle \xi_2(\mathbf{r}) \xi_2(\mathbf{r}') \rangle = N_0 \delta(\mathbf{r} - \mathbf{r}'), \\ \langle \xi_0(\mathbf{r}) \xi_2(\mathbf{r}') \rangle &= 0 . \end{aligned}$$

Consequently, the charge fluctuations are

$$\langle \rho(\mathbf{r}) \rho(\mathbf{r}') \rangle = 2e^2 N_0 \delta(\mathbf{r} - \mathbf{r}') . \quad (10.5)$$

Let us now consider a sphere of radius R where there is $\sim N_0 R^3$ complexes. The typical charge in the sphere is $e^2 (N_0 R^3)^{1/2}$, the resultant potential being $e^2 (N_0 R^3)^{1/2} / R$. It diverges as $R \rightarrow \infty$, and one has to allow for *screening*. We will check later that the screening potential varies little over a distance between the complexes. Therefore, one can employ the self-consistent field approximation.

As a result, we end at the Poisson equation

$$\Delta \phi = -\frac{4\pi}{\kappa} \rho(\mathbf{r}) - \frac{4\pi e}{\kappa} [N_2(\mu + e\phi) - N_0(\mu + e\phi)] .$$

Here $\rho(\mathbf{r})$ is a Gaussian random function whose correlator is given by (10.5). This approach is consistent at

$$|e\phi(\mathbf{r})| \ll \mu$$

when only small number of complexes are responsible for screening. At the same time, the majority of complexes contribute to charge fluctuations and are uncorrelated. In such a way we obtain the equation

$$\Delta \phi = -\frac{4\pi\rho}{\kappa} + \frac{\phi}{r_0^2}$$

where the screening length r_0 is given by the expression

$$\frac{1}{r_0^2} = \frac{4\pi e}{\kappa} \frac{d}{d\phi} [N_2(\mu + e\phi) - N_0(\mu + e\phi)]_{\phi=0} .$$

Substituting the expressions for the complex concentrations we obtain

$$r_0 = 0.58 N_A^{-1/2} N_D^{1/6} = 0.58 N_D^{-1/3} K^{-1/2} .$$

In a standard way, one can determine the distribution function near the Fermi level. It is Gaussian,

$$F(e\phi) = \frac{1}{\gamma\sqrt{pi}} \exp[-(e\phi)^2/\gamma^2], \quad \gamma = 2e^2\langle\phi(\mathbf{r})\rangle^2 = 0.26\epsilon_D K^{1/4}.$$

All the above results are applicable only at very small K . Indeed, to get a Gaussian fluctuations one has to assume $r_0 \gg N_0^{-1/3}$ or

$$4\pi N_0 r_0^3 / 3 \gg 1.$$

The condition can be rewritten as $K^{-1/2} \ll 0.05$.

High degrees of compensation

Now we turn to the case

$$1 - K \ll 1.$$

In this case, the concentration of occupied donors,

$$n = N_D - N_A \ll N_D.$$

Thus *all the electrons* are able to find proper donors whose potential is lowered by the potential of charges neighborhood. Thus the Fermi level is situated well *below* $-E_0$, see Fig. 10.7

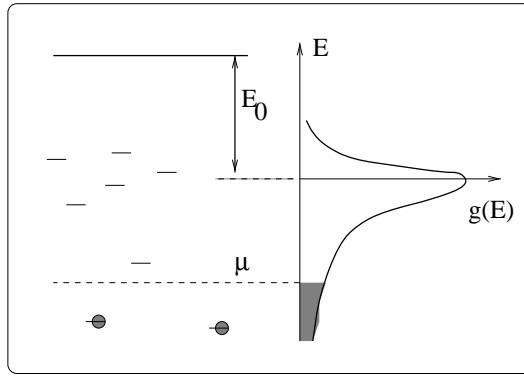


Figure 10.7: Energy diagram of highly compensated semiconductor. Solid line shows the conduction band edge, occupied states are shaded.

To understand the structure of the DOS tail consider a certain donor having at small ($r \ll N_D^{-1/3}$) another positively charged donor. Its influence at $r \gg a$ is just $\epsilon = -e^2/\kappa r$. It is assumed that the second donor is empty, the binding energy being $\sim E_0$. Thus a pair can contain only 1 electron.

To find $g(\epsilon)$ let us calculate the concentration of pairs having the energy in the interval $(\epsilon, \epsilon + d\epsilon)$. The probability to find another donor is $4\pi N_D r^2 (dr/d\epsilon) d\epsilon$, where $r(\epsilon) = e^2/\kappa\epsilon$. One has to multiply this quantity by N_D and divide by 2 (pairs!) to get

$$g(\epsilon) = \frac{3}{2} \frac{\epsilon_D^3}{\epsilon^4} N_D.$$

Now the Fermi level (at $T = 0$) is easily found from the conservation law

$$\int_{-\infty}^{\mu} g(\epsilon) d\epsilon = n.$$

As a result, we get

$$\mu = -\frac{\epsilon_D}{2^{1/3}(1-K)^{1/3}}.$$

This is purely classical result. It is valid only at $r_\mu \gg a$.

Long-range fluctuations

At $1 - K \ll 1$ it is a large and important effect because screening is weak. To obtain an estimates we can repeat the discussion for $K \ll 1$ and replace the donor concentration by the total concentration, N_t , of donors and acceptors. In this way we get for a typical potential energy of an electron,

$$\gamma(R) = \frac{e^2}{\kappa R} (N_t R^3)^{1/2}.$$

It also diverges at large R .

How the screening takes place. The excess fluctuating density is

$$\Delta N = (N_t R^3)^{1/2} / R^3.$$

They can be neutralized at $\Delta N = n$ leading to the expression for the screening length,

$$n = \frac{N_t r_s^3)^{1/2}}{r_s^3} \quad \rightarrow \quad r_s = \frac{2^{2/3} N_t^{-1/3}}{(1-K)^{2/3}}.$$

The random potential amplitude is

$$\gamma(r_s) = \frac{e^2 N_t^{2/3}}{\kappa n^{1/3}}.$$

It increases with decreasing n .

Here we disregarded the states with several extra electrons which are important very deep in the gap.

10.4 AC conductance due to localized states

As we have seen, at low temperatures dc conductance vanishes in the insulating phase, the electronic states being localized. However, ac conductance remains finite. The reason is that an electron (or hole) can hop between the adjacent localized states giving rise to a finite energy dissipation.

Deeply in the insulating phase the most probable is to find only pairs of localized states which are separated by the distances much less than the average. To analyze the physics of dissipation, let us consider such a pair. We used such a concept to discuss Anderson localization.

Consider a close pair of localized states. As we have seen, the quantum states of an electron sharing the pair can be expressed through one-center wave functions as

$$\psi_{\pm} = c_1 \phi_1 \pm c_2 \phi_2,$$

which must satisfy matrix Schrödinger equation,

$$\begin{pmatrix} \Delta/2 - E & I \\ I^* & -\Delta/2 - E \end{pmatrix} \begin{pmatrix} \psi^+ \\ \psi^- \end{pmatrix} = 0.$$

Here the origin for energy is taken at $(\epsilon_1 + \epsilon_2)/2$, while $\Delta \equiv \epsilon_1 - \epsilon_2$. The secular equation is thus

$$E^2 - (\Delta/2)^2 - |I|^2 = 0 \rightarrow E_{\pm} = \pm \sqrt{(\Delta/2)^2 + |I|^2}.$$

Consequently,

$$E_+ - E_- \equiv W = \sqrt{\Delta^2 + 4|I|^2}, \quad (10.6)$$

$$\frac{c_1}{c_2} = \frac{2I(\mathbf{r})}{\Delta \pm W}. \quad (10.7)$$

Thus at $\Delta \gg I$ either c_1 or c_2 is close to 1, and collectivization does not occur.

To find the dissipation one has to calculate the contribution of a single pair, and then sum the contributions of different pairs.

Dissipation by an isolated pair

One can discriminate between two absorption mechanisms. The first one is *resonant* absorption due to direct absorption of photons accompanied by transition between the states ψ^+ and ψ^- . The second mechanism is due to phonon-assistant transitions – an external field modulates the occupation numbers of close pairs. The modulation lags in phase comparing to the field due to relaxation. As a result, a finite dissipation appears. Below we consider both mechanisms.

Resonant contribution

The resonant absorption is due to transition of an electron from the state with the energy E^- to the state E^+ . The energy absorbed by a pair per unit time due to an electric field

$$\mathcal{E} = \mathcal{E}_0 \cos \omega t = \frac{1}{2} \mathcal{E}_0 [\exp(i\omega t) + \exp(-i\omega t)] \quad (10.8)$$

can be written as (Fermi golden rule!):

$$q = \frac{2\pi \hbar \omega}{\hbar} |e\mathcal{E}_0 \langle -|\mathbf{r}|+ \rangle|^2 \delta(\hbar\omega - W) (n_- - n_+) , \quad (10.9)$$

Occupation numbers

The occupation numbers n_{\pm} are determined from the following considerations. Let us write down a two-site Hamiltonian

$$H_{1,2} = \epsilon_1 n_1 + \epsilon_2 n_2 + \frac{e^2}{\kappa r} n_1 n_2 + I(r)(a_1^+ a_2 + a_2^+ a_1) . \quad (10.10)$$

Here n_i are the occupation numbers, while ϵ_i include Coulomb interaction with other neighbors.

The Hamiltonian (10.10) describes 4 states of the pair:

1. The pair has no electrons. The energy $E_0 = 0$.
2. The pair has 1 electron. There are two states with energies

$$E_1^{\pm} = \frac{\epsilon_1 + \epsilon_2}{2} \pm \frac{W}{2} .$$

3. The pair has 2 electrons. There is one state with the energy

$$E_2 = \epsilon_1 + \epsilon_2 + \frac{e^2}{\kappa r} .$$

Consequently, the probability to find a pair with 1 electron, the lower level to be occupied is

$$\begin{aligned} n_- &= \frac{1}{Z} \exp\left(-\frac{E_1^- - \mu}{kT}\right) , \\ Z &= 1 + \exp\left(-\frac{E_1^- - \mu}{kT}\right) + \exp\left(-\frac{E_1^+ - \mu}{kT}\right) + \exp\left(-\frac{E_2 - 2\mu}{kT}\right) . \end{aligned}$$

The occupation number $n_+ = n_- \exp(-W/kT)$, and we obtain finally,

$$q = \frac{2\pi \hbar \omega}{\hbar} \frac{1}{4Z} |e\mathcal{E}_0 \langle -|\mathbf{r}|+ \rangle|^2 \delta(\hbar\omega - W) \exp\left(-\frac{E_1^- - \mu}{kT}\right) \left[1 - \exp\left(-\frac{\hbar\omega}{kT}\right)\right] , \quad (10.11)$$

Relaxational contribution

To analyze this contribution one has to consider the balance equation, say for $n_+(t)$,

$$\frac{\partial n_+}{\partial t} = \frac{n_+ - n_0(t)}{\tau}. \quad (10.12)$$

Here

$$n_0(t) = \frac{1}{\exp[W(t)/kT] + 1}, \quad W(t) = \sqrt{[\Delta + e\mathcal{E}(t) \cdot \mathbf{r}]^2 + 4I(\mathbf{r})^2}, \quad (10.13)$$

while τ is the population relaxation time. Substituting

$$n_+(t) = n_0(t) + n_1(t), \quad n_1(t) \propto [e^{-i\omega t} + h.c.]$$

one easily obtains the relevant contribution to the absorbed energy as

$$q = \frac{\omega}{2\pi} \int_0^{2\pi/\omega} dt \dot{W}(t) n_1(t).$$

We get

$$q = \frac{|e\mathcal{E}_0 \cdot \mathbf{r}|^2}{2} \left(\frac{\Delta}{W} \right)^2 \frac{\omega^2 \tau(W, r)}{1 + [\omega \tau(W, r)]^2} \frac{1}{4kT \cosh(W/2kT)}. \quad (10.14)$$

The last factor is just $-(\partial n_0 / \partial W)$.

To calculate the dissipation one has to specify the relaxation time, which depends in general on W and \mathbf{r} . To do that let us specify the Hamiltonian to describe coupling between localized electrons and phonons. To construct the Hamiltonian, let us start with the unperturbed one,

$$\mathcal{H}_0 = \frac{1}{2} \begin{pmatrix} \Delta & 2I(\mathbf{r}) \\ 2I(\mathbf{r}) & -\Delta \end{pmatrix} = \frac{\Delta}{2} \sigma_3 + I(\mathbf{r}) \sigma_1. \quad (10.15)$$

Here we introduce Pauli matrices,

$$\sigma_1 = \begin{pmatrix} 0 & 1 \\ 1 & 0 \end{pmatrix}, \quad \sigma_2 = \begin{pmatrix} 0 & -i \\ i & 0 \end{pmatrix}, \quad \sigma_3 = \begin{pmatrix} 1 & 0 \\ 0 & -1 \end{pmatrix}.$$

Under influence of the phonon-induced strain the energy of each (j) component of the pair acquires the term proportional to the strain tensor,

$$u_{ik}(\mathbf{r}_j) = \frac{1}{2} \left(\frac{\partial u_i(\mathbf{r}_j)}{\partial x_k} + \frac{\partial u_k(\mathbf{r}_j)}{\partial x_i} \right).$$

Thus,

$$\tilde{\mathcal{H}}_{\text{int}} = \frac{1}{2} \sum_{ik} \left[\Lambda_{ik}^{(1)} u_{ik}(\mathbf{r}_1) - \Lambda_{ik}^{(2)} u_{ik}(\mathbf{r}_2) \right] \sigma_3, \quad (10.16)$$

where $\Lambda_{ik}^{(j)}$ are the component of the *deformational potential tensor* for each component.

Now we can make the transformation to a new basis which makes the Hamiltonian \mathcal{H}_0 diagonal. Technically, it is convenient to rewrite (10.16) in the form

$$\mathcal{H}_0 = \frac{W}{2} \begin{pmatrix} \cos \chi & \sin \chi \\ \sin \chi & -\cos \chi \end{pmatrix}, \quad \cos \chi \equiv \frac{\Delta}{W}.$$

Then one can represent the old basis through the new one as

$$\begin{pmatrix} \phi_1 \\ \phi_2 \end{pmatrix} = \hat{T} \begin{pmatrix} \psi_+ \\ \psi_- \end{pmatrix}, \quad \hat{T} = \begin{pmatrix} \cos \chi & -\sin \chi \\ \sin \chi & \cos \chi \end{pmatrix} = \hat{1} \cos \chi - i\sigma_2 \sin \chi.$$

Having in mind the algebra for Pauli matrices,

$$\sigma_i^2 = 1, \quad \sigma_2 \sigma_3 = i\sigma_1, \quad \sigma_3 \sigma_1 = i\sigma_2, \quad \sigma_1 \sigma_2 = i\sigma_3$$

we obtain the interaction Hamiltonian in a new basis,

$$\mathcal{H}_{\text{int}} = \hat{T}^{-1} \tilde{\mathcal{H}}_{\text{int}} \hat{T} = \frac{1}{2} \sum_{ik} \left[\Lambda_{ik}^{(1)} u_{ik}(\mathbf{r}_1) - \Lambda_{ik}^{(2)} u_{ik}(\mathbf{r}_2) \right] \left(\frac{\Delta}{W} \sigma_3 - \frac{2I(\mathbf{r})}{W} \sigma_1 \right). \quad (10.17)$$

We are interested in the item proportional to σ_1 which is responsible for phonon-assisted transitions between the levels. Using Fermi golden rule to calculate the relaxation rate, we get

$$\frac{1}{\tau(W, r)} = \frac{1}{\tau_{\min}(W)} \left(\frac{2I(r)}{W} \right)^2. \quad (10.18)$$

Here we have extracted the coordinate-dependent factor $(2I(r)/W)^2 = 2I_0 \exp(-2r/a)$. The quantity τ_{\min} has a transparent physical meaning of the *minimal* relaxation time for a pair with given interlevel spacing W . It is dependent on several characteristics of the electron-phonon interaction which we do not discuss now.

Summation over the relevant pairs.

Now we can proceed adding the contributions of different pairs that appears rather tricky. What we need is to find the so-called *pair* distribution function which is the probability to find a pair with bare energy spacing W and spatial distance r .

Resonant contribution

For simplicity, let us assume low temperatures, $T \leq \hbar\omega/k$. Then $n_- - n^+ \approx 1$ at

$$E_1^- - \mu < 0, \quad E_1^- - \mu < E_2 - 2\mu.$$

It means that one can introduce the variables $\Delta = \epsilon_1 - \epsilon_2$ and $E_1^- = (\epsilon_1 + \epsilon_2 - W)/2$ instead of ϵ_1 and ϵ_2 . One can show that $\mathcal{P} \approx 1$ at

$$-\frac{e^2}{\kappa r} - W < E_1^- - \mu < 0,$$

and

$$\int dE_1^- (n_- = n_+) \dots \rightarrow \left(W + \frac{e^2}{\kappa r} \right) \dots$$

One can explain qualitatively this factor as follows from Fig. 10.8. When the center of

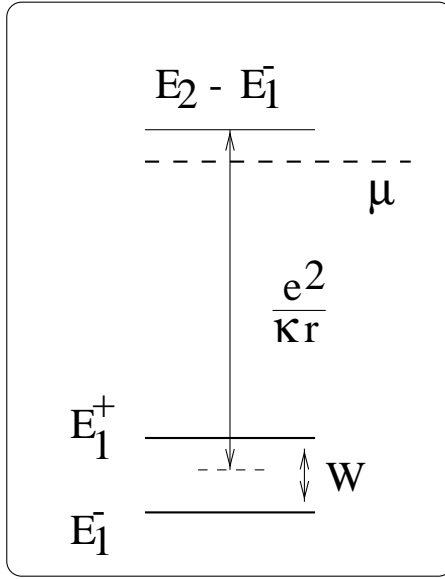


Figure 10.8: Energy scheme of absorption by a pair with the length r with allowance of Coulomb interaction.

gravity $(\epsilon_1 + \epsilon_2)/2$ falls into the region of the width $\sim e^2/\kappa r$ below the Fermi level the pair remains singly ionized and contains only 1 electron.

The full scheme of calculations can be described as follows. We define

$$\sigma(\omega) = \frac{2 \sum_i q_i}{\mathcal{E}_0^2} = \frac{1}{\mathcal{E}_0^2} \int d\mathbf{r} \int d\epsilon_2 g(\epsilon_2) \int_{\epsilon_2} d\epsilon_1 g(\epsilon_1) q(\epsilon_1, \epsilon_2, \mathbf{r}). \quad (10.19)$$

For the simplest (Anderson) model

$$g(\epsilon) = g_0 \Theta(A/2 - |\epsilon|).$$

Another important simplification arises from exponential decay of the overlap integral, $I(r) \propto \exp(-r/a)$. As a result, the coupling matrix element in the case of resonant contribution (as well as relaxation time in the case of the relaxational contribution) depend on r much stronger than other quantities. As a result, one can replace r apart from exponential functions by a proper characteristic length r_c (which is different for the resonant and the relaxational contributions).

Now we are ready to specify the results for low temperatures.. Substituting expression

(10.20) for the contribution of a single pair we get (at $T = 0$)

$$\begin{aligned}\sigma(\omega) &= \frac{8\pi^2 e^2 g_0^2}{3\hbar} \int_{r_\omega}^\infty \left(\hbar\omega + \frac{e^2}{\kappa r} \right) \frac{r^4 I^2(r) dr}{[(\hbar\omega)^2 - 4I^2(r)]^{1/2}} \\ &= \frac{2\pi^2}{3} e^2 g_0^2 a \omega r_\omega^4 \left(\hbar\omega + \frac{e^2}{\kappa r_\omega} \right)\end{aligned}\quad (10.20)$$

where

$$r_\omega = a \ln(2I_0/\hbar\omega). \quad (10.21)$$

The case of finite temperatures is more complicated. At the region

$$\hbar\omega \ll kT \ll e^2/\kappa r_\omega$$

the width of integration over E_1^- remains essentially the same. However the occupation numbers of the states E_1^\pm become very close, and

$$(n_- - n^+) \approx \tanh(\hbar\omega/2kT).$$

This estimate is valid within all the region

$$\hbar\omega, kT \ll e^2/\kappa r_\omega.$$

The case of very large temperatures can be considered in a similar way. At

$$kT \gg e^2/\kappa r_\omega, \hbar\omega$$

both states E_1^\pm fall into the layer $\leq kT$ around the Fermi level, the difference $(n_- - n^+)$ being

$$(n_- - n^+) \approx \frac{1}{4 \cosh^2[(E_1^- - \mu)/2kT]}.$$

Thus,

$$\sigma(\omega) = \frac{2}{3} \pi^2 e^2 a g_0^2 \hbar \omega^2 r_\omega^4.$$

Relaxational contribution

Let us start with expression (10.14) which assumes that there are only the pairs with one electron. Introducing the distribution function $F(W, r)$ of the energy and spatial spacings (W and r) one obtains

$$\sigma(\omega) = \frac{e^2 \pi}{3kT} \omega^2 \int_0^\infty r^4 dr \int_0^\infty \frac{F(W, r) dW}{\cosh^2(W/2kT)} \frac{\tau}{1 + \omega^2 \tau^2}. \quad (10.22)$$

We will see later that $F(W, r)$ is a smooth function of r comparing to

$$\tau(W, r) \propto \exp(2r/a).$$

Thus let us define

$$\tau = \tau_0 \exp(2r/a)$$

where τ_0 is a smooth function of W and (in general) r . The properties of the ratio

$$G = \frac{\omega\tau}{1 + \omega^2\tau^2} = \frac{\omega\tau_0 \exp(2r/a)}{1 + \omega^2\tau_0^2 \exp(4r/a)}$$

depend strongly on the product $\omega\tau_0$. At

$$\omega\tau_0 \geq 1, \quad r \geq a$$

one has

$$G \approx \frac{1}{\omega\tau_0} \exp(-2r/a).$$

As a result,

$$\sigma(\omega) = \frac{e^2\pi}{3kT} \int_0^\infty r^4 e^{-2r/a} dr \int_0^\infty \frac{F(W, r) dW}{\cosh^2(W/2kT)} \frac{1}{\tau_0(W, r)}. \quad (10.23)$$

Thus, σ appears ω -independent, the temperature dependence being determined by the properties of the functions $F(W, r)$ and $\tau_0(W, r)$. It is important that for the relevant pairs $W \sim kT$, $r = r_T \sim (a/2) \ln(2I_0/kT)$.

At

$$\omega\tau_0 \ll 1$$

the ratio G has a sharp maximum at

$$r = r_{c\omega} = (a/2) \ln(1/\omega\tau_0)$$

and we can express G as

$$G \approx \frac{4a}{\pi} \delta(r - r_{c\omega}).$$

In this way we obtain

$$\sigma(\omega) = \frac{4e^2}{3kT} \omega a r_{c\omega}^4 \int_0^\infty \frac{F(W, r_{c\omega}) dW}{\cosh^2(W/2kT)} \propto \omega. \quad (10.24)$$

Let us discuss a bit the distribution function F which is just the probability to find a *single-electron* pair with the energy distance W , spatial distance r . In the absence of Coulomb interaction,

$$\begin{aligned} F(W, r) &= \int d\epsilon_1 d\epsilon_2 g(\epsilon_1)g(\epsilon_2) \delta \left(W - \sqrt{(\epsilon_1 - \epsilon_2)^2 + 4I^2(r)} \right) \\ &\times \{ [f_0(E_1^-)[1 - f_0(E_1^+)] + f_0(E_1^+)(1 - f_0(E_1^-))] \}. \end{aligned}$$

Here f_0 is the Fermi function. The integration is very simple for the Anderson model ($g = g_0 = \text{const}$). In that case

$$F(W, r) = g_0^2 \frac{[W^2 - 4I^2(r)]^{1/2}}{\tanh(W/2kT)} \sim g_0^2 kT.$$

Coulomb interaction changes the situation, and one has to calculate the number of pairs taking into account electron repulsion at the same center. At low enough at $kT \ll e^2/\kappa r_{c\omega}$ that leads to the result similar to the one discussed above,

$$F(W, r) = g_0^2 \frac{[W^2 - 4I^2(r)]^{1/2}}{W} \left(W + \frac{e^2}{\kappa r} \right).$$

Thus at $kT \ll e^2/\kappa r_{c\omega}$ the absorption is essentially temperature-independent at $\omega\tau_0 \ll 1$.

10.5 Interband light absorption

A typical experimental picture of frequency-dependent light absorption in heavily doped degenerate GaAs is shown in Fig. 10.9. The main features are:

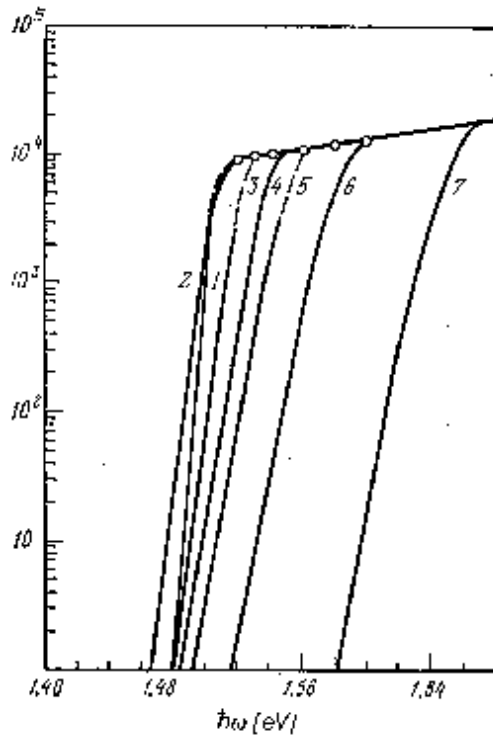


Figure 10.9: The absorption coefficient as a function of the energy of light quanta at 77 K in n -GaAs. $n \cdot 10^{-17}$, cm^{-3} : 1 – 0.02, 2 – 2.2, 3 – 5.3, 4 – 12, 5 – 16.2, 6 – 31.5, 6 – 65.

- rapid decrease of absorption (4 orders of magnitude) inside the forbidden gap (1.51 eV at 77 K).
- Shift towards short waves with increasing concentration (Moss-Burstein shift).

The last feature is due to Pauli principle which requires that the transitions should take place only into empty states (above the Fermi level). For indirect transitions the shift is equal to μ while for direct ones it is $\mu(1 + m_e/m_h)$, see Fig. 10.10. This picture is

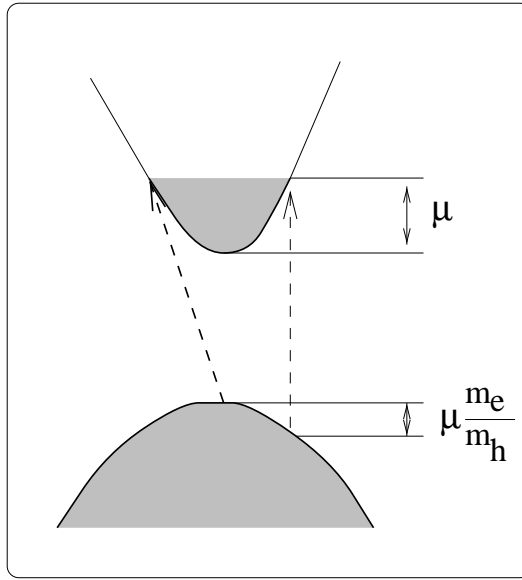


Figure 10.10: Scheme of typical interband absorption processes.

relevant to very low temperatures. At finite temperatures there is an absorption below the threshold because one can find a hole in the conduction band with the energy $\mu - \epsilon$ with the probability $\exp(-\epsilon/kT)$. Thus,

$$\alpha \propto \exp[-(\mu + E_g \hbar \omega)/kT].$$

Another important source which we are going to discuss are transitions from *fluctuation levels* above the top of valence gap, Fig. 10.11 We see that the absorption is proportional to the probability to find a level with the energy $\epsilon_h = E_g + \mu - \hbar\omega$ which decays exponentially with ϵ_h . This probability must be multiplied by the transition probability which is not exponentially small in many important cases.

Thus, the frequency dependence of absorption in degenerate doped semiconductors reproduces the DOS profile for *minority carriers*.

The situation is somewhat different in the case of non-degenerate materials where the Fermi level is situated deep in the forbidden gap. The situation is realized at high temperatures or degrees of compensation, as well as in indirect materials.

Assume that there are impurities of both signs, $N_t = N_D + N_A$. The impurity potential is regarded as Coulombic at short distances $r \leq r_0$ and screened at large distances. Let

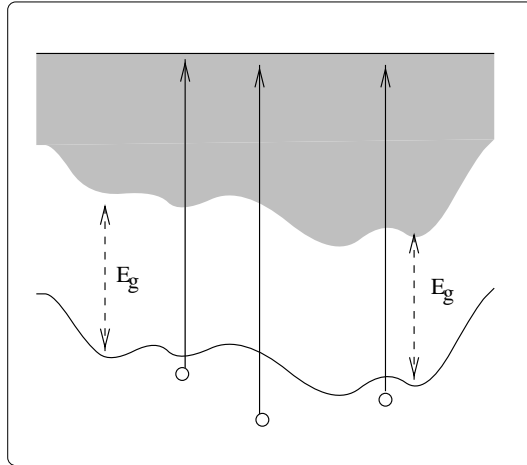


Figure 10.11: Scheme of interband transitions in a degenerate semiconductor at $T = 0$.

r_0 be large enough to consider the potential as classical; we also neglect the correlation in defect positions. Mathematically, that can be expressed as

$$\frac{\hbar^2}{m_e r_0^2}, \frac{\hbar^2}{m_h r_0^2} \ll \gamma, \quad \gamma = \frac{e^2}{\kappa r_0} (N_t r_0^3)^{1/2}.$$

One can show that in such a case the DOS tail can be represented as

$$g(\epsilon) = g(0) \exp(-\epsilon^2/\gamma^2).$$

In such an important case the absorption behavior *does not* represent the behavior of DOS, see Fig. 10.12 Suppose we are studying the transition which results in the formation of an

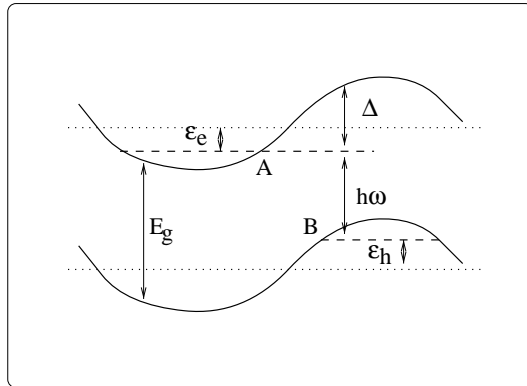


Figure 10.12: Absorption of a quantum of deficit Δ in a non-degenerate semiconductor.

electron of energy ϵ_e and a hole of energy ϵ_h ,

$$\Delta = \epsilon_h - \epsilon_e$$

(here the energies are calculated from the non-perturbed band edges). We observe that the electron and hole are *spatially separated*. Thus the matrix element involves *overlap integral* which has almost nothing to do with DOS. What we meet here, is the Franz-Keldysh effect in a random field.

To derive the result we use the conventional *optimum fluctuation method*. Here we demonstrate a simplified version of the method.

Consider a volume with linear dimension R . Charge fluctuations in the volume create a uniform electric field E , determined by the condition

$$eER = \Delta.$$

The excess number Z of charge defects to create the field $E = Ze^2/\kappa R^2$ must be

$$Z = \frac{E\kappa R^2}{e} = \frac{\kappa R\Delta}{e^2}. \quad (10.25)$$

The contribution of such a fluctuation to the absorption coefficient is proportional to

1. the probability to find Z excess charges in the given volume,

$$\exp(-Z^2/N_t R^2)',$$

2. the probability for an electron to tunnel the distance R to meet the hole,

$$\exp\left(-R\sqrt{m_2\Delta}/\hbar\right)$$

(we assume $m_h \gg m_2$).

Substituting Z from Eq. (10.25) we obtain the probability to be proportional to

$$\exp\left(-\frac{\kappa^2\Delta^2}{e^2 N_t R} - \frac{R\sqrt{m_e\Delta}}{\hbar}\right).$$

Maximizing the exponent, we obtain

$$\tilde{R} = a \left(\frac{\Delta}{E_0} \right)^{1/2} \frac{1}{(N_t a^3)^{1/2}}.$$

Consequently,

$$\frac{\alpha(\Delta)}{\alpha(0)} = \exp\left[-\beta \left(\frac{\Delta}{E_0} \right)^{1/2} \frac{1}{(N_t a^3)^{1/2}}\right]$$

where β is the number of the order 1. The derivation is valid at

$$\tilde{R} \leq r_0.$$

In the opposite case, the probability to find the proper fluctuation decreases, and the optimal cluster has the size r_0 . In that situation one has to substitute r_0 instead of \tilde{R} to obtain

$$\frac{\alpha(\Delta)}{\alpha(0)} = \exp\left(-\frac{\Delta^2}{\gamma^2}\right).$$

Part III

Basics of quantum transport

Chapter 11

Preliminary Concepts

11.1 Two-Dimensional Electron Gas

An important system where quantum effects were observed is two-dimensional electron gas (2DEG). There are two basic systems where 2DEG has been studied. One of them is Si MOSFETs (metal-oxide-semiconductor field-effect transistors). A very good review of such systems is given in Ref. [7]. A typical device is shown in Fig. 11.1. A (100)Si surface serves

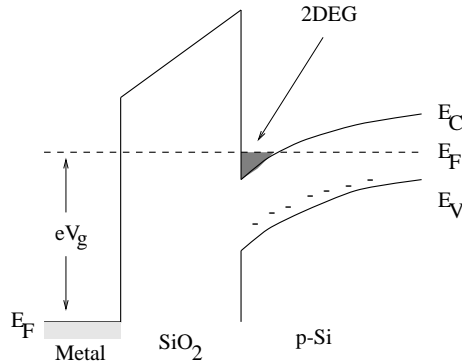


Figure 11.1: Band diagram showing conductance band E_C , valence band E_V and quasi-Fermi level E_F . A 2DEG is formed at the interface between the oxide (SiO_2) and p -type silicon substrate as a consequence of the gate voltage V_g .

as a substrate while SiO_2 layer behaves as an insulator. 2DEG is induced electrostatically by application a positive voltage V_g . The sheet density of 2DEG can be described as

$$n_s = \frac{\epsilon_{\text{ox}}}{ed_{\text{ox}}} (V_g - V_t)$$

where V_t is the threshold voltage for the barrier's creation

Another important systems with 2DEG involve modulation-doped GaAs-AlGaAs heterostructures. The bandgap in AlGaAs is wider than in GaAs. By variation of doping it is possible to move the Fermi level inside the forbidden gap. When the materials are

put together, a unified level of chemical potential is established, and an inversion layer is formed at the interface.

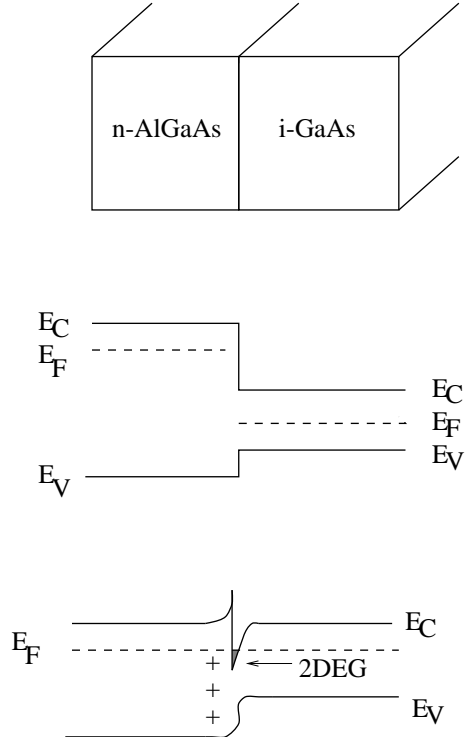


Figure 11.2: Band structure of the interface between n -AlGaAs and intrinsic GaAs, (a) before and (b) after the charge transfer.

The 2DEG created by a modulation doping can be squeezed into narrow channels by selective depletion in spatially separated regions. The simplest lateral confinement technique is to create split metallic gates in a way shown in Fig. 11.3. A typical nanostructure is shown in Fig. 11.4.

11.2 Basic Properties of Low-Dimensional Systems

Wave Functions

Let us direct z -axis perpendicular to the plane of 2DEG. The wave function can be decoupled as

$$\Psi(\mathbf{r}, z) = \chi(z) \psi(\mathbf{r})$$

where \mathbf{r} is the vector in plane of 2DEG. Throughout our considerations we will assume that all the distances are much larger than interatomic distance and thus we will use the effective

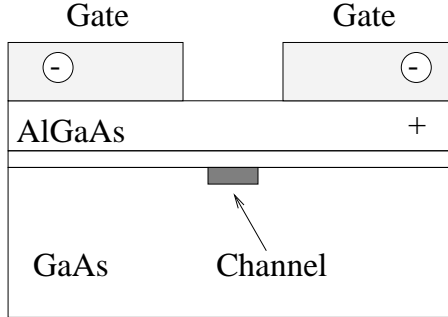


Figure 11.3: On the formation of a narrow channel by a split gate.

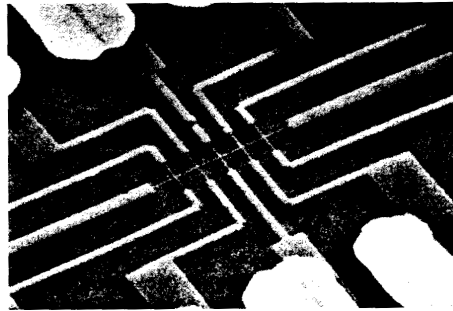


Figure 11.4: Scanning electron microphotographs of nanostructures in GaAs-AlGaAs heterostructures. Taken from M. L. Roukes *et al.*, Phys. Rev. Lett. **59**, 3011 (1987).

mass approximation. A good approximation for the confining potential is a triangular one,

$$U(z) = \begin{cases} \infty & \text{at } z < 0; \\ Fz & \text{at } z > 0. \end{cases}$$

Then one can write the Schrödinger equation for the wave function $\chi(z)$ as

$$\frac{\partial^2 \chi}{\partial z^2} + \frac{2m}{\hbar^2} (E - Fz) \chi = 0. \quad (11.1)$$

Instead z we introduce a dimensionless variable

$$\zeta = \left(z - \frac{E}{F} \right) \left(\frac{2mF}{\hbar^2} \right)^{1/3}.$$

The quantity

$$\ell_F = \left(\frac{2mF}{\hbar^2} \right)^{-1/3}$$

plays the role of characteristic localization length in z direction. Then Eq. (11.1) acquires the form

$$\chi'' - \zeta \chi = 0$$

which should be solved with the boundary conditions of finiteness at infinity and zero at $z = 0$. Such a solution has the form

$$\chi(\zeta) = A \text{Ai}(\zeta).$$

Here $\text{Ai}(\zeta)$ is the *Airy function* defined as

$$\text{Ai}(\zeta) = \frac{1}{\sqrt{\pi}} \int_0^\infty \cos(u^3/3 + u\zeta) du.$$

For large positive ζ it decays exponentially,

$$\text{Ai}(\zeta) \approx \frac{1}{2\zeta^{1/4}} e^{-(2/3)\zeta^{3/2}},$$

while for large negative *zeta* it is oscillatory,

$$\text{Ai}(\zeta) \approx \frac{1}{|\zeta|^{1/4}} \sin\left(\frac{2}{3}|\zeta|^{3/2} + \frac{\pi}{4}\right).$$

The energy spectrum E is defined by the roots ζ_n of the equation

$$\text{Ai}(\zeta) = 0, \quad \rightarrow \quad E_n = -E_0 \zeta_n.$$

Here

$$E_0 = \left(\frac{\hbar^2 F^2}{2m} \right)^{1/3}.$$

We have $\zeta_1 \approx -2.337$, $\zeta_2 \approx -4.088$. The normalization constants A_n for each level are defined as

$$A_n^{-1} = \int_0^\infty dz |\chi_n(z)|^2.$$

Normalized electron densities $A_n |\chi_n(z)|^2$ are shown in Fig. 11.5. Each level creates a subband for the in-plane motion, the energy being

$$E_{n,\mathbf{k}} = E_n + E(\mathbf{k}) = E_n + \frac{\hbar^2 k^2}{2m}.$$

Note that the effective mass m is considerably smaller than the mass of a free electron.

Density of States

The density of states $g(\epsilon)$ is defined as number of states per the energy interval $\epsilon, \epsilon + d\epsilon$. It is clear that

$$g(\epsilon) = \sum_\alpha \delta(\epsilon - \epsilon_\alpha)$$

where α is the set of quantum numbers characterizing the states. In the present case it includes the subband quantum number n , spin quantum number σ , valley quantum number

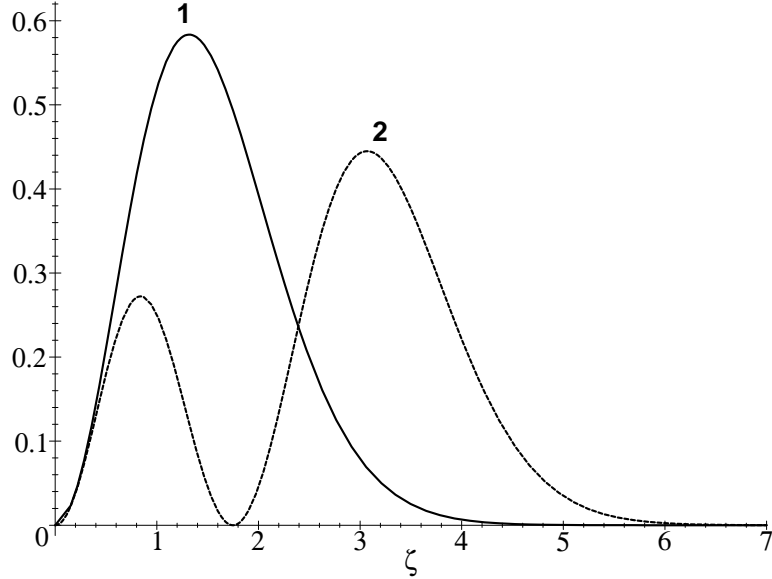


Figure 11.5: Normalized electron densities $A_n|\chi_n(z/\ell_F)|^2$ for the first (1) and second (2) subbands in a triangle potential with the slope F , $\ell_F = (\hbar^2/2mF)^{1/3}$.

v (for n -type materials), and in-plane quasimomentum \mathbf{k} . If the spectrum is degenerate with respect to spin and valleys one can define the spin degeneracy ν_s and valley degeneracy ν_v to get

$$g(\epsilon) = \frac{\nu_s \nu_v}{(2\pi)^d} \sum_n \int d^d k \delta(\epsilon - E_{n,\mathbf{k}}).$$

Here we calculate the number of states per unit volume, d being the dimension of the space. For 2D case we obtain easily

$$g(\epsilon) = \frac{\nu_s \nu_v m}{2\pi \hbar^2} \sum_n \Theta(\epsilon - E_n).$$

Within a given subband it appears energy-independent. Since there can exist several subbands in the confining potential (see Fig. 11.6, inset), the total density of states can be represented as a set of steps, as shown in Fig. 11.6. At low temperature ($kT \ll E_F$) all the states are filled up to the Fermi level. Because of energy-independent density of states the sheet electron density is linear in the Fermi energy,

$$n_s = \mathcal{N} \frac{\nu_s \nu_v m E_F}{2\pi \hbar^2} + \text{const}$$

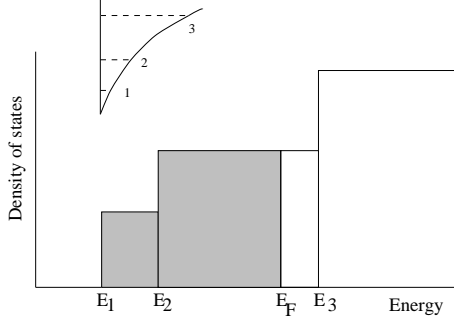


Figure 11.6: Density of states for a quasi-2D system.

while the Fermi momentum in each subband can be determined as

$$k_{Fn} = \frac{1}{\hbar} \sqrt{2m(E_F - E_n)}.$$

Here \mathcal{N} is the number of transverse modes having the edges E_n below the Fermi energy. The situation is more complicated if the gas is confined into a narrow channel, say, along y -axis. In a similar way, the in-plane wave function can be decoupled as a product

$$\psi(\mathbf{r}) = \eta(y) \frac{1}{N} e^{ik_x x},$$

where N is a proper normalization factor, the energy being

$$E_{n,s,k} = E_n + E_s(k_x) = E_n + E_s + \frac{\hbar^2 k_x^2}{2m}.$$

Here $E_{ns} \equiv E_n + E_s$ characterizes the energy level in the potential confined in both (z and y) directions. For square-box confinement the terms are

$$E_s = \frac{(s\pi\hbar)^2}{2mW^2},$$

where W is the channel width, while for the parabolic confinement $U(y) = (1/2)m\omega_0^2 y^2$ (typical for split-gate structures)

$$E_s = (s - 1/2)\hbar\omega_0.$$

It is conventional to introduce partial densities of states for the states with $k_x > 0$ and $k_x < 0$, g^\pm , respectively. We have,

$$g_s^+(\epsilon) = \frac{\nu_s \nu_v}{2\pi} \left(\frac{dE_s(k_x)}{dk_x} \right)^{-1} = \frac{\nu_s \nu_v \sqrt{m}}{2^{3/2} \pi \hbar} \frac{1}{\sqrt{\epsilon - E_{ns}}}. \quad (11.2)$$

The total density of states is

$$g^+(\epsilon) = \frac{\nu_s \nu_v \sqrt{m}}{2^{3/2} \pi \hbar} \sum_{ns} \frac{\Theta(\epsilon - E_{ns})}{\sqrt{\epsilon - E_{ns}}}. \quad (11.3)$$

The energy dependence of the density of states for the case of parabolic confinement is shown in Fig. 11.7.

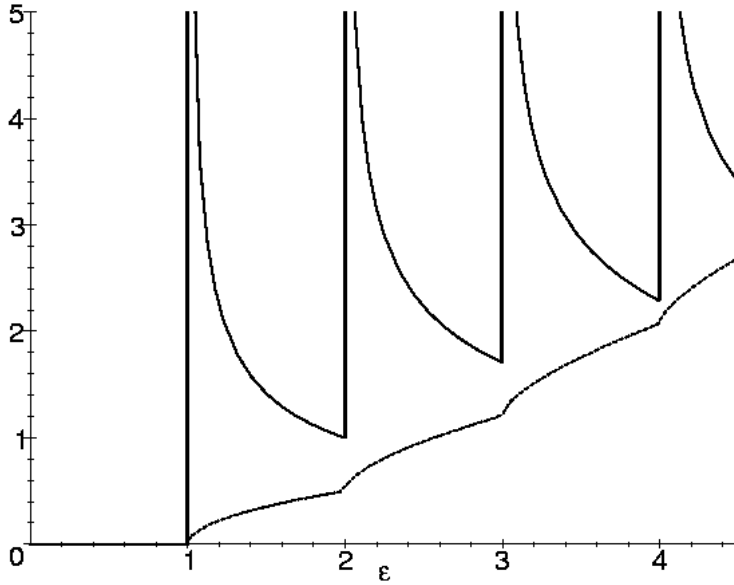


Figure 11.7: Density of states for a quasi-1D system (solid line) and the number of states (dashed lines).

Motion in a perpendicular magnetic field

2DEG in a perpendicular magnetic field gives an example of 0-dimensional electronic system. Indeed, according to the classical theory the Hamilton's function of a charged particle in an external electromagnetic field is

$$\mathcal{H} = \frac{1}{2m} \left(\mathbf{p} - \frac{e}{c} \mathbf{A} \right)^2 + e\phi,$$

where ϕ is the scalar and \mathbf{A} is the vector potential of the field, and \mathbf{p} is the generalized momentum of the particle. According to the rules of quantum mechanics, one should replace the canonical momentum \mathbf{p} by the operator

$$\mathbf{p} \rightarrow \hat{\mathbf{p}} = -i\hbar\nabla$$

and add also an extra spin term $-\boldsymbol{\mu}\mathbf{H}$ where $\boldsymbol{\mu} = \mu_B \hat{\mathbf{s}}/s$. Here $\mu_B = e/2mc$ is the Bohr magneton while $\hat{\mathbf{s}}$ is the spin operator. Generally, interaction with periodic potential of the crystalline lattice leads to renormalization of the spin splitting $\mu_B \rightarrow \mu^= g_f \mu_B$ where g_f is called the spectroscopic spin splitting factor.

Finally we get,

$$\begin{aligned} \mathcal{H} &= \frac{1}{2m} \left(\hat{\mathbf{p}} - \frac{e}{c} \mathbf{A} \right)^2 - \boldsymbol{\mu}\mathbf{H} + e\phi \\ &= \frac{\mathbf{p}^2}{2m} - \frac{e}{2mc} (\mathbf{A} \cdot \mathbf{p} + \mathbf{p} \cdot \mathbf{A}) + \frac{e^2 \mathbf{A}^2}{mc^2} - \frac{\mu}{s} \hat{\mathbf{s}} \cdot \mathbf{H} + e\phi. \end{aligned}$$

Since

$$\hat{\mathbf{p}} \cdot \mathbf{A} - \mathbf{A} \cdot \hat{\mathbf{p}} = -i\hbar \operatorname{div} \mathbf{A},$$

those operator commute if $\operatorname{div} \mathbf{A} = 0$. It holds in a uniform field with

$$\mathbf{A} = \frac{1}{2} \mathbf{H} \times \mathbf{r}.$$

The wave function in a magnetic field is not uniquely defined: it is defined only within the *gauge transform*

$$\mathbf{A} \rightarrow \mathbf{A} + \nabla f, \quad \phi \rightarrow \phi - \frac{1}{c} \frac{\partial f}{\partial t},$$

where f is an arbitrary function of coordinates and time. Under such a transform only the phase of wave function is changed by the quantity $ef/\hbar c$ that does not affect the observable quantities.

In classical mechanics, the generalized momentum of the particle is related to its velocity by the Hamilton equations,

$$m\mathbf{v} = \mathbf{p} - e\mathbf{A}/c.$$

According to the quantum mechanics we arrive at a similar expression. However different components of velocity do not commute, the commutation rules being

$$\begin{aligned} \{\hat{v}_x, \hat{v}_y\} &= i(e\hbar/m^2c)H_z, \\ \{\hat{v}_y, \hat{v}_z\} &= i(e\hbar/m^2c)H_x, \\ \{\hat{v}_z, \hat{v}_x\} &= i(e\hbar/m^2c)H_y. \end{aligned}$$

That means that the particle cannot simultaneously have definite velocities in all three directions.

Let us determine the energy levels in a 3-dimensional system embedded into a uniform magnetic film with a vector potential

$$A_x = -Hy, \quad A_y = A_z = 0.$$

The Hamiltonian then becomes

$$\mathcal{H} = \frac{1}{2m} \left(\hat{p}_x + \frac{eHy}{c} \right)^2 + \frac{\hat{p}_y^2}{2m} + \frac{\hat{p}_z^2}{2m} - \frac{\mu}{s} \hat{s}_z H.$$

First, the operator \hat{s}_z commutes with the Hamiltonian. Thus z -component of spin is conserved and can be replaced by its eigenvalue σ . Thus one can analyze the Schrödinger equation for an ordinary coordinate function,

$$\frac{1}{2m} \left[\left(\hat{p}_x + \frac{eH}{c}y \right)^2 + \hat{p}_y^2 + \hat{p}_z^2 \right] \psi - \frac{\mu}{s} \sigma H \psi = E\psi.$$

It is naturally to search for solution in the form

$$\psi = e^{i(p_x x + p_z z)/\hbar} \phi(y).$$

The eigenvalues p_x and p_z take all values from $-\infty$ to ∞ . Since $A_z = 0$ we get

$$p_z = mv_z.$$

Thus the motion along magnetic field in 3D system is not quantized. For a motion in the xy -plane we have the following Schrödinger equation,

$$\phi'' + \frac{2m}{\hbar^2} \left[\left(E + \frac{\mu\sigma}{s} H - \frac{p_z^2}{2m} \right) - \frac{1}{2} m\omega_c^2 (y - y_0)^2 \right] \phi = 0. \quad (11.4)$$

Here

$$y_0 = -cp_x/eH = -a_H^2 k_x, \quad a_H = (c\hbar/eH)^{1/2}, \quad \omega_c = |e|H/mc. \quad (11.5)$$

Since this equation is the same as the Schrödinger equation for a harmonic oscillator, we obtain

$$E = (n + 1/2)\hbar\omega_c - (\mu\sigma/s)H + p_z^2/2m, \quad n = 0, 1, \dots \quad (11.6)$$

The first term gives discrete levels which corresponds to the finite motion in the xy -plane, they are called *Landau levels*. For an electron, $\mu/s = -|e|\hbar/mc$, and the energy spectrum reads as

$$E = \left(n + \frac{1}{2} + \sigma \right) \hbar\omega_c + \frac{p_z^2}{2m}. \quad (11.7)$$

The eigenfunctions $\phi_n(y)$ are

$$\phi_n(y) = \frac{1}{\pi^{1/4} a_H^{1/2} \sqrt{2^n n!}} \exp \left[-\frac{(y - y_0)^2}{2a_H^2} \right] H_n \left[\frac{y - y_0}{a_H} \right]. \quad (11.8)$$

Here H_n is the Hermite polynomial.

In classical mechanics the motion in a magnetic field in xy -plane takes place in a circle about a fixed center. Here the conserved quantity y_0 corresponds to y coordinate of the center of the circle. It is easy to see that the combination

$$x_0 = cp_y/eH + x$$

is also conserved, it commutes with the Hamiltonian. The quantity x_0 corresponds to a classical x coordinate of the circle center. However, the operators \hat{y}_0 and \hat{x}_0 do not commute. That means that the coordinates x_0 and y_0 cannot take definite values simultaneously.¹

One can ask: why the coordinates x and y are not equivalent? The reason is that the wave functions (11.8) correspond to the energy independent of k_y . Consequently, any function of the type

$$\sum_{k_x} C(k_x) \psi_{N,k_x,k_z}$$

¹ In a classical mechanics, the radius of the circle is $r_c = cmv_t/eH = v_t/\omega_c$. Here v_t is the tangential component of the velocity. Thus we have,

$$y = y_0 + r_c(v_x/v_t), \quad x = x_0 - r_c(v_y/v_t).$$

corresponds to the same energy and one can chose convenient linear combinations to get correct asymptotic behavior.

To calculate the density of states in a magnetic field first we should count the number of the values k_y corresponding to the energy ε_α (the so-called *degeneracy factor*). As usual, we apply cyclic boundary conditions along y and z -axes and get

$$k_x = \frac{2\pi}{L_x} n_y, \quad k_z = \frac{2\pi}{L_z} n_z.$$

At the same time, we assume that the solution exists only in the region

$$0 < y_0 < L_y.$$

So, the degeneracy factor is

$$\frac{L_x}{2\pi} |k_x|^{\max} = \frac{L_x}{2\pi a_H^2} y_0^{\max} = \frac{L_y L_x}{2\pi a_H^2}. \quad (11.9)$$

This is very important relation which shows that one can imagine Landau states as cells with the area a_H^2 . We will come back to this property later.

Now it is easy to calculate number of states in a 3D system treating the k_z variable as for the usual 1D motion

$$\frac{2|k_z|L_z}{2\pi} = \frac{2\sqrt{2m}L_z}{2\pi\hbar} \sqrt{\varepsilon - \hbar\omega_c(N + 1/2)}$$

for each state with a given N . Finally, the total number of states per volume for a given spin is

$$Z_s(\varepsilon) = \sum_N Z_{sN}(\varepsilon) = \frac{2\sqrt{2m}}{(2\pi)^2 \hbar a_H^2} \sum_N \sqrt{\varepsilon - \hbar\omega_c(N + 1/2)}$$

where one has to sum over all the values of N with non-negative $\varepsilon - \hbar\omega_c(N + 1/2)$. The total number of states is $Z(\varepsilon) = 2Z_s(\varepsilon)$. To get DOS one should differentiate this equation with respect to ε . The result is

$$g_s(\varepsilon) = \frac{dZ(\varepsilon)}{d\varepsilon} = \frac{\sqrt{2m}}{(2\pi)^2 \hbar a_H^2} \sum_N \frac{\Theta[\varepsilon - \hbar\omega_c(N + 1/2)]}{\sqrt{\varepsilon - \hbar\omega_c(N + 1/2)}}.$$

Here

$$\Theta(x) = \begin{cases} 1 & \text{for } x > 0; \\ 1/2 & \text{for } x = 0; \\ 0 & \text{for } x < 0 \end{cases}$$

is the Heaviside step function. To take the spin into account one should add the spin splitting $\pm\mu_B g_f H$ to the energy levels. If we ignore the spin splitting we can assume spin degeneracy and multiply all the formulas by the factor 2. We take it into account automatically using $g(\varepsilon) = 2g_s(\varepsilon)$.

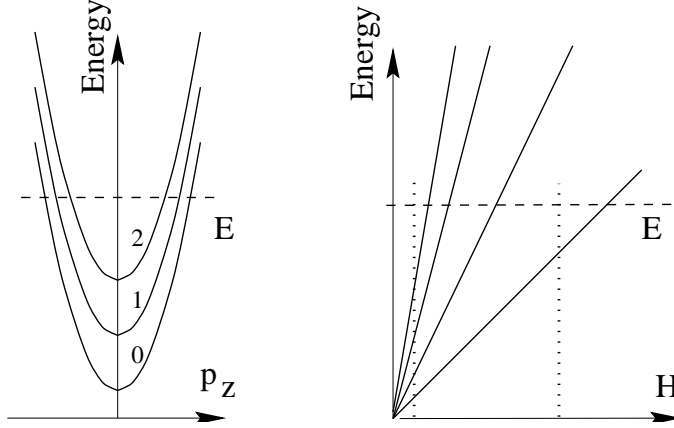


Figure 11.8: Landau levels as functions of p_z (left panel) and of H (right panel). The Fermi level is assumed to be fixed by external conditions.

The behavior of the density of states could be interpreted qualitatively in the following way. The Landau levels as functions of magnetic field for a given value of p_z are shown in Fig. 11.8. As a function of magnetic field, they form the so-called *Landau fan*. The Fermi level is also shown. At low magnetic fields its dependence on magnetic field is very weak. We see that if magnetic field is small many levels are filled. Let us start with some value of magnetic field and follow the upper filled level N . As the field increases, the slopes of the “fan” also increase and at a given threshold value H_N for which

$$\varepsilon_N(H_N) = \epsilon_F.$$

As the field increases the electrons are transferred from the N -th Landau level to the other ones. Then, for the field H_{N-1} determined from the equation $\varepsilon_{N-1}(H_{N-1}) = \epsilon_F$ the $(N-1)$ becomes empty. We get

$$H_N \approx \frac{m_c c \epsilon_F}{e \hbar} \frac{1}{N}, \quad \text{so} \quad \Delta \left(\frac{1}{H} \right) \approx \frac{e \hbar}{m_c c \epsilon_F}.$$

Here m_c is the so-called cyclotron effective mass which in the case of isotropic spectrum is the same as the density-of-states effective mass. We observe that DOS in a given magnetic field oscillated with the increase in energy just similar to the case of quasi 1D systems. Here Landau sub-bands play the same role as the modes of transverse quantization for quantum channels.

For a 2DEG the motion along z -direction is quantized, and instead of $e^{ip_z z/\hbar}$ we have $\chi_s(z)$. The means that for each subband of spatial quantization we have a sharp Landau level, the density of states (per area) being

$$g(\epsilon) = \frac{\nu_v e H}{4\pi^2 \hbar^2 c} \sum_{n,s,\sigma} \delta(\epsilon - E_{n,s,\sigma}).$$

Thus the density of states has sharp maxima at the energy levels that is a feature of so-called 0-dimensional system. In real samples the peaks are smeared by disorder.

11.3 Degenerate and non-degenerate electron gas

At equilibrium the states are filled according to the Fermi function

$$f_0(\epsilon) = \frac{1}{\exp[(\epsilon - \mu)/kT] + 1},$$

where μ is the chemical potential while k is the Boltzmann constant. The chemical potential is determined by the normalization to the total number of electrons as

$$n = \int_0^\infty g(\epsilon) f_0(\epsilon) d\epsilon$$

where n is the *electron density*. At zero temperature the chemical potential is called *the Fermi energy*, ϵ_F . The graph of the Fermi function and its energy derivative is given in Fig. 11.9

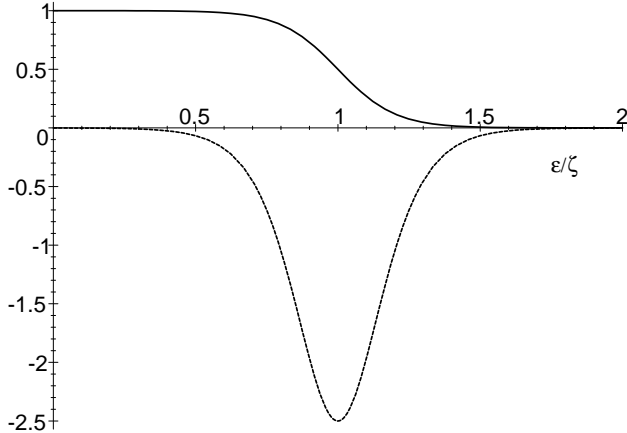


Figure 11.9: The Fermi distribution (solid line) and its energy derivative multiplied by kT (dashed line) for $\zeta/kT = 10$.

Since at $T = 0$

$$f_0(\epsilon) \approx \Theta(\epsilon - \zeta),$$

the Fermi energy is given by the equation

$$n = \int_0^{\epsilon_F} g(\epsilon) d\epsilon. \quad (11.10)$$

The limiting case $T = 0$ is actually means the the inequality $kT \ll \epsilon_F$ is met. In the opposite limiting case, $kT \gg \epsilon_F$, we get

$$f_0(\epsilon) \approx e^{(\zeta-\epsilon)/kT}, \quad n = e^{\zeta/kT} \int_0^\infty g(\epsilon) e^{-\epsilon/kT} d\epsilon.$$

Thus,

$$f_0(\epsilon) = A(T) e^{-\epsilon/kT}, \quad \frac{1}{A(T)} = \frac{1}{n} \int_0^\infty g(\epsilon) e^{-\epsilon/kT} d\epsilon. \quad (11.11)$$

This distribution is called the *Boltzmann* one.

11.4 Relevant length scales

One can discriminate between several important length scales in low-dimensional systems. They are shown in the Table 11.1.

1 mm	Mean free path in the quantum Hall regime
100 μm	Mean free path/Phase relaxation length in high-mobility semiconductor at $T < 4$ K
10 μm	
1 μm	Commercial semiconductor devices (1990)
100 nm	de Broglie wave length in semiconductors. Mean free path in polycrystalline metallic films
10 nm	
1 nm	de Broglie wave length in metals Distance between atoms
1 Å	

Table 11.1: A few relevant length scales. Note that $1 \mu\text{m} = 10^{-6} \text{ m} = 10^{-4} \text{ cm}$; $1 \text{ nm} = 10^{-9} \text{ m} = 10 \text{ Å}$.

The above mentioned scales have the following physical meaning:

De Broglie wave length, λ . This length is defined as

$$\lambda = \frac{2\pi\hbar}{p} = \frac{2\pi}{k}$$

where p (k) is the typical electron momentum (wave vector). For Fermi gas the characteristic momentum is just the Fermi momentum. For the case of a single filled band in 2DEG,

$$\lambda = 2\pi/k_F = \sqrt{2\pi/n_s}$$

where n_s is the sheet density. For the Boltzmann gas, $p \approx \sqrt{2mkT}$, and

$$\lambda = \frac{2\pi\hbar}{\sqrt{2mkT}}.$$

Mean free path, ℓ . This is a characteristic length between the collisions with impurities or phonons. It is defined as

$$\ell = v\tau_{\text{tr}}$$

where v is the typical velocity while τ_{tr} is the so-called *transport relaxation time*. It is defined as

$$\frac{1}{\tau_{\text{tr}}} \propto \int d\theta \sin \theta W(\theta) (1 - \cos \theta)$$

where θ is the scattering angle while $W(\theta)$ is the scattering probability. Usually the transport is characterized by the *mobility*

$$u = \frac{e\tau_{\text{tr}}}{m}.$$

The physical meaning of mobility is that a typical electron drift velocity acquired in an external electric field E is given by the relation

$$v_d = uE.$$

Phase-relaxation length, L_φ . This is a specially quantum mechanical relaxation length which has no analogs in classical physics. Namely, classical motion can be described as evolution of the *probability* to find a particle at a given point at a given time. However, in quantum mechanics the state is characterized by the *wave function* which has a *phase*. The phase is important in the so-called interference phenomena, where the electron wave functions having different pre-history are collected at the same point. If the phases of the waves are not destroyed, a specific quantum interference phenomena can be observed and important. The phase-relaxation time, τ_φ , describes relaxation of the phase memory.

It is clear that scattering against any static spin-independent potential cannot lead to the phase relaxation. Indeed, in any stationary potential the equations of motion are *time-reversible*. The only processes which can be responsible for phase relaxation are the ones which broke the symmetry with respect to time-reversal. Among them are inelastic scattering by phonons, electron-electron collisions, spin-flip processes, etc. An important feature of such processes is that an electron suffers many elastic collisions during a typical time τ_φ . Since it moves *diffusively* a proper way to estimate the relevant length L_φ is as follows:

$$L_\varphi = \sqrt{D\tau_\varphi},$$

where $D = (1/d)v\ell$ is the diffusion constant (d is the dimensionality of the electron gas).

Thermal dephasing length, L_T . The above mentioned relaxation process is relevant to the interference of the wave functions belonging to a single-electron state. However, interference can be also important for the interaction of *two electrons* having close

energies. Indeed, if the energy difference between the electrons is $\approx kT$ they travel almost coherently during the time \hbar/kT . Thus the characteristic length of coherent propagation is estimated as

$$L_T = \sqrt{\hbar D/kT}.$$

Comparing mean free path ℓ with characteristic dimensions of the system, L , one can discriminate between *diffusive*, $\ell \ll L$ and *ballistic*, $\ell \geq L$, transport. Such a classification appears incomplete in the situation where different dimensions of the sample are substantially different. The situation is illustrated in Fig. 11.10 for the case where the length L of the sample is much larger than its width, W . If phase coherence is taken into account, the

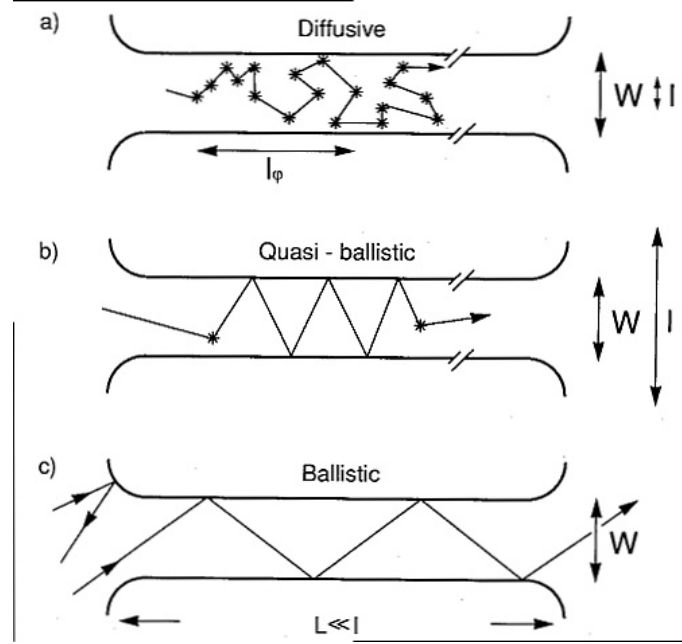


Figure 11.10: Electron trajectories for the diffusive ($\ell < W, L$), quasi-ballistic ($W < \ell < L$) and ballistic ($\ell > W, L$) transport regimes. From [11].

scales L_φ and L_T become important, and the situation appears more rich and interesting. Mesoscopic conductors are usually fabricated by patterning a planar conductor that has one very small dimension to start with. Although some of the pioneering experiments in this field were performed using metallic conductors, most of the recent work has been based on the gallium arsenide (GaAs)–aluminum gallium arsenide (AlGaAs) material system. Some important parameters for such systems are shown in Fig. 11.11.

		GaAs(100)	Si (100)	UNITS
Effective Mass	m	0.067	0.19	$m_e = 9.1 \times 10^{-28} \text{ g}$
Spin Degeneracy	g_s	2	2	
Valley Degeneracy	g_v	1	2	
Dielectric Constant	ϵ	13.1	11.9	$\epsilon_0 = 8.9 \times 10^{-12} \text{ F m}^{-1}$
Density of States Electronic Sheet	$\rho(E) = g_s g_v (m/2\pi\hbar^2)$	0.28	1.59	$10^{11} \text{ cm}^{-2} \text{ meV}^{-1}$
Density ^a	n_s	4	1-10	10^{11} cm^{-2}
Fermi Wave Vector	$k_F = (4\pi n_s/g_s g_v)^{1/2}$	1.58	0.56-1.77	10^6 cm^{-1}
Fermi Velocity	$v_F = \hbar k_F/m$	2.7	0.34-1.1	10^7 cm/s
Fermi Energy	$E_F = (\hbar k_F)^2/2m$	14	0.63-6.3	meV
Electron Mobility ^a	μ_e	10^4 - 10^6	10^4	$\text{cm}^2/\text{V s}$
Scattering Time	$\tau = m\mu_e/e$	0.38-38	1.1	ps
Diffusion Constant	$D = v_F^2 \tau / 2$	140-14000	6.4-64	cm^2/s
Resistivity	$\rho = (n_s e \mu_e)^{-1}$	1.6-0.016	6.3-0.63	$\text{k}\Omega$
Fermi Wavelength	$\lambda_F = 2\pi/k_F$	40	112-35	nm
Mean Free Path	$l = v_F \tau$	10^2 - 10^4	37-118	nm
Phase Coherence Length ^b	$l_\phi = (D\tau_\phi)^{1/2}$	200-...	40-400	$\text{nm}(T/\text{K})^{-1/2}$
Thermal Length	$l_T = (\hbar D/k_B T)^{1/2}$	330-3300	70-220	$\text{nm}(T/\text{K})^{-1/2}$
Cyclotron Radius	$l_{cycl} = \hbar k_F/eB$	100	37-116	$\text{nm}(B/\text{T})^{-1}$
Magnetic Length	$l_m = (\hbar/eB)^{1/2}$	26	26	$\text{nm}(B/\text{T})^{-1/2}$
	$k_F l$	15.8-1580	2.1-21	
	$\omega_c \tau$	1-100	1	(B/T)
	$E_F/\hbar\omega_c$	7.9	1-10	$(B/\text{T})^{-1}$

Figure 11.11: Electronic properties of the 2DEG in GaAs-AlGaAs and Si inversion layers. From [10].

Chapter 12

Ballistic transport

12.1 Landauer formula

We start this chapter by a description of a very powerful method in physics of small systems - so-called *Landauer approach*.

The main principle of this approach is the assumption that the system in question is coupled to large reservoirs where all inelastic processes take place. Consequently, the transport through the systems can be formulated as a quantum mechanical *scattering problem*. Thus one can reduce the non-equilibrium transport problem to a quantum mechanical one.

Another important assumption is that the system is connected to reservoirs by *ideal quantum wires* which behave as waveguides for the electron waves. We start our analysis from the discussion of the properties of an ideal quantum wire.

Ideal quantum wire

Consider 2 large reservoirs of electron gas reservoirs having the difference δn in the electron density and separated by a pure narrow channel. For small δn one can assume that there is a difference in a chemical potential, $\delta\mu = \delta n/g(\epsilon_F)$. In the following we shall use the Fermi level of non-biased system as the origin for the chemical potentials. So the difference between the chemical potential in α -th reservoir will be denoted as μ_α .

If the channel is long and uniform, then the total current carried by the state characterized by a transverse mode n and a given direction of spin which propagates without scattering is

$$J_n = e \int \frac{dk_z}{2\pi\hbar} \frac{\partial\varepsilon_n(k_z)}{\partial k_z} = \frac{2}{2\pi\hbar} \int_{\epsilon_F+\mu_\alpha}^{\epsilon_F+\mu_\beta} d\varepsilon \frac{\partial\varepsilon_n(k_z)/\partial k_z}{|\partial\varepsilon_n(k_z)/\partial k_z|} = \frac{2}{h}\delta\mu.$$

If we take into account electron spin and N transverse modes are open, then the conductance is given by the expression $G = \frac{2e^2}{h}N$.

We come to a very important conclusion: an *ideal* quantum wire has *finite* resistance $h/2e^2N$ which is independent of the length of the wire.

As we have seen, even an ideal quantum wire has a finite resistance. That means a finite heat generation even in the absence of any inelastic processes inside the wire. Below we will discuss the physical picture of heat release by a current-carrying nanostructure (here we follow the considerations of Ref. [23]).

First of all let us specify what heat release is. It will be convenient to consider an isolated system. Therefore we will have in mind the following physical situation. There is a capacitor which is discharged through the conductor of interest. The product RC of the whole system, R and C being the resistance and capacitance respectively, is much bigger than any relaxation time characterizing the electron or phonon system of the conductor. This means that for all the practical purposes the conduction process can be looked upon as a stationary one. The total energy of the system, \mathcal{U} , is conserved, while its total entropy, $\hat{\mathcal{S}}$, is growing. The rate of heat generation is expressed through $T\partial\hat{\mathcal{S}}/\partial t$, where T is the temperature, i.e. through the applied voltage and characteristics of the nanostructure itself. This means that the result is independent of the assumption that the considered system is isolated, which is made only for the sake of derivation. This thermodynamically defined heat is generated in the classical reservoirs over the length having a physical meaning of the electron mean free path. That is the same mean free path that enters the Drude formula, which determines the conductivity of the reservoirs themselves, the amount of heat generated per second in both reservoirs being the same.

It is interesting to indicate that even purely elastic collisions can result in a heat generation although they of course cannot establish full equilibrium. This has a clear physical meaning. The amount of order in the electron distribution resulting in electric current can bring about mechanical work. For instance, one can let the current flow through a coil, and a magnetic rod can be drawn into the coil. In such a way the electrons transferring the current can execute a work on the rod. As a result of scattering, the amount of order in the electrons' distribution diminishes, and this means dissipation of mechanical energy into the heat. It has been shown that the heat release is symmetric in both reservoirs even if the scatterers in the system are asymmetric.

All the above considerations do not mean that the collisions that give the main contribution to the heat release, also establish *full equilibrium*. What equilibrium needs is inelastic collisions which transfer the energy of electrons taking part in charge transfer to other degrees of freedom, such as to other electrons and phonons. In particular, a *local equilibrium electron distribution* is established over the length scale determined by *electron-electron* interaction. Such a distribution can be characterized by a local electro-chemical potential and sometimes an electron temperature. The latter can in principle be measured by optical methods. On the other hand, the *equilibrium with respect to the lattice* is established at the scales of *electron-phonon* and *phonon-phonon* mean free paths. Only over those distances from the channel one can treat the results in terms of the true local temperature.

Resistance of a quantum resistor

Consider a system shown in Fig. 12.1 consisting of a barrier connected to reservoirs by ideal quantum wires. If there is some reflection only a part of the current is transmitted.

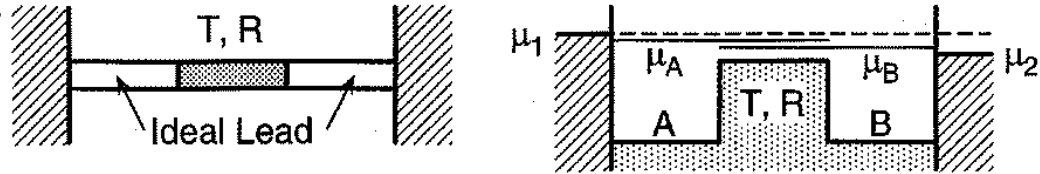


Figure 12.1: On the resistance of a quantum resistor.

In this case one can introduce the transmission probability of the mode n , T_n , to obtain (including spin degeneracy)

$$J = \frac{2}{h} \delta\mu \sum_{n=1}^N T_n.$$

As a result,

$$G = \frac{2e^2}{h} \sum_{n=1}^N T_n = \frac{2e^2}{h} \text{Tr } \mathbf{t}\mathbf{t}^\dagger. \quad (12.1)$$

Here \mathbf{t} is the matrix of *scattering amplitudes* while the expression is called *two-terminal* Landauer formula.

This very important and looking simple formula was confusing during a long period. Indeed, this is the conductance which is measured between two reservoirs. Having in mind that the resistance of the connecting ideal wires (per one conducting mode) is $h/2e^2$ we can ascribe to the scattering region the resistance

$$\frac{h}{2e^2} \left[\frac{1}{T} - 1 \right] = \frac{h}{2e^2} \frac{R}{T},$$

where R is the reflection coefficient. Consequently, in the original formulation the quantum resistance was described as

$$G = \frac{2e^2}{h} \sum_{n=1}^N \frac{T_n}{1 - T_n}. \quad (12.2)$$

However, the quantity which is usually measured is given by Eq. (12.1).

Now we derive the Landauer formula for finite-temperature and so-called multichannel case when the leads have several transverse modes. Consider ideal wires which lead to a general elastic scattering system. Let each lead has the cross section A and have N_\perp transverse channels characterized by wave vectors k_i so that,

$$E_i + \frac{\hbar^2 k_i^2}{2m} = E_F.$$

The incoming channels are fed from the electron baths with the same temperature and chemical potentials μ_1, μ_2, \dots . The outgoing channels are fed up to *thermal equilibrium population*. We shall assume that the particles are absorbed in the outgoing baths. The sources are assumed to be *incoherent*, the differences $\mu_1 - \mu_2$ are also assumed small to yield linear transport. We introduce the scattering amplitudes t_{ij} for the transmission from j th incoming to i th outgoing channel. Reflection amplitudes r_{ij} are introduced in a similar way for reflection into the i th incoming channel. If we replace the incoming and outgoing channels, we denote the proper amplitudes by primes. In this way it is convenient to introduce $2N_\perp \times 2N_\perp$ scattering matrix as

$$S = \begin{pmatrix} r & t' \\ t & r' \end{pmatrix}.$$

From the current conservation we must require unitarity while from time reversal symmetry $S = \tilde{S}$. Thus we have also $SS^* = I$ where star stays for complex conjugation while tilde for transposition. In a magnetic field the Onsager relation requires $S(H) = \tilde{S}(-H)$.

If one defines the total transmission and reflection into i th channel as

$$T_i = \sum_j |t_{ij}|^2, \quad R_i = \sum_j |r_{ij}|^2.$$

then from unitarity condition we get

$$\sum_i T_i = \sum_i (1 - R_i).$$

Since the densities of states in each channel are 1D like, $g_i(E) = (\pi\hbar v_i)^{-1}$ we write the current through outgoing channels as

$$\begin{aligned} I &= \frac{e}{\pi\hbar} \sum_i \int dE [f_1(E)T_i(E) + f_2(E)R'(E) - f_2(E)] \\ &= \frac{(\mu_1 - \mu_2)e}{\pi\hbar} \int dE \left(-\frac{\partial f}{\partial E} \right) \sum_i T_i(E). \end{aligned}$$

Thus the conductance becomes

$$G = \frac{2e^2}{h} \int dE \left(-\frac{\partial f}{\partial E} \right) \text{Tr } \mathbf{t}\mathbf{t}^\dagger.$$

This is the *two-terminal* conductance measured between the *outside* reservoirs which includes contact resistances.

Multiterminal resistance

For simplicity we shall discuss the case of zero temperature. Let us introduce the total transmission probability from the bath α to the bath β ,

$$T_{\alpha \rightarrow \beta} = \sum_{n=1}^{N_\alpha} \sum_{m=1}^{N_\beta} |t_{\beta\alpha,mn}|^2.$$

Here N_i is the number of propagating modes in each lead connected to i th reservoir. Counting all the chemical potentials from the Fermi level, we see that the reservoir α injects the current $(2e/h)N_\alpha\mu_\alpha$ into the lead α . The fraction $T_{\alpha \rightarrow \beta}/N_\alpha$ is transmitted to the reservoir β while the fraction $T_{\alpha \rightarrow \alpha}/N_\alpha = R_\alpha/N_\alpha$ is reflected back into reservoir α . The net current I_α is given by the following set of equations,

$$\frac{h}{2e}I_\alpha + (N_\alpha - R_\alpha)\mu_\alpha - \sum_{\beta \neq \alpha} T_{\beta \rightarrow \alpha}\mu_\beta. \quad (12.3)$$

Introducing vectors \vec{I} and $\vec{\mu}$ with components I_α and μ_α , respectively, we can write

$$\vec{I} = \hat{G}\vec{\mu}, \quad (12.4)$$

where the conductance matrix \hat{G} is defined as

$$\begin{aligned} G_{\alpha\beta} &= \frac{2e^2}{h} [(N_\alpha - R_\alpha)\delta_{\alpha\beta} - T_{\beta \rightarrow \alpha}(1 - \delta_{\alpha\beta})] \\ &= \frac{2e^2}{h} [N_\alpha\delta_{\alpha\beta} - T_{\beta \rightarrow \alpha}]. \end{aligned} \quad (12.5)$$

Here we use the relation $T_{\alpha \rightarrow \alpha} = R_\alpha$. The sum of rows of this matrix is zero because of current conservation, the sum of the elements of each row also vanishes because if one changes all the chemical potentials by the same amount no current will be induced. Thus

$$N_\alpha - R_\alpha = \sum_{\beta \neq \alpha} T_{\beta \rightarrow \alpha} = \sum_{\beta \neq \alpha} T_{\alpha \rightarrow \beta}.$$

The equations (12.4) and (12.5) are called often the *Landauer-Büttiker formalism*. They

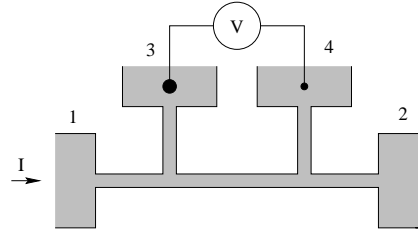


Figure 12.2: On the resistance of 4-terminal device.

allow us to find, e. g. 4-terminal resistance. Indeed, we can put $I_1 = -I_2 = I$, $I_3 = I_4 = 0$. Then $\vec{I} = I\vec{j}$ where

$$\vec{j} = I \begin{pmatrix} 1 \\ -1 \\ 0 \\ 0 \end{pmatrix}.$$

Thus

$$\mathcal{R}_{34} = \frac{\mu_4 - \mu_3}{I} = \left(\hat{G}^{-1} \vec{j} \right)_4 - \left(\hat{G}^{-1} \vec{j} \right)_3.$$

Having in mind the properties of the scattering amplitudes we have,

$$T_{\alpha \rightarrow \beta}(H) = T_{\beta \rightarrow \alpha}(-H)$$

that results in the *reciprocity relation*

$$\mathcal{R}_{\alpha\beta,\gamma\delta}(H) = \mathcal{R}_{\gamma\delta,\alpha\beta}(-H).$$

Here $\mathcal{R}_{\alpha\beta,\gamma\delta}$ stands for the resistance measured for voltage contacts γ, δ while the current passes through the contacts α, β . Note that this relation works even in the case when the concept of local conductivity is not applicable. What we only need is linear response and absence of inelastic scattering inside the device under consideration.

One can easily generalize the above expressions for the case of finite temperatures by replacement of the element of \hat{G} -matrix by their thermal averages,

$$\langle A \rangle_T = \frac{\int_0^\infty dE g(E) (\partial f_0 / \partial E) A(E)}{\int_0^\infty dE g(E) (\partial f_0 / \partial E)}.$$

12.2 Application of Landauer formula

Point ballistic contact

The most clean system is the so-called quantum point contact (QPC) - short and narrow constrictions in 2d electron gas. A sketch of QPC is shown in Fig. 12.3. The conductance of

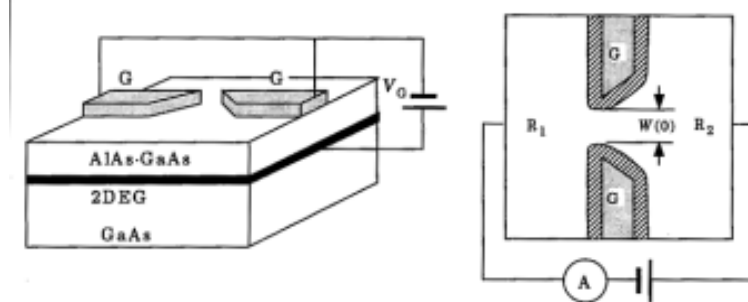


Figure 12.3: A sketch of QPC formed by splitted gates.

QPC is quantized in the units of $2e^2/h$. The quantization is not that accurate as in quantum Hall effect (about 1%) because of non-unit transparencies T_n and finite temperature. It is interesting to compare quantum and classical behavior of QPC. In a classical picture one can write

$$J = W(\delta n)v_F \int_{-\pi/2}^{\pi/2} \frac{d\alpha}{2\pi} \cos \alpha = \frac{1}{\pi} W v_F (\delta n).$$

Thus the “diffusion constant” is

$$D_{eff} = \frac{J}{\delta n} = \frac{1}{\pi} W v_F \quad \rightarrow \quad G = e^2 g(\epsilon_F) D_{eff} = \frac{2e^2 k_F W}{h} \frac{1}{\pi}.$$

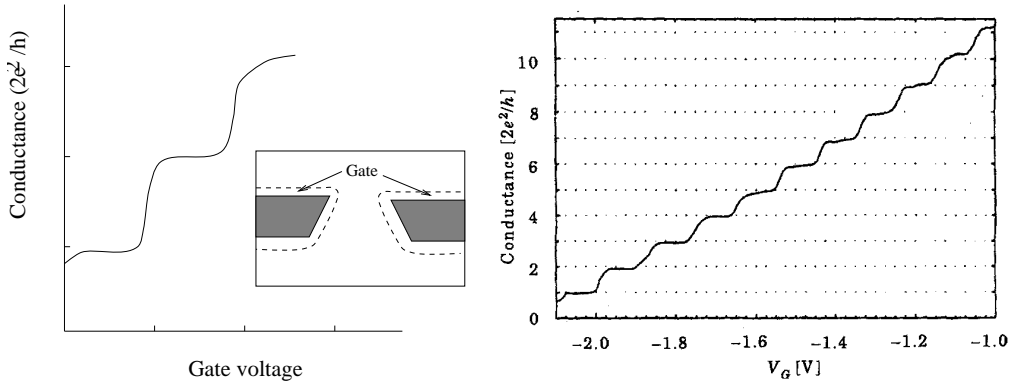


Figure 12.4: Quantization of conductance of a point contact: Schematic picture (left) and experimental result (right).

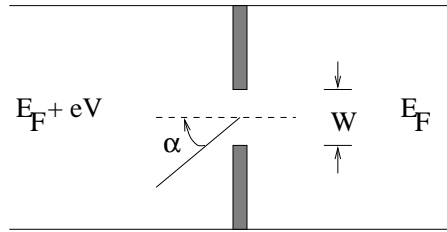


Figure 12.5: On the classical conductance of a point contact.

Note that the integer part of the quantity $k_F W / \pi$ is just the number of occupied modes according to quantum mechanics.

Series addition of quantum resistors

Assume that we have two obstacles in series. Let the wave with unit amplitude is incident to the region, the amplitude of the reflected wave is A while D is the amplitude the wave transmitted through device. The obstacles are connected by an ideal conductor, the phase shift of the wave along which being ϕ . Let the wave emerging from the obstacle

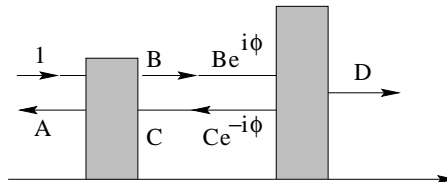


Figure 12.6: On series of quantum resistors.

1 is $B \exp(kx - \omega t)$. It reaches the obstacle 2 gaining the phase ϕ , having the complex amplitude $B \exp(i\phi)$. The reverse wave C gains the phase $-\phi$. In this way we get the

following set of equations,

$$\begin{aligned} A &= r_1 + t_1 C, & B &= t_1 + r'_1 C \\ Ce^{-i\phi} &= r_2 B e^{i\phi}, & D &= t_2 B e^{i\phi} \end{aligned}$$

Solving this equation we obtain,

$$D = \frac{e^{i\phi} t_1 t_2}{1 - e^{2i\phi} r_2 r'_1},$$

that yields for the total transmittance:

$$T = |D|^2 = \frac{T_1 T_2}{1 + R_1 R_2 - 2\sqrt{R_1 R_2} \cos \theta} \quad (12.6)$$

where $\theta = 2\phi + \arg(r_2 r'_1)$. The ratio between reflection and transmission which should be understood as a reduced resistance (in units $h/2e^2$) of the system excluding wires is

$$\mathcal{G}^{-1} \equiv \frac{R}{T} = \left| \frac{A}{D} \right|^2 = \frac{R_1 + R_2 - 2\sqrt{R_1 R_2} \cos \theta}{T_1 T_2}, \quad \mathcal{G} \equiv \frac{hG}{2e^2}. \quad (12.7)$$

This is a very strange formula. Assume that we made an ensemble of the systems which differ only by the distance between the obstacles, i. e. by the phase ϕ . Let the distribution of ϕ will be constant in the interval $(0, 2\pi)$. The averaging over ϕ we get

$$\langle \mathcal{G}^{-1} \rangle = \frac{R_1 + R_2}{(1 - R_1)(1 - R_2)},$$

while the Ohm's law will provide

$$\mathcal{G}^{-1} = \frac{R_1}{1 - R_1} + \frac{R_2}{1 - R_2}.$$

As a result the Ohm's law survives only at small reflections.

Let us construct a chain of n resistors with very small reflections. Then the total reflection first increases linearly in n . Finally the total transmission becomes substantially less than 1. Now let us add a very good conductor to this chain. We get

$$\langle \mathcal{G}^{-1} \rangle_{n+1} = \frac{R_n + R}{T_n} = \langle \mathcal{G}^{-1} \rangle_n + \frac{R}{T_n}.$$

Thus an addition a good conductor increases the resistance by $R/T_n > R$. Such a behavior can be formulated as a “renormalization group”

$$\frac{1}{R} \frac{d}{dn} \langle \mathcal{G}^{-1} \rangle_n = \langle \mathcal{G}^{-1} \rangle_n + 1.$$

Thus the average resistance grows exponentially with the length which has something to do with 1D localization. This considerations are not fully satisfactory because resistance

is not the proper quantity to be averaged. Following Anderson, the proper quantity to be averaged is $\ln(1 + \mathcal{G}^{-1})$. Indeed,

$$1 + \mathcal{G}^{-1} = 1 + R/T = 1/T \rightarrow \ln(1 + \mathcal{G}^{-1}) = -\ln T.$$

The quantity $-\ln T$ plays the role of extinction exponent and it should be additive to successive scatterers if the relative phases are averaged out. We get this relation using

$$\int_0^{2\pi} d\theta \ln(a + b \cos \theta) = \pi \ln \frac{1}{2} \left[a + \sqrt{a^2 - b^2} \right].$$

So the exact scaling is given by the relation

$$\langle \ln(1 + \mathcal{G}_n^{-1}) \rangle = n(Rh/2e^2).$$

Parallel addition of quantum resistors.

Let us now discuss the parallel addition of two single-channeled quantum resistors. The geometry of the problem is shown in Fig. 12.7. All the phases and scattering effects along

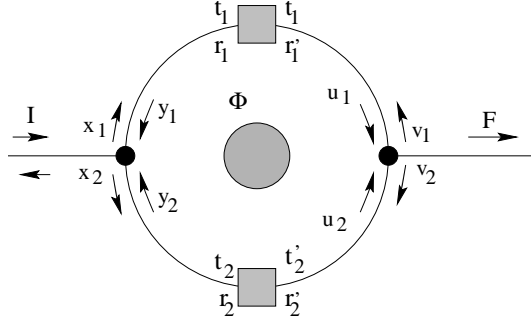


Figure 12.7: On the parallel addition of quantum resistances.

the branches are absorbed by the scattering parameters. Time-reversal symmetry requires $t_i = t'_i$ while the current conservation requires

$$-t_i/t_i'^* = r_i/r_i'^*.$$

In the presence of Aharonov-Bohm flux Φ through the loop, following from the gauge invariance the scattering amplitudes are renormalized as

$$t_1 \rightarrow t_1 e^{-i\theta}, \quad t'_1 \rightarrow t_1 e^{+i\theta}, \quad t_2 \rightarrow t_2 e^{+i\theta}, \quad t'_2 \rightarrow t_2 e^{-i\theta}, \quad r_i \rightarrow r_i, \quad r'_i \rightarrow r'_i.$$

Here $\theta = \pi\Phi/\Phi_0$.

This point needs some more explanation. An Aharonov-Bohm flux Φ through the opening can be represented as $\oint \mathbf{A} \cdot d\mathbf{l}$ along the path circulating the opening. Here \mathbf{A} is the vector potential. One can eliminate this flux by a gauge transform

$$\psi' = \psi \exp \left[\frac{ie}{\hbar c} \sum_j \chi_j(\mathbf{r}_j) \right],$$

where χ is defined as $A_l = \nabla\chi$. The transformed Schrödinger equation has $A_l = 0$. However, the price for this is that the transformed wave function, ψ' , does not satisfy periodic boundary conditions. When the electron coordinate is rotated once around the ring the phase of χ' is changed by $\delta\chi = 2\pi\Phi/\Phi_0$. In our calculation this phase shift is absorbed into the expressions for the transition amplitudes.

To find the transmitted wave one has to determine 10 unknown amplitudes, $x_1, x_2, y_1, y_2, u_1, u_2, v_1, v_2, F, \dots$. It can be done solving the set of matching equations at the scatterers and the triple connections. It is assumed that the connections do not introduce additional scattering and can be described by the unitary scattering matrix

$$S = \begin{pmatrix} 0 & -1/\sqrt{2} & -1/\sqrt{2} \\ -1/\sqrt{2} & 1/2 & -1/2 \\ -1/\sqrt{2} & -1/2 & 1/2 \end{pmatrix}.$$

Here S_{ii} denote the reflection amplitude of the i th channel while off-diagonal elements S_{ij} are the transition amplitudes from the channel i to j . The subscript 1 is used for left incoming channel and right outgoing channel. After rather long algebra made originally in Ref. [24] we arrive at the solution,

$$T \equiv |F|^2 = 4 \frac{\alpha + \beta \cos 2\theta}{\gamma + \delta \cos 2\theta + \epsilon \cos 4\theta}, \quad (12.8)$$

where $\alpha, \beta, \gamma, \delta, \epsilon$ are rather complicated functions of the scattering amplitudes,

$$\begin{aligned} \alpha &= |A|^2 + |B|^2, \quad \beta = 2 \operatorname{Re}(AB^*), \quad \gamma = |D|^2 + |E|^2, \\ \delta &= 2 \operatorname{Re}(DC^* + EC^*), \quad \epsilon = 2 \operatorname{Re}(DE^*), \\ A &= t_1^2 t_2 + t_2(r_1 - 1)(1 - r'_1), \quad B = t_2^2 t_1 + t_1(r_2 - 1)(1 - r'_2), \\ D &= E = t_1 t_2, \quad C = t_1^2 + t_2^2 - (2 - r_1 - r_2)(2 - r'_1 - r'_2). \end{aligned}$$

This expression describes a rich physical picture. Even in the absence of magnetic field, $\theta = 0$ the transmittance can be strongly dependent on the phases of the complex scattering amplitude. If we make one branch fully non-conducting, $t_1 = 0$, still the appropriate choice of phases of the reflection amplitudes r_1 and r'_1 can result either in $T = 0$ or $T = 1$. Indeed, in this case,

$$\begin{aligned} A &= t_2(r_1 - 1)(1 - r'_1), \quad B = D = E = 0, \quad C = t_2^2 - (2 - r_1 - r_2)(2 - r'_1 - r'_2), \\ \alpha &= |t_2|^2 |(r_1 - 1)(1 - r'_1)|^2, \quad \beta = 0, \quad \gamma = |t_2^2 - (2 - r_1 - r_2)(2 - r'_1 - r'_2)|^2, \\ \delta &= \epsilon = 0. \end{aligned}$$

As a result we get

$$T = \frac{|t_2|^2 |(r_1 - 1)(1 - r'_1)|^2}{|t_2^2 - (2 - r_1 - r_2)(2 - r'_1 - r'_2)|^2}.$$

Putting $r_1 = 1$ we obtain $T = 0$. Thus we observe that non-conducting branch can influence the total conductance strongly.

Of course, all the discussed effects are due to interference. If the size of the system exceeds L_φ we come back to classical laws.

12.3 Additional aspects of ballistic transport

Adiabatic point contacts

The results of first observations of conductance quantization were surprising. Indeed, from quantum mechanics it is well known that any sharp potential barrier produces oscillations in the transmission coefficient as a function of the energy. However, the experimental steps were more or less rectangular. An explanation of such a behavior was given in Ref. [25]. The authors showed that if the point contact has a smooth profile, i. e. if its width d depends on the longitudinal coordinate x in a smooth way, then the $T(E)$ dependence is very close to a perfect step. To make the results simple, let us consider a channel with rectangular confinement. Let us assume that we can separate the variables in an adiabatic way, $\Psi_n(x, y) = \psi_n(x)\varphi_{n,x}(y)$, and first solve the Schrödinger equation for a given width d . In this way we get the transverse wave functions

$$\varphi_{n,x}(y) = \sqrt{\frac{2}{d(x)}} \sin \left[\pi n \frac{2y + d(x)}{d(x)} \right].$$

The Schrödinger equation for the longitudinal motion has the form

$$-\frac{\hbar^2}{2m} \frac{d^2\psi}{dx^2} + \epsilon_n(x)\psi = E\psi, \quad \epsilon_n(x) = \frac{\pi^2 n^2 \hbar^2}{2m[d(x)]^2}.$$

If the variation $d(x)$ is smooth at the scale of de Broglie wave length, k_F^{-1} , the potential $\epsilon_n(x)$ is semiclassical. Then one can use the semiclassical scheme for scattering problem and choose

$$\psi_n(x) = \sqrt{\frac{p_n(\infty)}{p_n(x)}} \exp \left[\frac{i}{\hbar} \int_0^x p_n(x') dx' \right], \quad p_n(x) = \sqrt{2m[E - \epsilon_n(x)]}.$$

The transmittance step depends occurs when the Fermi energy crosses the maximum of

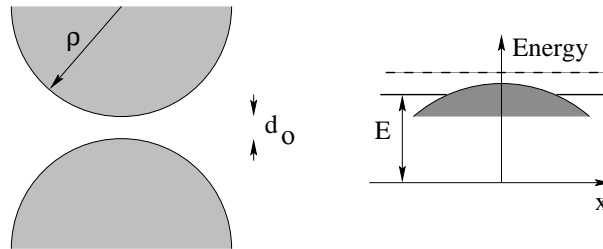


Figure 12.8: On the adiabatic quantum point contact.

the potential $\epsilon_n(x)$ for the upper transverse mode, see Fig. 12.8. Expanding the potential near its maximum we get

$$\epsilon_n(x) = \epsilon_n(0) \left[1 - \left(\frac{\partial^2 d(x)}{\partial x^2} \right)_{x=0} \frac{x^2}{d} \right].$$

Since $\partial^2 d/\partial x^2 = 2/\rho$ where ρ is the curvature radius of the center of constriction, we get the barrier as

$$U(x) = \epsilon_n(0) \left[1 - \frac{2x^2}{d\rho} \right].$$

The transmission through a parabolic barrier is known,

$$T(E) = \frac{1}{1 + \exp[-\pi^2(kd_0/\pi - n_0)\sqrt{2\rho/d_0}]}. \quad (12.9)$$

Here d_0 is the minimal width of the constriction, n_0 is the number of upper level, while $k = \hbar^{-1}\sqrt{2mE}$. We observe that the shape of the step is almost n independent, the transition being sharp at $\rho \geq d_0$. It is important that the numerical factor $\pi^2\sqrt{2}$ makes the transitions sharp even at $R \sim d_0$. The same numerical factor helps for the semiclassical condition to be valid. This criterion reads $\pi^2\sqrt{2\rho/d_0} \gg 1$. To make the motion through the contact ballistic the elastic mean free path should exceed $\sqrt{\rho d_0}$.

12.4 Electron-electron interaction in ballistic systems

The case of pure 3D metal. Concept of Fermi liquid

Let us begin with the estimate of the electron-electron scattering in a Fermi gas. Suppose that we have a particle 1 outside the Fermi sea, see Fig. 12.9. If this particle interacts

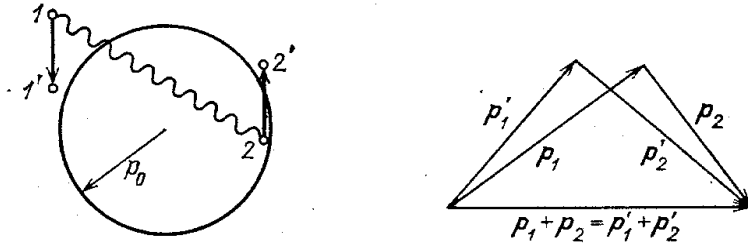


Figure 12.9: Scattering processes for electron-electron interaction.

with another one, 2, inside the Fermi sea both final states should be outside the Fermi sea (Pauli principle!). According to the momentum conservation law,

$$\mathbf{p}_1 + \mathbf{p}_2 = \mathbf{p}'_1 + \mathbf{p}'_2,$$

and, as we have seen,

$$p_1, p'_1, p'_2 > p_F; \quad p_2 < p_F.$$

The momentum conservation law is shown graphically in the right panel of Fig. 12.9. One should keep in mind that the planes $(\mathbf{p}_1, \mathbf{p}_2)$ and $(\mathbf{p}'_1, \mathbf{p}'_2)$ are not the same, they are

shown together for convenience. To get the escape probability for the particle 1 one should integrate over the intermediate momenta

$$W \propto \int \delta(\varepsilon_1 + \varepsilon_2 - \varepsilon'_1 - \varepsilon'_2) (dp_2) (dp'_1)$$

(\mathbf{p}'_2 is fixed by the momentum conservation). The energy conservation law actually determines the angle between \mathbf{p}'_1 and \mathbf{p}'_2 for given absolute values of these vectors. Consequently, the rest is to integrate over $p_2 = |\mathbf{p}_2|$ and $p'_1 = |\mathbf{p}'_1|$.

Let p_1 be close to p_F . It means that all the momenta are close to p_F and the angles with the vector $\mathbf{p}_1 + \mathbf{p}_2$ are almost the same. So let us assume cosines to be the same and from the relation between the projections write down

$$p'_1 \approx p_1 + p_2 - p'_2.$$

Now let us recall that $p'_2 > p_F$. Consequently, $p'_1 < p_1 + p_2 - p_F$. But at the same time, $p'_1 > p_F$. Thus

$$p_1 + p_2 - p_F > p_F, \text{ or } p_2 > 2p_F - p_1.$$

But from the Pauli principle, the upper limit for p_2 is p_F . As a result, we come to the following chain of inequalities

$$0 > p_2 - p_F > p_F - p_1, \quad 0 < p'_1 - p_F < (p_1 - p_F) + (p_2 - p_F).$$

Finally,

$$\int dp_2 dp'_1 = \int_{-\alpha_1}^0 d\alpha_2 \int_0^{\alpha_1 + \alpha_2} d\alpha'_1 = \frac{\alpha_1^2}{2}$$

where we have introduced $\alpha_i = p_i - p_F$. Now we should remember that $\varepsilon - \epsilon_F = v_F(p - p_F)$. So $W \propto (\varepsilon - \epsilon_F)^2$. The simplest way to estimate τ is to use dimensionality approach. Indeed, the average potential and kinetic energies are of the order of ϵ_F . Consequently, the only quantity which is proportional to $(\varepsilon - \epsilon_F)^2$ and has the time dimensionality is

$$\tau \sim \frac{\hbar \epsilon_F}{(\varepsilon - \epsilon_F)^2}.$$

We came to important conclusion: if one is interested in quasiparticles near the Fermi level, $|\varepsilon - \epsilon_F| \ll \epsilon_F$, he can treat them as to near classical ones provided

$$\frac{\hbar}{(\varepsilon - \epsilon_F)\tau} \approx \frac{\varepsilon - \epsilon_F}{\epsilon_F} \ll 1.$$

The typical value for the quasiparticle energy is $k_B T$. This is why the electron-electron interaction can be treated in the leading approximation in a self-consistent approximation. The estimates above based on the conservation laws provide background of the theory of *Fermi liquid*. The essence of this concept is that the excitations in the vicinity of the the Fermi surface can be treated as *quasiparticles* which behave as particles with renormalized velocity. Consequently, the effects of electron-electron interaction are not crucially important in pure 3D systems.

One-dimensional systems. Tomonaga-Luttinger liquid

For 1D interacting systems the above considerations are not valid because for a single branch linear dispersion near the Fermi points the energy spectrum is close to linear, $E - E_F \approx v(p - p_F)$. That means that the energy and momentum conservation laws are actually the same, and this is why they are not restrictive as in a 3D case. For this reason, the perturbative corrections describing even weak electron-electron interaction are divergent. A proper model for interactive 1D electrons is the so-called Tomonaga-Luttinger model. According to this model, collective electron modes (plasmons) with linear spectra are described by new, *boson* modes. Creation of a real electron in this model is equivalent to excitation an infinite number of plasmons. Because of that, the space and time dependence of density (and spin) correlation functions are substantially different from the ones for non-interacting systems. That manifests itself in various kinetic quantities. For example, the Drude conductivity is predicted to vary as power law with temperature.

The *Luttinger liquid* model which was previously used for 1D organic conductors now became important for high-mobility quantum wires, as well as for edge states under conditions of quantum Hall effect (see below). One can find a good review of this model in Ref. [16].

A 1D quantum wire is appropriately characterized by a conductance. If the absence of interactions, the conductance of an ideal single-mode quantum wire, adiabatically connected to leads, is quantized, $G = 2e^2/h$. In the presence of a scatterer, the conductance drops to $G = 2e^2T/h$, where T is the transmission coefficient.

The electron-electron interaction modifies dramatically the low-energy excitations in a quantum wire that leads to striking predictions for the transport. The new features manifest itself only if there is one (or several) scatterers inside the quantum wire - otherwise the correlation effects are canceled out at the contacts between the interacting quantum wire and non-interacting reservoirs. All that together leads to a rich and very interesting physical picture.

To get a flavor of the theory ¹ let us consider a spinless electrons hopping on 1D lattice with the Hamiltonian

$$\mathcal{H} = -t \sum_j c_j^\dagger c_{j+1} + \frac{V}{2} \sum_j c_j^\dagger c_j c_{j+1}^\dagger c_{j+1} + h.c.. \quad (12.10)$$

When the interaction $V = 0$ this Hamiltonian can be diagonalized as $E_k = -t \cos k$, $|k| < \pi$. The low-energy excitation exist near $\pm k_F$. Consider a single particle excitation near $+k_F$ where we remove one electron with $k < k_F$ and place it into a free state with $k + q > k_F$. Then the energy of excitation is $\hbar\omega_k = \hbar q v_F$. Adding a similar state near $-k_F$ we have a situation similar to phonons in one dimension. When the interaction is turned on this dispersion law remains, however the velocity is renormalized.

Linear spectrum implies a boson-like description. Mathematically in can be done using

¹Here we follow Ref. [16].

(Jordan-Wigner) canonical transform,

$$c_j = \exp \left(i\pi \sum_{k>j} c_k^\dagger c_k \right) b_j ,$$

that keeps the Hamiltonian (12.10) in the same form with replacement $c \rightarrow b$. One can check that the b operators at different lattice points *commute*, and therefore they are *bosons*. Now, the boson operators can be approximately decoupled as $b_j \rightarrow \sqrt{n_j} \exp(i\phi_j)$, $n_j \equiv c_j^\dagger c_j$. Then we can proceed to continuum limit, focusing on scales long compared to the lattice constant. In this way we replace

$$\phi_j \rightarrow \phi(x) , \quad n_j \rightarrow \tilde{\rho}(x) .$$

Extracting from the total electron density its average value, $\rho_0 = k_F/\pi$ and introducing the “displacement” operator, θ , as $\tilde{\rho} - \rho_0 = \partial_x \theta(x)/\pi$ we arrive at the phonon-like commutation rule,

$$[\phi(x), \theta(x')] = \frac{i\pi}{2} \delta(x - x') .$$

We observe that $\partial_x \phi$ is the momentum conjugate to θ . As a result, we arrive at the effective Hamiltonian,

$$\mathcal{H} = \frac{v}{2\pi} [g(\partial_x \phi)^2 + g^{-1}(\partial_x \theta)^2] . \quad (12.11)$$

From the commutation relations it can be seen that the Hamiltonian leads to the equation of motion

$$\partial_t^2 \theta = v^2 \partial_x^2 \theta$$

and a similar equation for ϕ . the velocity v , as well as an additional dimensionless constant g depend on the strength of interaction. For non-interacting electrons, $v = v_F$ and $g = 1$.

It is convenient to expand the original Fermion operator into two part corresponding to the motion around the points $\pm k_F$,

$$\phi(x) \approx \psi_R + \psi_L = e^{k_F x} e^{i\Phi_R} + e^{-k_F x} e^{i\Phi_L},$$

where $\Phi_{R/L} \equiv \phi \pm \theta$. These two field commute with one another and satisfy the relations,

$$[\Phi_R(x), \Phi_R(x')] = -[\Phi_L(x), \Phi_L(x')] = i\pi \operatorname{sgn}(x - x') .$$

The right and left moving electron densities can be reconstructed as

$$N_{B/L} = \pm \partial_x \Phi_{R/L} .$$

Then we can rewrite the Hamiltonian (12.11) as

$$\mathcal{H} = \pi v_0 [N_R^2 + N_L^2 + 2\lambda N_R N_L] \quad (12.12)$$

with

$$v_0 = \frac{v}{2} \left(g + \frac{1}{g} \right), \quad \lambda = \frac{1-g^2}{1+g^2}.$$

This Hamiltonian describes interacting system of right and left moving electrons. We identify v_0 to v_F , the case $g < 1$ corresponds to $\lambda > 0$ (repulsion) while $g > 1$ corresponds to attraction.

It is not straightforward how one can relate the parameters v and g with the original lattice model because we have only the effective theory for low-energy excitations. There are analytical expressions only for some models, e. g. for the case of long-range interaction comparing to the scale k_F^{-1} .

A very important point is that the parameter g has a physical meaning of dimensionless (in units e^2/h per spin) conductance of an infinite ideal Luttinger liquid. That can been traced introducing new variables, $\phi_{R/L} = g\phi \pm \theta$, that diagonalize the Hamiltonian (12.10) as

$$\mathcal{H} = \frac{\pi v}{g} (n_R^2 + n_L^2), \quad n_{R/L} = \pm \frac{1}{2\pi} \partial_x \phi_{R/L}. \quad (12.13)$$

The operators $n_{R/L}$ correspond to the densities of right and left moving *interacting* electrons. The Hamiltonian allows chiral general solutions $f(x \pm vt)$. Now we can raise the chemical potential of right chiral mode n_R by an amount μ_R Them $\delta\mathcal{H} = -e\mu_R n_R$, and minimizing (12.13) we get $n_R = (ge/2\pi v)\mu_R$. Since the additional current to the right is $I_R = en_R v$ we get

$$G = g \frac{e^2}{h}. \quad (12.14)$$

As is was already mentioned, in a quantum wire it is impossible to couple only to one chiral mode. As a result, the d.c. conductance of a finite Luttinger liquid wire coupled to noninteracting leads appears the same as for noninteracting case. However, interaction effects can be revealed in a.c. experiments, as well as in the presence of some scatterers. Because of long-range correlations, the scatterers “undress” the excitations of interacting systems. As a result, may interesting and important effects can be observed. In particular, the interaction leads to a strong renormalization of density of states near an obstacle. For example, if the Luttinger liquid wire has a large barrier with low transmission coefficient T_0 one can employ the results for the density of states in a semi-infinite liquid. That results in the nonlinear current-voltage curve at low temperatures.

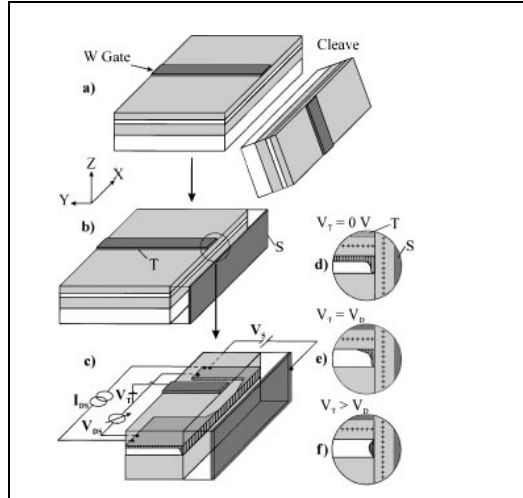
$$I \propto T_0 |V|^{2(g-1)/g} V \rightarrow G(V) \equiv \frac{dI}{dV} \propto T_0 |V|^{2(g-1)/g}.$$

Thus, got the repulsive case the linear conductance is *zero*. At finite temperature it does exist. However it is proportional to $T^{2(g-1)/g}$. It the case of weak scattering the results are substantially different.

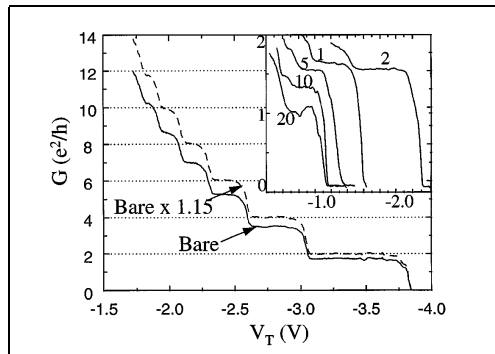
There are several experiments where some deviations from the predictions of single-electron theory were observed, such as unusual conductance quantization and anomalous temperature dependences. Unfortunately, the electron-electron correlations are effectively

destroyed by disorder and electron-phonon scattering. Therefore, to observe the interaction effect one needs extremely pure samples and low temperatures. The results of such experiment is demonstrated in Fig. 12.10.

The concept of Luttinger liquid is specifically important for quantum Hall effect systems. We shall see that near the edges of a Hall bar a specific edge states appear which can be described by the above mentioned model. This system is much more pure than quantum wires, and interaction effects are crucially important. We are going to discuss quantum Hall systems later.



(a) Wire preparation by cleaved edge overgrowth of GaAs-AlGaAs by MBE. The wire is fabricated by cleaving the specimen [see also panel (b)]. Edge states (d) form the quantum wire. Panels (e) and (f) show different charge distributions for different top voltages. The panel (c) shows a blowup of critical device region. The mean free path is estimated as 10 μm , the length of the channel is about 2 μm .



Linear response conductance of a 2 μm log wire in a 25 nm quantum well vs. the top-gate voltage (V_T) measured at a temperature 0.3 K. Solid line is the measured conductance. The dashed curve is the measured conductance multiplied by an empirical factor 1.15. Inset: Linear response conductance of the last plateau for wires of different lengths fabricated consecutively along the edge of a single 25 nm cleaved edge overgrowth specimen. The numbers denote the wire lengths in microns.

Figure 12.10: Non-universal Conductance Quantization in Quantum wires [From A. Yacoby, *et al.*, Physical Review Letters, **77**, 4612 (1996).]

Chapter 13

Tunneling and Coulomb blockage

13.1 Tunneling

Modern technology allows to fabricate various structures involving tunneling barriers. One of the ways is a split-gate structure. Such a system can be considered as a specific example

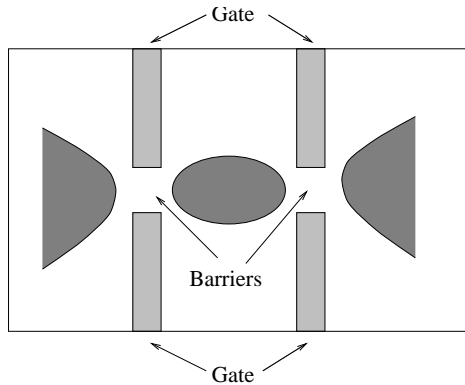


Figure 13.1: Split-gate structure allowing resonant tunneling.

of series connection of two obstacles. The complex amplitude of the wave transmitted through the whole system is

$$D = \frac{t_1 t_2 e^{i\phi}}{1 - e^{2i\phi} r_2 r'_1} = \frac{t_1 t_2 e^{i\phi}}{1 - e^\theta \sqrt{R_1 R_2}}, \quad (13.1)$$

where $\theta = 2\phi + \arg(r_2 r'_1)$. It is clear that the transmittance

$$T = \frac{T_1 T_2}{1 + R_1 R_2 - 2\sqrt{R_1 R_2} \cos \theta} \quad (13.2)$$

is maximal at some specific value of θ where $\cos \theta = 1$, the maximal value being

$$T_{\max} = \frac{T_1 T_2}{(1 - \sqrt{R_1 R_2})^2}. \quad (13.3)$$

This expression is specifically simple at $T_1, T_2 \ll 1$,

$$T_{\max} = \frac{4T_1 T_2}{(T_1 + T_2)^2}. \quad (13.4)$$

Thus we observe that two low-transparent barriers in series can have a unit transmittance if they have the same partial transparencies, $T_1 = T_2 = T$. The reason of this fact in quantum interference in the region between the barriers which makes wave functions near the barriers very large to overcome low transmittance of each barrier.

An important point is that the phase θ gained in the system is a function of the electron energy. Thus near a particular value $E^{(r)}$ defined by the equality

$$\cos \theta(E^{(r)}) = 0 \rightarrow \theta(E_k^{(r)}) = 2\pi k$$

one can expand $\cos \theta$ as

$$1 - \frac{1}{2} \left(\frac{\partial \theta}{\partial E} \right)^2 (E - E^{(r)})^2.$$

Thus at low transmittance we arrive at a very simple formula of a Breit-Wigner type,

$$\begin{aligned} T &\approx \frac{T_1 T_2}{(T_1 + T_2)^2 / 4 + (\theta')^2 (E - E^{(r)})^2} \\ &= \frac{\Gamma_1 \Gamma_2}{(\Gamma_1 + \Gamma_2)^2 / 4 + (E - E^{(r)})^2}. \end{aligned} \quad (13.5)$$

Here we denote $\theta' \equiv (\partial \theta / \partial E)_{E=E^{(r)}}$ and introduce $\Gamma_i = T_i / |\theta'|$.

The physical meaning of the quantities Γ_i is transparent. Let us assume that all the phase shift is due to ballistic motion of an electron between the barriers. Then,

$$\theta = 2ka = 2ah^{-1}\sqrt{2mE} \rightarrow \theta' = \frac{a}{\hbar} \sqrt{\frac{2m}{E}} = \frac{2a}{\hbar v}$$

where v is the electron velocity. As a result, the quantity Γ_i can be rewritten as $\Gamma = \hbar\nu_a T_i$, where $\nu_a = v/2d$ is the frequency of oscillations inside the inter-barrier region, the so-called *attempt frequency*. Thus it is clear that Γ_i are the escape rates through i -th barrier.

To specify the transition amplitudes let us consider a 1D model for a particle in a well between two barriers. We are interested in the scattering problem shown in Fig. 13.2. To find a transmission probability one has to match the wave functions and their gradients at the interfaces 1-4 between the regions **A-C**. They have the following form

$e^{ikx} + re^{-ikx}$	in the region A;
$a_1 e^{\kappa_B x} + a_2 e^{-\kappa_B x}$	in the region B;
$b_1 e^{ikx} + b_2 e^{-ikx}$	in the region C; .
$c_1 e^{\kappa_D x} + c_2 e^{-\kappa_D x}$	in the region D;
$t e^{ikx}$	in the region E

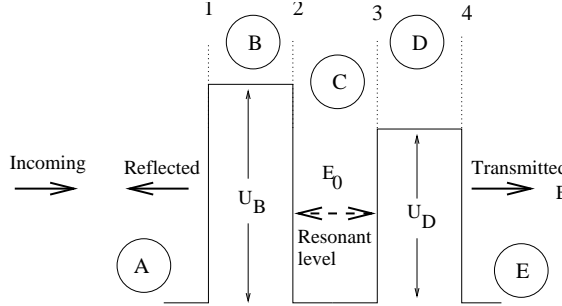


Figure 13.2: On the resonant tunneling in a double-barrier structure.

Here

$$k = \hbar^{-1} \sqrt{2mE}, \quad \kappa_i = \sqrt{\kappa_{0i}^2 - k^2}, \quad \kappa_{0i} = \hbar^{-1} \sqrt{2mU_i}.$$

The transmission amplitude is given by the quantity t while the reflection amplitude – by the quantity r . In fact we have 8 equations for 8 unknowns (r, t, a_i, b_i, c_i) , so after some tedious algebra we can find everything. For a single barrier one would get

$$T(E) = \frac{4k^2\kappa^2}{\kappa_0^4 \sinh^2(\kappa d) + 4k^2\kappa^2} \approx \frac{k^2\kappa^2}{\kappa_0^4} e^{-2\kappa d}.$$

Here d is the barrier's thickness. So the transparency exponentially decays with increase of the product κd . The calculations for a double-barrier structure is tedious, so we consider a simplified model of the potential

$$U(x) = U_0 d [\delta(x) + \delta(x - a)].$$

In this case we have 3 regions,

$$\begin{aligned} & e^{ikx} + r e^{-ikx} && x < 0. \\ & A \sin kx + B \cos kx && 0 < x < a, \\ & t e^{ik(x-a)} && x > a \end{aligned} \tag{13.7}$$

The matching conditions for the derivatives at the δ -functional barrier has the form

$$\psi'(x_0 + 0) - \psi'(x_0 - 0) = \kappa^2 d \psi(x_0). \tag{13.8}$$

Here $\kappa^2 = 2mU_0/\hbar^2$. One can prove it by integration of the Schrödinger equation

$$(\hbar^2/2m)\nabla^2\psi + U_0 d \delta(x - x_0) \psi = E\psi$$

around the point x_0 . Thus we get the following matching conditions

$$\begin{aligned} B &= 1 + r, \\ kA - ik(1 - r) &= \kappa^2 a(1 + r), \\ A \sin ka + B \cos ka &= t, \\ ikt - k(A \cos ka - B \sin ka) &= t\kappa^2 a. \end{aligned}$$

First one can easily see that there is a solution with *zero reflectance*, $r = 0$. Substituting $r = 0$ we get the following requirement for the set of equation to be consistent

$$k = k_0, \quad \tan k_0 a = -\frac{2k_0}{\kappa^2 d}. \quad (13.9)$$

We immediately observe that at $k = k_0$ the total transmission amplitude $|t| = 1$ and there is no reflection.

Equation (13.9) can be rewritten as

$$\tan z = -\eta z, \quad \text{where } \eta \equiv 2/\kappa^2 da = \hbar^2/mU_0 ad.$$

The solution of this equation can be found graphically. For “strong barriers”, $\eta \ll 1$ the solution tends to

$$k_0 a = s\pi, \quad s = 0, \pm 1, \dots$$

while for “weak” barriers

$$k_0 a = (s + 1/2)\pi.$$

Physically, that means that an electron gains the phase $2\pi s$ during its round trip (cf. with optical interferometer). Thus two barriers in series can have perfect transparency even if the transparency of a single barrier is exponentially small. The physical reason is *quantum interference*.

The condition (13.9) defines the energy

$$E_0 = \frac{\hbar^2 k_0^2}{2m}$$

where the transparency is maximal. Near the peak one can expand all the quantities in powers of

$$k - k_0 \approx \frac{E - E_0}{(\partial E / \partial k)_{k_0}} \approx k_0 \frac{E - E_0}{2E_0}.$$

The result for a general case can be expressed in the Breit-Wigner form

$$T(E) = \frac{\Gamma_L \Gamma_R}{(E - E_0)^2 + \frac{1}{4}(\Gamma_L + \Gamma_R)^2}.$$

Here $\Gamma_{L(R)}/\hbar$ are the *escape rates* for the electron inside the well to the left(right) lead. They are given by the attempt frequency $v_0/2a = \hbar k_0/2ma$ times the transparency of a given barrier.

Of course, if voltage across the system is zero the total number of electrons passing along opposite directions is the same, and the current is absent. However, in a biased system we obtain the situation shown in Fig. 13.3. *Negative* differential conductance, $dJ/dV \leq 0$, allows one to make a generator. One can also control the system moving the level E_0 with respect to the Fermi level by the gate voltage. In this way, one can make a *transistor*.

Commercial resonant tunneling transistors are more complicated than the principle scheme described above. A schematic diagram of a real device is shown in Fig. 13.4. In

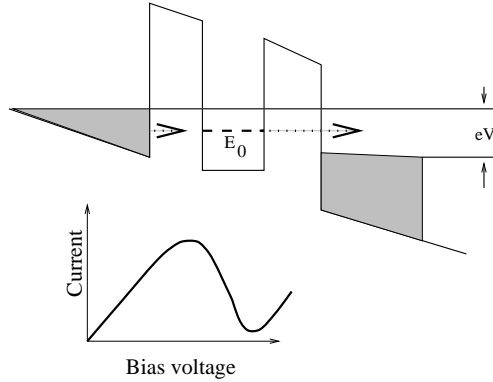


Figure 13.3: Negative differential conductance in double-barrier resonant-tunneling structure.

this device resonant tunneling takes place through localized states in the barrier. There exist also transistors with two quantum wells where electrons pass through the resonant levels in two quantum wells from the emitter to collector if the levels are aligned. The condition of alignment is controlled by the collector-base voltage, while the number of electrons from emitter is controlled by the base-emitter voltage.

13.2 Coulomb blockade

Now let us discuss a specific role of Coulomb interaction in a mesoscopic system. Consider a system with a dot created by a split-gate system (see above).

If one transfers the charge Q from the source to the grain the change in the energy of the system is

$$\Delta E = QV_G + \frac{Q^2}{2C}.$$

Here the first item is the work by the source of the gate voltage while the second one is the energy of Coulomb repulsion at the grain. We describe it by the effective capacitance C to take into account polarization of the electrodes. The graph of this function is the parabola with the minimum at

$$Q = Q_0 = -CV_G,$$

So it can be tuned by the gate voltage V_G . Now let us remember that the charge is transferred by the electrons with the charge $-e$. Then, the energy as a function of the number n of electrons at the grain is

$$\Delta E(n) = -neV_G + \frac{n^2e^2}{2C}.$$

Now let us estimate the difference

$$\Delta E(n+1) - \Delta E(n) = -eV_G + n\frac{e^2}{C}.$$

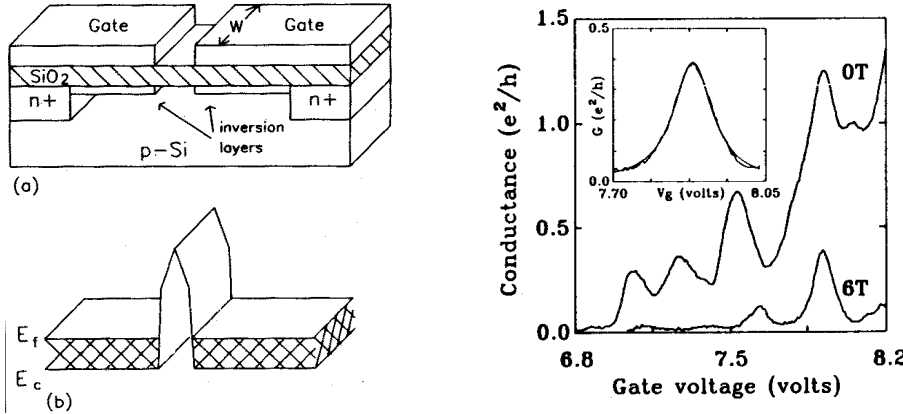


Figure 13.4: Schematic diagram of a Si MOSFET with a split gate (a), which creates a potential barrier in the inversion layer (b). In the right panel oscillations in the conductance as a function of gate voltage at 0.5 K are shown. They are attributed to resonant tunneling through localized states in the barrier. A second trace is shown for a magnetic field of 6 T. From T. E. Kopley *et al.*, Phys. Rev. Lett. **61**, 1654 (1988).

We observe that at certain values of V_G ,

$$V_{Gn} = n \frac{e}{C}, \quad (13.10)$$

the difference vanishes. It means that only at those values of the gate voltage resonant transfer is possible. Otherwise one has to pay for the transfer that means that only inelastic processes can contribute. As a result, at

$$k_B T \leq \frac{e^2}{2C}$$

the linear conductance is exponentially small if the condition (13.10) is met. This phenomenon is called the Coulomb blockade of conductance.

As a result of the Coulomb blockade, electron tunnel *one-by-one*, and the conductance vs. gate voltage dependence is a set of sharp peaks. That fact allows one to create a so-called *single-electron transistor* (SET) which is now the *most sensitive* electrometer. Such a device (as was recently demonstrated) can work at room temperature provided the capacitance (size!) is small enough.

Coulomb blockade as a physical phenomenon has been predicted by Kulik and Shekhter [26]. There are very good reviews [13, 14, 15] about single-change effects which cover both principal and applied aspects. Below we shall review the simplest variant of the theory, so called “orthodox model”.

A simple theory of single charge tunneling

For simplicity, let us ignore discrete character of energy spectrum of the grain and assume that its state is fully characterized by the number n of excess electrons with respect to

an electrically neutral situation. To calculate the energy of the systems let us employ the equivalent circuit shown in Fig. 13.5. The left (emitter) and right (collector) tunnel

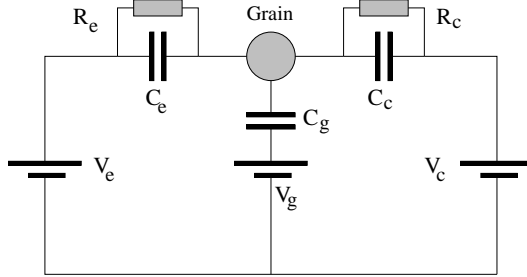


Figure 13.5: Equivalent circuit for a single-electron transistor. The gate voltage, V_g , is coupled to the grain via the gate capacitance, C_g . The voltages V_e and V_c of emitter and collector are counted from the ground.

junctions are modeled by partial resistances and capacitances.

The charge conservation requires that

$$\begin{aligned} -ne &= Q_e + Q_c + Q_g \\ &= C_e(V_e - U) + C_c(V_c - U) + C_g(V_g - U), \end{aligned} \quad (13.11)$$

where U is the potential of the grain. The effective charge of the grain is hence

$$Q = CU = ne + \sum_{i=e,c,g} C_i V_i, \quad C \equiv \sum_i C_i.$$

This charge consists of 4 contributions, the charge of excess electrons and the charges induced by the electrodes. Thus, the electrostatic energy of the grain is

$$E_n = \frac{Q^2}{2C} = \frac{(ne)^2}{2C} + \frac{ne}{C} \sum_i C_i V_i + \frac{1}{2C} \left(\sum_i C_i V_i \right)^2. \quad (13.12)$$

The last item is not important because it is n -independent. In the stationary case, the currents through both junctions are the same. Here we shall concentrate on this case. In the non-stationary situation, an electric charge can be accumulated at the grain, and the currents are different.

To organize a transport of one electron one has to transfer it first from emitter to grain and then from grain to collector. The energy cost for the first transition,

$$E_{n+1} - E_n = \frac{(2n+1)e^2}{2C} + \frac{e}{C} \sum_i C_i V_i \quad (13.13)$$

must be less than the voltage drop eV_e . In this way we come to the criterion

$$E_n - E_{n+1} + eV_e \geq 0. \quad (13.14)$$

In a similar way, to organize the transport from grain to collector we need

$$E_{n+1} - E_n - eV_c \geq 0. \quad (13.15)$$

The inequalities (13.15) and (13.14) provide the relations between V_e , V_c and V_g to make the current possible. For simplicity let us consider a symmetric system, where

$$G_e = G_c = G, \quad C_e = C_c \approx C/2 \quad (C_g \ll C), \quad V_e = -V_c = V_b/2$$

where V_b is bias voltage. Then we get the criterion,

$$V_b \geq (2n + 1)|e|/C - 2(C_g/C)V_g.$$

We observe that there is a threshold voltage which is necessary to exceed to organize transport. This is a manifestation of *Coulomb blockade*. It is important that the threshold linearly depends on the gate voltage which makes it possible to create a transistor. Of course, the above considerations are applicable at zero temperature.

The current through the emitter-grain transition we get

$$I = e \sum_n p_n [\Gamma_{e \rightarrow g} - \Gamma_{g \rightarrow e}]. \quad (13.16)$$

Here p_n is the stationary probability to find n excess electrons at the grain. It can be determined from the balance equation,

$$p_{n-1}\Gamma_{n-1}^n + p_{n+1}\Gamma_{n+1}^n - (\Gamma_n^{n-1} + \Gamma_{n+1}^n)p_n = 0. \quad (13.17)$$

Here

$$\Gamma_{n-1}^n = \Gamma_{e \rightarrow g}(n-1) + \Gamma_{c \rightarrow g}(n-1); \quad (13.18)$$

$$\Gamma_{n+1}^n = \Gamma_{g \rightarrow e}(n+1) + \Gamma_{g \rightarrow c}(n+1). \quad (13.19)$$

The proper tunneling rates can be calculated from the golden rule expressions using tunneling transmittance as perturbations. To do that, let us write down the Hamiltonian as

$$\begin{aligned} \mathcal{H}_0 &= \mathcal{H}_e + \mathcal{H}_g + \mathcal{H}_{ch} + \mathcal{H}_{bath}; \\ \mathcal{H}_{e,c} &= \sum_{\mathbf{k}\sigma} \epsilon_{\mathbf{k}} c_{\mathbf{k}\sigma}^\dagger c_{\mathbf{k}\sigma}, \\ \mathcal{H}_g &= \sum_{\mathbf{q}\sigma} \epsilon_{\mathbf{q}} c_{\mathbf{q}\sigma}^\dagger c_{\mathbf{q}\sigma}, \\ \mathcal{H}_{ch} &= (\hat{n} - Q_0)/2C, \quad \hat{n} = \sum_{\mathbf{q}\sigma} c_{\mathbf{q}\sigma}^\dagger c_{\mathbf{q}\sigma} - N^+. \end{aligned}$$

Here \mathcal{H}_{bath} is the Hamiltonian for the thermal bath. We assume that emitter and collector electrodes can have different chemical potentials. N^+ is the number of positively charged

ions in the grain. To describe tunneling we introduce the tunneling Hamiltonian between, say, emitter and grain as

$$\mathcal{H}_{e \leftrightarrow g} = \sum_{\mathbf{k}, \mathbf{q}, \sigma} T_{\mathbf{kq}} c_{\mathbf{k}\sigma}^\dagger c_{\mathbf{q}\sigma} + \text{h.c.}$$

Applying the golden rule we obtain

$$\Gamma_{e \rightarrow g}(n) = \frac{G_e}{e^2} \int_{-\infty}^{\infty} d\epsilon_k \int_{-\infty}^{\infty} d\epsilon_q f_e(\epsilon_k) [1 - f_g(\epsilon_q)] \delta(E_{n+1} - E_n - eV_e).$$

Here we have introduced the tunneling conductance of $e - g$ junction as

$$G_e = (4\pi e^2/\hbar) g_e(\epsilon_F) g_g(\epsilon_F) \mathcal{V}_e \mathcal{V}_g \langle |T_{\mathbf{kq}}|^2 \rangle.$$

along the Landauer formula, $\mathcal{V}_{e,g}$ being the volumes of the lead and grain, respectively. In this way one arrives at the expressions

$$\Gamma_{e \rightarrow g}(n, V_e) = \Gamma_{g \rightarrow e}(-n, -V_e) = \frac{2G_e}{e^2} \mathcal{F}(\Delta_{+,e}); \quad (13.20)$$

$$\Gamma_{g \rightarrow c}(n, V_c) = \Gamma_{c \rightarrow g}(-n, -V_c) = \frac{2G_c}{e^2} \mathcal{F}(\Delta_{-,c}). \quad (13.21)$$

Here

$$\mathcal{F}(\epsilon) = \frac{\epsilon}{1 + \exp(-\epsilon/kT)} \rightarrow \epsilon \Theta(\epsilon) \text{ at } T \rightarrow 0,$$

while

$$\Delta_{\pm,\mu}(n) = E_n - E_{n\pm1} \pm eV_\mu = \frac{1}{C} \left[\frac{e^2}{2} \mp en \mp e \sum_i C_i V_i \right] \pm eV_\mu$$

is the energy cost of transition. The temperature-dependent factor arise from the Fermi occupation factor for the initial and final states, physically they describe thermal activation over Coulomb barrier. The results of calculation of current-voltage curves for a symmetric transistor structure are shown in Fig. 13.6. At low temperatures and low bias voltages, $VC/e < 1$, only two charge states play a role. At larger bias voltage, more charge states are involved. To illustrate this fact, a similar plot is made for symmetrically biased transistor, $V_e = -V_g = V/2$, for different values of Q_0 , Fig. 13.7.

Cotunneling processes

As we have seen, at low temperature the sequential tunneling can be exponentially suppressed by Coulomb blockade. In this case, a higher-order tunneling process transferring electron charge coherently through two junctions can take place. For such processes the excess electron charge at the grain exists only virtually.

A standard next-order perturbation theory yields the rate

$$\Gamma_{i \rightarrow f} = \frac{2\pi}{\hbar} \left| \sum_{\psi} \frac{\langle i | \mathcal{H}_{\text{int}} | \psi \rangle \langle \psi | \mathcal{H}_{\text{int}} | i \rangle}{E_\psi - E_i} \right|^2 \delta(E_i - E_f).$$

Two features are important.

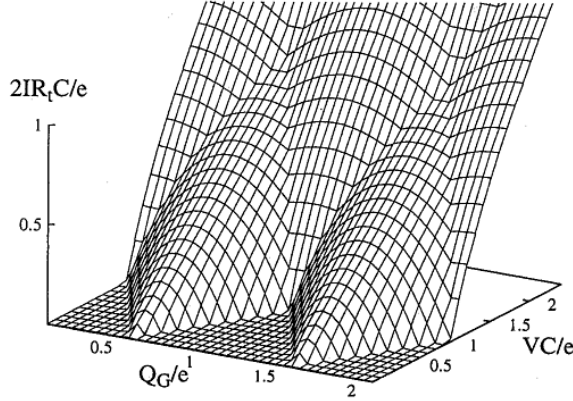


Figure 13.6: The current of a symmetric transistor as a function of gate and bias voltage at $T = 0$ (from the book [5]).

- There are 2 channel which add coherently: (i) $e \rightarrow g, g \rightarrow c$ with the energy cost $\Delta_{-,e}(n+1)$, and (ii) $g \rightarrow c, e \rightarrow g$ with the energy cost $\Delta_{+,c}(n-1)$.
- The leads have macroscopic number of electrons. Therefore, with overwhelming probability the outgoing electron will come from a different state than the one which the incoming electron occupies. Hence, after the process an *electron-hole excitation* is left in the grain.

Transitions involving different excitations are added incoherently, the result being

$$\begin{aligned} \Gamma_{\text{cot}} &= \frac{\hbar G_e G_c}{2\pi e^4} \int_e d\epsilon_k \int_g d\epsilon_q \int_g d\epsilon_{q'} \int_c d\epsilon_{k'} f(\epsilon_k)[1-f(\epsilon_q)]f(\epsilon_{q'})[1-f(\epsilon_{k'})] \\ &\quad \times \left[\frac{1}{\Delta_{-,e}(n+1)} + \frac{1}{\Delta_{+,c}(n-1)} \right]^2 \delta(eV + \epsilon_k - \epsilon_q + \epsilon_{q'} - \epsilon_{k'}). \end{aligned}$$

At $T = 0$ the integrals can be done explicitly, and one obtains

$$\Gamma_{\text{cot}} = \frac{\hbar G_e G_c}{12\pi e} \left[\frac{1}{\Delta_{-,e}(n+1)} + \frac{1}{\Delta_{+,c}(n-1)} \right]^2 V^3 \quad \text{for } eV \ll \Delta_i.$$

As a result, the current appears proportional to V^3 that was observed experimentally. The situation is not that simple for the degenerate case when $\Delta_i = 0$. In that case the integrals are divergent and the divergence must be removed by a finite life time of a state. A detailed treatment of that case is presented in the book [5].

There is also a process when an electron tunnels through the system leaving no excitations in the grain. The probability of such *elastic cotunneling* has a small factor $(g_g V_g)^{-1}$. However, it leads to the current, proportional to V , thus it can be important at very low bias voltage.

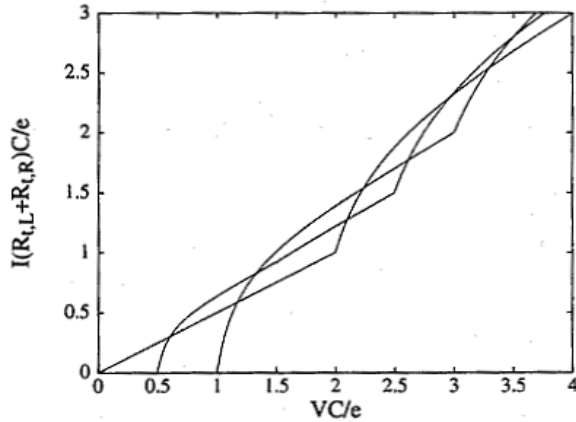


Figure 13.7: The current of asymmetric transistor, $G_e = 10G_c$, as a function of bias voltage at $T = 0$ and different $Q_0/e = 0, 0.25$ and 1 (from the book [5]). At $Q_0 = 0$ the Coulomb blockade is pronounced, while at $Q_0/e = 0.5$ the current-voltage curve is linear at small bias voltage. The curves of such type are called the *Coulomb staircase*.

Concluding remarks

There are many experiments where Coulomb-blockaded devices are investigated. Probably most interesting are the devices where tunneling takes place through a small quantum dot with discrete spectrum. An example of such device is shown in Fig. 13.8. The linear conductance of such a structure as a function of the gate electrode C is shown in Fig. 13.9. An important point is that at present time the devices can be fabricated so small that the criterion $kT \leq e^2/C$ can be satisfied at room temperatures. Now several room temperature operating Coulomb blockade devices were reported. Among them are devices consisting of large molecules with the probes attached in different ways. This is probably a starting point for new extremely important field - *molecular electronics*. Such devices are extremely promising both because they are able to operate at room temperatures and because they will allow high integration. This is one of important trends. Another one concerns with single-electron devices which include superconducting parts. There is a lot of interesting physics regarding transport in such systems.

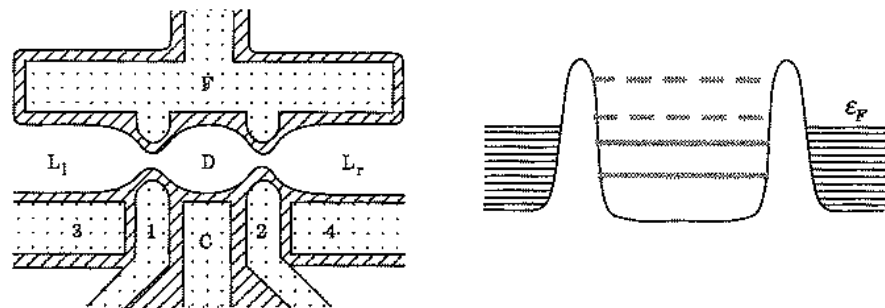


Figure 13.8: (a) A typical structure of a quantum dot. The depleted (shaded) areas are controlled by electrodes 1-4, C, and F. Electrode C also controls the electrostatic potential in the dot. (b) a model of a quantum dot. From [7].

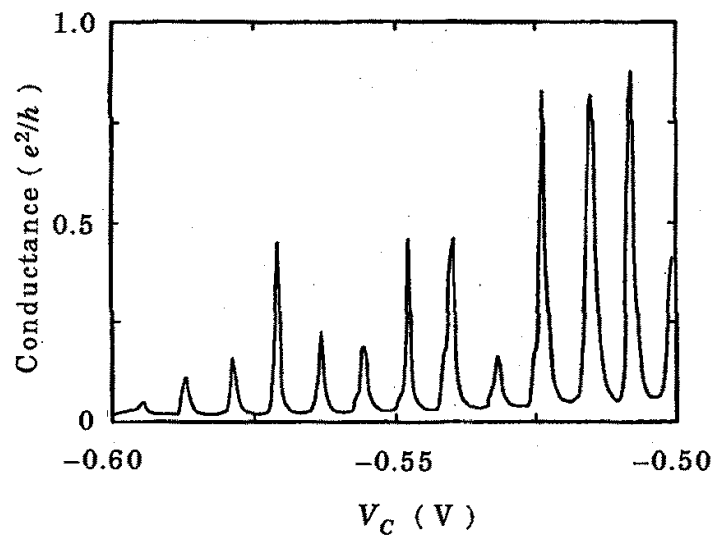


Figure 13.9: Conductance of a quantum dot vs. the voltage of gate electrode C. From L. P. Kouwenhoven *et al.*, Z. Phys. B **85**, 367 (1991).

Chapter 14

Quantum Hall Effect and Adiabatic Transport

14.1 Ordinary Hall effect

In a magnetic field electrons' trajectories are curved because of Lorentz force. As a result,

$$\mathbf{j} = \sigma_0 (\mathbf{E} + [\mathbf{j} \times \mathbf{H}]/nec) , \quad \sigma_0 = ne^2\tau/m .$$

One can solve this vector equation to obtain the resistivity tensor

$$\hat{\rho} = \begin{bmatrix} \rho_0 & H/enc \\ -H/enc & \rho_0 \end{bmatrix} , \quad \rho_0 = 1/\sigma_0 .$$

The inversion of this tensor gives the *conductivity tensor* with the components (in 2d case)

$$\sigma_{xx} = \frac{\sigma_0}{1 + (\omega_c\tau)^2} , \quad \sigma_{xy} = \frac{nec}{H} + \frac{1}{\omega_c\tau}\sigma_{xx} . \quad (14.1)$$

There is a striking similarity between the quantization of the conductance of a ballistic channel in units of e^2/h and of the Hall conductance.

14.2 Integer Quantum Hall effect - General Picture

In the quantum case one faces the Landau levels. We have seen that the number of states per unit area for a filled Landau level is

$$n_H = 1/2\pi a_H^2 = eH/ch .$$

Usually the *filling factor*

$$\nu = n/n_H$$

for a fractionally filled level is introduced. The total degeneracy of a Landau level in the absence of disorder is $N = An_B = A/2\pi a_H^2$ where A is the sample area. The average density of states is $An_B/\hbar\omega_c$.

If one expresses the Hall component of the conductivity tensor through the filling factor ν and assumes $\omega_c\tau \rightarrow \infty$ he obtains $\sigma_{xy} = \nu e^2/h$. This result seems very fundamental. Indeed, according to the electrodynamics, one can eliminate the electric field on a *spatially-homogeneous* system by assuming a drift velocity

$$\mathbf{v} = c [\mathbf{E} \times \mathbf{H}] / H^2.$$

Thus, the result seems fundamental independently whether classical or quantum mechanics is discussed.

Experimentally, the following picture was observed. It is clear that only violation of

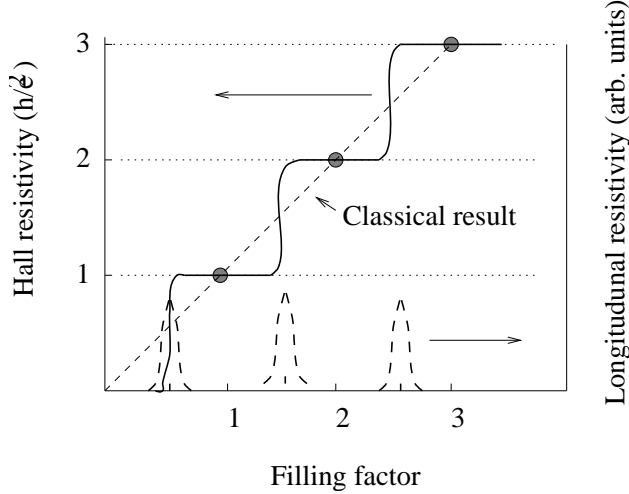


Figure 14.1: Schematic dependence of Hall resistance on filing factor.

the translational invariance can lead to such a picture. Thus one has to consider either impurities, or edges.

The generally accepted picture is as follows. Impurities violate the translational invariance. As a result, p_y is not a good quantum number any more, and Landau levels smear into sub-bands. The crucial point that the most of the states are *localized* and cannot carry the current.

To make the analysis as simple as possible let us discuss a 2d electrons in crossed electric and magnetic fields ($\mathbf{E} \parallel \mathbf{x}$, $\mathbf{H} \parallel \mathbf{z}$) and a single impurity at the point $\mathbf{r}_0 = \{x_0, y_0\}$. As we have seen (see Sec. 6.9, *Shubnikov-de Haas effect*), the weak electric field leads to the energy shift $p_y v$ where $v = cE/H$ is the drift velocity in y -direction, as well as to the shift in the center-of-motion co-ordinate is shifted in x -direction by v/ω_c . Using the corresponding states as a basis, we can now expand the exact wave function as

$$\Psi = \sum_{np_y} c_{np_y} \psi_{np_y}(\mathbf{r}).$$

We get

$$\sum_{np_y} c_{np_y} [\hat{\mathcal{H}}_0 + V] \psi_{np_y} = \sum_{np_y} c_{np_y} [E_{np_y} + V] \psi_{np_y} = E \sum_{np_y} c_{np_y} \psi_{np_y}.$$

Let us now express the potential as

$$V = \lambda \delta(\mathbf{r} - \mathbf{r}_0)$$

where λ is a proper coupling constant. Then one can write

$$c_{np_y} = \lambda \frac{\psi_{np_y}^*(\mathbf{r}_0) \Psi(\mathbf{r}_0)}{E - E_{np_y}}.$$

Now we recall that $\sum_{np_y} c_{np_y} \psi_{np_y}(\mathbf{r}_0) = \Psi(\mathbf{r}_0)$. Substituting the previous expression into this equation and dividing by $\Psi(\mathbf{r}_0)$, we get the exact condition for eigen energy

$$\frac{1}{\lambda} = \sum_{n,p_y} \frac{|\psi_{n,p_y}(\mathbf{r}_0)|^2}{E - E_{n,p_y}}.$$

The right hand side of this equation as a function of the energy is shown below. One can

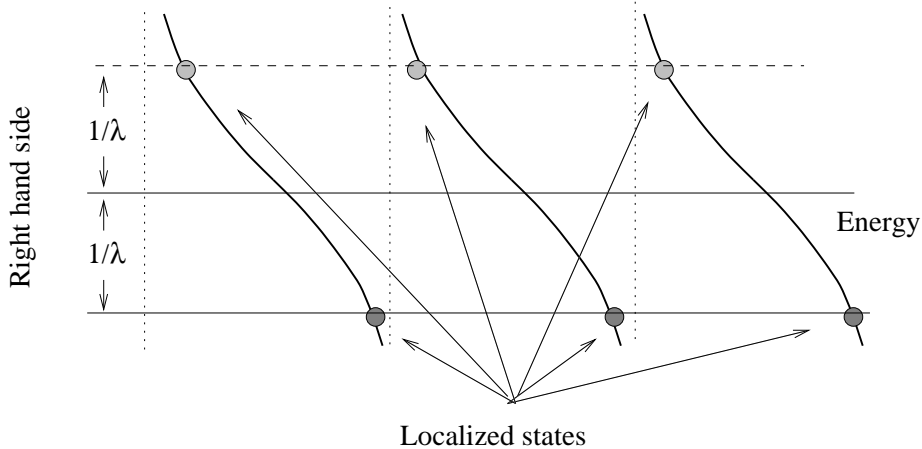


Figure 14.2: Formation of localized states in 2DEG in magnetic field.

find from this equation one completely localized state for each Landau level, its energy shift being proportional to λ . The lowest such state can be represented as (for $\mathbf{r}_0 = 0$)

$$\psi_{\text{loc}} \sim \exp \left[\frac{ixy}{2a_H^2} - \frac{x^2 + y^2}{4a_H^2} \right].$$

The other levels are almost unperturbed and extended.

Now let us take into account only the lowest Landau level which we assume to be completely filled. We have one localized state and $N - 1$ extended ones where $N = A/2\pi a_H^2$, which we can label by the discrete quantum number k as

$$k = \frac{p_y L_y}{2\pi\hbar}.$$

Each mode behaves just as the transverse mode in a quantum channel, and the current is given as

$$I = -\frac{2}{h} \sum_{nk} (E_{n,k+1} - E_{nk}) = -\frac{2}{h} \sum_{nk} (E_{n,k_{\max}} - E_{n,k_{\min}}).$$

It is not trivial to prove this equation. It was done by R. Prange using gauge considerations.

Proof :

The main procedure is as follows. We have specified periodic boundary conditions along y -axis. Consider the system as a cylinder and introduce an auxiliary constant vector-potential $\tilde{\mathbf{A}}$ along y axis as

$$\tilde{A}_y = \frac{\hbar c}{e} \frac{2\pi\alpha}{L_y}. \quad (14.2)$$

Increase of the parameter α by one corresponds to increase the magnetic flux in the sample by 1 quantum, Φ_0 .

If one applies periodic boundary conditions then the vector-potential such as given by Eq. (14.2) can be eliminated by the gauge transform

$$\psi \rightarrow \exp(2\pi\alpha y/L_y)\psi$$

only if α is integer. Thus the *extended* states which extend from 0 to L_y *must* depend on α while localized states satisfy boundary conditions automatically since their amplitude at the boundaries vanish. The extended states in the presence of the auxiliary have the same form as in its absence, with the replacement

$$k \rightarrow k + \alpha.$$

The vector potential $\tilde{\mathbf{A}}$ leads to an additional item in the effective Hamiltonian,

$$\delta\mathcal{H} = -\frac{1}{c}(\mathbf{I} \cdot \tilde{\mathbf{A}}).$$

Thus, the current operator can be written as

$$\hat{I}_y = -\frac{1}{c} \frac{\partial \delta\mathcal{H}}{\partial \tilde{A}_y} = -\frac{e}{h} \frac{\partial \mathcal{H}}{\partial \alpha},$$

while the average current is

$$I = \langle \hat{I} \rangle = -\frac{e}{h} \frac{d}{d\alpha} \sum_{nk} E_{nk}(\alpha).$$

As we have already mentioned, according to the construction of the quantum number k the introduction of the vector-potential leads to the replacement $k \rightarrow k + \alpha$. Thus

$$E_{n,k}|_{\alpha=1} = E_{n,k+1}|_{\alpha=0}.$$

Replacing the derivative by the average value over the region $0 \leq \alpha \leq 1$ we get the result given above.

Thus we come to the following picture. as the Fermi level passes the regions of the

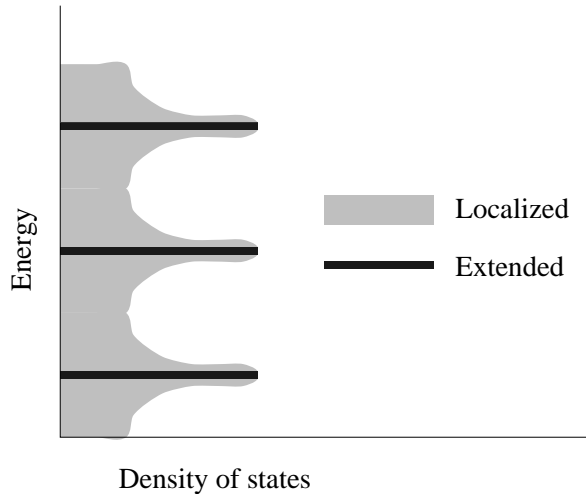


Figure 14.3: Density of states in 2DEG in magnetic field.

extended states the steps in Hall resistance and peaks at the longitudinal resistance occur. As we have shown, the current is *independent* of the density of states, only the number of occupied extended states is important.

Now we have to remember that the state with $k_{\max}(k_{\min})$ correspond to the upper (lower) edge of the sample if we map the quantum number k to the centers of gravity of the states. Thus we come in a natural way to edge states.

14.3 Edge Channels and Adiabatic Transport

The quantization of the conductance of the ballistic channel arises from the finite number of *propagating modes* each of which can carry only a very specific current. Thus it is tempting to consider the modes of an ideal finite system embedded into an external magnetic field. In

this simplified picture we can obtain some understanding concerning the nature of localized and extended states.

Let us start from a *ideal* electron system confined by the potential $V(x)$ in the presence of the magnetic field $\mathbf{H} \parallel \mathbf{z}$. For a single spin component we have the Hamiltonian

$$\mathcal{H} = \frac{p_x^2}{2m} + \frac{[p_y + (eH/c)x]^2}{2m} + V(x).$$

It is natural to look for a solution in the form (\mathcal{H} commutes with p_y !)

$$|n, k\rangle = \psi_{nk}(x)e^{iky}$$

where $\hbar k$ is the eigenvalue of p_y . The average velocity for such a state is

$$v_n(k) = \left\langle n, k \left| \frac{p_y + (eH/c)x}{m} \right| n, k \right\rangle = \left\langle n, k \left| \frac{\partial \mathcal{H}}{\partial p_y} \right| n, k \right\rangle = \frac{1}{\hbar} \frac{dE_n(k)}{dk}.$$

It is easy to calculate such a velocity for a parabolic confinement,

$$V(x) = \frac{1}{2}m\omega_0^2x^2.$$

The result is

$$v(k) = \frac{\hbar k}{M} = \frac{\hbar k}{m} \frac{1}{1 + (\omega_c/\omega_0)^2}.$$

To understand what is going on let us consider a classical orbit with the center (X, Y) . Then one can write

$$x = X + v_y/\omega_c, \quad y = Y - v_x/\omega_c.$$

The quantity $r_c = v/\omega_c$ is the cyclotron radius of the orbit. We have two constants of motion, the energy E and X . In a long strip of width W the trajectories can be classified as a cyclotron orbits , skipping orbits, or traversing trajectory. In the (X, E) space such trajectories are separated by the line

$$(X \pm W/2)^2 = r_c^2.$$

According to quantum mechanics, the motion is quantized, and we come to the following picture of quantum terms The cyclotron orbits (solid lines) correspond to Landau level, and they have zero group velocities. We have not shown traversing trajectories which correspond to higher energies. Dashed lines reproduce two sets of edge states (corresponding to skipping orbits). These sets carry the currents in opposite directions.

If the Fermi level is situated *between* the Landau levels, only the edge states can contribute to the current. Their dispersion law can be obtained (approximately) from the Bohr-Sommerfeld quantization condition,

$$\hbar^{-1} \oint p_x dx + \gamma = 2\pi n, \quad n = 1, 2, \dots$$

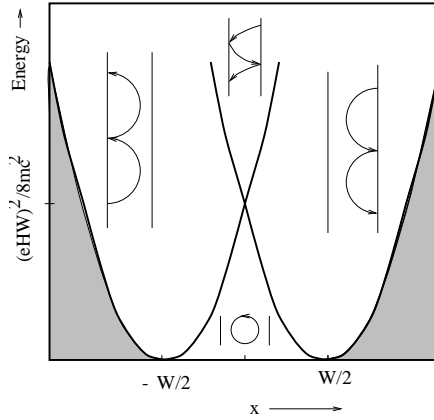


Figure 14.4: Typical electron trajectories in a 2D strip in magnetic field.

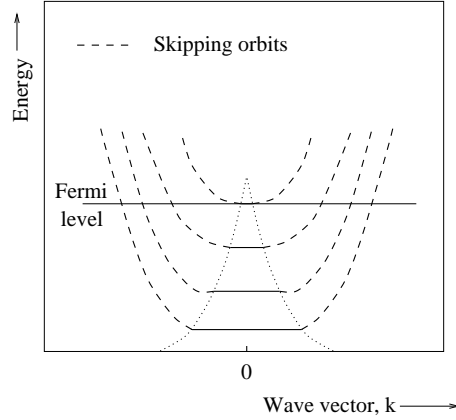


Figure 14.5: Electron terms in a 2D strip in magnetic field.

One can show that for the rigid boundary the phase shift of the skipping orbit $\gamma = \pi/2$, while

$$p_x = mv_x = (eH/c)(Y - y).$$

Thus,

$$\frac{1}{a_H^2} \oint (Y - y) dx = 2\pi \frac{\Phi}{\Phi_0} = 2\pi \left(n - \frac{\gamma}{2\pi} \right).$$

Consider an electron at the Fermi level. Its energy consists of $(n - 1/2)\hbar\omega_c$ (+ spin contribution which I do not discuss now), as well the the part

$$E_G = \epsilon_F - (n - 1/2)\hbar\omega_c$$

due to electrostatic potential created by the edges, as well as by disorder. In an external potential, the center of the orbit moves with the drift velocity

$$v_d(\mathbf{R}) = \frac{c}{eH} [\nabla V(\mathbf{R}) \times \mathbf{H}]$$

which is parallel to the equipotentials. That can be easily shown from classical mechanics in a magnetic field. The typical spread of the wave function along the guiding center is spread within the range of magnetic length a_H . Now we can map the classical picture to quantum mechanics according to $\hbar k \rightarrow -x(eH/c)$. Thus, if the typical scale of the random potential of the disorder is greater than the magnetic length, we arrive at the picture.



Figure 14.6: Electron terms in the presence of long-range disorder.

Assume that the edges are in a local equilibrium. Thus if there is a difference $\delta\zeta$ chemical potentials *between the edges*, then each channel contributes $(e/h)\delta\zeta$ to the current in the *Hall direction*. The system appears robust because to obtain a inter-channel exchange one needs tunneling with exponentially low probability. Actually we have an almost ideal ballistic conductor and the only difference with the systems discussed earlier is that the edge channels with different directions of the current do not overlap in space.

In a typical realistic situation, the contacts are out of local equilibrium and the measured resistance depends on the properties of contacts. Consider for example, a situation when the edge channel at the lower edge are in equilibrium at chemical potential E_F , while the edge channel at the upper edge are not in local equilibrium. Then the current at the upper edge is not equipartitioned between N modes. Let f_n is the fraction of the total current I that is carried by states above E_F in the n th channel at the upper edge, $I_n = f_n I$. The voltage contact at the upper edge will measure a chemical potential which depends on how it is coupled to each of the edge channels. The transmission probability T_n is the fraction of the current I_n that is transmitted through the voltage probe to a reservoir at chemical potential $E_F + \delta\zeta$. The incoming current

$$I_{\text{in}} = \sum_n^N T_n f_n I, \quad \text{with} \quad \sum_n f_n = 1, \quad (14.3)$$

has to be balanced by an outgoing current,

$$I_{\text{out}} = \frac{e}{h} \delta\zeta (N - R) = \frac{e}{h} \delta\zeta \sum_n T_n, \quad (14.4)$$

since the voltage probe draws no net current. Thus the Hall resistance,

$$R_h = \frac{\delta\zeta}{eI} = \frac{h}{e^2} \left(\sum_n T_n f_n \right) \left(\sum_n T_n \right)^{-1}. \quad (14.5)$$

The Hall conductance remains quantized only if $f_n = 1/N$, or at $T_n = 1$. The first case corresponds to local equilibrium, while the second case corresponds to an ideal contact. The Landauer-Büttiker formalism forms the basis on which anomalies in the QHE due to absence of local equilibrium in combination with non-ideal contacts can be treated theoretically.

This is a simplified picture of the integer quantum Hall effect in the random potential. The real life is much more complicated. In particular, there exists an extremely interesting *fractional* quantum Hall effect, which manifests itself at fractional values of the filling factor. We do not discuss this effect in the present course.

Role of localization

As we have seen, at $H = 0$ a 2D system with disorder should have its states localized at all energies. However, only extended states are sensitive to the flux and can provide the QHE. At the same time, ranges of energies with only localized states are needed to pin E_F there and have finite plateaus. Thus, introduction of magnetic field must *delocalize some states*. As we have seen, extended modes appear near edges. However, extended states in a magnetic field are present also in the bulk of the conductor.

To discuss this phenomenon let us recall the main relevant quantities. First, let us note that the condition

$$\omega_c \tau \gg 1, \quad \text{or} \quad r_c \ll \ell, \quad r_c = v_F/0_c$$

for cyclotron motion is fully classical. In terms of quantum mechanical length, $a_H = \sqrt{cH/eH}$ the classical cyclotron radius r_c can be written as

$$r_c \sim k_F a_H^2 \sim a_H \sqrt{E_F \hbar \omega_c} \sim a_H \sqrt{N}$$

where N is the number of full Landau levels. The *weak localization regime* corresponds to the inequality

$$a_H \ll \ell,$$

while the intermediate regime where $a_H \ll r_c$ while r_c can be comparable with ℓ also exists.

Strong magnetic field, $\omega_c \tau \gg 1, r_c \ll \ell$.

As we have discussed, in a uniform electric field the drift velocity directed along $[\mathbf{E} \times \mathbf{H}]$ appears, $v_d = c(E/H)$. This concept can be generalized for the case of a smooth random potential $V(x)$ which does not change a lot on the scale of cyclotron motion. Then, if r_c is much less than the correlation length d of the random potential, the guiding center moves

along the equipotential line $V(\mathbf{r}) = V$. If its orbit is closed and embeds the area $A(V)$, then the typical frequency is

$$\frac{\omega_d}{2\pi} = \left[\oint \frac{dl}{v_d} \right]^{-1} = \frac{2c}{H} \left[\int \frac{dl dx_\perp}{dV} \right]^{-1} = \frac{2c}{H} \frac{\Delta V}{\Delta A},$$

where dx_\perp is an element of length in the direction of the potential gradient. Such a slow motion can be quantized for any Landau levels into locally equidistant levels with the separation $\hbar\omega_d$. The area between two quantized orbits is given by the relation

$$H \Delta A = \frac{\hbar c}{e} = \Phi_0; \quad \Delta A = 2\pi a_H^2.$$

Thus the flux of H in the area per state in a given Landau level corresponds to a flux quantum, as for free electron.

Let us assume that the amplitude of the random potential is much less than $\hbar\omega_c$, so there is no inter-Landau-level mixing. Then the potential energy of a properly quantized levels should be added to $\hbar\omega_c(j + 1/2)$ for j th Landau band. The levels correspond to the orbits running around the potential “hills”, or inside potential “lakes”. Both kinds of states are localized. There is one and only one energy, E_c , (in 2D case) at which the equipotential curves span the whole system (imagine filling up of the potential $V(\mathbf{r})$ “terrain” with water). The characteristic size of the orbit, ξ_p , may be defined by the r.m.s. of the area enclosed by the equipotential contours for the localized states. It must blow up at $E \rightarrow E_c$,

$$\xi_p \sim |E - E_c|^{-\nu_p}, \quad \nu_p \gtrsim 1.$$

Such an orbit provides the way to transfer an electron between the edges.

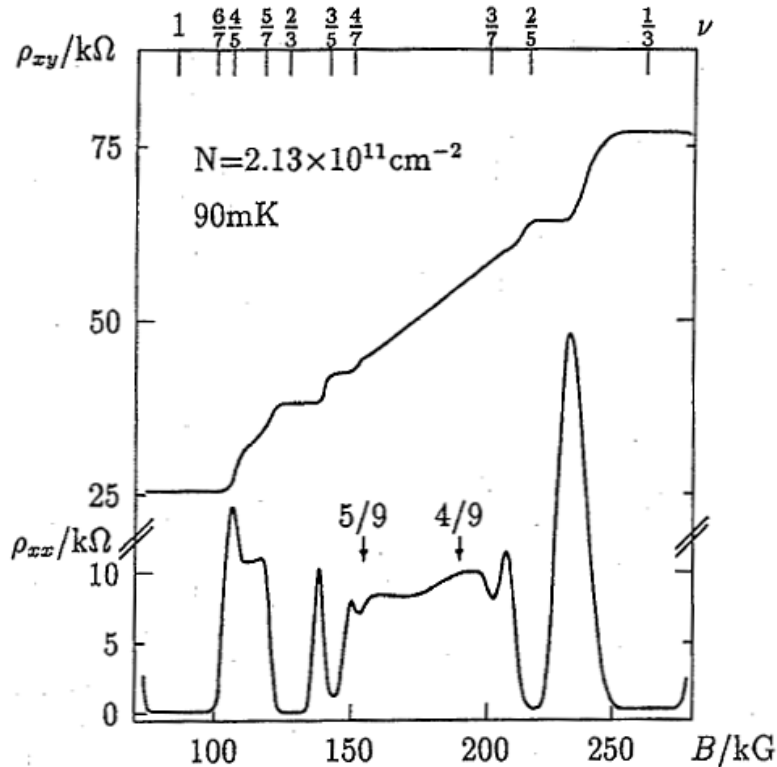
There is also a very interesting intermediate situation when

$$a_H \ll \ell \ll r_c, \quad \text{or} \quad \omega_c \tau \ll 1.$$

As was shown by Khmelnitskii (1984), even in this region QHE plateaus can exist which are irrelevant to Landau levels.

14.4 Fractional Quantum Hall Effect

Fractional quantum Hall effect (FQHE) was discovered by the group of Tsui et Bell Laboratories [31]. Using a high-mobility GaAs/AlGaAs heterostructures they observed quantization of Hall conductance at filling factors $\nu = 1/3$ and $2/3$ at very low temperatures (below 1 K). Later more rich structure, as shown in Figs. 14.7 and 14.8 at fractional filling factors was discovered. It appears that only account of Coulomb interaction leads to understanding of the problem. Now the studies of FQHE belong to the most active area of research. Below we shall provide a very brief sketch of the problems regarding electron-electron interaction in magnetic field and FQHE.



The fractional quantum Hall effect. The Hall resistivity (upper curve) of the inversion layer in a high mobility AlGaAs/GaAs heterostructure shows plateaus at magnetic inductions B that correspond to the indicated filling factors ν . At the same filling factors, the magnetoresistivity (lower curve) shows minima

Figure 14.7:

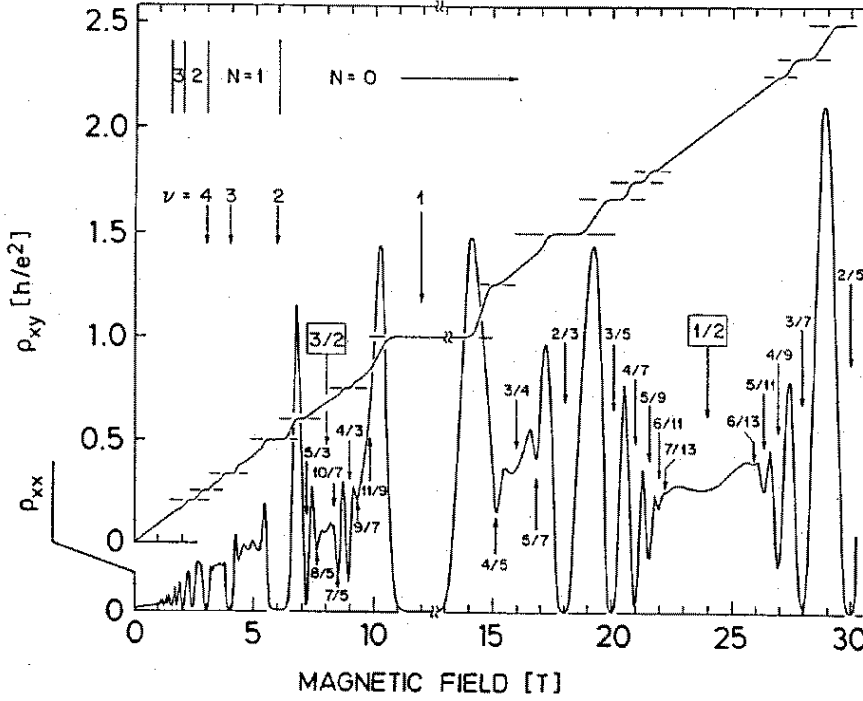
Few electron with Coulomb interaction

The role of electron-electron interaction is determined by the relation between the mean free distance between electrons, r_s , and the Bohr radius, $a_B = \epsilon\hbar^2/me^2$. At $r_s \ll a_B$ one can use the usual mean field description of interacting electrons, considering screening, plasmons, charge density waves, etc. However, at $r_s \geq a_B$ the interaction energy becomes larger than the average kinetic energy. As a result, there exists a strong electron-electron correlation, and the electrons tend to crystallize. It is known that magnetic field enhances these effects.

To get some understanding let us start with more simple problem of few electrons in a magnetic field. Historically, these studies appeared important because they led to discovery of a new state, the *incompressible electron liquid*, that is believed to transform into (Wigner) crystal at very low densities.

Two electrons. Let us discuss the case of 2 electrons in a very strong magnetic field, $\hbar\omega_c \geq e^2/\epsilon a_H$. This inequality means that Landau levels are not mixed by the Coulomb interaction (see below).

Using symmetric gauge, $\mathbf{A} = (-Hy/2, Hx/2, 0)$ and introducing polar coordinates we



The lowest Landau level corresponds to $n = 0$, $m > 0$. The Coulomb energy for the lowest state can be easily calculated as

$$E_C = \langle 0m | e^2 / \epsilon r | 0m \rangle = \frac{e^2}{\epsilon a_H} \frac{\Gamma(m + 1/2)}{m!}. \quad (14.8)$$

At large m it decays as $m^{-1/2}$.

Two electrons are described by the Hamiltonian

$$\mathcal{H}_0(1) + \mathcal{H}_0(2) + \mathcal{H}_{\text{int}}.$$

It can be rewritten through the center-of-mass coordinate, $\mathbf{R} = (\mathbf{r}_1 + \mathbf{r}_2)/\sqrt{2}$, and the relative coordinate, $\mathbf{r} = (\mathbf{r}_1 - \mathbf{r}_2)/\sqrt{2}$, as

$$\mathcal{H}_0(\mathbf{R}) + \mathcal{H}_0(\mathbf{r}) + \mathcal{H}_{\text{int}}(\mathbf{r}\sqrt{2}).$$

As a result, the center-of-mass motion is separated, and we look for a solution in the form

$$\Psi(\mathbf{R}, \mathbf{r}) = \phi(\mathbf{R})\psi(\mathbf{r}).$$

Now we are left with a *single-particle* problem for the relative motion.

Since the interaction energy is radially-symmetric one can look for a solution in the form

$$\psi(\mathbf{r}) = \mathcal{R}(r)e^{-im\varphi}$$

with odd m because of the Pauli principle [$\psi(-\mathbf{r}) = -\psi(\mathbf{r})$]. The radial Schrödinger equation is easily written in the dimensionless units as

$$-\frac{1}{2} \frac{d^2 \mathcal{R}}{dr^2} - \frac{1}{r} \frac{d\mathcal{R}}{dr} + \frac{1}{2} \left(\frac{m^2}{r^2} + m + \frac{r^2}{4} - \frac{\alpha}{r} \right) \mathcal{R} = E\mathcal{R}, \quad (14.9)$$

where r is measured in units of a_H , E is measured in the units of $\hbar\omega_c$, while dimensionless interaction constant is $\alpha = \sqrt{2}e^2/\epsilon a_H \hbar\omega_c$. At large magnetic field this equation can be solved perturbatively with respect to α . In the lowest approximation we obtain:

$$E_{0m}^{(1)} = \frac{\hbar\omega_c}{2} + \frac{e^2}{\epsilon a_H} \frac{\Gamma(m + 1/2)}{m!}. \quad (14.10)$$

The energy of the center-of-mass motion must be added.

We find that the interaction *destroys* the degeneracy of the lowest Landau level. At large m the correction decreases because the electrons are less sensitive to interaction at long distances.

Three electrons. For 3 electrons we can also strip the center-of-mass motion. It can be done by the transform $\boldsymbol{\rho} = \mathcal{O}\mathbf{r}$ where

$$\mathcal{O} = \begin{pmatrix} 1/\sqrt{2} & -1/\sqrt{2} & 0 \\ 1/\sqrt{6} & 1/\sqrt{6} & -2/\sqrt{6} \\ 1/\sqrt{3} & 1/\sqrt{3} & 1/\sqrt{3} \end{pmatrix}.$$

After the transform the interaction Hamiltonian can be written as

$$\mathcal{H}_{\text{int}} = \frac{e^2}{\epsilon\sqrt{2}} \left(\frac{1}{|\boldsymbol{\rho}_1|} + \frac{2}{|\boldsymbol{\rho}_1 + \sqrt{3}\boldsymbol{\rho}_2|} + \frac{2}{|\sqrt{3}\boldsymbol{\rho}_2 - \boldsymbol{\rho}_1|} \right). \quad (14.11)$$

Again, we can write the eigen function as a product

$$\Psi(\boldsymbol{\rho}_1, \boldsymbol{\rho}_2, \boldsymbol{\rho}_3) = \phi(\boldsymbol{\rho}_3)\psi(\boldsymbol{\rho}_1, \boldsymbol{\rho}_2)$$

and in this way to reduce the problem to a two-particle one.

An important point is that the probability density must be invariant under rotation about multiples of $\pi/3$. The resulting Hamiltonian also commutes with the total angular momentum, \mathbf{L} . Then the states can be classified according to eigenvalues M of the orbital momentum. It was shown by R. Laughlin that a proper complete set to diagonalize a 3-electron system can be written as

$$|m, m'\rangle = \frac{F}{2} [(z_2 + iz_1)^{3m} - (z_2 - iz_1)^{3m}] (z_1^2 + z_2^2)^{m'} e^{-(|z_1|^2 + |z_2|^2)}. \quad (14.12)$$

Here $z_i = \xi_i + \eta_i$, ξ, η are the Cartesian components of the vector $\boldsymbol{\rho}_i/a_H$, F is a normalization factor. The states (14.12) are the eigenstates of the total angular momentum with $M = 3(m + m')$.

To diagonalize the system one has to solve the secular equation

$$\det |e\delta_{mm}\delta_{m'm'} - \langle mm'|\mathcal{H}_{\text{int}}|mm'\rangle| = 0.$$

The crucial point is that the basis (14.12) is an extremely good starting approximation since off-diagonal elements of \mathcal{H}_{int} are typically at least 10 times less than the diagonal ones.

The minimum angular momentum for which a non-degenerate solution exists is $M = 3$ ($m = 0, m' = 1$). The next solution corresponds to $M = 9$, it is combined from the states (3,0) and (1,3). These states have the lowest energy at $\mathcal{H}_{\text{int}} = 0$. The “charge density” for the state with $M = 9$ is 1/3 comparing to the state with $M = 3$. Since the angular momentum is conserved and the angular momentum corresponds to the area of an electronic state, the 3 electrons are “incompressible”.

Fractional quantum Hall states

It is impossible to diagonalize exactly the system of many electron states. An extremely effective approximate guess was suggested by R. Laughlin which we shall discuss for the case of very large magnetic field when only the lowest Landau level is important. The single-electron states for that case can be written as

$$\langle \mathbf{r}|0m\rangle = \frac{N_m}{a_H} z^m e^{-|z|^2/4},$$

where $z = x + iy$. The complete set of N -electron states with total angular momentum $M = \sum_{\nu=1}^N m_{\nu}$ are the Slater determinants

$$\Psi(1 \dots N) = \sum_{P(\nu_1 \dots \nu_N)} (-1)^P \prod_{\mu=1}^N N_{m_{\mu}} z_{\nu_{\mu}}^{m_{\mu}} \exp \left(-\frac{1}{4} \sum_{\alpha=1}^N |z_{\alpha}|^2 \right).$$

Since the ground state in the independent band approximation is a combination of Slater determinants, its general form is

$$\Psi(1 \dots N) = \prod_{j < k} f(z_j - z_k) \exp \left(-\frac{1}{4} \sum_{\alpha=1}^N |z_{\alpha}|^2 \right).$$

There are several requirements to the functions $f(z)$:

- The function $f(z)$ must be a polynomial of z ;
- Since Ψ should be a Fermion state, $f(-z) = -f(z)$;
- Ψ can be chosen as an eigenfunction of the total angular momentum. Therefore, the function $f(z)$ has to be *homogeneous*.

The simplest choice is

$$f(z) = z^m, \quad (n \text{ odd}).$$

Thus the approximate wave function has the form

$$\Psi(1 \dots N) = \prod_{j < k} (z_j - z_k)^m \exp \left(-\frac{1}{4} \sum_{\alpha=1}^N |z_{\alpha}|^2 \right). \quad (14.13)$$

The *Laughlin state* (14.13) describes a liquid-like system. The two-particle correlation function

$$g_2^{(m)}(z_1, z_2) = \int \prod_{\nu=3}^N d\mathbf{r}_{\nu} |\Psi(1 \dots N)|^2$$

at small distances is proportional to $|z_1 - z_2|^m$ that reflects the Pauli principle for the electrons. The smallest possible value of m is 3. The total angular momentum is just

$M = Nm$, while the area covered by the electrons is $A = N(2\pi ma_H^2)$. Thus the average electron density is $(2\pi ma_H^2)^{-1}$, and the filling factor is $\nu = 1/m$. To keep electrostatic stability one has to add the positive background.

The estimate for the Coulomb energy for the Laughlin state can be obtained as

$$E_C^{(m)} = \frac{N(N-1)}{2A} \frac{e^2}{\epsilon} \int \frac{d^2r}{r} \left[g_2^{(m)}(r) - 1 \right].$$

Because the correlation function decay strongly at small distances the incompressible liquid state appears more stable than the Wigner crystal. An interesting fact is that the Laughlin state appears the exact ground state for $\nu = 1/m$ in the case of contact interaction, $\mathcal{H}_{\text{int}}(\mathbf{r}) \propto \delta(\mathbf{r})$.

As a consequence of the electron-hole symmetry it is easy to find the state corresponding to the filling factor $(1-\nu)$ if the state for ν is known.

Elementary excitations

Elementary excitation are important both for transport and dynamics. Changing of energy of the electron system can be achieved by its compression, or, equivalently, by changing of angular momentum while keeping the neutralizing background.

In other words, it means that new quasielectrons of quasiholes are introduced into the state Ψ_ν if $\nu \neq 1/m$. An introduction of a quasihole can be represented as

$$\Psi_\nu^+ = A^+(z_0)\Psi_\nu(z_1 \dots z_n), \quad A^+(z_0) = \prod_{j=1}^N (z_j - z_0).$$

Let us estimate the effective charge of this excitation. The average area per particle which is covered in the state with filling factor $\nu = 1/m$ is $(N-1)(2\pi ma_H^2)$. It can be seen by direct calculation of the integral. The corresponding charge density is

$$\rho_0 = \frac{-Ne}{(N-1)(2\pi ma_H^2)} \approx -\frac{e}{2\pi ma_H^2}.$$

Thus, each electron occupies the area with m flux quanta. Its charge must be compensated by a positive background.

In the state Ψ_ν^+ the maximum angular momentum per particle is increased by $2\pi a_H^2$. This corresponds to the change in the charge density which is equivalent to the positive charge $+e/m$.

Quasielectrons can be created in a similar way,

$$\Psi_\nu^- = A^-(z_0)\Psi_\nu(z_1 \dots z_n), \quad A^-(z_0) = \prod_{j=1}^N \left(\frac{\partial}{\partial z_j} - z_0^* \right).$$

Here the partial derivative acts only on the polynomial part of the wave function Ψ_ν , leaving alone the Gaussian part. It can be shown that the effective charge of the quasielectron is $-e/m$.

The gaps between the ground and excited states were observed directly from temperature dependences of conductance. It appears that the quasiparticles can be considered as particles with so-called fractional statistics – *anyons*. Very interesting *collective excitations* were also predicted and observed experimentally by inelastic light scattering. H. Störmer, D. Tsui and R. Laughlin were awarded by the Nobel Prize 1998 for their discovery of FQHE.

However, the story is not over. Very specific features of Hall conductance were observed at $\nu = p/q$ where p, q are integers, both for odd and even denominator q . These features were not explained by original theory by Laughlin. It appears, that at odd denominators the electrons also condense in some quantum liquids. However, the properties of that liquids differ significantly from those of the incompressible Laughlin liquid.

The above discussion is definitely not an “explanation” of FQHE. It just demonstrates some basic trends in the field. More work has to be done to understand the whole physical picture and to construct a proper transport theory.

Bibliography

Books

- [1] B. L. Altshuler, A. G. Aronov, D. E. Khmelnitskii, and A. I. Larkin, in: *Quantum Theory of Solids*, edited by I. M. Lifshits, pp. 130-237, Advances in Science and Technology in the USSR, Mir Publishers, Moscow 1982.
- [2] H. Fukuyama and S. Hikami, *Anderson Localization*, Springer, Berlin (1982).
- [3] S. Datta, *Transport in Mesoscopic Systems*, Cambridge University Press (1996).
- [4] Y. Imry, “*Introduction to Mesoscopic Physics*”, Oxford University Press (1997).
- [5] T. Dittrich, P. Hänggi, G.-L. Ingold, B. Kramer, G. Schön, W. Zwerger, *Quantum Transport and Dissipation*, Wiley-VCH (1998).
- [6] T. Ando, Y. Arakawa, K. Furuya, S. Komiyama, H. Nakashima (Eds.), *Mesoscopic Physics and Electronics*, Springer (1998).

Review articles

- [7] T. Ando, A. B. Fowler, and F. Stern, Rev. Mod. Phys. **54**, 437 (1982).
- [8] B. L. Altshuler and A. G. Aronov, In: *Electron-Electron Interactions in Disordered Systems*, ed. by M. Pollak and A. L. Efros, pp. 1-151, In: Modern Problems in Condensed Matter Physics, North Holland (1985).
- [9] H. Fukuyama, In: *Electron-Electron Interactions in Disordered Systems*, ed. by M. Pollak and A. L. Efros, pp. 155-230, In: Modern Problems in Condensed Matter Physics, North Holland (1985).
- [10] C. W. J. Beenakker and H. van Houten, in “Solid State Physics” (H. Ehrenreich and D. Turnbull, eds.), v. 44, p. 1. Academic Press, Inc., 1991.
- [11] H. van Houten *et al.*, in “Physics and Technology of Submicron Structures” (H. Heinrich, G. Bauer, and F. Kuchar, eds.). Springer, Berlin, 1988.

- [12] C. W. J. Beenakker, H. van Houten and B. van Wees, *Superlattices and Microstructures*, **5**, 127 (1989)
- [13] D. A. Averin, K. K. Likharev, in: *Quantum Effects in Small Disordered Systems*, ed. by B. L. Altshuler, P. A. Lee and R. A. Webb (Elsevier, Amsterdam, 1991).
- [14] *Single Charge Tunneling*, Vol. 294 of *NATO Advanced Study Institute, Series B: Physics*, ed. by H. Grabert and M. H. Devoret (Plenum, New York, 1992).
- [15] *Single-Electron Tunneling and Mesoscopic Devices*, ed. by H. Koch and H. Lübbig (Springer-Verlag, Berlin Heidelberg, 1995).
- [16] M. P. A. Fisher, L. I. Glazman, preprint cond-mat/96010037.
- [17] C. W. J. Beenakker, Rev. Mod. Phys. **69**, 731 (1997).
- [18] A. D. Stone, in: *Physics of Nanostructures*, ed by J. H. Davies and A. R. Long, p. 65 (1991).
- [19] M. J. M. de Jong and C. W. J. Beenakker, *Shot Noise in mesoscopic systems*, preprint cond-mat/9611140.

Selected papers

- [20] B. L. Altshuler, A. G. Aronov and B. Z. Spivak, JETP Lett. **33**, 94 (1981).
- [21] D. Yu. Sharvin and Yu. V. Sharvin, JETP Lett. **34**, 272 (1981)
- [22] D. E. Khmelnitskii, Physica **126b**, 235 (1984).
- [23] V. L. Gurevich, Phys. Rev. B **55**, 4522 (1997).
- [24] Y. Gefen, Y. Imry, and M. Ya. Azbel, Phys. Rev. Lett. **52**, 129 (1984).
- [25] L. I. Glazman, G. B. Lesovik, D. E. Khmelnitskii, R. I. Shekhter, JETP Letters, **48**, 238 (1988).
- [26] I. O. Kulik and R. I. Shekhter, Sov. Phys.-JETP, **41**, 308 (1975).
- [27] P. A. Lee, Physica **140A**, 169 (1986).
- [28] B. L. Altshuler, JETP Lett. **41**, 648 (1985).
- [29] B. L. Altshuler and B. I. Shklovskii, JETP **64**, 127 (1986) [Zh. Eksp. Teor. Fiz. **91**, 220 (1986)].
- [30] Y. Imry, Europhys. Lett. **1**, 249 (1986).

- [31] D. C. Tsui, H. L. Störmer and A. C. Gossard, Phys. Rev. Lett. **48**, 1559 (1982).
- [32] M. Reznikov, M. Heiblum, H. Shtrikman, and D. Mahalu, Phys. Rev. Lett. **75**, 3340 (1995).
- [33] C. W. J. Beenakker and M. Büttiker, Phys. Rev. B **46**, 1889 (1992).
- [34] H. Birk, M. J. M. de Jong, and C. Schönenberger, Phys. Rev. Lett. **75**, 1610 (1995).
- [35] A. H. Steinbach, J. M. Martinis, and M. H. Devoret, Phys. Rev. Lett. **76**, 3806 (1996).

Part IV

Superconductivity

Chapter 15

Fundamental Properties of Superconductors

15.1 General properties.

We review here the most important properties of superconductors which are definitely well known. They are

- Zero resistance (*Kammerlingh-Onnes, 1911*) at $T < T_c$. The temperature T_c is called the *critical* one.
- Superconductivity can be destroyed also by an external magnetic field H_c which is also called the *critical* one (*Kammerlingh-Onnes, 1914*). Empirically,

$$H_c(T) = H_c(0) [1 - (T/T_c)^2] .$$

- If the superconductivity is destroyed by a current the critical current is just the one which produces the field H_c at the surface (the *Silsby rule*). (This rule is not valid for thin samples, see below).
- The *Meissner-Ochsenfeld effect* (1933). Magnetic field does not penetrate the sample, the magnetic induction being zero, $B = 0$ (see Fig. 15.1). In many important cases this effect can be not complete. We will come back to the problem later.
- To be more exact, the field does exist inside a surface region with the thickness $\delta \sim 10^{-5} - 10^{-6}$ cm where persistent screening currents flow. Empirical temperature dependence of the penetration depth is

$$\delta(T) = \delta(0) \frac{1}{\sqrt{1 - (T/T_c)^4}}$$

so $\delta \rightarrow \infty$ at $T \rightarrow T_c$.

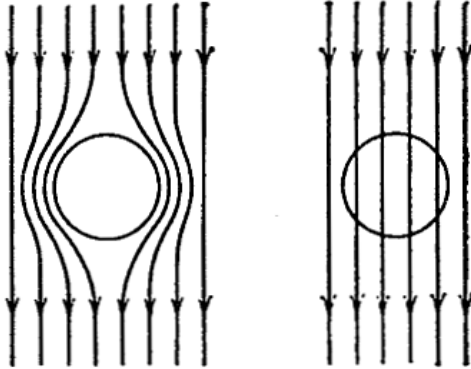


Figure 15.1: The Meissner effect.

- The phase transition to the superconducting (SC) state in the absence of magnetic field is the type II one. So, there is no hidden heat. Rather, there is a discontinuity of the specific heat. Contrary, if $H \neq 0$ (i.e. at $T < T_c$) the transition is the type I one.
- The penetration depth continuously changes from the finite value to infinity at T_c . It means that the properties of electron system change also continuously. At the same time, resistivity changes abruptly. One could imagine that electrons do not interact with the lattice in the SC state. In this case one would expect great increase of the thermal conductivity. Nevertheless, it is continuous at the transition point.
- The last property which is very important is that electron contribution to the specific heat behaves at low temperatures as $\exp(-\Delta/k_B T)$ that means that there is a *gap* in the elementary excitation spectrum. But this gap is strongly temperature dependent contrary to semiconductors. Indeed, it should vanish at the transition point.
- There are other arguments in favor of the gap in the excitation spectrum, namely, electromagnetic and sound absorption which has the threshold $\hbar\omega = 2\Delta$ (because a pair of excitations is created by a quantum), tunnel effect and so on.

As a result, one comes to the conclusion that it is a *new type* of condensed state.

The London Equation

In the following, it is convenient to use the local magnetic field $\mathbf{h}(\mathbf{r})$, the induction being the spatial average of the local magnetic field, $\mathbf{B} = \bar{\mathbf{h}}$. One can write the free energy as

$$\mathcal{F} = \int F_s dV + E_{kin} + E_{mag}$$

where F_s is the free energy on the condensed system, while E_{kin} is connected with persistent currents. If we denote

$$\mathbf{j}_s = -n_s e \mathbf{v}(\mathbf{r})$$

with the *density of superconducting electrons*, n_s ,¹

$$E_{\text{kin}} = \frac{1}{2} \int n_s m v^2 d\mathcal{V}.$$

The energy of the magnetic field is

$$E_{\text{mag}} = \int \frac{h^2}{8\pi} d\mathcal{V}.$$

Then,

$$\text{curl } \mathbf{h} = \frac{4\pi}{c} \mathbf{j}_s. \quad (15.1)$$

As a result,

$$\mathcal{F} = \mathcal{F}_0 + \frac{1}{8\pi} \int (\mathbf{h}^2 + \delta_L^2 |\text{curl } \mathbf{h}|^2) d\mathcal{V}$$

with

$$\mathcal{F}_0 = \int F_s d\mathcal{V}, \quad \delta_L = \sqrt{\frac{mc^2}{4\pi n_s e^2}}. \quad (15.2)$$

At low temperature it is natural to assume that $n_s = n_e$. Then, for order-of-magnitude estimates we get for $\delta_L \sim 500 \text{ \AA}$ for simple metals like Al and Sn ($m \sim m_0$) and $\sim 2000 \text{ \AA}$ for transition metals with large m .

Now we get the equation for \mathbf{h} that provides the minimal free energy. We get

$$\delta\mathcal{F} = \frac{1}{4\pi} \int (\mathbf{h} \cdot \delta\mathbf{h} + \delta_L^2 \text{curl } \mathbf{h} \cdot \text{curl } \delta\mathbf{h}) d\mathcal{V} = \frac{1}{4\pi} \int (\mathbf{h} + \delta_L^2 \text{curl curl } \mathbf{h}) \cdot \delta\mathbf{h} d\mathcal{V}$$

(the second expression is obtained by the interacting by parts, check!). As a result, for the minimum we get the London equation

$$\mathbf{h} + \delta_L^2 \text{curl curl } \mathbf{h} = 0. \quad (15.3)$$

which should be analyzed together with the Maxwell equation (15.1).

The Meissner effect

For the simplest geometry, Fig. 15.2, the surface is the (x, y) plane, field and current depend only on z . We have

$$\begin{aligned} \mathbf{h} + \delta_L^2 \text{curl curl } \mathbf{h} &= 0, \\ \text{curl } \mathbf{h} &= (4\pi/c) \mathbf{j}_s, \\ \text{div } \mathbf{h} &= 0. \end{aligned}$$

¹We assume that the velocity is a slow-varying function of co-ordinates.

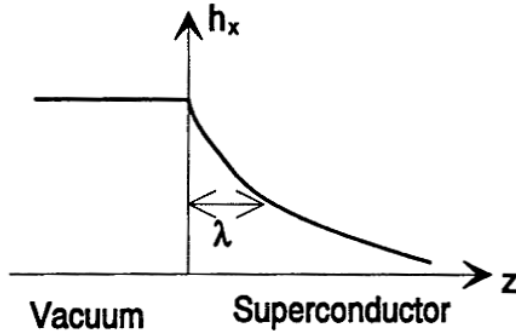


Figure 15.2: The Meissner effect. Penetration depth.

1. If $\mathbf{h} \parallel \mathbf{z}$, we obtain $\partial h / \partial z = 0$, $h = \text{const}$. Consequently, $\text{curl } \mathbf{h} = 0$, $\mathbf{j}_s = 0$. From the London equation, $h = 0$. **The field cannot be normal to the superconductor surface.**

2. If $\mathbf{h} \parallel \mathbf{x}$ the equation $\text{div } \mathbf{h} = 0$ is automatically met, and we get $\mathbf{j} \parallel \mathbf{y}$. So, the Maxwell equation is

$$\frac{dh}{dz} = \frac{4\pi}{c} j_s$$

and the London one

$$\frac{d j_s}{dz} = \frac{n_s e^2}{mc} h = \frac{h}{\delta_L^2} \frac{c}{4\pi}.$$

The solution is

$$h(z) = h(0) e^{-z/\delta_L}.$$

Thus, we have proved the concept of the penetration depth. p

Chapter 16

Magnetic Properties of Type I Superconductors

16.1 Thermodynamics in a Magnetic Field.

Consider a long cylinder with length L and a coil with N shown in Fig. 16.1.

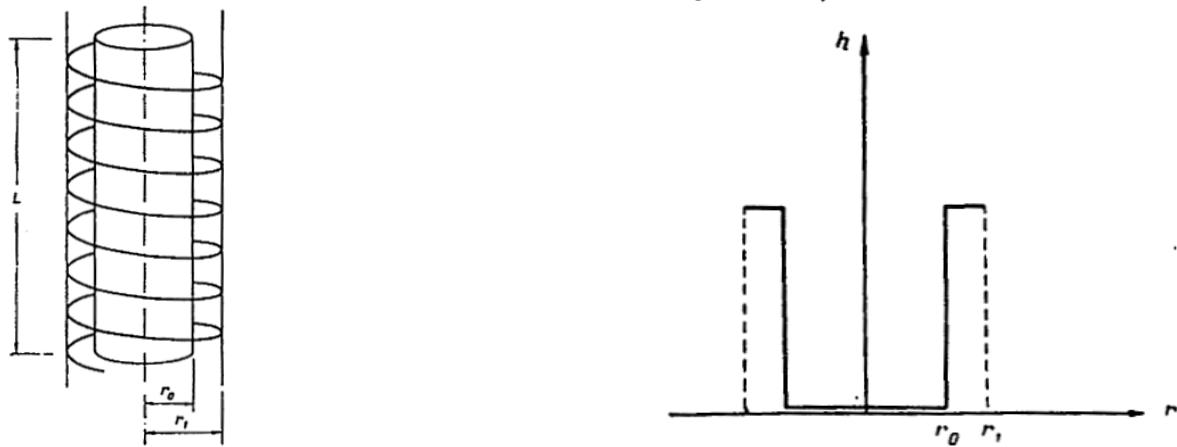


Figure 16.1: Magnetic properties of a long cylinder.

1. In a normal state, the field is homogeneous

$$h = \frac{4\pi NI}{cL},$$

$$\mathcal{F}_n = \pi r_0^2 L F_n + \pi r_1^2 L \frac{h^2}{8\pi}.$$

2. In a SC state

$$\mathcal{F}_s = \pi r_0^2 L F_s + \pi(r_1^2 - r_0^2)L \frac{h^2}{8\pi}.$$

Here we have neglected surface effects – penetration of the field inside the sample and kinetic energy of surface currents ($r_0 \gg \delta$).

Let us find the difference $F_n - F_s$. At the transition the magnetic flux Φ decreases. As a result, the voltage V is induced, the work being

$$\int VI dt = - \int_n^s \left(\frac{N}{c} \frac{d\Phi}{dt} \right) I dt.$$

If we keep the current constant

$$\int VI dt = \frac{NI}{c} (\Phi_n - \Phi_s) = \frac{NI}{c} \pi r_0^2 h = \pi r_0^2 L \frac{h^2}{4\pi}.$$

In the equilibrium, at $h = H_c$,

$$\mathcal{F}_n - \mathcal{F}_s = \int VI dt = \pi r_0^2 L \frac{H_c^2}{8\pi}.$$

As a result,

$$F_n - F_s = \frac{H_c^2}{4\pi}.$$

Now we can derive several important relations.

1. Let us fix the current I and change the temperature. The entropy

$$S_n = - \frac{dF_n}{dT}, \quad S_s = - \frac{dF_s}{dT} \rightarrow$$

$$S_n - S_s = - \frac{1}{4\pi} H_c \frac{dH_c}{dT}$$

the hidden heat being

$$L = T(S_n - S_s) = - \frac{T}{4\pi} H_c \frac{dH_c}{dT} > 0.$$

It is known that at $T \rightarrow T_c$ $H_c \rightarrow 0$ while dH_c/dT remains finite. We have proved that at $H = 0$ $L = 0$ (type II transition). The specific heat step is

$$C_n - C_s = \left[T \frac{d}{dT} (S_n - S_s) \right]_{T_c} = - \frac{1}{4\pi} \left[T \left(\frac{dH_c}{dT} \right)^2 \right]_{T_c}.$$

This relation is confirmed by experiments.

16.2 Penetration Depth

Relation Between the Current and the Field

It is very convenient to use the vector potential according to the relation

$$h = \text{curl } \mathbf{A}.$$

To make this equation definite one should chose the gauge and the boundary conditions. Usually the gauge

$$\operatorname{div} \mathbf{A} = 0, \quad [\mathbf{A}_n = 0]_{\text{surface}}$$

is chosen. In such a gauge the current response is

$$\mathbf{j}_s = -\frac{n_s e^2}{mc} \mathbf{A} \quad (16.1)$$

with

$$\operatorname{div} \mathbf{j} = 0, \quad [\mathbf{j}_n = 0]_{\text{surface}}.$$

The first condition is just the continuity equation while the second is met in the absence of the currents flowing into the sample.

Eq. (16.1) is valid if both the current and field slowly vary in space. As the same time, if there is a gap Δ in the excitations spectrum the electrons in the layer

$$\epsilon_F - \Delta < p^2/2m < \epsilon_F + \Delta$$

are correlated. The width of the layer in the p -space is

$$\delta p \sim 2\Delta/v_F.$$

According to the uncertainty principle, it means that the spatial size of the package is

$$\zeta_0 = \frac{\hbar v_F}{\pi \Delta}$$

(the factor $1/\pi$ is introduced for convenience). The quantity ζ_0 is called the *coherence length*.

We see that the London equation is valid at

$$\delta_L \gg \zeta_0.$$

The materials with $\delta_L \gg \zeta_0$ are called the *type II* superconductors. In this section we are interested in the opposite limiting case, $\delta_L \ll \zeta_0$, for *type I* materials.

To get the relation between the current and the vector-potential usually the *Pippard's* phenomenological expression is used

$$\mathbf{j}(\mathbf{r}) = C \int \frac{(\mathbf{A}(\mathbf{r}') \cdot \mathbf{R}) \mathbf{R}}{R^4} e^{-R/\zeta_0} dV', \quad \mathbf{R} = \mathbf{r} - \mathbf{r}'. \quad (16.2)$$

To get C we apply this expression to the case of slow-varying vector potential. In this case the potential can be considered as constant, and we should come to the London expression. As a result (see *Problem 16.1*)

$$C = -\frac{3n_s e^2}{4\pi mc\zeta_0}. \quad (16.3)$$

The exact result can be obtained from the microscopic theory and it is much more complicated. Nevertheless, the Eq. (16.2) is a very good approximation and we will use it extensively.

Penetration depth.

The integration in Eq. (16.2) is performed over the whole sample. Near the surface it is obviously incorrect. One can use the following rule. Let us keep Eq. (16.2) but perform the integration only over the points \mathbf{r}' which are accessible from the point \mathbf{r} along the straight line (see Fig. 16.2).

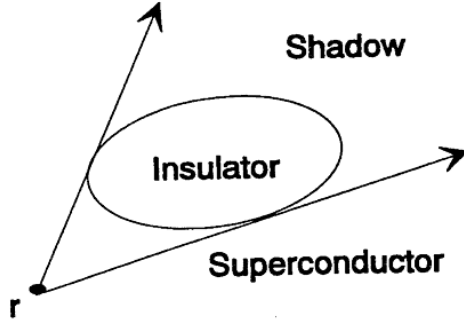


Figure 16.2: On the shadow effect.

The exact theory is very complicated for this case, and we will apply the model considerations (*Pippard*).

Let us return to our geometry, Fig. 15.2. Let the vectors \mathbf{A} , \mathbf{j} are parallel to \mathbf{z} . If the vector-potential would be constant near the surface one would obtain

$$\mathbf{j} = -\frac{n_s e^2}{mc} \mathbf{A}.$$

In reality, \mathbf{A} is not very small only in the layer with the thickness $\delta \ll \zeta_0$. Consequently, one should multiply this expression by δ/ζ_0 to get

$$\mathbf{j} = -\frac{n_s e^2}{mc} \frac{\delta}{\zeta_0} \mathbf{A}.$$

Substituting this relation to the Maxwell equation (15.1) we get

$$h(z) = h(0) e^{-z/\delta}$$

with the following self-consistent equation for δ

$$\delta^{-2} = \frac{4\pi n_s e^2}{mc^2} \frac{\delta}{\zeta_0} \rightarrow \delta^3 = \delta_L^2 \zeta_0.$$

The exact theory leads to the extra factor 0.62 in this equation:

$$\delta^3 = 0.62 \delta_L^2 \zeta_0. \quad (16.4)$$

Metal	δ_L , Å	ζ_0 , Å	δ_{th} , Å	δ_{exp} , Å
Al	157	16000	530	490-515
Sn	355	2300	560	510
Pb	370	830	480	390

Table 16.1: Values of δ and ζ_0 for 3 metals.

As a result

$$\frac{\delta}{\delta_L} \sim \left(\frac{\zeta_0}{\delta_L} \right)^{1/3} \gg 1, \quad \text{while} \quad \frac{\delta}{\zeta_0} \sim \left(\frac{\delta_L}{\zeta_0} \right)^{2/3} \ll 1.$$

There are several conventional ways to measure the penetration depth: by magnetic susceptibility of small SC particles, or thin films. Another way is measuring the inductance of a coil near the SC surface, or the inductance of a coil with long SC cylinder as a kernel (the Kazimir method). The best way is study a cavity with SC walls.

Filed Penetration into Clean Metals and Alloys.

Clean Metals

Now we briefly discuss the experimental picture. It interesting to check the relation (16.4). For clean metals one can obtain the ratio n_e/m and v_F from the specific heat data and calculate δ_L , while $\Delta(0)$ can be obtained from the similar measurements in the SC state, so we can determine ζ_0 . The comparison is given in the table 16.1.

Alloys

The idea to take impurities into account in the simplest way belongs also to Pippard. It is just to introduce the facto $\exp(-|\mathbf{r} - \mathbf{r}'|/\ell)$ in the integrand of Eq. (16.2) to get

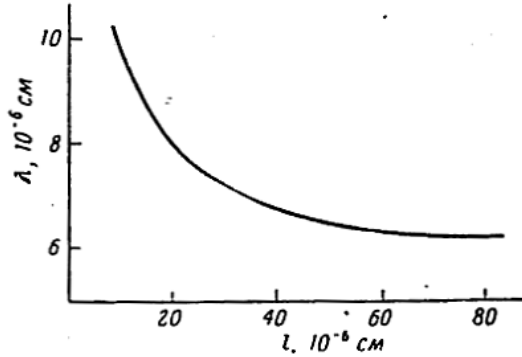
$$\mathbf{j}(\mathbf{r}) = C \int \frac{(\mathbf{A}(\mathbf{r}') \cdot \mathbf{R}) \mathbf{R}}{R^4} \exp \left[-R \left(\frac{1}{\zeta_0} + \frac{1}{\ell} \right) \right] dV', \quad \mathbf{R} = \mathbf{r} - \mathbf{r}'. \quad (16.5)$$

This way was successful to explain many experimental results, in particular, on the alloys SnIn, Fig. 16.3. We see that the penetration depth increases with the increase of the impurity concentration. Thus, **Impure materials are type II superconductors.** At $\delta \gg \ell$ one can integrate over R considering $\mathbf{A}(\mathbf{r}')$ as constant. The result is

$$\mathbf{j}(\mathbf{r}) = C \frac{4\pi}{3} \frac{1}{\zeta_0^{-1} + \ell^{-1}} \mathbf{A}(\mathbf{r}).$$

We returned to the London equation

$$\mathbf{j}(\mathbf{r}) = -\frac{n_s e^2}{mc} \frac{\ell}{\zeta_0} \mathbf{A}(\mathbf{r})$$

Figure 16.3: The dependence δ vs ℓ in SnIn alloys.

which leads to the penetration depth

$$\delta = \delta_L \sqrt{\frac{\zeta_0}{\ell}} \quad \text{at} \quad \ell \ll \delta, \zeta_0. \quad (16.6)$$

Temperature Dependence of the Penetration Depth

As a prescription, the Pippards relations (16.2) and (16.5) remain valid at finite temperatures. One can retain the quantity ζ_0 obtained for zero temperature while the factor C becomes temperature-dependent. Near T_c

$$C \propto T_c - T.$$

We will discuss this complete dependence after considering microscopic theory. People often use the *empirical* relation given above which works relatively well.

16.3 Magnetic Properties of Samples with an Arbitrary Shape

Nature of the Intermediate State.

To discuss the penetration depth we have always used the long cylinder configuration which provides constant magnetic field at the surface. To understand what happens for a sample with an arbitrary shape let us consider a SC sphere with the radius a embedded in the external magnetic field H_0 , Fig. 16.4. If the field is very low, we have the Meissner effect and $\mathbf{h} = 0$ inside the sphere. To get the field outside one should write the Maxwell equation

$$\operatorname{div} \mathbf{h} = \operatorname{curl} \mathbf{h} = 0, \quad \mathbf{h} \rightarrow \mathbf{H}_0 \text{ at } r \rightarrow \infty.$$

Another boundary condition is

$$(h_n)_{r=a} = 0$$

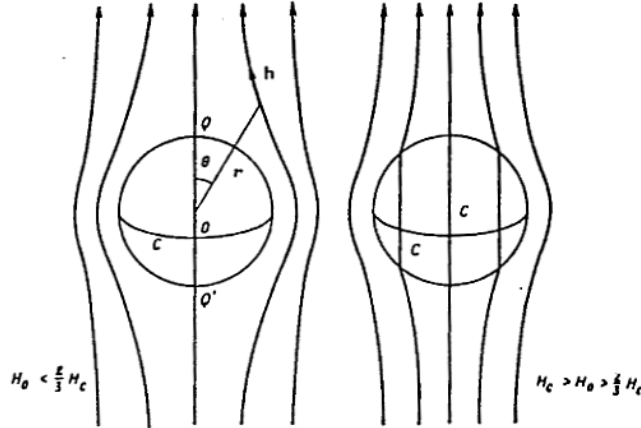


Figure 16.4: Field distribution near a SC sphere with the radius a .

(the field cannot be normal to a SC). As a result, we get the solution for the region outside the sphere

$$\mathbf{h} = \mathbf{H}_0 + H_0 \frac{a^3}{2} \nabla \left(\frac{\cos \theta}{r^2} \right)$$

that is just the field of a magnetic dipole. At the surface, the tangential field component is

$$(h_\theta)_{r=a} = \frac{3}{2} H_0 \sin \theta.$$

Thus, at the equator ($\theta = \pi/2$) $h_\theta = (3/2)H_0$ and at $H_0 = (2/3)H_c$ the maximal field is just H_c . What happens at

$$\frac{2}{3} H_c < H_0 < H_c? \quad (16.7)$$

In this region the normal and SC phases *co-exist*. This state is called the *intermediate* one. It is clear that condition (16.7) is *shape dependent*. For example, in a very thin plate intermediate state exists at any field $H < H_c$.

To study the system in more detail, let us consider the plate in a perpendicular magnetic field, Fig.(16.5). We see the set in N and S layers, the field at the interface being H_c . In the N -regions $\mathbf{h} \parallel \mathbf{z}$, i.e. $\text{div } \mathbf{h} = \text{curl } \mathbf{h} = 0$. As a result, $h = \text{const}$. In S -layers $h = 0$.

To keep the flux constant we should fix the fraction of SC volume to be

$$\rho = \frac{d_s}{d_n + d_s}.$$

Indeed, far away the field is homogeneous, $h = H_0$, and the flux is AH_0 where A is the film's area. Inside the film the total flux penetrated only the normal regions, the area being $A(1 - \rho)$ while the field is equal to H_c . As a result,

$$AH_0 = A(1 - \rho)H_c \rightarrow \rho = 1 - \frac{H_0}{H_c}.$$

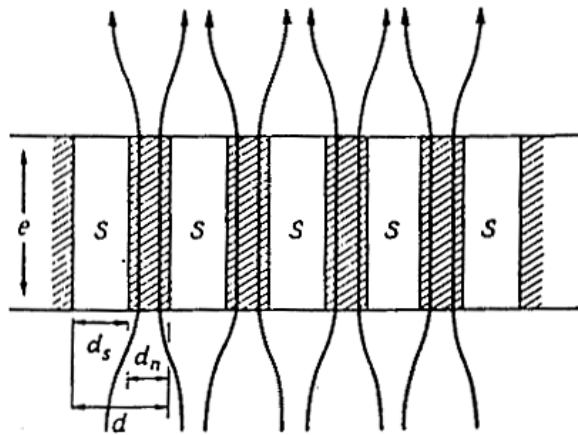


Figure 16.5: Field distribution in a plate embedded in a transverse field.

We cannot determine the thickness $d_{n,s}$ from geometry consideration and need to discuss thermodynamics.

Important Thermodynamics Relations

Now we introduce the most important concepts of thermodynamics to use them in the following chapters.

Free energy

Consider a system consisting of the sample and external objects (coils, generators, etc.). The *energy* of the electrons can be written as (we put the electron charge $-e$)

$$U = \sum_i \left[\frac{1}{2m} \left(\mathbf{p}_i + \frac{e}{c} \mathbf{A} \right)^2 + V_i \right] + \sum_{i \neq j} V_{ij}.$$

To get the *free energy* one should add the *entropy* contribution $-TS$. Thus

$$U - TS \equiv \int_{\text{sample}} F_s dV.$$

Adding the magnetic energy $\int(h^2/8\pi) dV$ we get

$$\mathcal{F} = \int_{\text{sample}} F_s dV + \int_{\text{all space}} (h^2/8\pi) dV. \quad (16.8)$$

Magnetic induction

In many cases, we will face the problems when the field changes at the scale Δx which is small in comparison with the sample's size. In those case it is convenient to introduce *magnetic induction* $\mathbf{B}(\mathbf{r})$ as the average field at the distances $\gg \Delta x$, but much less than the sample's size. According to this definition

$$\begin{aligned}\mathbf{B} &= \bar{\mathbf{h}} \quad \text{inside the sample} \\ \mathbf{B} &= \mathbf{h} \quad \text{outside.}\end{aligned}$$

From the local Maxwell equations we get

$$\operatorname{curl} \mathbf{B} = \frac{4\pi}{c} \bar{\mathbf{j}}, \quad \operatorname{div} \mathbf{B} = 0. \quad (16.9)$$

Magnetic field strength

Assume that the field $\mathbf{h}(\mathbf{r})$ has changed because of the variation of the currents in the coils. As a result, the induction \mathbf{B} should also change. Expanding the free energy in powers of $\delta\mathbf{B}(\mathbf{r})$ we get

$$\delta\mathcal{F} = \frac{1}{4\pi} \int \mathbf{H}(\mathbf{r}) \delta\mathbf{B}(\mathbf{r}) dV \quad (16.10)$$

where we have introduced the factor $(1/4\pi)$ just for convenience. The function $\mathbf{H}(\mathbf{r})$ *defined* in such a way is called the *magnetic field*. Outside the sample

$$\frac{\mathbf{h} \delta\mathbf{h}}{4\pi} = \frac{\mathbf{H} \delta\mathbf{B}}{4\pi}, \quad \mathbf{h} = \mathbf{B}.$$

Consequently, outside the sample the thermodynamic field \mathbf{H} is the same as the microscopic field.

The definition (16.10) is rather formal. To understand its physical meaning we consider the situation when *no external currents* flow into the sample. In this case

$$\bar{\mathbf{j}} = \bar{\mathbf{j}}_s + \mathbf{j}_e$$

where \mathbf{j}_e is the current density in the external coils, etc. We have

$$\operatorname{curl} \mathbf{H} = \frac{4\pi}{c} \mathbf{j}_e. \quad (16.11)$$

To prove this expression let us assume that the induction $\mathbf{B}(\mathbf{r})$ has the variation $\delta\mathbf{B}(\mathbf{r})$ for the time δt . As a results, the electric field \mathbf{E} appears in the external circuit according to the Maxwell equation

$$\operatorname{curl} \mathbf{E} = -\frac{1}{c} \frac{\delta \mathbf{B}}{\delta t}.$$

This electric field leads to the work $\delta t \int \mathbf{j}_e \mathbf{E} d\mathcal{V}$ upon the external currents, while the work produced by these currents is

$$\delta W = -\delta t \int \mathbf{j}_e \mathbf{E} d\mathcal{V}. \quad (16.12)$$

On the other hand, it is known from the thermodynamics that for reversible processes this work should be equal to the variation of the free energy, $\delta W = \delta \mathcal{F}$. Now we return to the definition (16.10)

$$\begin{aligned} \delta \mathcal{F} &= \delta t \frac{1}{4\pi} \int \mathbf{H} \frac{\delta \mathbf{B}}{\delta t} d\mathcal{V} = -\delta t \frac{c}{4\pi} \int \mathbf{H} \operatorname{curl} \mathbf{E} d\mathcal{V} \\ &= -\delta t \frac{c}{4\pi} \int \mathbf{E} \operatorname{curl} \mathbf{H} d\mathcal{V} - \delta t \frac{c}{4\pi} \int [\mathbf{E} \times \mathbf{H}] d\mathbf{s} \end{aligned}$$

where the last integral is calculated over the surface of the *whole system* and it is equal to the emitted energy. Neglecting the last term and comparing the result with Eq. (16.12) we prove Eq. (16.11).

Thermodynamic potential at fixed T and \mathbf{j}_e

If both the temperature and field are changed

$$\delta \mathcal{F} = \frac{1}{4\pi} \int \mathbf{H} \delta \mathbf{B} d\mathcal{V} - S \delta T.$$

To get the equilibrium at fixed T and \mathbf{B} one should minimize \mathcal{F} .

Usually, experimentally both the external currents and the temperature are kept fixed. To take it into account it is convenient to construct a special thermodynamic potential

$$\mathcal{G} = \mathcal{F} - \frac{1}{4\pi} \int \mathbf{B} \cdot \mathbf{H} d\mathcal{V}.$$

Consequently,

$$\delta \mathcal{G} = -\frac{1}{4\pi} \int \mathbf{B} \cdot \delta \mathbf{H} d\mathcal{V} - S \delta T. \quad (16.13)$$

Because $\operatorname{div} \mathbf{B} = 0$ one can put $\mathbf{B} = \operatorname{curl} \bar{\mathbf{A}}$ where $\bar{\mathbf{A}}$ is the “macroscopic” vector-potential. Then, after the integration by parts,

$$S \delta T + \delta \mathcal{G} = -\frac{1}{4\pi} \int \operatorname{curl} \bar{\mathbf{A}} \cdot \delta \mathbf{H} d\mathcal{V} = \frac{1}{4\pi} \int \bar{\mathbf{A}} \cdot \operatorname{curl} \delta \mathbf{H} d\mathcal{V} = \frac{1}{c} \int \bar{\mathbf{A}} \cdot \delta \mathbf{j}_e d\mathcal{V}.$$

This is just the potential which should be minimized at fixed T and \mathbf{j}_e .

Magnetization Curve in the Intermediate State

To get the magnetization curve $\mathbf{B}(\mathbf{H})$ let us calculate the \mathcal{G} -potential for the sample. If the magnetic field in a normal state if h_n

$$B = (1 - \rho)h_n + \rho \cdot 0 = (1 - \rho)h_n.$$

The free energy density is

$$F = F_n - \underbrace{\frac{\rho H_c^2}{8\pi}}_{\text{condensation energy}} + (1 - \rho) \frac{h_n^2}{8\pi}.$$

Here we dropped the interface energy at $S - N$ -boundaries, as well as the field distortion near the surface. Introducing B we get

$$F = F_n - \frac{\rho H_c^2}{8\pi} + \frac{B^2}{8\pi(1 - \rho)}.$$

Now

$$\mathcal{G}(B, \rho) = \mathcal{F} - \frac{BH}{4\pi} = F_n - \frac{\rho H_c^2}{8\pi} + \frac{B^2}{8\pi(1 - \rho)} - \frac{BH}{4\pi}.$$

1. Minimization with respect to ρ :

$$|B| = H_c(1 - \rho) \rightarrow h_n = H_c.$$

2. Minimization with respect to B :

$$B = H(1 - \rho).$$

That means: i) $\mathbf{B} \parallel \mathbf{H}$, ii) the quantity H is constant over the sample and equal to H_c . These relation are equivalent to the conventional relation $\mathbf{B} = \mu \mathbf{H}$ for a paramagnet. The only (but very important) difference is that in SC it is *non-linear*.

The distribution of magnetic field can be obtained from the set of equations

$$\begin{aligned} \operatorname{div} \mathbf{B} &= 0, \\ \operatorname{curl} \mathbf{H} &= 0, \\ \mathbf{H} &= \frac{\mathbf{B}}{B} H_c \end{aligned}$$

and usual boundary condition of continuity of B_n and H_t (normal component of induction and tangential component of the field).

Applications.

1. Force lines are the straight ones.

Proof. We have $H^2 = H_c^2$, so

$$0 = \nabla H^2 = 2(\mathbf{H} \cdot \nabla)\mathbf{H} + 2 \left[\mathbf{H} \times \underbrace{\text{curl } \mathbf{H}}_0 \right].$$

Consequently, $(\mathbf{H} \cdot \nabla)\mathbf{H} = 0$ - vector \mathbf{H} does not change along the force line and it is the straight one.

2. Field distribution in a sphere.

We chose \mathbf{z} -axis along \mathbf{B} and \mathbf{H} , which are constant. We know that inside $H = H_c$. Let us denote B as B_0 . Outside the sample

$$\mathbf{H} = \mathbf{B} = \mathbf{H}_0 - H_1 \frac{a^3}{2} \nabla \left(\frac{\cos \theta}{r^2} \right)$$

where H_1 is a constant. Then we apply boundary conditions:

$$\begin{aligned} \text{Continuity of } H_t &\rightarrow \left(H_0 + \frac{H_1}{2} \right) \sin \theta = H_c \sin \theta, \\ \text{Continuity of } B_n &\rightarrow (H_0 - H_1) \cos \theta = B_0 \cos \theta. \end{aligned}$$

As a result,

$$\begin{aligned} B_0 &= 3H_0 - 2H_c, \\ H_1 &= 2(H - H_c). \end{aligned}$$

We come to the conclusion the fraction of SC regions in a sphere is

$$\rho = 1 - \frac{B_0}{H_c} = 1 - \frac{3H_0 - 2H_c}{H_c} = 3 \frac{H_c - H_0}{H_c}, \quad \frac{2}{3}H_c < H_0 < H_c.$$

The field at the equator and at the poles of a sphere is shown in Fig. 16.6.

3. Critical current of a SC wire.

Consider a wire with the radius a , Fig. 16.7 carrying the current I . The field at the surface is $H(a) = 2I/ca$. If $H(a) < H_c$ all the wire is in a SC state. So, the critical current is

$$I_c = \frac{ca}{2} H_c.$$

At $I > I_c$ the surface is to become normal. On the other hand, in this case the current would be uniform that leads to the condition $H < H_c$ near the central part. Thus, we conclude that the external part (at $R < r < a$) should be normal while the internal part ($0 < r < R$) should be in an intermediate state.

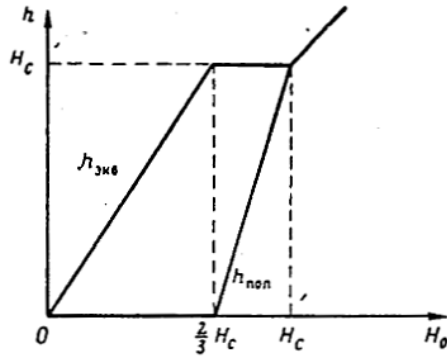


Figure 16.6: Field distribution at the equator (1) and poles (2) of a SC sphere.

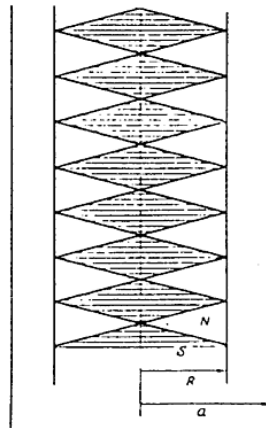


Figure 16.7: Field distribution in a wire.

At the boundary, at $r = R$, one has $H(R) = H_c$ and we get the condition for the current inside the tube $r < R$

$$H(R) = H_c = \frac{2I_1}{cR} \rightarrow I_1 = \frac{cRH_c}{2} = I_c \frac{R}{a} < I_c < I.$$

We come to the conclusion that the current $I - I_1$ should flow through the *normal* external part. As a result, this current should produce a constant electric field \mathbf{E} (remember: $\text{curl } \mathbf{E} = 0$). So, the central part cannot be completely SC. The picture of the intermediate state in a wire is shown in Fig. 16.7.

Microscopic Structure of the Intermediate State.

Let us discuss the structure of the intermediate state in more detail. Consider a plate shown in Fig. 16.8 and placed in a perpendicular magnetic field H_0 . Let us *assume* that

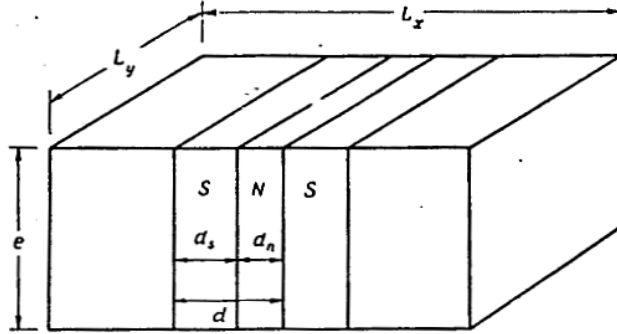


Figure 16.8: Microscopic domain structure.

the normal and SC regions form a layered structure. Our aim is to determine the widths $d_{n,s}$ of the layers.

The way is to minimize the free energy with respect to $d_{n,s}$ at given H_0 . That means the fixed *flux* through the plate and one has to use \mathcal{G} -potential. If the interfaces are flat and the surface energy is neglected

$$\mathcal{F} = -\underbrace{\frac{H_c^2}{8\pi} L_x L_y e \frac{d_s}{d}}_{\text{condens. magn. energy for } h = H_0(d/d_n)} + \underbrace{\frac{H_0^2}{8\pi} L_x L_y e \frac{d}{d_n}}_{\text{magn. energy for } h = H_0(d/d_n)},$$

Now we come to the next approximation. We have to take into account

1. Creation of the $N - S$ interfaces. We allow for the interfaces introducing a specific surface energy

$$\gamma = \frac{H_c^2}{8\pi} \lambda, \quad \lambda \sim 10^3 - 10^4 \text{ \AA}.$$

The corresponding contribution to \mathcal{F} is

$$\gamma e L_y \times (\text{number of interfaces}) = \frac{H_c^2}{8\pi} \lambda e L_y \frac{2L_x}{d}.$$

2. Deformation of the force lines near the surface. As shown in Fig. 16.9, SC domains become thinner near the surface. The energy "loss" is of the order $\sim d_s^2 L_y$ for each interface. The total loss is

$$\frac{H_c^2}{8\pi} d_s^2 L_y \frac{L_x}{d} U_0 \left(\frac{d_s}{d} \right)$$

where U_0 is the dimensionless function which depends on the shape of the regions.

3. Magnetic energy is also changed near the surface which we take into account by another dimensionless function V_0

$$\frac{H_0^2}{8\pi} d_s^2 L_y \frac{L_x}{d} V_0 \left(\frac{d_s}{d} \right).$$

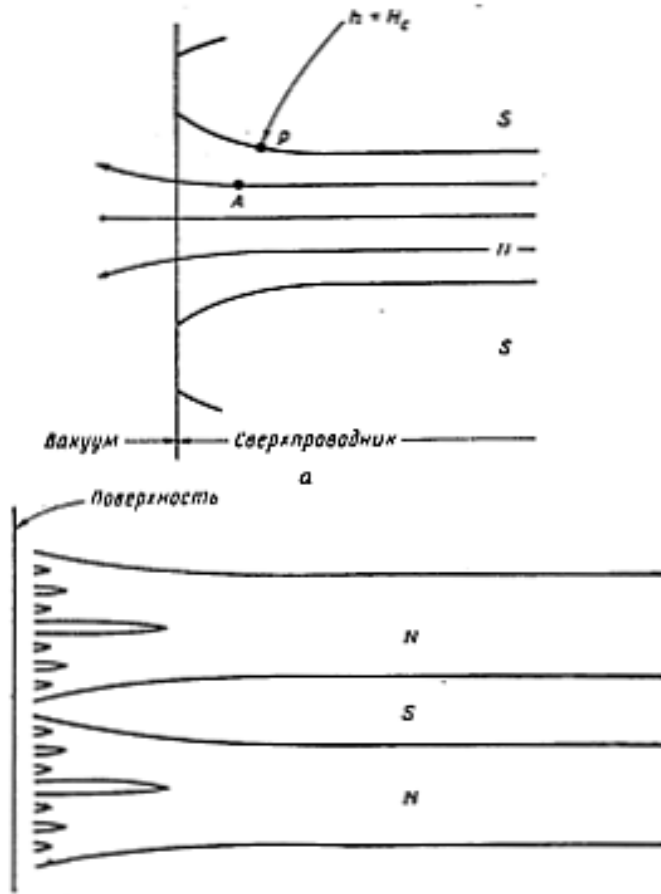


Figure 16.9: Domain structure near the surface.

Let us consider the quantities ρ_s and d as independent variables. As we have seen earlier, for a macroscopic material

$$1 - \rho_s = \frac{H_0}{H_c}.$$

We fix the SC density ρ_s according to this expression and get

$$\mathcal{F} = \mathcal{F}_{\text{macro}} + \frac{H_c^2}{8\pi} e L_x L_y \left\{ \frac{2\lambda}{d} + [\rho_s^2 U_0 + \rho_s^2 (1 - \rho_s^2) V_0] \frac{d}{e} \right\}.$$

Minimizing with respect to d we get

$$d = \sqrt{\frac{\lambda e}{\varphi(\rho_s)}}, \quad \varphi(\rho_s) = \frac{1}{2} [\rho_s^2 U_0 + \rho_s^2 (1 - \rho_s^2) V_0].$$

The typical estimates are: for $H_0/H_c \sim 0.7$, $\varphi = 10^{-2}$, we get $d \sim \sqrt{\lambda e}$. Taking $e \sim 1$ cm, $\lambda \sim 3000 \text{ \AA}$, we obtain $d \approx 0.06 \text{ cm}$.

There are several methods to observe the domain structure.

1. Change of the resistance of a thin wire while motion along the sample's surface (*Meshkovskii, Shal'nikov, 1947*).
2. Decoration by ferromagnetic powder.
3. Optical methods (using Faraday rotation).

We have discussed a simplified picture. The surface domain structure is much more complicated because of the surface winding (see the lower panel of Fig. 16.9).

16.4 The Nature of the Surface Energy.

In the end of the chapter we discuss qualitatively the nature of the interface contribution to the energy.

Consider two limiting cases.

1. $\zeta_0 \gg \delta$. In our previous macroscopic treatment we have assumed the sharp $N - S$ boundary. In the N -region the thermodynamic potential \mathcal{G} decreases due to magnetic contribution $(H_c^2/8\pi) - (H_c^2/4\pi)$ while in the S -region it decreases according to the condensation energy as $-(H_c^2/8\pi)$. What is the difference if we come to the microscopics? The new feature is that the superconductivity becomes "spoiled" at the distance $\sim \zeta_0$ that leads to the *loss* of the condensation energy. Consequently, $\lambda \sim \zeta_0$ and $\gamma \sim (H_c^2/8\pi)\zeta_0$.
2. $\zeta_0 \ll \delta$. The contribution discussed above is very small and we return to the London equation for the field. We have $h = H_c$ in the N -region while $h = H_s \exp(-x/\delta)$ in the S -region. The \mathcal{G} -potential has the form

$$\mathcal{G} = \int_{x>0} dV \left[F_n - \frac{H_c^2}{8\pi} + \frac{h^2}{8\pi} - \frac{Hh}{8\pi} + \frac{\delta^2}{8\pi} \left(\frac{dh}{dx} \right)^2 \right]$$

The specification of the items is

- 1 → free energy of normal phase at $H = 0$,
- 2 → condensation energy of the S -region,
- 3 → energy of magnetic field,
- 4 → microscopic analog of the quantity $-(BH/4\pi)$,
- 5 → kinetic energy of the currents.

We write the previous expression as

$$\mathcal{G} = \int dV \left(F_n - \frac{H_c^2}{8\pi} \right) + \gamma A$$

extracting the surface contribution. As a result,

$$\gamma = \frac{1}{8\pi} \int_0^\infty dx \left[h^2 + \delta^2 \left(\frac{dh}{dx} \right)^2 - 2hH_c \right] = -\frac{H_c^2}{8\pi}\delta.$$

We see that surface energy is *negative*. So the system "wants" to make as many surfaces as possible. It is not surprising that superconductors with $\zeta_0 \ll \delta$ have specific magnetic properties. They are called the type II superconductors and we will discuss these materials in the next chapter.

16.5 Problems

16.1. Derive Eq. (16.3).

Chapter 17

Magnetic Properties of Type II Superconductors

17.1 Magnetization Curve for a Long Cylinder

Type II superconductors have the following general properties

1. The Meissner effect in a long cylinder is complete only in very weak fields, $H < H_{c1}$. The *lower critical field* H_{c1} is much less than the thermodynamic field H_c defined as

$$F_n - F_s = \frac{H_c^2}{8\pi}.$$

2. At $H > H_{c1}$ magnetic field lines penetrate the cylinder. Nevertheless, even in the equilibrium state the penetration is not complete. The flux Φ is less than in the normal state. It means that persistent currents still exist. Such a situation holds at $H_{c1} < H < H_{c2}$ where H_{c2} is the so-called *upper critical field* which is much greater than H_c .
3. At $H > H_{c2}$ a macroscopic sample does not repel the flux, and $B \equiv H$. At the same time, at $H_{c2} < H < H_{c3}$ a surface SC layer still exists, the thickness being $\sim 10^3$ Å. Usually, $H_{c3} = 1.69H_{c2}$. One can observe the layer measuring surface conductivity. The physical reason is similar to the bubbles creation at the wall of the glass with beer (see later).

The values of critical fields for V₃Ga at $T = 0$ are: $H_{c1} = 200$ G, $H_c = 6\,000$ G, $H_{c2} = 300\,000$ G.

The temperature dependencies of the critical fields are shown in Fig. 17.1. Now we will concentrate on the region $H_{c1} < H < H_{c2}$ with partial field penetration. Such a region has been discovered by Shubnikov (1937) and is called the *Shubnikov phase*. Another names for this region are the *vortex state* (see below), and the *mixed state* (do not mix with the intermediate state for type I SC). The magnetization curve $B(H)$ is shown in Fig. 17.2.

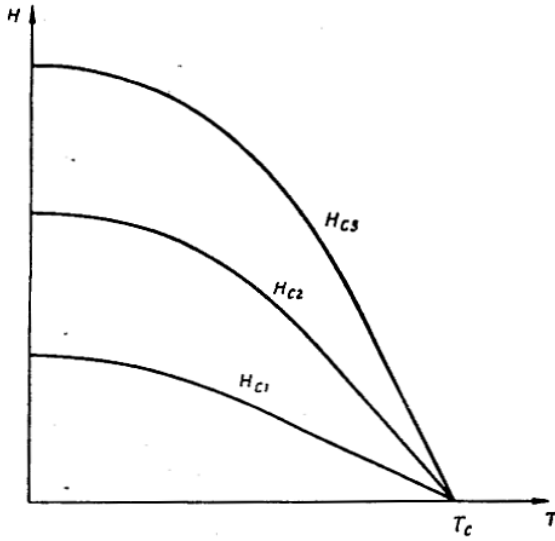


Figure 17.1: Phase diagram of a long cylinder of type II superconductor.

In some experimental works people prefer to plot magnetization

$$M = \frac{M - H}{4\pi}$$

(see Fig. 17.3). It is interesting that the areas below the curves in Fig. 17.2 are the same for type I and type II SC (*Problem 17.1*).

Now let us discuss the phase transition at H equal to the critical value H_{c1} or H_{c2} . We start with $H = H_{c2}$. According to experimental results,

1. The curve $B(H)$ is *continuous* at $H = H_{c2}$.
2. There is no hidden heat while there is a discontinuity of the specific heat.

So we face the typical type II transition. Let us consider thermodynamics for this transition. Let us consider two phases: the Shubnikov one i , and the "normal" one, j , in which most of the sample is in the normal state ($B = H$). We have

$$G_i = F_i(T, B) - \frac{B_i H}{4\pi},$$

the dependence $B(H)$ is determined from the condition

$$\frac{\partial}{\partial B_i} F_i(T, B_i) = \frac{H}{4\pi}, \quad (17.1)$$

while the entropy is

$$S_i = - \left(\frac{\partial G_i}{\partial T} \right)_H = - \frac{\partial F_i}{\partial T}.$$

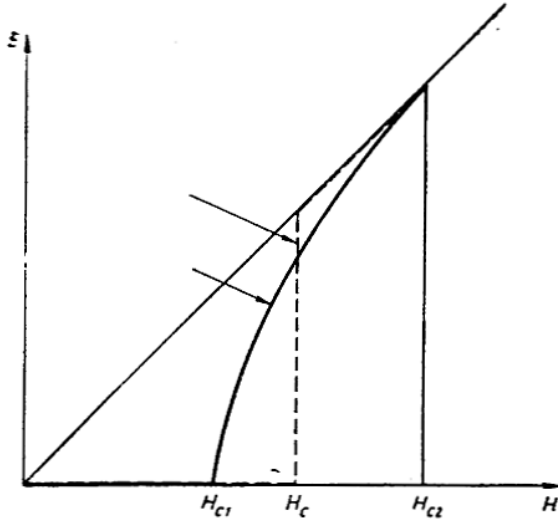


Figure 17.2: B vs H curves for type I (dashed line) and type II (solid line) superconductors.

Let the SC and normal state are in equilibrium at some field H^* (in our case $H^* = H_{c2}$) that means

$$G_i = G_j.$$

If there is no hidden heat the entropies should be also equal,

$$S_i = S_j.$$

That leads to the continuity of the curve $B(H)$ along the equilibrium line $H = H^*(T)$. Indeed, we have at the line

$$\frac{dF_i}{dT} = \frac{\partial F_i}{\partial T} + \frac{\partial F_i}{\partial B_i} \frac{dB_i}{dT}$$

Using the magnetization curve (17.1) we obtain $[dH = (dH^*/dT)dT]$

$$\frac{dG_i}{dT} = -S_i - \frac{B_i}{4\pi} \frac{dH^*}{dT}.$$

Then, along the equilibrium curve ($G_i = G_j$) we have

$$dG_i/dT = dG_j/dT, \quad S_i = S_j.$$

Thus $B_i = B_j$.

Now we can calculate the specific heat at given magnetic field as

$$C_i = T \left(\frac{\partial S_i}{\partial T} \right)_H.$$

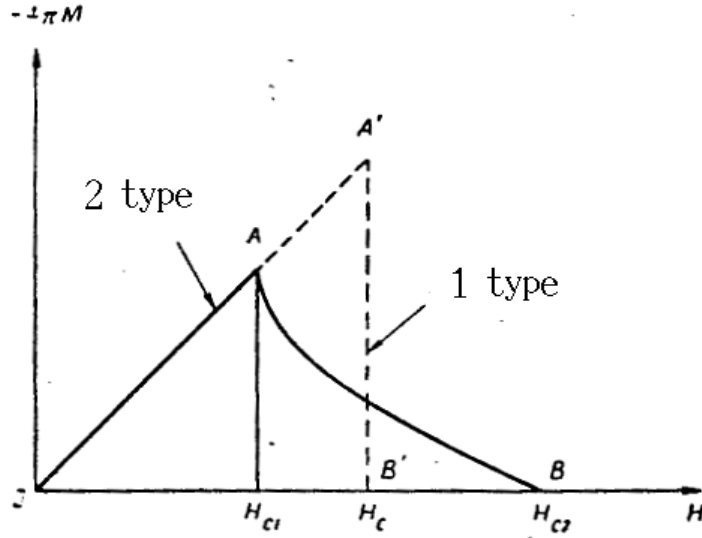


Figure 17.3: Magnetization curves for type I (dashed line) and type II (solid line) superconductors.

As earlier, we express

$$\frac{dS_i}{dT} = \left(\frac{\partial S_i}{\partial T} \right)_H + \left(\frac{\partial S_i}{\partial H} \right)_T \frac{dH^*}{dT}.$$

We should remember that along the magnetization curve

$$\frac{dS_i}{dT} = \frac{dS_j}{dt}.$$

As a result, we get

$$C_j - C_i = T \frac{dH^*}{dT} \left[\left(\frac{\partial S_i}{\partial H} \right)_T - \left(\frac{\partial S_j}{\partial H} \right)_T \right].$$

The last part of the calculation is to express the derivative $(\partial S_i / \partial H)_T$ through magnetic characteristics. We have

$$\left(\frac{\partial S_i}{\partial H} \right)_T = \left(\frac{\partial S_i}{\partial B_i} \right)_T \left(\frac{\partial B_i}{\partial H} \right)_T = -\frac{\partial^2 F_i}{\partial B_i \partial T} \left(\frac{\partial B_i}{\partial H} \right)_T = -\frac{1}{4\pi} \frac{\partial H(B_i, T)}{\partial T} \left(\frac{\partial B_i}{\partial H} \right)_T. \quad (17.2)$$

Then

$$\frac{dH^*}{dT} = \left(\frac{\partial H}{\partial T} \right)_{B_i} + \left(\frac{\partial H}{\partial B_i} \right)_T \frac{dB}{dT} \quad (17.3)$$

where

$$\frac{dB}{dT} = \frac{dB_i}{dT} = \frac{dB_j}{dT}$$

is the induction derivative along the equilibrium line. Substituting $(\partial H / \partial T)_{B_i}$ from (17.3) into (17.2) we get

$$\left(\frac{\partial S_i}{\partial H} \right)_T = -\frac{1}{4\pi} \frac{dH^*}{dT} \left(\frac{\partial B_i}{\partial H} \right)_T + \frac{1}{4\pi} \frac{dB}{dT}$$

$$C_j - C_i = \frac{T}{4\pi} \left(\frac{dH^*}{dT} \right)^2 \left[\left(\frac{\partial B_j}{\partial H} \right)_T - \left(\frac{\partial B_i}{\partial H} \right)_T \right]$$

Consequently, if one knows both the dependence $H^*(T)$ and magnetic susceptibility $\left(\frac{\partial B_j}{\partial H} \right)_T$ for both phases he can predict the specific heat discontinuity. Looking at the curves in Fig. 17.2 we see that $C_i > C_j$. This relation can be checked experimentally.

However one should keep in mind that it is rather difficult to reach true equilibrium conditions in type II SC (see below).

Check of thermodynamic properties is very important to prove that you observe the true bulk effects.

17.2 Microscopic Structure of the Mixed State

Physical Picture

The first important feature of type II SC is that the surface energy is negative (see Sec. 9.4). It is clear that in this case the system “wants” to form a fine mixture of normal and SC regions, the surface contribution to the free energy being *very important*.

To get the physical picture we start with the case of a mixed state with small B ($H - H_{c1} \ll H_{c1}$). One can imagine 2 types of the structure: thin layers (with the width $\sim \zeta$), or filaments with the radius $\sim \zeta$. One can show that at $\delta \gg \zeta$ the latter is more advantageous, and we discuss it in more detail.

Consider an isolated filament (see Fig. 17.4) which is called the *Abrikosov vortex line* (Abrikosov, 1956). It has a *core* with a radius ζ in which the density n_s of SC electrons decays to zero in the center. The magnetic field is maximal in the center while at $r > \delta$ it decays as a result of screening by circular currents.

As we will see later, the structure of the core is not important for many applications, at least at $\delta \gg \zeta$ (the core’s characteristics usually enter under the sign of logarithm). According to the results both of the experiment and the theory (we will discuss it in detail), the magnetic flux through a hole in a massive SC is *quantized*:

$$\Phi = k\Phi_0, \quad \Phi_0 = \frac{ch}{2e} = 2 \cdot 10^7 \text{ G} \cdot \text{cm}^2.$$

Thus, we can expect that the magnetic flux

$$\Phi = \int \mathbf{h} \cdot d\mathbf{S}$$

is equal to Φ_0 (maximal mixing in the system). The condition $\Phi = \Phi_0$ determines all the structure of an isolated line at $\delta \gg \zeta$.

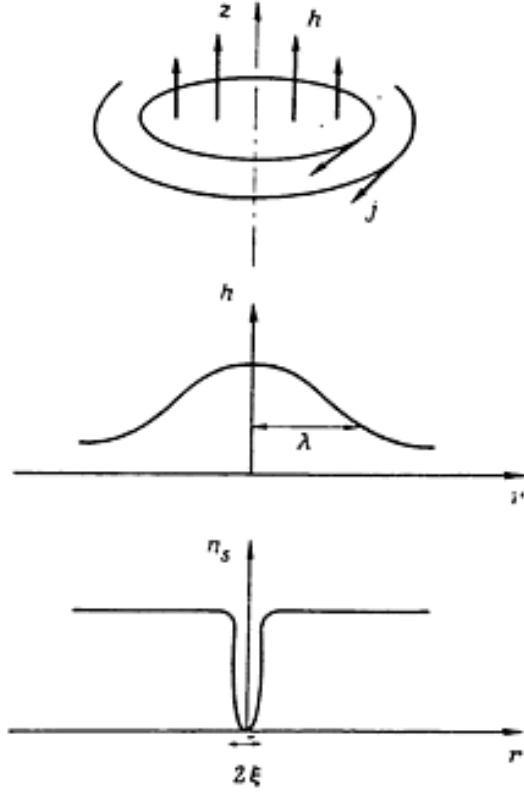


Figure 17.4: Structure of an isolated filament in a type II superconductor.

Properties of a isolated vortex line.

Because we are interested in the case $\delta \gg \zeta$, let us neglect the core contribution to the free energy. As was shown in Sec. 8.1.1, the contribution of an isolated line can be expressed as

$$\mathcal{F} = \frac{1}{8\pi} \int_{r>\zeta} [\mathbf{h}^2 + \delta_L^2 (\operatorname{curl} \mathbf{h})^2] dV. \quad (17.4)$$

We are interested in the *linear tension*, i.e. in the value of \mathcal{F} for a unit length. Outside the core the field is determined by the London equation

$$\mathbf{h} + \delta_L^2 \operatorname{curl} \operatorname{curl} \mathbf{h} = 0, \quad r > \zeta.$$

The presence of the core we take into account as a boundary condition at $r \rightarrow \zeta$. Because $\delta \gg \zeta$ we can express it introducing a δ -function source in the London equation as

$$\mathbf{h} + \delta_L^2 \operatorname{curl} \operatorname{curl} \mathbf{h} = \mathbf{z} \Phi_0 \delta_2(\mathbf{r}) \quad (17.5)$$

where \mathbf{z} is the unit vector directed along z -axis. To prove this assumption let us integrate the Eq. (17.5) over the area of a circular contour with the center at the axis and the radius

r . Using the Stokes theorem we get

$$\int \mathbf{h} \cdot d\mathbf{S} + \delta_L^2 \oint \operatorname{curl} \mathbf{h} \cdot d\mathbf{l} = \Phi_0.$$

The first integral in the l.h.s. is just the magnetic flux through the contour. Remembering that

$$\mathbf{j} = \frac{c}{4\pi} \operatorname{curl} \mathbf{h}$$

we see that for $r \gg \delta$ it is possible to neglect the contour integral. Thus we prove that the total flux is equal to Φ_0 .

Now we will find the structure of the field. It is easy to calculate it for

$$\zeta \ll r \ll \delta.$$

Indeed, one can neglect the first integral in the l.h.s. of Eq. (17.5) and get

$$\delta_L^2 2\pi r |\operatorname{curl} \mathbf{h}| = \Phi_0 \rightarrow |\operatorname{curl} \mathbf{h}| \equiv -\frac{\partial h}{\partial r} = \frac{\Phi_0}{2\pi\delta_L^2} \frac{1}{r}.$$

As a result,

$$h = \frac{\Phi_0}{2\pi\delta_L^2} \left(\ln \frac{\delta_L}{r} + \text{const} \right), \quad \zeta \ll r \ll \delta.$$

In principle, one can find exact solution of the London equation (17.5) together with the condition $\operatorname{div} \mathbf{h} = 0$. It has the form

$$h = \frac{\Phi_0}{2\pi\delta_L^2} K_0 \left(\frac{r}{\delta_L} \right) \quad (17.6)$$

where K_0 is the Bessel function. Comparing the exact solution (17.6) with the asymptotic one we get: const = 0. The large-distance asymptotics of the field, according to (17.6) is

$$h = \frac{\Phi_0}{2\pi\delta_L^2} \sqrt{\frac{\pi\delta_L}{2r}} e^{-r/\delta_L}, \quad r \gg \delta.$$

Now we can easily calculate the free energy. After integration of the second term in the integrand of (17.4) we get

$$\mathcal{F} = \frac{\delta_L^2}{8\pi} \int [\mathbf{h} \times \operatorname{curl} \mathbf{h}] d\mathbf{S}$$

where the integral is to be calculated over the surface of the core (the cylinder with the radius ζ). We have

$$\mathcal{F} = \frac{\delta_L^2}{8\pi} 2\pi\zeta h(\zeta) |\operatorname{curl} \mathbf{h}|_{r=\zeta} = \left(\frac{\Phi_0}{4\pi\delta_L} \right)^2 \ln \frac{\delta_L}{\zeta}. \quad (17.7)$$

Discussion of the last formula.

1. \mathcal{F} is only logarithmically dependent on ζ .
2. \mathcal{F} is proportional to Φ_0^2 . Consequently it is more profitable to create 2 vortices with the flux Φ_0 than one with the flux $2\Phi_0$.
3. We can rewrite the formula for $T = 0$ using the expression for Φ_0 and the relations (see below)

$$\zeta_0 = \frac{\hbar v_F}{\pi \Delta(0)}, \quad \frac{H_c^2}{8\pi} = \frac{1}{2} g(\epsilon_F) \Delta^2(0) \quad (17.8)$$

which follow from the BCS microscopic theory. We get

$$\mathcal{F} = \frac{\pi^2}{3} \frac{H_c^2}{8\pi} \zeta^2 \ln \frac{\delta_L}{\zeta}.$$

Now we can compare this energy with the core contribution which is of the order

$$\delta \mathcal{F}_{\text{core}} \sim \frac{H_c^2}{8\pi} \zeta^2.$$

We prove that the core contribution appears small in comparison with the one due to the supercurrent.

Isolated Vortex in a Slab

Now we discuss the properties of the isolated vortex in a thin slab ($d \ll \delta$) (Pearl). Inside we have the London equation

$$\mathbf{h} + \frac{4\pi\delta_L^2}{c} \operatorname{curl} \mathbf{j} = \mathbf{z} \Phi_0 \delta_2(\mathbf{r}).$$

It is convenient to come to the vector-potential \mathbf{A} ,

$$\mathbf{h} = \operatorname{curl} \mathbf{A}, \quad \operatorname{div} \mathbf{A} = 0.$$

We have

$$\mathbf{A} + \frac{4\pi\delta_L^2}{c} \mathbf{j} = \mathbf{F} \quad (17.9)$$

where in the cylindric co-ordinates

$$F_r = F_z = 0, \quad F_\theta = \frac{\Phi_0}{2\pi r}.$$

Now let us average Eq. (17.9) over z -co-ordinate. Because $d \ll \delta$ the quantities \mathbf{A} and \mathbf{F} are almost z -independent. Denoting the total current as $\mathbf{J} = \mathbf{j}d$ we get

$$\mathbf{J} = \frac{c}{4\pi} \frac{1}{\delta_{\text{eff}}} (\mathbf{F} - \mathbf{A}), \quad \delta_{\text{eff}} = \frac{\delta_L^2}{d}.$$

To solve the problem we need the field distribution outside the slab. We can make calculations assuming that we have a plane with the current $\mathbf{J}\delta(z)$:

$$\operatorname{curl} \operatorname{curl} \mathbf{A} = \frac{4\pi}{c} \mathbf{j} = \frac{1}{\delta_{\text{eff}}} (\mathbf{F} - \mathbf{A}) \delta(z) \rightarrow \nabla^2 \mathbf{A} + \frac{1}{\delta_{\text{eff}}} (\mathbf{F} - \mathbf{A}) \delta(z) = 0. \quad (17.10)$$

To get the last equation we used the London gauge ($\operatorname{curl} \operatorname{curl} \mathbf{A} = -\nabla^2 \mathbf{A}$).

To solve Eq. (17.10) we introduce Fourier components

$$\begin{aligned} \mathbf{A}_{\mathbf{q}k} &= \int \mathbf{A}(\mathbf{s}, z) e^{i(\mathbf{qs}+kz)} d\mathcal{V}, \quad \mathbf{A}_{\mathbf{q}} = \frac{1}{2\pi} \int dk A_{\mathbf{q}k} = \int \mathbf{A}(\mathbf{s}, z) \delta(z) e^{i\mathbf{qs}} d\mathcal{V}, \\ \mathbf{F}_{\mathbf{q}} &= \int \mathbf{F}(\mathbf{s}) \delta(z) e^{i\mathbf{qs}} d\mathcal{V} = i \frac{\Phi_0}{q^2} [\mathbf{z} \times \mathbf{q}] . \end{aligned} \quad (17.11)$$

where \mathbf{s} is the in-plane co-ordinate. We come to the very simple equation

$$-(q^2 + k^2) \mathbf{A}_{\mathbf{q}k} + \frac{1}{\delta_{\text{eff}}} \mathbf{A}_{\mathbf{q}} = \frac{1}{\delta_{\text{eff}}} \mathbf{F}_{\mathbf{q}}.$$

We can find $\mathbf{A}_{\mathbf{q}k}$ from this equation and then substitute it to the definition (17.11) of $\mathbf{A}_{\mathbf{q}}$. The result is

$$\mathbf{A}_{\mathbf{q}} = \frac{1}{2\pi} \int dk \frac{1}{q^2 + k^2} \frac{1}{\delta_{\text{eff}}} (\mathbf{A}_{\mathbf{q}} - \mathbf{F}_{\mathbf{q}}) = \frac{1}{2q\delta_{\text{eff}}} (\mathbf{A}_{\mathbf{q}} - \mathbf{F}_{\mathbf{q}}).$$

Finally,

$$\mathbf{A}_{\mathbf{q}} = \frac{1}{1 + 2q\delta_{\text{eff}}} \mathbf{F}_{\mathbf{q}}.$$

Now we know everything: the current

$$\mathbf{J}_{\mathbf{q}} = \frac{c}{4\pi} \frac{1}{\delta_{\text{eff}}} (\mathbf{F}_{\mathbf{q}} - \mathbf{A}_{\mathbf{q}}) = \frac{c}{4\pi\delta_{\text{eff}}} \frac{2q\delta_{\text{eff}}}{1 + 2q\delta_{\text{eff}}} \mathbf{F}_{\mathbf{q}},$$

magnetic field:

$$\mathbf{h}_{\mathbf{q}} = i [\mathbf{q} \times \mathbf{A}_{\mathbf{q}}] = \frac{\Phi_0}{1 + 2q\delta_{\text{eff}}} \mathbf{z}.$$

Small distances correspond to large q ($q\delta_{\text{eff}} \gg 1$). We have

$$h_{zq} \approx \frac{\Phi_0}{2q\delta_{\text{eff}}} \rightarrow h_z \approx \frac{\Phi_0}{4\pi\delta_{\text{eff}}} \frac{1}{r}.$$

For large distances ($q\delta_{\text{eff}} \ll 1$)

$$\begin{aligned} \mathbf{J}_{\mathbf{q}} &\approx \frac{c}{4\pi\delta_{\text{eff}}} 2q\delta_{\text{eff}} \mathbf{F}_{\mathbf{q}} = \frac{c\Phi_0}{2\pi} \frac{i[\mathbf{z} \times \mathbf{q}]}{q} \rightarrow J(r) = \frac{c\Phi_0}{4\pi^2 r^2}, \\ h_z(r) &= -\frac{4\pi\delta_{\text{eff}}}{c} \frac{1}{r} \frac{d}{dr} (Jr) \approx \frac{2\Phi_0\delta_{\text{eff}}}{\pi r^3}. \end{aligned}$$

The free energy of the vortex is

$$\mathcal{F} = \left(\frac{\Phi_0}{4\pi} \right)^2 \frac{1}{\delta_{\text{eff}}} \ln \frac{\delta_{\text{eff}}}{\zeta}.$$

It is important that the vortices in a slab have long range interaction. Indeed

$$\mathbf{F}_{12} = \frac{\Phi_0}{c} [\mathbf{z} \times \mathbf{J}(R_{12})] \propto R_{12}^{-2},$$

the interaction (repulsion) energy decays only as R_{12}^{-1} .

Interaction between Abrikosov Vortices.

Now we return to the bulk material and consider interaction of 2 vortex lines parallel to z -axis. We have

$$\mathbf{h} + \delta_L^2 \operatorname{curl} \operatorname{curl} \mathbf{h} = \mathbf{z} \Phi_0 [\delta_2(\mathbf{r} - \mathbf{r}_1) + \delta_2(\mathbf{r} - \mathbf{r}_2)].$$

Its solution is a superposition of the two fields

$$\mathbf{h}(\mathbf{r}) = \mathbf{h}_1(\mathbf{r}) + \mathbf{h}_2(\mathbf{r}), \quad \mathbf{h}_i(\mathbf{r}) = \mathbf{z} \frac{\Phi_0}{2\pi\delta_L^2} K_0 \left(\frac{|\mathbf{r} - \mathbf{r}_i|}{\delta_L} \right).$$

As usual, the free energy is

$$\mathcal{F} = \frac{\delta_L^2}{8\pi} \int [\mathbf{h} \times \operatorname{curl} \mathbf{h}] d\mathbf{S}$$

where one should integrate over the both cores' surfaces. As a result, the energy is

$$\mathcal{E} = \frac{\delta_L^2}{8\pi} \int [(\mathbf{h}_1 + \mathbf{h}_2) \times (\operatorname{curl} \mathbf{h}_1 + \operatorname{curl} \mathbf{h}_2)] (d\mathbf{S}_1 + d\mathbf{S}_2).$$

One can separate the $2^3 = 8$ items into 3 groups.

1. Sum of the free energies of separate lines

$$2\mathcal{F} = \frac{\delta_L^2}{8\pi} \left[\int [\mathbf{h}_1 \times \operatorname{curl} \mathbf{h}_1] d\mathbf{S}_1 + \int [\mathbf{h}_2 \times \operatorname{curl} \mathbf{h}_2] d\mathbf{S}_2 \right],$$

2. Item

$$\int (\mathbf{h}_1 + \mathbf{h}_2) \cdot ([\operatorname{curl} \mathbf{h}_1 \times d\mathbf{S}_2] + [\operatorname{curl} \mathbf{h}_2 \times d\mathbf{S}_1])$$

which is small at $\zeta \ll \delta_L$ (currents and fields remain finite at the axis of the opposite vortex),

3. The interaction energy

$$\mathcal{U}_{12} = \frac{\delta_L^2}{8\pi} \left[\int [\mathbf{h}_1 \times \operatorname{curl} \mathbf{h}_2] d\mathbf{S}_2 + \int [\mathbf{h}_2 \times \operatorname{curl} \mathbf{h}_1] d\mathbf{S}_1 \right].$$

Using the relation

$$|\operatorname{curl} \mathbf{h}| = \frac{\Phi_0}{2\pi\delta_L^2} \frac{1}{r}$$

we get

$$\mathcal{U}_{12} = \frac{\Phi_0}{4\pi} h_{12}, \quad h_{12} = \frac{\Phi_0}{2\pi\delta_L^2} K_0 \left(\frac{|\mathbf{r}_1 - \mathbf{r}_2|}{\delta_L} \right).$$

We see that lines repulse and the interaction energy decays as $R_{12}^{-1/2} \exp(-R_{12}/\delta_L)$ at long distances and behaves as $\ln |\delta_L/R_{12}|$ at small distances.

Interaction of a Vortex with a Surface

Now we discuss an important problem - interaction of a flux line with the sample's surface. Assume that we have a vortex line directed along z -axis and parallel to a plane surface (yz -plane), the external magnetic field being H . Let SC occupy the semi space $x \geq 0$. The London equation for the problem is

$$\mathbf{h} + \delta_L^2 \operatorname{curl} \operatorname{curl} \mathbf{h} = \mathbf{z} \Phi_0 \delta_2(\mathbf{r} - \mathbf{r}_L)$$

where $\mathbf{r}_L = (x_L, 0)$ is the "line co-ordinate". The boundary conditions at the surface are

$$\mathbf{h} = \mathbf{H}, \quad (\operatorname{curl} \mathbf{h})_x = 0, \quad \text{at } x = 0$$

(the second condition is just the vanishing of the current normal to the surface). We search solution as

$$\mathbf{h} = \mathbf{h}_1 + \mathbf{h}_2$$

where $\mathbf{h}_1 = \mathbf{H} \exp(-\mathbf{x}/\delta_L)$ is the penetration of the external field. The field \mathbf{h}_2 is due to the vortex. It can be calculated with the help of the *image approach*.

Let us add the *auxiliary* image vortex placed at the point $\bar{\mathbf{r}}_L = (-x_L, 0)$ with all the currents flowing in the opposite directions (mirror image), Fig. 17.5. It is clear that the sum of the fields produced by the both lines meet the boundary conditions. Thus we can prove that the field \mathbf{h}_2 is equal to this sum.

The resulting London equation becomes

$$\mathbf{h} + \delta_L^2 \operatorname{curl} \operatorname{curl} \mathbf{h} = \mathbf{z} \Phi_0 [\delta_2(\mathbf{r} - \mathbf{r}_L) - \delta_2(\mathbf{r} - \bar{\mathbf{r}}_L)]$$

and the total field is

$$h = H e^{-x/\delta_L} + \frac{\Phi_0}{2\pi\delta_L^2} \left[K_0 \left(\frac{|\mathbf{r} - \mathbf{r}_L|}{\delta_L} \right) - K_0 \left(\frac{|\mathbf{r} - \bar{\mathbf{r}}_L|}{\delta_L} \right) \right].$$

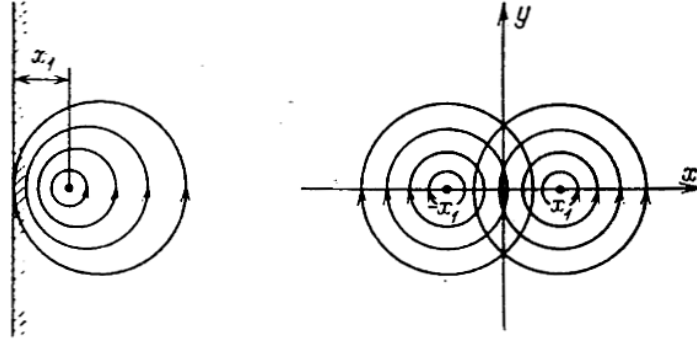


Figure 17.5: On the mirror image approach.

Then we go along the old way. The \mathcal{G} free energy

$$\mathcal{G} = \int dV \left[\frac{\mathbf{h}^2 + \delta_L^2 (\operatorname{curl} \mathbf{h})^2}{8\pi} - \frac{\mathbf{h} \cdot \mathbf{H}}{4\pi} \right].$$

We are interested in the energy per unit length. This integral is evaluated on the total volume of the sample ($x_1 \geq 0$) excluding the core region.

Transferring to the surface integral we get the first contribution

$$\delta\mathcal{G} = \frac{\delta_L^2}{4\pi} \int_{S_1+S_2} d\mathbf{S} \left[\left(\frac{1}{2}\mathbf{h} - \mathbf{H} \right) \times \operatorname{curl} \mathbf{h} \right].$$

where S_1 is the core's surface while S_2 is the sample's one. We denote the corresponding contributions as \mathcal{G}_1 and \mathcal{G}_2 . As usual, at $\zeta \rightarrow 0$ the main contribution to S_1 is the diverging part of $\operatorname{curl} \mathbf{h}$ and

$$\mathcal{G}_1 = \frac{\Phi_0}{4\pi} \left[\frac{1}{2} h(\mathbf{r}_L) - H \right].$$

The second contribution can be written as

$$\mathcal{G}_2 = -\frac{\delta_L^2}{8\pi} \int_{S_2} d\mathbf{S} [\mathbf{h}_1 \times \operatorname{curl} \mathbf{h}]$$

because at the surface $\mathbf{h}_2 = 0$, $\mathbf{h}_1 = \mathbf{H}$. Now we can split the field as $\mathbf{h} = \mathbf{h}_1 + \mathbf{h}_2$ and consider the part, proportional to $[\mathbf{h}_1 \times \operatorname{curl} \mathbf{h}_1]$ as an additive constant which is present in the absence of the vortex. The remainder is

$$\mathcal{G}_2 = \frac{\delta_L^2}{8\pi} \int_{S_2} d\mathbf{S} [\mathbf{h}_1 \times \operatorname{curl} \mathbf{h}_2].$$

To get the result, we do the following trick. The integral could be rewritten as

$$\int_{S_2} = \int_{S_1+S_2} - \int_{S_1}$$

According to the London equation

$$\int_{S_1+S_2} d\mathbf{S} [\mathbf{h}_1 \times \operatorname{curl} \mathbf{h}_2] = \int_{S_1+S_2} d\mathbf{S} [\mathbf{h}_2 \times \operatorname{curl} \mathbf{h}_1]$$

We can see that the integral is very small. Indeed, at the surface S_1 the field \mathbf{h}_1 is non-singular while at the surface the field \mathbf{h}_2 is zero because of the boundary conditions. As a result,

$$\mathcal{G}_2 = \frac{\delta_L^2}{8\pi} \int_{S_1} d\mathbf{S} [\mathbf{h}_1 \times \operatorname{curl} \mathbf{h}_2] = \frac{\Phi_0}{8\pi} h_1(\mathbf{r}_l).$$

The result is

$$\mathcal{G} = \frac{\Phi_0}{4\pi} \left[H e^{-x/\delta_L} + \frac{1}{2} h_2(\mathbf{r}_L) - H \right].$$

It is clear that $\mathcal{G} = 0$ if the line is at the surface ($h_2 = 0$). Now we should remember that the field h_2 consists from the initial and the mirror fields. The first contribution leads to the free energy of a isolated vortex

$$\mathcal{G} = \frac{\Phi_0 H_{c1}}{4\pi}$$

while the second is just the interaction energy between the line and the image

$$-\frac{\Phi_0}{8\pi} h(2x_L) \quad \text{with} \quad h(r) = \frac{\Phi_0}{2\pi\delta_L^2} K_0\left(\frac{r}{\delta_L}\right).$$

The final result is

$$\mathcal{G} = \frac{\Phi_0}{4\pi} \left[H e^{-x/\delta_L} - \frac{1}{2} h(2x_L) + H_{c1} - H \right].$$

The graphs of the function $\mathcal{G}(x_L)$ for different H are shown in Fig. 17.6. In these graphs the magnetic field is measured in units $\Phi_0/4\pi\delta_L^2$. We see that at finite magnetic fields a surface barrier appears (Bean-Livingstone barrier). This barrier is a consequence of interplay between the tendency to penetrate the sample and attraction to the image "antivortex". The barrier is very important for the real life and should be taken into account interpreting experimental results.

17.3 Magnetization curves.

Now we discuss the magnetization curves for type II SC. The free energy is

$$\mathcal{G} = n_L \mathcal{F} - \sum_{i,j} \mathcal{U}_{ij} - \frac{BH}{4\pi} \tag{17.12}$$

where n_L is the density of vortex lines, $B = n_L \Phi_0$.

To make explicit estimates we separate 3 regions

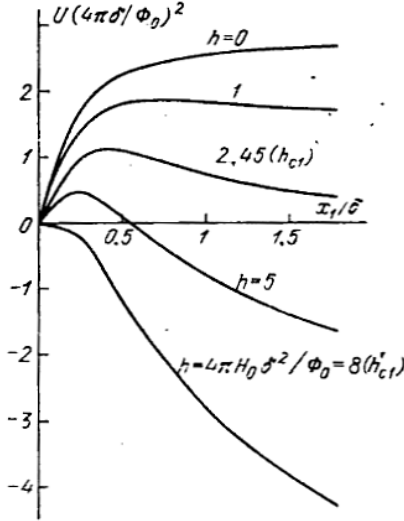


Figure 17.6: Surface barrier in type II superconductors.

1. Small B ($n_L \delta_L^2 \ll 1$) where only nearest neighbor's interaction is important.
2. Intermediate B ($n_L \delta_L^2 \gg 1$) where there are many vortices inside the interaction region.
3. High B where $n_L \zeta^2 \sim 1$ and the cores overlap.

The Lower Critical Field H_{c1} .

To get H_{c1} one can neglect interaction at all. We have

$$\mathcal{G} \approx B \left(\frac{\mathcal{F}}{\Phi_0} - \frac{H}{4\pi} \right).$$

The bracket vanishes at $H = H_{c1} = 4\pi\mathcal{F}/\Phi_0$. Indeed, at $H < H_{c1}$ the free energy \mathcal{G} increases with the increases of B , so the equilibrium value is $B = 0$. At the same time, at $H > H_{c1}$ there is a possibility to get a minimum at $B \neq 0$. Consequently, we get

$$H_{c1} = \frac{4\pi\mathcal{F}}{\Phi_0} = \frac{\Phi_0}{4\pi\delta_L^2} \ln \frac{\delta_L}{\zeta}. \quad (17.13)$$

Making use of the relations (17.8) we get for $T = 0$

$$\frac{H_{c1}}{H_c} = \frac{\pi}{\sqrt{24}} \frac{\zeta_0}{\delta_L} \ln \frac{\delta_L}{\zeta_0}$$

that is usually $\ll 1$.

The vicinity of H_{c1} .

Repulsion of vortices becomes important and one should use the general equation (17.12). A detailed calculation show that for all the values of B the most stable is *triangle* lattice vortices (see Fig. 17.7). Taking into account that only nearest neighbors are important

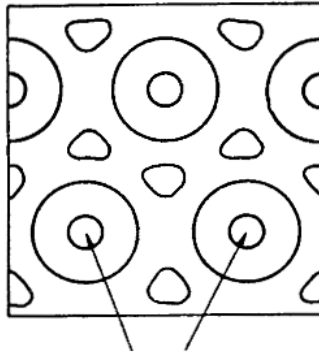


Figure 17.7: Triangle vortex lattice. Solid lines correspond to constant values of n_s .

we get

$$\mathcal{G} \approx \frac{B}{4\pi} \left[H_{c1} - H + \frac{1}{2} z \frac{\Phi_0}{2\pi\delta_L^2} K_0 \left(\frac{d}{\delta_L} \right) \right],$$

where z is the number of nearest neighbors ($z = 6$) while the lattice constant d is determined from the relation

$$B = n_L \Phi_0 = \frac{2}{\sqrt{3}} \frac{\Phi_0}{d^2}. \quad (17.14)$$

The result of calculations according to this scheme is shown in Fig. 17.8. We see the

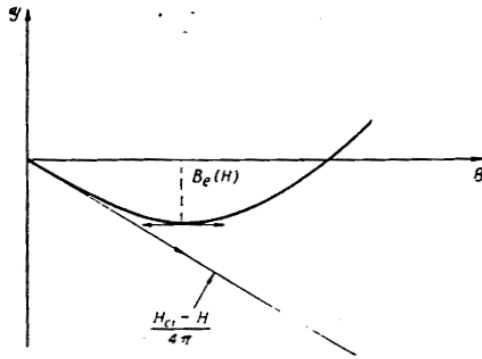


Figure 17.8: Dependence \mathcal{G} vs. B .

minimum which corresponds to the equilibrium value of induction B for a given H . The magnetization curve calculated from this model, as well as experimental results for the alloy More are shown in Fig. 17.9.

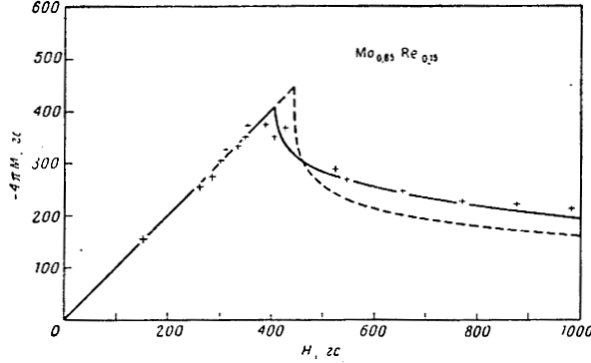


Figure 17.9: Magnetization curves for the vicinity of H_{c1} . Crosses - experiment, dashed line - calculations for a laminar model.

Intermediate magnetic fields.

In this case one should sum interaction energies for many vortices and we discuss the way to perform calculations. We start with the London equation

$$\mathbf{h} + \delta_L^2 \operatorname{curl} \operatorname{curl} \mathbf{h} = \mathbf{z} \Phi_0 \sum_i \delta_2(\mathbf{r} - \mathbf{r}_i)$$

where the sites \mathbf{r}_i form a 2D *periodic lattice*. Introducing the primitive cell we get the Fourier component

$$\mathbf{h}_{\mathbf{m}} = n_L \int_{Cell} \mathbf{h}(\mathbf{r}) e^{i\mathbf{m}\mathbf{r}} d^2r.$$

Certainly, $\mathbf{h}_{\mathbf{m}} \neq 0$ only for the vectors proportional to the reciprocal lattice vector. From the London equation we get

$$\mathbf{h}_{\mathbf{m}} = \frac{n_L \Phi_0}{1 + m^2 \delta_L^2}.$$

Then we write¹

$$\begin{aligned} \mathcal{F} &= \frac{1}{8\pi} \int [\mathbf{h}^2 + \delta_L^2 (\operatorname{curl} \mathbf{h})^2] d^2r = \frac{1}{8\pi} \sum_{\mathbf{m}} h_{\mathbf{m}}^2 (1 + m^2 \delta_L^2) = \\ &= \frac{B^2}{8\pi} \sum_{\mathbf{m}} \frac{1}{(1 + m^2 \delta_L^2)} = \frac{B^2}{8\pi} + \frac{B^2}{8\pi} \sum_{\mathbf{m} \neq 0} \frac{1}{(1 + m^2 \delta_L^2)}. \end{aligned}$$

The minimal value of m in the last sum is of the order $1/d \sim \sqrt{n_L}$. Thus, in our region $m^2 \delta_L^2 \gg 1$ and we can drop 1 in the denominator. The sum $\sum_{\mathbf{m} \neq 0} m^{-2}$ depends only on the properties of the lattice. To get an estimate one can replace the sum by the integral

$$\sum_{\mathbf{m} \neq 0} \frac{1}{m^2} \rightarrow \frac{1}{(2\pi)^2} \frac{1}{n_L} \int \frac{d^2m}{m^2} = \frac{1}{2\pi} \frac{1}{n_L} \int \frac{m dm}{m^2} = \frac{1}{2\pi n_L} \ln \left| \frac{m_{\max}}{m_{\min}} \right|$$

¹We calculate the energy per 1 cm.

with $m_{\max} \sim 1/d$, $m_{\min} \sim 1/\zeta$. Finally,

$$\mathcal{F} = \frac{B^2}{8\pi} + \frac{BH_{c1}}{4\pi} \frac{\ln(\beta d/\zeta)}{\ln(\delta_L/\zeta)}, \quad \beta = 0.381 \quad (\text{triangle lattice, exact solution}).$$

Then, as usual, we put $\partial\mathcal{G}/\partial B = \partial(\mathcal{F} - \frac{BH}{4\pi})/\partial B = 0$ and obtain (we should not forget that B is related to d according Eq. (17.14))

$$H = B + H_{c1} \frac{\ln(\beta' d/\zeta)}{\ln(\delta_L/\zeta)}, \quad \beta' = \beta/\sqrt{e}.$$

This result is in a good agreement with the experiment.

High field region

In this region where cores overlap our approach is definitely not sufficient. We return to this region later after the analysis of the Ginzburg-Landau theory and show that the upper critical field has the order Φ_0/ζ^2 .

17.4 Non-Equilibrium Properties. Pinning.

General Properties. Pinning.

It is clear that people are interested to fabricate a SC which is able to carry large supercurrent and, consequently, superconductivity should exist in a high magnetic field. We know that in type II SC the upper critical field can be very high. At the same time, the question arises:

Is the mixed state superconducting?

Indeed, in a magnetic field a force should act upon the vortices and leads them to move. But moving vortices should produce non-steady magnetic fields and, consequently, energy loss.

To make the estimates assume that there is one vortex with the current \mathbf{j} and the external current density is equal to \mathbf{j}^{ex} , the total current being $\mathbf{j} + \mathbf{j}^{ex}$. Assuming that the corresponding contribution to the free energy is $n_s m v_s^2 / 2 = (n_s m / 2)(j/n_s e)^2 = (4\pi/c^2 \delta_L^2) j^2 / 2$ we get for the interaction energy

$$\mathcal{U} = \frac{4\pi}{c^2 \delta_L^2} \int \mathbf{j}^{ex} \cdot \mathbf{j} d\mathcal{V}.$$

Then we remember that \mathbf{j} depends only on the difference $\mathbf{r} - \mathbf{r}_L$ (where \mathbf{r} is the 2D coordinate in the plane perpendicular to the line). The force is

$$F_k = -\frac{\partial \mathcal{U}}{\partial r_{Lk}} \propto -\sum_i \int d\mathcal{V} j_i^{ex} \frac{\partial j_i}{\partial r_{Lk}} = \sum_i \int d\mathcal{V} j_i^{ex} \frac{\partial j_i}{\partial r_k} =$$

$$= \sum_i \int dV j_i^{ex} \left(\frac{\partial j_i}{\partial r_k} - \frac{\partial j_k}{\partial r_i} \right) + \sum_i \int dV j_i^{ex} \frac{\partial j_k}{\partial r_i}.$$

The last item vanishes because by integration by parts we get $\operatorname{div} \mathbf{j}^{ex} = 0$. Thus

$$\mathbf{F} = \frac{4\pi}{c^2 \delta_L^2} \int [\mathbf{j}^{ex} \times \operatorname{curl} \mathbf{j}] dV.$$

Substituting the expression for $\operatorname{curl} \mathbf{j}$ we get

$$\mathbf{f}_L = \frac{\Phi_0}{c} [\mathbf{j}^{ex} \times \mathbf{z}]$$

for a separate vortex. The total force acting upon the vortex structure is just the Lorentz force

$$\mathbf{F}_L = \frac{1}{c} [\mathbf{j}^{ex} \times \mathbf{B}].$$

Now let us assume that a vortex moves with a given velocity \mathbf{v}_L and there is a viscous braking force

$$\mathbf{f}_v = -\eta \mathbf{v}_L.$$

As a result of force balance,

$$\mathbf{v}_L = \frac{\Phi_0}{\eta c} [\mathbf{j}^{ex} \times \mathbf{z}].$$

We see that $\mathbf{v}_L \perp \mathbf{j}^{ex} \perp \mathbf{B}$. According to the laws of electrodynamics, such a motion produces the electric field

$$\mathbf{E} = \frac{1}{c} [\mathbf{B} \times \mathbf{v}_L] = \frac{\Phi_0 B}{\eta c^2} \mathbf{j}^{ex}.$$

We observe the Ohm's law with the resistivity

$$\rho = \frac{\Phi_0 B}{\eta c^2}.$$

If we assume that at $B = H_{c2}$ $\rho = \rho_n$ (i.e. to the resistivity of the normal phase) we get

$$\eta(H_{c2}) = \frac{\Phi_0 H_{c2}}{\rho_n c^2} \quad \rightarrow \quad \rho = \rho_n \frac{B}{H_{c2}}.$$

This expression is only a very rough order-of-magnitude estimate. In fact the viscosity η is a very complicated and interesting function of both the temperature and magnetic field. From this point of view we get the conclusion that the superconductivity is destroyed at $H = H_{c1}$.

Fortunately, this statement is wrong. In real materials there is *pinning*, i.e. the vortices become pinned by the defects. One kind of pinning is the surface barrier we have discussed earlier. It is clear that large-scale defects with size greater than ζ should be very effective.

To get a simple estimate let us consider a cavity in the SC with $d \gg \zeta$. Suppose that the core is in the normal state that leads to the extra energy $\sim H_c^2 \zeta^2$ per unit length. If the

vortex passes through the cavity, this energy is absent. Consequently, there is attraction between the line and the cavity the force being of the order

$$f_p \sim H_c^2 \zeta$$

(we have taken into account that at the distance $\sim \zeta$ the vortex collides with its image). Combining this expression with the expression for the Lorentz force we find the critical current density able to start the motion

$$j_c \sim H_c \frac{c}{\delta_L}$$

(we have used the relations $f_L = j^{ex} \Phi_0 / c$ and $H_c \sim \Phi_0 / \delta_L \zeta$).

This discussion is oversimplified for many reasons.

- The pinning force acts upon a small part of the line while the Lorentz force is applied to the whole line.
- Vortices interact, and one should take into account the deformation energy of the lattice. So the problem is collective.
- It is not clear in general case what is the external current distribution inside the sample because the critical current is B -dependent. This property will be discussed in more detail in the following section.

As a result, the pinning is a very complicated property, and it is not completely understood today (especially for high- T_c materials).

Fluctuations, Flux Creep

One can imagine that at very $j < j_c$ the resistance is zero while at $j = j_c$ the resistance appears in a step-like character. This statement is wrong at finite temperatures. In fact, pinning centers create a potential profile for the vortices which can hop between the valleys due to thermally activated fluctuations. As a result, the resistance becomes finite (but exponentially small) at any finite temperature. This phenomenon is called the *flux creep*. In other words, the true critical current is zero at any finite temperature. That is why one should be very accurate in interpreting relevant experiments.

One of the consequences of the creep is dumping of the "persistent current". In practice, for many materials it can be not so important.

Another consequence are current instabilities. Assume that at some region a bunch of vortices hop from one position to another. Immediately this region becomes heated that leads to *decrease* of the critical current. As a result, the heating *increases*. Those instabilities are extremely important for superconductor engineering. The typical way to fight with them is the thermal shunting (composite materials).

The theory of creep and thermal instabilities is very complicated, and we do not discuss it in detail.

Critical State at $T = 0$.

In this section we discuss a very popular simplified model to treat the external current distribution in a type II SC - the critical state model.

Suppose that the SC is in a mixed state with the field $\mathbf{H} \parallel \mathbf{z}$. In the equilibrium the vortex density is constant and equal to $B(H)/\Phi_0$. If we come to a metastable state

- the vortex density is position dependent,
- there is the macroscopic current

$$j = \frac{c}{4\pi} \frac{\partial B}{\partial x}.$$

Now let us discuss the interaction forces. The first type is the repulsion one, we can describe them as a *pressure* p in the 2D vortex system. The total force acting upon the unit volume is $-\partial p / \partial x$. Another type is the pinning force which has the maximal value α_m . the necessary condition of the *mechanical equilibrium* is just

$$\left| \frac{\partial p}{\partial x} \right| \leq \alpha_m.$$

The *critical state model* uses the condition

$$\left| \frac{\partial p}{\partial x} \right| = \alpha_m$$

to determine the flux distribution.

To be more precise, we estimate the force from the thermodynamic considerations. Consider a piece of the xy -plane with the area S having N vortices (the external field is parallel to z -axis). We have

$$\mathcal{G} = SG, \quad p = - \left(\frac{\partial \mathcal{G}}{\partial S} \right)_N = -G - S \frac{\partial G}{\partial S}$$

At the same time, $B = N\Phi_0/S$, and

$$\frac{dS}{S} = -\frac{dB}{B}.$$

As a result

$$p = -G + B \frac{\partial G}{\partial B}.$$

Inserting the definition of the .thermodynamic potential G

$$G(B) = F(B) - \frac{BH}{4\pi}$$

and taking into account that in the equilibrium

$$\frac{\partial G}{\partial B} = 0 \quad \rightarrow \quad H(B) = 4\pi \frac{\partial F}{\partial B}$$

we get (*Problem 17.2*)

$$\frac{\partial p}{\partial x} = \frac{B}{4\pi} \frac{\partial H(B)}{\partial x} \quad (17.15)$$

In the most important cases at $H_{c2} \gg H \gg H_{c1}$ we have $H(B) \approx B$, and

$$-\frac{\partial p}{\partial x} = -\frac{B}{4\pi} \frac{\partial B}{\partial x} = \frac{Bj_y}{c}.$$

In this case the current distribution is given by the equation

$$\left| \frac{B}{4\pi} \frac{\partial B}{\partial x} \right| = \left| \frac{Bj_y}{c} \right| = \alpha_m \quad \text{at } H(B) \gg H_{c1}.$$

To solve the problem one needs the dependence $\alpha_m(B)$. According to *Bean's model* This dependence is *linear* and $j_y = \text{const}$. According to the *Kim-Anderson model* the quantity α_m is B -independent. The profiles of the magnetic induction for both models are shown in Fig. 17.10. Usual ways to study pinning is to observe the penetration of slow-varying

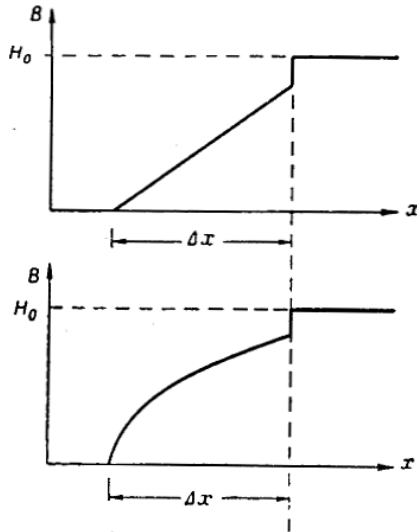


Figure 17.10: Magnetic induction profiles for the Bean and Kim-Anderson models.

magnetic field in a bulk or hollow cylinder.

17.5 Problems

17.1. Prove that the areas under magnetization curves are the same for type I and type II SC with the same H_c .

17.2. Derive Eq. (17.15).

Chapter 18

Microscopic Theory of Superconductivity. Basic Concepts

18.1 Phonon-Mediated Attraction

The first important motivation to study electron-phonon interaction was discovery of the *isotopic effect*, i.e. the dependence of the critical parameters on the atomic mass

$$T_c \propto M^{-1/2}, \quad H_c \propto M^{-1/2}.$$

Relying upon this fact the concept of phonon-mediated electron-electron attraction has been introduced (Frölich, Bardin, 1950).

To understand what happens let us discuss the scattering process shown in the left panel of Fig. 18.1. The amplitude of this second-order process is

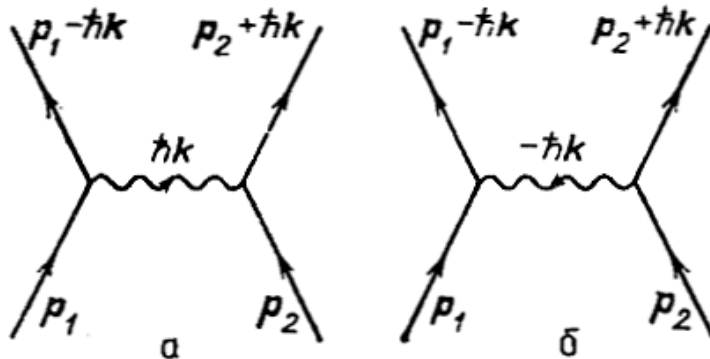


Figure 18.1: Electron-phonon processes.

$$\frac{|V_{\mathbf{q}}|^2}{\varepsilon_{\mathbf{k}_1} - \varepsilon_{\mathbf{k}_1 - \mathbf{q}} - \hbar\omega_{\mathbf{q}}}, \quad V_{\mathbf{q}} \equiv V_{\mathbf{k} - \mathbf{q}, \mathbf{k}}.$$

One should also add the amplitude of the process with phonon absorption shown in the right panel,

$$\frac{|V_{\mathbf{q}}|^2}{\varepsilon_{\mathbf{k}_2} - \varepsilon_{\mathbf{k}_1 + \mathbf{q}} - \hbar\omega_{\mathbf{q}}}.$$

We have taken into account that $\omega_{-\mathbf{q}} = \omega_{\mathbf{q}}$, $|V_{-\mathbf{q}}| = |V_{\mathbf{q}}|$. If we take into account the conservation law

$$\varepsilon_{\mathbf{k}_1} + \varepsilon_{\mathbf{k}_2} = \varepsilon_{\mathbf{k}'_1} + \varepsilon_{\mathbf{k}'_2}$$

we obtain

$$-\frac{2|V_{\mathbf{q}}|^2 \hbar\omega_{\mathbf{q}}}{(\hbar\omega_{\mathbf{q}})^2 - (\varepsilon_{\mathbf{k}_1} - \varepsilon_{\mathbf{k}_1 - \mathbf{q}})^2}.$$

Remembering that

$$V_q \sim -i \frac{p_F}{\sqrt{\mathcal{V}nm}}$$

we get the following expression for the total amplitude

$$-\frac{\hbar^3}{p_F m \mathcal{V}} \frac{(\hbar\omega_{\mathbf{q}})^2}{(\hbar\omega_{\mathbf{q}})^2 - (\varepsilon_{\mathbf{k}_1} - \varepsilon_{\mathbf{k}_1 - \mathbf{q}})^2}.$$

At $|\varepsilon_{\mathbf{k}_1} - \varepsilon_{\mathbf{k}_1 - \mathbf{q}}| \ll \hbar\omega_{\mathbf{q}}$ this amplitude is *negative*, and **k-independent**. Thus it is equivalent to a *short-range attraction*. Another feature is that it is the interaction with the total orbital moment equal to 0 (it is independent on **k**-direction). Consequently, the wave function should be *symmetric* with respect to the interchange of the electron co-ordinates. But, at the same time, electrons are Fermi particles, and the total wave function should be *antisymmetric*. Thus the spin wave function should be also antisymmetric, i.e. the spins should be *opposite*. It is the only way to meet the Pauli principle. It is clear that phonons with maximal q are most important (density of states increases with q). Consequently we can say that electrons within a thin layer $|\varepsilon_{\mathbf{k}_1} - \varepsilon_{\mathbf{k}'_1}| \sim \hbar\omega_D$ near the Fermi surface attract, that in the momentum space means $\Delta p \sim \hbar\omega_D/v_F$.

Let us find a typical spatial spread of the corresponding quantum state from the uncertainty principle

$$\Delta r \sim \hbar/\Delta p \sim v_F/\omega_D \sim (v_F/s)a \sim a\sqrt{M/m}.$$

Thus, phonon attraction is a *long-range one*, its order-of-magnitude estimate being \hbar^3/mp_F . At the same time, there is Coulomb repulsive forces. It is a short-range one due to screening and it can be written as

$$e^2 a^2 \delta(\mathbf{r}_1 - \mathbf{r}_2).$$

The ratio is

$$\frac{e^2 a^2}{\hbar^3/mp_F} \sim \frac{e^2}{\hbar v_F} \sim 1.$$

Actually, this is a very rough estimate, and in real metals the contributions to the interaction differ strong enough. In the following we neglect Coulomb effects and will model the interaction as constant $-\lambda$ where

$$\lambda \sim \frac{\hbar^3}{mp_F} \sim \frac{1}{g(\epsilon_F)}$$

in the interval

$$\epsilon_F - \hbar\omega_{\mathbf{q}} < \varepsilon < \epsilon_F + \hbar\omega_{\mathbf{q}}$$

and $\lambda = 0$ outside this interval (the so-called *BCS model*).

18.2 Cooper Pairs

Attraction does not mean formation of a bound state. Indeed, in 3D case the bound state is formed only if the potential is strong enough. The situation in 1D case is completely different: one can form a bounded state at *any* attraction strength. At the first glance, this model has nothing to do with the real life, but L. Cooper (1956) was first to understand that it is the case. Unfortunately, his original paper had a mistake and we shall follow the correct derivation below.

To start, let us reformulate the quasiparticle concept which has been used for normal metals. We know, the electron states near the Fermi surface are very similar to ordinary particles, they decay very weakly. Thus, it is natural to use the Fermi level as the origin of the energies. As a result, we can classify the particles with $\varepsilon > \epsilon_F$ as *particle-like* excitations. We write their energies as

$$\xi^{(e)} = \frac{p^2}{2m} - \frac{p_F^2}{2m} \approx v_F(p - p_F).$$

The excitations with $\varepsilon < \epsilon_F$ behave as *anti-particles* (or holes). It is conventional to write their energy as

$$\xi^{(h)} = -\xi^{(e)} = \frac{p_F^2}{2m} - \frac{p^2}{2m} \approx v_F(p_F - p)$$

to have positive energy. As a result, one can describe the quasiparticle spectrum in a normal metal as

$$\xi(p) = v_F(p - p_F).$$

This spectrum is shown in Fig. 18.2, the right branch corresponding to particle-like excitations while the left branch - to antiparticle-like ones. One should remember that anti-particles have the electric charge of the opposite sign.

Consider the interaction of 2 quasiparticles with the same $|\mathbf{k}|$. The SE is

$$[\mathcal{H}_0(\mathbf{r}_1) + \mathcal{H}_0(\mathbf{r}_2) + U(\mathbf{r}_1, \mathbf{r}_2)] \Psi(\mathbf{r}_1, \mathbf{r}_2) = E\Psi(\mathbf{r}_1, \mathbf{r}_2) \quad (18.1)$$

where $\mathcal{H}_0(\mathbf{r}_1)$ is the *free quasiparticle Hamiltonian*

$$\mathcal{H}_0(\mathbf{r}_1)\psi_{\mathbf{k}}(\mathbf{r}_1) = |\xi_{\mathbf{k}}|\psi_{\mathbf{k}}(\mathbf{r}_1)$$

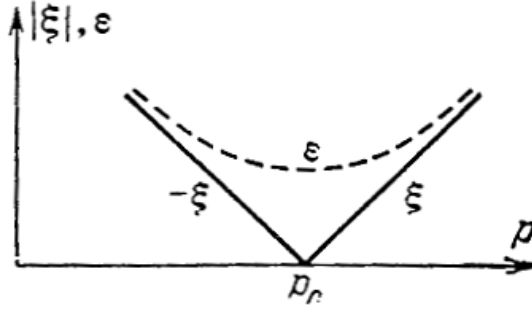


Figure 18.2: Quasiparticle spectra in normal (solid line) and SC (dashed line) states.

[for free particles $\psi_{\mathbf{k}}(\mathbf{r}_1) = (\mathcal{V})^{-1/2} \exp(i\mathbf{k}\mathbf{r}_1)$].

In the ground state both the total momentum and total spin should vanish. As a result, one can construct the wave function as

$$\Psi(\mathbf{r}_1, \mathbf{r}_2) = \sum_{\mathbf{k}} c_{\mathbf{k}} \psi_{\mathbf{k}\uparrow}(\mathbf{r}_1) \psi_{-\mathbf{k}\downarrow}(\mathbf{r}_2) \quad (18.2)$$

where arrows mean the spin projections. Substituting (18.2) into Eq. (18.2) we get (Check!) the following integral equation

$$2|\xi_{\mathbf{k}}|c_{\mathbf{k}} + \sum_{\mathbf{k}'} U_{\mathbf{k}\mathbf{k}'} c_{\mathbf{k}'} = E c_{\mathbf{k}}$$

To solve the equation we use the model

$$U_{\mathbf{k}\mathbf{k}'} = \begin{cases} -\lambda, & k_F - \omega_D/v_F < |\mathbf{k}|, |\mathbf{k}'| < k_F + \omega_D/v_F \\ 0, & \text{outside the interval} \end{cases} \quad (18.3)$$

Denoting

$$I = \sum_{\substack{|\mathbf{k}'|=k_F+\omega_D/v_F \\ |\mathbf{k}'|=k_F-\omega_D/v_F}} c_{\mathbf{k}'} \quad (18.4)$$

we get

$$c_{\mathbf{k}} = \frac{\lambda I}{2|\xi_{\mathbf{k}}| - E}$$

Substituting this equation into Eq. (18.4) we get the *self-consistency equation*

$$I = \sum_{\substack{|\mathbf{k}'|=k_F+\omega_D/v_F \\ |\mathbf{k}'|=k_F-\omega_D/v_F}} \frac{\lambda I}{2|\xi_{\mathbf{k}}| - E}$$

Now recall that we are interested in a bound state with *negative* energy. Denoting $E = -2\Delta$ and transferring the sum into the integral we get

$$1 = \frac{\lambda g(\epsilon_F)}{2} \ln \left(\frac{\hbar\omega_D}{\Delta} \right)$$

(the factor 1/2 is due to the fact that we sum over the states with one spin projections while g is defined as the sum over spin projections) or

$$\Delta = \hbar\omega_D \exp \left[-\frac{2}{\lambda g(\epsilon_F)} \right]. \quad (18.5)$$

The exact calculation has an extra factor 2 which is due to the fact that all the matrix elements are to be calculated in the renormalized state (see below).

Let us discuss Eq. (18.5).

- As we have seen, $\lambda g(\epsilon_F) \sim 1$. Actually, this product is small enough to make $\Delta \ll \hbar\omega_D$.
- We see that $\Delta \neq 0$ at *any interaction strength*. The reason is that we have integrated only in *the vicinity of the Fermi surface*. Indeed, our rule

$$\int \frac{d^3 k}{(2\pi)^3} \rightarrow \frac{g(\epsilon_F)}{2} \int d\xi$$

corresponds to 1D problem.

- We see that presence of the Fermi surface is very important. So we can suspect that its temperature smearing will strongly influence upon superconductivity.

18.3 Energy Spectrum

Now we come to a more detailed calculation. For this we need to minimize the free energy with respect to the wave functions. To do this we need to calculate the ground state energy for attracting electrons.

As we have mentioned, it is convenient to come to the quasiparticle description. Then means that we will keep the *chemical potential* ϵ_F fixed as the origin of the energy reference frame. Technically, we transfer the Hamiltonian to $\mathcal{H} - \epsilon_F N$ where $N = \sum_{\mathbf{k}\sigma} a_{\mathbf{k}\sigma}^\dagger a_{\mathbf{k}\sigma}$ is the operator of number of particles.

We have

$$\mathcal{H} - \epsilon_F N = \sum_{\mathbf{k}\sigma} \xi_{\mathbf{k}} a_{\mathbf{k}\sigma}^\dagger a_{\mathbf{k}\sigma} - \frac{\lambda}{\mathcal{V}} \sum_{\substack{\mathbf{k}_1 + \mathbf{k}_2 = \mathbf{k}'_1 + \mathbf{k}'_2 \\ \mathbf{k}_1 \neq \mathbf{k}'_1}} a_{\mathbf{k}'_1 \uparrow}^\dagger a_{\mathbf{k}'_2 \downarrow}^\dagger a_{\mathbf{k}_2 \downarrow} a_{\mathbf{k}_1 \uparrow}. \quad (18.6)$$

All the sums are calculated over the thin interval $\sim \hbar\omega_D$ near the Fermi surface. Now we come to a very important point - introduction of *quasiparticle operators*. In a normal metal we can define

$$\begin{aligned} \text{at } p > p_F : \quad a_{\mathbf{k}\sigma} &= \alpha_{\mathbf{k}\sigma}, \\ \text{at } p < p_F : \quad a_{\mathbf{k}\sigma} &= \alpha_{-\mathbf{k}-\sigma}^\dagger \end{aligned}$$

where $\alpha(\alpha^\dagger)$ are the *quasiparticle operators*. The physical meaning is transparent: annihilation of an electron below the Fermi surface is just the same as creation of a hole with opposite values of momentum and spin.

In a superconductor, the ground state is more complicated, and the simplest way to calculate the spectrum is to use the *Bogolyubov transform*

$$\begin{aligned} a_{\mathbf{k}\uparrow} &= u_{\mathbf{k}} \alpha_{\mathbf{k}\uparrow} + v_{\mathbf{k}} \alpha_{-\mathbf{k}\downarrow}^\dagger, \\ a_{\mathbf{k}\downarrow} &= u_{\mathbf{k}} \alpha_{\mathbf{k}\downarrow} - v_{\mathbf{k}} \alpha_{-\mathbf{k}\uparrow}^\dagger. \end{aligned}$$

Note that this transform conserves the momentum. Then we use the coefficients $u_{\mathbf{k}}, v_{\mathbf{k}}$ as parameters to minimize the free energy. The key idea - to diagonalize the Hamiltonian (18.6).

Let us check the commutation rules for the quasiparticle operators. We have

$$\begin{aligned} \left\{ a_{\mathbf{k}\sigma}, a_{\mathbf{k}'\sigma'}^\dagger \right\} &= u_{\mathbf{k}}^2 \left\{ \alpha_{\mathbf{k}\sigma}, \alpha_{\mathbf{k}'\sigma'}^\dagger \right\} + v_{\mathbf{k}}^2 \left\{ \alpha_{-\mathbf{k}-\sigma}, \alpha_{-\mathbf{k}'-\sigma'}^\dagger \right\} \\ &\quad + \sigma u_{\mathbf{k}} v_{\mathbf{k}} \left\{ \alpha_{\mathbf{k}\sigma}, \alpha_{-\mathbf{k}'-\sigma} \right\} + \sigma u_{\mathbf{k}} v_{\mathbf{k}} \left\{ \alpha_{-\mathbf{k}-\sigma}^\dagger, \alpha_{\mathbf{k}'\sigma'}^\dagger \right\} = 1. \end{aligned}$$

If we request the usual Fermi commutation rules for the quasiparticle commutators we obtain the relation

$$u_{\mathbf{k}}^2 + v_{\mathbf{k}}^2 = 1 \tag{18.7}$$

that leaves only one free variable, say $v_{\mathbf{k}}$.

Now we can express the energy through the quasiparticle numbers $n_{\mathbf{k}\sigma} = \langle \alpha_{\mathbf{k}\sigma}^\dagger \alpha_{\mathbf{k}\sigma} \rangle$. We get

$$\begin{aligned} \langle \mathcal{H} - \epsilon_F N \rangle &= \sum_{\mathbf{k}} \xi_{\mathbf{k}} [u_{\mathbf{k}}^2 (n_{\mathbf{k}\uparrow} + n_{\mathbf{k}\downarrow}) + v_{\mathbf{k}}^2 (2 - n_{\mathbf{k}\uparrow} - n_{\mathbf{k}\downarrow})] - \\ &\quad - \lambda \sum_{\mathbf{k}} u_{\mathbf{k}} v_{\mathbf{k}} (1 - n_{\mathbf{k}\uparrow} - n_{\mathbf{k}\downarrow}) \sum_{\mathbf{k}'} u_{\mathbf{k}'} v_{\mathbf{k}'} (1 - n_{\mathbf{k}'\uparrow} - n_{\mathbf{k}'\downarrow}) \equiv E - \epsilon_F N. \end{aligned} \tag{18.8}$$

Now we calculate the variation with respect to $v_{\mathbf{k}}$ taking into account (18.7). We get (*Problem 18.1*)

$$2\xi_{\mathbf{k}} u_{\mathbf{k}} v_{\mathbf{k}} = \Delta (1 - 2v_{\mathbf{k}}^2), \tag{18.9}$$

$$\Delta = \lambda \sum_{\mathbf{k}} u_{\mathbf{k}} v_{\mathbf{k}} (1 - n_{\mathbf{k}\uparrow} - n_{\mathbf{k}\downarrow}). \tag{18.10}$$

The solution of the equation is

$$u_{\mathbf{k}}^2 = \frac{1}{2} \left(1 + \frac{\xi_{\mathbf{k}}}{\varepsilon_{\mathbf{k}}} \right), \quad v_{\mathbf{k}}^2 = \frac{1}{2} \left(1 - \frac{\xi_{\mathbf{k}}}{\varepsilon_{\mathbf{k}}} \right) \tag{18.11}$$

where

$$\varepsilon_{\mathbf{k}} = \sqrt{\xi_{\mathbf{k}}^2 + \Delta^2}. \quad (18.12)$$

In the following we consider isotropic model where the spectrum is independent of the direction of \mathbf{k} .

Now we can calculate the *quasiparticle energy* as a variational derivative of the total energy with respect to the distribution function. Thus we have

$$\delta\mathcal{E} = \sum_{\mathbf{k}} (\varepsilon_{\mathbf{k}\uparrow} \delta n_{\mathbf{k}\uparrow} + \varepsilon_{\mathbf{k}\downarrow} \delta n_{\mathbf{k}\downarrow}).$$

Because of the symmetry of the problem we get $\varepsilon_{\mathbf{k}\uparrow} = \varepsilon_{\mathbf{k}\downarrow}$, $n_{\mathbf{k}\uparrow} = n_{\mathbf{k}\downarrow}$. After the variation of (18.8) with respect to, say, $n_{\mathbf{k}\uparrow}$ at constant $u_{\mathbf{k}}, v_{\mathbf{k}}$ we get

$$\varepsilon_{\mathbf{k}\uparrow} = \frac{\delta\mathcal{E}}{\delta n_{\mathbf{k}\uparrow}} = \sqrt{\xi_{\mathbf{k}}^2 + \Delta^2} = \varepsilon_k$$

So we come to the following conclusion

- There is the gap Δ in the quasiparticle spectrum.
- At $|\xi_k| \gg \Delta$ we come to the normal metal properties: $\varepsilon_k \rightarrow |\xi_k|$, at $\xi_k > 0$ $u_k \rightarrow 1$, $v_k \rightarrow 0$, at $\xi_k < 0$ $u_k \rightarrow 0$, $v_k \rightarrow 1$. Thus, we come to the quasiparticles of the normal metal.

The presence of the gap is very important. It means that there is no low-energy excitations and the electron liquid may be *superfluid*. Indeed, if the liquid moves as total with the velocity \mathbf{v} the energy in the laboratory frame of reference is

$$\varepsilon(p) + \mathbf{p}\mathbf{v}.$$

Consequently, to create a new quasiparticle one needs the condition $\varepsilon(p) + \mathbf{p}\mathbf{v} < 0$ to be met, or

$$v < v_c = \min \frac{\varepsilon(p)}{p}.$$

In the presence, of the gap we come to the relation¹

$$v_c \sim \frac{\Delta}{p_F}.$$

We have discussed here the simplest variant of the theory with the *s*-state pairing. The pairing with non-zero orbital moment has been discussed in connection with superconductivity in the so-called heavy fermion compounds and with superfluid ${}^3\text{He}$.

¹The life is not so simple. One can imagine also *collective* excitations which may have no gap. As has been shown, it is not the case because of the finite electron charge.

18.4 Temperature Dependence of the Energy Gap

Now we are prepared to discuss the temperature dependence of the gap. From Eq. (18.10) we get

$$1 = \frac{\lambda}{2} \int dk \frac{1 - 2n_0(\varepsilon_k)}{\varepsilon_k} = \frac{\lambda g(\epsilon_F)}{2} \int_0^{\hbar\omega_D} d\xi \frac{\tanh(\sqrt{\xi^2 + \Delta^2}/2k_B T)}{\sqrt{\xi^2 + \Delta^2}}. \quad (18.13)$$

At $T \rightarrow 0$ $\tanh(\sqrt{\xi^2 + \Delta^2}/2k_B T) \rightarrow 1$ and

$$1 = \frac{\lambda g(\epsilon_F)}{2} \ln \frac{2\hbar\omega_D}{\Delta(0)} \rightarrow \Delta(0) = 2\hbar\omega_D \exp(-2/\lambda g(\epsilon_F)) \quad (18.14)$$

(note the extra factor 2). At $T \rightarrow T_c$ $\Delta \rightarrow 0$, and

$$1 = \frac{\lambda g(\epsilon_F)}{2} \int_0^{\hbar\omega_D} d\xi \frac{\tanh(\xi/2k_B T_c)}{\xi} = \frac{\lambda g(\epsilon_F)}{2} \ln \frac{2\hbar\omega_D \gamma}{\pi k_B T_c}, \quad \gamma = 1.78.$$

Thus

$$k_B T_c = \frac{2\hbar\omega_D \gamma}{\pi} \exp(-2/\lambda g(\epsilon_F)) \quad (18.15)$$

and

$$\Delta(0) = \frac{\pi}{\gamma} k_B T_c = 1.76 k_B T_c. \quad (18.16)$$

To discuss the temperature dependence one can simply calculate the integral in (18.13). It is interesting to show the analytical formula, so we analyze briefly this integral. At low temperatures we can rewrite the formula as

$$\ln \frac{\Delta(0)}{\Delta} = \int_0^\infty \frac{1 - \tanh(\sqrt{\xi^2 + \Delta^2}/2k_B T)}{\sqrt{\xi^2 + \Delta^2}} d\xi = 2f\left(\frac{\Delta}{k_B T}\right)$$

where

$$f(x) = \int_1^\infty \frac{dy}{(1 + e^{yx}) \sqrt{y^2 - 1}}, \quad y = \frac{\sqrt{\xi^2 + \Delta^2}}{\Delta}.$$

Here we have used the expression (18.14) and expanded the integration region to infinity (the important region is $\sim \Delta$). We are interested in large values of x ,

$$f(x) = \int_1^\infty dy \sum_{n=1}^\infty (-1)^{n+1} \frac{e^{-nyx}}{\sqrt{y^2 - 1}}.$$

Then we use the integral representation for the McDonald function

$$K_\nu(z) = \frac{\Gamma(1/2)}{\Gamma(\nu + 1/2)} \left(\frac{z}{2}\right)^\nu \int_1^\infty e^{-yz} (y^2 - 1)^{\nu-1/2} dy$$

and get

$$f(x) = \sum_{n=1}^{\infty} (-1)^{n+1} K_0(nx) \sim \sqrt{\frac{\pi}{2x}} e^{-x}.$$

Thus, at $T \ll T_c$

$$\Delta(T) = \Delta(0) - \underbrace{\sqrt{2\pi\Delta(0)k_B T} e^{-\Delta(0)/k_B T}}_{\sim \text{number of quasiparticles}}. \quad (18.17)$$

At $T \rightarrow T_c$ it is convenient to expand over $\Delta \rightarrow 0$. To do this we also divide the expression (18.13) by $(\lambda g(\epsilon_F)/2)$ and subtract its limit at $\Delta = 0$. We get

$$\ln \frac{T_c}{T} = \int_0^\infty d\xi \left[\frac{\tanh \xi}{\xi} - \frac{\tanh(\sqrt{\xi^2 + \Delta^2}/2k_B T)}{\sqrt{\xi^2 + \Delta^2}} \right].$$

Then we use the formula

$$\tanh\left(\frac{\pi x}{2}\right) = \left(\frac{4x}{\pi}\right) \sum_{k=0}^{\infty} \frac{1}{(2k+1)^2 + x^2}.$$

Substituting this formula into the previous one, expanding over Δ and integrating over ξ we get

$$\ln \frac{T_c}{T} = 2 \sum_{n=1}^{\infty} (-1)^{n+1} \frac{(2n-1)!!}{(2n)!!} \left(\frac{\Delta}{\pi k_B T}\right)^{2n} \sum_{k=0}^{\infty} \frac{1}{(2k+1)^{2n+1}}.$$

The first item leads to

$$\Delta \approx 3.06 \sqrt{\frac{T_c}{T_c - T}}.$$

The graph of the dependence $\Delta(T)$ is given in Fig. 18.3.

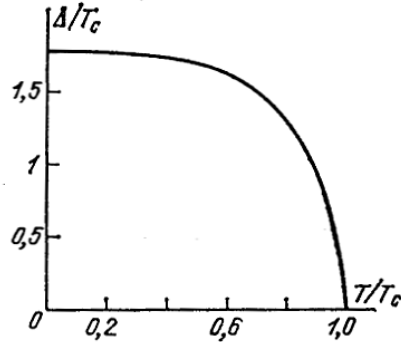


Figure 18.3: Temperature dependence of the energy gap.

18.5 Thermodynamics of a Superconductor

According to statistical physics, the thermodynamic potential Ω depending on the variables T, \mathcal{V} , and chemical potential ϵ is

$$\Omega = -k_B T \ln Z,$$

with the partition function

$$Z = \sum_{s,N} \exp \left[-\frac{E_{sN} - N\epsilon}{k_B T} \right] = \text{Tr} \left[\exp \left(-\frac{\mathcal{H} - \epsilon N}{k_B T} \right) \right].$$

Splitting the Hamiltonian as $\mathcal{H}_0 + \mathcal{H}_{int}$ and differentiating with respect to the interaction constant λ we get

$$\frac{\partial \Omega}{\partial \lambda} = \frac{1}{\lambda} \frac{\text{Tr} \left[\mathcal{H}_{int} \exp \left(-\frac{\mathcal{H} - \epsilon N}{k_B T} \right) \right]}{\text{Tr} \left[\exp \left(-\frac{\mathcal{H} - \epsilon N}{k_B T} \right) \right]} = \frac{1}{\lambda} \langle \mathcal{H}_{int} \rangle.$$

Substituting the expression for the interaction Hamiltonian²

$$\mathcal{H}_{int} = -\lambda \sum_{\mathbf{k}_1 + \mathbf{k}_2 = \mathbf{k}'_1 + \mathbf{k}'_2, \mathbf{k}_1 \neq \mathbf{k}'_1} a_{\mathbf{k}'_1 \uparrow}^\dagger a_{\mathbf{k}'_2 \downarrow}^\dagger a_{\mathbf{k}_2 \downarrow} a_{\mathbf{k}_1 \uparrow}$$

and expressing the electron operators through the quasiparticle ones as

$$a_{\mathbf{k}\uparrow} = u_{\mathbf{k}} \alpha_{\mathbf{k}\uparrow} + v_{\mathbf{k}} \alpha_{-\mathbf{k}\downarrow}^\dagger, \quad a_{\mathbf{k}\downarrow} = u_{\mathbf{k}} \alpha_{\mathbf{k}\downarrow} - v_{\mathbf{k}} \alpha_{-\mathbf{k}\uparrow}^\dagger$$

we get (*Problem 18.2*)

$$\frac{\partial \Omega}{\partial \lambda} = -\frac{\Delta^2}{\lambda^2}. \tag{18.18}$$

Then we can integrate over λ to get

$$\Omega_s - \Omega_n = - \int_0^\lambda \frac{d\lambda_1}{\lambda_1^2} \Delta^2(\lambda_1).$$

It is more convenient to change variables to introduce inverse function $\lambda_1(\Delta_1)$ to get $d\lambda_1 = (d\lambda_1/d\Delta_1)d\Delta_1$. We get

$$\Omega_s - \Omega_n = \int_0^\Delta \frac{d\lambda_1^{-1}(\Delta_1)}{d\Delta_1} \Delta_1^2 d\Delta_1.$$

We can obtain the integrand from the self-consistency equation

$$\ln \frac{\Delta(0)}{\Delta} = \int_0^\infty \frac{1 - \tanh(\sqrt{\xi^2 + \Delta^2}/2k_B T)}{\sqrt{\xi^2 + \Delta^2}} d\xi = 2f \left(\frac{\Delta}{k_B T} \right),$$

²For brevity we assume $\mathcal{V} = \infty$.

$$\Delta(0) = 2\hbar\omega_D \exp(-2/\lambda g(\epsilon_F)).$$

Finally,

$$\lambda^{-1}(\Delta) = \frac{g(\epsilon)}{2} \left[\ln \frac{2\hbar\omega_D}{\Delta} - 2f\left(\frac{\Delta}{2k_B T}\right) \right].$$

As a result, we get the exact formula

$$\Omega_s - \Omega_n = \frac{g(\epsilon)}{2} \int_0^\Delta \frac{d}{d\Delta_1} \left[\ln \frac{2\hbar\omega_D}{\Delta_1} - 2f\left(\frac{\Delta_1}{2k_B T}\right) \right] \Delta_1^2 d\Delta_1.$$

It is easy to calculate asymptotic behavior because we know all the functions. At $T = 0$

$$\Omega_s(0) = -\frac{g(\epsilon)\Delta^2(0)}{4}.$$

This formula is clear enough: the bonding energy $\sim \Delta$ while the number of electron in the actual region $\sim g(\epsilon)\Delta$. The temperature-dependent part at low temperatures is

$$\Omega_s(T) - \Omega_s(0) \sim g(\epsilon)\sqrt{2\pi(k_B T)^3 \Delta(0)} e^{-\Delta(0)/k_B T}.$$

As a result, we get

$$S_s = -\frac{\partial \Omega_s}{\partial T} \approx g(\epsilon) \sqrt{\frac{2\pi\Delta^3(0)}{k_B T}} e^{-\Delta(0)/k_B T},$$

$$C_s = T \frac{\partial S_s}{\partial T} = k_B g(\epsilon) \sqrt{\frac{2\pi\Delta^5(0)}{(k_B T)^3}} e^{-\Delta(0)/k_B T}.$$

Near T_c we get

$$\Omega_s - \Omega_n = -g(\epsilon) \frac{7\zeta(3)}{32} \frac{\Delta^4}{(\pi k_B T)^2}$$

where $\zeta(3)$ is the Riemann zeta function

$$\zeta(x) = \sum_1^\infty \frac{1}{n^x}.$$

In the same way, we can obtain the specific heat

$$C_s(T_c) = C_n(T_c) + \frac{4}{7\zeta(3)} k_B \frac{p_F m(k_B T_c)}{\hbar^3}, \quad C_n(T_c) = k_B \frac{p_F m(k_B T_c)}{3\hbar^3}.$$

Making use of all the relations we get near T_c

$$\frac{C_s(T)}{C_n(T_c)} = 2.42 + 4.76 \frac{T - T_c}{T_c}.$$

The temperature dependence of the specific heat is shown in Fig. 18.4. We can also de-

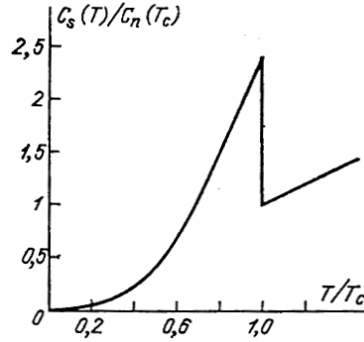


Figure 18.4: Temperature dependence of the specific heat.

termine the critical magnetic field. Indeed, the additional terms to all the thermodynamic potentials are equal if they are expressed in the corresponding variables. In particular,

$$(\delta F)_{N,T,V} = (\delta \Omega)_{\epsilon,T,V}$$

and

$$\Omega_n - \Omega_s = \frac{H_c^2}{8\pi}.$$

Thus,

$$H_c(0) = \sqrt{2\pi g(\epsilon)} \Delta(0).$$

At low temperatures we have

$$H_c(T) = H_c(0) \left[1 - \frac{\pi^2}{3} \frac{(k_B T)^2}{\Delta^2(0)} \right]$$

while near T_c

$$H_c = k_B \sqrt{\frac{16\pi}{7\zeta(3)} \frac{mp_F}{\hbar^3}} (T_c - T) \approx 1.735 H_c(0) \frac{T_c - T}{T_c}.$$

In conclusion to this section, we should mention that one very important assumption has been extensively used, namely the interaction assumed to be *weak*:

$$\lambda g(\epsilon) \ll 1.$$

There are some materials where this condition is invalid. The theory should be generalized to treat those materials.

18.6 Electromagnetic Response of a Superconductor

In this section we analyze the applicability of the London equation and its generalization.

Qualitative Discussion

When we've derived the London equation

$$\mathbf{j} = -Q\mathbf{A}, \quad Q = \frac{n_e e^2}{mc^2}$$

we thought that the current is transferred by the electrons. Now we know that *Cooper pairs* are responsible for the superconductivity. The main difference is that Cooper pairs have quite large size $\zeta \sim \hbar v_F / \Delta \gg a$ (at $\Delta \approx 10$ K $\zeta \sim 10^{-4}$ cm). So we face the problem: why Cooper pairs do not scatter each other? The answer is that they represent eigenstates of the SE and their wave function are orthogonal. That means that one can discuss the *correlation length* rather than the *size* of pairs.

Because of the correlation, the relation current-vectorial potential becomes *non-local*

$$j_i = - \sum_k \int Q_{ik}(\mathbf{r} - \mathbf{r}') A_k(\mathbf{r}') dV'$$

where $Q_{ik}(\mathbf{r})$ decays at $|\mathbf{r}| > \zeta$. The London equation is the case at very slow variation of $\mathbf{A}(\mathbf{r})$. In this situation one can replace $\mathbf{A}(\mathbf{r}') \rightarrow \mathbf{A}(\mathbf{r})$ and

$$\int Q_{ik}(\mathbf{r} - \mathbf{r}') dV' = \delta_{ik} Q.$$

We know that the characteristic scale for the variation of \mathbf{A} is δ , consequently we return to the London limit at $\delta \gg \zeta$. In the opposite limiting case, $\delta \ll \zeta$, we can assume that only the electron which live for a long time in the surface region $\sim \delta$ are effective. The number of those electrons is proportional to the angle $\theta \sim \delta/\zeta$ and $n_{eff} \approx n_e \delta/\zeta$. As a result,

$$\delta \sim \sqrt{\frac{mc^2 \zeta}{4\pi n_e e^2 \delta}} \rightarrow \delta_P \sim \left[\frac{mc^2 \zeta}{4\pi n_e e^2} \right]^{1/3}.$$

As was mentioned, most of pure materials are type I (or *Pippard*) ones. Nevertheless, one can decrease the ratio ζ/δ introducing defects, impurities, etc. Moreover, we'll see later that near T_c all the SC are type II ones.

It is interesting that all the formulas do not feel if the carriers are single electrons, or pairs (one can check it replacing $e \rightarrow 2e$, $n_e \rightarrow n_e/2$).

Theory of the Meissner Effect at $T = 0$.

Here we consider only the simplest case: response of a SC to a weak steady magnetic field at $T = 0$. The aim is just to show the way of microscopic calculations.

According to quantum mechanics, in the presence of a magnetic field the Hamilton acquires the additional factor

$$\delta\mathcal{H} = -\frac{1}{c} \int \mathbf{j} \delta\mathbf{A} dV \text{ that leads to } \delta E = -\frac{1}{c} \int \langle \mathbf{j} \rangle \delta\mathbf{A} dV$$

where $\langle \mathbf{j} \rangle$ is the quantum mechanical average of the current (in the following we omit the angular brackets $\langle \dots \rangle$). We will do like this: we calculate the contribution to the energy and then find the variation with respect to $\delta \mathbf{A}$. It is clear that in a weak field we need 2nd order of the perturbation theory because the current is proportional to \mathbf{A} .

The prescription to take the field into account is to replace³

$$\mathbf{p} = -i\hbar\nabla \rightarrow -i\hbar\nabla + \frac{e}{c}\mathbf{A}$$

As a result, for a bare electron the Hamiltonian is

$$\frac{1}{2m} \left[-\hbar^2 \nabla^2 - i\hbar \frac{e}{c} (\mathbf{A} \nabla + \nabla \mathbf{A}) + \left(\frac{e}{c}\right)^2 \mathbf{A}^2 \right].$$

We see that only the first item conserves the particle momentum. To take the lack of conservation into account we expand the vector potential in the Fourier series

$$\mathbf{A}(\mathbf{r}) = \sum_{\mathbf{q}} \mathbf{A}_{\mathbf{q}} e^{i\mathbf{qr}},$$

the component $\mathbf{A}_{\mathbf{q}}$ can be understood as the absorption of electromagnetic quantum with the momentum $\hbar\mathbf{q}$. Using the second quantization, we write the interaction Hamiltonian as a sum of 2 parts

$$\mathcal{H}_1 = \frac{e}{mc} \sum_{\mathbf{p}, \mathbf{q}, \sigma} [(\mathbf{p} - \hbar\mathbf{q}) a_{\mathbf{p}\sigma}^\dagger a_{\mathbf{p}-\hbar\mathbf{q}, \sigma} + \mathbf{p} a_{\mathbf{p}\sigma}^\dagger a_{\mathbf{p}-\hbar\mathbf{q}, \sigma}] \mathbf{A}_{\mathbf{q}},$$

$$\mathcal{H}_2 = \frac{e^2}{2mc^2} \sum_{\mathbf{p}, \mathbf{q}, \mathbf{q}', \sigma} a_{\mathbf{p}\sigma}^\dagger a_{\mathbf{p}-\hbar\mathbf{q}-\hbar\mathbf{q}', \sigma} \mathbf{A}_{\mathbf{q}} \mathbf{A}_{\mathbf{q}'}. \quad \text{---}$$

Then we transform $\sum_{\sigma} a_{\mathbf{p}\sigma}^\dagger a_{\mathbf{p}', \sigma}$ through quasiparticle operators

$$\begin{aligned} \sum_{\sigma} a_{\mathbf{p}\sigma}^\dagger a_{\mathbf{p}', \sigma} &= u_p u_{p'} (\alpha_{\mathbf{p}\uparrow}^\dagger \alpha_{\mathbf{p}'\uparrow} + \alpha_{\mathbf{p}\downarrow}^\dagger \alpha_{\mathbf{p}'\downarrow}) + v_p v_{p'} (\alpha_{-\mathbf{p}\downarrow}^\dagger \alpha_{-\mathbf{p}'\downarrow}^\dagger + \alpha_{-\mathbf{p}\uparrow}^\dagger \alpha_{-\mathbf{p}'\uparrow}^\dagger) + \\ &+ u_p v_{p'} (\alpha_{\mathbf{p}\uparrow}^\dagger \alpha_{-\mathbf{p}'\downarrow}^\dagger - \alpha_{\mathbf{p}\downarrow}^\dagger \alpha_{-\mathbf{p}'\uparrow}^\dagger) + v_p u_{p'} (\alpha_{-\mathbf{p}\downarrow}^\dagger \alpha_{\mathbf{p}'\uparrow} - \alpha_{-\mathbf{p}\uparrow}^\dagger \alpha_{\mathbf{p}'\downarrow}). \end{aligned}$$

The part \mathcal{H}_2 is of the 2nd order and it is enough to average it over the ground state. We see that only the item proportional to $v_p v_{p'}$ gives a finite contribution, and $\mathbf{k} = \mathbf{k}'$, $\mathbf{q} = -\mathbf{q}'$. At low temperatures $n_{\mathbf{p}\uparrow} = n_{\mathbf{p}\downarrow} = 0$, and

$$E_2 = \frac{e^2}{mc^2} \sum_{\mathbf{p}, \mathbf{q}} v_p^2 \mathbf{A}_{\mathbf{q}} \mathbf{A}_{-\mathbf{q}}.$$

³Remember: the charge is denoted as $-e$.

The first order contribution from \mathcal{H}_1 vanishes because $\sum_{\mathbf{p}} \mathbf{p} v_p^2 \delta_{\mathbf{q},0} = 0$. Thus, in the second order

$$E_1 = \sum_{m \neq 0} \frac{|\langle 0 | \mathcal{H}_1 | m \rangle|^2}{E_{(0)} - E_{(m)}}.$$

Then, in the ground state there is no quasiparticles, and only transitions involving 2 quasiparticles are important. As a result

$$\langle 0 | \mathcal{H}_1 | m \rangle = \frac{2}{mc} (u_p v_{\mathbf{p}-\hbar\mathbf{q}} - v_p u_{\mathbf{p}-\hbar\mathbf{q}}) (2\mathbf{p} - \hbar\mathbf{q}), \quad \mathbf{E}_{(0)} - E_{(m)} = -(\varepsilon_{\mathbf{p}} + \varepsilon_{\mathbf{p}-\hbar\mathbf{q}}).$$

Finally

$$E_1 = - \left(\frac{e}{2mc} \right)^2 \sum_{\mathbf{p}, \mathbf{q}} (u_p v_{\mathbf{p}-\hbar\mathbf{q}} - v_p u_{\mathbf{p}-\hbar\mathbf{q}})^2 \frac{((2\mathbf{p} - \hbar\mathbf{q}) \cdot \mathbf{A}_{\mathbf{q}}) ((2\mathbf{p} - \hbar\mathbf{q}) \cdot \mathbf{A}_{-\mathbf{q}})}{\varepsilon_{\mathbf{p}} + \varepsilon_{\mathbf{p}-\hbar\mathbf{q}}}.$$

We have taken into account that $\mathbf{A}_{\mathbf{q}} = [\mathbf{A}_{-\mathbf{q}}]^*$ and that quasiparticle operators for different momenta anti-commute. Now we use the gauge $\text{div } \mathbf{A} = 0$, or $(\mathbf{q} \mathbf{A}_{\mathbf{q}}) = 0$. We change $\mathbf{p} \rightarrow \mathbf{p} + \hbar\mathbf{q}/2$ and denote

$$\xi_{\mathbf{p} + \hbar\mathbf{q}/2} \equiv \xi_+, \quad \xi_{\mathbf{p} - \hbar\mathbf{q}/2} = \xi_-.$$

As a result

$$E_1 = - \frac{1}{2} \left(\frac{e}{mc} \right)^2 \sum_{\mathbf{p}, \mathbf{q}} \frac{(\mathbf{p} \mathbf{A}_{\mathbf{q}})(\mathbf{p} \mathbf{A}_{-\mathbf{q}})(\varepsilon_+ \varepsilon_- - \xi_+ \xi_- - \Delta^2)}{\varepsilon_+ \varepsilon_- (\varepsilon_+ + \varepsilon_-)}.$$

Remembering that

$$\delta E = - \frac{1}{c} \sum_{\mathbf{q}} \mathbf{j}_{\mathbf{q}} \delta \mathbf{A}_{-\mathbf{q}}$$

we get

$$\mathbf{j}_{\mathbf{q}} = - \frac{2e^2}{mc} \sum_{\mathbf{p}} v_p^2 \mathbf{A}_{\mathbf{q}} + \frac{e^2}{m^2 c} \sum_{\mathbf{p}} \frac{\mathbf{p}(\mathbf{p} \mathbf{A}_{\mathbf{q}})(\varepsilon_+ \varepsilon_- - \xi_+ \xi_- - \Delta^2)}{\varepsilon_+ \varepsilon_- (\varepsilon_+ + \varepsilon_-)}.$$

In the first integral $2 \sum_{\mathbf{p}} v_p^2 = n_e$. In the second integral we put $\hbar q \ll p_F$ and

$$\xi_{\pm} = \frac{(\mathbf{p} \pm \hbar\mathbf{q}/2)^2 - p_F^2}{2m} \approx \xi \pm \hbar q v_F \cos \theta$$

(z -axis is directed along \mathbf{q}). Finally, coming to the integral over momenta and calculating the perpendicular current we get

$$\begin{aligned} Q(q) &= \frac{n_e e^2}{mc} - \frac{e^2 p_F^4}{m^2 c v_F} \frac{1}{(2\pi\hbar)^3} \int_{-\infty}^{\infty} d\xi \int \cos^2 \theta \sin^2 \theta \frac{(\varepsilon_+ \varepsilon_- - \xi_+ \xi_- - \Delta^2)}{\varepsilon_+ \varepsilon_- (\varepsilon_+ + \varepsilon_-)} d\Omega = \\ &= \frac{n_e e^2}{mc} \mathcal{F} \left(\frac{\hbar q v_F}{2\Delta(0)} \right), \quad \mathcal{F}(z) = \frac{3}{2z} \int_0^1 \frac{(1-t^2) dt}{t} \frac{\text{arsh}(zt)}{\sqrt{1+z^2 t^2}} \end{aligned}$$

(we have introduced $t = \cos \theta$). This integral could be analyzed in limiting cases. At small q ($z \rightarrow 0$) $\mathcal{F}(z) \rightarrow 1$ (London limiting case). At large q only small values of t are important. Thus we can neglect t^2 in comparison with 1 and get

$$\mathcal{F}(z) = \frac{\pi^2}{4z} \rightarrow Q(q) = \frac{3\pi^2 n_e e^2}{4 mc} \frac{\Delta(0)}{\hbar v_F} \frac{1}{q}.$$

This formula is not enough to calculate the penetration depth because it is determined for inhomogeneous space. The result depends on the scattering conditions for the electron at the surface. The result for mirror reflection has the form

$$\delta_P = \frac{2^{8/3}}{3^{11/6} \pi^{2/3}} \delta_L^{2/3} \left(\frac{\hbar v_F}{\Delta(0)} \right)^{1/3},$$

i.e. it corresponds to the qualitative estimates.

Electrodynamics at $T \neq 0$ (London limit).

Now we briefly discuss the influence of finite temperature. First, we emphasize that near T_c all the SC meet the London limit. Indeed, at all the temperatures the correlation length is of the order of $\zeta_0 \sim \hbar v_F / T_c$. At the same time, the penetration depth diverges at $T \rightarrow T_c$.

The influence of the finite temperature leads to creation of quasiparticles, i.e. to *decrease* of the number of superconducting electrons. To estimate the number of SC electrons let us calculate the momentum of the system if all the particles move with the same velocity \mathbf{u} . We get

$$\mathbf{P} = \int \mathbf{p} n_F(\varepsilon - \mathbf{p}\mathbf{u}) (dp) \approx \int \mathbf{p}(\mathbf{p}\mathbf{u}) \left(-\frac{\partial n_F}{\partial \varepsilon} \right) (dp) = g(\epsilon_F) \int d\xi \int \frac{d\Omega}{4\pi} \mathbf{p}(\mathbf{p}\mathbf{u}) \left(-\frac{\partial n_F}{\partial \varepsilon} \right).$$

Then, we have

$$\int \frac{d\Omega}{4\pi} \mathbf{p}(\mathbf{p}\mathbf{u}) \approx \frac{1}{3} p_F^2 \mathbf{u}.$$

Introducing new variable φ as $\xi = \Delta \sinh \varphi$ we get

$$\mathbf{P} = \frac{1}{3} p_F^2 \mathbf{u} g(\epsilon_F) \mathcal{G} \left(\frac{\Delta}{k_B T} \right), \quad \mathcal{G}(z) = 2z \int_0^\infty \frac{\cosh \varphi d\varphi}{(e^{z \cosh \varphi} + 1)(e^{-z \cosh \varphi} + 1)}$$

We denote

$$\mathbf{P} = n_n m \mathbf{u}$$

where n_n is the number of "normal electrons". We see that

$$\frac{n_n}{n_e} = \mathcal{G} \left(\frac{\Delta}{k_B T} \right) = \frac{1}{T} \frac{d\Delta}{dT} \left(\frac{d\Delta}{dT} \right)^{-1}.$$

We check the last formula remembering that

$$\ln \frac{\Delta(0)}{\Delta(T)} = 2 \int_0^\infty \frac{d\varphi}{(e^{(\Delta/k_B T) \cosh \varphi} + 1)}.$$

One can show that at $T \rightarrow T_c$ $n_s/n_e \rightarrow 1$ ($\Delta \propto \sqrt{T_c - T}$). At the same time, at $T < T_c$ this ratio is less than 1. It means that displacement of quasiparticles is not the same as displacement of all the liquid, the rest being *superconducting electrons*. We have

$$\frac{n_s}{n_e} = 1 - \frac{n_n}{n_e} = - \left[\frac{d \ln(\Delta/T)}{d \ln T} \right]^{-1}.$$

It is just the number which enters the London penetration depth at finite temperatures. At $T \rightarrow T_c$

$$\frac{n_s}{n_e} = 2 \frac{T_c - T}{T_c} \quad \rightarrow \quad \delta_L(T) = \delta_L(0) \sqrt{\frac{T_c}{2(T_c - T)}}.$$

At the end of this section one should mention that although all the SC come to the London limit near T_c this transition takes place very close to T_c if $\delta_L(0) \ll \zeta_0$. In the Pippard region

$$\delta_P(T) = \delta_P(0) \left[\frac{\Delta}{\Delta(0)} \tanh \left(\frac{\Delta}{2k_B T} \right) \right]^{-1/3} \propto \left(\frac{T_c}{T_c - T} \right)^{1/3} \text{ near } T_c.$$

18.7 Kinetics of Superconductors

Formulas for Transition Probabilities

Consider the case where a weak a.c. field acts upon a SC. Such a field can be created by acoustic wave, or by electromagnetic wave.

Acoustic Wave

As we know, acoustic field create a perturbation $\Lambda_{ik} u_{ik}(\mathbf{r}, t)$. Denoting the interaction matrix element as $\Lambda u_{\mathbf{k}-\mathbf{k}'}$ we get

$$\mathcal{H}_{int} = \sum_{\mathbf{k}, \mathbf{k}', \sigma} \Lambda u_{\mathbf{k}-\mathbf{k}'} a_{\mathbf{k}\sigma}^\dagger a_{\mathbf{k}'\sigma}.$$

Microwave Field

In the linear approximation the perturbation is $(e/2mc)(\mathbf{pA} + \mathbf{Ap})$. As a result

$$\mathcal{H}_{int} = \frac{e}{mc} \sum_{\mathbf{k}, \mathbf{k}', \sigma} (\mathbf{A}_{\mathbf{k}-\mathbf{k}'} \cdot (\mathbf{k} + \mathbf{k}')) a_{\mathbf{k}\sigma}^\dagger a_{\mathbf{k}'\sigma}.$$

Thus in general case

$$\mathcal{H}_{int} = \sum_{\mathbf{k}, \mathbf{k}', \sigma} \langle \mathbf{k}'\sigma' | \hat{B} | \mathbf{k}\sigma \rangle a_{\mathbf{k}\sigma}^\dagger a_{\mathbf{k}'\sigma'}. \quad (18.19)$$

There are two kinds of processes induced by \mathcal{H}_{int} .

1. Transitions between different states, described by quasiparticle operators. To analyze them we transform the Hamiltonian (18.19) to the quasiparticle operators α . We have done this transformation earlier. In a compact form it can be written as (*Problem 18.3*)

$$a_{m\sigma}^\dagger = u_m \alpha_{m\sigma}^\dagger + \sum_{\sigma'} \rho_{\sigma\sigma'} \alpha_{-m\sigma'}, \text{ where } \rho = \begin{pmatrix} 0 & -1 \\ 1 & 0 \end{pmatrix}. \quad (18.20)$$

As a result

$$\begin{aligned} a_{\mathbf{k}\sigma}^\dagger a_{\mathbf{k}'\sigma'} &= u_k u_{k'} \alpha_{\mathbf{k}\sigma}^\dagger \alpha_{\mathbf{k}'\sigma'} + v_k v_{k'} \sum_{\sigma_1 \sigma_2} \rho_{\sigma\sigma_1} \rho_{\sigma'\sigma_2} \alpha_{-\mathbf{k}\sigma_1}^\dagger \alpha_{-\mathbf{k}'\sigma_2}^\dagger + \\ &+ u_k v_{k'} \sum_{\sigma_1} \rho_{\sigma'\sigma_1} \alpha_{\mathbf{k}\sigma}^\dagger \alpha_{-\mathbf{k}'\sigma_1}^\dagger + v_k u_{k'} \sum_{\sigma_1} \rho_{\sigma\sigma_1} \alpha_{-\mathbf{k}\sigma_1} \alpha_{\mathbf{k}'\sigma'}. \end{aligned} \quad (18.21)$$

Note that the items $\alpha_{\mathbf{k}\sigma}^\dagger \alpha_{\mathbf{k}'\sigma'}$ and $\alpha_{\mathbf{k}\sigma_1} \alpha_{\mathbf{k}'\sigma_2}^\dagger$ describe scattering of quasiparticles while $\alpha_{\mathbf{k}\sigma}^\dagger \alpha_{-\mathbf{k}'\sigma_1}^\dagger$ and $\alpha_{-\mathbf{k}\sigma_1} \alpha_{\mathbf{k}'\sigma'}$ describe creation and annihilation of pairs of quasiparticles. (**The number of quasiparticles is not conserved!**).

2. The perturbation can also modulates the system's parameters. Usually it is not so important.

Now we analyze different processes.

Scattering processes.

Making use of anti commutation of quasiparticle operators we get the following expression for transition matrix element

$$M(\mathbf{k}\sigma|\mathbf{k}'\sigma') = u_k u_{k'} \left\langle \mathbf{k}'\sigma' \left| \hat{B} \right| \mathbf{k}\sigma \right\rangle - v_k v_{k'} \sum_{\sigma_1 \sigma_2} \rho_{\sigma_2 \sigma'} \rho_{\sigma_1 \sigma} \left\langle -\mathbf{k}'\sigma' \left| \hat{B} \right| -\mathbf{k}\sigma \right\rangle.$$

In fact, $\sum_{\sigma_1 \sigma_2} \rho_{\sigma_2 \sigma'} \rho_{\sigma_1 \sigma} \left\langle -\mathbf{k}'\sigma' \left| \hat{B} \right| -\mathbf{k}\sigma \right\rangle$ is the matrix element where all the momenta and spins are reversed which means time reversion. It is clear that they can differ only by signs:

$$\sum_{\sigma_1 \sigma_2} \rho_{\sigma_2 \sigma'} \rho_{\sigma_1 \sigma} \left\langle -\mathbf{k}'\sigma' \left| \hat{B} \right| -\mathbf{k}\sigma \right\rangle = \eta \left\langle \mathbf{k}'\sigma' \left| \hat{B} \right| \mathbf{k}\sigma \right\rangle$$

where

$$\eta = \begin{cases} +1, & \text{for the case 1} \\ -1, & \text{for the case 2} \end{cases}.$$

Thus

$$M(\mathbf{k}\sigma|\mathbf{k}'\sigma') = (u_k u_{k'} - \eta v_k v_{k'}) \left\langle \mathbf{k}'\sigma' \left| \hat{B} \right| \mathbf{k}\sigma \right\rangle$$

where the coefficient $(u_k u_{k'} - \eta v_k v_{k'})$ is called the *coherence factor*. This factor is very important. The resulting contribution to the transition rate is

$$\nu_{\mathbf{kk}'} = \frac{2\pi}{\hbar} |M(\mathbf{k}\sigma|\mathbf{k}'\sigma')|^2 \{n_F(\varepsilon_{\mathbf{k}'}) [1 - n_F(\varepsilon_{\mathbf{k}})] - n_F(\varepsilon_{\mathbf{k}}) [1 - n_F(\varepsilon_{\mathbf{k}'})]\} \times \delta(\varepsilon_{\mathbf{k}} - \varepsilon_{\mathbf{k}'} - \hbar\omega). \quad (18.22)$$

Consequently, the absorbed power is

$$W_1 = \sum_{\mathbf{kk}'} \hbar\omega \nu_{\mathbf{kk}'}.$$

Denoting $B^2 \equiv \overline{\left| \left\langle \mathbf{k}'\sigma' \left| \hat{B} \right| \mathbf{k}\sigma \right\rangle \right|^2}$ where the bar means angle average over the Fermi surface we get

$$W_1 = 2\pi\omega B^2 \int_{\Delta}^{\infty} d\varepsilon d\varepsilon' g_s(\varepsilon) g_s(\varepsilon') (u_k u_{k'} - \eta v_k v_{k'})^2 \times \\ \times [n_F(\varepsilon') - n_F(\varepsilon)] \delta(\varepsilon - \varepsilon' - \hbar\omega).$$

Here we have introduced the density of states with respect to the energy ε

$$g_s(\varepsilon) = g(\epsilon_F) \left| \frac{d\xi}{d\varepsilon} \right| = g(\epsilon_F) \frac{\varepsilon}{\sqrt{\varepsilon^2 - \Delta^2}}.$$

According to the definition,

$$(u_k u_{k'} - \eta v_k v_{k'})^2 = \frac{1}{2} \left[1 + \frac{\xi\xi'}{\varepsilon\varepsilon'} - \eta \frac{\Delta^2}{\varepsilon\varepsilon'} \right].$$

Finally

$$W_1 = 2\pi\omega B^2 g^2(\epsilon_F) \int_{\Delta}^{\infty} d\varepsilon \int_{\Delta}^{\infty} d\varepsilon' \frac{\varepsilon\varepsilon' - \eta\Delta^2}{\sqrt{(\varepsilon^2 - \Delta^2)(\varepsilon'^2 - \Delta^2)}} \times \\ \times [n_F(\varepsilon') - n_F(\varepsilon)] \delta(\varepsilon - \varepsilon' - \hbar\omega). \quad (18.23)$$

We can make the same calculation for the second part, corresponding to creation and annihilation of quasiparticles which is nonzero at $\hbar\omega > 2\Delta$. The result can be formulated as

$$\frac{W_s}{W_n} = \frac{1}{\hbar\omega} \int_{-\infty}^{\infty} d\varepsilon \int_{-\infty}^{\infty} d\varepsilon' \frac{\varepsilon\varepsilon' - \eta\Delta^2}{\sqrt{(\varepsilon^2 - \Delta^2)(\varepsilon'^2 - \Delta^2)}} \Theta(|\varepsilon| - \Delta) \Theta(|\varepsilon'| - \Delta) \times \\ \times [n_F(\varepsilon') - n_F(\varepsilon)] \delta(\varepsilon - \varepsilon' - \hbar\omega). \quad (18.24)$$

Now we discuss the applications of the formula.

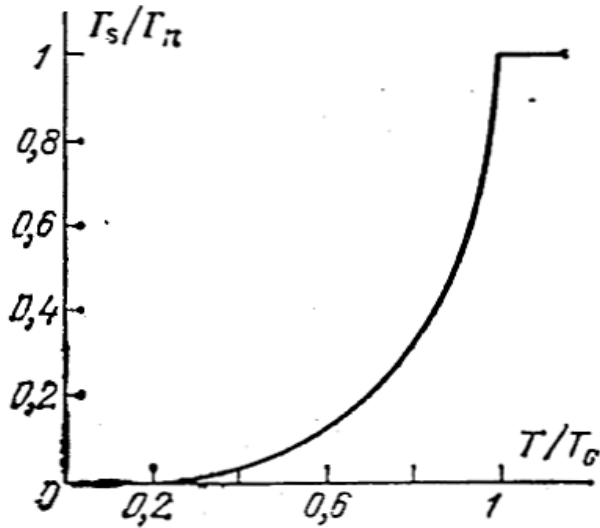


Figure 18.5: Temperature dependence of sound absorption.

Ultrasonic Absorption

We have $\eta = 1$. At $\hbar\omega \ll \Delta$

$$\frac{W_s}{W_n} = \int_{|\varepsilon| > \Delta} d\varepsilon \frac{\varepsilon^2 - \Delta^2}{\varepsilon^2 - \Delta^2} \left(-\frac{\partial n_F}{\partial \varepsilon} \right) = \frac{2}{1 + e^{\Delta/k_B T}}.$$

At $T = 0$ the absorption takes place only at $\hbar\omega > 2\Delta$. The graph of this function is shown in Fig. 18.5.

Response to Microwave Field

The quantitative analysis is more difficult. The key results are the follows. At $T = 0$ the absorption takes place only at $\hbar\omega > 2\Delta$ (see Fig. 18.6). At low frequencies and temperatures, $k_B T, \hbar\omega \ll \Delta(0)$ we have

$$\text{Im } Q \approx -4\pi \sinh \left(\frac{\hbar\omega}{2k_B T} \right) K_0 \left(\frac{\hbar\omega}{2k_B T} \right) \exp \left(-\frac{\Delta(0)}{k_B T} \right)$$

Note that the condition $\hbar\omega = 2\Delta$ corresponds to the frequencies $\sim 10^{11} - 10^{12} \text{ Hz}$. Consequently, in the optical frequency range the electromagnetic properties of SC and normal conductors are practically the same.

Finally, we discuss also the very important limiting case of the vicinity of T_c and small frequencies

$$\hbar\omega \ll \Delta \ll k_B T_c.$$

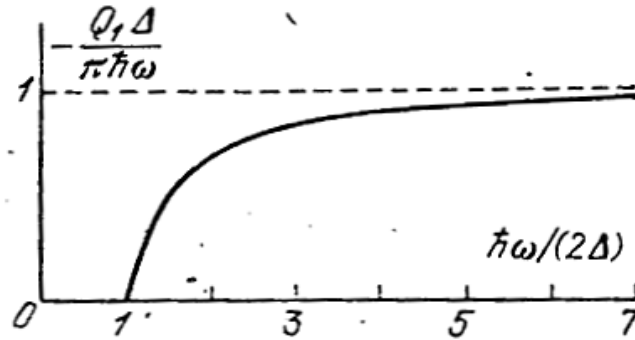


Figure 18.6: Frequency dependence of microwave absorption at $T = 0$.

In this region

$$\mathbf{j} = \left[-\frac{c}{4\pi\delta^2} + \frac{i\omega\sigma}{c} \right] \mathbf{A}.$$

Remembering that $\mathbf{E} = -(1/c)\dot{\mathbf{A}}$ we see that the second item is just $\sigma\mathbf{E}$ and

$$\mathbf{j} = \mathbf{j}_s + \mathbf{j}_n.$$

Note that such a *two-fluid hydrodynamics* is not the case beyond the vicinity of T_c .

Electron Thermal Conductivity

The main electronic contribution to thermal conductivity can be calculated from the Boltzmann-like equation for quasiparticles ⁴

$$\frac{\partial \varepsilon}{\partial \mathbf{p}} \frac{\partial n}{\partial \mathbf{r}} - \frac{\partial \varepsilon}{\partial \mathbf{r}} \frac{\partial n}{\partial \mathbf{p}} = I(n)$$

where $\varepsilon(\mathbf{p}, \mathbf{r})$ is the quasiparticle energy. To estimate the scattering rate we assume impurity scattering,

$$\mathcal{H}_{int} = \sum_{\mathbf{k}, \mathbf{k}', \sigma} V_{\mathbf{k}\mathbf{k}'} a_{\mathbf{k}\sigma}^\dagger a_{\mathbf{k}'\sigma}$$

where the matrix element $V_{\mathbf{k}\mathbf{k}'}$ depends only on the angle $\theta = (\widehat{\mathbf{k}}, \widehat{\mathbf{k}'})$. After Bogolyubov transform neglecting creation-annihilation terms we get

$$\mathcal{H}_{int} = \sum_{\mathbf{k}, \mathbf{k}', \sigma} V_{\mathbf{k}\mathbf{k}'} \alpha_{\mathbf{k}\sigma}^\dagger \alpha_{\mathbf{k}'\sigma} (u_k u_{k'} - v_k v_{k'}).$$

⁴This equation is oversimplified, but appropriate for the problem.

For elastic scattering $\xi_{\mathbf{k}} = \pm \xi_{\mathbf{k}'}$. For the sign + we get $\xi_{\mathbf{k}}/\varepsilon_{\mathbf{k}}$ for the coherence factor while for the sign - this factor vanishes. As a result,

$$\begin{aligned}\frac{1}{\tau_s} &= \frac{2\pi}{\hbar} \int |V_{\mathbf{k}\mathbf{k}'}|^2 (1 - \cos \theta) (u_k u_{k'} - v_k v_{k'})^2 \delta(\varepsilon_{\mathbf{k}} - \varepsilon_{\mathbf{k'}})(dk') = \\ &= \frac{\pi}{\hbar} g(\epsilon_F) \left(\frac{\xi_{\mathbf{k}}}{\varepsilon_{\mathbf{k}}} \right)^2 \left| \frac{d\xi_{\mathbf{k}}}{d\varepsilon_{\mathbf{k}}} \right| \int \frac{d\Omega}{4\pi} |V(\theta)|^2 (1 - \cos \theta) = \frac{1}{\tau_{tr}} \frac{|\xi_{\mathbf{k}}|}{\varepsilon_{\mathbf{k}}}\end{aligned}$$

Now we can do everything:

$$\frac{\partial n_F}{\partial \mathbf{r}} = -\frac{\varepsilon}{T} \frac{\partial n_F}{\partial \varepsilon} \nabla T, \quad \frac{\partial \varepsilon}{\partial \mathbf{p}} = \frac{\partial n_F}{\partial \xi} \frac{\partial \xi}{\partial \mathbf{p}} = \mathbf{v} \frac{\xi_{\mathbf{k}}}{\varepsilon_{\mathbf{k}}}, \quad I(n) = \frac{n - n_F}{\tau_{tr}} \frac{|\xi_{\mathbf{k}}|}{\varepsilon_{\mathbf{k}}}.$$

Finally,

$$n^{(1)} = \frac{\varepsilon}{T} \frac{\partial n_F}{\partial \varepsilon} \tau_{tr} \operatorname{sign} \xi_{\mathbf{k}} \mathbf{v} \nabla T. \quad (18.25)$$

It is easy to calculate the thermal current

$$\mathbf{Q} = \int \varepsilon_{\mathbf{p}} \frac{\partial \varepsilon}{\partial \mathbf{p}} n^{(1)}(dp) = -\frac{n_e \tau_{tr}}{2m k_B T^2} \int_{\Delta}^{\infty} \frac{\varepsilon^2 d\varepsilon}{\cosh^2(\varepsilon/2k_B T)} \nabla T.$$

Thus

$$\kappa = \frac{n_e \tau_{tr} k_B T}{2m} \int_{\Delta/k_B T}^{\infty} \frac{x dx}{\cosh^2(x/2)}.$$

The graph of this function is shown in Fig. 18.7.

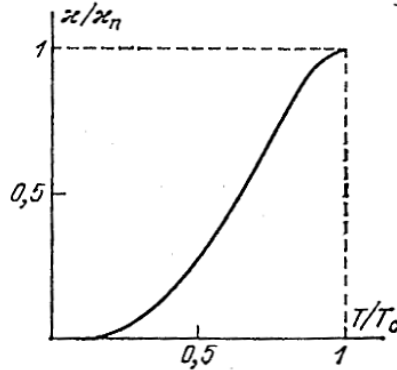


Figure 18.7: Temperature dependence of thermal conductivity.

Thermoelectric Phenomena

For many years it was thought that one cannot observe thermoelectric phenomena because the drag current of quasiparticles is compensated by the counter flow of supercurrent. Then

it was shown that there are ways to observe the supercurrent and in such a way to study the thermoelectric effect. It is not so easy to calculate the thermoelectric current because of some important features of superflow. Here we use a simplified approach.

Assume that the condensate moves as a whole with the velocity \mathbf{v}_s , the Cooper pair momentum being $\mathbf{p}_s = 2m\mathbf{v}_s$. The motion as a whole means that the superconducting coupling should be the case for the momenta \mathbf{p} and $-\mathbf{p} + \mathbf{p}_s$. As a result, instead of the Bogolyubov transform we get

$$\begin{aligned} a_{\mathbf{p}\uparrow} &= u_{\mathbf{p}}\alpha_{\mathbf{p}\uparrow} + v_{\mathbf{p}}\alpha_{-\mathbf{p}+\mathbf{p}_s\downarrow}^\dagger, \\ a_{\mathbf{p}\downarrow} &= u_{-\mathbf{p}+\mathbf{p}_s}\alpha_{\mathbf{p}\downarrow} - v_{-\mathbf{p}+\mathbf{p}_s}\alpha_{-\mathbf{p}+\mathbf{p}_s\uparrow}^\dagger. \end{aligned}$$

(we have chosen the subscripts in the second line to fulfill the anti commutation condition

$$\{a_{\mathbf{p}\uparrow}, a_{-\mathbf{p}+\mathbf{p}_s\downarrow}\} = -u_{\mathbf{p}}v_{\mathbf{p}} + u_{\mathbf{p}}v_{\mathbf{p}} = 0.$$

Then we make the same procedure as earlier and get

$$\begin{aligned} \langle \mathcal{H} - \epsilon N \rangle &= \sum_{\mathbf{p}} \left\{ \xi [n_{\mathbf{p}\uparrow} + |v_{\mathbf{p}}|^2 (1 - n_{\mathbf{p}\uparrow} - n_{-\mathbf{p}+\mathbf{p}_s\downarrow})] + \right. \\ &\quad \left. + \xi' [n_{-\mathbf{p}+\mathbf{p}_s\downarrow} + |v_{\mathbf{p}}|^2 (1 - n_{\mathbf{p}\uparrow} - n_{-\mathbf{p}+\mathbf{p}_s\downarrow})] \right\} - \frac{\Delta^2}{\lambda}. \end{aligned}$$

Here

$$\begin{aligned} \Delta &= \lambda \sum_{\mathbf{p}} u_{\mathbf{p}}v_{\mathbf{p}}(1 - n_{\mathbf{p}\uparrow} - n_{-\mathbf{p}+\mathbf{p}_s\downarrow}), \\ \xi' &= \xi(-\mathbf{p} + \mathbf{p}_s). \end{aligned} \tag{18.26}$$

Minimizing the energy, we get

$$\begin{aligned} u_{\mathbf{p}}^2 &= u_{-\mathbf{p}+\mathbf{p}_s}^2 = \frac{1}{2} \left[1 + \frac{\xi + \xi'}{2\varepsilon} \right], \\ v_{\mathbf{p}}^2 &= v_{-\mathbf{p}+\mathbf{p}_s}^2 = \frac{1}{2} \left[1 - \frac{\xi + \xi'}{2\varepsilon} \right], \\ \varepsilon &= \sqrt{\frac{(\xi + \xi')^2}{4} + \Delta^2}. \end{aligned}$$

Consequently, after variation over $n_{\mathbf{p}\sigma}$ we obtain the quasiparticle energies

$$\varepsilon_{\mathbf{p}\uparrow} = \varepsilon + \frac{\xi - \xi'}{2}, \quad \varepsilon_{-\mathbf{p}+\mathbf{p}_s\downarrow} = \varepsilon - \frac{\xi - \xi'}{2}$$

In a more symmetric way, it is reasonable to shift the momentum by $\mathbf{p}_s/2$. In this case we can denote $\xi_{\pm} \equiv \xi(\mathbf{p} \pm \mathbf{p}_s/2)$, $\xi + \xi' = 2\xi(\mathbf{p}) + \mathbf{p}_s/4m$, $\xi - \xi' = \mathbf{p}\mathbf{p}_s/m = 2\mathbf{p}\mathbf{v}_s$. At small \mathbf{p}_s one can obtain

$$\varepsilon_{\mathbf{p}+\mathbf{p}_s/2\uparrow} = \varepsilon_0 + \mathbf{p}\mathbf{v}_s, \quad \varepsilon_{-\mathbf{p}+\mathbf{p}_s/2\downarrow} = \varepsilon_0 - \mathbf{p}\mathbf{v}_s$$

that means just the Doppler shift of the energy.

One should be careful to calculate the current. We get

$$\mathbf{j} = -\frac{e}{m} \sum_{\mathbf{p}\sigma} \mathbf{p} a_{\mathbf{p}\sigma}^\dagger a_{\mathbf{p}\sigma} = -\frac{e}{m} \sum_{\mathbf{p}} \mathbf{p} [u_{\mathbf{p}}^2 n_{\mathbf{p}\uparrow} + v_{\mathbf{p}}^2 (1 - n_{-\mathbf{p}+\mathbf{p}_s\downarrow}) + u_{\mathbf{p}}^2 n_{\mathbf{p}\downarrow} + v_{\mathbf{p}}^2 (1 - n_{-\mathbf{p}+\mathbf{p}_s\uparrow})].$$

Then we shift the variables as $\mathbf{p} \rightarrow \mathbf{p} + \mathbf{p}_s/2$ and assume $p_s \ll \Delta/p_F$ to get

$$\mathbf{j} = -\frac{2e}{m} \sum_{\mathbf{p}\sigma} (\mathbf{p} + \mathbf{p}_s/2) [u_{\mathbf{p}+\mathbf{p}_s/2}^2 n_{\mathbf{p}+\mathbf{p}_s/2,\sigma} + v_{\mathbf{p}+\mathbf{p}_s/2}^2 (1 - n_{-\mathbf{p}+\mathbf{p}_s/2,\sigma})].$$

Expanding in terms of $\mathbf{p}\mathbf{v}_s$ we get $[n_F(\varepsilon + \mathbf{p}\mathbf{v}_s) = n_F(\varepsilon) + \mathbf{p}\mathbf{v}_s(\partial n_F/\partial \varepsilon)]$

$$\mathbf{j} = -2e\mathbf{v}_s \sum_{\mathbf{p}} [u_{\mathbf{p}}^2 n_F + v_{\mathbf{p}}^2 (1 - n_F)] - \frac{2e}{m} \sum_{\mathbf{p}} \mathbf{p}(\mathbf{p}\mathbf{v}_s) \left(\frac{\partial n_F}{\partial \varepsilon} \right) - \frac{2e}{m} \sum_{\mathbf{p}} \mathbf{p}n^{(1)}.$$

The two first item can be grouped as $-en_s\mathbf{v}_s$ while the last one is the thermoelectric current of normal excitations. Substituting the expression for $n^{(1)}$ from (18.25) we get

$$\mathbf{j} = -\eta_s \nabla T, \quad \eta_s = -\frac{e}{\epsilon_F} \kappa.$$

We will come back to this problem later to explain how one can observe this current.

18.8 Problems

18.1. Prove the Eqs. (18.9) and (18.10).

18.2. Prove Eq. (18.18).

18.3. Check Eq. (18.20)

Chapter 19

Ginzburg-Landau Theory

In this chapter we consider a very powerful macroscopic theory which is very useful for many problems in SC.

19.1 Ginzburg-Landau Equations

Derivation

Let us formulate the theory of SC transition as the one for a general type II transition. First, one should define the order parameter. As the order parameter it is natural to chose the *wave function of the Bose condensate*, Ψ . According to the principles of SC, it is natural to assume that the ground state corresponds to the total momentum equal to 0, the wave function being the same for all the Bose particles.

Near the critical temperature, the modulus of the order parameter is small, and one can expand the thermodynamic potential as

$$\Omega_s = \Omega_n + a|\Psi|^2 + \frac{b}{2}|\Psi|^4 + \dots$$

Because we are interested in the vicinity of T_c we can expand the coefficients in power of

$$\tau = \frac{T - T_c}{T_c}.$$

According the definition of T_c , above T_c the stable state corresponds to $\Psi = 0$, while below T_c $\Psi \neq 0$. Thus the coefficient a should change the sign at the transition point:

$$a = \alpha\tau, \quad \alpha > 0.$$

As a result, we describe the equilibrium values of the order parameter as

$$\begin{aligned} \Psi &= 0 && \text{at } T > T_c \\ |\Psi|^2 &= -\frac{\alpha}{b}\tau = |\Psi_0|^2 && \text{at } T < T_c. \end{aligned}$$

Inserting the equilibrium value if $|\Psi_0|^2$ into the expansion and comparing the result with the known relation for the critical field, we get

$$\Omega_s - \Omega_n = \frac{(\alpha\tau)^2}{2b} = \frac{H_c^2}{8\pi}.$$

Consequently, using the microscopic theory we have

$$\frac{\alpha^2}{2b} = \frac{4}{7\zeta(3)} \frac{(k_B T_c)^2 m p_F}{\hbar^3} = \frac{4\pi^2}{7\zeta(3)} g(\epsilon_F) (k_B T_c)^2.$$

The most interesting case is the case of external magnetic field. In this case Ψ is *coordinate dependent*. Thus we should add both the energy of magnetic field $H^2/8\pi$ and the energy connected with the inhomogeneity. Near the critical point it is enough to add $|\nabla\Psi|^2$. Here we come to the most important point: Cooper pairs are *charged particles*. Consequently, because of gauge invariance, only combination

$$-i\hbar\nabla + \frac{2e}{c}\mathbf{A}$$

is possible. To make a proper dimension we write the corresponding term as

$$\frac{1}{4m} \left| \left(-i\hbar\nabla + \frac{2e}{c}\mathbf{A} \right) \Psi \right|^2.$$

Finally, we get

$$\int (\Omega_s - \Omega_n^{(0)}) dV = \int dV \left\{ \alpha\tau|\Psi|^2 + \frac{b}{2}|\Psi|^4 + \frac{1}{4m} \left| \left(-i\hbar\nabla + \frac{2e}{c}\mathbf{A} \right) \Psi \right|^2 + \frac{H^2}{8\pi} \right\}.$$

Here $\Omega_n^{(0)}$ is the thermodynamic potential of the normal state *without magnetic field*. To get the minimum we calculate variation with respect to Ψ^* :

$$\int dV \left\{ \alpha\tau\Psi\delta\Psi^* + b|\Psi|^2\Psi\delta\Psi^* + \frac{1}{4m} \left(-i\hbar\nabla + \frac{2e}{c}\mathbf{A} \right) \Psi \left(i\hbar\nabla + \frac{2e}{c}\mathbf{A} \right) \delta\Psi^* \right\}$$

The item with the $\nabla\delta\Psi^*$ can be integrated by parts. Using the Gauss theorem we get

$$\frac{i\hbar}{4m} \int_{surface} \delta\Psi^* \left(-i\hbar\nabla + \frac{2e}{c}\mathbf{A} \right) \Psi dS + \frac{1}{4m} \int dV \delta\Psi^* \left(-i\hbar\nabla + \frac{2e}{c}\mathbf{A} \right)^2 \Psi.$$

Then we put $\delta\Psi^* = 0$ at the surface and arbitrary inside. As a result, we get the following equation for the order parameter

$$\frac{1}{4m} \left(-i\hbar\nabla + \frac{2e}{c}\mathbf{A} \right)^2 \Psi + \alpha\tau\Psi + b|\Psi|^2\Psi = 0.$$

If now we put $\delta\Psi^*$ at the surface to be arbitrary, we obtain the boundary condition

$$\mathbf{n} \left(-i\hbar\nabla + \frac{2e}{c}\mathbf{A} \right) \Psi|_{surface} = 0.$$

The variation with respect to $\delta\Psi$ leads to the complex conjugate expressions.

Now it is important to get the equation for electric current. To obtain it one should calculate the variation with respect to the vector potential \mathbf{A} . The variation of H^2 leads to

$$\delta(\operatorname{curl} \mathbf{A})^2 = 2 \operatorname{curl} \mathbf{A} \operatorname{curl} \delta\mathbf{A}.$$

Then we can use the relation

$$\operatorname{div} [\mathbf{a} \times \mathbf{b}] = \mathbf{b} \operatorname{curl} \mathbf{a} - \mathbf{a} \operatorname{curl} \mathbf{b}$$

to get

$$\delta(\operatorname{curl} \mathbf{A})^2 = 2\delta\mathbf{A} \operatorname{curl} \operatorname{curl} \mathbf{A} + 2\operatorname{div} [\delta\mathbf{A} \times \operatorname{curl} \mathbf{A}].$$

The second integral can be transformed into the surface one, thus it is not important. On the other hand, from the Maxwell equations

$$\operatorname{curl} \operatorname{curl} \mathbf{A} = \operatorname{curl} \mathbf{H} = \frac{4\pi}{c}\mathbf{j} \quad \rightarrow \quad \delta(\operatorname{curl} \mathbf{A})^2 = 2\mathbf{j}\delta\mathbf{A}.$$

The rest of the free energy can be calculated in a straightforward way, and equating the total variation to zero we obtain

$$\mathbf{j} = \frac{ie\hbar}{2m} (\Psi^* \nabla \Psi - \Psi \nabla \Psi^*) - \frac{2e^2}{mc} |\Psi|^2 \mathbf{A}$$

This is just the quantum mechanical expression for the current for a particle with the charge $(-2e)$ and the mass $2m$. The set

$$(1/4m) \left(-i\hbar\nabla + \frac{2e}{c}\mathbf{A} \right)^2 \Psi + \alpha\tau\Psi + b|\Psi|^2\Psi = 0,$$

$$\mathbf{j} = (ie\hbar/2m) (\Psi^* \nabla \Psi - \Psi \nabla \Psi^*) - (2e^2/mc)|\Psi|^2 \mathbf{A}$$

forms the *Ginzburg-Landau equations*.

Dimensionless Parameters and Their Meaning

To make the equations simple new dimensionless parameters are usually introduced:

$$\Psi' = \frac{\Psi}{\Psi_0}, \quad \mathbf{H}' = \frac{\mathbf{H}}{H_c\sqrt{2}}, \quad \mathbf{r}' = \frac{\mathbf{r}}{\delta}, \quad \mathbf{A}' = \frac{\mathbf{A}}{H_c\delta\sqrt{2}}$$

$$\text{with } \delta = \sqrt{\frac{2mc^2}{4\pi(2e)^2\Psi_0^2}}, \quad H_c = 2\sqrt{\pi}\frac{\alpha\tau}{\sqrt{b}}, \quad \Psi_0^2 = \frac{\alpha|\tau|}{b}.$$

In the following we will omit primes and use these variables. As a result, the set of equations can be expressed as

$$\begin{aligned} \left(\frac{i}{\kappa} \nabla - \mathbf{A} \right)^2 \Psi - \Psi + |\Psi|^2 \Psi &= 0, \\ \mathbf{n} \left(\frac{i}{\kappa} \nabla - \mathbf{A} \right) \Psi_{surface} &= 0, \quad \text{boundary condition}, \\ \operatorname{curl} \operatorname{curl} \mathbf{A} &= \frac{i}{2\kappa} (\Psi^* \nabla \Psi - \Psi \nabla \Psi^*) - |\Psi|^2 \mathbf{A}. \end{aligned} \quad (19.1)$$

This set contains only one dimensionless parameter

$$\kappa = 2\sqrt{2} \frac{eH_c\delta^2}{\hbar c} \quad (19.2)$$

which is called the *Ginzburg-Landau (GL) parameter*.

To understand the meaning of the parameters let us consider the simplest problem, namely penetration of a weak field into the superconductor $x > 0$. Let $\mathbf{H} \parallel \mathbf{z}$, $\mathbf{A} \parallel \mathbf{y}$, i.e.

$$H(x) = \frac{dA_y}{dx}.$$

It is natural to consider Ψ as a function only of x . We get

$$-\frac{1}{\kappa^2} \frac{d^2\Psi}{dx^2} - \Psi + A^2 |\Psi| = 0, \quad \frac{d\Psi}{dx} \Big|_{surf} = 0.$$

At $k \ll 1$ one can assume $\Psi = \text{const}$, in the bulk of material it is natural to assume $|\Psi|^2 = 1$, we chose Ψ real. Immediately we get from the second GL equation

$$\frac{d^2A}{dx^2} - A = 0 \rightarrow H = H_0 e^{-x}, \quad \text{in usual units } H = H_0 e^{-x/\delta}.$$

Thus δ is just the London penetration depth near T_c . Immediately we get

$$|\Psi_0|^2 = \frac{n_s}{2} \rightarrow -\frac{\alpha}{b}\tau = \frac{n_s}{2}.$$

Comparing this expression with the microscopic formula for n_s obtained in the previous chapter we get

$$\frac{\alpha}{b} = n_e.$$

Then it is possible to express the constants α and b through the microscopic parameters. Indeed,

$$\frac{\alpha^2}{2b} = \frac{4\pi^2}{7\zeta(3)} g(\epsilon_F) (k_B T_c)^2 \rightarrow \alpha = \frac{8\pi^2 n_e}{7\zeta(3)} g(\epsilon_F) (k_B T_c)^2, \quad b = \frac{\alpha}{n_e}.$$

One can show using these expressions that

$$\kappa = a_1 \frac{\delta_L(0)}{\zeta_0}, \quad a_1 = \sqrt{\frac{24}{7\zeta(3)\pi}} \approx 0.96.$$

Thus we determined the meaning of all the parameters. The last thing is to discuss the physics of the order parameter. It is clear that $\Psi \propto \Delta$ (both are proportional to $\sqrt{|\tau|}$). Computing the coefficients at $\tau \rightarrow 0$ we obtain

$$\Psi(\mathbf{r}) = a_2 \frac{1}{\sqrt{n_e}} \frac{\Delta(\mathbf{r})}{k_B T_c}, \quad a_2 = \frac{1}{\pi} \sqrt{\frac{7\zeta(3)}{8}}.$$

Modification for SC Alloys.

As we have discussed, impurities change strongly the penetration depth δ . To take this change into account we substitute the expression for the penetration depth for dirty SC into Eq. (19.2). According to exact theory, at $\ell \ll \zeta_0$

$$\delta(T) = \delta_L(0) \sqrt{\frac{\hbar}{\Delta \tau_{tr} \tanh(\Delta/2k_B T)}} \sim \delta_L(0) \sqrt{\frac{\zeta}{\ell}}.$$

At the same time, let us take into account that the coherence length ζ can be expressed as the electron path during the time \hbar/Δ : $\zeta \sim \hbar v_F / \Delta$. If the electron moves diffusely due to impurity scattering, the coherence length can be expressed as the characteristic electron path during the time \hbar/Δ :

$$\zeta_{eff} \sim \sqrt{D \frac{\hbar}{\Delta}} \sim \sqrt{v_F^2 \tau_{tr} \frac{\hbar}{\Delta}} \sim \sqrt{\zeta \ell}$$

where D is the electron diffusion coefficient. Thus

$$\kappa \sim \frac{\delta}{\zeta_{eff}} \sim \frac{\delta_L(0)}{\ell}$$

(the exact theory leads to the coefficient 0.72 in this formula). Note that in this case the coefficient

$$\frac{1}{4m\kappa^2} \sim \frac{\ell^2}{4m\delta_L^2(0)} \sim \frac{3D}{4p_F \delta_L^2(0)}.$$

Thus one can express the GL equation for alloys in the form

$$\frac{\pi D \hbar}{8k_B T_c} \left(\nabla + \frac{2ie}{\hbar c} \mathbf{A} \right)^2 \Delta + \frac{T_c - T}{T_c} \Delta - \frac{7\zeta(3)}{8\pi^2} \frac{|\Delta|^2}{(k_B T_c)^2} \Delta = 0$$

and the current is expressed in the form

$$\mathbf{j} = \frac{ieg(\epsilon_F)D}{4k_B T_c} \left[\frac{1}{2} (\Delta^* \nabla \Delta - \Delta \nabla \Delta^*) + \frac{2ie}{\hbar c} |\Delta|^2 \mathbf{A} \right].$$

Finally, we will derive an auxiliary expression for the free energy which will be used below. Using dimensionless notations we get

$$\int (\Omega_s - \Omega_n^{(0)}) d\mathcal{V} = \frac{H_c^2}{4\pi} \int d\mathcal{V} \left\{ -|\Psi|^2 + \frac{|\Psi|^4}{2} + \left| \left(\frac{i\nabla}{\kappa} - \mathbf{A} \right) \Psi \right|^2 + H^2 \right\}.$$

Then we integrate the item with $\nabla\Psi^*$ by parts, the surface integral being zero. In the rest integral we take into account that Ψ obeys the GL equation. As a result,

$$\int (\Omega_s - \Omega_n^{(0)}) d\mathcal{V} = \frac{H_c^2}{4\pi} \int d\mathcal{V} \left[H^2 - \frac{|\Psi|^4}{2} \right].$$

If one keeps the external field \mathbf{H}_0 fixed the corresponding thermodynamic potential can be obtained by subtracting $\mathbf{H}_0\mathbf{B}/4\pi$. In a normal phase, correspondingly $\Omega_{nH} = \Omega_n^{(0)} - H_0^2/8\pi$. As a result,

$$\int (\Omega_{sH} - \Omega_{nH}) d\mathcal{V} = \frac{H_c^2}{4\pi} \int d\mathcal{V} \left[(H - H_0)^2 - \frac{|\Psi|^4}{2} \right]. \quad (19.3)$$

Range of Applicability for the GL Theory.

As we have mentioned, one of the conditions is the vicinity of the transition, $|\tau| \ll 1$. Another condition is the local relation between the current and vector potential, $\delta \ll \zeta_0$. In fact, it is possible to combine these equations taking into account that $\delta(T) \sim \delta_L(0)|\tau|^{-1/2}$. The criterion reads as

$$|\tau| \ll \min(\kappa^2, 1).$$

In fact, the theory works not so bad even beyond the vicinity of T_c .

There is another limitation of the range of GL theory: at very small $|\tau|$ where fluctuations become important and the self consistent approach becomes invalid. This limitation is not important for bulk materials but may be very important for layered and low dimensional SC.

19.2 Applications of the GL Theory

Surface Energy at N-S Interface

Consider the problem where all the quantities depend only upon one co-ordinate, say x , while $\mathbf{A} \perp \mathbf{x}$. The set of equations has the form (we'll see that Ψ is *real*)

$$\begin{aligned} \kappa^{-2}(d^2\Psi/dx^2) + \Psi(1 - A^2) - \Psi^3 &= 0, \\ (d\Psi/dx)|_{\text{surface}} &= 0, \\ d^2A/dx^2 - \Psi^2 A &= 0. \end{aligned}$$

It is easy to find the integral of this set. Let us multiply the first equation by $d\Psi/dx$, the last one - by dA/dx and them add the equation and integrate over x :

$$\int_0^x dx \left[\frac{1}{\kappa^2} \frac{d^2\Psi}{dx^2} \frac{d\Psi}{dx} + \Psi \frac{d\Psi}{dx} (1 - A^2) - \frac{d\Psi}{dx} \Psi^3 + \frac{d^2A}{dx^2} \frac{dA}{dx} - \Psi^2 A \frac{dA}{dx} \right] = 0.$$

We obtain

$$\frac{1}{\kappa^2} \left(\frac{d\Psi}{dx} \right)^2 + \Psi^2 (1 - A^2) - \frac{\Psi^4}{2} + \left(\frac{dA}{dx} \right)^2 = \text{const} = \frac{1}{2}$$

(the constant being determined from the boundary conditions.

To find the surface energy we formulate the boundary conditions

$$\begin{aligned} x \rightarrow \infty & (\text{superconductor}) : \Psi = 1, \quad H = A = 0, \quad d\Psi/dx = 0, \\ x \rightarrow -\infty & (\text{normal conductor}) : \Psi = 0, \quad H = H_0 = 1/\sqrt{2}, \quad d\Psi/dx = 0. \end{aligned}$$

At $\kappa \ll 1$ ($\zeta \gg \delta$) the most important region where A and H are small. Thus, we get

$$\frac{1}{\kappa^2} \left(\frac{d\Psi}{dx} \right)^2 + \Psi^2 - \frac{\Psi^4}{2} = \frac{1}{2} \rightarrow \frac{d\Psi}{dx} = \frac{\kappa}{\sqrt{2}} (1 - \Psi^2).$$

The solution is

$$\Psi = \tanh \frac{\kappa x}{\sqrt{2}},$$

it is wrong in the region where the field penetrates, but this region is small. Now we can employ Eq. (19.3) and put $H_0 = 1/\sqrt{2}$, $H = 0$. We obtain

$$\sigma_{ns} = \frac{H_c^2}{8\pi} \int \left[1 - \tanh^2 \frac{\kappa x}{\sqrt{2}} \right] dx = \frac{H_c^2}{8\pi} \frac{4\sqrt{2}}{3\kappa}.$$

In dimensional units that means

$$\sigma_{ns} = \frac{4\sqrt{2}}{3} \frac{H_c^2}{8\pi} \frac{\delta}{\kappa}.$$

The opposite limiting case can be treated only numerically. The result is that σ_{ns} at $\kappa = 1/\sqrt{2}$ and at $\kappa > 1/\sqrt{2}$ it is negative. The order-of magnitude estimate has been made earlier.

Quantization of Magnetic Flux.

Consider a hollow cylinder placed into a longitudinal magnetic field. Assume that the cylinder is in the Meissner state. If the order parameter has the form

$$\Psi = |\Psi| e^{i\chi}$$

the current is

$$\mathbf{j} = -\frac{e\hbar}{m}|\Psi|^2 \left[\nabla\chi + \frac{2e}{\hbar c} \mathbf{A} \right].$$

We can divide the current density by $|\Psi|$ and integrate over a closed circuit in the bulk of superconductor:

$$\oint_0 \underbrace{\frac{\mathbf{j}}{|\Psi|^2} d\mathbf{l}}_{-\frac{e\hbar}{m}} = -\frac{e\hbar}{m} \left[\underbrace{\oint \nabla\chi d\mathbf{l}}_{-2\pi k} + \underbrace{\frac{2e}{\hbar c} \oint \mathbf{A} d\mathbf{l}}_{\text{flux}} \right].$$

Thus

$$\Phi = k\Phi_0, \quad \Phi_0 = \pi\hbar c/e = 2.07 \cdot 10^{-7} \text{G} \cdot \text{cm}^2.$$

It is interesting that the effect has been predicted by F. London (1950) before the concept of Cooper pairs. He assumed the quantum to be $\pi\hbar c/e = 2\Phi_0$.

In any case the quantized quantity is in fact *fluxoid*

$$\oint \nabla\chi d\mathbf{l}$$

which is equal to the total flux through the hole and the surface layer. As a result, the flux quantization through the hole is not exact.

Experimentally, the SC is cooled in a fixed magnetic field and the flux is frozen inside the hole. To determine the trapped flux one should minimize the free energy difference

$$\int (\Omega_{sH} - \Omega_{nH}) d\mathcal{V} = \frac{H_c^2}{4\pi} \left\{ \underbrace{(H_{int} - H_0)^2 \pi R_1^2}_{\text{hole}} + \underbrace{\int_{R_1}^{R_2} \left[(H - H_0)^2 - \frac{|\Psi|^4}{2} \right] 2\pi\rho d\rho}_{\text{SC walls}} \right\}.$$

Here $R_{1,2}$ are internal (external) radius of the SC pipe. The second term is not important for a macroscopic pipe ($R_2 - R_1 \gg \Delta$) and one should find H_{int} to minimize the previous expression under the quantization condition. It is clear to understand that the internal magnetic flux is equal to

$$\Phi = n\Phi_0 \quad \text{at} \quad \left(n - \frac{1}{2} \right) \Phi_0 < \Phi_{ext} < \left(n + \frac{1}{2} \right) \Phi_0$$

(see Fig. 19.1).

This kind of behavior has been demonstrated in a very interesting experiments by Little and Parks (1962). Let us make the hollow cylinder from a very thin film with the thickness $\ll \delta$. Such a film does not screen the magnetic field. If the film radius is $\gg \delta$ one

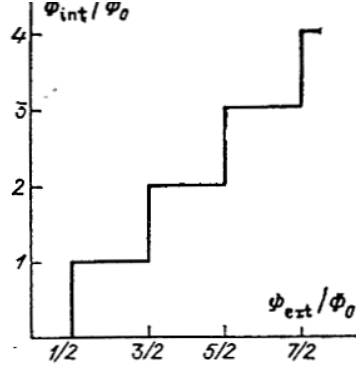


Figure 19.1: Quantization of magnetic flux through a SC cylinder.

can consider the vector potential to be constant in the film. We can come to cylindric co-ordinates and assume that the only component of \mathbf{A} as A_φ . Expressing the order parameter as $\Psi e^{i\chi}$ we have

$$\begin{aligned} \int (\Omega_s - \Omega_n^{(0)}) dV &= \int dV \left\{ \alpha\tau|\Psi|^2 + \frac{b}{2}|\Psi|^4 + \frac{1}{4m} \left| \left(-i\hbar\nabla + \frac{2e}{c}\mathbf{A} \right) \Psi \right|^2 + \frac{H^2}{8\pi} \right\} \rightarrow \\ \Omega_s - \Omega_n^{(0)} &= \alpha\tau|\Psi|^2 + \frac{b}{2}|\Psi|^4 + \frac{\hbar^2}{4m} \left(\nabla\chi + \frac{2e}{\hbar c}\mathbf{A} \right)^2 + \frac{H^2}{8\pi}. \end{aligned} \quad (19.4)$$

In our case $|\Psi| = \text{const}$, as well as the quantities $\nabla\chi$ and \mathbf{A} are constant along the film. So we can replace the gauge-invariant difference $\nabla\chi + \frac{2e}{\hbar c}\mathbf{A}$ by its average value

$$\nabla\chi + \frac{2e}{\hbar c}\mathbf{A} = \frac{1}{2\pi R} \oint \left(\nabla\chi + \frac{2e}{\hbar c}\mathbf{A} \right) d\mathbf{l} = \frac{1}{R} \left(n - \frac{\Phi}{\Phi_0} \right).$$

Now we can substitute this expression into (19.4) to get

$$\Omega_s - \Omega_n^{(0)} = \alpha\tau|\Psi|^2 + \frac{b}{2}|\Psi|^4 + \frac{\hbar^2}{4mR^2} \left(n - \frac{\Phi}{\Phi_0} \right)^2 |\Psi|^2 + \frac{H^2}{8\pi},$$

the number n is within the interval

$$\left(n - \frac{1}{2} \right) \Phi_0 < \Phi_{ext} < \left(n + \frac{1}{2} \right) \Phi.$$

We see that the magnetic field leads to the renormalization of the critical temperature

$$\tau \rightarrow \tau' = \tau + \frac{\hbar^2}{4mR^2\alpha} \left(n - \frac{\Phi}{\Phi_0} \right)^2$$

or

$$\frac{\delta T_c}{T_c} = -\frac{\hbar^2}{4mR^2\alpha} \left(n - \frac{\Phi}{\Phi_0} \right)^2.$$

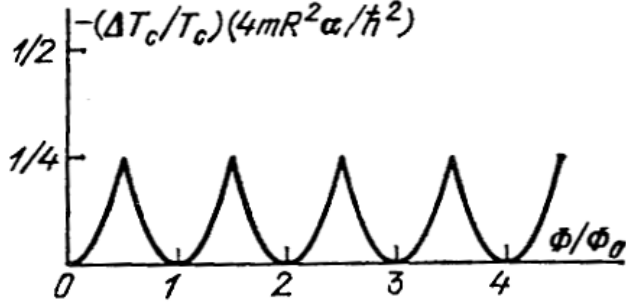


Figure 19.2: On the experiments by Little and Parks.

The graph of the experimental dependence is shown in Fig. 19.2. Note that to observe the change of magnetic flux in a SC cylinder with thick walls one should wait several years because the life time of the metastable state with "wrong" numbers of quanta is very long. The key feature of the experiment discussed is the thin walls of the cylinder.

Thermoelectric Phenomena

Now we can discuss how to observe the thermoelectric effects we've considered earlier. For this reason we write the supercurrent as

$$\mathbf{j} = \mathbf{j}_T + \mathbf{j}_s, \quad \mathbf{j}_T = -\eta_s \nabla T, \quad \mathbf{j}_s = -\frac{\hbar e n_s}{2m} \left(\nabla \chi + \frac{2e}{\hbar c} \mathbf{A} \right)$$

(we have substituted $|\Psi|^2 = n_s/2$. Now consider a cylindric system shown in Fig. 19.3, the branches a and b being fabricated from different materials. In the bulk of materials $\mathbf{j} = 0$,

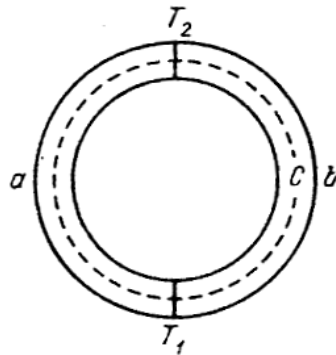


Figure 19.3: On the thermoelectric effect.

and

$$\nabla \chi = \frac{2m\eta_s}{\hbar e n_s} \nabla T - \frac{2e}{\hbar c} \mathbf{A}.$$

Integrating over the closed loop we get

$$\begin{aligned} 2\pi n &= \frac{2m}{\hbar e} \oint \frac{\eta_s}{n_s} \nabla T d\mathbf{l} - \frac{2e}{\hbar c} \oint \frac{\eta_s}{n_s} \mathbf{A} d\mathbf{l} = \\ &= \frac{2m}{\hbar e} \int_{T_1}^{T_2} \left[\left(\frac{\eta_s}{n_s} \right)_a - \left(\frac{\eta_s}{n_s} \right)_b \right] dT - 2\pi \frac{\Phi}{\Phi_0}. \end{aligned}$$

As a result,

$$\frac{\Phi}{\Phi_0} = -n + \frac{m}{\pi \hbar e} \int_{T_1}^{T_2} \left[\left(\frac{\eta_s}{n_s} \right)_a - \left(\frac{\eta_s}{n_s} \right)_b \right] dT.$$

We see that there is non-quantized contribution to the magnetic flux. This contribution is small but observable.

Surface Superconductivity

Now we discuss the surface superconductivity. To start let us discuss stability of the SC region in the normal phase. We have different possibilities (see Fig. 19.4 where the order parameter is shown). For all the cases one should use the boundary condition

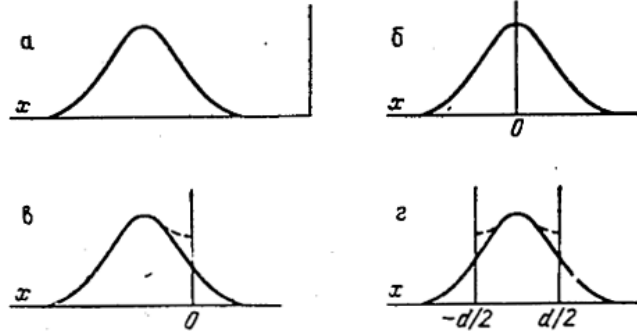


Figure 19.4: On the surface superconductivity.

$$\left(\frac{d\Psi}{dx} \right)_{surface} = 0.$$

Assume that the field is parallel to the surface. We chose

$$A = H(x - x_0)$$

where x_0 is the parameter. The GL equation has the form

$$-\frac{d^2\Psi}{dx^2} + \kappa^2 H_0^2 (x - x_0)^2 \Psi = \kappa^2 \Psi$$

It is convenient to transform the equation to dimensionless variable $x' = x\sqrt{\kappa H_0}$, and we have

$$-\Psi'' + (x' - x'_0)^2 \Psi = \frac{\kappa}{H_0} \Psi.$$

This equation has 2 parameters: $\beta = \kappa/H_0$, and $x'_0 = x_0\sqrt{\kappa H_0}$. There is an exact solution of this equation that can be expressed in terms of hypergeometric function. It has the form

$$\Psi = e^{-x'^2/2} \left\{ C_1 F \left[\frac{1-\beta}{4}, \frac{1}{2}, (x' - x'_0)^2 \right] + C_2 x' F \left[\frac{3-\beta}{4}, \frac{3}{2}, (x' - x'_0)^2 \right] \right\}$$

where $F(\alpha, \gamma, z)$ obeys the equation

$$zF'' + (\gamma - z)F - \alpha F = 0.$$

We can find the ratio C_1/C_2 and β from the boundary conditions at the surface and at infinity (they can be expressed as the function of x'_0). Then one can minimize β with respect to x'_0 , the quantity β_{\min} corresponds to $H_{0\max}$. The result is

$$H_{c3} = 1.69\kappa = 1.695H_{c2}.$$

19.3 N-S Boundary

Proximity Effect

In this section we briefly discuss important physics for the N-S boundary. To make the discussion as simple as possible we discuss the case of the temperature close to T_c , so we can use the GL theory.

The most important feature that one should modify the boundary condition for the order parameter. It has the form

$$\mathbf{n} \left[\nabla + \frac{2ie}{c\hbar} \mathbf{A} \right] \Psi \Big|_{surface} = \frac{1}{\mu} \Psi \Big|_{surface}. \quad (19.5)$$

To calculate μ one needs the microscopic theory but it is clear that $\mu \sim \zeta$. The exact result is

$$\mu = \begin{cases} 0.6\zeta_0, & \text{pureSC} \\ 0.3\sqrt{\zeta_0\ell}, & \text{"dirty"SC.} \end{cases}$$

Let us consider the plain surface $x = 0$. The integral of the GL equation at $A = 0$ is

$$\zeta^2 \left(\frac{d\Psi}{dx} \right)^2 + \Psi^2 - \frac{\Psi^4}{2} = \frac{1}{2}.$$

The length ζ is just the coherence length . We know the solution

$$\Psi = \tanh \left(\frac{x - x_0}{\zeta\sqrt{2}} \right),$$

the parameter x_0 is to be determined from the boundary condition (19.5)

$$\sinh\left(\frac{x_0\sqrt{2}}{\zeta}\right) = -2\frac{\mu}{\zeta}.$$

Near T_c $\zeta \propto 1/\sqrt{T_c - T}$ and $x_0 \approx -\mu\sqrt{2}$. Thus

$$\Psi = \tanh\left(\frac{x}{\zeta\sqrt{2}} + 1\right).$$

That means that the order parameter is non-zero also in the thin layer of former normal phase. At the same time, normal conductor "spoils" the superconductivity near the surface.

Andreev Reflection

Let us discuss the N-S boundary in more detail. At the interface the chemical potentials in both phases should be equal. At the same time, in the SC the electrons exist as Cooper pairs. As a result, the chemical potential of the pair of electrons should be the same as the chemical potential of a Cooper pair.

Now let one electron come to the SC. It has no partner, and consequently its energy is greater by Δ . Consequently, if the excitation energy of the electron above the Fermi level is less than Δ it should be *reflected* from the boundary.

To discuss the physical picture in more detail let us assume that metal s are the same (say, we discuss the N-S boundary in the intermediate state). In this case the order parameter penetrates into the normal phase up to the thickness $\sim \zeta \approx \hbar v_F / \Delta$. The energy spectrum $\varepsilon = \sqrt{\xi^2 + \Delta^2}$ is shown in Fig. 19.5. As we have discussed, the quasiparticle

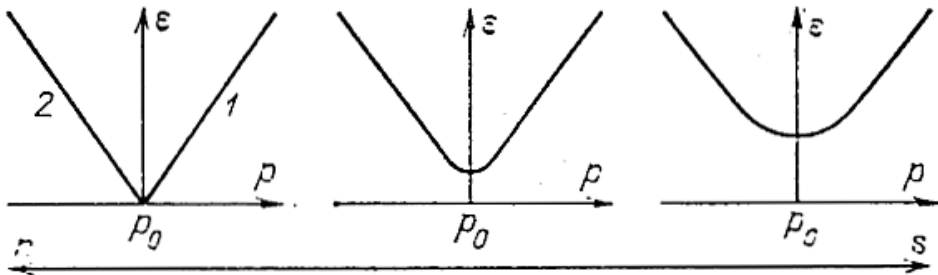


Figure 19.5: Quasiparticle spectrum near the surface.

from the normal metal (left panel) is reflected, its energy being conserved. At the same time, the momentum change can be estimated as follows: $\delta p \sim (dp/dt)\delta t$ where δt is the time to be inside SC: $\delta t \sim \zeta/v_F$. The derivative

$$dp/dt \sim -dU/dx \sim \Delta/\zeta.$$

Thus

$$\delta p \sim (\Delta/\zeta)(\zeta/v_F) \sim p_F(\Delta/\epsilon_F) \ll p_F.$$

The only way to meet these conditions is to make inter-branch transition (from particle-like to antiparticle-like branch and vice versa). We see that both energy and momentum are almost the same. At the same time, the group velocity will have an opposite direction. Actually the process is

$$\text{particle} \rightarrow \text{anti-particle}, \quad \varepsilon_1 = \varepsilon_2, \quad \mathbf{p}_1 \approx \mathbf{p}_2, \quad \mathbf{v}_1 = -\mathbf{v}_2.$$

Such a process is called the *Andreev reflection* (Andreev, 1964).

What happens with the charge? In fact, such a reflection is assisted with the creation of a Cooper pair in the SC region which carries the charge.

This is the mechanism for charge transfer from normal conductor to SC.
Andreev reflection is very important for many effects in superconductors.

Chapter 20

Tunnel Junction. Josephson Effect.

20.1 One-Particle Tunnel Current

Tunneling is the famous problem of quantum mechanics. It is important that a quantum particle can penetrate the barrier with the energy less than the barrier height. The tunnel transparency, up to the main approximation, is given by the formula

$$W \sim \exp \left[\int \text{Imp}_x \, dx \right] = \exp \left[-\frac{2\sqrt{2m}}{\hbar} \int_{x_1}^{x_2} \sqrt{U(x) - E} \, dx \right] \quad (20.1)$$

(see Fig. 20.1).

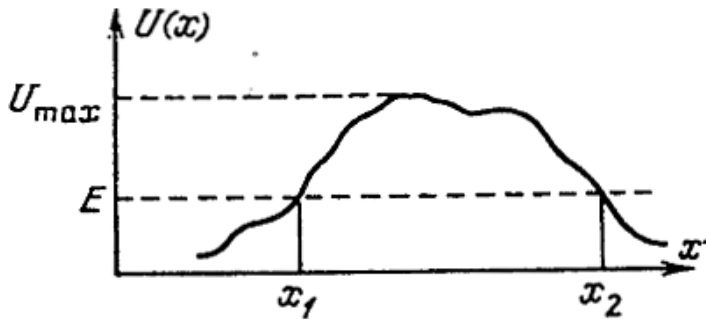


Figure 20.1: Quantum tunneling.

We start with the case of two normal metals. In the equilibrium their chemical potentials are equal. At a fixed bias, all the voltage is dropped across the barrier (the resistance being maximal), so the difference of the electro-chemical potentials is $-eV$ (Fig. 20.2). We see that the number of the electron which can penetrate the barrier is proportional to eV , and we get the Ohm's law (Fig. 20.3, curve 1).

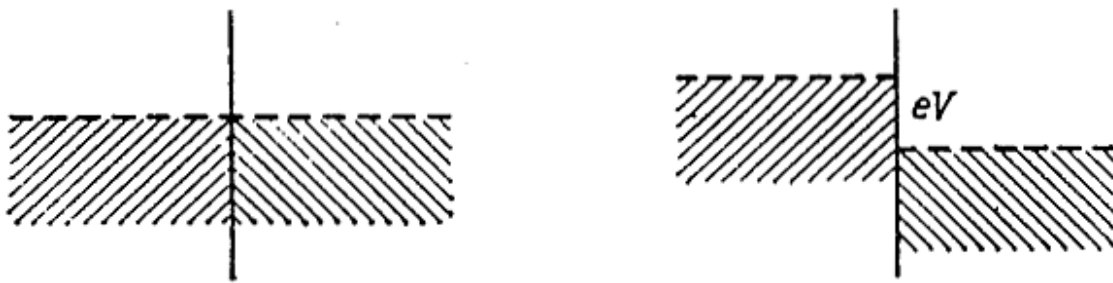
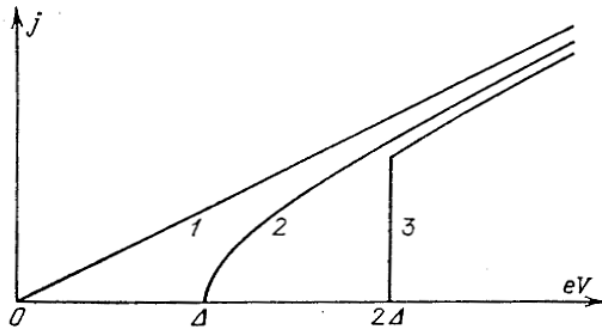


Figure 20.2: Tunnel junction at a given bias.

Figure 20.3: $I - V$ -curves for normal conductors (1), one-electron (2), and two-electron (3) tunneling.

Now let us discuss the N-S case at $T = 0$. In a SC the electrons form Cooper pairs, their chemical potentials are just the same as the energy level of the Bose condensate. In a normal conductor, we have two free quasi-particles at the Fermi level.

Let us suppose that 1 electron made the N \rightarrow S transition through the junction. In a SC its energy is greater by Δ than the energy of an electron inside the Cooper pair. Thus, *an extra energy should be given to the electron*. Energy cost for the reverse transition is just the same because one should destroy the Cooper pair, the energy per electron being Δ .

Why the electron pairs cannot tunnel as a whole? The total charge transferred is $-2e$ that doubles $U(x)$ in Eq. (20.1), while the mass is $2m$ that leads to the extra $\sqrt{2}$. We see that the probability decreases drastically.

To understand the situation let us look at Fig. 20.4. This is the so-called quasi-particle scheme, and we see that the cost is Δ . Consequently, there is a threshold at $eV = \Delta$.

To calculate the current one needs the densities of states: $g_s = g(\epsilon_F)$ for the normal metal and

$$g_s(\varepsilon) = g_n \frac{\varepsilon}{\sqrt{\varepsilon^2 - \Delta^2}}, \quad \varepsilon > \Delta.$$

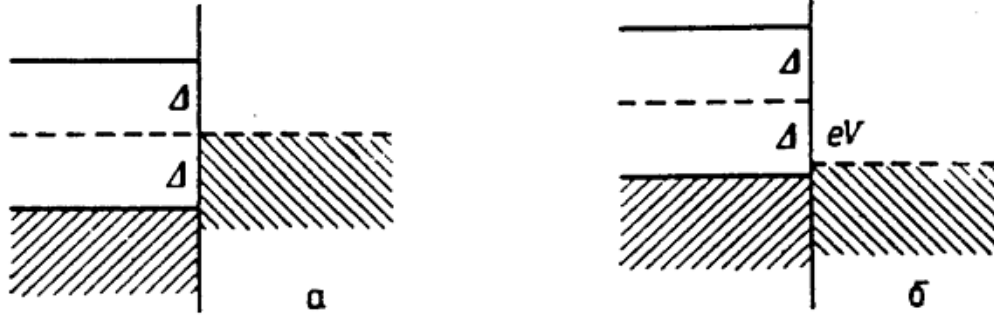


Figure 20.4: Energy diagram for N-S tunneling (S – left side, N – right side of each panel).

This is real density of states. To use the scheme depicted in Fig. 20.4 we should assume both signs of ε . So we define

$$g_s(\varepsilon) = \begin{cases} g_n |\varepsilon| / \sqrt{\varepsilon^2 - \Delta^2}, & |\varepsilon| > \Delta \\ 0, & |\varepsilon| < \Delta \end{cases}.$$

Here positive ε corresponds to N→S tunnel transitions while $\varepsilon < 0$ corresponds to destruction of Cooper pairs assisted by S→N transitions.

The current is given by the golden rule formula

$$\begin{aligned} j &\propto \int d\varepsilon W g_1(\varepsilon - eV) g_2(\varepsilon) \times \\ &\quad \times \{n_1(\varepsilon - eV) [1 - n_2(\varepsilon)] - n_2(\varepsilon) [1 - n_1(\varepsilon - eV)]\} = \\ &= \int d\varepsilon W g_1(\varepsilon - eV) g_2(\varepsilon) [n_1(\varepsilon - eV) - n_2(\varepsilon)] \approx \\ &\approx W g_{1n} g_{2n} \int d\varepsilon \frac{|\varepsilon - eV|}{\sqrt{(\varepsilon - eV)^2 - \Delta^2}} [n_1(\varepsilon - eV) - n_2(\varepsilon)]. \end{aligned}$$

At zero temperature, $n(\varepsilon) = \Theta(\varepsilon)$ and we get

$$j \propto W g_{1n} g_{2n} \int_0^{eV-\Delta} d\varepsilon \frac{|\varepsilon - eV|}{\sqrt{(\varepsilon - eV)^2 - \Delta^2}} = W g_{1n} g_{2n} \sqrt{(eV)^2 - \Delta^2}.$$

One can easily obtain the coefficient taking into account that at $eV \gg \Delta$ the result should be the same as for N-N system. Thus

$$\frac{j}{j_n} = \frac{\sqrt{(eV)^2 - \Delta^2}}{eV}.$$

Now let us discuss the S-S junction. We have

$$j \propto W g_{1n}^2 \int_{\Delta}^{eV-\Delta} d\varepsilon \frac{eV - \varepsilon}{\sqrt{(\varepsilon - eV)^2 - \Delta^2}} \frac{\varepsilon}{\sqrt{\varepsilon^2 - \Delta^2}}.$$

We see that threshold value is $eV = 2\Delta$, the result being

$$\frac{j}{j_n} = E \left(\frac{\sqrt{(eV)^2 - (2\Delta)^2}}{eV} \right) - 2 \left(\frac{\Delta}{eV} \right)^2 K \left(\frac{\sqrt{(eV)^2 - (2\Delta)^2}}{eV} \right)$$

where E, K are the *elliptic integrals*

$$\begin{aligned} K(k) &= \int_0^{\pi/2} (1 - k^2 \sin^2 \varphi)^{-1/2} d\varphi, \\ E(k) &= \int_0^{\pi/2} (1 - k^2 \sin^2 \varphi)^{1/2} d\varphi. \end{aligned}$$

At $eV = 2\Delta$ $j/j_n = \pi/4$ (see Fig. 20.3, curve 3).

At final temperatures, the threshold singularity is smeared, nevertheless even at finite temperatures it is convenient to measure the dependence $\Delta(T)$ from the derivative $\partial j / \partial V$.

It is interesting to consider the case of 2 different superconductors with $T_{c2} > T_{c1} \geq T$. At low temperatures the singularity takes place at

$$eV = \Delta_1 + \Delta_2.$$

To see what happens at finite temperatures let us look at Fig. 20.5 (left panel) where the density of states are plotted. At the increase of voltage the left side of the picture moves



Figure 20.5: S-S tunnelling. Left – Energy diagram, right – $I - V$ -curve.

up and the current *increases* because of the increase of the thermally excited states which can tunnel into the free states in the right side. Then, when $eV \geq (\Delta_2 - \Delta_1)$, the number of free states decreases with the voltage increase. Consequently, the current decreases. The situation changes at $eV = (\Delta_2 + \Delta_1)$ where the *upper limit* of the *left lower band* coincides with the *lower limit* of the *right upper band*. The $I - V$ -curve is shown in Fig. 20.5 (right panel).

Tunneling experiments appear extremely informative to study properties of SC.

20.2 Josephson Effect

Up to now, we have considered *incoherent processes*. Actually, the complete theory should take into account *coherent transfer* of the electron wave function. As a result, the order parameters overlap, and there is a possibility to form a *united condensate*. As a result, a finite supercurrent can flow through S-I-S system *almost* like through a bulk SC (Josephson, 1962).

Let us calculate the *Josephson current* in a very simple way. Namely, let us find the contribution of the coupling to the energy up to the lowest order. The simplest expression

$$E = C \int dy dz (\Delta_1 \Delta_2^* + \Delta_1^* \Delta_2) = 2C \int dy dz |\Delta_1 \Delta_2| \cos(\chi_2 - \chi_1).$$

Here C is a constant, (y, z) is the plane of the contact.

Why the phase difference is dependent on $(\chi_2 - \chi_1)$? Let us consider the magnetic field $\mathbf{H} \parallel (yz)$. According to the gauge invariance, all the physical quantities depend on

$$\nabla \chi + \frac{2e}{\hbar c} \mathbf{A}$$

Now we can chose $\mathbf{A} \parallel \mathbf{x}$ and integrate the relation along x between the points 1 and 2 which are placed inside the left (and right) SC parts. We get

$$\chi_2 - \chi_1 + \frac{2e}{\hbar c} \int_1^2 A_x dx.$$

Thus,

$$E = 2C \int dy dz |\Delta_1 \Delta_2| \cos \left(\chi_2 - \chi_1 + \frac{2e}{\hbar c} \int_1^2 A_x dx \right).$$

After variation with respect to A_x is

$$\delta E = -\frac{4e}{\hbar c} C \int |\Delta_1 \Delta_2| \sin \left(\chi_2 - \chi_1 + \frac{2e}{\hbar c} \int_1^2 A_x dx \right) \delta A_x dV.$$

Comparing this equation with the general formula of electrodynamics

$$\delta E = -\frac{1}{c} \int \mathbf{j} \delta \mathbf{A} dV$$

we obtain

$$j = \frac{4e}{\hbar} C |\Delta_1 \Delta_2| \sin \left(\chi_2 - \chi_1 + \frac{2e}{\hbar c} \int_1^2 A_x dx \right) = j_c \sin \left(\chi_2 - \chi_1 + \frac{2e}{\hbar c} \int_1^2 A_x dx \right).$$

In particular, in the absence of magnetic field,

$$j = j_c \sin (\chi_2 - \chi_1).$$

Thus the phase difference is connected with the supercurrent.

It is clear that the critical current is proportional to the tunneling probability. At the same time, the normal conductance R^{-1} is also proportional to the tunneling probability. The microscopic formula for two identical SC at $T = 0$ (Ambegaokar, Baratoff, 1963) is

$$j_c = \frac{\pi \Delta(0)}{2eR}$$

while at finite temperature

$$j_c = \frac{\pi \Delta(T)}{2eR} \tanh \left(\frac{\Delta(T)}{k_B T} \right).$$

Experimentally, $j_c \sim 10^3 - 10^4$ A/cm² that is 5-6 orders less than the critical current in a bulk sample. Consequently, Josephson effect and related topics are called the *weak superconductivity*. Actually, the current is tuned by the ballast resistor and the transition from zero voltage to the finite one is observed. In fact, this transition is assisted by many interesting nonlinear phenomena (see e.g. *Problem 20.1*).

Josephson Effect in a Weak Link

It is important that the analogs of the Josephson effect can take place not only in S-I-S systems but in any kind of inhomogeneous structures with the part where superconductivity is suppressed. Among such systems are

- S – I – S (SC – insulator – SC, tunneljunction)
- S – N – S (SC – normalconductor – SC, proximitybridge)
- S – C – S (SC – constriction – SC, bridge or point contact)

To explain the reason we discuss here a very simple derivation based on the GL theory.

Consider the GL equation

$$-\frac{1}{\kappa^2} \nabla^2 \Psi - \Psi + |\Psi|^2 \Psi = 0$$

and suppose that the length L of the bridge is much less than ζ (in our units $L/\delta \ll \kappa^{-1}$). In this case, inside the bridge the first item is the most important, and we have in the lowest approximation

$$\nabla^2 \Psi = 0.$$

In the bulk of the "banks" $\Psi \rightarrow \text{const}$. Let us assume that

$$\begin{aligned} \text{const} &= e^{i\chi_1}, \quad \text{in the left side} \\ \text{const} &= e^{i\chi_2}, \quad \text{in the right side} \end{aligned}.$$

Thus we can search the solution of the GL equation as

$$\Psi = f(\mathbf{r})e^{i\chi_1} + [1 - f(\mathbf{r})]e^{i\chi_2} \quad (20.2)$$

where $f(\mathbf{r})$ obeys the equation

$$\nabla^2 f(\mathbf{r}) = 0$$

and tends to 1 in the bank 1 and to 0 in the bank 2. We will not discuss the exact form of the solution which depends on the concrete system. Rather we substitute Eq. (20.2) into the expression for the super-current and transform it to dimensional units. The result is

$$j = \underbrace{\frac{2\hbar}{m}\Psi_0^2\nabla f(\mathbf{r})}_{\text{critical current}} \sin(\chi_2 - \chi_1).$$

20.3 Josephson Effect in a Magnetic Field

Narrow Junction

Suppose that there is an external magnetic field $\mathbf{H} \parallel \mathbf{y}$ (the junction plane is yz one). The field can be described by the vector potential

$$A_x = H_y(x)z$$

We also neglect the field created by the current. In this case

$$\int_1^2 A_x dx = H_{y0} z d, \quad \text{where } d = 2\delta(T) + d' \approx 2\delta(T),$$

d' is the thickness of the insulating region (we have taken into account that the field decays as $\exp(-x/\delta)$ in SC regions). As a result, we have

$$j = j_c \sin \left[\chi_1 - \chi_2 - 2 \frac{eH}{c\hbar} \right].$$

The experimentally measurable quantity is the average current,

$$\bar{j} = \frac{1}{L} \int_0^L j(z) dz = j_c \underbrace{\frac{c\hbar}{2eHLd}}_{\text{flux through the contact}} \left\{ \cos \left[\chi_1 - \chi_2 - 2 \frac{eH}{c\hbar} \right] - \cos (\chi_1 - \chi_2) \right\}.$$

Denoting $\theta_0 = \chi_1 - \chi_2$ we get

$$\bar{j} = \underbrace{\frac{j_c}{\pi} \frac{\Phi}{\Phi_0} \sin\left(\pi \frac{\Phi}{\Phi_0}\right)}_{j_{c\max}-\text{maximal critical current}} \sin\left(\theta_0 + \pi \frac{\Phi}{\Phi_0}\right)$$

As a result, the maximal critical current is

$$j_{c\max} = j_c \left| \frac{\sin(\pi\Phi/\Phi_0)}{\pi\Phi/\Phi_0} \right|.$$

The graph of this function is shown in Fig. 20.6.

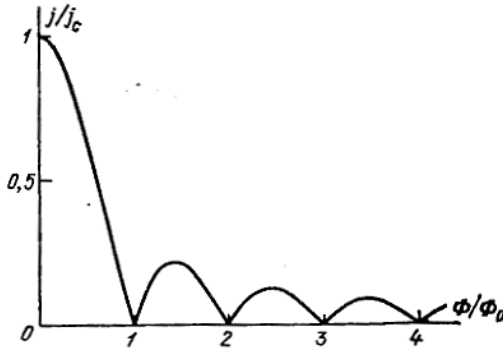


Figure 20.6: Josephson effect in a magnetic field.

Wide Junction

One can neglect the field produced by the own current only if the width of the junction is small. In a wide junction the field becomes z -dependent due to the field produced by the transport current. To take this dependence into account we denote

$$\chi_2 - \chi_1 + \frac{2e}{\hbar c} \int_1^2 A_x dx \equiv \theta(z)$$

and write

$$\theta(z + dz) - \theta(z) = \frac{2e}{c\hbar} dH_y(z) dz = \frac{2\pi}{\Phi_0} dH_y(z) dz.$$

Thus

$$H_y(z) = \frac{\Phi_0}{2\pi d} \frac{d\theta}{dz}.$$

On the other hand, from the Maxwell equation

$$j = \frac{c}{4\pi} \frac{dH_y}{dz}$$

while according to the Josephson relation

$$j = j_c \sin \theta.$$

As a result, we come to the equation

$$\begin{aligned} j_c \sin \theta &= \frac{c}{4\pi} \frac{dH_y}{dz} = \frac{c\Phi_0}{8\pi^2 d} \frac{d^2\theta}{dz^2} \rightarrow \\ \frac{d^2\theta}{dz^2} &= \frac{1}{\delta_J^2} \sin \theta. \end{aligned} \quad (20.3)$$

This is the *Ferrell-Prange equation*. Here

$$\delta_J = \sqrt{\frac{c\Phi_0}{8\pi^2 dj_c}}$$

is the so-called *Josephson penetration depth*.

To understand the situation let us consider the case of weak magnetic field with no transport current. In this case we can replace $\sin \theta \rightarrow \theta$, and the solution is

$$\theta = \theta_0 e^{-z/\delta_J} \rightarrow H = H_0 e^{-z/\delta_J}.$$

For $j_c \sim 10^2$ A/cm² $\delta_J \sim 10^{-2}$ cm $\gg \delta_L$. Thus the junction can be considered as narrow if

$$L \ll \delta_J.$$

In wide junctions we come to a very interesting picture – the junction behaves as 2D superconductor with the specific Meissner effect. The current distribution is shown in Fig. 20.7, left panel.

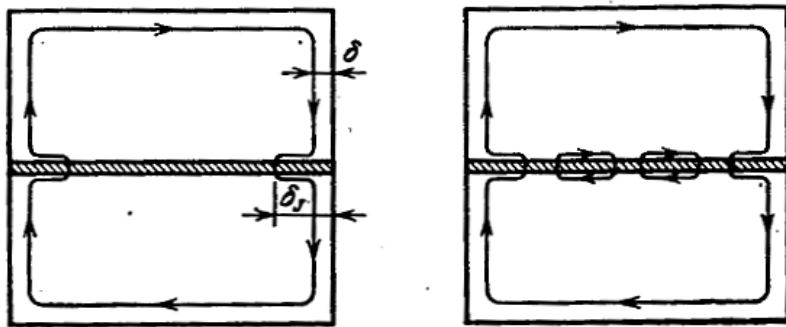


Figure 20.7: Josephson effect in a wide junction. Left panel - weak magnetic field, right panel - strong magnetic field.

In a strong enough field we return to Eq. (20.3) multiply it by $d\theta/dz$ and integrate over z . As a result, we get the integral

$$\left(\frac{d\theta}{dz}\right)^2 = -\frac{2}{\delta_J^2} \cos \theta + C.$$

The solution can be written as

$$z - z_0 = \int_{\pi}^{\theta} \frac{d\theta_1}{\sqrt{C - 2\delta_J^{-2} \cos \theta_1}}.$$

To study the structure of the magnetic field we discuss the solution of the soliton type with the boundary condition

$$\frac{d\theta}{dz} \rightarrow 0 \quad \text{at} \quad z \rightarrow \pm\infty.$$

To find the constants C note that

$$\frac{d\theta}{dz} = \left[\frac{d}{d\theta} \int_{\pi}^{\theta} \frac{d\theta_1}{\sqrt{C - 2\delta_J^{-2} \cos \theta_1}} \right]^{-1} = \sqrt{C - 2\delta_J^{-2} \cos \theta}$$

We can get the solution assuming that $\theta \rightarrow 0$ at $z \rightarrow -\infty$ and $\theta \rightarrow 2\pi$ at $z \rightarrow \infty$. We get $C = 2\delta_J^{-2}$ and

$$\theta(z) = 4 \arctan \left[\exp \left(\frac{z - z_0}{\delta_L} \right) \right].$$

The distribution of current is shown in Fig 20.7, right panel, while the graphs of the phase, field and current are shown in Fig. 20.8.

In general, there is a chain of vortexes. The magnetic flux in each one is

$$\Phi = d \int_{-\infty}^{\infty} H dz = \frac{\Phi_0}{2\pi d} d [\theta(\infty) - \theta(0)] = \Phi_0.$$

Thus we come to the picture similar to the type II SC. One can show that the analog of the field H_{c1} is

$$H_{c1} = \frac{2\Phi_0}{\pi^2 d \delta_J}.$$

The important difference that the Josephson vortexes have no normal core. Consequently, there is no upper critical field H_{c2} . At high field vortexes overlap and the field is almost uniform.

Superconductor Interferometers

Let us discuss the principle of a very important application of quantum interference in superconductors. Consider a system show in Fig. 20.9. . The total current through the

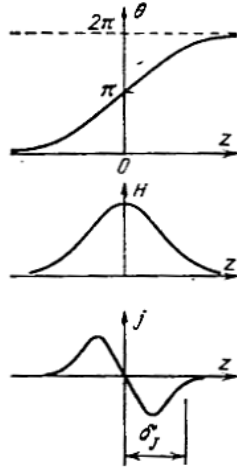


Figure 20.8: Josephson effect in a wide junction. Distributions of phase, current, and field.

external circuit is

$$I = I_{c1} \sin \theta_1 + I_{c2} \sin \theta_2.$$

If magnetic field is directed perpendicular to the loop's plane, the phase of the order parameter in the bulk of material is

$$\nabla \chi = \frac{2e}{\hbar c} \mathbf{A} \quad (\text{current is absent, } \mathbf{j} = 0).$$

Integrating along the dashed line we get for the total phase variation:

$$\theta_1 - \theta_2 + \frac{2e}{\hbar c} \Phi = 2\pi n \rightarrow \theta_1 - \theta_2 + 2\pi \frac{\Phi}{\Phi_0} = 2\pi n.$$

Consequently, we can denote

$$\theta_1 = \theta - \pi \frac{\Phi}{\Phi_0} + 2\pi n, \quad \theta_2 = \theta + \pi \frac{\Phi}{\Phi_0}.$$

If the field is weak enough in order not to affect upon the currents I_{c1}, I_{c2} we have

$$I = I_{c1} \sin \left(\theta - \pi \frac{\Phi}{\Phi_0} \right) + I_{c2} \sin \left(\theta + \pi \frac{\Phi}{\Phi_0} \right).$$

The result has the simplest form at $I_{c1} = I_{c2} = I_c$:

$$I = I_c^{eff} \sin \theta, \quad I_c^{eff} = 2I_c \cos \left(\pi \frac{\Phi}{\Phi_0} \right).$$

We see that the critical current of the interferometer oscillates with the external magnetic field.

We have described only one possible scheme of a SQUID (Superconductor Quantum Interference Device). In fact, SQUIDs are very important for applications and there are different schemes to use them.

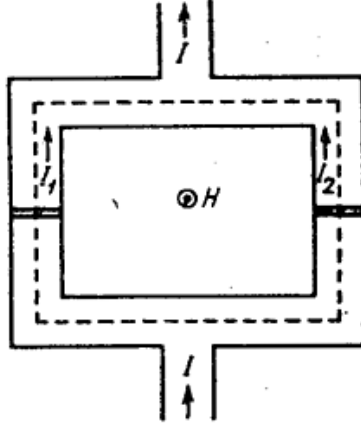


Figure 20.9: Superconductor interferometer.

20.4 Non-Stationary Josephson Effect

According to the gauge invariance, the electric potential enters all the equations in a combination

$$2e\varphi + \hbar \frac{\partial \chi}{\partial t}.$$

It means that the phase acquires the additional factor

$$\frac{2e}{\hbar} \int^t \varphi(t') dt'$$

or

$$\frac{\partial \theta}{\partial t} = \frac{2e}{\hbar} V.$$

This is the so-called *not-stationary Josephson effect*. Thus, if the voltage V at the junction kept constant

$$j = j_c \sin [\theta_0 + \omega_J t], \quad \omega_j = \frac{2e}{\hbar} V$$

(for $V = 10^{-4}$ V $\omega_J \sim 10^{11}$ s $^{-1}$). Usually, the voltage is never kept constant. Rather a series circuit is constructed with a battery and a load tunable resistor. In this case an interesting and complicated picture can be observed (see *Problem 20.1*).

It is important that at finite temperature in the presence of voltage the one-particle tunneling is present, the normal current being $V/R = (\hbar/2eR) \partial \theta / \partial t$. Thus

$$j = j_c \sin \theta + (\hbar/2eR) \partial \theta / \partial t.$$

According to the Josephson formula,

$$\frac{d\theta}{dt} = \frac{2e}{\hbar} V = \frac{2e}{\hbar} (U - J_c R \sin \theta) = \omega_J (1 - \lambda \sin \theta), \quad \lambda = \frac{J_c R}{U}.$$

As a result

$$\omega_j(t - t_0) = \int \frac{d\theta}{1 - \lambda \sin \theta}$$

At $\lambda > 1$ there is a pole in the integrand at $\theta_0 = \arcsin(1/\lambda)$. Thus at $t \rightarrow \infty$ $\theta \rightarrow \theta_0$, the current being U/R while the voltage at the junction is zero. At $\lambda > 1$ (or $J > J_c$) one can calculate the integral exactly: assuming $m = \tan(\theta/2)$ we get

$$m = \lambda + \sqrt{1 - \lambda^2} \tan \left[\frac{1}{2} \sqrt{1 - \lambda^2} \omega_J (t - t_0) \right]$$

The current being

$$I = \frac{2_c m}{1 + m^2}.$$

We see that the current oscillates with the period $2\pi/\omega = 2\pi/\omega_J \sqrt{1 - \lambda^2}$.

Having in mind that $V = (\hbar/2e)(\partial\theta / \partial t)$ we obtain

$$V(t) = R \frac{j(j^2 - j_c^2)}{j^2 + j_c^2 \cos \omega t + j_c \sqrt{j^2 - j_c^2} \sin \omega t}, \quad \omega = \frac{2eR}{\hbar} \sqrt{j^2 - j_c^2}.$$

One can show that the time average is equal to

$$\overline{V(t)} = \frac{1}{2\pi} \int_0^{2\pi} d(\omega t) V(t) = \frac{\hbar\omega}{2e}.$$

This property is employed in metrology.

Another important property is the reaction of the Josephson junction to the external a.c. field. Suppose that one modulates the voltage as

$$V(t) = V_0 + v \cos \Omega t.$$

We obtain

$$\theta(t) = \frac{2e}{\hbar} \left[V_0 t + \theta_0 + \frac{v}{\Omega} \sin \Omega t \right],$$

$$\frac{j}{j_c} = \sin \theta(t) = \sin \left[\frac{2e}{\hbar} (V_0 t + \theta_0) \right] \cos \left[\frac{2eV}{\hbar\Omega} \sin \Omega t \right] + \cos \left[\frac{2e}{\hbar} (V_0 t + \theta_0) \right] \sin \left[\frac{2eV}{\hbar\Omega} \sin \Omega t \right].$$

Then, one should remember that

$$\begin{aligned} \cos(a \sin \Omega t) &= \sum_{-\infty}^{\infty} J_{2k}(a) e^{i2k\Omega t} = 2 \sum_0^{\infty} J_{2k}(a) \cos 2k\Omega t, \\ \sin(a \sin \Omega t) &= \sum_{-\infty}^{\infty} J_{2k+1}(a) e^{i(2k+1)\Omega t} = 2 \sum_1^{\infty} J_{2k-1}(a) \sin (2k-1)\Omega t. \end{aligned}$$

Consequently we can plug in these series into the previous equation denoting $a \equiv 2eV/\hbar\Omega$. Now, we can recall that

$$\begin{aligned} 2 \sin \left[\frac{2e}{\hbar} (V_0 t + \theta_0) \right] \cos 2k\Omega t &= \sin \left[\left(\frac{2eV_0}{\hbar} + 2k\Omega \right) t + \theta_0 \right] \\ &\quad + \sin \left[\left(\frac{2eV_0}{\hbar} - 2k\Omega \right) t + \theta_0 \right], \\ 2 \cos \left[\frac{2e}{\hbar} (V_0 t + \theta_0) \right] \sin (2k-1)\Omega t &= \sin \left[\left(\frac{2eV_0}{\hbar} + (2k-1)\Omega \right) t + \theta_0 \right] \\ &\quad - \sin \left[\left(\frac{2eV_0}{\hbar} - (2k-1)\Omega \right) t + \theta_0 \right]. \end{aligned}$$

We see that at

$$\frac{2eV}{\hbar} = n\Omega$$

a time-independent item appears, the amplitude being

$$\overline{j_n} = (-1)^n J_n(2ev/\hbar\Omega) \sin \theta_0.$$

Thus we get resonant additional contributions to the current.

Such a formulation does not coincide with the experiment where usually the current is kept constant. To describe the situation one should solve the corresponding problem which is more difficult mathematically but is not too difficult qualitatively. As a result, the steps at the current-voltage curves appear (Shapira steps, Fig. 20.10).

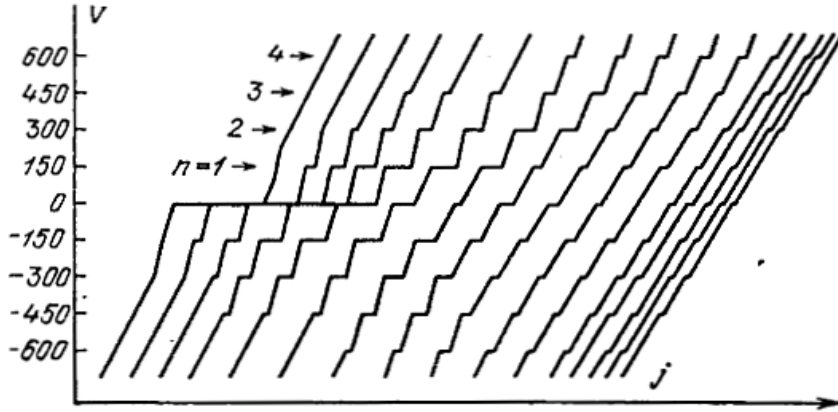


Figure 20.10: Shapira steps. Different curves are measured for different amplitudes of microwave and shifted along the x -axis.

Registration of the steps is one way to construct Josephson detectors for microwave fields.

20.5 Wave in Josephson Junctions

Josephson waves

Suppose that we place a Josephson junction in a magnetic field and keep a given potential difference. In this case,

$$j = j_c \sin [\theta_0 + (2eV/\hbar)t + (2eHd/\hbar c)z] . \quad (20.4)$$

This is just the wave propagating along z axis, the wave vector being $k = 2eHd/\hbar c$, and the phase velocity being

$$v_0 = \omega/k = cV/Hd . \quad (20.5)$$

Swihart waves

Do not forget that the junction has a finite capacitance, and the current has a contribution

$$\frac{\partial Q}{\partial t} = C \frac{\partial V}{\partial t} = \frac{C\hbar}{2e} \frac{\partial^2 \theta}{\partial t^2} .$$

Thus

$$j = j_c \sin \theta + \frac{\hbar}{2eR} \frac{\partial \theta}{\partial t} + \frac{C\hbar}{2e} \frac{\partial^2 \theta}{\partial t^2} . \quad (20.6)$$

If we substitute this expression to the Maxwell equation

$$j = \frac{c}{4\pi} \frac{dH}{dz} , \quad H(z) = \frac{\Phi_0}{2\pi d} \frac{d\theta}{dz}$$

we obtain *nonlinear* wave equation

$$\frac{\partial^2 \theta}{\partial z^2} - \frac{1}{c_0^2} \frac{\partial^2 \theta}{\partial t^2} - \frac{\gamma}{c_0^2} \frac{\partial \theta}{\partial t} = \frac{1}{\delta_J^2} \sin \theta . \quad (20.7)$$

Here

$$\begin{aligned} c_0 &= \sqrt{\frac{ec}{4\pi^2 d C \hbar \Phi_0}} = c \sqrt{\frac{d'}{\kappa d}} , \quad d' = \frac{\kappa}{4\pi C} , \\ \gamma &= \frac{1}{RC} \end{aligned}$$

At $j_c \rightarrow 0$, $\gamma \rightarrow 0$ one obtains eigen modes with velocity $c_0 \ll c$. These waves are called the *Swihart waves*.

In the presence of Josephson current they interact with the Josephson waves. To study such a coupling let us assume that $j_c \rightarrow 0$ and iterate the r.h.s. of Eq. (20.7):

$$\theta = \theta_0 + \omega t + kz + \theta_1 , \quad \theta_1 \ll \omega t + kz .$$

In this case we have

$$\frac{\partial^2 \theta_1}{\partial z^2} - \frac{1}{c_0^2} \frac{\partial^2 \theta_1}{\partial t^2} - \frac{\gamma}{c_0^2} \frac{\partial \theta_1}{\partial t} = \frac{1}{\delta_J^2} \sin(\theta_0 + kz + \omega t). \quad (20.8)$$

From this equation,

$$\theta_1 = \frac{c_0^2}{\delta_J^2} \operatorname{Im} \left[\frac{\exp[i(\theta_0 + kz + \omega t)]}{\omega^2 - k^2 c_0^2 - i\omega\gamma} \right].$$

Now we can calculate the average current,

$$\bar{J} \equiv \lim_{T,L \rightarrow \infty} \frac{1}{T} \int_0^T dt \int_0^L dz j(z,t).$$

Expanding the expression as

$$\sin \theta(z,t) = \cos(\theta_0 + \omega t + kz) \sin(\theta_1(z,t)) + \text{vanishing items}$$

we get

$$\bar{J} = j_c \frac{\omega c_0^2 \gamma}{2\delta_J^2} \frac{1}{(\omega^2 - c_0^2 k^2)^2 + \omega^2 \gamma^2}.$$

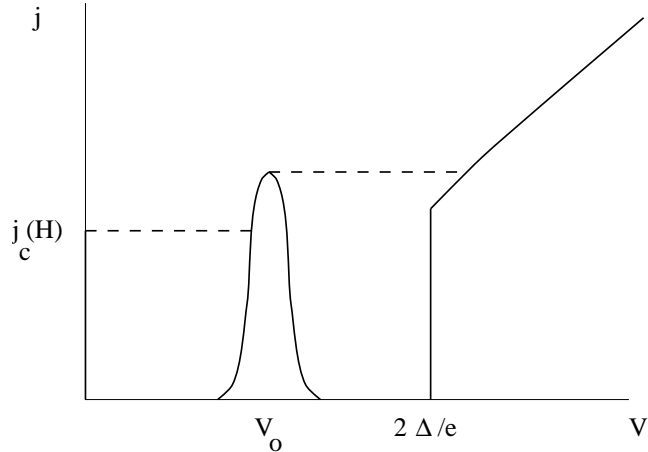
As a result, one obtains a clear peak (resonance) at

$$v_0 = c_0, \quad \rightarrow \quad V = \frac{c_0}{e} H d.$$

Note that the criterion of applicability is

$$\bar{j} \ll j_c \quad \rightarrow \quad \frac{c_0^2}{\delta_J^2} \ll \omega \gamma.$$

Usually the *current* rather than the voltage is kept constant. Then one observes the steps at the $V - I$ curve.



20.6 Problems

20.1. Consider the current in a series circuit containing a Josephson junction, load resistor, and a battery.

Chapter 21

Mesoscopic Superconductivity

21.1 Introduction

Recent experiments on conduction between a semiconductor and a superconductor have revealed a variety of new mesoscopic phenomena. Here is a review of the present status of this rapidly developing field. A scattering theory is described which leads to a conductance formula analogous to Landauer's formula in normal-state conduction. The theory is used to identify features in the conductance which can serve as "signatures" of phase-coherent Andreev reflection, i.e. for which the phase coherence of the electrons and the Andreev-reflected holes is essential. The applications of the theory include a quantum point contact (conductance quantization in multiples of $4e^2/h$), a quantum dot (non-Lorentzian conductance resonance), and quantum interference effects in a disordered normal-superconductor junction (enhanced weak-localization and reflectionless tunneling through a potential barrier).

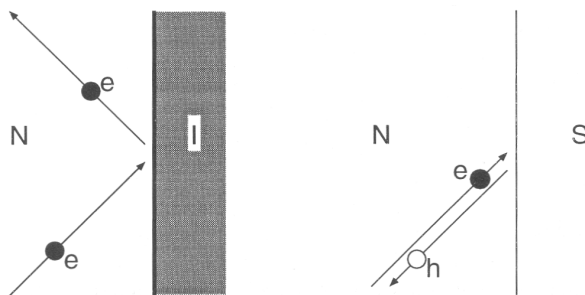


Figure 21.1: Normal reflection by an insulator (I) versus Andreev reflection by a superconductor (S) of an electron excitation in a normal metal (N) near the Fermi level. Normal reflection (left) conserves charge but does not conserve momentum. Andreev reflection (right) conserves momentum but does not conserve charge: The electron (e) is reflected as a hole (h) with the same momentum and opposite velocity. The missing charge of $2e$ is absorbed as a Cooper pair by the superconducting condensate.

21.2 Bogoliubov-de Gennes equation

Electrons are subjected to a scalar potential $U(\mathbf{r})$, then the single-electron Hamiltonian is

$$\hat{\mathcal{H}}_0 = \frac{[\hat{\mathbf{p}} + (e/c)\mathbf{A}]^2}{2m} + V(\mathbf{r}). \quad (21.1)$$

where $\mathbf{A}()$ is the vector-potential.

One can define eigenfunctions, $w_n(\mathbf{r})|\sigma\rangle$, of the operator $\hat{\mathcal{H}}_0$, where $w_n(\mathbf{r})$ describes orbital motion while $|\sigma\rangle$ is the spin state. There are two solutions corresponding to a given excitation energy, ξ_n , measured relatively to the Fermi energy –

$$w_n = w_n(\mathbf{r})|\uparrow\rangle \quad \text{and} \quad w_{\bar{n}} = w_n^*(\mathbf{r})|\downarrow\rangle.$$

If electron-electron interaction is present, then these states are not independent any more. To find the ground state one has to minimize the proper thermodynamic potential which includes the interaction.

The way suggested by Bogoliubov is the following. Let us construct the so-called field operators as

$$\Psi(\mathbf{r}\alpha) = \sum_n w_n a_n, \quad \Psi^+(\mathbf{r}\alpha) = \sum_n w_{\bar{n}} a_n^+. \quad (21.2)$$

Here α is the spin index. The field operators meet the commutation rules.

$$\begin{aligned} \Psi(\mathbf{r}\alpha)\Psi(\mathbf{r}'\beta) + \Psi(\mathbf{r}'\beta)\Psi(\mathbf{r}\alpha) &= 0, \\ \Psi^+(\mathbf{r}\alpha)\Psi^+(\mathbf{r}'\beta) + \Psi^+(\mathbf{r}'\beta)\Psi^+(\mathbf{r}\alpha) &= 0, \\ \Psi^+(\mathbf{r}\alpha)\Psi(\mathbf{r}'\beta) + \Psi(\mathbf{r}'\beta)\Psi^+(\mathbf{r}\alpha) &= \delta_{\alpha\beta} \delta(\mathbf{r} - \mathbf{r}'). \end{aligned} \quad (21.3)$$

The operator for the particle number is then

$$\hat{N} = \sum_{\alpha} \int d\mathbf{r} \Psi^+(\mathbf{r}\alpha)\Psi(\mathbf{r}\alpha), \quad (21.4)$$

while the Hamiltonian can be expressed as

$$\hat{H} = \hat{H}_0 + \hat{H}_{\text{int}}$$

where

$$\begin{aligned} \hat{H} &= \sum_{\alpha} \int d\mathbf{r} \Psi^+(\mathbf{r}\alpha)\mathcal{H}_0\Psi(\mathbf{r}\alpha), \\ \hat{H}_{\text{int}} &= -\frac{g}{2} \sum_{\alpha} \int d\mathbf{r} \Psi^+(\mathbf{r}\beta)\Psi^+(\mathbf{r}\alpha)\Psi(\mathbf{r}\beta)\Psi(\mathbf{r}\alpha). \end{aligned} \quad (21.5)$$

Since we are interested in the thermodynamic potential, we replace

$$\mathcal{H}_0 \rightarrow \mathcal{H}_e = \mathcal{H}_0 + V(\mathbf{r}) - \epsilon_F$$

and the interaction $g\Psi^+\Psi^+\Psi\Psi$ by the interaction with the *mean field* $\Delta(\mathbf{r})$. Here $V(\mathbf{r})$ is some effective potential due to electron-electron interaction.

Then we arrive at the effective Hamiltonian,

$$\begin{aligned}\hat{H}_{\text{eff}} = & \int d\mathbf{r} \left[\sum_{\alpha} \Psi^+(\mathbf{r}\alpha) \mathcal{H}_e(\mathbf{r}) \Psi(\mathbf{r}\alpha) \right. \\ & \left. + \Delta(\mathbf{r}) \Psi^+(\mathbf{r}\uparrow) \Psi^+(\mathbf{r}\downarrow) + \Delta^*(\mathbf{r}) \Psi(\mathbf{r}\downarrow) \Psi(\mathbf{r}\uparrow) \right].\end{aligned}\quad (21.6)$$

Let us suppose now that we know $\Delta(\mathbf{r})$ and find the energy levels for the effective Hamiltonian (21.6). Since it is *quadratic* in Ψ -operators we can use a unitary transform to diagonalize it,

$$\begin{aligned}\Psi(\mathbf{r}\uparrow) = & \sum_n [\gamma_{n\uparrow} u_n(\mathbf{r}) - \gamma_{n\downarrow}^+ v_n^*(\mathbf{r})], \\ \Psi(\mathbf{r}\downarrow) = & \sum_n [\gamma_{n\downarrow} u_n(\mathbf{r}) + \gamma_{n\uparrow}^+ v_n^*(\mathbf{r})].\end{aligned}\quad (21.7)$$

Here γ is the system of new operators obeying the commutation relations

$$\gamma_{n\alpha}^+ \gamma_{m\beta} + \gamma_{m\beta} \gamma_{n\alpha}^+ = \delta_{mn} \delta_{\alpha\beta}, \quad \gamma_{n\alpha} \gamma_{m\beta} + \gamma_{m\beta} \gamma_{n\alpha} = 0. \quad (21.8)$$

The functions $u(\mathbf{r})$ and $v(\mathbf{r})$ are unknown, and we need to derive the equation for it.

Since after the transform (21.7) the effective Hamiltonian must be *diagonal*, i. e. it must take the form

$$\hat{H}_{\text{eff}} = E_g + \sum_{n\alpha} \epsilon_n \gamma_{n\alpha}^+ \gamma_{n\alpha},$$

the following commutation rules must be met,

$$[\hat{H}_{\text{eff}}, \gamma_{n\alpha}] = -\epsilon_n \gamma_{n\alpha}, \quad [\hat{H}_{\text{eff}}, \gamma_{n\alpha}^+] = \epsilon_n \gamma_{n\alpha}^+. \quad (21.9)$$

This equation can be used to determine the functions u and v . Indeed, using Eq. (21.6) and commutation properties of the field operators we get

$$\begin{aligned}[\Psi(\mathbf{r}\uparrow), \hat{H}_{\text{eff}}] &= \mathcal{H}_e \Psi(\mathbf{r}\uparrow) + \Delta(\mathbf{r}) \Psi^+(\mathbf{r}\downarrow), \\ [\Psi(\mathbf{r}\downarrow), \hat{H}_{\text{eff}}] &= -\mathcal{H}_e^* \Psi(\mathbf{r}\downarrow) + \Delta(\mathbf{r}) \Psi^+(\mathbf{r}\uparrow).\end{aligned}\quad (21.10)$$

Then we can use Eq. (21.7) to express Ψ -functions in terms of u, v and γ , and then use commutation relations (21.8) for γ -operators. In this way we arrive at the Bogoliubov-de Gennes equations

$$\begin{aligned}\mathcal{H}_e u(\mathbf{r}) + \Delta(\mathbf{r}) v(\mathbf{r}) &= \epsilon u(\mathbf{r}) \\ \Delta^* u(\mathbf{r}) - \mathcal{H}_e^* v(\mathbf{r}) &= \epsilon v(\mathbf{r}).\end{aligned}\quad (21.11)$$

There is a convenient matrix form of these equations,

$$\begin{pmatrix} \mathcal{H}_e & \Delta \\ \Delta^* & -\mathcal{H}_e^* \end{pmatrix} \begin{pmatrix} u(\mathbf{r}) \\ v(\mathbf{r}) \end{pmatrix} = \epsilon \begin{pmatrix} u(\mathbf{r}) \\ v(\mathbf{r}) \end{pmatrix}. \quad (21.12)$$

Notes

- Hamiltonians \mathcal{H}_e and \mathcal{H}_e^* are different in magnetic field since the quantities $[\mp i\hbar\nabla + (e/c)\mathbf{A}]^2$ are different.
- One can easily show that solutions of BdG equations for different n are orthogonal.
- if $\{u, v\}$ is the solution for some ϵ , then $\{v^*, u^*\}$ is the solution corresponding to $-\epsilon$.

The last point of the derivation is to determine the potentials V and Δ . For that we have to minimize the free energy,

$$F = \langle \hat{H} \rangle - TS,$$

calculated for the basis diagonalizing \hat{H}_{eff} . After rather tedious calculations we obtain the following conditions:

$$\begin{aligned} V(\mathbf{r}) &= -g\langle\Psi^+(\mathbf{r}\downarrow)\Psi(\mathbf{r}\downarrow)\rangle, \\ \Delta(\mathbf{r}) &= g\langle\Psi(\mathbf{r}\uparrow)\Psi(\mathbf{r}\downarrow)\rangle. \end{aligned} \quad (21.13)$$

The 1st equation is the usual Hartree result for point interaction. Substituting Ψ -operators from Eq. (21.7) and using the relationship

$$\langle\gamma_{n\alpha}^+\gamma_{m\beta}\rangle = \delta_{nm}\delta_{\alpha\beta}f_n, \quad \text{where } f_n = [e^{\epsilon_n/kT} + 1]^{-1} \quad (21.14)$$

is the Fermi function, we obtain

$$V(\mathbf{r}) = -g \sum_n [|u_n(\mathbf{r})|^2 f_n + |v_n(\mathbf{r})|^2 (1 - f_n)], \quad (21.15)$$

$$\Delta(\mathbf{r}) = +g \sum_n u_n(\mathbf{r})v_n(\mathbf{r})^*(1 - 2f_n). \quad (21.16)$$

Equations (21.12) together with the *self-consistency equation* (21.16) constitute a powerful scheme to solve spatially-inhomogeneous problems.

21.3 N-S interface

Model

The model considered is illustrated in Fig. 21.2. It consists of a disordered normal region (hatched) adjacent to a superconductor (S). The disordered region may also contain a geometrical constriction or a tunnel barrier. To obtain a well-defined scattering problem we insert ideal (impurity-free) normal leads N_1 and N_2 to the left and right of the disordered region. The NS interface is located at $x = 0$.

We assume that the only scattering in the superconductor consists of Andreev reflection at the NS interface, i.e. we consider the case that the disorder is contained entirely

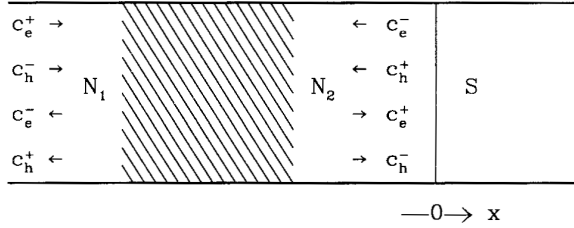


Figure 21.2: Normal-metal–superconductor junction containing a disordered normal region (hatched). Scattering states in the two normal leads N_1 and N_2 are indicated schematically.

within the normal region. The spatial separation of Andreev and normal scattering is the key simplification which allows us to relate the conductance directly to the normal-state scattering matrix. The model is directly applicable to a superconductor in the clean limit (mean free path in S large compared to the superconducting coherence length ξ), or to a point-contact junction (formed by a constriction which is narrow compared to ξ). In both cases the contribution of scattering within the superconductor to the junction resistance can be neglected.

The scattering states at energy ε are eigenfunctions of the Bogoliubov-de Gennes (BdG) equation (21.12). To simplify construction of the scattering basis we assume that the magnetic field \mathbf{B} (in the z -direction) vanishes outside the disordered region. One can then choose a gauge such that $\mathbf{A} \equiv 0$ in lead N_2 and in S , while $A_x, A_z = 0$, $A_y = A_1 \equiv \text{constant}$ in lead N_1 .

The pair potential in the bulk of the superconductor ($x \gg \xi$) has amplitude Δ_0 and phase ϕ . The spatial dependence of $\Delta(\mathbf{r})$ near the NS interface is determined by the self-consistency relation (21.16). The coefficient g is the interaction constant of the BCS theory of superconductivity. At an NS interface, g drops abruptly (over atomic distances) to zero, in the assumed absence of any pairing interaction in the normal region. Therefore, $\Delta(\mathbf{r}) \equiv 0$ for $x < 0$. At the superconducting side of the NS interface, $\Delta(\mathbf{r})$ recovers its bulk value $\Delta_0 e^{i\phi}$ only at some distance from the interface. We will neglect the suppression of $\Delta(\mathbf{r})$ on approaching the NS interface, and use the step-function model

$$\Delta(\mathbf{r}) = \Delta_0 e^{i\phi} \theta(x). \quad (21.17)$$

This model is also referred to in the literature as a “rigid boundary-condition”. The conditions for its validity: If the width W of the NS junction is small compared to ξ , the non-uniformities in $\Delta(\mathbf{r})$ extend only over a distance of order W from the junction (because of “geometrical dilution” of the influence of the narrow junction in the wide superconductor). Since non-uniformities on length scales $\ll \xi$ do not affect the dynamics of the quasiparticles, these can be neglected and the step-function model holds. A point contact or microbridge belongs in general to this class of junctions. Alternatively, the step-function model holds also for a wide junction if the resistivity of the junction region is much bigger than the resistivity of the bulk superconductor. A semiconductor — superconductor

junction is typically in this second category. Note that both the two cases are consistent with our assumption that the disorder is contained entirely within the normal region.¹

Scattering theory for N-S systems: Basic expressions

We now construct a basis for the scattering matrix (\hat{s} -matrix). In the normal lead N_2 the eigenfunctions of the BdG equation (21.12) can be written in the form

$$\begin{aligned}\psi_{n,e}^{\pm}(N_2) &= \begin{pmatrix} 1 \\ 0 \end{pmatrix} (k_n^e)^{-1/2} \Phi_n(y, z) \exp(\pm i k_n^e x), \\ \psi_{n,h}^{\pm}(N_2) &= \begin{pmatrix} 0 \\ 1 \end{pmatrix} (k_n^h)^{-1/2} \Phi_n(y, z) \exp(\pm i k_n^h x),\end{aligned}\quad (21.19)$$

where the wavenumbers k_n^e and k_n^h are given by

$$k_n^{e,h} \equiv (2m/\hbar^2)^{1/2} (E_F - E_n + \sigma^{e,h} \varepsilon)^{1/2}, \quad (21.20)$$

and we have defined $\sigma^e \equiv 1$, $\sigma^h \equiv -1$. The labels e and h indicate the electron or hole character of the wavefunction. The index n labels the modes, $\Phi_n(y, z)$ is the transverse wavefunction of the n -th mode, and E_n its threshold energy:

$$[(p_y^2 + p_z^2)/2m + V(y, z)]\Phi_n(y, z) = E_n\Phi_n(y, z). \quad (21.21)$$

The eigenfunction Φ_n is normalized to unity, $\int dy \int dz |\Phi_n|^2 = 1$. With this normalization each wavefunction in the basis (21.19) carries the same amount of quasiparticle current. The eigenfunctions in lead N_1 are chosen similarly, but with an additional phase factor $\exp[-i\sigma^{e,h}(eA_1/\hbar)y]$ from the vector potential.

A wave incident on the disordered normal region is described in the basis (21.19) by a vector of coefficients

$$c_N^{\text{in}} \equiv (c_e^+(N_1), c_e^-(N_2), c_h^-(N_1), c_h^+(N_2)). \quad (21.22)$$

¹ It is worth emphasizing that the absence of a pairing interaction in the normal region ($g(\mathbf{r}) \equiv 0$ for $x < 0$) implies a vanishing pair potential $\Delta(\mathbf{r})$, according to Eq. (21.16), but does not imply a vanishing order parameter $\Psi(\mathbf{r})$, which is given by

$$\Psi(\mathbf{r}) = \sum_{\varepsilon > 0} v^*(\mathbf{r}) u(\mathbf{r}) [1 - 2f(\varepsilon)]. \quad (21.18)$$

Phase coherence between the electron and hole wave functions u and v leads to $\Psi(\mathbf{r}) \neq 0$ for $x < 0$. The term “proximity effect” can therefore mean two different things: One is the suppression of the pair potential Δ at the superconducting side of the NS interface. This is a small effect which is often neglected in the present work. The other is the induction of a non-zero order parameter Ψ at the normal side of the NS interface. This effect is fully included here, even though Ψ does not appear explicitly in the expressions which follow. The reason is that the order parameter quantifies the degree of phase coherence between electrons and holes, but does not itself affect the dynamics of the quasiparticles. (The BdG equation (21.12) contains Δ not Ψ .)

(The mode-index n has been suppressed for simplicity of notation.) The reflected and transmitted wave has vector of coefficients

$$c_N^{\text{out}} \equiv (c_e^-(N_1), c_e^+(N_2), c_h^+(N_1), c_h^-(N_2)). \quad (21.23)$$

The \hat{s} -matrix s_N of the normal region relates these two vectors,

$$c_N^{\text{out}} = \hat{s}_N c_N^{\text{in}}. \quad (21.24)$$

Because the normal region does not couple electrons and holes, this matrix has the block-diagonal form

$$\hat{s}_N(\varepsilon) = \begin{pmatrix} \hat{s}_0(\varepsilon) & 0 \\ 0 & \hat{s}_0(-\varepsilon)^* \end{pmatrix}, \quad \hat{s}_0 \equiv \begin{pmatrix} r_{11} & t_{12} \\ t_{21} & r_{22} \end{pmatrix}. \quad (21.25)$$

Here \hat{s}_0 is the unitary \hat{s} -matrix associated with the single-electron Hamiltonian \mathcal{H}_0 . The reflection and transmission matrices $r(\varepsilon)$ and $t(\varepsilon)$ are $N \times N$ matrices, $N(\varepsilon)$ being the number of propagating modes at energy ε . (We assume for simplicity that the number of modes in leads N_1 and N_2 is the same.)

The matrix s_0 is unitary ($\hat{s}_0^\dagger \hat{s}_0 = 1$) and satisfies the symmetry relation $\hat{s}_0(\varepsilon, B)_{ij} = \hat{s}_0(\varepsilon, -B)_{ji}$.

Andreev reflection

For energies $0 < \varepsilon < \Delta_0$ there are no propagating modes in the superconductor. We can then define an \hat{s} -matrix for Andreev reflection at the NS interface which relates the vector of coefficients $(c_e^-(N_2), c_h^+(N_2))$ to $(c_e^+(N_2), c_h^-(N_2))$. The elements of this \hat{s} -matrix can be obtained by matching the wavefunctions (21.19) at $x = 0$ to the decaying solutions in S of the BdG equation. If terms of order Δ_0/ϵ_F are neglected (the so-called Andreev approximation, the result is simply

$$\begin{aligned} c_e^-(N_2) &= \alpha e^{i\phi} c_h^-(N_2), \\ c_h^+(N_2) &= \alpha e^{-i\phi} c_e^+(N_2), \end{aligned} \quad (21.26)$$

where $\alpha \equiv \exp[-i \arccos(\varepsilon/\Delta_0)]$. Andreev reflection transforms an electron mode into a hole mode, without change of mode index. The transformation is accompanied by a phase shift, which consists of two parts:

1. A phase shift $-\arccos(\varepsilon/\Delta_0)$ due to the penetration of the wavefunction into the superconductor.
2. A phase shift equal to plus or minus the phase of the pair potential in the superconductor (*plus* for reflection from hole to electron, *minus* for the reverse process).

General relations

We can combine the $2N$ linear relations (21.26) with the $4N$ relations (21.24) to obtain a set of $2N$ linear relations between the incident wave in lead N_1 and the reflected wave in the same lead:

$$\begin{aligned} c_e^-(N_1) &= \hat{s}_{ee} c_e^+(N_1) + \hat{s}_{eh} c_h^-(N_1), \\ c_h^+(N_1) &= \hat{s}_{he} c_e^+(N_1) + \hat{s}_{hh} c_h^-(N_1). \end{aligned} \quad (21.27)$$

The four $N \times N$ matrices \hat{s}_{ee} , \hat{s}_{hh} , \hat{s}_{eh} , and \hat{s}_{he} form together the scattering matrix \hat{s} of the whole system for energies $0 < \varepsilon < \Delta_0$. An electron incident in lead N_1 is reflected either as an electron (with scattering amplitudes \hat{s}_{ee}) or as a hole (with scattering amplitudes \hat{s}_{he}). Similarly, the matrices \hat{s}_{hh} and \hat{s}_{eh} contain the scattering amplitudes for reflection of a hole as a hole or as an electron. After some algebra we find for these matrices the expressions

$$\hat{s}_{ee}(\varepsilon) = r_{11}(\varepsilon) + \alpha^2 t_{12}(\varepsilon) r_{22}^*(-\varepsilon) \hat{M}_e t_{21}(\varepsilon), \quad (21.28)$$

$$\hat{s}_{hh}(\varepsilon) = r_{11}^*(-\varepsilon) + \alpha^2 t_{12}^*(-\varepsilon) r_{22}(\varepsilon) \hat{M}_h t_{21}^*(-\varepsilon), \quad (21.29)$$

$$\hat{s}_{eh}(\varepsilon) = \alpha e^{i\phi} t_{12}(\varepsilon) \hat{M}_h t_{21}^*(-\varepsilon), \quad (21.30)$$

$$\hat{s}_{he}(\varepsilon) = \alpha e^{-i\phi} t_{12}^*(-\varepsilon) \hat{M}_e t_{21}(\varepsilon), \quad (21.31)$$

where we have defined the matrices

$$\begin{aligned} \hat{M}_e &\equiv [1 - \alpha^2 r_{22}(\varepsilon) r_{22}^*(-\varepsilon)]^{-1}, \\ \hat{M}_h &\equiv [1 - \alpha^2 r_{22}^*(-\varepsilon) r_{22}(\varepsilon)]^{-1}. \end{aligned} \quad (21.32)$$

One can verify that the \hat{s} -matrix constructed from these four sub-matrices satisfies unitarity ($\hat{s}^\dagger \hat{s} = 1$) and the symmetry relation $\hat{s}(\varepsilon, B, \phi)_{ij} = \hat{s}(\varepsilon, -B, -\phi)_{ji}$, as required by quasiparticle-current conservation and by time-reversal invariance, respectively.

Conductance of N-S boundary

For the linear-response conductance G_{NS} of the NS junction at zero temperature we only need the \hat{s} -matrix at the Fermi level, i.e. at $\varepsilon = 0$. We restrict ourselves to this case and omit the argument ε in what follows. We apply the general formula

$$G_{\text{NS}} = \frac{2e^2}{h} \text{Tr} (1 - \hat{s}_{ee} s_{ee}^\dagger + \hat{s}_{he} s_{he}^\dagger) = \frac{4e^2}{h} \text{Tr} \hat{s}_{he} \hat{s}_{he}^\dagger. \quad (21.33)$$

The second equality follows from unitarity of \hat{s} , which implies $1 - \hat{s}_{ee} \hat{s}_{ee}^\dagger = \hat{s}_{eh} \hat{s}_{eh}^\dagger = (s_{ee}^\dagger)^{-1} \hat{s}_{he}^\dagger \hat{s}_{he} \hat{s}_{ee}^\dagger$, so that $\text{Tr} (1 - \hat{s}_{ee} \hat{s}_{ee}^\dagger) = \text{Tr} \hat{s}_{he} \hat{s}_{he}^\dagger$. We now substitute Eq. (21.31) for $\varepsilon = 0$ ($\alpha = -i$) into Eq. (21.33), and obtain the expression

$$G_{\text{NS}} = \frac{4e^2}{h} \text{Tr} \hat{t}_{12}^\dagger \hat{t}_{12} (1 + \hat{r}_{22}^* \hat{r}_{22})^{-1} \hat{t}_{21}^* \hat{t}_{21}^\text{T} (1 + \hat{r}_{22}^\dagger \hat{r}_{22}^\text{T})^{-1}, \quad (21.34)$$

where $\hat{M}T \equiv (\hat{M}^*)^\dagger$ denotes the transpose of a matrix. The advantage of Eq. (21.34) over Eq. (21.33) is that the former can be evaluated by using standard techniques developed for quantum transport in the normal state, since the only input is the normal-state scattering matrix. The effects of multiple Andreev reflections are fully incorporated by the two matrix inversions in Eq. (21.34).

In the absence of a magnetic field the general formula (21.34) simplifies considerably. Since the \hat{s} -matrix \hat{s}_0 of the normal region is symmetric for $B = 0$, one has $\hat{r}_{22} = \hat{r}_{22}^T$ and $\hat{t}_{12} = \hat{t}_{21}^T$. Equation (21.34) then takes the form

$$\begin{aligned} G_{\text{NS}} &= \frac{4e^2}{h} \text{Tr} \hat{t}_{12}^\dagger \hat{t}_{12} (1 + \hat{r}_{22}^\dagger \hat{r}_{22})^{-1} \hat{t}_{12}^\dagger \hat{t}_{12} (1 + \hat{r}_{22}^\dagger \hat{r}_{22})^{-1} \\ &= \frac{4e^2}{h} \text{Tr} \left(\hat{t}_{12}^\dagger \hat{t}_{12} (2 - \hat{t}_{12}^\dagger \hat{t}_{12})^{-1} \right)^2. \end{aligned} \quad (21.35)$$

In the second equality we have used the unitarity relation $\hat{r}_{22}^\dagger \hat{r}_{22} + \hat{t}_{12}^\dagger \hat{t}_{12} = 1$. The trace (21.35) depends only on the eigenvalues of the Hermitian matrix $\hat{t}_{12}^\dagger \hat{t}_{12}$. We denote these eigenvalues by T_n ($n = 1, 2, \dots, N$). Since the matrices $\hat{t}_{12}^\dagger \hat{t}_{12}$, $\hat{t}_{12} \hat{t}_{12}^\dagger$, $\hat{t}_{21}^\dagger \hat{t}_{21}$, and $\hat{t}_{21} \hat{t}_{21}^\dagger$ all have the same set of eigenvalues, we can omit the indices and write simply $\hat{t}\hat{t}^\dagger$. We obtain the following relation between the conductance and the transmission eigenvalues:

$$G_{\text{NS}} = \frac{4e^2}{h} \sum_{n=1}^N \frac{T_n^2}{(2 - T_n)^2}. \quad (21.36)$$

This is the central result for NS interface.

A formula of similar generality for the normal-metal conductance G_N is the multi-channel Landauer formula

$$G_N = \frac{2e^2}{h} \text{Tr} \hat{t}\hat{t}^\dagger \equiv \frac{2e^2}{h} \sum_{n=1}^N T_n. \quad (21.37)$$

In contrast to the Landauer formula, Eq. (21.36) for the conductance of an NS junction is a *non-linear* function of the transmission eigenvalues T_n . When dealing with a non-linear multi-channel formula as Eq. (21.36), it is of importance to distinguish between the transmission eigenvalue T_n and the modal transmission probability $\mathcal{T}_n \equiv \sum_{m=1}^N |t_{nm}|^2$. The former is an eigenvalue of the matrix $t\hat{t}^\dagger$, the latter a diagonal element of that matrix. The Landauer formula (21.37) can be written equivalently as a sum over eigenvalues or as sum over modal transmission probabilities:

$$\frac{h}{2e^2} G_N = \sum_{n=1}^N T_n \equiv \sum_{n=1}^N \mathcal{T}_n. \quad (21.38)$$

This equivalence is of importance for (numerical) evaluations of the Landauer formula, in which one calculates the probability that an electron injected in mode n is transmitted, and then obtains the conductance by summing over all modes. The non-linear scattering formula (21.36), in contrast, can not be written in terms of modal transmission probabilities alone: The off-diagonal elements of $\hat{t}\hat{t}^\dagger$ contribute to G_{NS} in an essential way.

Simple examples

Quantum point contact

Consider first the case that the normal metal consists of a ballistic constriction with a normal-state conductance quantized at $G_N = 2N_0e^2/h$ (a *quantum point contact*). The integer N_0 is the number of occupied one-dimensional subbands (per spin direction) in the constriction, or alternatively the number of transverse modes at the Fermi level which can propagate through the constriction. Note that $N_0 \ll N$. An “ideal” quantum point contact is characterized by a special set of transmission eigenvalues, which are equal to either zero or one:

$$T_n = \begin{cases} 1 & \text{if } 1 \leq n \leq N_0, \\ 0 & \text{if } N_0 < n \leq N, \end{cases} \quad (21.39)$$

where the eigenvalues have been ordered from large to small. We emphasize that Eq. (21.39) does not imply that the transport through the constriction is adiabatic. In the case of adiabatic transport, the transmission eigenvalue T_n is equal to the modal transmission probability \mathcal{T}_n . In the absence of adiabaticity there is no direct relation between T_n and \mathcal{T}_n . Substitution of Eq. (21.39) into Eq. (21.36) yields

$$G_{\text{NS}} = \frac{4e^2}{h} N_0. \quad (21.40)$$

The conductance of the NS junction is quantized in units of $4e^2/h$. This is *twice* the conductance quantum in the normal state, due to the current-doubling effect of Andreev reflection.

In the classical limit $N_0 \rightarrow \infty$ we recover the well-known result $G_{\text{NS}} = 2G_N$ for a *classical* ballistic point contact. In the quantum regime, however, the simple factor-of-two enhancement only holds for the conductance plateaus, where Eq. (21.39) applies, and not to the transition region between two subsequent plateaus of quantized conductance. To illustrate this, we compare in Fig. 21.3 the conductances G_{NS} and $2G_N$ for a saddle-point constriction model in a two-dimensional electron gas. Appreciable differences appear in the transition region, where G_{NS} lies below twice G_N . This is actually a rigorous inequality, which follows from Eqs. (21.36) and (21.37) for *arbitrary* transmission matrix:

$$G_{\text{NS}} \leq 2G_N, \quad \text{for all } t. \quad (21.41)$$

Quantum dot

Consider next a small confined region (of dimensions comparable to the Fermi wavelength), which is weakly coupled by tunnel barriers to two electron reservoirs. We assume that transport through this *quantum dot* occurs via resonant tunneling through a single bound state. Let ε_{res} be the energy of the resonant level, relative to the Fermi level in the reservoirs, and let γ_1/\hbar and γ_2/\hbar be the tunnel rates through the two barriers. We denote

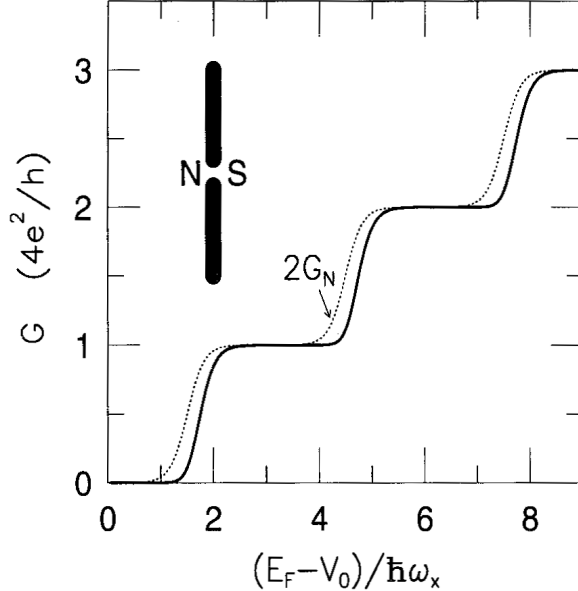


Figure 21.3: Solid curve: Conductance G_{NS} versus Fermi energy of a quantum point contact between a normal and a superconducting reservoir (shown schematically in the inset). The dotted curve is twice the conductance G_N for the case of two normal reservoirs. The constriction is defined by the 2D saddle-point potential $V(x, y) = V_0 - \frac{1}{2}m\omega_x^2x^2 + \frac{1}{2}m\omega_y^2y^2$, with $\omega_y/\omega_x = 3$; G_{NS} is calculated from eq. (21.36), with $T_n = [1 + \exp(-2\pi\varepsilon_n/\hbar\omega_x)]^{-1}$, $\varepsilon_n \equiv E_F - V_0 - (n - \frac{1}{2})\hbar\omega_y$.

$\gamma \equiv \gamma_1 + \gamma_2$. If $\gamma \ll \Delta E$ (with ΔE the level spacing in the quantum dot), the conductance G_N in the case of non-interacting electrons has the form

$$\frac{h}{2e^2}G_N = \frac{\gamma_1\gamma_2}{\varepsilon_{\text{res}}^2 + \frac{1}{4}\gamma^2} \equiv T_{\text{BW}}, \quad (21.42)$$

with T_{BW} the Breit-Wigner transmission probability at the Fermi level. The normal-state transmission matrix $t_{12}(\varepsilon)$ which yields this conductance has matrix elements

$$t_{12}(\varepsilon) = U_1\tau(\varepsilon)U_2, \quad \tau(\varepsilon)_{nm} \equiv \frac{\sqrt{\gamma_{1n}\gamma_{2m}}}{\varepsilon - \varepsilon_{\text{res}} + \frac{1}{2}i\gamma}, \quad (21.43)$$

where $\sum_n \gamma_{1n} \equiv \gamma_1$, $\sum_n \gamma_{2n} \equiv \gamma_2$, and U_1 , U_2 are two unitary matrices (which need not be further specified).

Let us now investigate how the conductance (21.42) is modified if one of the two reservoirs is in the superconducting state. The transmission matrix product $t_{12}t_{12}^\dagger$ (evaluated at the Fermi level $\varepsilon = 0$) following from Eq. (21.43) is

$$t_{12}t_{12}^\dagger = U_1 M U_1^\dagger, \quad M_{nm} \equiv \frac{T_{\text{BW}}}{\gamma_1} \sqrt{\gamma_{1n}\gamma_{1m}}. \quad (21.44)$$

Its eigenvalues are

$$T_n = \begin{cases} T_{\text{BW}} & \text{if } n = 1, \\ 0 & \text{if } 2 \leq n \leq N. \end{cases} \quad (21.45)$$

Substitution into eq. (21.36) yields the conductance

$$G_{\text{NS}} = \frac{4e^2}{h} \left(\frac{T_{\text{BW}}}{2 - T_{\text{BW}}} \right)^2 = \frac{4e^2}{h} \left(\frac{2\gamma_1\gamma_2}{4\varepsilon_{\text{res}}^2 + \gamma_1^2 + \gamma_2^2} \right)^2. \quad (21.46)$$

The conductance on resonance ($\varepsilon_{\text{res}} = 0$) is maximal in the case of equal tunnel rates ($\gamma_1 = \gamma_2$), and is then equal to $4e^2/h$ — independent of γ . The lineshape for this case is shown in Fig. 21.4 (solid curve). It differs substantially from the Lorentzian lineshape (21.42) of the Breit-Wigner formula (dotted curve). The amplitude and lineshape of the

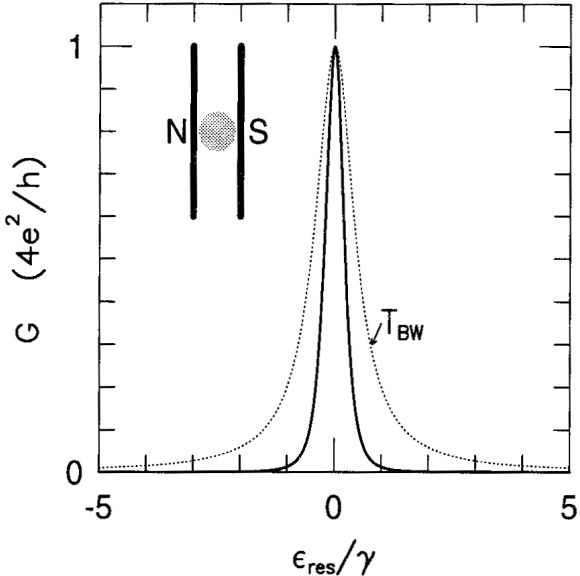


Figure 21.4: Conductance versus energy of the resonant level, from eq. (21.46) for the case of equal tunnel barriers (solid curve). The dotted curve is the Breit-Wigner transmission probability (21.42). The inset shows schematically the normal-metal — quantum-dot — superconductor junction.

conductance resonance (21.46) does not depend on the relative magnitude of the resonance width γ and the superconducting energy gap Δ_0 . This is in contrast to the supercurrent resonance in a superconductor — quantum dot — superconductor Josephson junction, which depends sensitively on the ratio γ/Δ_0 . The difference can be traced to the fact that the conductance (in the zero-temperature, zero-voltage limit) is strictly a Fermi-level property, whereas all states within Δ_0 of the Fermi level contribute to the Josephson effect. Since we have assumed non-interacting quasiparticles, the above results apply to a quantum dot with a small charging energy U for double occupancy of the resonant state.

Disordered junction

We now turn to the regime of diffusive transport through a disordered point contact or microbridge between a normal and a superconducting reservoir. The model considered is that of an NS junction containing a disordered normal region of length L much greater than the mean free path l for elastic impurity scattering, but much smaller than the localization length Nl . We calculate the average conductance of the junction, averaged over an ensemble of impurity configurations. We begin by parameterizing the transmission eigenvalue T_n in terms of a channel-dependent localization length ζ_n :

$$T_n = \frac{1}{\cosh^2(L/\zeta_n)}. \quad (21.47)$$

A fundamental result in quantum transport is that the inverse localization length is *uniformly* distributed between 0 and $1/\zeta_{\min} \simeq 1/l$ for $l \ll L \ll Nl$. One can therefore write

$$\frac{\left\langle \sum_{n=1}^N f(T_n) \right\rangle}{\left\langle \sum_{n=1}^N T_n \right\rangle} = \frac{\int_0^{L/\zeta_{\min}} dx f(\cosh^{-2} x)}{\int_0^{L/\zeta_{\min}} dx \cosh^{-2} x} = \int_0^\infty dx f(\cosh^{-2} x), \quad (21.48)$$

where $\langle \dots \rangle$ indicates the ensemble average and $f(T)$ is an arbitrary function of the transmission eigenvalue such that $f(T) \rightarrow 0$ for $T \rightarrow 0$. In the second equality in eq. (21.48) we have used that $L/\zeta_{\min} \simeq L/l \gg 1$ to replace the upper integration limit by ∞ .

Combining Eqs. (21.36), (21.37), and (21.48), we find

$$\langle G_{\text{NS}} \rangle = 2\langle G_{\text{N}} \rangle \int_0^\infty dx \left(\frac{\cosh^{-2} x}{2 - \cosh^{-2} x} \right)^2 = \langle G_{\text{N}} \rangle. \quad (21.49)$$

We conclude that — although G_{NS} according to Eq. (21.36) is of *second* order in the transmission eigenvalues T_n — the ensemble average $\langle G_{\text{NS}} \rangle$ is of *first* order in l/L . The resolution of this paradox is that the T 's are not distributed uniformly, but are either exponentially small (closed channels) or of order unity (open channels). Hence the average of T_n^2 is of the same order as the average of T_n . Off-diagonal elements of the transmission matrix tt^\dagger are crucial to arrive at the result (21.49). Indeed, if one would evaluate Eq. (21.36) with the transmission eigenvalues T_n replaced by the modal transmission probabilities \mathcal{T}_n , one would find a totally wrong result: Since $\mathcal{T}_n \simeq l/L \ll 1$, one would find $G_{\text{NS}} \simeq (l/L)G_{\text{N}}$ — which underestimates the conductance of the NS junction by the factor L/l .

The present derivation, in contrast, is fully quantum mechanical. It applies to the “mesoscopic” regime $L < l_\phi$, in which transport is phase coherent. If the condition $L \ll Nl$ is relaxed, differences between $\langle G_{\text{NS}} \rangle$ and $\langle G_{\text{N}} \rangle$ appear.

21.4 Andreev levels and Josephson effect

Consider a SNS weak link schematically depicted in Fig. 21.5. We assume that the only

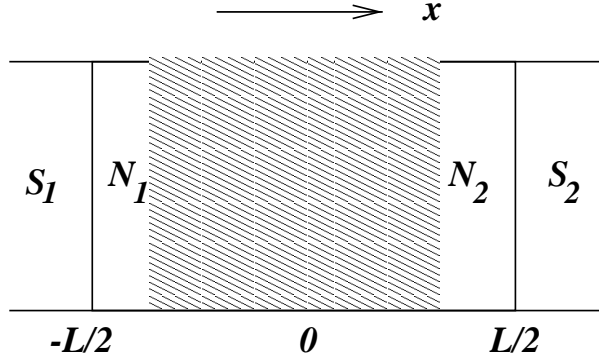


Figure 21.5: S-N-S Josephson junction containing a disordered normal region (hatched)

scattering on the NS interfaces $x = \pm L/2$ is the Andreev one. The key simplification is to separate in space normal and Andreev scattering, its applicability range being $\xi_0 \ll l_S$ where l_S is the mean free path in the superconductor. The junction width is assumed to be much smaller than the Josephson penetration depth, so the vector-potential can be disregarded, as well as reduction of the order parameter Δ . Thus we approximate

$$\Delta = \begin{cases} \Delta_0 \exp(\pm i\phi/2) & \text{for } |x| > L/2, \\ 0 & \text{for } |x| < L/2. \end{cases} \quad (21.50)$$

This model is rather universal, it works also for S-S-S junctions with a constriction provided its size is $\lesssim \xi$.

Andreev levels

Since Josephson effect is the *equilibrium* property let us start with the excitation spectrum. For that we have to solve the BdG equation (21.12) with proper boundary conditions. In the normal lead N_1 the eigenfunctions are

$$\begin{aligned} \psi_{n,e}^\pm(N_1) &= \begin{pmatrix} 1 \\ 0 \end{pmatrix} (k_n^e)^{-1/2} \Phi_n \exp[\pm ik_n^e(x + L/2)], \\ \psi_{n,h}^\pm(N_1) &= \begin{pmatrix} 0 \\ 1 \end{pmatrix} (k_n^h)^{-1/2} \Phi_n \exp[\pm ik_n^h(x + L/2)]. \end{aligned} \quad (21.51)$$

Here $k_n^{e,h} = (2m/\hbar^2)^{1/2}(E_F - E_n + \sigma^{e,h}\epsilon)^{1/2}$ and $\sigma^e = 1$, $\sigma^h = -1$. The index n labels the transverse modes, $\Phi_n(y, x)$ is the transverse wave function for the n th mode, and E_n its threshold energy. The wave functions for the lead N_2 are chosen in a similar way with the substitution $L \rightarrow -L$.

In the superconducting lead S_1 , where $\Delta = \Delta_0 \exp(i\phi/2)$, the eigenfunctions are

$$\psi_{n,e}^\pm(S_1) = \begin{pmatrix} e^{i\eta^e/2} \\ e^{-i\eta^e/2} \end{pmatrix} (2q_n^e)^{-1/2} (\epsilon^2/\Delta^2 - 1)^{-1/4} \Phi_n \exp[\pm iq_n^e(x + L/2)], \quad (21.52)$$

while for $\psi_{n,h}^\pm(S_1)$ the label e replaced by h . Here

$$q_n^{e,h} = (2m/\hbar^2)^{1/2}[E_F - E_n + \sigma^{e,h}(\epsilon^2 - \Delta_0^2)^{1/2}]^{1/2}, \quad \eta^e = \phi/2 + \sigma^{e,h} \arccos(\epsilon/\Delta_0).$$

The complex functions are defined such that $\operatorname{Re} q^{e,h} \geq 0$, $\operatorname{Im} q^2 \geq 0$, $\operatorname{Im} q^h \leq 0$. The function $\arccos t \in (0, \pi/2)$ for $0 < t < 1$, while $\arccos t \equiv -i \ln [t + (t^2 - 1)^{1/2}]$ for $t > 1$. The eigenfunctions for S_2 are obtained by substitution $\phi \rightarrow -\phi$, $L \rightarrow -L$. The functions (21.51) and (21.52) are normalized to carry the same amount of quasiparticle current since we are going to use them as a basis for the scattering problem.

Now we have to introduce the proper scattering matrices. The wave incident on the disordered normal region is described in the basis (21.51) by the vector of the coefficients

$$\mathbf{c}_N^{\text{in}} \equiv \left(c_e^+(N_1), c_e^-(N_2), c_h^-(N_1), c_h^+(N_2) \right).$$

(The mode index is omitted for brevity). The reflected and transmitted waves have vector of coefficients

$$\mathbf{c}_N^{\text{out}} \equiv \left(c_e^-(N_1), c_e^+(N_2), c_h^+(N_1), c_h^-(N_2) \right).$$

The matrix \hat{s}_N relates the above two vectors as

$$\mathbf{c}_N^{\text{out}} = \hat{s}_N \mathbf{c}_N^{\text{in}}.$$

An important simplification is that the disordered region does not couple electrons and holes. As result the matrix \hat{s}_N has a block-diagonal form,

$$\hat{s}_N(\epsilon) = \begin{pmatrix} \hat{s}_0(\epsilon) & 0 \\ 0 & \hat{s}_0^*(-\epsilon) \end{pmatrix}, \quad \hat{s}_0(\epsilon) = \begin{pmatrix} r_{11} & t_{12} \\ t_{21} & r_{22} \end{pmatrix}. \quad (21.53)$$

\hat{s}_0 is the unitary and symmetric s -matrix associated with the Hamiltonian \mathcal{H}_0 . The elements r_{ik} and t_{ik} are $N \times N$ matrices in the mode space, where N is the number of propagating modes for given ϵ .

In a superconductor, there is no propagating modes for $\epsilon < \Delta$. We can then define s -matrix for the *Andreev reflection*, \hat{s}_A , at the NS interfaces as

$$\mathbf{c}_N^{\text{out}} = \hat{s}_A \mathbf{c}_N^{\text{in}}.$$

The elements of \hat{s}_A can be obtained by matching the functions (21.51) at $|x| = \pm L/2$ to the *decaying* wave functions (21.52). The result is

$$\hat{s}_A(\epsilon) = a \begin{pmatrix} 0 & r_A \\ r_A^* & 0 \end{pmatrix}, \quad \hat{r}_A(\epsilon) = \begin{pmatrix} e^{\phi/2} & 0 \\ e^{-\phi/2} & 0 \end{pmatrix}. \quad (21.54)$$

Here $a = \arccos(\epsilon/\Delta_0)$.

For $\epsilon > \Delta_0$ we have to define the s -matrix of the whole junction as

$$\mathbf{c}_S^{\text{out}} = \hat{s}_{SNS} \mathbf{c}_S^{\text{in}}.$$

The vectors $\mathbf{c}_S^{\text{in,out}}$ are the coefficients of the expansion of the incoming and outgoing waves in leads S_1 and S_2 in terms of the wave functions (21.52). By matching the wave functions (21.51) and (21.52) at $|x| = L/2$ one can obtain

$$\hat{s}_{SNS} = \hat{U}^{-1}(1 - \hat{M})^{-1}(1 - \hat{M}^\dagger)\hat{s}_N\hat{U} \quad (21.55)$$

where

$$\hat{U} = a \begin{pmatrix} r_A & 0 \\ 0 & r_A^* \end{pmatrix}, \quad \hat{M} = a\hat{s}_N \begin{pmatrix} 0 & r_A \\ r_A^* & 0 \end{pmatrix}.$$

Now we are ready to find the excitation spectrum. For $\epsilon < \Delta_0$ there is no outgoing waves, and $\hat{s}_N\hat{s}_A = 1$. Consequently, $\det(\hat{s}_N\hat{s}_A - 1) = 0$. Using the identity

$$\det \begin{pmatrix} \hat{a} & \hat{b} \\ \hat{c} & \hat{d} \end{pmatrix} = \det(\hat{a}\hat{d} - \hat{a}\hat{c}\hat{a}^{-1}\hat{b})$$

we get the dispersion relation for the *Andreev levels* ϵ_p ,

$$\det \left(1 - a^2(\epsilon_p)r_A^*\hat{s}_0((\epsilon_p)r_A\hat{s}_0^*(-\epsilon_p)) \right) = 0. \quad (21.56)$$

Short junction. The above equation allows further simplification for a *short* junction with $L \ll \xi$. This inequality is equivalent to $\Delta_0 \ll E_c \equiv \hbar/\tau$ where τ is the *traversal time* through the junction. Since the elements of \hat{s}_0 change significantly at the energies of the order of E_c one can put $\hat{s}_0(\epsilon) \approx \hat{s}_0(-\epsilon) \approx \hat{s}_0(0)$. Then instead of Eq. (21.56) we get

$$\det \left[(1 - \epsilon_p^2/\Delta_0^2)\hat{\mathbf{1}} - \hat{t}_{12}\hat{t}_{21}^* \sin^2(\phi/2) \right] = 0. \quad (21.57)$$

Denoting T_p the eigenvalues of the $N \times N$ matrix $\hat{t}_{12}\hat{t}_{21}^*$ we have

$$\epsilon_p = \Delta_0 \left[1 - T_p \sin^2(\phi/2) \right]. \quad (21.58)$$

Josephson current

The Josephson current can be derived from the known expression for the BCS free energy F for the superconductor as

$$I(\phi) = (2e/\hbar)(dF/d\phi).$$

After rather tedious calculations one can obtain the following result:

$$I = I_1 + I_2 + I_3, \quad (21.59)$$

$$I_1 = -\frac{2e}{\hbar} \sum_p \tanh(\epsilon_p/2kT) \frac{d\epsilon_p}{d\phi},$$

$$I_2 = -\frac{2e}{\hbar}(2kT) \int_{\Delta_0}^{\infty} d\epsilon \ln[2 \cosh(\epsilon/2kT)] \frac{d\rho}{d\phi}, \quad (21.60)$$

$$I_3 = \frac{2e}{\hbar} \frac{d}{d\phi} \int d\mathbf{r} |\Delta|^2/g. \quad (21.61)$$

The 1st term is the contribution of the discrete states (Andreev levels), the 2nd one is due to the continuous spectrum with density of states $\rho(\epsilon)$, the 3d one vanishes for ϕ -independent Δ . For s shot junction the contribution of the continuous spectrum *vanishes*. Substituting Eq. (21.58) into Eq. (21.60) we get

$$I = \frac{e\Delta_0^2}{2\hbar} \sin \phi \sum_{p=1}^N \frac{T_p}{\epsilon_p(\phi)} \tanh \left(\frac{\epsilon_p(\phi)}{2kT} \right). \quad (21.62)$$

We see that, contrary to the Landauer conductance, the Josephson current is a *nonlinear* function of the transmittance T_p .

For a ballistic point contact, $L \gg l$,

$$T_p = \begin{cases} 1 & \text{for } p \leq N_0 \\ 0 & \text{for } p \geq N_0 \end{cases},$$

and

$$I = I_c \sin \phi, \quad I_c = N_0 e \Delta_0 / \hbar \quad (\text{quantized}). \quad (21.63)$$

In the opposite limiting case, $L \ll l$, the transmittance is small, and

$$I_c = \frac{e\Delta_0}{\hbar} \text{Tr } \hat{t}\hat{t}^\dagger \tanh \frac{\Delta_0}{2kT} = \frac{\pi\Delta_0}{2e} G \quad (21.64)$$

where conductance G is calculated according to the Landauer formula. The above result coincides with the Ambegaokar-Baratoff formula for a tunnel junction.

21.5 Superconducting nanoparticles

Coulomb blockade of Andreev reflection

Consider at an ideal superconducting electrode between normal bulk electrodes forming two tunnel junctions in series, Fig. 21.6. The superconducting part modifies strongly

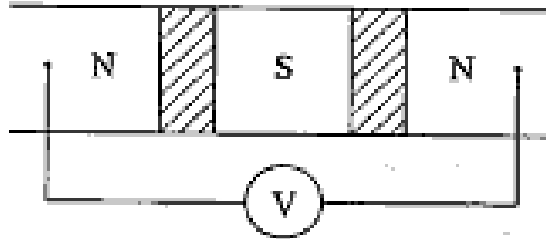


Figure 21.6: An ideal superconducting electrode between normal bulk electrodes forming two tunnel junctions in series.

tunneling through the system which becomes sensitive to the *parity* of the electron number

N in the superconductor. When N is even, inelastic tunneling cannot take place (at zero temperature) at voltages below $2\Delta/e$, and only elastic tunneling is allowed. For odd N a quasiparticle exists unavoidably in the superconductor, which opens an inelastic channel.

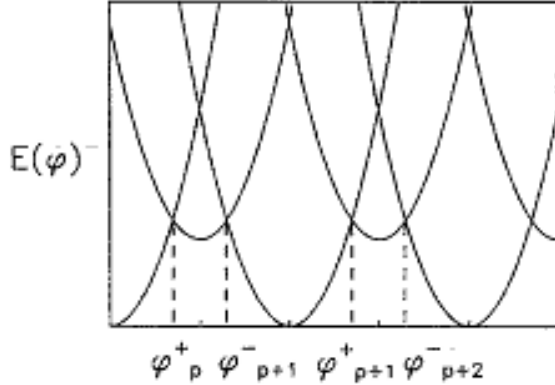
The total number N of the free electrons in the superconductor depends on the electrostatic energy,

$$U = \frac{Q^2}{2C} - \frac{eV}{C}(C_1 n_2 + C_2 n_1), \quad Q = en - \varphi C, \quad n = n_1 - n_2, \quad C = C_1 + C_2. \quad (21.65)$$

Here n_i is the number of particles that have tunneled through i th junction, C_i are junction capacitances, and φ is the potential difference between the middle of the grain and the leads at vanishing bias voltage V . The total energy can be written as

$$E(N) = \frac{[e(N - N_0) - C\varphi]^2}{2C} + E_0(N), \quad E_0(N) = \begin{cases} \Delta & \text{for odd } N \\ 0 & \text{for even } N. \end{cases} \quad (21.66)$$

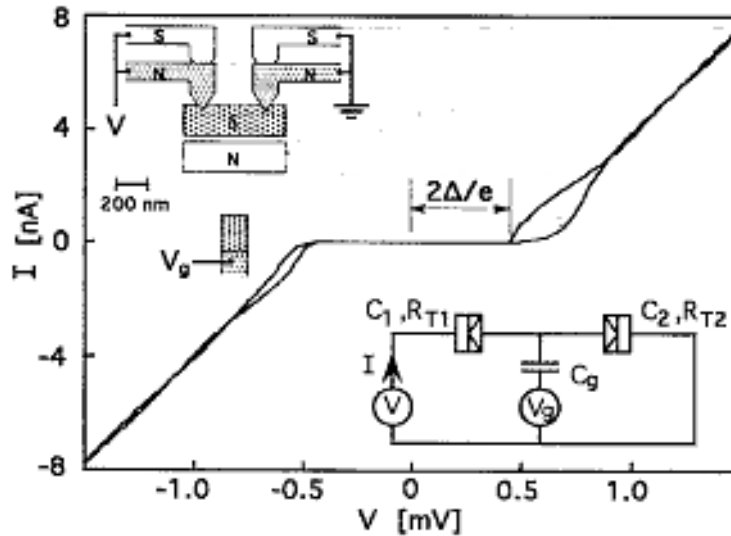
Here N_0 is the electron number at $\phi = 0$, while E_0 allows for the quasiparticle energy. The graph of $E(N)$ is schematically shown in Fig. 21.7. The curves correspond to different n ,



Ground-state energy (2) of the superconducting island as a function of externally induced potential difference φ between the island and bulk external electrodes. The upper and lower sets of parabolas correspond, respectively, to odd and even numbers of electrons in the island. The lowest parabola at a given φ determines the ground-state energy. The intersections of parabolas give the φ values at which the number of electrons in the island is changed.

Figure 21.7: From Averin & Nazarov, Phys. Rev. Lett. **69**, 1993 (1992).

and the lowest curve at a given φ corresponds to the equilibrium number n of the excess electrons. One can see that the parity of the electrons is changed at the intersections. Since the potential difference φ can be changed by the gate the system under consideration behaves as a *parity-sensitive* single-electron transistor.



Current-voltage characteristic of NSN Coulomb blockade electrometer. Two traces are for gate voltage V_g adjusted for minimum and maximum gap at positive voltage. Arrow indicates the value of $2\Delta/e = 470 \mu\text{V}$, where the nominal value of Δ is obtained from our aluminum SSS electrometers. Lower inset shows electrical schematic for the electrometer, where the boxed symbols represent ultrasmall tunnel junctions. Upper inset depicts the device layout. Normal and superconducting metals are indicated by N and S, respectively. The shaded regions indicate metals used for the NSN electrometer. The gate is actually $3 \mu\text{m}$ from the island.

Figure 21.8: From Eiles *et al.*, Phys. Rev. Lett. **70**, 1862 (1993).

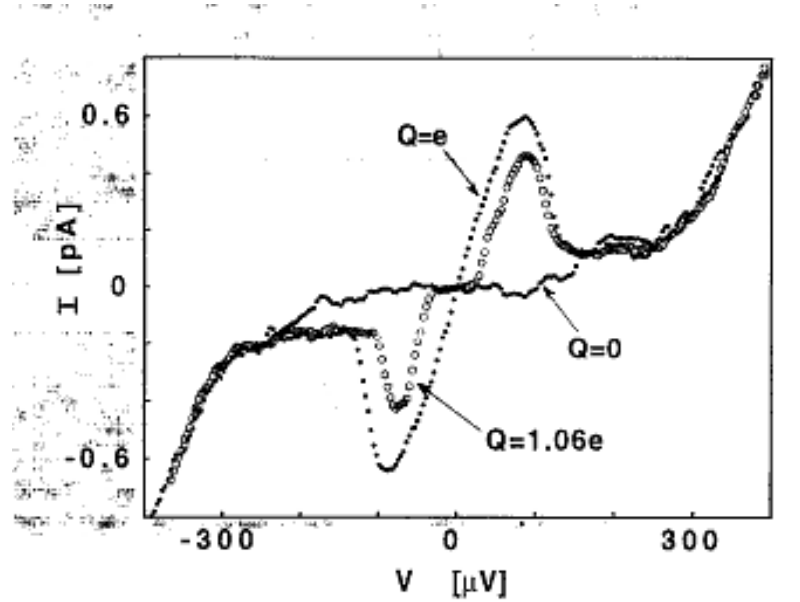
The experimental $I - V$ -curve for such a device is shown in Fig. 21.8 Specifying the Coulomb energy for the system under consideration as

$$E(N) = \frac{(Ne)^2}{2C} + \frac{Ne}{C}(C_l V_l + C_r V_r + C_g V_g), \quad C = C_l + C_r + C_g, \quad (21.67)$$

we observe that $E(N) = E(N+2)$ at $V_g^{(N)} = -(N+1)e/C_g$.

Parity-sensitive transport

To compute the current near the resonances one needs to estimate the tunneling rates Γ_l and Γ_r for the tunneling *from the left lead* and *from the right lead* to the grain, respectively.



Fine scale current-voltage characteristics for $Q = C_g V_g \text{mod} 2e = 0, e$, and $1.06e$. A small Coulomb gap is seen for the $Q = 1.06e$ data.

Figure 21.9: From Eiles *et al.*, Phys. Rev. Lett. **70**, 1862 (1993).

They depend on the energy differences $\epsilon_i = E(N+2) - E(N) - 2eV_i$ as

$$\Gamma_i = \frac{2\pi}{\hbar} \gamma_i \frac{\epsilon_i}{\exp(\epsilon_i/kT) - 1}. \quad (21.68)$$

This is a golden-rule expression which differs from the normal-state expression by two features: (i) the excitation energy corresponds to transfer of two electrons, (ii) the dimensionless parameters γ_i should be calculated in the *second* order in tunneling transparency since we are interested in the transfer of a pair of electrons,

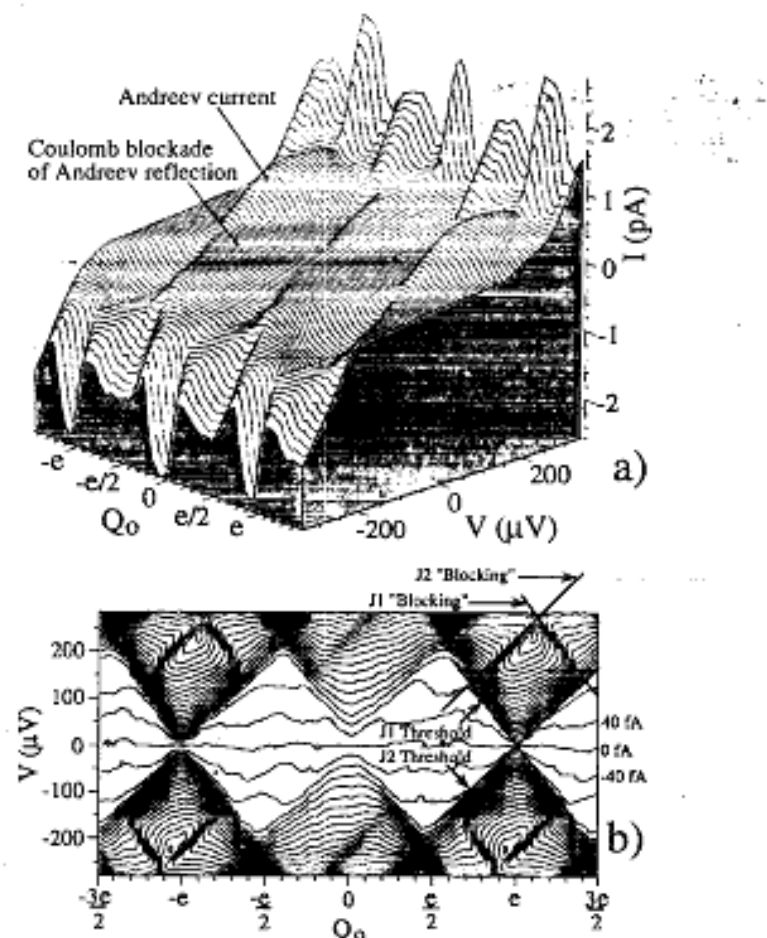
$$\gamma_i = \frac{1}{N_i} \left(\frac{G_i \hbar}{2\pi e^2} \right)^2 \frac{4\Delta^2}{\Delta^2 - E_c^2} \left[\arctan \sqrt{\frac{\Delta + E_c}{\Delta - E_c}} \right]^2, \quad E_c = e^2/2C. \quad (21.69)$$

Here N_i is the geometric factor of the order of the number of transverse modes in the tunneling junction, while G_i is its normal-state conductance. The result for Ohmic conductance is

$$G = \frac{4\pi e^2}{\hbar} \frac{\gamma_l \gamma_r}{\gamma_l + \gamma_r} \frac{\mathcal{V}}{\sinh \mathcal{V}}, \quad \mathcal{V} \equiv 2eC_g(V_g - V_g^{(N)})/CkT. \quad (21.70)$$

The G vs. V_g dependence is a set of sharp peaks at $V_g = V_g^{(N)}$. The non-Ohmic $I-V$ -curves for different gate voltages are shown in Fig. 21.9.

In general, the “phase diagram” in the coordinates $V - V_g$ showing an interplay between single-electron and pair tunneling is observed. In general, the “phase diagram” in the



(a) Complete experimental $I(V, Q_0)$ surface for $T = 15$ mK and zero magnetic field showing the $2e$ -periodic Andreev current and the Coulomb blockade of Andreev reflection.
 (b) A contour plot representation of the same data showing the thresholds for Andreev reflection at each junction and the "blocking" thresholds. The contour interval is 40 fA.

Figure 21.10: From Hergenrother *et al.*, Phys. Rev. Lett. **72**, 1742 (1994).

coordinates $V - V_g$ showing an interplay between single-electron and pair tunneling is observed.

There are other effects regarding parity-effect tunneling which are beyond the scope of this course. Among them are quantum co-tunneling through virtual states which competes with the blockaded transport, non-perturbative effects for high-transparency contacts, influence of magnetic field, etc.

Part V

Appendices

Chapter 22

Solutions of the Problems

Chapter 1

Problem 1.1. Show that $(\mathbf{a}_1[\mathbf{a}_2\mathbf{a}_3]) = (\mathbf{a}_3[\mathbf{a}_1\mathbf{a}_2]) = (\mathbf{a}_2[\mathbf{a}_3\mathbf{a}_1])$.

Solution. Direct calculation.

Problem 1.2. Show that only $n = 1, 2, 3, 6$ are available.

Solution.

i	$\cos \phi$	ϕ
-2	-1	π
-1	-1/2	$2\pi/3$
0	0	$\pi/2$
1	1/2	$\pi/2$
2	1	0

Problem 1.3. We have mentioned that primitive vectors are not unique. New vectors can be defined as

$$\mathbf{a}'_i = \sum_k \beta_{ik} \mathbf{a}_k,$$

the sufficient condition for the matrix $\hat{\beta}$ is

$$\det(\beta_{ik}) = \pm 1. \quad (22.1)$$

Show that this equality is sufficient.

Solution. The inverse transform is

$$\mathbf{a}_k = \sum_k \beta_{ki}^{-1} \mathbf{a}'_i,$$

where

$$\beta_{ki}^{-1} = \frac{A(\beta_{ik})}{\det(\beta_{ik})}$$

where $A(\beta_{ik})$ is the algebraic augment. Then, for any lattice vector we have

$$\mathbf{a} = \sum_k n_k \mathbf{a}_k = \sum_{k,i} n_k \frac{A(\beta_{ik})}{\det(\beta_{ik})} \mathbf{a}'_i.$$

All the coefficients are to be integer, so we return to the condition (22.1).

Problem 1.4. Derive the expressions (1.10) for reciprocal lattice vectors.

Solution. Let us expand the unknown vector \mathbf{b} in terms of 3 non-coplanar vectors $[\mathbf{a}_i \mathbf{a}_k]$

$$\mathbf{b} = \alpha [\mathbf{a}_1 \mathbf{a}_2] + \beta [\mathbf{a}_2 \mathbf{a}_3] + \gamma [\mathbf{a}_3 \mathbf{a}_1]. \quad (22.2)$$

Then we can substitute Eq. (22.2) into (1.9) we get

$$\{\alpha, \beta, \gamma\} = \frac{2\pi g_i}{V_0}.$$

Problem 1.5. Find the reciprocal lattice vectors for fcc lattice.

Solution We write lattice vectors for fcc as

$$\begin{aligned} \mathbf{a}_1 &= \frac{a}{2}(\mathbf{y} + \mathbf{z}), \\ \mathbf{a}_2 &= \frac{a}{2}(\mathbf{z} + \mathbf{x}), \\ \mathbf{a}_3 &= \frac{a}{2}(\mathbf{x} + \mathbf{y}) \end{aligned}$$

(see Fig.1.6). The volume of the cell is $V_0 = a^3/4$. Making use of the definition (1.10) we get

$$\begin{aligned} \mathbf{b}_1 &= \frac{2\pi}{a}(-\mathbf{x} + \mathbf{y} + \mathbf{z}), \\ \mathbf{b}_2 &= \frac{2\pi}{a}(-\mathbf{y} + \mathbf{z} + \mathbf{x}), \\ \mathbf{b}_3 &= \frac{2\pi}{a}(-\mathbf{z} + \mathbf{x} + \mathbf{y}). \end{aligned}$$

Problem 1.6. Find the width of the scattering peak at the half intensity due to finite size of the chain with N sites.

Solution Introducing the dimensionless quantity $x = Na\Delta k'/2$ where $\Delta k'$ is the peak's width *at the half intensity* we get the following equation

$$\sin^2 x = x^2/2.$$

The solution is $x \approx 1.38$.

Problem 2.1. Derive the dispersion relation (2.9).

Solution. Substituting (2.8) into Eq. (2.7) we get

$$-m\omega^2 = -C(2 - e^{-iqa} - e^{iqa}).$$

Then one can use the relations (B.1) and (B.2) of the Appendix B.

Problem 2.2. Derive the expression (2.13).

Solution From the Eqs. (2.9), (2.12) we get $d\omega = a\sqrt{\frac{C}{m}}|\cos \frac{qa}{2}|dq$ and $dq = \frac{2\pi}{aL}dg$. The number dz of the vibration modes within the interval $(-\pi/a, \pi/a)$ is equal to $2z$ because one has to sum over $\pm q$. Collecting these expressions and using the formula

$$\cos \frac{aq}{2} = \sqrt{1 - \sin^2 \frac{aq}{2}} = \sqrt{1 - \frac{\omega^2}{4C/m}}$$

we get the formula (2.13).

Problem 2.3. Derive Eq. (2.25).

Solution Substitute expressions (2.23) to Eq. (2.24) and do algebra.

Problem 2.4. Prove the relation of the Section 4.

Solution To prove the relations it is enough to apply the equilibrium condition $\left(\frac{\partial\Phi}{\partial u_{n\alpha k}}\right)_0 = 0$ for *constant* displacement u_0 of all the atoms.

Problem 2.5. Prove the relation (2.35).

Solution Use the definition (2.34) of the dynamic matrix and its property (2.29).

Problem 2.6. Prove the equation (2.74).

Solution. We express the displacements according to the definition (2.72) and get

$$\begin{aligned}\mathcal{T} &= \frac{1}{2N} \sum_{nka} \left[\sum_{qj} e_{jka}(\mathbf{q}) \dot{a}_j(\mathbf{q}, t) e^{i\mathbf{q}\mathbf{a}_n} \right]^2 = \\ &= \frac{1}{2N} \sum_{nka} \sum_{\mathbf{q}\mathbf{q}'j'} \left[e_{jka}(\mathbf{q}) \dot{a}_j(\mathbf{q}, t) e^{i\mathbf{q}\mathbf{a}_n} e_{j'k\alpha}^*(\mathbf{q}) \dot{a}_{j'}^*(\mathbf{q}', t) e^{-i\mathbf{q}'\mathbf{a}_n} \right].\end{aligned}$$

Then we use the condition

$$\sum_n e^{i(q-q')a_n} = N\delta_{qq'}.$$

Problem 2.7. Prove the expression (2.75) for the potential energy.

Solution. We have

$$\begin{aligned}\Phi &= \frac{1}{2} \sum_{all} \Phi_{\alpha\beta} \binom{kk'}{\mathbf{n}\mathbf{n}'} u_{n\alpha}^k u_{n'\beta}^{k'} = \\ &= \frac{1}{2N} \sum_{all} \Phi_{\alpha\beta} \binom{kk'}{\mathbf{n}\mathbf{n}'} \frac{1}{\sqrt{m_k m_{k'}}} \times \\ &\quad \times \sum_{\mathbf{q}\mathbf{j}\mathbf{q}'j'} e_{jka}(\mathbf{q}) \dot{a}_j(\mathbf{q}, t) e^{i\mathbf{q}\mathbf{a}_n} e_{j'k\alpha}^*(\mathbf{q}) \dot{a}_{j'}^*(\mathbf{q}', t) e^{-i\mathbf{q}'\mathbf{a}_{n'}}.\end{aligned}$$

Then, let us transform

$$\begin{aligned} & \sum_{nn'} \frac{1}{\sqrt{m_k m_{k'}}} \Phi_{\alpha\beta} \left(\begin{array}{c} kk' \\ nn' \end{array} \right) e^{i(\mathbf{q}'\mathbf{a}_{n'} - \mathbf{q}\mathbf{a}_n)} = \\ &= \sum_n e^{i(\mathbf{q}' - \mathbf{q})\mathbf{a}_n} \sum_{n'} \frac{1}{\sqrt{m_k m_{k'}}} \Phi_{\alpha\beta} \left(\begin{array}{c} kk' \\ nn' \end{array} \right) e^{i\mathbf{q}'(\mathbf{a}_{n'} - \mathbf{a}_n)} = \\ &= N \delta_{\mathbf{q}\mathbf{q}'} D_{\alpha\beta}^{kk'}(\mathbf{q}). \end{aligned}$$

Now we can sum over q' and use the equation of motion (2.20) and normalization condition for eigenvectors e_j .

Problem 2.8. Prove the expression (2.79).

Solution. According to the definition and equation of motion

$$\begin{aligned} \dot{a}_j(\mathbf{q}) &= \frac{1}{2} [\dot{Q}_j(\mathbf{q}) + \dot{Q}_j(-\mathbf{q})] + \\ &+ \frac{i\omega_j(\mathbf{q})}{2} [Q_j(-\mathbf{q}) - Q_j(\mathbf{q})]. \end{aligned}$$

Combining this expression with the expression for a_j and inserting into the expression for the energy (2.76) we get the expression (2.79).

Problem 2.9. Prove the expression (2.90).

Solution. One can use the definition (2.89) and the recursion formula

$$H'_N(\xi) = 2NH_{N-1}(\xi).$$

Chapter 3

Problem 3.1. Derive Eq. (3.15).

Solution. Substituting (3.14) into (3.15) we get

$$\psi_p(x) = \frac{1}{N} \sum_{n,p'} e^{i(p-p')na/\hbar} \psi_{p'}(x) = \psi_p(x).$$

Problem 3.2 Prove the orthogonality of the Wannier functions.

Solution.

$$\begin{aligned} \int w_n^*(x) w_m(x) dx &= \frac{1}{N} \sum_{pp'} e^{i(pn-p'm)a/\hbar} \int \psi_p^*(x) \psi_{p'}(x) dx = \\ &= \frac{1}{N} \sum_p e^{ip(n-m)a/\hbar} = \frac{a}{2\pi\hbar} \int_{-\pi\hbar/a}^{\pi\hbar/a} e^{ip(n-m)a/\hbar} dp = \\ &= \begin{cases} \sin[\pi(n-m)]/[\pi(n-m)] = 0, & n \neq m \\ 1, & n = m \end{cases} = \delta_{n,m}. \end{aligned}$$

Problem 3.3 Derive expression (3.16).

Solution. Expand both numerator and denominator in powers of h and I .

Problem 3.4 Derive expression (3.24).

Solution. The number of nearest neighbors is 6. We have

$$\sum_0^{1-6} e^{ika_0} = \sum_i (e^{ik_i a} + e^{-ik_i a}) .$$

Problem 3.5 Prove the identity (3.39).

Solution. We expand the exponential in the series

$$\exp(a\nabla) = 1 + a\nabla + \frac{1}{2}(a\nabla)^2 + \dots$$

and we see that it is just the same as the expansion of the shifted function.

Problem 3.6. Prove the formula (3.41).

Solution. We start from the SE for the Bloch function

$$\nabla^2\psi + \frac{\hbar^2}{2m} [\varepsilon(k) - V(r)] \psi = 0 .$$

Then we take the partial derivative of the equation with respect to, say, k_x with the account of relations

$$\frac{\partial}{\partial k_x} [\varepsilon(k) - V] \psi = \frac{\partial \varepsilon}{\partial k_x} \psi + (\varepsilon - V) \frac{\partial \psi}{\partial k_x} , \quad (22.3)$$

$$\frac{\partial \psi}{\partial k_x} = \frac{\partial}{\partial k_x} (ue^{kr}) = ix\psi + e^{kr} \frac{\partial u}{\partial k_x} , \quad (22.4)$$

and

$$\nabla^2 \frac{\partial \psi}{\partial k_x} = 2i \frac{\partial \psi}{\partial x} + ix \nabla^2 \psi + \nabla^2 \left(e^{ikr} \frac{\partial u}{\partial x} \right) . \quad (22.5)$$

As a result, we get

$$\begin{aligned} 2i \frac{\partial \psi}{\partial x} &+ \frac{2m}{\hbar^2} \frac{\partial \varepsilon}{\partial k_x} \psi + ix \left\{ \nabla^2 \psi + \frac{2m}{\hbar^2} (\varepsilon - V) \psi \right\} + \\ &+ \left[\nabla^2 + \frac{2m}{\hbar^2} (\varepsilon - V) \right] e^{ikr} \frac{\partial u}{\partial k_x} = 0 \end{aligned} \quad (22.6)$$

where the curly bracket vanishes according to SE. Then we multiply the equation by ψ^* and integrate over r :

$$\begin{aligned} 2i \int \psi^* \frac{\partial \psi}{\partial x} d^3 r &+ \frac{2m}{\hbar^2} \frac{\partial \varepsilon}{\partial k_x} \int \psi^* \psi d^3 r + \\ &+ \int e^{ikr} \frac{\partial u}{\partial k_x} \left[\nabla^2 + \frac{2m}{\hbar^2} (\varepsilon - V) \right] \psi^* d^3 r = 0 , \end{aligned} \quad (22.7)$$

where we have used the integration by parts. The last item in the l.h.s. is also equal to zero (SE) and we come to the result.

Chapter 4

Problem 4.1. Calculate the partition function for a harmonic oscillator.

Solution. Using the definition, we get

$$Z = e^{-\hbar\omega/2k_B T} \sum_{N=0}^{\infty} e^{-N\hbar\omega/k_B T}.$$

The we use the formula for geometric progression to get the result.

Problem 4.2. Prove the expression (4.11).

Solution. Use the formulas $\varepsilon_k = \hbar^2 k^2 / 2m$ and

$$\delta[z - f(y)] = \frac{\delta(y - z_y)}{|f'(z_y)|}$$

where z_y is determined by the condition $f(z_y) = z$.

Problem 4.3. Calculate temperature-dependent corrections to the chemical potential of a Fermi gas.

Solution. To calculate the integrals with the Fermi function

$$I = \int_0^\infty \chi(\varepsilon) f(\varepsilon) d\varepsilon$$

it is convenient first to integrate by parts. If we introduce

$$\varphi(\varepsilon) = \int_0^\varepsilon \chi(x) dx$$

it is easy to show that

$$I = \int_0^\infty \varphi(\varepsilon) \left(-\frac{\partial f_0}{d\varepsilon} \right) d\varepsilon.$$

At low temperatures the function $\left(-\frac{\partial f_0}{d\varepsilon} \right)$ behaves as δ -function at we will take advantage of this fact. Namely, we expand $\varphi(\varepsilon)$ as

$$\varphi(\varepsilon) = \varphi(\epsilon_F) + \varphi'(\epsilon_F)(\varepsilon - \epsilon_F) + \frac{1}{2}\varphi''(\epsilon_F)(\varepsilon - \epsilon_F)^2 + \dots$$

and introduce dimensionless variable $\eta = (\varepsilon - \epsilon_F)/k_B T$. We have

$$\left(-\frac{\partial f_0}{d\varepsilon} \right) d\varepsilon = \frac{e^{-\eta}}{(e^{-\eta} + 1)^2} d\eta.$$

Finally,

$$I = \varphi(\epsilon_F) + k_B T \varphi'(\epsilon_F) I_1 + (k_B T)^2 \varphi''(\epsilon_F) I_2 + \dots$$

where

$$I_1 = 0, \quad I_2 = \int_0^\infty \frac{\eta^2 e^{-\eta} d\eta}{2(e^{-\eta} + 1)^2} = \frac{\pi^2}{6}.$$

Making use of the last expression we get

$$\epsilon_F^{2/3} = \mu^{2/3} \left[1 + \frac{\pi^2}{8} \left(\frac{k_B T}{\epsilon_F} \right)^2 \right]$$

that leads to the expression we are interested in.

Problem 4.4. Calculate specific heat for the Boltzmann gas.

Solution. Use the general expression (4.16) with the Boltzmann distribution function.

Problem 4.5. Derive expression (4.22) for magnetic susceptibility.

Solution. Use the general procedure outlined in the Problem 4.3 with

$$\varphi(\varepsilon) = g(\varepsilon).$$

Problem 4.6. Derive the formula (4.33).

Solution. We chose the integration variable to

$$y = \frac{\varepsilon - N - 1/2}{k_B T}$$

and take into account that

$$\int_0^\infty y^{3/2} e^{-y} dy = \frac{3\sqrt{\pi}}{4}.$$

Then the sum over N can be done as the sum of geometric progression.

Chapter 6

Problem 6.1. An electron with a energy spectrum

$$\varepsilon(\mathbf{p}) = \frac{p_x^2}{2m_x} + \frac{p_y^2}{2m_y} + \frac{p_z^2}{2m_z}$$

is placed into a magnetic field parallel to \mathbf{z} -axis. Find the cyclotron effective mass and compare it with the density-of-states effective mass defined as

$$g(\varepsilon) = \frac{\sqrt{2}m_d^{3/2}\varepsilon^{1/2}}{\pi^2\hbar^3}.$$

Solution. The equation for the electron trajectory, $\varepsilon(\mathbf{p}) = \varepsilon$ for a given p_z , has the form

$$\frac{1}{2\varepsilon - p_z^2/m_z} \left(\frac{p_x^2}{m_x} + \frac{p_y^2}{m_y} \right) = 1.$$

This is the ellipse having the area

$$S(\varepsilon, p_z) = \pi(2\varepsilon - p_z^2/m_z)\sqrt{m_x m_y}.$$

Thus, according to definition,

$$m_c = \frac{1}{2\pi} \frac{\partial S(\varepsilon, p_z)}{\partial \varepsilon} = \sqrt{m_x m_y}.$$

According to the definition of the density of states,

$$g(\varepsilon) = \frac{2}{(2\pi\hbar)^3} \int dp_x dp_y dp_z \delta[\varepsilon(\mathbf{p}) - \varepsilon].$$

Introducing new variables as

$$p_x = \xi\sqrt{2m_x}, \quad p_y = \eta\sqrt{2m_y}, \quad p_z = \zeta\sqrt{2m_z}$$

we obtain that

$$m_d = (m_x m_y m_z)^{1/3}.$$

Problem 6.2. Derive the Drude formula (6.17).

$$\sigma = \frac{ne^2\tau_{tr}}{m}.$$

from the expression

$$\sigma = e^2 D(\epsilon_F) g(\epsilon_F).$$

Solution. For zero temperature we have

$$g(\epsilon_F) = \frac{\partial n}{\partial \epsilon_F} = \frac{3}{2} \frac{n}{\epsilon_F} = \frac{3n}{mv_F^2}.$$

Problem 6.3. Assume that the electrons obey Boltzmann statistics,

$$f_0(\varepsilon) = \exp\left(\frac{\zeta - \varepsilon}{T}\right),$$

and that

$$\tau_{tr}(\varepsilon, T) \propto \varepsilon^r.$$

Expressing the transport relaxation time as

$$\tau_{tr}(\varepsilon, T) = \tau_0(T)(\varepsilon/kT)^r$$

find the expressions for Drude conductance at $\omega\tau_0 \ll 1$ and $\omega\tau_0 \gg 1$.

Solution Using the definition of Drude conductance we get

$$\langle \tau_{\text{tr}} \rangle = \tau(T) \frac{\Gamma(r + 5/2)}{\Gamma(5/2)}.$$

Thus, $\sigma_0 \propto \tau_0(T)$.

At large frequencies,

$$\operatorname{Re} \sigma(\omega) = \frac{ne^2}{m\omega^2} \left\langle \frac{1}{\tau_{\text{tr}}} \right\rangle = \frac{ne^2}{m\omega^2 \tau_0(T)} \frac{\Gamma(5/2 - r)}{\Gamma(5/2)}.$$

Problem 6.4. Compare thermoelectric coefficients η for degenerate and non-degenerate electron gas. Assume

$$\tau_{\text{tr}}(\varepsilon, T) = \tau_0(T)(\varepsilon/kT)^r.$$

Solution. It is practical to introduce the integration variable $x = \varepsilon/T$ and denote $\zeta^* = \zeta/T$ (here we skip the Boltzmann constant k for brevity). Then

$$\left(-\frac{\partial f_0}{\partial \varepsilon} \right) = \frac{1}{T} \exp(\zeta^* - x), \quad g(\varepsilon)D(\varepsilon)(\varepsilon - \zeta) = g(T)D(T)T(x - \zeta^*)x^{r+3/2}.$$

Thus

$$\begin{aligned} \eta &= -eg(T)D(T)e^{\zeta^*} \int_0^\infty dx (x - \zeta^*)x^{r+3/2}e^{-x} \\ &= -eg(T)D(T)e^{\zeta^*}[\Gamma(r + 7/2) - \zeta^*\Gamma(r + 5/2)]. \end{aligned}$$

Similarly,

$$\sigma_0 = e^2 g(T)D(T)e^{\zeta^*}\Gamma(r + 5/2).$$

Thus, introducing k we get

$$\alpha = -\frac{k}{e}(r + 5/2 - \zeta^*).$$

Note that

$$n = e^{\zeta^*} g(T)T\Gamma(3/2) \rightarrow \zeta^* = -\ln \frac{\sqrt{\pi}g(T)T}{2n}.$$

In the Fermi gas,

$$\frac{d}{\zeta} g(\zeta)D(\zeta) = (r + 3/2) \frac{g(\zeta)D(\zeta)}{\zeta}.$$

Thus according to the definition,

$$\alpha = -\frac{k}{e}(r + 3/2) \frac{\pi^2}{3} \frac{kT}{\zeta}.$$

Problem 6.5. Using the Wiedemann-Franz law compare the coefficients κ and β for a typical metal.

Solution. We have the relation $\kappa = \beta - T\eta\alpha$. The ratio $T\eta\alpha/\beta$ (according to the Wiedemann-Franz law) has the order

$$\frac{T\eta^2 e^2}{\sigma T \sigma k_B^2} \approx \left(\frac{k_B T}{\epsilon_F} \right)^2.$$

Problem 6.6. Derive the expression (6.26) for the screened Coulomb potential.

$$\varphi = \frac{Ze}{r} e^{-r/r_s},$$

Solution. In a spherical symmetric system it is natural to chose spherical co-ordinates, the Laplace operator for the angle-independent case being

$$\nabla^2 \varphi = \frac{1}{r^2} \frac{d}{dr} \left(r^2 \frac{d\varphi}{dr} \right).$$

If we search the solution as $u(r)/r$ the equation for u has the form

$$\begin{aligned} \frac{1}{r^2} \frac{d}{dr} \left[r^2 \frac{d}{dr} \left(\frac{u}{r} \right) \right] &= \frac{1}{r^2} \frac{d}{dr} r^2 \left[\frac{u'}{r} - \frac{u}{r^2} \right] = \\ &= \frac{1}{r^2} \frac{d}{dr} (ru' - u) = \frac{u''}{r}. \end{aligned}$$

Substituting this expression to the Poisson equation we get

$$u'' - \frac{1}{r_s^2} u = 0 \rightarrow u \propto \exp \left(-\frac{r}{r_s} \right).$$

Problem 6.7. Derive the expression (6.27).

$$W(\theta) = 4\pi n_i v \left[\frac{e^2 / \epsilon}{2\epsilon(1 - \cos \theta) + \hbar^2 / 2mr_s^2} \right]^2$$

Solution. One should calculate the matrix element

$$\mathbf{v} \propto M = \int d^3 r e^{i\mathbf{qr}} \frac{e^{-r/r_s}}{r}$$

where $\mathbf{q} = \mathbf{k}' - \mathbf{k}$. We have

$$\begin{aligned} M &= 2\pi \int_0^\infty r dr \int_{-1}^1 d(\cos \beta) \exp(iqr \cos \beta) \cdot \exp \left(-\frac{r}{r_s} \right) = \\ &= 4\pi \int_0^\infty dr \frac{\sin(qr)}{q} \exp \left(-\frac{r}{r_s} \right) = \frac{4\pi}{q} \operatorname{Im} \int_0^\infty dr \exp(iq - \frac{1}{r_s}) r = \frac{2\pi}{q^2 + r_s^{-2}}. \end{aligned}$$

Using the property $k = k'$ and the equality

$$q^2 = 2k^2(1 - \cos \theta) = 2\epsilon(2m/\hbar^2)(1 - \cos \theta)$$

we get the result.

Problem 6.10. Derive the expression for the solution of the Boltzmann equation

$$\mathbf{G} = e\tau_{tr} \frac{\partial f_0}{\partial \varepsilon} \frac{\mathbf{E} + (\mu/c)^2(\mathbf{H}\mathbf{E})\mathbf{H} + (\mu/c)[\mathbf{EH}]}{1 + \mu^2 H^2/c^2}.$$

Use this expression to find the conductivity tensor.

Solution Use the relation (6.51), determine the coefficients α , β and γ and then substitute them into initial expression for \mathbf{G} . The calculation of the conductivity tensor is straightforward.

Problem 6.12. Using the expression (6.71) find imaginary part of $1/\epsilon(\mathbf{q}, \omega)$ which is responsible for damping of the wave of electrical polarization.

Solution We have

$$\text{Im } \frac{1}{\epsilon(\mathbf{q}, \omega)} = -\frac{1}{\epsilon_0} \frac{\omega/\tau_M}{(q^2 D + 1/\tau_M)^2 + \omega^2} = -\frac{1}{\epsilon_0} \frac{\omega\tau_M}{(1 + q^2/\kappa^2)^2 + \omega^2\tau_M^2}.$$

Chapter 7

Problem 7.1. Derive the equation (7.3).

$$\delta = \frac{1}{\text{Im } q} = \frac{2}{\sqrt{3}} \left(\frac{c^2 \ell}{4\pi\sigma\omega_0 b} \right)^{1/3}.$$

Solution. Start from the equation $q^2 = 4\pi i\omega\sigma/c^2$ and substitute $\sigma = ia\sigma_0/ql$. We get

$$q^3 = -4\pi a\omega\sigma_0/c^2\ell = (4\pi a\omega\sigma_0/c^2\ell) e^{i\pi}.$$

The following way is straightforward.

Problem 7.2. Derive the dispersion law for plasmons.

Solution. We have

$$\frac{1}{-\omega(1 - \mathbf{qv}/\omega)} = -i \frac{1}{\omega} \left[1 + \frac{\mathbf{qv}}{\omega} + \left(\frac{\mathbf{qv}}{\omega} \right)^2 + \dots \right]$$

The longitudinal conductivity contains

$$\overline{v_z^2} \left[1 + \frac{q_z v_z}{\omega} + \left(\frac{q_z v_z}{\omega} \right)^2 + \dots \right] = v^2 \overline{\cos^2 \theta} + \frac{q^2 v^4}{\omega^2} \overline{\cos^4 \theta} = \frac{1}{3} v^2 \left(1 + \frac{3}{5} \frac{q^2 v^2}{\omega^2} \right).$$

Consequently, the dispersion equation for the Fermi gas has the form

$$1 - \frac{\omega_p^2}{\omega^2} \left(1 + \frac{3}{5} \frac{q^2 v_F^2}{\omega_p^2} \right) = 0 \rightarrow \omega^2 = \omega_p^2 \left(1 + \frac{3}{5} \frac{q^2 v_F^2}{\omega_p^2} \right) = \omega_p^2 \left(1 + \frac{9}{5} (qr_{TF})^2 \right).$$

Thus, we come to the dispersion equation

$$1 - \frac{\omega_p^2}{\omega^2} \frac{(1 + (9/5)(qr_{TF})^2)}{1 - (\omega_p^2/\omega^2)(qr_{TF})^2} = 0.$$

or

$$\omega \approx \omega_p(1 + 7q^2r_{TF}^2/5).$$

Problem 7.3. Derive the dispersion relation for electromagnetic waves in metals.

$$\det \left[q^2 \delta_{ik} - q_i q_k - \frac{4\pi i \omega}{c^2} \sigma_{ik} \right] = 0.$$

Solution. We start from the Maxwell equations

$$\text{curl } \mathbf{H} = \frac{4\pi}{c} \mathbf{j}, \quad \text{curl } \mathbf{E} = -\frac{1}{c} \frac{\partial \mathbf{H}}{\partial t}$$

and take the curl of the second one with the identity

$$\text{curl curl } \mathbf{E} = \text{grad div } \mathbf{E} - \nabla^2 \mathbf{E}.$$

After the substitution $j_i = \sum_k \sigma_{ik} E_k$ we come to the result.

Chapter 8

Problem 8.1. Compare electrical and mechanical energies carried by the wave in a piezodielectric.

Solution. The density of electrical energy in the insulating sample is

$$Q_e = \frac{\langle \mathbf{E} \mathbf{D} \rangle}{4\pi} = \frac{\epsilon_0 q^2 |\phi|^2}{8\pi} = \frac{1}{2} \frac{4\pi |\beta_{i,kl} q_i q_l u_k|^2}{\epsilon_0 q^2}.$$

The mechanical energy can be estimated as

$$Q_m = 2\rho \frac{\omega^2 \langle u_i^2 \rangle}{2} = \frac{1/2}{\rho} w^2 q^2 |u_i|^2.$$

Thus

$$\frac{Q_e}{Q_m} = \chi = \frac{4\pi |\beta_{i,kl} q_i q_l u_k|^2}{\epsilon_0 \rho w^2 q^4 |u_i|^2}.$$

Problem 8.2 . Find the relation between the amplitudes of electric fields and deformation for the case of acoustic wave in a piezoelectric semiconductor. Compare electrical and mechanical energies carried by the wave.

Solution. Taking into account the Poisson equation

$$\operatorname{div} \mathbf{D} = 4\pi e(\delta n)$$

together with the expression (8.7) for the electrical induction \mathbf{D} and expression (8.10) yields

$$\phi = i \frac{4\pi \beta_{i,kl} q_i u_{kl}}{q^2 \epsilon(\mathbf{q}, \omega)} = i \frac{4\pi \beta_{i,kl} q_i u_{kl}}{q^2 \epsilon_0} \frac{-i\omega + q^2 D}{-i\omega + q^2 D + 1/\tau_m}. \quad (22.8)$$

Problem 8.3 Find dc current induced by a acoustic wave in a non-degenerate piezoelectric semiconductor.

Hint: A dc current appears in the second approximation in the wave amplitude. Thus

$$\begin{aligned} j_{dc} &= \langle \sigma E - eD(\partial \delta n / \partial x)_{\text{time}} \rangle \\ &\approx \langle (\delta\sigma) E \rangle \\ &= \frac{\sigma}{n} \langle (\delta n) E \rangle. \end{aligned}$$

Solution. Using the hint we write

$$\begin{aligned} j_{dc} &= \frac{\sigma}{2en} \operatorname{Re}[(\delta n)_\omega E_\omega^*] \\ &= -\frac{q\sigma}{2en} \operatorname{Im}[(\delta n)_\omega \phi_\omega^*]. \end{aligned}$$

Then, we have from (8.10)

$$(\delta n)_\omega = -\frac{\sigma}{e(-i\omega + Dq^2)} q^2 \phi_\omega.$$

As a result,

$$j_{dc} = \frac{\sigma}{en} \left(\frac{\epsilon_0 |\phi_\omega|^2 q^2}{4\pi} \right) q \frac{\omega/\tau_m}{\omega^2 + (q^2 D)^2}.$$

Now we can express the actual potential ϕ_ω through the bare one, ϕ_ω^0 , as

$$\phi_\omega = \phi_\omega^0 / \epsilon(\mathbf{q}, \omega).$$

As a result,

$$j_{dc} = \frac{\sigma}{enw} \left(\frac{|\phi_\omega^0|^2 q^2}{4\pi \epsilon_0} \right) q \frac{\omega \tau_m}{(1 + q^2/\kappa^2)^2 + \omega^2 \tau_m^2}.$$

Here w is the sound velocity The coefficient

$$\left(\frac{w \epsilon_0 |\phi_\omega^0|^2 q^2}{4\pi} \right)$$

has the meaning of the flux of electric energy due to the wave which is connected to the flux in mechanical energy, S as χS . The the product

$$\chi q \frac{\omega \tau_m}{(1 + q^2/\kappa^2)^2 + \omega^2 \tau_m^2}$$

is nothing else than the absorption coefficient Γ . Finally we obtain

$$j_{dc} = \frac{\sigma \Gamma S}{s}.$$

Chapter 9

Problem 9.1. Calculate dipole matrix element for the transitions between adjacent subbands in a rectangular quantum well with infinite potential barriers. Assume that light is polarized perpendicular to the well.

Solution Normalized wave functions are

$$g^n(z) = \sqrt{\frac{2}{W}} \begin{cases} \cos(\pi nz/W), & n \text{ odd} \\ \sin(\pi nz/W), & n \text{ even} \end{cases}$$

Thus, for odd n

$$\begin{aligned} \langle n | p_z | n + s \rangle &= \langle n + s | p_z | n \rangle \\ &= -i \frac{2\hbar}{W} \int_{-W/2}^{W/2} dz \cos(\pi nz/W) (\partial/\partial z) \sin[\pi(n+s)z/W] \\ &= \frac{2\hbar}{iW} \frac{[2 \sin(\pi sn/2) + \sin(\pi s^2/2) + \sin(\pi ns + \pi s^2/2)](n+s)}{s(2n+s)}. \end{aligned}$$

For $s = 1$ the matrix element is

$$-\frac{4i\hbar}{W} \frac{n(n+1)}{2n+1}.$$

Problem 4.2. Make a similar calculation for a parabolic confinement

$$U(z) = (1/2)m\omega^2 z^2.$$

Define ω from the request that the typical spread of the ground state wave function is W and compare the result with the case of rectangular confinement.

Solution. The solution is similar. The typical confinement length is related to the frequency ω as

$$W = \sqrt{\hbar/m\omega} \rightarrow \omega = \hbar^2/mW^2.$$

From textbooks in quantum mechanics,

$$\langle n | p_z | n + s \rangle = i \frac{\hbar}{W\sqrt{2}} [\sqrt{n}\delta_{s,-1} - \sqrt{n+1}\delta_{s,1}].$$

Chapter 16

Problem 16.1. Derive Eq. (16.3).

Solution. For $\mathbf{A} \parallel \mathbf{z}$

$$\begin{aligned} \int \frac{(\mathbf{A}(\mathbf{r}')\mathbf{R})\mathbf{R}}{R^4} e^{-R/\zeta_0} dV' &\rightarrow A \int R^2 dR d(\cos \theta) d\varphi \frac{(\mathbf{z}\mathbf{R})\mathbf{R}}{R^4} e^{-R/\zeta_0} = \\ &= \mathbf{A} \int R^2 dR d(\cos \theta) d\varphi \frac{\cos^2 \theta}{R^2} e^{-R/\zeta_0} = \frac{4\pi}{3\zeta_0} \end{aligned}$$

Chapter 17

Problem 17.1. Prove that the areas under magnetization curves are the same for type I and type II SC with the same H_c .

Solution. Introducing G -potential as

$$G_s = F_s(B) - \frac{BH}{4\pi}$$

we note that it should be minimal in an equilibrium state with fixed H :

$$\left(\frac{\partial G_s}{\partial B} \right)_H = 0.$$

For a normal state

$$G_n = F_n + \frac{B^2}{8\pi} - \frac{BH}{4\pi}.$$

From the stability condition for the normal state $\left(\frac{\partial G_n}{\partial B} \right)_H = 0$ we get $B = H$ and

$$G_n = F_n - \frac{H^2}{8\pi}.$$

Now let us change H by δH . We get

$$\frac{\partial}{\partial H} (G_n - G_s) = \frac{B - H}{4\pi} = M.$$

Now we can integrate this relation over H from 0 to H_{c2} (where $G_n = G_s$ —equilibrium!). At the same time, at $H = 0$ $G_i = F_i$ and $(F_n - F_s)_{B=0} = H_c^2/8\pi$. We get

$$\int_0^{H_{c2}} M dH = -\frac{H_c^2}{8\pi}.$$

Consequently, it depends only on H_c .

Problem 17.2. Derive Eq. (17.15).

Solution.

$$\frac{\partial p}{\partial x} = B \frac{\partial^2 G}{\partial B^2} \frac{\partial B}{\partial x} = \frac{B}{4\pi} \frac{\partial H(B)}{\partial B} \frac{\partial B}{\partial x} = \frac{B}{4\pi} \frac{\partial H(B)}{\partial x}.$$

Chapter 18

Problem 18.1. Prove the Eqs. (18.9) and (18.10).

Solution. For Eq. (18.8)

$$\mathcal{E} = E - \epsilon_F N = \sum_{\mathbf{k}} \xi_{\mathbf{k}} [(n_{\mathbf{k}\uparrow} + n_{\mathbf{k}\downarrow}) + 2v_{\mathbf{k}}^2(1 - n_{\mathbf{k}\uparrow} - n_{\mathbf{k}\downarrow})] - \frac{\Delta^2}{\lambda}$$

with

$$\Delta = \lambda \sum_{\mathbf{k}} u_{\mathbf{k}} v_{\mathbf{k}} (1 - n_{\mathbf{k}\uparrow} - n_{\mathbf{k}\downarrow}).$$

We get

$$\begin{aligned} \frac{\delta \mathcal{E}}{\delta v_{\mathbf{k}}} &= 4v_{\mathbf{k}} \xi_{\mathbf{k}} (1 - n_{\mathbf{k}\uparrow} - n_{\mathbf{k}\downarrow}) - 2 \frac{\Delta}{\lambda} \frac{\delta \Delta}{\delta v_{\mathbf{k}}} = \\ &= 4v_{\mathbf{k}} \xi_{\mathbf{k}} (1 - n_{\mathbf{k}\uparrow} - n_{\mathbf{k}\downarrow}) - 2 \frac{\Delta}{\lambda} \lambda (u_{\mathbf{k}} + v_{\mathbf{k}} \frac{du_{\mathbf{k}}}{dv_{\mathbf{k}}}) (1 - n_{\mathbf{k}\uparrow} - n_{\mathbf{k}\downarrow}) = \\ &= 4v_{\mathbf{k}} \xi_{\mathbf{k}} (1 - n_{\mathbf{k}\uparrow} - n_{\mathbf{k}\downarrow}) - 2 \frac{\Delta}{u_{\mathbf{k}}} (1 - 2v_{\mathbf{k}}^2) (1 - n_{\mathbf{k}\uparrow} - n_{\mathbf{k}\downarrow}) = 0. \end{aligned}$$

This is just the result we need.

Problem 18.2. Prove Eq. (18.18).

Solution. We have

$$\begin{aligned} \mathcal{H}_{int} &= -\lambda \sum a_{\mathbf{k}'_1\uparrow}^\dagger a_{\mathbf{k}'_2\downarrow}^\dagger a_{\mathbf{k}_2\downarrow} a_{\mathbf{k}_1\uparrow} = -\lambda \sum \left(u_{\mathbf{k}'_1} \alpha_{\mathbf{k}'_1\uparrow}^\dagger + v_{\mathbf{k}'_1} \alpha_{-\mathbf{k}'_1\downarrow} \right) \left(u_{\mathbf{k}'_2} \alpha_{\mathbf{k}'_2\downarrow}^\dagger - v_{\mathbf{k}'_2} \alpha_{-\mathbf{k}'_2\uparrow} \right) \times \\ &\quad \times \left(u_{\mathbf{k}_2} \alpha_{\mathbf{k}_2\downarrow} - v_{\mathbf{k}_2} \alpha_{-\mathbf{k}_2\uparrow}^\dagger \right) \left(u_{\mathbf{k}_1} \alpha_{\mathbf{k}_1\uparrow} + v_{\mathbf{k}_1} \alpha_{-\mathbf{k}_1\downarrow}^\dagger \right). \end{aligned}$$

We get

$$\begin{aligned} &\left(u_{\mathbf{k}'_1} u_{\mathbf{k}'_2} \alpha_{\mathbf{k}'_1\uparrow}^\dagger \alpha_{\mathbf{k}'_2\downarrow}^\dagger - v_{\mathbf{k}'_1} v_{\mathbf{k}'_2} \alpha_{-\mathbf{k}'_1\downarrow} \alpha_{-\mathbf{k}'_2\uparrow} + v_{\mathbf{k}'_1} u_{\mathbf{k}'_2} \alpha_{-\mathbf{k}'_1\downarrow} \alpha_{\mathbf{k}'_2\downarrow}^\dagger - u_{\mathbf{k}'_1} v_{\mathbf{k}'_2} \alpha_{\mathbf{k}'_1\uparrow}^\dagger \alpha_{-\mathbf{k}'_2\uparrow} \right) \times \\ &\quad \times \left(u_{\mathbf{k}_2} u_{\mathbf{k}_1} \alpha_{\mathbf{k}_2\downarrow} \alpha_{\mathbf{k}_1\uparrow} - v_{\mathbf{k}_2} v_{\mathbf{k}_1} \alpha_{-\mathbf{k}_2\uparrow}^\dagger \alpha_{-\mathbf{k}_1\downarrow}^\dagger + u_{\mathbf{k}_2} v_{\mathbf{k}_1} \alpha_{\mathbf{k}_2\downarrow} \alpha_{-\mathbf{k}_1\downarrow}^\dagger - v_{\mathbf{k}_2} u_{\mathbf{k}_1} \alpha_{-\mathbf{k}_2\uparrow}^\dagger \alpha_{\mathbf{k}_1\uparrow} \right) \end{aligned}$$

Now we should remember that $\mathbf{k}'_1 \neq \mathbf{k}_1$. Consequently only the following combinations lead to non-zero averages

$$\begin{aligned} &\left(v_{\mathbf{k}'_1} u_{\mathbf{k}'_2} \alpha_{-\mathbf{k}'_1\downarrow} \alpha_{\mathbf{k}'_2\downarrow}^\dagger - u_{\mathbf{k}'_1} v_{\mathbf{k}'_2} \alpha_{\mathbf{k}'_1\uparrow}^\dagger \alpha_{-\mathbf{k}'_2\uparrow} \right) \left(u_{\mathbf{k}_2} v_{\mathbf{k}_1} \alpha_{\mathbf{k}_2\downarrow} \alpha_{-\mathbf{k}_1\downarrow}^\dagger - v_{\mathbf{k}_2} u_{\mathbf{k}_1} \alpha_{-\mathbf{k}_2\uparrow}^\dagger \alpha_{\mathbf{k}_1\uparrow} \right) \rightarrow \\ &\rightarrow v_{\mathbf{k}'_1} u_{\mathbf{k}'_2} u_{\mathbf{k}_2} v_{\mathbf{k}_1} \left\langle \alpha_{-\mathbf{k}'_1\downarrow} \alpha_{\mathbf{k}'_2\downarrow}^\dagger \alpha_{\mathbf{k}_2\downarrow} \alpha_{-\mathbf{k}_1\downarrow}^\dagger \right\rangle - u_{\mathbf{k}'_1} v_{\mathbf{k}'_2} u_{\mathbf{k}_2} v_{\mathbf{k}_1} \left\langle \alpha_{\mathbf{k}'_1\uparrow}^\dagger \alpha_{-\mathbf{k}'_2\uparrow} \alpha_{\mathbf{k}_2\downarrow} \alpha_{-\mathbf{k}_1\downarrow}^\dagger \right\rangle - \\ &- v_{\mathbf{k}_2} u_{\mathbf{k}_1} v_{\mathbf{k}'_1} u_{\mathbf{k}'_2} \left\langle \alpha_{-\mathbf{k}'_1\downarrow} \alpha_{\mathbf{k}'_2\downarrow}^\dagger \alpha_{-\mathbf{k}_2\uparrow}^\dagger \alpha_{\mathbf{k}_1\uparrow} \right\rangle + u_{\mathbf{k}'_1} v_{\mathbf{k}'_2} v_{\mathbf{k}_2} u_{\mathbf{k}_1} \left\langle \alpha_{\mathbf{k}'_1\uparrow}^\dagger \alpha_{-\mathbf{k}'_2\uparrow} \alpha_{-\mathbf{k}_2\uparrow}^\dagger \alpha_{\mathbf{k}_1\uparrow} \right\rangle \end{aligned}$$

To get nonzero averages we put $\mathbf{k}'_2 = -\mathbf{k}'_1$, $\mathbf{k}_1 = -\mathbf{k}_2$. Consequently, we have

$$\begin{aligned} & v_{\mathbf{k}'_1} u_{\mathbf{k}'_1} u_{\mathbf{k}_1} v_{\mathbf{k}_1} \times \\ & \left(\left\langle \alpha_{-\mathbf{k}'_1\downarrow} \alpha_{-\mathbf{k}'_1\downarrow}^\dagger \alpha_{-\mathbf{k}_1\downarrow} \alpha_{-\mathbf{k}_1\downarrow}^\dagger \right\rangle - \left\langle \alpha_{\mathbf{k}'_1\uparrow}^\dagger \alpha_{\mathbf{k}'_1\uparrow} \alpha_{-\mathbf{k}_1\downarrow} \alpha_{-\mathbf{k}_1\downarrow}^\dagger \right\rangle - \right. \\ & \left. - \left\langle \alpha_{-\mathbf{k}'_1\downarrow} \alpha_{-\mathbf{k}'_1\downarrow}^\dagger \alpha_{\mathbf{k}_1\uparrow}^\dagger \alpha_{\mathbf{k}_1\uparrow} \right\rangle + \left\langle \alpha_{\mathbf{k}'_1\uparrow}^\dagger \alpha_{\mathbf{k}'_1\uparrow} \alpha_{\mathbf{k}_1\uparrow}^\dagger \alpha_{\mathbf{k}_1\uparrow} \right\rangle \right) = \\ & = v_{\mathbf{k}'_1} u_{\mathbf{k}'_1} u_{\mathbf{k}_1} v_{\mathbf{k}_1} \left[(1 - n_{-\mathbf{k}'_1\downarrow}) (1 - n_{-\mathbf{k}_1\downarrow}) - n_{\mathbf{k}'_1\uparrow} (1 - n_{-\mathbf{k}_1\downarrow}) - (1 - n_{-\mathbf{k}'_1\downarrow}) n_{\mathbf{k}_1\uparrow} + n_{\mathbf{k}'_1\uparrow} n_{\mathbf{k}_1\uparrow} \right] \end{aligned}$$

Combining the formulas we come to the final result.

Problem 18.3. Check Eq. (18.20).

Solution. It is checked directly by use of Bogoliubov transform.

Chapter 20

Problem 20.1. Consider the current in a series circuit containing a Josephson junction, load resistor R , and a battery.

Solution. The voltage is

$$V = U - RI = U - J_c R \sin \theta.$$

According to the Josephson formula,

$$\frac{d\theta}{dt} = \frac{2e}{\hbar} V = \frac{2e}{\hbar} (U - J_c R \sin \theta) = \omega_J (1 - \lambda \sin \theta), \quad \lambda = \frac{J_c R}{U}.$$

As a result

$$\omega_j(t - t_0) = \int \frac{d\theta}{1 - \lambda \sin \theta}$$

At $\lambda > 1$ there is a pole in the integrand at $\theta_0 = \arcsin(1/\lambda)$. Thus at $t \rightarrow \infty$ $\theta \rightarrow \theta_0$, the current being U/R while the voltage at the junction is zero. At $\lambda > 1$ (or $J > J_c$) one can calculate the integral exactly: assuming $m = \tan(\theta/2)$ we get

$$m = \lambda + \sqrt{1 - \lambda^2} \tan \left[\frac{1}{2} \sqrt{1 - \lambda^2} \omega_J (t - t_0) \right]$$

The current being

$$I = \frac{2_c m}{1 + m^2}.$$

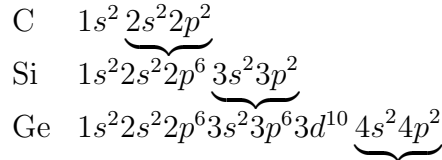
We see that the current oscillates with the period $2\pi/\omega_J \sqrt{1 - \lambda^2}$.

Appendix A

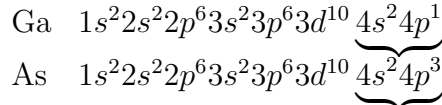
Band structure of semiconductors

Let us start with atomic structure of few important semiconductors.

IV Semiconductors



III-V Semiconductors



Important feature - outermost valence electrons are made of either s or p orbitals.

We will classify the band structure of following a simple tight-binding approximation. Namely, we look for the wave function in the form

$$\psi_{\mathbf{k}}(\mathbf{r}) = \sum_{\mathbf{R}} e^{i\mathbf{k}\mathbf{R}} \sum_n b_n \phi(\mathbf{r} - \mathbf{R})$$

where $\phi_n(\mathbf{r})$ are atomic eigenfunctions. From the Schrödinger equation we have

$$\begin{aligned} [E(\mathbf{k}) - E_m] b_m &\approx \sum_n b_n \left[\int d^3 r \phi_m^*(\mathbf{r}) \phi_n(\mathbf{r}) \Delta U(\mathbf{r}) \right. \\ &\quad \left. + \sum_{\mathbf{R} \neq 0} \int d^3 r \phi_m^*(\mathbf{r}) \phi_n(\mathbf{r}) \Delta U(\mathbf{r}) e^{i\mathbf{k}\mathbf{R}} \right] \end{aligned}$$

Here ΔU is the deviation of the real potential from the superposition of atomic ones. It is not small only in the places where atomic wave functions are small. Usually, the integrals

$$\int d^3 r \phi_m^*(\mathbf{r}) \phi_n(\mathbf{r}) \Delta U(\mathbf{r}) \propto \delta_{nm}$$

and thus lead to a renormalization of the on-site energy.

Single atomic s -level

In this case, $b_s = 1$. Denoting

$$\begin{aligned}\alpha(\mathbf{R}) &= \int d^3r \phi_s^*(\mathbf{r})\phi_s(\mathbf{r} - \mathbf{R}) \\ \beta_s &= - \int d^3r \phi_s^*(\mathbf{r})\phi_s(\mathbf{r})\Delta U(\mathbf{r}) \\ \gamma(\mathbf{R}) &= - \int d^3r \phi_m^*(\mathbf{r})\phi_n(\mathbf{r} - \mathbf{R})\Delta U(\mathbf{r})\end{aligned}$$

and neglecting (for simplicity) $\alpha(\mathbf{R})$ we obtain

$$E(\mathbf{k}) = E_s - \beta_s - \sum_{\mathbf{R} \neq 0} \gamma(\mathbf{R})e^{i\mathbf{k}\mathbf{R}}.$$

It is reasonable to keep nearest neighbors. A simple example is fcc cubic lattice, where 12 nearest neighbors are situated at

$$\frac{a}{2}(\pm 1, \pm 1, 0); \quad \frac{a}{2}(\pm 1, 0, \pm 1); \quad \frac{a}{2}(0, \pm 1, \pm 1).$$

In this case,

$$E(\mathbf{k}) = E_s - \beta_s - 4\gamma \left[\cos \frac{k_x a}{2} \cos \frac{k_y a}{2} + \cos \frac{k_y a}{2} \cos \frac{k_z a}{2} + \cos \frac{k_x a}{2} \cos \frac{k_z a}{2} \right].$$

Let us examine important points, Fig. A.1.

- $\Gamma \Rightarrow (0, 0, 0)$, zone center,
- $X \Rightarrow (1, 0, 0)$ and 5 other equivalent points,
- $L \Rightarrow (1/2, 1/2, 1/2)$ and 7 other equivalent points,
- $L \Rightarrow (3/4, 3/4, 0)$
- $L \Rightarrow (1, 1/2, 0)$.

The opposite L points are connected by a reciprocal lattice vector, and real degeneracy is only 4-fold. X -point has only 3 distinct analogs in the 1st BZ. We get the following band structure

$$\begin{array}{lll} \text{Along } \Gamma X & k_x = 2\pi\alpha/a & 0 \leq \alpha \leq 1 \\ & k_y = k_z = 0 & \\ & E(\mathbf{k}) = E_s - \beta_s - 4\gamma(1 + 2 \cos \pi a) & \\ \text{Along } \Gamma L & k_x = k_y = k_z = 2\pi\alpha/a & 0 \leq \alpha \leq 1/2 \\ & E(\mathbf{k}) = E_s - \beta_s - 12\gamma \cos^2 \pi a & \\ \text{Along } \Gamma K & k_x = k_y = 2\pi\alpha/a & 0 \leq \alpha \leq 3/4 \\ & k_z = 0 & \\ & E(\mathbf{k}) = E_s - \beta_s - 4\gamma(\cos^2 \pi a + 2 \cos \pi a) & \end{array}$$

Near the Γ point,

$$E(\mathbf{k}) = E_s - \beta_s - 12\gamma + \gamma^2 k^2 a^2.$$

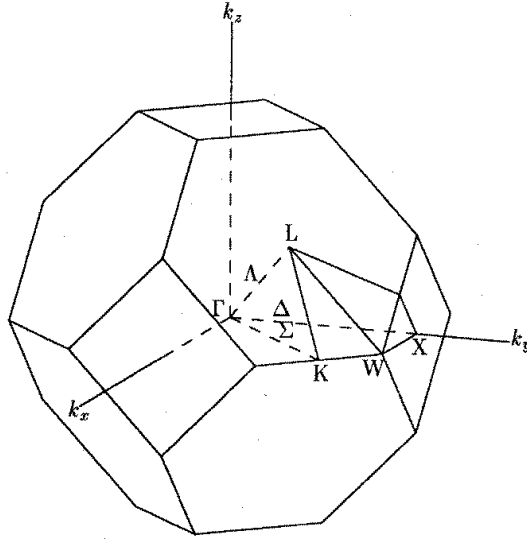


Figure A.1: Brillouin zone of fcc lattice.

The case of s and p orbitals

In this case, we have 4 wave functions, s and p_i , $i = x, y, z$. Moreover, there are 2 atoms per unit cell, $j = 1, 2$,

$$\psi(\mathbf{k}, \mathbf{r}) = \sum_{\mathbf{R}_i} \sum_{m=1}^4 \sum_{j=1}^2 C_{mj}(\mathbf{k}) \phi_{mj}(\mathbf{r} - \mathbf{r}_j - \mathbf{R}_i)$$

where \mathbf{R}_i stand for unit cells.

The coefficients are determined from the Schrödinger equation,

$$\langle \phi_{m'j'} | \mathcal{H} - E | \psi(\mathbf{k}) \rangle = 0.$$

This is impossible to do in general, and there are many approximate methods. One of the simplest is sp^2 nearest neighbor expansion, which ignores spin degrees of freedom. We shall not go along this way leaving this for special courses.

Spin-orbit coupling

It is difficult to calculate spin-orbit interaction in crystals, and it is usually done with adjustable parameters.

Here we consider simple examples using tight-binding approximation,

$$\mathcal{H} = \mathcal{H}_{tb} + \mathcal{H}_{so}.$$

The interaction Hamiltonian is usually written as

$$\mathcal{H}_{\text{SO}} = \lambda \mathbf{L} \cdot \mathbf{S},$$

the total angular momentum being

$$\mathbf{J}^2 = (\mathbf{L} + \mathbf{S})^2 = \mathbf{L}^2 + \mathbf{S}^2 + 2\mathbf{LS}.$$

Thus,

$$2\langle \mathbf{LS} \rangle = \langle \mathbf{J}^2 - \mathbf{L}^2 - \mathbf{S}^2 \rangle = \hbar^2[j(j+1) - l(l+1) - s(s+1)].$$

Here we face a problem – all this considerations are applicable to the eigenfunctions of a given total angular momentum. So first one must decouple electronic states into the eigenfunctions of a given angular momentum. Original p -states are in fact *linear combinations* of such functions, e.g.

$$\begin{aligned} p_x &= \frac{1}{\sqrt{2}}(-\phi_{1,1} + \phi_{1,-1}) \\ p_y &= \frac{i}{\sqrt{2}}(\phi_{1,1} + \phi_{1,-1}) \\ p_z &= \phi_{1,0} \\ \phi_{1,\pm 1} &= \mp \sqrt{\frac{3}{8\pi}} \sin \theta e^{\pm i\phi} \\ \phi_{1,0} &= \sqrt{\frac{3}{4\pi}} \cos \theta. \end{aligned}$$

Here ϕ_{ij} are eigenfunctions of the operators \mathbf{L}^2 and L_z with respective quantum numbers $l = i$ and $l_z = j$. Then we must add spin and decompose mixed states to get eigenfunctions for total angular momentum. In this way one gets (see Quantum Mechanics)

$$\begin{aligned} \Phi_{3/2,3/2} &= -\frac{1}{\sqrt{2}}(p_x + ip_y) \uparrow \\ \Phi_{3/2,1/2} &= -\frac{1}{\sqrt{6}}[(p_x + ip_y) \downarrow - 2p_z \uparrow] \\ \Phi_{3/2,-1/2} &= -\frac{\sqrt{2}}{\sqrt{3}}[(p_x - ip_y) \uparrow + 2p_z \downarrow] \\ \Phi_{3/2,-3/2} &= \frac{1}{\sqrt{2}}(p_x - ip_y) \downarrow \\ \Phi_{1/2,1/2} &= -\frac{1}{\sqrt{3}}[(p_x + ip_y) \downarrow + p_z \uparrow] \\ \Phi_{1/2,-1/2} &= -\frac{1}{\sqrt{3}}[(p_x - ip_y) \uparrow - p_z \downarrow] \end{aligned}$$

Then one can invert this set of equations to express $|p_i, s\rangle$ through the functions $\Phi_{l,m}$. For references,

$$\begin{aligned}
p_x \uparrow &= \frac{1}{\sqrt{2}} \left[-\Phi_{3/2,3/2} + \frac{1}{\sqrt{3}}\Phi_{3/2,-1/2} - \frac{\sqrt{2}}{\sqrt{3}}\Phi_{1/2,-1/2} \right] \\
p_x \downarrow &= \frac{1}{\sqrt{2}} \left[+\Phi_{3/2,-3/2} - \frac{1}{\sqrt{3}}\Phi_{3/2,1/2} - \frac{\sqrt{2}}{\sqrt{3}}\Phi_{1/2,1/2} \right] \\
p_y \uparrow &= \frac{i}{\sqrt{2}} \left[\Phi_{3/2,3/2} + \frac{1}{\sqrt{3}}\Phi_{3/2,-1/2} - \frac{\sqrt{2}}{\sqrt{3}}\Phi_{1/2,-1/2} \right] \\
p_y \downarrow &= \frac{i}{\sqrt{2}} \left[+\Phi_{3/2,-3/2} + \frac{1}{\sqrt{3}}\Phi_{3/2,1/2} + \frac{\sqrt{2}}{\sqrt{3}}\Phi_{1/2,1/2} \right] \\
p_z \uparrow &= \frac{\sqrt{2}}{\sqrt{3}}\Phi_{3/2,1/2} - \frac{\sqrt{2}}{\sqrt{3}}\Phi_{1/2,1/2} \\
p_z \downarrow &= \frac{\sqrt{2}}{\sqrt{3}}\Phi_{3/2,-1/2} - \frac{\sqrt{2}}{\sqrt{3}}\Phi_{1/2,-1/2}.
\end{aligned}$$

Finally, we can write the spin-orbit Hamiltonian as

$$\mathcal{H}_{so} = \frac{\lambda\hbar^2}{2}[j(j+1) - l(l+1) - s(s+1)].$$

For p -orbitals, $l = 1$, $s = 1/2$ while j is given by the first index of Φ_{ij} . One can prove that the only non-vanishing matrix elements in p representation are

$$\begin{aligned}
\langle p_x \uparrow | \mathcal{H}_{so} | p_y \uparrow \rangle &= -i\frac{\Delta}{3} \\
\langle p_x \uparrow | \mathcal{H}_{so} | p_z \downarrow \rangle &= \frac{\Delta}{3} \\
\langle p_y \uparrow | \mathcal{H}_{so} | p_z \downarrow \rangle &= -i\frac{\Delta}{3} \\
\langle p_x \downarrow | \mathcal{H}_{so} | p_y \downarrow \rangle &= i\frac{\Delta}{3} \\
\langle p_x \downarrow | \mathcal{H}_{so} | p_z \uparrow \rangle &= -\frac{\Delta}{3} \\
\langle p_y \downarrow | \mathcal{H}_{so} | p_z \uparrow \rangle &= -i\frac{\Delta}{3}.
\end{aligned}$$

Here $\Delta = 3\lambda\hbar^2/2$ is the *spin-orbit splitting*. As a result, we arrive at the following structure of valence band, Fig. A.2 Spin-orbit splitting is given in the table A

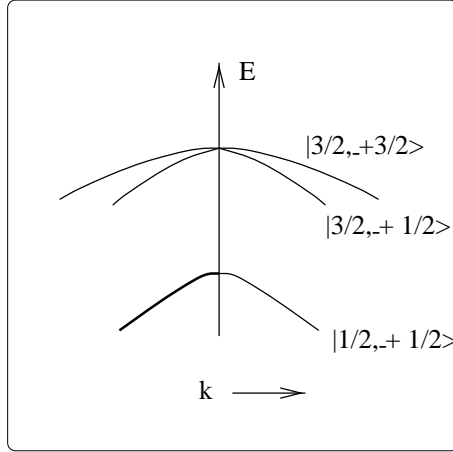


Figure A.2: The general form of the valence band including spin-orbit coupling.

Semiconductor	Δ (eV)
Si	0.044
Ge	0.29
GaAs	0.35
InAs	0.41
InSb	0.82
InP	0.14
GaP	0.094

Table A.1: Spin-orbit splitting for different semiconductors

A.1 Symmetry of the band edge states

One has to discriminate between direct gap (GaAs, InAs) and indirect gap (Si, Ge) materials, Fig. A.3. In direct gap materials the conduction band minimum occurs at Γ -point and have a spherically symmetric central cell function. So they are made of s atomic states. As one goes apart, admixture of p -states appears. This implies important limitations for selection rules.

In the valence band, he have

Heavy holes:

$$\begin{aligned}\Phi_{3/2,3/2} &= -\frac{1}{\sqrt{2}}(|p_x\rangle + i|p_y\rangle) \uparrow \\ \Phi_{3/2,-3/2} &= \frac{1}{\sqrt{2}}(|p_x\rangle - i|p_y\rangle) \downarrow\end{aligned}$$

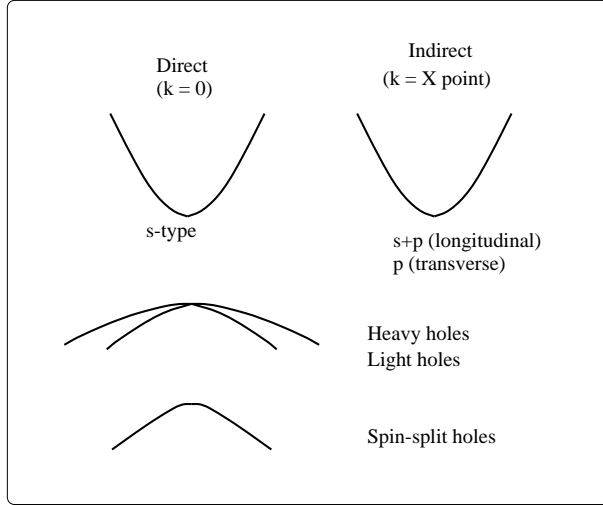


Figure A.3: Schematic description of the nature of central cell functions.

Light holes:

$$\begin{aligned}\Phi_{3/2,1/2} &= -\frac{1}{\sqrt{6}} [(|p_x\rangle + i|p_y\rangle) \downarrow -2|p_z\rangle \uparrow] \\ \Phi_{3/2,-1/2} &= \frac{1}{\sqrt{6}} [(|p_x\rangle - i|p_y\rangle) \uparrow +2|p_z\rangle \downarrow]\end{aligned}$$

Split-off hole states:

$$\begin{aligned}\Phi_{1/2,1/2} &= -\frac{1}{\sqrt{3}} [(|p_x\rangle + i|p_y\rangle) \downarrow +|p_z\rangle \uparrow] \\ \Phi_{1/2,-1/2} &= -\frac{1}{\sqrt{3}} [(|p_x\rangle - i|p_y\rangle) \uparrow +|p_z\rangle \downarrow]\end{aligned}$$

A Brillouin zone for silicon is shown in Fig. A.2

A.2 Modifications in heterostructures.

An important feature is how the bands align. Three type are usually studied, Fig. A.5.

The problem of band offsets is very complicated, and several theories exist.

Quantum wells

Let us discuss the case where the well region is made of direct gap material, so conduction band states are of *s*-type while valence band states are *p*-type. For simplicity we discuss square-box confinement, Fig- A.6. Within the effective mass approach the Schrödinger

equation for the electron states is (in the following we do not discriminate between m^* and m)

$$\left[-\frac{\hbar^2}{2m^*} \nabla^2 + V(z) \right] \psi = E\psi.$$

Looking for the solution as

$$\Psi(\mathbf{r}) = e^{i(k_y y + k_x x)} f(z)$$

we have the equation for f

$$\left[-\frac{\hbar^2}{2m^*} \frac{\partial^2}{\partial z^2} + V(z) \right] \psi = E_n \psi.$$

For an infinite barrier, its solution has the form

$$\begin{aligned} f(z) &= \cos \frac{\pi n z}{W}, & \text{if } n \text{ is even} \\ &= \sin \frac{\pi n z}{W}, & \text{if } n \text{ is odd} \\ E_n &= \frac{\pi^2 \hbar^2 n^2}{2m W^2}. \end{aligned}$$

Then the total energy is

$$E = E_n + \frac{\hbar^2 k_{\parallel}^2}{2m}.$$

The situation for the valence band is much more complicated because the heavy- and light-hole states mix away from $\mathbf{k} = 0$.

A.3 Impurity states

A typical energy level diagram is shown on Fig. A.7 Shallow levels allow a universal description because the spread of wave function is large and the potential can be treated as from the point charge,

$$U(r) = e^2/\epsilon r.$$

To find impurity states one has to treat Schrödinger equation (SE) including periodic potential + Coulomb potential of the defect.

Extremum at the center of BZ

Then for small k we have

$$E_n(k) = \frac{\hbar^2 k^2}{2m}.$$

We look for solution of the SE

$$(\mathcal{H}_0 + U)\psi = E\psi$$

in the form

$$\psi = \sum_{n'k'} B_{n'}(\mathbf{k}') \phi_{n'k'}(\mathbf{r}),$$

where $\phi_{n'k'}(\mathbf{r})$ are Bloch states. By a usual procedure (multiplication by $\phi_{nk}^*(\mathbf{r})$ and integration over \mathbf{r}) we get the equation

$$\begin{aligned} [E_n(\mathbf{k}) - E] B_n(\mathbf{k}) + \sum_{n'k'} U_{n'k'}^{nk} B_{n'}(\mathbf{k}) &= 0 \\ U_{n'k'}^{nk} &= \frac{1}{V} \int u_{nk}^* u_{n'k'} e^{i(k'-k)\mathbf{r}} U(\mathbf{r}) d\mathbf{r}. \end{aligned}$$

Then, it is natural to assume that $B(\mathbf{k})$ is nonvanishing only near the BZ center, and to replace central cell functions u by their values at $\mathbf{k} = 0$. These function rapidly oscillate within the cell while the rest varies slowly. Then within each cell

$$\int_{\text{cell}} u_{n0}^* u_{n'0} d\mathbf{r} = \delta_{nn'}$$

because Bloch functions are orthonormal. Thus,

$$\begin{aligned} [E_n(\mathbf{k}) - E] B_n(\mathbf{k}) + \sum_{n'} U(\mathbf{kk}') B_n(\mathbf{k}') &= 0 \\ U(\mathbf{kk}) &= \frac{1}{V} \int e^{i(\mathbf{k}-b\mathbf{k}')\mathbf{r}} U(r) d\mathbf{r} = -\frac{4\pi e^2}{\epsilon V |\mathbf{k} - \mathbf{k}'|^2}. \end{aligned}$$

Finally we get

$$\left[\frac{\hbar^2 k^2}{2m} - E \right] B_n(\mathbf{k}) - \frac{4\pi e^2}{\epsilon V} \sum_{\mathbf{k}'} \frac{1}{|\mathbf{k} - \mathbf{k}'|^2} B_n(\mathbf{k}')$$

where one can integrate over \mathbf{k} in the infinite region (because $B_n(\mathbf{k})$ decays rapidly).

Coming back to the real space and introducing

$$F(\mathbf{r}) = \frac{1}{\sqrt{V}} \sum_{\mathbf{k}} B_n(\mathbf{k}) e^{i\mathbf{kr}}$$

we come to the SE for a hydrogen atom,

$$\left[-\frac{\hbar^2}{2m} \nabla^2 - \frac{e^2}{\epsilon r} \right] F(r) = E F(r).$$

Here

$$\begin{aligned} E_t &= -\frac{1}{t^2} \frac{e^4 m}{2\epsilon^2 \hbar^2}, \quad t = 1, 2 \dots \\ F(r) &= (\pi a^3)^{-1/2} \exp(-r/a), \quad a = \hbar^2 \epsilon / m e^2. \end{aligned}$$

For the total wave function one can easily obtain

$$\psi = u_{n0}(\mathbf{r}) F(\mathbf{r}).$$

The results are summarized in the table.

Material	ϵ	m/m_0	E_{1s} (th.) (meV)	E_{1s} (exp.) (meV)
GaAs	12.5	0.066	5.67	Ge: 6.1 Si: 5.8 Se: 5.9 S: 6.1 S: 5.9
InP	12.6	0.08	6.8	7.28
CdTe	10	0.1	13	13.*

Table A.2: Characteristics of the impurity centers.

Several equivalent extrema

Let us consider silicon for example. The conduction band minimum is located at $k_z = 0.85(2\pi/a)$ in the [100] direction, the constant energy surfaces are ellipsoids of revolution around [100]. There must be 6 equivalent ellipsoids according to cubic symmetry. For a given ellipsoid,

$$E = \frac{\hbar^2}{2m_\ell}(k_z - k_z^0)^2 + \frac{\hbar^2}{2m_t}(k_x^2 + k_y^2).$$

Here $m_\ell = 0.916m_0$, $m_t = 0.19m_0$. According to the effective mass theory, the energy levels are N -fold degenerate, where n is the number of equivalent ellipsoids. In real situation, these levels are split due to short-range corrections to the potential. These corrections provide inter-extrema matrix elements. The results for an arbitrary ration $\gamma = m_t/m_\ell$ can be obtained only numerically by a variational method (Kohn and Luttinger). The trial function was chosen in the form

$$F = (\pi a_\parallel a_\perp^2)^{-1/2} \exp \left\{ - \left[\frac{x^2 + y^2}{a_\perp^2} + \frac{z^2}{a_\parallel} \right]^{1/2} \right\},$$

and the parameters a_i were chosen to minimize the energy at given γ . Excited states are calculated in a similar way. The energies are listed in table A.3.

Material	E_{1s} (meV)		E_{2p_0} (meV)
Si (theor.)		31.27	11.51
Si(P)	45.5	33.9	11.45
Si(As)	53.7	32.6	11.49
Si(Sb)	42.7	32.9	11.52
Ge(theor/)		9.81	4.74
Ge(P)	12.9	9.9	4.75
Ge(As)	14.17	10.0	4.75
Ge(Sb)	10.32	10.0	4.7

Table A.3: Donor ionization energies in Ge and Si. Experimental values are different because of chemical shift

Impurity levels near the point of degeneracy

Degeneracy means that there are $t > 1$ functions,

$$\phi_{n\mathbf{k}}^j, \quad j = 1, 2..t$$

which satisfy Schrödinger equation without an impurity. In this case (remember, $\mathbf{k} \approx 0$),

$$\psi = \sum_{j=1}^t F_j(\mathbf{r}) \phi_{n0}^j(br) .$$

The functions F_j satisfy matrix equation,

$$\sum_{j'=1}^t \left[\sum_{\alpha,\beta=1}^3 H_{jj'}^{\alpha\beta} \hat{p}_\alpha \hat{p}_\beta + U(\mathbf{r}) \delta_{jj'} \right] F_{j'} = EF_j . \quad (\text{A.1})$$

If we want to include spin-orbital interaction we have to add

$$\mathcal{H}_{so} = \frac{1}{4m_0^c c^2} [\boldsymbol{\sigma} \times \nabla V] \cdot \hat{\mathbf{p}} .$$

Here $\boldsymbol{\sigma}$ is the spin operator while V is periodic potential. In general \mathcal{H} -matrix is complicated. Here we use the opportunity to introduce a simplified (the so-called invariant) method based just upon the symmetry.

For simplicity, let us start with the situation when spin-orbit interaction is very large, and split-off mode is very far. Then we have 4-fold degenerate system. Mathematically, it can be represented by a pseudo-spin 3/2 characterized by a pseudo-vector \mathbf{J} .

There are only 2 invariants quadratic in \mathbf{p} , namely $\hat{\mathbf{p}}^2$ and $(\hat{\mathbf{p}} \cdot \mathbf{J})^2$. Thus we have only two independent parameters, and traditionally the Hamiltonian is written as

$$\mathcal{H} = \frac{1}{m_0} \left[\frac{\hat{\mathbf{p}}^2}{2} \left(\gamma_1 + \frac{5}{2}\gamma \right) - \gamma(\hat{\mathbf{p}} \cdot \mathbf{J})^2 \right] . \quad (\text{A.2})$$

That would be OK for spherical symmetry, while for cubic symmetry one has one more invariant, $\sum_i \hat{p}_i^2 J_i^2$. As a result, the Hamiltonian is traditionally expressed as

$$\mathcal{H} = \frac{1}{m_0} \left[\frac{\hat{\mathbf{p}}^2}{2} \left(\gamma_1 + \frac{5}{2}\gamma_2 \right) - \gamma_3(\hat{\mathbf{p}} \cdot \mathbf{J})^2 + (\gamma_3 - \gamma_2) \sum_i \hat{p}_i^2 J_i^2 \right] . \quad (\text{A.3})$$

This is the famous Luttinger Hamiltonian. Note that if the lattice has no inversion center there also linear in \mathbf{p} terms.

Now we left with 4 coupled Schrödinger equations (A.1). To check the situation, let us first put $U(\mathbf{r}) = 0$ and look for solution in the form

$$F_j = A_j(\mathbf{k}/k) e^{i\mathbf{kr}}, \quad k \equiv |\mathbf{k}| .$$

The corresponding matrix elements can be obtained by substitution $\hbar\mathbf{k}$ instead of the operator \hat{p} into Luttinger Hamiltonian. The Hamiltonian (A.2) does not depend on the direction of \mathbf{k} . Thus let us direct \mathbf{k} along z axis and use representation with diagonal J_z^2 . Thus the system is decoupled into 4 independent equation with two different eigenvalues,

$$E_\ell = \frac{\gamma_1 + 2\gamma}{2m_0} \hbar^2 k^2, \quad E_h = \frac{\gamma_1 - 2\gamma}{2m_0} \hbar^2 k^2.$$

If

$$\gamma_1 \pm 2\gamma > 0$$

both energies are positive (here the energy is counted inside the valence band) and called the light and heavy holes. The effective masses are

$$m_{\ell(h)} = m_0 / (\gamma_1 \pm \gamma).$$

The calculations for the full Luttinger Hamiltonian (A.3) require explicit form of \mathbf{J} -matrices. Its solutions lead to the anisotropic dispersion law

$$E_{\ell,h} = \frac{\hbar^2}{2m_0} \left\{ \gamma_1 k^2 \pm 4 [\gamma_2^2 k^4 + 12(\gamma_3^2 - \gamma_2^2)(k_x^2 k_y^2 + k_y^2 k_z^2 + k_z^2 k_x^2)]^{1/2} \right\}.$$

The parameters of Ge and Si are given in the Table A.3

Material	γ_1	γ_2	γ_3	Δ	ϵ
Ge	4.22	0.39	1.44	0.044	11.4
Si	13.35	4.25	5.69	0.29	15.4

Table A.4: Parameters of the Luttinger Hamiltonian for Ge and Si

The usual way to calculate acceptor states is variational calculation under the spherical model (A.2). In this case the set of 4 differential equations can be reduced to a system of 2 differential equation containing only 1 parameter, $\beta = m_\ell/m_h$.

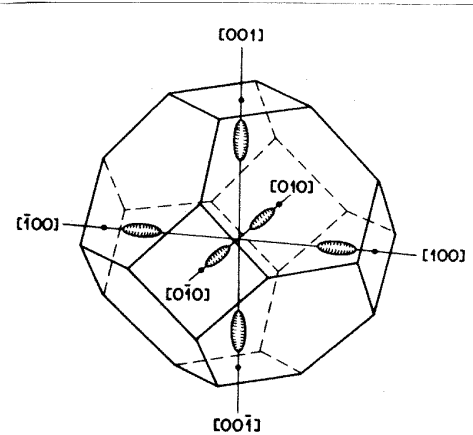


Figure A.4: Constant energy ellipsoids for Si conduction band. There are 6 equivalent valleys resulting in a very large density of states.

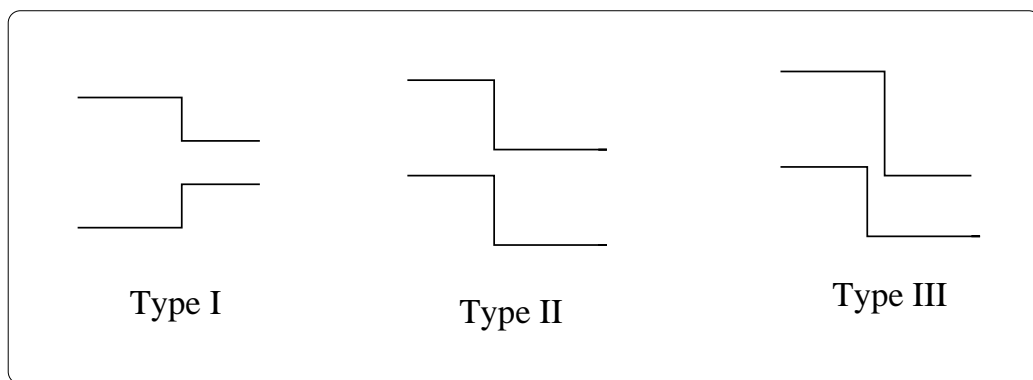


Figure A.5: Various possible band lineups in heterostructures.

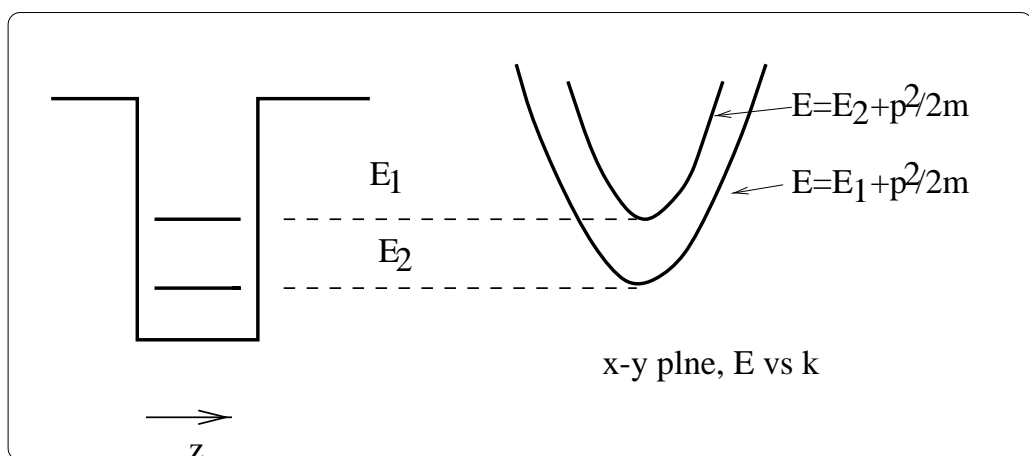


Figure A.6: Subband levels in a quantum well.

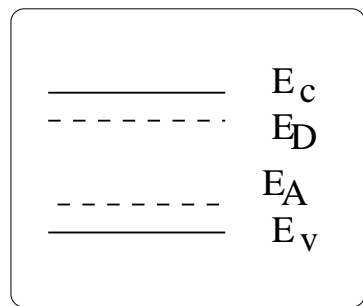


Figure A.7: band diagram of a semiconductor.

Appendix B

Useful Relations

B.1 Trigonometry Relations

$$\begin{pmatrix} \cos x \\ \sin x \end{pmatrix} = \frac{1}{2} (e^{ix} \pm e^{-ix}) \quad (\text{B.1})$$

$$\begin{pmatrix} \cos^2 x \\ \sin^2 x \end{pmatrix} = \frac{1}{2} (1 \pm \cos x) \quad (\text{B.2})$$

B.2 Application of the Poisson summation formula

The Poisson formula reads

$$\sum_{N=-\infty}^{\infty} \varphi(2\pi N + t) = \frac{1}{2\pi} \sum_{l=-\infty}^{\infty} e^{ilt} \int_{-\infty}^{\infty} \varphi(\tau) e^{-il\tau} d\tau.$$

In our case

$$\varphi(2\pi N + t) = \frac{1}{(2\pi)^{3/2}} (2\pi N + t)^{3/2} \quad (\text{B.3})$$

if we replace $N \rightarrow -N$ and put $t = 2\pi x - \pi$. The other difference is that the function φ is finite. So, if we introduce the maximal integer in the quantity x as $[x]$ we get the limits of the φ

$$\text{from } 2\pi \left(x - \frac{1}{2} - [x] - \frac{1}{2} \right) \text{ to } t.$$

The lower limit we replace by 0 that is good for large x . Finally we get the for $\Phi(x)$

$$\Phi(x) = \frac{1}{(2\pi)^{5/2}} \sum_{l=-\infty}^{\infty} e^{ilt} \int_0^t \tau^{3/2} e^{-il\tau} d\tau.$$

Then we take into account that for $l = 0$

$$\int_0^t \tau^{3/2} d\tau = \frac{2}{5} t^{5/2},$$

and combine the item with $\pm l$. As a result, we get

$$\begin{aligned} & (-1)^l \left\{ e^{2\pi ilx} \int_0^t \tau^{3/2} e^{-il\tau} d\tau + \right. \\ & \quad \left. + e^{-2\pi ilx} \int_0^t \tau^{3/2} e^{il\tau} d\tau \right\} = \\ & = (-1)^l 2 \int_0^t \tau^{3/2} \cos [2\pi l(x - \tau)] d\tau. \end{aligned}$$

Then we integrate by parts twice to transform $\tau^{3/2} \rightarrow \tau^{-1/2}$ and changing $\tau \rightarrow (\pi/2l)z^2$ we get

$$\begin{aligned} \Phi(x) &= \frac{1}{(2\pi)^{5/2}} \left[\frac{2}{5} (2\pi x)^{5/2} + 3 \sum_{l=1}^{\infty} \frac{(-1)^l}{l^{5/2}} \left\{ (2\pi lx)^{1/2} - \right. \right. \\ &\quad \left. \left. - \sqrt{\frac{\pi}{2}} \left[\sin(2\pi lx) S(\sqrt{4lx}) + \cos(2\pi lx) C(\sqrt{4lx}) \right] \right\} \right]. \end{aligned}$$

Here we have introduced the Fresnel integrals

$$\begin{aligned} S(u) &= \int_0^u \sin\left(\frac{\pi}{2}x^2\right) dx \\ C(u) &= \int_0^u \cos\left(\frac{\pi}{2}x^2\right) dx. \end{aligned}$$

These function oscillate with the period ≈ 1 and with dumping amplitudes; the asymptotic behavior being 0.5 at $u \rightarrow \infty$. The non-oscillating term can be easily summed over l :

$$\sum_{l=1}^{\infty} \frac{(-1)^l}{l^{5/2}} (2\pi lx)^{1/2} = (2\pi x)^{1/2} \sum_{l=1}^{\infty} \frac{(-1)^l}{l^2} = -\frac{\pi^2}{12} (2\pi x)^{1/2}$$

Appendix C

Vector and Matrix Relations

Vector \mathbf{A} is a column A_i . Usually, two kind of vector products are defined: the *scalar product*

$$\mathbf{AB} = \mathbf{A} \cdot \mathbf{B} = \sum_i A_i B_i$$

and the *vector product*

$$[\mathbf{AB}] = [\mathbf{A} \times \mathbf{B}] = \det \begin{vmatrix} \mathbf{i}_1 & \mathbf{i}_2 & \mathbf{i}_3 \\ A_1 & A_2 & A_3 \\ B_1 & B_2 & B_3 \end{vmatrix}$$

where \mathbf{i}_i are the unit vectors. We have $\mathbf{AB} = \mathbf{BA}$, $[\mathbf{A} \times \mathbf{B}] = -[\mathbf{B} \times \mathbf{A}]$.

Matrix \hat{A} is a table with the elements A_{ik} . If

$$A_{ik} = A_i \delta_{ik}$$

the matrix is called the *diagonal*, the unit matrix $\hat{1}$ has the elements δ_{ik} . We have $\hat{1}\hat{A} = \hat{A}\hat{1} = \hat{A}$. 0-matrix has all the elements equal to 0; $(\hat{A} + \hat{B})_{ik} = A_{ik} + B_{ik}$.

Trace of the matrix defined as

$$\text{Tr } \hat{A} = \sum_i A_{ii}; \quad \text{Tr}(\hat{A}\hat{B}) = \text{Tr}(\hat{B}\hat{A}).$$

Matrix dot product is defined as

$$(\hat{A}\hat{B})_{ik} = \sum_l A_{il} B_{lk}.$$

It is important that $\hat{A}\hat{B} \neq \hat{B}\hat{A}$. At the same time, $\hat{C}(\hat{B}\hat{A}) = (\hat{C}\hat{B})\hat{A}$. The *inverse matrix* is defined by the relation

$$\hat{A}\hat{A}^{-1} = \hat{A}^{-1}\hat{A} = \hat{1}.$$

We have

$$(\hat{A}\hat{B})^{-1} = \hat{B}^{-1}\hat{A}^{-1}.$$

The *conjugate* matrix is defined as

$$\left(\hat{A}^\dagger\right)_{ik} = A_{ki}^*.$$

If $\hat{A}^\dagger = \hat{A}$ the matrix is called the *Hermitian*. The matrix is called *unitary* if

$$\hat{A}^\dagger = \hat{A}^{-1}, \text{ or } \hat{A}^\dagger \hat{A} = \hat{1}.$$

Sometimes it is useful to introduce a row \mathbf{A}^\dagger with the elements A_i . We get $\mathbf{A}^\dagger \mathbf{A} = \sum_i A_i^2$.

Eigenvectors \mathbf{u} and eigenvalues λ of the matrix \hat{A} are defined as solutions of matrix equation:

$$\hat{A}\mathbf{u} = \lambda\mathbf{u} \quad \text{or} \quad \sum_k (A_{ik} - \lambda\delta_{ik})u_k = 0.$$

It is a set of i equations. The number of solutions is equal to the matrix's range. They exist only if

$$\det(\hat{A} - \lambda\hat{1}) = 0,$$

it is just the equation for the eigenvalues λ_i . If the matrix \hat{A} is Hermitian, its eigenvalues are real

Bibliography

- [1] N. W. Ashcroft, and N. D. Mermin, *Solid State Physics* (Holt, Rinehart and Winston, New York, 1976).
- [2] C. Kittel, *Quantum Theory of Solids* (John Wiley and Sons, New York, 1987).
- [3] K. Seeger “*Semiconductor Physics*”, Springer (1997)
- [4] Jasprit Singh, *Physics of Semiconductors and their Heterostructures* (McGraw-Hill, Inc., New York, 1993).
- [5] R. B. Leighton, *Principles of Modern Physics* (McGraw-Hill, Inc., New York, 1959).
- [6] H. Haug and S. W. Koch *Quantum theory of the optical and electronic properties of semiconductors*, World Scintific, 1990.